Stable isotope dendroclimatology at Forfjorddalen in northwestern Norway.

Young, Giles Hugh Findlay

Stable Isotope Dendroclimatology at Forfjorddalen in Northwestern Norway

Giles Hugh Findlay Young

Submitted to the University of Wales in fulfillment of the requirements for the Degree of Doctor of Philosophy

Department of Geography
School of the Environment and Society
Swansea University
January 2008

ProQuest LLC.
789 East Eisenhower Parkway
P.O. Box 1346
Ann Arbor, MI 48106 – 1346

"... isn't it good Norwegian wood"

Lennon and McCartney (1965)

SUMMARY

Climate change has become a key issue for the 21st century and producing future climatic scenarios has become a priority. However, to model future climate scenarios successfully and to understand their implications it is important to have a clear picture of past climate. Stable isotopes from tree rings may have the potential to reconstruct past climate at all temporal frequencies. This thesis presents a reconstruction of temperature (AD 1394-2001) and precipitation (AD 1765-2001) from Forfjorddalen in northwest Norway based on $\delta^{13}C$ and $\delta^{18}O$, respectively. Tree cores were dated and the annual growth rings cut and extracted to α-cellulose, measurements of $\delta^{13}C$ and $\delta^{18}O$ were then made. Corrected $\delta^{13}C_{pin}$ was calibrated with temperature ($r = 0.71$) and $\delta^{18}O$ with precipitation ($r = 0.57$). A conceptual model of the relationship between $\delta^{13}C$ and $\delta^{18}O$ and temperature and precipitation is presented to explain a period of non-linearity in the relationship between $\delta^{13}C$ and temperature. The $\delta^{13}C$ temperature reconstruction suggests periods with warmer summer temperatures than the late twentieth century during the mid 18th and early 17th centuries; the coldest periods occur in the early 15th and late 19th centuries. This reconstruction compares favorably with long Scandinavian temperature records form Tornedalen (AD 1802) and Uppsala (AD 1722) and a recent tree-ring density based reconstruction from Torneträsk. It also exhibits much greater multi-decadal variability than the previous, ring-width based, Forfjorddalen temperature reconstruction. A precipitation reconstruction (AD 1765 to 2001) shows wet conditions during the late 18th and early 19th centuries followed by a dry period in the late 19th century, becoming wetter again through the 20th century. Spatial field correlations demonstrate the potential for proxy data from Forfjorddalen to reconstruct climate on a regional scale; combination with data from Torneträsk yields correlations $> r = 0.70$ with much of northwestern Scandinavian temperature.

DECLARATION

This work has not previously been accepted in substance for any degree and is not being concurrently submitted in candidature for any degree.

Signed ..... (Candidate)

Date 26th June 2008

STATEMENT 1

This thesis is the result of my own investigations, except where otherwise stated. Other sources are acknowledged in Harvard (author-year) style. A bibliography is appended.

Signed ..... (Candidate)

Date 26th June 2008

STATEMENT 2

I hereby give consent for my thesis, if accepted, to be available for photocopying and for inter-library loan, and for the title and summary to be made available to outside organisations.

Signed ..... (Candidate)

Date 26th June 2008

ACKNOWLEDGMENTS

I would like to take this opportunity to acknowledge my gratitude to the people an organisations that have helped to make this PhD research project possible.

Firstly I would like to thank my supervisory panel: Professor Danny McCarroll for all his support, and his many helpful and stimulating ideas and insights; Dr Neil Loader, for passing on to me so much of his knowledge and experience of fieldwork, laboratory techniques and mass spectrometry; and Dr Andreas Kirchhefer (of Tromsø University), for all his help with fieldwork and tree-core dating and his invaluable local knowledge.

There are numerous other people whose help I would like to acknowledge. Firstly, the other members of the Swansea University dendroclimatology group: Dr Iain Robertson, Dr Mary Gagen, Dr Penny Blackmore, Paula Santillo, Jonathan Woodman-Ralph, Roderick Bale, Rochelle Campbell, Tommy Wils and Ewan Woodley. Other members of the Geography Department I would like to thank are (in no particular order): Professor John Matthews, Dr Sietse Los, Professor Rory Walsh, Professor Alayne Street-Perrott, Nathan Scott, Dr William Grey, Alan Cutliffe, Philip Bevan, Steve Shaw, Gill Oliver, Anna Ratcliffe and Nicola Jones. Outside of Swansea University I would like to thank: Professor Roy Switsur, Professor John Waterhouse, Dr Håkan Grudd, Dr Hans Linderholm and Dr Björn Gunnarson.

I would also like to acknowledge the University of Swansea and Swansea University Geography Department for offering me the opportunity, and providing me with the facilities, to undertake this PhD, and the National Environment Research Council (NERC) for funding my research.

Finally I would especially like to acknowledge my debt two people: Roderick Bale, who started this journey with me just over three years ago, and has helped to make it all seem like fun; and Joanne Demmler who has helped me more often and in more ways than I could possibly hope to list here. Thank You.

Contents

List of Figures

List of Tables

1

Research Background

1.1 Introduction

Climatic change has become one of the key issues of the twenty first century. Not only is it now recognised that global temperatures are generally rising (with a mean increase of 0.76°C ±0.19°C from AD 1850-1899 to AD 2001-2005), and increasingly so since around AD 1950 (mean decadal temperature rises over the past 50 years of 0.13°C ±0.13°C) (IPCC, 2007). There is a mounting body of evidence suggesting that these recent temperature rises may be due to an anthropogenically enhanced greenhouse affect. The four reports of Intergovernmental Panel on Climate Change (IPCC) have increasingly come to the conclusion (IPCC, 1990, 1996, 2001, 2007) that a discernible human influence on climate exists and this anthropogenic affect on climate is also expected to continue. Future prediction of global climate change from the latest IPCC report suggests that even were greenhouse gas levels to remain stable at the AD 2000 levels global mean temperatures would still rise by between 0.3°C and 0.9°C by the end of the century (IPCC, 2007). Under their most extreme (A1F1) scenario global mean temperatures are expected to rise between 2.4°C and 6.4°C (best estimate of 4°C), while even under the most conservative (B1) scenario the IPCC (2007) expects a global mean temperature rise of between 1.1 and 2.9°C (best estimate 1.6°C).

While major climate fluctuations have been recognised during much of the Quaternary (Bond et al., 1993; Dansgaard et al., 1993; Petit et al., 1999) and to a lesser extent during the Holocene, most recently in the shape of the so called Medieval Warm Period (MWP) and Little Ice Age (LIA) (Lamb, 1965, 1995; Bradley and Jones, 1992a; Matthews and

Briffa, 2005), there is an increasing consensus amongst scientists, with a few notable exceptions (e.g. Soon and Baliunas, 2003; McIntyre and McKitrick, 2005), that recent global temperatures have no analogue within the last millennium (Mann et al., 1999; Briffa, 2000; Crowley and Lowery, 2000; Esper et al., 2002; Moberg et al., 2005) and that human agency may well be behind this warming trend (IPCC, 2007).

Under IPCC emissions scenarios, General Circulation Models (GCM) have suggested that high latitude land masses in the Northern Hemisphere will experience the highest magnitude of warming (IPCC, 2001, 2007), including northern Fennoscandia. It is however vital to test such models to determine how accurate they may prove to be, and so as we have no data available for future climate the only way to achieve this is retrodictively, on past climate. Unfortunately instrumental data, for which there is a reasonable network for the past 150 years (Parker et al., 2000), are not sufficient to take in the full range of Holocene climatic variation and so detailed, high resolution proxy data sets are required for a wide network of site specific locations to reconstruct real past climatic variability. Of the available climatic proxy archives tree rings offer several unique advantages: they have a perfect annual resolution; are extremely widespread; easily accessible; and highly sensitive to climatic change. They also contain within each annual growth ring a variety of individual proxies which can be used to reconstruct climate individually or combined for a multiproxy reconstruction (McCarroll and Loader, 2004, 2006).

This research aims to provide a detailed climatic reconstruction using this multiproxy dendroclimatic technique for the past 600 years on the Vesterålen archipelago in northwest Norway. The period under examination may encompass the end of the Medieval Warm Period, the Little Ice Age and twentieth century climate. The area chosen is strongly influenced by the North Atlantic with its large scale climatic influences such as the North Atlantic Oscillation and the North Atlantic Drift.

1.2 Climate change

It was in the early years of the nineteenth century that scientists began to question the history of the world described in the Bible. Until then the glaciogenic sediments that cover much of the northern hemisphere were interpreted as being the result of the 'biblical flood'. The nineteenth century development of the 'glacial theory' by scientists such as Louis Agassiz led to a more rational cause of these features and by the early years of the twentieth century was widely accepted. The mechanisms that drove such dramatic climatic change were explained by the theoretical work of Milutin Milankovitch who demonstrated that cyclical variations in the Earth's orbit may explain insolation changes that could lead to the onset of glaciations. They could not however explain the magnitude of these changes or what the timing of the four glaciations recognised at the time in the terrestrial record. It was not until the analysis of the stable oxygen isotope ratios of marine cores that the full extent of Quaternary climatic fluctuation was glimpsed and the predictive ability of the Milankovitch hypothesis realised (Imbrie and Imbrie, 1979). Detailed studies of the proxy climatic record contained in ice cores has shed further light on the climate of the late Quaternary (Alley, 2000; Bond et al., 1993; Dansgaard et al., 1993; Petit et al., 1999). Figure 1.1 shows the $\delta^{18}O$ record of the GRIP ice core for the last 125,000 years, with extreme fluctuations up until the last 10,000 years, followed by the relative stability of the Holocene.

Although on a rather more modest scale, climatic fluctuations have been recognised within the Holocene. At the end of the Younger Dryas stadial there was a rapid warming to the Holocene climatic optimum or hypsithermal when temperatures may have been 2-3°C warmer than at present (Roberts, 1998). Although early Holocene warming appears to have been interrupted by a short cold event at around 8200 BP (Alley et al., 1997). Climate then gradually deteriorated and what has been termed a neoglaciation ensued. At this time glaciers and ice caps are thougt to have reformed after their early Holocene disappearance (Nesje and Kvamme, 1991; Matthews and Kárlen, 1992; Nesje et al., 2001). The timing of the onset of this is far from clear but much of the evidence

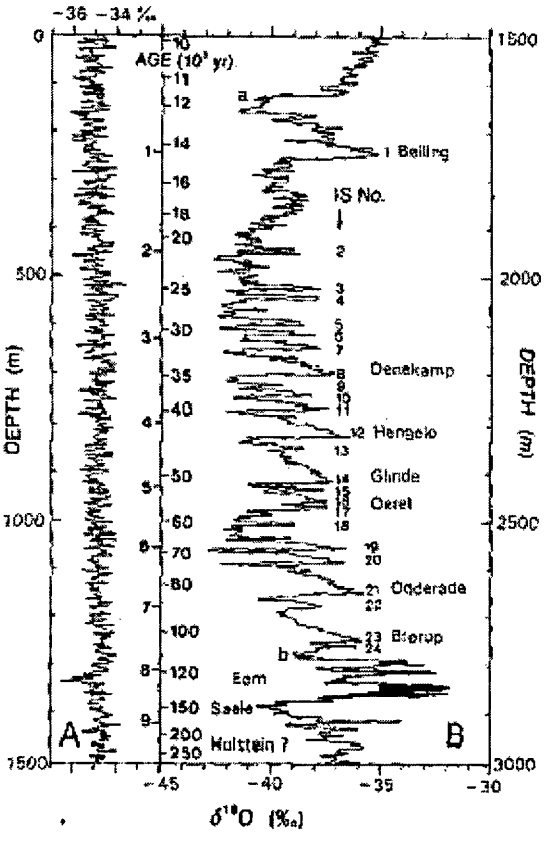

Figure 1.1: The GRIP δ^{18}O profile plotted on a linear depth scale.
Note the stability of the Holocene record (A), on the left, compared to previous 250k years (B), on the right, with the timescale in the centre (Dansgaard et al., 1993).

points to ~4000-5000 years BP (Grove, 1988). At lower latitudes the picture is more complex but much of the evidence suggests that tropical and sub-tropical regions may have experienced greater climatic instability throughout the Holocene than observed at higher latitudes (Bradley et al., 2003a).

Over the past past ~1100 years researchers have described a distinct warm and cold period which have been called the Medieval Warm Period (MWP) and Little Ice Age (LIA). The MWP was first recognised and named by (Lamb, 1965) referring to a period of supposed warmth between around AD 900 and AD 1300. Little Ice Age was a term first used by Matthes (1939), when referring to early Holocene neoglaciation, the term has however become most strongly associated with a supposed cold epoch stretching from around

AD 1300 to AD 1900 (Grove, 1988). The reality, scale and global extent of these two phenomena have often figured in the debate on late twentieth century global warming and its possible anthropogenic origins. If medieval warmth were demonstrated to be of similar or greater magnitude and extent to late twentieth century global temperatures it could not have been as a result of the extensive burning of fossil fuels and so recent warming would have a recent natural analogue.On the other hand, if there are no recent analogues for modern temperatures this may lend weight to the idea that there is some additional driving force to recent temperature increases (anthropogenically released greenhouse gasses), which may be expected to continue to affect climate many decades into the future IPCC (2007).

The prospect has also been raised of abrupt and threshold changes in climate (Jansen et al., 2007). Various abrupt climate changes have been identified, either as large changes in climate in less than 30 years and/or threshold transitions, where climate moves from one steady state to another, but with different base levels (Clark et al., 2002; Alley et al., 2003). Changes of this nature appear to have been common during the Quaternary (Dansgaard et al., 1993). The most notable of which were the Dansgaard-Oescher (D-O) events, characterised by warming in Greenland of 8°C to 16°C within a few decades (Seveinghaus and Brook, 1999). While in the North Atlantic Heinrich events, large flotillas of icebergs discharged into the North Atlantic (diagnosed by drop-stones in sea sediments) have been characterised by large reductions in sea surface salinity (Bond et al., 1993). The cold event at around 8200 BP which is a prominent feature of Greenland ice cores with inferred cooling of between 2°C to 6°C (Alley et al., 1997) is the largest identified rapid climate event during the Holocene. A likely cause for this event is the outburst flood discharge of fresh water into the North Atlantic from the pro-glacial Lake Agassiz, possibly as much as 5 Sv (1 Sv (Svedrup) = $10^6 m^3$per second) over half a year into Hudson Bay (Clarke et al., 2004). GCMs have been used to test this hypothesis and to assess the risks that the current addition of fresh water, especially into the North Atlantic, may cause such events in the future (Alley and Agustsdottir, 2005), and indeed some GCMs are able to broadly simulate what has been observed of the 8.2 event (Jansen

et al., 2007). However, making analogies between conditions which prevailed around the 8.2 event (essentially a late glacial climate, with extremely large pro-glacial lakes) and modern conditions may not be especially realistic (Mayewski et al., 2004). It has, however, been suggested that Holocene climate may not have been as stable as had previously been supposed with several researchers identifying periods of relatively rapid climate change (Mayewski et al., 2004; Jansen et al., 2007)

1.3 Climate of the Past 1000 Years

Instrumental climatic data, which exist for relatively large areas of the northern hemisphere back to the mid-1850s (Jones et al., 1999; Parker et al., 2000) have indicated a general average warming of 0.6°C since AD 1861, with a marked seasonal contrast: winters have warmed by 0.8°C and summers by only 0.4°C . This warming has occurred principally in two phases, from around AD 1920 to 1945 and AD 1975 to present (Jones et al., 2001), the AD 1990s were the warmest decade on record while AD 1998 and AD 2005 were the warmest years (IPCC, 2007). The global temperature data sets that these data are derived from have been recently updated (Jones and Moberg, 2003; Brohan et al., 2006) and appear generally homogeneous (Vose et al., 2005; IPCC, 2007). However there is rather more debate surrounding earlier non-instrumental data covering the MWP and LIA.

The classic definition of the MWP of Lamb (1965) was based largely on evidence from western Europe, much of which was anecdotal. Lamb (1965) suggested that temperatures between AD 1000 and AD 1200 were ~1 to 2°C above present values, which probably meant the AD 1931-1961 average (Bradley et al., 2003b). Many subsequent researchers have questioned the reality of a MWP (Hughes and Diaz, 1994). Evidence for prolonged drought rather than warmth in the western United States led Stine (Stine, 1994, 1998) to suggest that the term Medieval Climate Anomaly would be more suitable. The LIA is a rather better recorded phenomenon: its end lies within the period widespread instrumental climate data (~AD 1850 to 1900); while physical features such as moraines bear witness

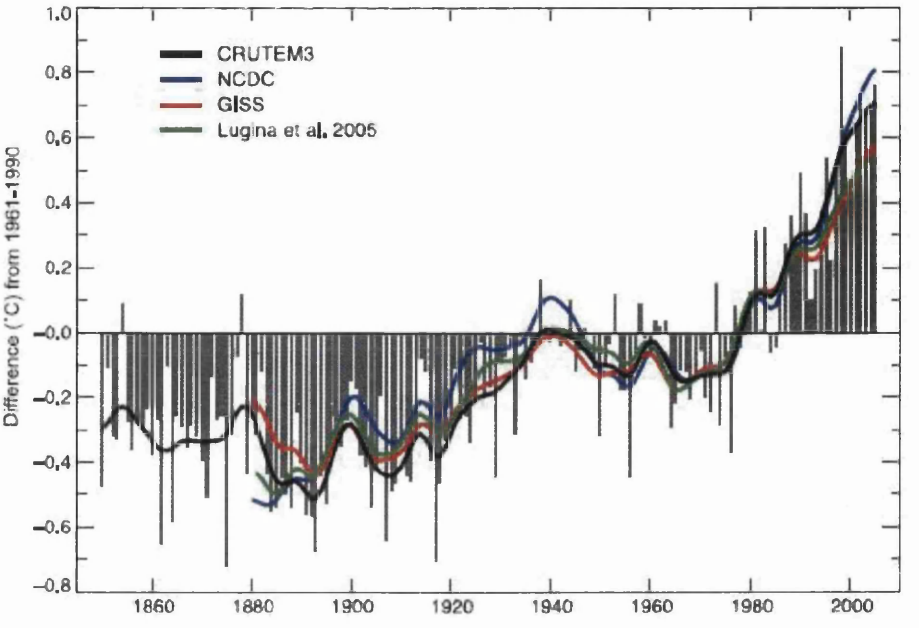

Figure 1.2: Annual anomalies of global-surface air temperature (°C) from 1850 to 2005. They are relative to the AD 1961 to AD1990 mean for the CRU/Hadley Centre gridded land-surface air temperature version 3 (CRUTEM3) updated from Brohan et al. (2006), with the black curve showing decadal variations. Compared to data from the National Climate Data Centre (NCDC) in blue (Smith and Reynolds, 2005), the Goddard Institute for Space Studies (GISS) in red (Hansen et al., 2001) and Lugina et al. (2006) in green (IPCC, 2007).

to significantly advanced glaciers; and historical records testify to events such as failed harvests, glacial surges and jökulhlaups (Grove, 1988). While there is strong evidence for cooler conditions from AD 1550 to 1850 it has proved difficult to bracket this event with precise dates (Bradley and Jones, 1992b; Bradley et al., 2003a). Largely due to its spatial extent and synchronicity appearing to be extremely variable (Matthews and Briffa, 2005). Indeed these two phenomena are so hard to precisely pin down that the usefulness of the terms MWP and LIA has even been questioned (Jones and Mann, 2004; Ogilvie and Jonsson, 2001).

Recent climate reconstructions of the past millennium have led to little consensus over the MWP and LIA, except perhaps in the need for more high resolution reconstructions covering these events (Jones and Mann, 2004; Jones et al., 2001; Matthews and Briffa,

2005). Mann et al. (1999), in their reconstruction of northern hemisphere temperatures for the last 1000 years, produced the now famous graph shown in Figure 1.3 (sometimes refered to as the *Hockey Stick*, due to its shape). This shows a general decline in average temperatures from ~AD 1000 to around ~AD 1900, followed by an abrupt warming over much of the twentieth century. This warming is mainly attributed to anthropogenic greenhouse gas emissions (Mann, 2001; Mann et al., 2003, 1999; Mann and Jones, 2003). Figure 1.3 is reconstructed from multiple proxy sources including tree ring and (post 1850) instrumental data. It shows a significant cool period which matches the LIA but no major earlier warm anomaly to match MWP. The Mann et al. (1999) reconstruction was included, in a slightly modified form, in the IPCC third report (IPCC, 2001) see Figure 1.4.

The Hockey Stick reconstruction of Mann et al. (1999) has been criticised by some researchers. Soon and Baliunas (2003) challenged their findings that the twentieth century was the warmest, at a hemispheric average scale, by looking at diverse proxy data sets for evidence of relatively warm/cool or wet/dry events occurring any time during pre-defined MWP or LIA time zones. The qualitative nature of the this research however, precludes quantitative comparisons with twentieth temperatures and so limits the value of the work (Mann and Jones, 2003; Osborn and Briffa, 2006; Jansen et al., 2007). Broecker (2001) disputed the finding of Mann et al. (1999) and concluded that there was a distinct MWP and that twentieth century warming was part of a natural Holocene climatic variability with a periodicity of around 1500 years (Bond et al., 2001). Broecker (2001) further suggested that a major problem with the Mann curve (Mann et al., 1999) was that tree ring chronologies were of little use in reconstructing long term climatic fluctuations due to problems associated with retaining low frequency variations (Cook et al., 1995), preferring instead data from borehole thermometry and snowline fluctuations. The use of snowline data has in turn has been criticised as a poor indicator of temperatures as other factors such as precipitation changes are also important for snow accumulation (Jones and Mann, 2004). McIntyre and McKitrick (2003) found that they were unable to reproduce the results of Mann et al. (1998), however Wahl and Ammann (2007) showed that

this was a consequence of differences in the way which McIntyre and McKitrick (2003) had implemented the methods of Mann et al. (1998) and that it was possible to closely reproduce the original reconstruction using the original proxy data. McIntyre and McKitrick (2005) raised further concerns over the details of Mann et al. (1998) concerning the verification of the reconstruction against independent nineteenth century temperature records and the use of principle component analysis to extract temperature signals from western North American tree ring series, which may not be the primary cause of tree-ring variability. This criticism may have some theoretical foundation (Jansen et al., 2007). However, Wahl and Ammann (2007) have demonstrated that the affect of this on the amplitude of the reconstruction is very small (~0.05°C). Indeed despite much debate and criticism focused on the, now famous, hockey stick of Mann et al. (1999) there is little evidence to suggest that, with data available to them, there are any fundamental problems with their reconstruction (NRC, 2006) .

While Mann et al. (1999) conclusions as to the reality and origins of twentieth century warmth are supported by many researchers (Alley, 2003; Bradley, 2000b,a, 2001; Briffa et al., 2001; Crowley, 2000; Crowley and Lowery, 2000; Huang, 2004; Huang et al., 2000) and generally accepted by the IPCC (2001, 2007) there has been less consensus around their reconstruction of the preceding 900 years and especially the MWP. Tree ring data from high latitudes in some areas of the northern hemisphere show summer temperatures in the MWP well above those of the 20th century (Briffa, 2000) and some north Atlantic records, although poorly temporally constrained, also support these findings (Keigwin, 1996; Keigwin and Pickart, 1999) while suggesting that MWP and LIA variability may be explicable in this area in terms of variations in the North Atlantic Oscillation (NAO) index. In an alternative reconstruction of northern hemisphere temperatures Esper et al. (2002) produced results that included a distinct MWP using a detrending technique designed to preserve low frequency climate variations, while Moberg et al. (2005) have published a reconstruction with an equally warm but more prolonged warm period after AD 1000. These three climate reconstruction and other notable recent reconstructions (Overpeck et al., 1997; Jones et al., 1998; Crowley and Lowery, 2000; Briffa, 2000; Briffa et al.,

2001) can be seen in Figure 1.5, which also includes instrumental temperature records for the past 150 years. In some respects the reconstructions in Figure 1.5 are quite similar, they follow a similar general pattern, and much of the high frequency variability appears similar, which is not surprising as they are based on similar proxy data sets. They are however rather more alike nearer to the present with more divergence further back in time and increasingly so before around AD 1600 (especially for the Esper et al. (2002) and Moberg et al. (2005) reconstructions.

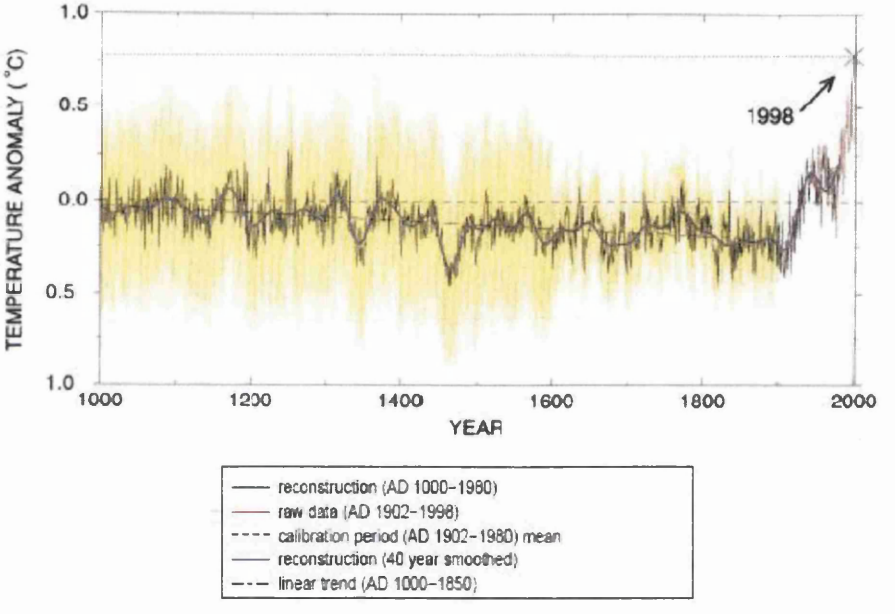

Figure 1.3: A multiproxy reconstruction of northern hemisphere mean annual temperatures, as departures from the 1902-1980 mean. The shaded area shows confidence limits of the temperature estimates, with uncertainty increasing back in time (Mann et al., 1999).

A number of studies that have attempted to reconstruct temperatures at a large spatial scale have arrived at the conclusion that warmth during the medieval period was not either spatially or temporally particularly homogeneous (Crowley and Lowery, 2000; Folland et al., 2001; Bradley et al., 2003a; Jones and Mann, 2004; D'Arrigo et al., 2006). This makes it rather difficult to make comparisons between modern temperatures and those during the medieval period and this is further exacerbated by the limited number of

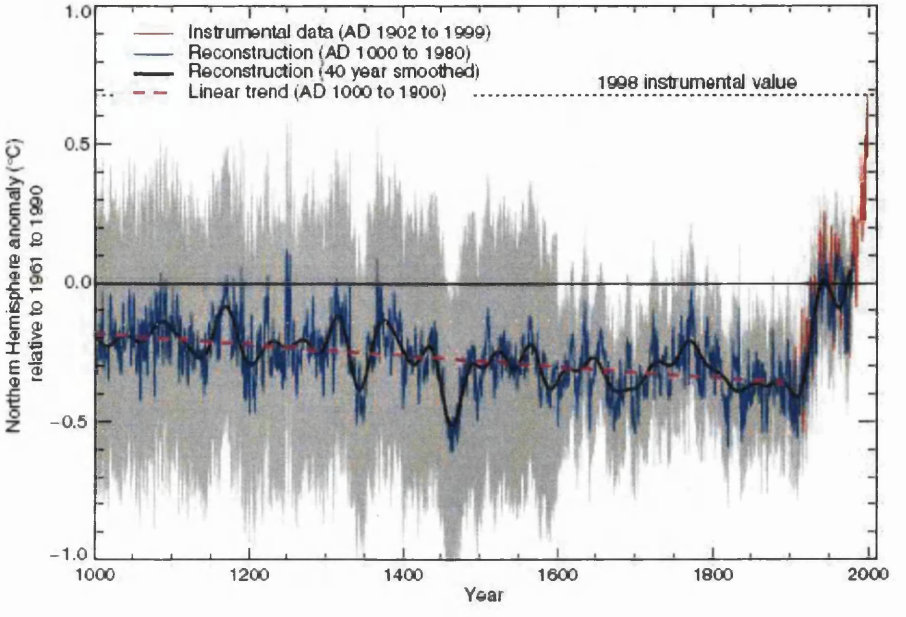

Figure 1.4: Millennial northern hemisphere temperature reconstruction (blue) and instrumental data (red) from AD 1000 to AD 1999 adapted from Mann et al. (1999), two standard error limits (grey shading) are shown (IPCC, 2001)

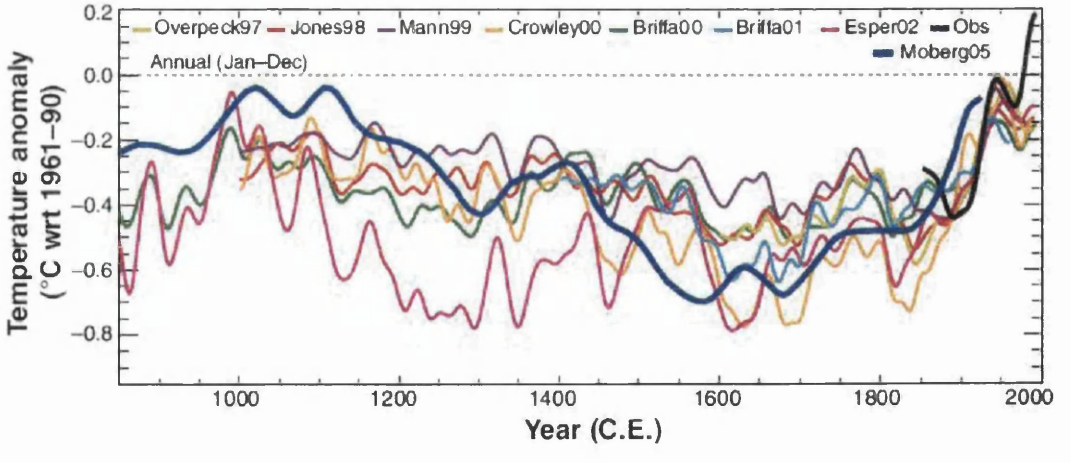

Figure 1.5: Comparison of climate reconstructions by Overpeck et al. (1997); Jones et al. (1998); Mann et al. (1999); Crowley and Lowery (2000); Briffa (2000); Briffa et al. (2001); Esper et al. (2002); Moberg et al. (2005) and observed temperatures.

high resolution proxy records available which span the last 1000 years (see Figure 1.6). Figure 1.6 shows that not only are the number of proxy records stretching back over the millennium limited, but also that they are quite spatially constrained. A disproportionate number are found in the northern hemisphere and even here they are mostly found at higher latitudes. The number of proxy records available increases through time, as can be seen in Figure 1.6. However, the geographical locations of these records are still strongly weighted to the higher latitudes of the northern hemisphere and the western coast of North America, where precipitation rather than temperature has often been found to be the major limiting factor in tree ring growth (e.g. Fritts, 1965; Cook et al., 1999, 2004b; Hughes and Funkhouser, 2003). This geographical weighting of proxy records is likely to affect the reconstruction of any climatic phenomena that is not spatially homogeneous as would appear to be the case for both the MWP and the LIA (Matthews and Briffa, 2005; Jones and Mann, 2004).

The evidence currently available would seem to suggest that northern hemisphere temperatures were warm during the medieval period (AD 950-1100), in a 2000 year climate context, and warmer in comparison to the subsequent period, especially the 17th century for which there is widespread evidence of cool conditions (Osborn and Briffa, 2006). However, there is not sufficient evidence to support the conjecture that northern hemisphere mean temperatures during the MWP were as warm as those during the 20th century for any of the medieval period (Jones et al., 2001; Bradley et al., 2003a,b; Osborn and Briffa, 2006). The evidence for this, as already discussed, is sparse, although rather less so for the LIA than the MWP (Figure 1.6). It is widely recognised that the evidence upon which these reconstructions are based is insufficient to reconstruct global mean temperatures during the medieval period in any meaningful way (Jansen et al., 2007) and uncertainties surrounding current estimates of northern hemisphere temperature are high prior to AD 1600 (Mann et al., 1999; Cook et al., 2004a). There is an urgent need for more, spatially disparate, high resolution, millennial length (and longer) proxy records

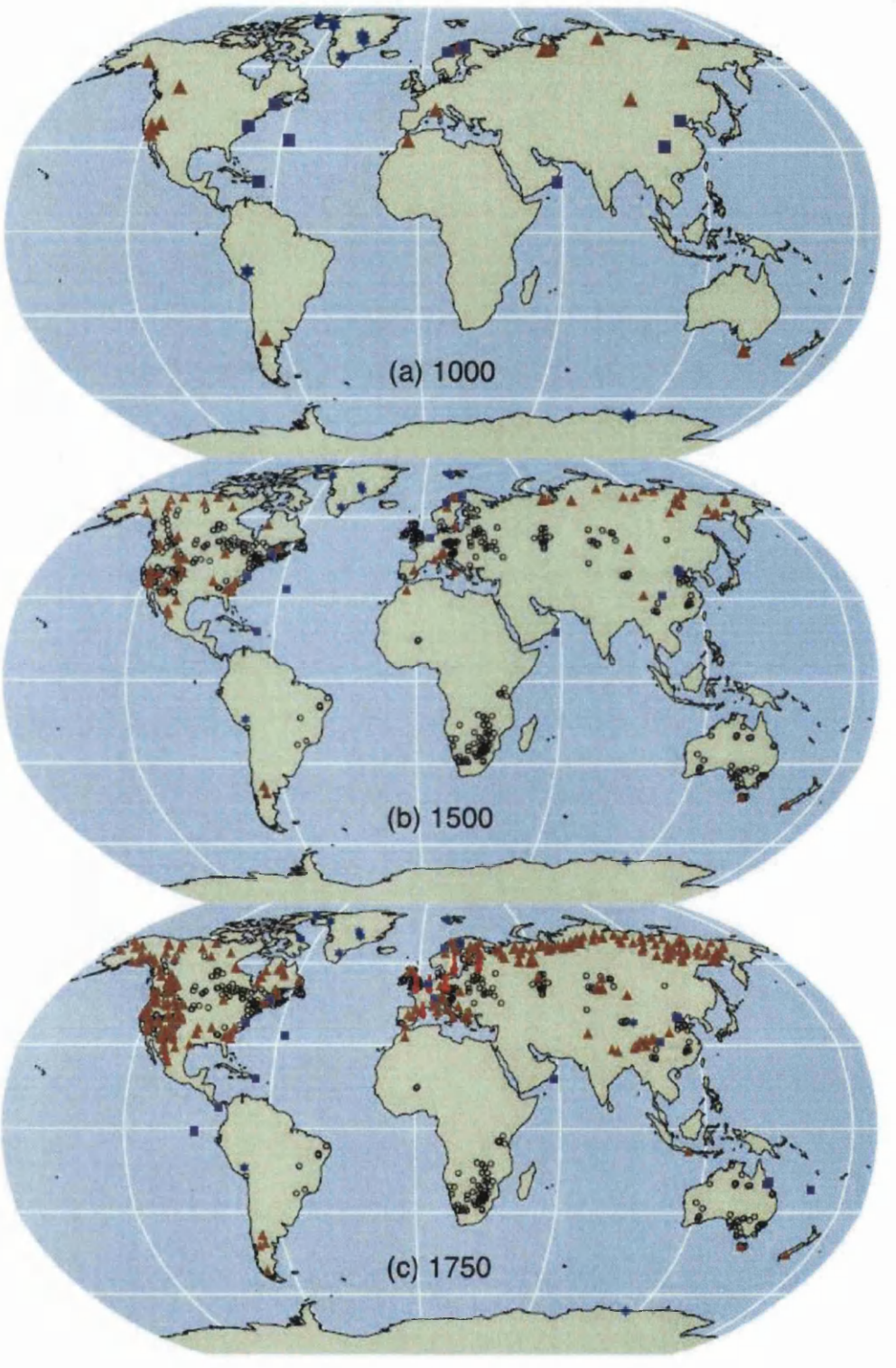

Figure 1.6: Location of proxy records dating back to AD 1000, 1500 and 1750. Instrumental data: red thermometers; tree ring: brown triangles; borehole: black circles; ice core/borehole: blue stars; other including low resolution records: purple squares (Jansen et al., 2007).

to gain a fuller understanding of climate change over the last 1000 years (IPCC, 2007). Also much of the evidence currently in use was collected up to 20 years ago and so needs to be brought up to date (Jansen et al., 2007).

1.4 Proxy Records

It would seem that the climatic history of the last millennium is far from resolved and since the instrumental climatic record is too short, at around 150 years, to adequately account for past climatic changes and thus to infer future changes, it has been necessary to employ proxy climatic indicators to more fully reconstruct past climates. A proxy or proxy record can be defined as a line of evidence that provides an indirect measure of former climates or environments (Bell and Walker, 1992). These line of evidence can include materials as diverse as pollen grains, glacial sediments, speleothems, animal bones, isotopic records and tree rings. As an archive of proxy records tree rings have several major advantages: they are widespread; and generally easily accessible; they have potentially perfect annual resolution; while their growth is strongly linked to climate; in addition each ring contains a variety of potential lines of proxy evidence.

1.4.1 Tree rings

The widely acknowledge father of dendrochronology is A. E. Douglass (Fritts, 1976) who, while working on the hypothesis that sunspot activity affected the earths climate and especially precipitation, came to the conclusion that ring widths may act as a proxy for precipitation with narrower ring widths in dryer years. He proceeded to use this insight to build up a chronology from many different trees, from the Flagstaff-Prescott area of Arizona in the American southwest, concluding that the most reliable patterns for cross-dating were found in narrow ring widths. He demonstrated, using available climate data, that ring width was directly related the previous winter's precipitation concluding that the replenishment of soil water by precipitation led to enhanced tree growth during

the following season (Douglass, 1919, 1928). The two major implications of Douglass' discovery were: firstly that cross-dating could be used as a chronological tool to identify the exact year in which any particular growth ring was laid down. All that was required was to know the date of the outermost ring of a tree and that the same relative pattern of growth rings were observable in many trees, then wood of an unknown age could be dated by matching its ring widths to that of a dated chronology; and secondly that ring-width patterns represent an environmental record over a region, because while some ring-width variations were attributable to local conditions, a large portion of the ring-width variations were observable in trees throughout a region and so could only mirror factors that affected the whole region (Fritts, 1976). One of the first results of Douglass' technique was the absolute dating of archaeological sites in the American south west such as the cliff dwelling of Mesa Verde by cross-dating building timbers (Fritts, 1976).

Since Douglass' pioneering work tree ring growth chronologies have been pieced together in many parts of the world where a discernible annual growing season occurs. By using dead wood (standing and fallen), building timbers and sub-fossil logs it has been possible to extend these chronologies over many tens of centuries (Baillie and Brown, 2003). In northern Europe these extend back in excess of 7000 years for pine (Eronen et al., 2002; Grudd et al., 2002) and in excess of 8000 years for oak (Friedrich et al., 1999; Leuschner et al., 2002; Spurk et al., 2002), while in western north America Bristlecone pines, which are reputed to be the oldest living organisms. Living in excess of 4700 years, have produced chronologies in excess of 8000 years (Briffa, 2003; Baillie and Brown, 2003). Indeed it was the availability of this absolutely dated Bristlecone pine wood along with European oak that allowed for the calibration of radiocarbon dates (Briffa, 2003; Baillie and Brown, 2003). Dendroclimatology as a branch of dendrochronology grew from the same premise that made precise dating possible, namely that tree growth is often affected by variations in climate and that the history of this climatic variation is recorded in the sequence of wide rings (for favorable years), and narrow rings (for unfavorable years) (Fritts, 1976).

As archives of proxy climate records tree rings have several advantages over other natural

archives such as marine sediments, peat bogs and speleothems: they can offer perfect annual resolution; are widely distributed globally; and are generally easily accessible. These advantages have various positive ramifications for the reconstruction of past climates. Firstly tree ring widths (TRW) and maximum latewood density (MXD) of trees at their ecological limit often respond to a single climatic factor (unlike trees growing in more optimal conditions). At high latitudes and elevations on sites with little or no moisture stress TRW and MXD often display a strong linear relationship with surface temperatures for part or all of the growing season (Hughes, 2002). This is not however an assumption that can be made in all situations, Touchan and Hughes (1999) for example, demonstrated that in seasonally arid Mediterranean type climates TRW may reflect the extent of soil water recharge in the antecedent wet season. Secondly unlike proxies with poorer dating resolution researchers can be sure, with tree rings, that they are comparing climate and tree ring variables for the same year (Hughes, 2002), while the use of precise cutting techniques such as laser ablation makes inter-annual resolution a distinct possibility (Schulze et al., 2004). Thirdly the wide geographical distribution of trees with annual rings makes climate reconstruction on hemispherical scales possible (Briffa, 2000; Esper et al., 2002; Mann et al., 1998, 1999) and means that large scale climatic phenomena such as the North Atlantic Oscillation can also be studied and potentially reconstructed (Cook et al., 1998, 2002; Cullen et al., 2001; D'Arrigo et al., 1993; Luterbacher et al., 2002).

While productive and innovative climatic reconstructions have been achieved in recent years using tree rings, there are potential problems associated with reconstructing climate using the ring widths of trees. Firstly these reconstructions are necessarily limited to parts of the globe where trees display annual growth rings, this excludes a large part of the earths surface, which are also the most dynamic in terms of energy budget and so it has been necessary to find other high resolution proxies for the tropics, for example corals (e.g. Knutson et al., 1972; McClanahan and Multhiga, 2000). Secondly there is an age related trend in tree ring widths, which is simply due to the fact that as trees age their ring widths decline. This age trend must be removed from each tree before

a meaningful climatic reconstruction can be made and is simply done putting linear or negative exponential function through the data set (Fritts, 1976). There is however, a potential problem which arises from this statistical detrending of maintaining climatic variability on multi-centennial timescales. This has been called *the segment length curse* (Cook et al., 1995), because any climatic signal with a temporal frequency equal to or longer than the life-span of the tree will be removed. This has led some researchers to the conclusion that dendroclimatology is only useful for relatively short term reconstructions (e.g. Broecker, 2001). More recent techniques of detrending such as *regional curve standardisation* (RCS) (Briffa et al., 1992) and *ageband decomposition* (ADC) (Briffa et al., 2001) have been developed to retain more of the low-frequency variability and these methods have been widely employed in large scale climatic reconstructions (e.g. Esper et al., 2002; Moberg et al., 2005). However, much of the debate surrounding the structure of climate over the past millennium, discussed above, centers around this detrending and whether or not it is possible to retain low-frequency climate signals in tree rings (Briffa and Osborn, 2002; Esper et al., 2002; Esper and Frank, 2004; Mann and Hughes, 2002). Indeed, Figure 1.5 shows the variety of reconstructions that can be achieved by the application of slightly different statistical methods to essentially similar data sets. To help to resolve some of these problems, it has been suggested that the measurement of stable isotope ratios in tree rings may allow for less a ambiguous low frequency climate signal to be retained, than has previously been achieved using ring width series alone (McCarroll et al., 2003).

1.4.2 Isotopes in Tree Rings

The basis of isotope theory is that while atoms are comprised of electrons, protons and neutrons, different isotopes of elements have the same number of protons and electrons but varying numbers of neutrons. This makes isotopes of an element almost chemically identical but slightly different in mass and it is this difference in mass that allows for discrimination against either the heavier or lighter isotope. These small variations in mass can be measured in a mass spectrometer. Trees are mainly composed of oxygen,

carbon and hydrogen all of which have more than one stable isotope:

- Oxygen – ^{16}O, ^{17}O and ^{18}O
- Carbon – ^{12}C and ^{13}C (plus the unstable ^{14}C, decay rate of which is used for dating)
- Hydrogen – ^{1}H, ^{2}H (Deuterium) and ^{3}H (Tritium)

It is the discrimination against either the lighter or heavier forms of these isotopes by either physical processes, such as evaporation, or biological processes, such as photosynthesis, which means that a climatic signal may be sought in isotopic ratios. The level of discrimination or fractionation is measured against a standard which in the case of Carbon was the ratio of a fossil belemnite from the Pee Dee (PDB) formation of South Carolina which has since been exhausted and been replaced by the Vienna-PDB (VPDB). For oxygen the ratio of ^{18}O to ^{16}O and ^{2}H to ^{1}H (D) are measured against 'standard mean ocean water' (SMOW) again now replaced by Vienna-SMOW or VSMOW (Coplen, 1995). These ratios are expressed by the delta (δ) notation to the standard in parts per mille (‰). So ratios are expressed as $\delta^{18}O$, $\delta^{13}C$ and δD, the calculation of which are made using Equation 1.1, where R is the $^{13}C/^{12}C$, $^{18}O/^{16}O$ or $^{1}H/D$ ratio of the sample and standard.

$$\delta_{sample} = \left(\frac{R_{sample}}{R_{standard}} - 1 \right) 1000 \tag{1.1}$$

It has long been recognised that global variations in $\delta^{18}O$ can be linked, albeit in a complex way, to climate (Dansgaard, 1964). Water containing the lighter ^{16}O isotope is preferentially evaporated meaning that source water is enriched in the heavier isotope, while evaporated water vapour is enriched in the lighter isotope. This effect is also temperature dependant with cold air masses collecting isotopically lighter moisture than warmer air masses. When water vapour condenses this process works in reverse, here the heavier isotopes condense more readily and once again isotope ratios are dependant on the temperature at which condensation occurs (McCarroll and Loader, 2004). It

was these isotopic variations in calcium carbonate marine shells found in deep sea cores that unraveled the true scale of Quaternary glaciations and confirmed the Milankovitch astronomical theory as their primary driving force (Imbrie and Imbrie, 1979).

It was the Nobel prize winning chemist and pioneer in the study of the solar system Harold C Urey who first mooted the idea that there may be a climatic signal in the $\delta^{13}C$ of cellulose when he suggested that carbon compounds synthesised at different temperatures may contain varying amounts of ^{13}C and that this may have important applications as a means of determining past temperatures (Urey, 1947). It was later suggested that a temperature signal may also be obtained from the ratios of oxygen ($\delta^{18}O$) and hydrogen (δD) isotopes in wood as their source is meteoric water, which has been demonstrated to contain a temperature signal, and so should preserve a record of past temperatures (Epstein et al., 1976). Since wood is primarily composed of carbon, oxygen and hydrogen an isotopic examination tree rings should provide a record of the climate at the time when wood containing these elements was formed (Switsur and Waterhouse, 1998), and this climate signal should be observable in the relative discrimination of isotopes in the cellulose or whole-wood of the annual tree rings. Indeed, it has been suggested that these ratios can be used as a palaeo-thermometer, with a rise in $\delta^{13}C$ per mil per °C of temperature (e.g. Leavitt and Long, 1985; Lipp et al., 1991; Sheu et al., 1996; Anderson et al., 1998). The real picture appears to be rather more complex than this (McCarroll and Loader, 2004).

Carbon fractionation in tree rings is governed by discrimination against the heavier ^{13}C isotope as CO_2 enters the stomata and during the utilisation of intercellular CO_2 by the photosynthetic enzyme to create sugars. The discrimination against ^{13}C at these two stages is normally nearly constant at around -4.4‰ and -27 ‰ respectively (Farquhar et al., 1982). As CO_2 diffuses through the stomata the difference in the diffusion of $^{13}CO_2$ and $^{12}CO_2$ is that as these molecules bounce around the light molecules bounce furthest and so are more likely to pass through the stomatal opening, which leads to the near constant fractionation due to diffusion of -4.4‰ (McCarroll and Loader, 2006). When photosynthesis produces sugars by combining leaf water and intercellular CO_2 there is

fractionation of both carbon and water isotopes (Farquhar et al., 1982, 1989; Ehleringer et al., 1993). The fractionation of $\delta^{13}C$ at this point is nearly constant at about -27‰, compared to that of the intercellular CO_2. If however, the rate at which photosynthesis uses CO_2 is faster than it can be replenished by stomatal conductance, the concentration of intracellular CO_2 will fall and become enriched in $^{13}CO_2$, and although fractionation remains constant (around -27‰) the ratio of ^{13}C will increase in the produced leaf sugars as the source (intercellular) ratio increases (McCarroll and Loader, 2006). Provided there is no change in $\delta^{13}C_{air}$ (ambient air), the $\delta^{13}C$ of leaf sugars is principally controlled by changes in the $\delta^{13}C$ of intercellular CO_2, which is in turn controlled by the concentration of internal leaf CO_2. Lower internal CO_2 concentrations lead to higher concentrations of ^{13}C and higher (less negative) $\delta^{13}C$ values in leaf sugars (McCarroll and Loader, 2004, 2006). That there have been changes in $\delta^{13}C$ of atmospheric CO_2 due to the introduction of isotopically light CO_2 from the burning of fossil fuels, especially since the onset of industrialisation, is well recognised (e.g Keeling et al., 1979; Mook et al., 1983), the implications that this has for $\delta^{13}C$ in tree rings will be discussed in Chapter 4.

For $\delta^{18}O$ ratios in tree ring cellulose the major influences on fractionation are: the $\delta^{18}O$ of soil water (antecedent precipitation); preferential evaporation of the lighter ^{16}O during photosynthesis; and exchanges with xylem water. The ^{18}O enrichment in the leaf can be as much as 20‰ (Saurer et al., 1998a), however dilution of this signal due to exchange with xylem water which can be as much as 40% (Sternberg et al., 1986, 2003) can mask this potentially very useful signal and make it difficult to interpret. For a clear palaeoenvironmental signal to be derived from the $\delta^{18}O$ of tree rings it is therefore important to have a clear idea of what proportion of oxygen atoms are exchanged (McCarroll and Loader, 2004), although one possible solution to this problem may be to isolate and measure the $\delta^{18}O$ of the oxygen atoms which are never exchanged (Sternberg et al., 2003). However this has not as yet been routinely achieved. The key climatic signal, internal to the tree, is preferential evaporation of the lighter $H_2^{16}O$ due to evaporation through the stomata, the dominant control is the leaf to air vapour pressure deficit which is controlled more by air humidity than temperature (McCarroll

and Loader, 2004). The climatic controls of δD are similar to those of δ^{18}O, however, the measurement of δD falls outside the scope of this research and so will not be dealt with here, reviews of the current work in this area can be found in McCarroll and Loader (2004, 2006).

In early work on isotopes in tree rings researchers tended to work with continuous blocks of between five and twenty rings and isotopically analyse wholewood (e.g. Craig, 1954; Farmer and Baxter, 1974). The disadvantage of this approach was, that it did not exploit the unique advantage of the annual resolution of tree rings (Switsur and Waterhouse, 1998), and since it was demonstrated that the different components of wood differ isotopically (Wilson and Grinstead, 1977), the results from extracted cellulose have generally been thought more valid than those of wholewood although this has been debated. Most recent studies have tended to analyse the signal of α-cellulose from the late wood of single or pooled rings. However the extraction of cellulose from tree rings (Loader et al., 1997, 2002) is a time consuming process and restricts the number of samples which can be analysed, and some research comparing the isotopic signals of wholewood and α-cellulose for δ^{13}C would seem to suggest that it may be unnecessary (Barbour et al., 2001; Loader et al., 2003; Schulze et al., 2004). Loader et al. (2003) demonstrate that the signals of cellulose and wholewood display the same temporal pattern of δ^{13}C ratios, with the values for wholewood depleted by $\sim 3‰$ from cellulose, they further suggest that the signal from modern wholewood provides the strongest climatic signal but caution that differential decay rates in sub-fossil wood may alter the lignin to cellulose ratio. The position is less clear with δ^{18}O (Borella et al., 2004), although the little work so far undertaken suggests that the δ^{18}O of cellulose correlates rather better with climate than that of wholewood (Borella et al., 1999).

Schulze et al. (2004) used online laser ablation to prepare samples of wholewood for combustion and mass spectrometry. The nature of the online process precludes the effective use of α-cellulose, however they ran a comparison of wholewood and α-cellulose samples and once again found a consistent positive offset of δ^{13}C for cellulose compared to wholewood and concluded that it was unnecessary to extract to cellulose for a clear

climatic signal. The major advantages of this process are speed (six minutes per sample), and cutting accuracy, which may allow for inter-annual signals to be measured raising the possibility that micro-dendroclimatology (Loader et al., 1995) may be a very real possibility. This technique has the additional advantage of being essentially non-destructive (Schulze et al., 2004), and so samples can be easily revisited.

In terms of precision it has been demonstrated that using stable isotopes from as few as four trees can yield a stronger climatic signal than the ring widths of more than 20 (McCarroll and Pawellek, 1998, 2001), and analysing the isotope ratio of each of these rings independently, rather than pooling samples (Leavitt and Long, 1984), allows variability and thus precision to be defined by placing statistical confidence limits around mean values (McCarroll and Loader, 2004). Indeed, as the between tree variability in isotope signals has been shown to vary considerably (McCarroll and Pawellek, 1998), the time expended extracting α-cellulose from tree rings, in the hope of extracting a more precise value from an individual sample, would seem ill used compared to sampling a greater number of trees, which would give much greater precision to the average value obtained (McCarroll and Loader, 2004). The problem of maintaining an accurate mean value will be returned to later in this thesis, but as yet it remains unclear the number of trees per year that are required to achieve a good estimate of the true mean δ^{13}C or δ^{18}O value.

Isotopes in tree rings have not universally been accepted as a useful approach to climatic reconstruction for a variety of reasons. Measuring the isotope ratios of individual rings is time consuming and relatively expensive in comparison to measuring ring widths and so may not be a cost affective advance in dendroclimatology (McCarroll and Pawellek, 1998; Hughes, 2002; Jones and Mann, 2004). However improvements in technology have meant that sample through-put has increased many fold in recent years, and online laser ablation techniques, discussed above (Schulze et al., 2004), are being developed in more than one laboratory. The lack of a clear understanding of the complex biological and environmental processes involved in stable isotope fractionation in trees (Hughes, 2002; Treydte et al., 2004) is a rather more difficult criticism to deal with however research into

these complex relationships is a vibrant ongoing field of endeavor (e.g. Barbour et al., 2001, 2002; Edwards et al., 2000; Farquhar et al., 1989; Körner, 2003, 2006; O'leary et al., 1992; Rebetez et al., 2003; Saurer, 2003; Saurer et al., 2004; Scheidegger et al., 2000) while the use of multiproxies within tree rings may be able to isolate the true climatic signal (McCarroll and Loader, 2004), see below. The concept of uniformitarianism, where the present is seen as analogous with the past, is also problematic for the use of δ^{13}C in isotope dendroclimatology due to changes in the atmospheric composition of CO_2 over the last 150 years, or so. The ratio of δ^{13}C is reducing as isotopically light CO_2 from fossil carbon is released into the atmosphere and so techniques are required for removing these trends, which are dealt with in Chapter 4.

The recent increases in the atmospheric concentrations of CO_2 may also be altering the way in which trees respond to climate (Feng and Epstein, 1995a; Marshall and Monserud, 1996; Feng, 1998, 1999; Krishnamurthy and Machavaram, 2000; Waterhouse et al., 2004), which may have serious implications for the use of δ^{13}C from thee rings as a tool for reconstructing climate. There is increasing evidence to suggest that trees have responded to increasing atmospheric CO_2 concentrations (c_a) by increasing their intrinsic water-use efficiency (IWUE), as c_a rises they are able to absorb the same amount of CO_2 while keeping their stomata open less and so reducing water loss, to maintain near constant intercellular CO_2 (c_i) (Waterhouse et al., 2004). However, in recent decades in seems that many trees have failed to further increase their IWUE leading to a sharp, non climatic related, decline in δ^{13}C values (McCarroll et al., 2007). As these changes most strongly affect the period for which instrumental climate data are available any non climatic changes in δ^{13}C during this period may significantly affect any climate reconstruction based on a calibration with climate made over this period. If such a trend exists it will again require some corrective measure (Treydte et al., 2001; McCarroll et al., 2007). This topic will be dealt with in more detail in Chapter 4.

δ^{13}C values also exhibit, what appears to be, a non-climatic age related trend (juvenile effect). Young trees appear to exhibit increasing δ^{13}C values for approximately the first 50-years of tree rings (McCarroll and Loader, 2004; Gagen et al., 2007). It has been

suggested that this is due to the recycling of more isotopically negative respired CO_2 in the forests understory (Schleser and Jayasekera, 1985). However, as trees in open canopy forests also exhibit this juvenile affect where recycling of respired air is likely to be minimal (Gagen et al., 2004), the explanation is likely to be more complex than this (McCarroll and Loader, 2004). An alternative explanation is that there are changes in hydraulic conductivity within trees as they get taller which may be responsible for this juvenile effect in $\delta^{13}C$ (Ryan and Yoder, 1997; McDowell et al., 2002). As height increases leaf water potential declines and so young trees are likely to have more moisture available at the leaves and so are able to keep there stomata open longer maintaining higher intercellular CO_2 concentrations and so more negative $\delta^{13}C$ values. This explanation is complicated by some trees having increased sapwood to leaf area ratios as age increases and so potentially more water availability (McCarroll and Loader, 2006). However, this combination of declining sapwood potential with higher sapwood to leaf area ratio has been used to explain the *juvenile effect* in coniferous and deciduous trees (Schäfer et al., 2000; Monserud and Marshall, 2001; McDowell et al., 2002). If the *juvenile effect* is due to changes in hydraulic conductivity one might expect it to also be found in $\delta^{18}O$ which is also controlled, to some extent, by stomatal conductance, with potentially more positive values if there is more evaporation as stomata remain open longer. That no *juvenile effect* has been demonstrated conclusively for $\delta^{18}O$ may be due to the paucity of data available for individual trees (McCarroll and Loader, 2006). There is some evidence, however, that it may be present in both $\delta^{18}O$ and δD (McCarroll and Loader, 2006).

In terms of palaeoenvironmental reconstruction the *juvenile effect* in $\delta^{13}C$ values poses some problems as it reflects changes in isotope values which are not related to an environmental signal and must be removed before the $\delta^{13}C$ results for a tree can be used. Statistical detrending of this trend should not prove to problematic, but this would probably also remove any environmental signal of the same length as the *juvenile effect (McCarroll and Loader, 2006),* and so would remove one of the major advantages which stable isotopes appear to have over ring widths and, to some extent, density, namely the problems associated with maintaining lower frequency signals from the data (Cook et al.,

1995; Gagen et al., 2007). An alternative approach is to simply not process the early part (around 50 years) of the trees cores which may contain the *juvenile effect (McCarroll and Loader, 2004, 2006)*, although careful comparison of the results from cores of different ages would seem prudent to check for aberrant behavior.

For palaeoclimatology the major problem of all three stable isotope ratios in tree rings is that they are not controlled by a single climatic variable (McCarroll and Loader, 2004). For example McCarroll and Pawellek (2001) in a study of *Pinus sylvestris* L. in northern Finland found that the $\delta^{13}C$ ratios were controlled by summer sunshine, temperature, antecedent precipitation and relative humidity. As these controls vary spatially and are likely to have varied locally throughout the Holocene they concluded that without an estimate of either photosynthetic rate (controlled by summer sunshine and temperature) or stomatal conductance (controlled by air humidity and soil moisture) there is little potential for using $\delta^{13}C$ alone to reconstruct palaeoenvironmental information from the long Fennoscandian pine chronologies. The solution to this problem may be in using the multiproxy approach of estimating a single climatic parameter using a variety of proxies, either using multiple regression models, or alternatively by using the method of McCarroll et al. (2003) of combining them by taking a weighted average. Provided these proxies carry the same 'signal' but with different sources of 'noise' this averaging should strengthen the 'signal' while dampening the 'noise' (McCarroll and Loader, 2004).

1.4.3 A multiproxy approach

Multiproxy and multiarchival reconstructions are increasingly seen as good practice in the field of palaeoclimatology (Mann, 2002; Bradley et al., 2003a; Huang, 2004; Jones and Mann, 2004). Climate proxies can be from physical archives (e.g. sedimentary deposits, speleothems and sediment or ice cores), biological archives (e.g. tree rings and corals) or historical archives (e.g. harvest dates and phenology). All proxies have limitations and potential biases and so it is generally seen as advisable to employ a multiproxy approach in an attempt to reduce uncertainties and to differentiate between those elements of the

various signals contained in natural archives that are climatic and non-climatic (Bradley et al., 2003a; Folland et al., 2001; Jones and Mann, 2004; Jones et al., 2001). This approach has been employed by researchers to reconstruct climatic on a hemispheric scale in the northern hemisphere (Briffa, 2000; Briffa et al., 2002a,b; Jones et al., 1998; Mann et al., 1998, 1999) and rather more tentatively for the southern hemisphere (Jones et al., 1998, 2001; Mann et al., 2000). Multiproxy reconstructions have also been made of climate related phenomena, such as tree line fluctuations (Ammann and Germann, 1996; Battarbee, 2000; Dahl and Nesje, 1996; Thompson et al., 1998); and the North Atlantic Oscillation (Cook et al., 2002; Cullen et al., 2001; Luterbacher et al., 2002).

For the dendroclimatologists a variety of potential climatic proxies are available: total ring widths; earlywood width; latewood width; earlywood density; latewood density; maximum density; annual height increment; needle production; pollen deposition; and stable isotope ratios (McCarroll et al., 2003) and while most multiproxy tree ring studies to date have focused on ring width and maximum latewood density to reconstruct palaeoclimate (Briffa, 2000; Briffa et al., 2002a,b) a more varied multiproxy study in northern Finland (McCarroll et al., 2003) has suggested that there may be a some potential for this approach for climatic reconstruction. In this study a variety of potential climate proxies were used to determine how well each proxy correlated with climate and which had potential for reconstructing palaeoclimate, they used simple linear correlation coefficients (r-values) between each proxy and mean monthly temperatures of the current and previous year taking r-value of 0.71 as a minimum acceptable value, with the independent variable explaining half of the variance of the dependent variable (McCarroll et al., 2003; McCarroll and Pawellek, 2001), of the eight proxies measured only height increment ($r = 0.87$) and needle production ($r = 0.84$) reach r-value of greater than 0.71, for any single calender month.

McCarroll et al. (2003) found that they could improve their climate correlations by combining proxies. By combining height increment ($r = 0.67$) and latewood density ($r = 0.63$) they achieved a correlation with mean July temperature of 0.79, see Figure 1.7. Similarly they were able to combine ring widths, latewood density and $\delta^{13}C$ for a corre-

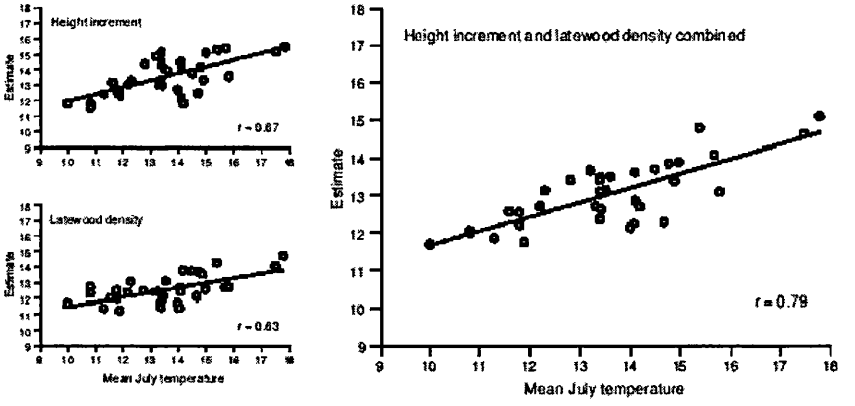

Figure 1.7: Individual and combined correlation with mean July temperature for height increment and latewood density (McCarroll et al., 2003).

lation of 0.73 with mean July temperature (Figure 1.8). They were also able to demonstrate that proxies with different responses to climatic controls can be used effectively to reconstruct climate, so while latewood density and δ^{13}C are correlated to summer sunshine and temperature, δ^{13}C ratios are also affected by variations in soil moisture (summer precipitation). When they regressed these two proxies (Figure 1.9) an effective correlation of 0.70 was found with the three distinct residuals (highlighted), these being the tree driest summers in the region (1979, 1980 and 1985). The chance of these being randomly identified as such was $p = 0.00015$ (McCarroll et al., 2003).

This technique has great potential for palaeoclimatic reconstruction, especially when the different controlling factors of each proxy can be identified, as shown in Figure 1.9 differentiating the years when temperature and moisture were the primary controls for δ^{13}C. Having demonstrated this potential McCarroll et al. (2003) conclude that this approach needs to be applied to longer tree series, using trees of a variety of ages and

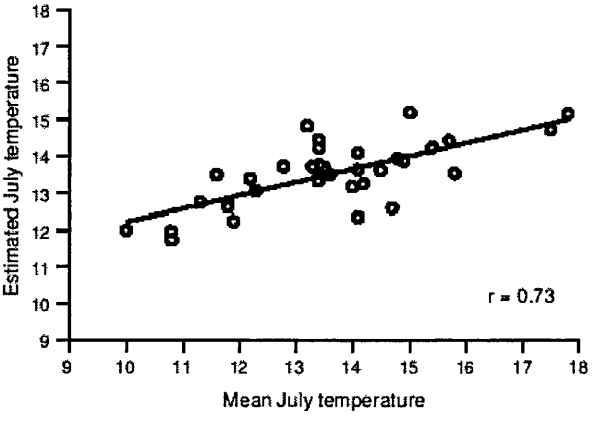

Figure 1.8: Effective correlation of ring width, latewood density and $\delta^{13}C$ (McCarroll et al., 2003).

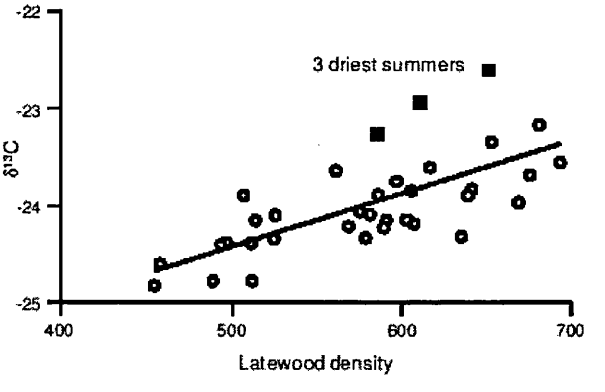

Figure 1.9: $\delta^{13}C$ regressed against latewood density, note three highlighted residuals which represent the driest summers (June – Aug precipitation) (McCarroll et al., 2003).

covering a wide latitudinal range, to better test the responses of the various proxies and to determine whether this technique can reliably reconstruct the low-frequency climate changes which are notoriously difficult to extract using ring widths (Cook et al., 1995). It is also concluded (McCarroll et al., 2003) that multiple proxies (including the isotopes of hydrogen and oxygen) may be used to model the relationship between tree growth and climate. This may help to circumvent the problems inherent in using the climate of the last century as the calibration period for reconstructing past climate. A century which has seen large changes in atmospheric composition due to human agency, which in turn may have affected the way that trees respond to climate

1.5 Northwest Norway

The site of this research is Forfjorddalen on the Lofoten-Vesterålen archipelago in north western Norway (Figure 1.10), located within the Arctic circle at 69°N (see Chapter 2 for more detailed site information), which is home to the oldest known living trees in Norway (Kirchhefer, 2001). The dominant tree species here is Scots pine (*Pinus sylvestris* L.), with individual trees reaching ages well in excess of 500 years.

An existing tree ring chronology for this area stretches back to AD 1228 for living trees, and back to AD 877 with the inclusion of standing dead wood (Kirchhefer, 2001). A palaeoclimatic reconstruction for this area based on ring widths (Kirchhefer, 2001) can be seen in Figure1.11 and while the correlation with climate is not strong ($r = 0.51$) it does pick out many of the coldest years of the LIA. As the trees in this area are at or near their ecological growth limits they should, in theory, display a strong climatic signal (Fritts, 1976, 1991). However the maritime nature of the locality means that it is difficult to extract a strong climate signal from ring widths alone. Tree growth here is not, it seems, limited by summer temperature alone ($r = 0.51$), winter temperatures also seem to strongly modify the low-frequency growth trends. Ring widths from this area are, it appears, on their own a relatively poor predictor for long term trends in past summer temperatures

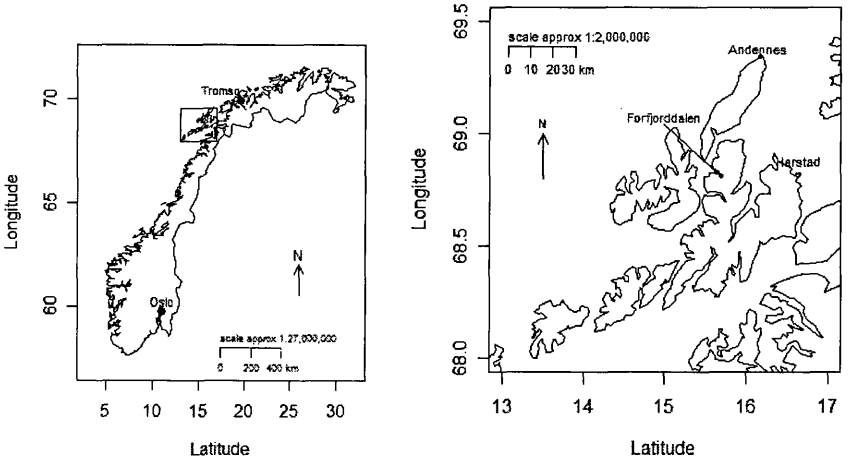

Figure 1.10: Location of the Lofoten-Vesterålen archipelago in north western Norway

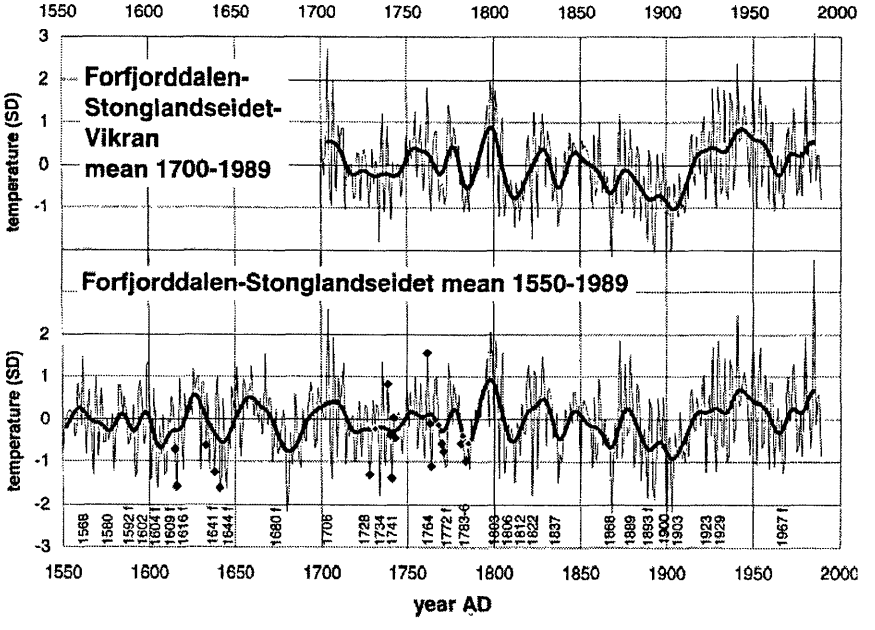

Figure 1.11: July-August temperature reconstruction as deviations from the 1874-1992 mean, dates for selected cold summers are shown with diamonds representing poor or failed barley harvests (Kirchhefer, 2001)

The employment of multiproxy dendroclimatology at this location with the inclusion of the existing ring width chronology and multiple individual measurement of $\delta^{13}C$ and $\delta^{18}O$ for each year, should make it possible to reconstruct climate at this location with greater degree of certainty than has already been achieved. While the inclusion of $\delta^{13}C$ measurements should, after some corrections (See Chapter 4), yield a more realistic low frequency climate signal than can be achieved using ring widths alone, with their inherent detrending problems (Cook et al., 1995; Gagen et al., 2007). Therefore a reconstruction based on stable isotopes may can be expected to lead to a fuller understanding of climatic variability over the past 600 years at this location.

1.6 Research Aims

This research seeks to answer the following questions.

- Is it possible to reconstruct successfully climate at Forfjorddalen using the stable isotopes of carbon and oxygen from tree-rings?
- Do these isotopes contain additional palaeoclimatic information to that available from the existing tree-ring width series?

2

Site Location and Description

2.1 Location

Forfjorddalen lies at 68°48'N and 15°44'E in the Vesterålen archipelago of north western Norway (see Figure 2.1). Locally forest is dominated by Birch (*Betula pendula* L.) however isolated forests of Scots pine (*Pinus sylvestris* L.) occur near the coast where soils are poor and dry, or on the margins of mires, many of these forests are undisturbed by man and individual trees can reach ages in excess of 500 years Kirchhefer (2001). Just such an isolated patch of Scots pine is located at Forfjorddalen (Figure 2.1).

2.2 Site Description

The geology of the Lofoten-Vesterålen archipelago is metamorphic and igneous, with the Forfjord valley being underlain by banded gneisses and granitic rocks. The field site itself is underlain by granite and granodiorite. The inner regions of the archipelago, including Forfjorddalen, have been extensively modified by the action of ice during the Quaternary. The geomorphology of this area displays many good examples of landforms associated with erosion and deposition by ice e.g. u-shaped valleys, moraines, cirques, aretes, horns & tarns (the walk to the field site crosses several good examples of De-Geer moraines). There are also a large number of relict rock glaciers in the area. The outer islands of the archipelago, by contrast, display little evidence of modification by ice, with a much

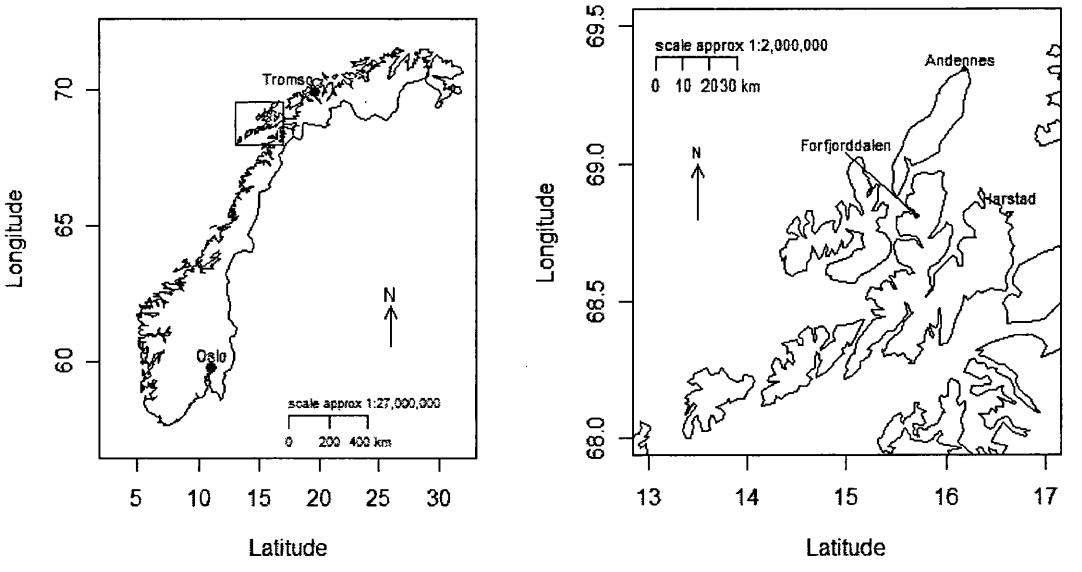

Figure 2.1: Location of Forfjorddalen

more rugged geomorphology. De-glaciated landscapes with steep sided valleys can be unstable and are prone to mass movements and there is much evidence of this in this area. Indeed the field site is located on what appears to be a medial moraine and this is overlain in many places by talus deposits and scree slopes. Many of these disturbances must of recent in origin as they have felled trees in their paths.

Near the coast of the Vesterålen archipelago mountains rise from the sea to heights of 500-1000 m a.s.l.. These act as barriers to the trajectory of North Atlantic air masses. As a result up to 2500 mm of precipitation falls in the alpine areas of the Lofoten-Vesterålen archipelago while the coastal pine forests are thought to receive $\sim$1000 mm annually (Kirchhefer, 2001). The pine forest sampled lies on the seaward margin of these coastal mountains.

Much of the Forfjord valley bottom and sides are sparsely forested with Scots Pine, hence the name Forf(Pine)fjord. The trees sampled lie on the eastern side of the valley as is curves south, on moraine and talus deposits in an area approximately 1.5 km by 0.5 km on the top and western facing slope of this moraine. This moraine descends in steps to

the valley bottom which is covered by a large mire. The altitudinal tree line for Scots Pine here is at around 200 m and the trees sampled for this study were between 50 m and 150 m a.s.l. (see Figure 2.2).

The moraine deposits on which the trees are growing seem to have relatively thin soils and the trees seem generally shallow rooting (see Figure 2.3). It is also generously covered with a large size range of boulders and in some areas with scree and talus deposits (see pictures in Figure 2.3). The typical slope on the western side of the moraine where the majority of trees were sampled is 15°, although many of the tree germinate on flatter areas, typically on the tops of boulders (Figure 2.3) where seedlings may face less competition.

The nature of the substrate and relatively thin soil development mean generally free draining conditions for tree growth, although occasional areas appear prone to water logging, so although precipitation is high moisture stress may be a factor for the trees during long dry periods. This is in distinct contrast to the valley bottom where the extensive mire coupled with high annual precipitation and spring runoff would require exceptional conditions for moisture stress to occur.

The forest canopy on the moraine is generally open (see Figure 2.3) with typically several metres between trees. Seedling regeneration of both birch and pine trees appears healthy to the pine tree line (there is no apparent birch tree-line at this location). The open nature of the canopy generally allows for a thick cover of ground plants including: *Calluna vulgaris* (ling), *Empetrum nigrum* (crowberry), *Vaccinium myrtillus* (bilberry), *Betula nana* (dwarf birch), *Melamphyrum* (cow-wheat) and *Vaccinium oxycoccus* (cranberry).

The growing season for Scots pine in boreal northern Europe does not typically exceed two months (Schweingruber, 1993) and requires mean monthly growing season temperatures in excess of around 10°C (Schweingruber, 1993). Here at Forfjorddalen, towards its northern tree-line, mean monthly summer temperatures only just exceed this threshold for July and August over the past 140 years (see Figure 2.4) and do not reach this level

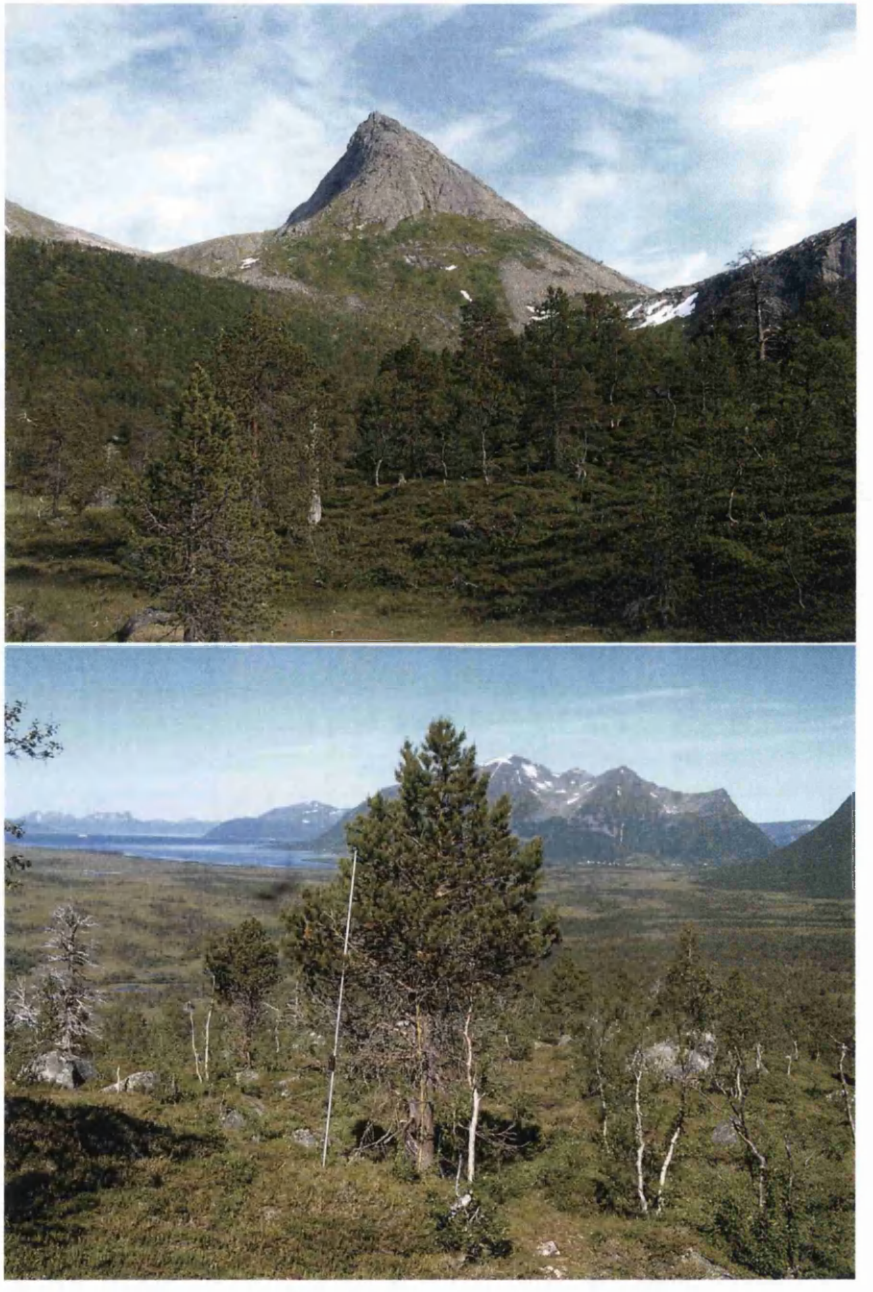

Figure 2.2: Pictures of site. The picture on top shows the ridge where the trees were sampled, rising to the right from the mire. The lower picture was taken from the altitudinal pine limit, looking down the moraine containing the trees .

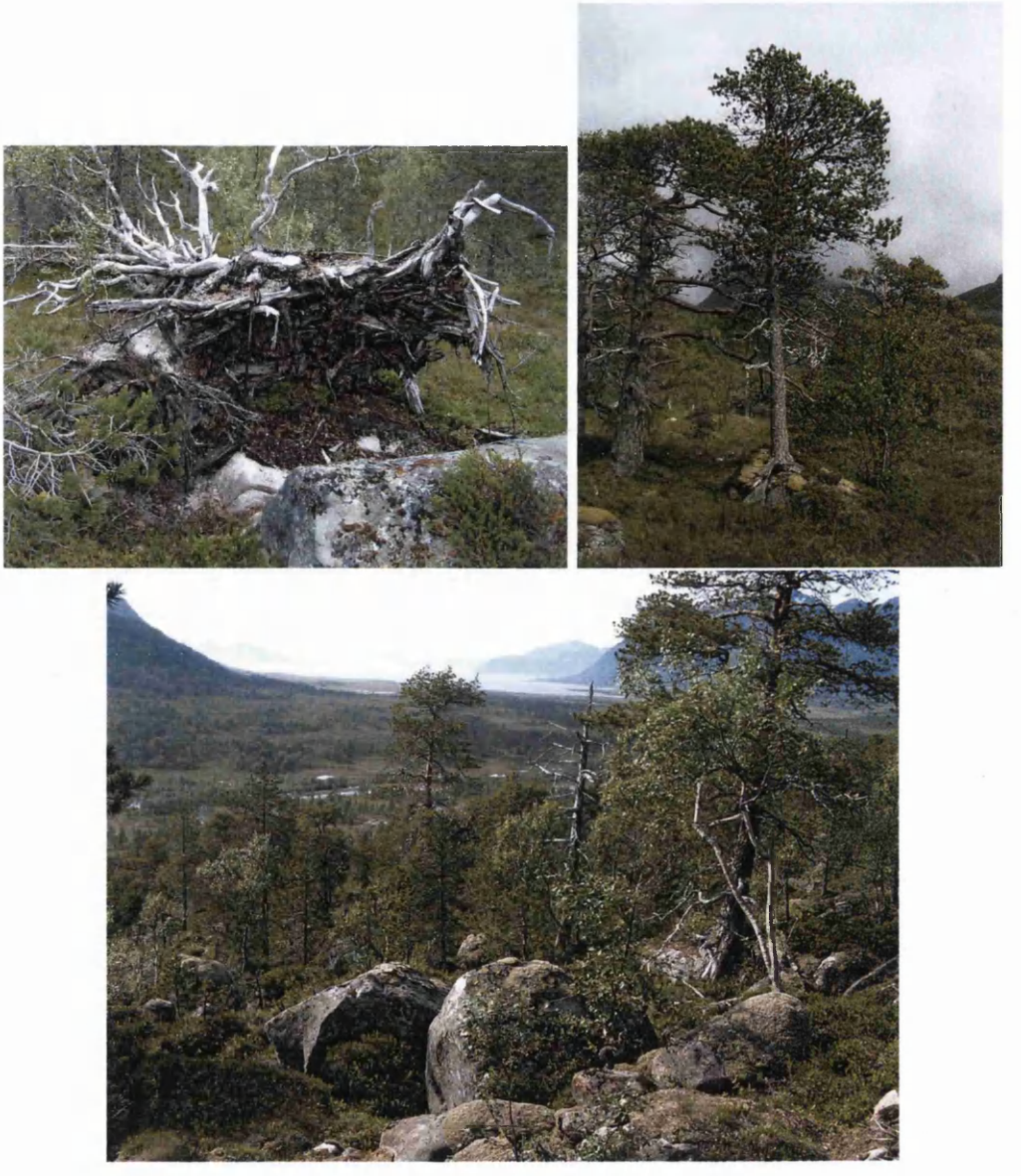

Figure 2.3: Example of tree roots, note shallow rooting (top left); tree growing over a boulder (top right); and general nature of site terrain and slope (bottom).

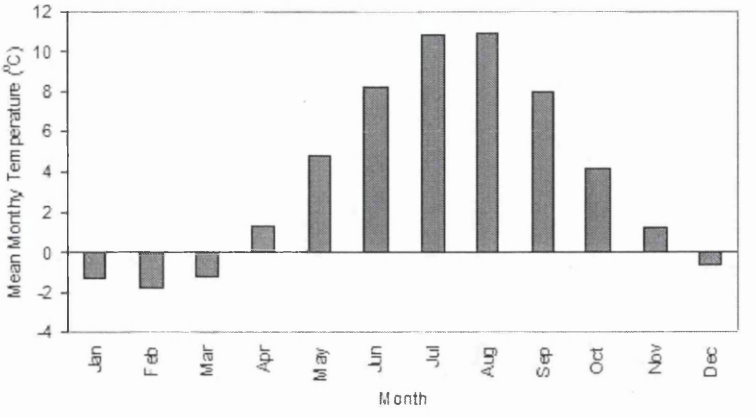

Figure 2.4: Monthly mean temperature for Andenes met station AD 1868-2003 in °C

for, by any means, all of the summers on record (see Figure 2.7). The growing season here is probably somewhat less than eight weeks. Evidence from tree rings and isotopes (see Chapter 5) suggests a period for the production of sugars for latewood formation contained within July and August, although the period is not precise and may vary year to year. Despite these marginal growing conditions only one of the trees used showed any evidence of missing rings (Tree 166).

2.3 Climate data

The nearest meteorological station to Forfjorddalen is Andenes (Figure 2.1) at the northern tip of the Vesterålen archipelago (69°18'N and 16°09'E). Andenes lies approximately 60 km north-east of Forfjorddalen. The temperature record here, at only 60 km distance, should reasonably reflect conditions at Forfjorddalen. However, in its rather more exposed position it may receive rather more precipitation than Forfjorddalen. Mean monthly temperature records from Andenes begin in AD 1868 and precipitation in AD 1910, which are sufficient for climate calibration. The mean monthly temperature record for this period cam be seen in Figure 2.4 and those for precipitation in Figure 2.5. Tabulated monthly mean climate data can be found in Appendices A.1 (temperature) and A.2 (precipitation).

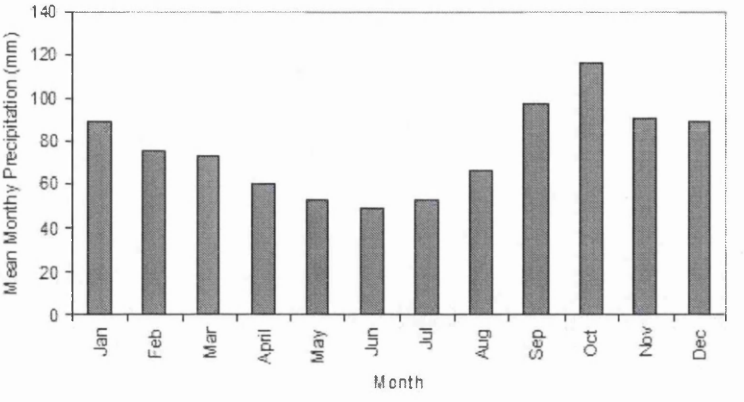

Figure 2.5: Monthly mean precipitation for Andenes met station for AD 1910-2003

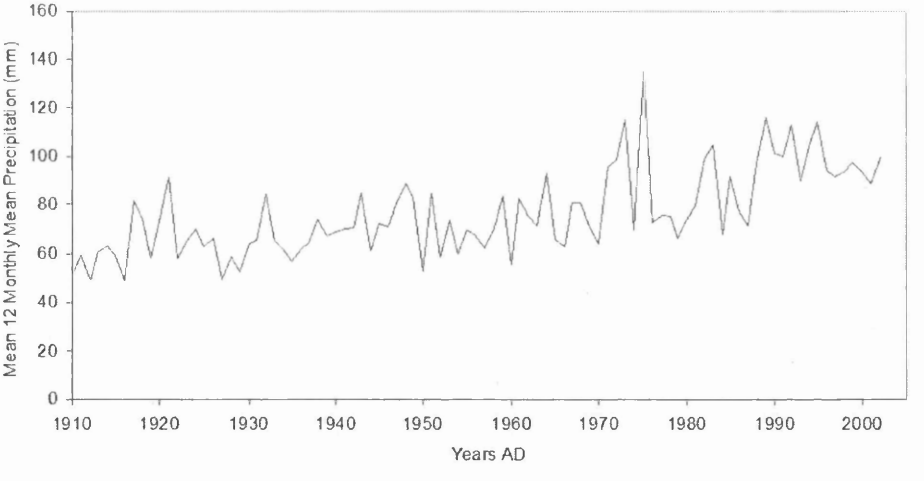

Figure 2.8: Mean 12 monthly (Jan-Dec) precipitation for Andenes from AD 1910-2002

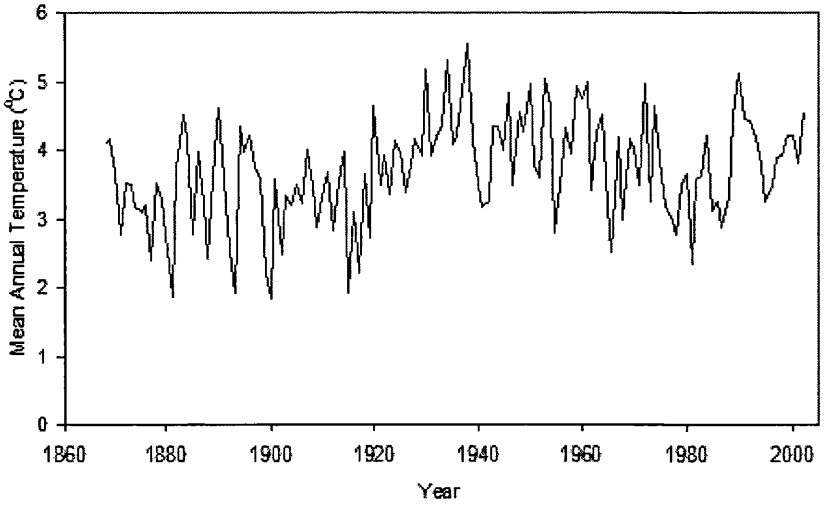

Figure 2.6: Annual mean temperature for Andenes from AD 1868-2002

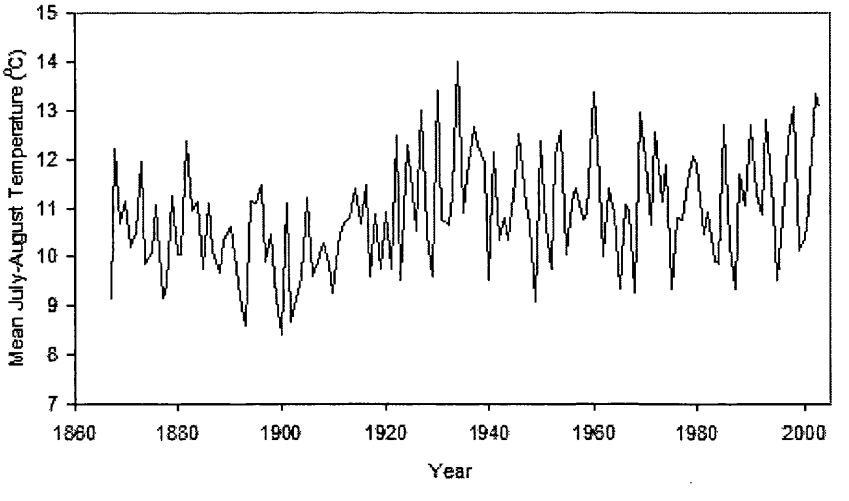

Figure 2.7: Mean temperature in July and August for Andenes from AD 1868-2002

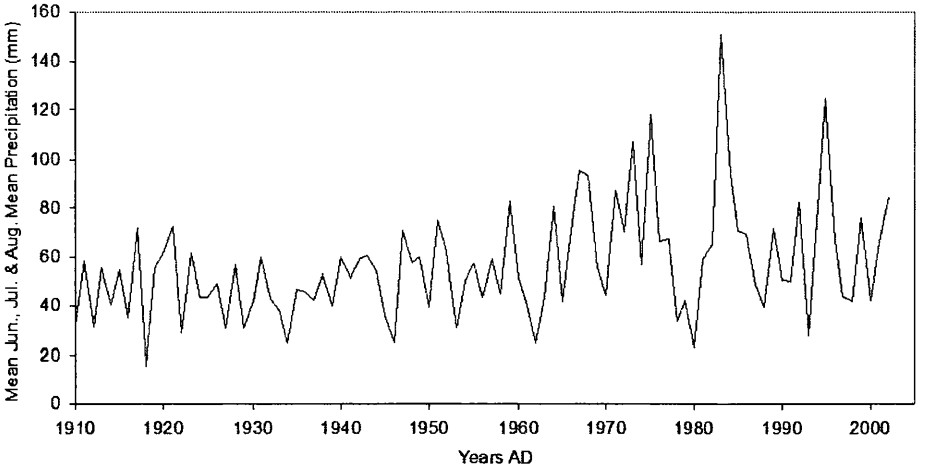

Figure 2.9: Mean of July and August mean precipitation for Andenes from AD 1910-2002

The trends for summer and annual temperature and precipitation from the Andenes meteorological station since records began can be seen in Figures 2.6 & 2.7 (for temperature) and Figures 2.8 & 2.9 (for precipitation). For both mean annual (Figure 2.6) and mean July and August (Figure 2.7) temperature after a period of rapid warming from around AD 1900-1930 temperature at this location seems to have remained relatively stable with little evidence of any significant warming trend up until AD 2002. The precipitation record (Figures 2.8 and 2.9) has a very apparent increasing trend in both the mean annual and mean summer precipitation (which are significant at $p<0.01$). Not only has there been an increase in the level of precipitation but also in its magnitude and variability, especially in summer precipitation over recent decades. Indeed, increasing wetness, over recent decades, has been noted as a trend over much of Fennoscandia (Hanssen-Bauer and Føland, 1998; Busuioc et al., 2001; Linderholm and Chen, 2005).

3

Methodology

3.1 Sampling

3.1.1 Species Selection

Many tree species from a variety of geographical locations have been analysed to determine the isotopic ratios of their tree rings including the oldest living trees, bristlecone pine (*Pinus longaeva*) (Tang et al., 1999; Leavitt, 1994; Feng and Epstein, 1994). Other tree species used from the Americas include beech, fir, fitzroya, juniper, maple, oak, pine, spruce and sequoia (Craig, 1954; Epstein and Yapp, 1976; Feng and Epstein, 1995a,b; Leavitt and Long, 1983; Leavitt, 2002).

In Asia isotopic analysis of tree rings has been conducted using: silver fir in India (Ramesh et al., 1985, 1986); juniper from the Himalayas in Pakistan (Treydte et al., 2006); Chinese pine, Qinghai fir (Liu et al., 2004) and spruce (Feng et al., 1999) in China; Taiwan fir in Taiwan (Sheu et al., 1996); cryptomeria (Libby et al., 1976; Kitagawa and Matsumoto, 1995), larch (Kagawa et al., 2006a,b), spruce and oak (Tsuji et al., 2006) in Japan; and juniper from the Tibetan Plateau (Zimmerman et al., 1997). In Africa work has been undertaken on juniper in Kenya (Krishnamurthy and Epstein, 1985) and on *the* long-lived *Widdringtonia cedarbergenis* in South Africa (February and Stock, 1999; Swanborough et al., 2003). In Australia isotope values from the the grasstree *Xanthorrhoea preissii* (Swanborough et al., 2003) have been analysed.

Pioneering work has also been undertaken to resolve a climatic signal from trees which have no obvious seasonal growth rings. In Kenya on the mangrove species *Rhizophora*

Figure 3.1: Examples of Scots pine (*Pinus Sylvestris* L.) from Forfjorddalen. from left to right Tree 82 & Tree 166

mucronata (Verheyden et al., 2004); in tropical Malaysia using *Shorea superba* (Robertson et al., 2004a); and on a *Prosopis* species coastal plantation in Peru (Evans and Schrag, 2004).

In Europe a variety trees have been analysed to determine the stable isotope ratios of their rings. Oak has been important in building multi-millennial length tree-ring chronologies as far back as 10,480 BP (Baillie, 1995; Friedrich et al., 1999; Leuschner et al., 2002; Spurk et al., 2002) and a number of studies have been carried out on stable isotope ratios in oak, for both carbon (Farmer and Baxter, 1974; Robertson et al., 1997a,b; Loader et al., 2003), water isotopes (Libby et al., 1976; Robertson et al., 2001b) and both (Danis et al., 2006; Raffalli-Delerce et al., 2004; Sass-Klaassen et al., 2005). Spruce (*Picea abies*) has been studied in Switzerland (Anderson et al., 1998, 2002; Jäggi et al., 2002), while isotopes from the fir (*Abies alba*) have been measured in trees from Germany (Edwards et al., 2000) and those of beech (*fagus sylvatica*) in Switzerland (Saurer et al., 1995, 1997a,b), Great Britain (Hemming et al., 1998) and France (Duquesnay et al., 1998).

Towards the northern European tree-line larch (*Larix spp.*), spruce (*Picea spp.*) and

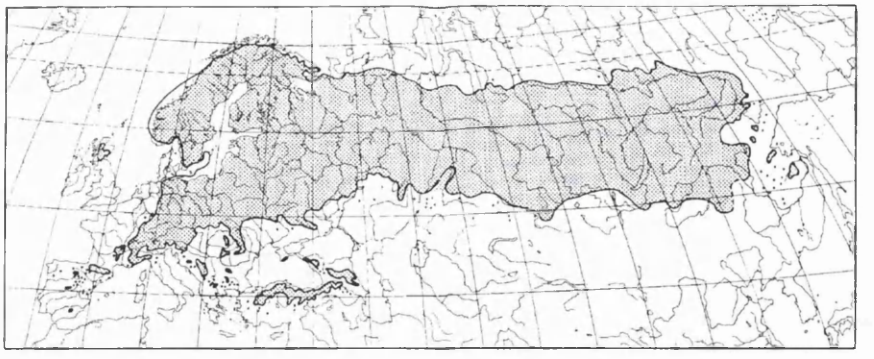

Figure 3.2: Distribution of Scots pine (*Pinus sylvestris* L.), (Zoller, 1981) in Schweingruber (1993)

Scots pine (*Pinus sylvestris*) are the major archive species (McCarroll and Loader, 2006). In northern Fennoscandia several Scots pine chronologies in excess of 1000 years have been built, with the longest greater than 7000 years (Eronen et al., 2002; Grudd et al., 2002) and here, near the northern tree-line, it is Scots pine that has mostly been used in isotope studies (Sonninen and Jungner, 1995; McCarroll and Pawellek, 2001; McCarroll et al., 2003). It has also been exploited at a variety of other locations through its natural range (see Figure 3.2) of Europe and Eurasia, including Russia (Waterhouse et al., 2000; Saurer et al., 2002), France (Gagen et al., 2004) and Great Britain (Loader and Switsur, 1996; Hemming et al., 1998). Scots pine (see Figure 3.1) is one of the most naturally widespread European species and can be found from the Mediterranean to the northern tree-line (Figure 3.2). It was once widespread throughout central Europe but is now restricted as a result of extensive felling and competition from other trees, for example in Great Britain there are a few native stands in Scotland, but not elsewhere (Phillips, 1978). Although restricted in range in central Europe it is the dominant forest tree in many areas of Fennoscandia.

Morphologically Scots pine can inhabit a variety of forms. In northern Europe and at high mountain sites its crown tends to be narrow, while in maritime and semi-arid climates crowns tend to be bushy and sometimes umbrella shaped. This conifer typically has well developed surface roots and tap roots (Schweingruber, 1993), although in Fennoscandia tap roots tend not to develop. Under optimal conditions Scots pine can reach heights

up to 40 m (Schweingruber, 1993; Phillips, 1978). *Pinus sylvestris* having such a wide distribution covers a large ecological spectrum (Figure 3.2). At its southern European locations temperatures range from an average ~8°C in winter, to 22°C in Summer. While at its northern European limits winter temperatures average only ~-15°C (with a minimum of around -40°C) and summer temperatures ~10°C (Schweingruber, 1993). Scots pine also tolerates a wide range of annual precipitation values, from 2500 mm (in western Europe) to 400 mm (in southern Europe). Its vegetation period in Fennoscandia is typically two months and is generally indifferent to soil acidity (Schweingruber, 1993). Under natural conditions Scots pine lives in excess of 300 years and, according to Schweingruber (1993), can reach a maximum age of about 600 years, expecially at dry sites. At Forfjorddalen, where site conditions are generally free draining, but annual precipitation is very high, individual trees can live well in excess of this. For example tree 166 (see 3.1) has been dated to AD 1270 and was still alive in July 2006 (726 years old).

For dendroclimatology and isotope-dendroclimatology, Scots pine is an ideal species. It has a wide geographical range, is long lived and has a generally homogeneous geographical signal within both ring widths and isotopes. This allows for precise cross-dating and typically good climatic signals, especially at sensitive sites such as at the northern tree-line. Species selection is, of course, inextricably linked to site selection. It is the combination of the long, precisely dated Scots pine chronology at Forfjorddalen and the advantageous nature of the site for climate reconstruction (see 3.1.2 below) that has led to both species and site selection.

3.1.2 Site Selection

A number of factors should be taken into account when selecting a site for work with stable isotopes, but perhaps the most important is that the trees used should be capable of being reliably cross-dated (McCarroll and Loader, 2006). Simply counting back from the bark is not a reliable way of producing an absolutely dated chronology even in mild and temperate environments (Fritts, 1976; Schweingruber, 1988). It is therefore essential

that trees be reliably cross-dated or the great advantage, which tree rings possess, of an absolute time scale is lost. At Forfjorddalen a continuous ring width sequence has been established back to AD 877.

In dendrochronology an expressed population signal (EPS) is typically used to estimate between-tree signal strength. EPS (Equation 3.1) is defined as the mean correlation calculated between all possible pairs of trees ($\overline{r}_{bt}$), which is equivalent to the fractional variance component in ANOVA. The noise or variance not common between trees is canceled in direct proportion to the number of trees (t). Values for EPS are very sensitive to the number of trees (t) used in the chronology and typically increases rapidly as additional trees are added up to around 10 trees, from then onwards the incremental advantage of adding extra trees rapidly decreases (Briffa and Jones, 1989). While there is no formal minimum limit for EPS that can be used for climatic reconstruction, a figure of EPS $= 0.85$ has been suggested as a reasonable value by Wigley et al. (1984) and is typically used.

$$\mathrm{EPS}(t) = \frac{(t \cdot \overline{r}_{bt})}{(t \cdot \overline{r}_{bt} + (1 - \overline{r}_{bt}))} \tag{3.1}$$

At Forfjorddalen ring width series from nine trees have proved enough for a chronology with an EPS of greater than 0.85. The current tree ring series at Forfjorddalen provides a well replicated series back to AD 1151 (Kirchhefer, 2001). The dating of cores collected for isotopic analysis will be discussed in detail in Section 3.3.

Site selection is critical in terms of the nature of the climatic reconstruction that is to be undertaken (Fritts, 1976; Schweingruber et al., 1989). In studies that use ring widths for climatic reconstruction it is usually recommended that site selection be guided by the aims of the study and that sites are selected for sensitivity to the climatic factor under investigation (Fritts, 1976; Schweingruber et al., 1989; McCarroll and Loader, 2006). For example, if precipitation is of interest, the selection of a dry well drained site where moisture is likely to be the major limiting factor on tree growth would be advisable; for temperature sites at the latitudinal or altitudinal tree line should be sought

out, where summer temperature is often the main growth limiting factor (Fritts, 1976; Schweingruber, 1988).

For the study of isotopes in tree rings, it is more important to base site selection on an understanding of isotope theory (McCarroll and Loader, 2004, 2006; Switsur and Waterhouse, 1998), rather than merely seeking out sensitive sites, as isotopes, unlike tree-rings, are not a proxy for net annual growth. So a factor that is strongly limiting to tree growth may not be the key factor in dominating isotopic fractionation (McCarroll and Loader, 2006). For example in northern Finland, where tree growth is strongly linked to summer temperature, the $\delta^{13}C$ of Scots pine tree-rings is also strongly linked to summer temperature, however there is also a response to very dry summers, to which other tree ring proxies (e.g. maximum latewood density) are seemingly unaffected (McCarroll et al., 2003).

Carbon isotopes in trees reflect the internal concentrations of CO_2, which are a result of the balance of the rate at which CO_2 enters and leaves the stomatal chambers. The dominant controls are stomatal conductance (the rate at which CO_2 enters) and photosynthetic rate (the rate at which it is removed). Stomatal conductance is governed by moisture stress and ambient air relative humidity, while photosynthetic rate is governed by photon-flux (sunlight and so indirectly by temperature). The isotopic values for oxygen in tree rings are controlled by antecedent precipitation and relative air humidity (vapour pressure deficit) (Switsur and Waterhouse, 1998; McCarroll and Loader, 2004) (a detailed discussion of isotope fractionation theory and its relationship with climate can be found in Section 3.5.1 for carbon and 3.5.2 for oxygen). So care must be taken in site selection depending on which climate parameter is being studied. If carbon isotopes are to be used to reconstruct temperature then a site should be selected where trees are likely to suffer little moisture limitation during their growing season. Shallow rooting trees on well drained substrates, especially in areas prone to summer drought should be avoided, in favour of sites where trees have abundant access to moisture.

At 68°48'N and 15°44'E, the forest at Forfjorddalen is an isolated outpost of Scots pine towards its northern tree-line. The combiniation of its tree line location with high mean

annual precipitation of ~1000mm (Kirchhefer, 2001) should make this an ideal site for reconstructing summer temperatures from isotopes, ring-widths and maximum late-wood density. However, the generally free draining nature of the substrate in which the trees are growing, which may account for their extreme longevity (Schweingruber, 1993), allows for the possibility of a precipitation signal in the stable carbon isotopes especially in extremely dry (and possibly wet) summers. The lack of a precipitation signal in the ring-widths (Kirchhefer, 2001) does not mean there will be none present in the isotopes (McCarroll and Loader, 2006); however this seems a reasonable working assumption. The inclusion of both stable oxygen isotopes (which should be sensitive to changes in precipitation) and ring-widths (which at this site have been demonstrated to be temperature sensitive (Kirchhefer, 2001)), should enable any mixed signal of temperature and precipitation to be recognised.

Site conditions preclude the availability of sub-fossil material at Forfjorddalen and so the tree ring archive is made (almost entirely) of living trees and standing and fallen dead-wood. The exception being Tree 63. This sample comes from a disc, in Tromsø museum, of a tree felled in the 1970s. There are both extremely long lived trees and abundant standing dead-wood available at the site. There are living trees in excess of 600 years old (see Section 3.3) and trees which have died but remained standing after death for many hundreds of years, see Figure 3.1 for examples of living trees and Figure 3.3 for examples of standing dead-wood. Tree 130 (Figure 3.3) is dated from AD 1050 to AD 1400, it appears to have lost all of it's sapwood (which at this location is typically 100 years) and so is likely to have died between 400 and 500 years ago. It is still standing and despite losing all of it's superstructure shows no signs of decay in the core taken. Tree 59 is the oldest dated standing timber in the forest dating to AD 877. All that is remains of this tree is approximately one metre of stump. While neither of these trees have been used in this study, they do demonstrate that with careful sampling enough material for a well replicated isotope chronology in excess of 1000 years should be possible at Forfjorddalen.

Why so many very old trees, living and dead, have remained in this forest of Scots pine in an area where pine trees are scarce and which has been inhabited for may generations

Figure 3.3: Examples of standing deadwood from Forfjorddalen. From left to right Trees 130, 59 and 133.

by the Norse and much longer by the indigenous Sami peoples, is a question beyond the scope of this study. The site is fairly remote and difficult to access in the summer months due to the extensive mire in the valley floor, which would make timber extraction difficult, however during the long winter months when the mire is frozen and snow lies on the ground it would be much less problematic. There is evidence that the Sami used the pine trees for more than just timber with evidence of cultural modification on some of the trees (these were not sampled). The land is divided between local landowners in strips, down the hill side, and it is clear that some have been logged more than others, so some areas have few old trees, while others have many, this distribution would seem very much dependent on whether the particular owners had need for timber. The area is now a designated nature reserve and so the forest is safe from further felling. This also means that permission to core trees must be sought in advance and that coring is limited.

In terms of the climatic importance of the sites geographical location, the The Vesterålen archipelago lies proximal to a key location for the moderation of Western European climate. The influence of the Gulf Stream ameliorates the climate of North-western Europe and the area of the Norwegian-Greenland Sea off southern Svalbard has been identified as a major area of downwelling in the thermohaline circulation system, producing North

Atlantic Deep Water (NADW) (Schmitz, 1995). It is the formation of this NADW which in turn drives the Gulf Stream. NADW formation has a considerable impact on climate of the North Atlantic region. The release of heat into the atmosphere by 'ventilation' of the ocean as warm surface water sinks generates ~25% of solar heating reaching the surface of the North Atlantic in the region north of 35°N (Broecker and Denton, 1990). Adjacent to this area of NADW formation in the Norwegian-Greenland Sea the Vesterålen archipelago may prove to be a key location for understanding Western European climate.

3.1.3 Sampling Strategy

Cores were collected in July AD 2002, July AD 2005 and June AD 2006. Cores were generally taken at breast height from dominant trees. Both 12 mm and 6 mm corers were used, 6 mm cores to gauge whether a particular tree might be suitable for isotope work and the 12 mm to extract the cores for isotopes measurements. While 12 mm corers are more difficult to use than 6 mm cores, being harder to insert and also harder to remove, if they become stuck, they have the major advantage of providing a core of approximately 10 mm diameter which yields more than six times as much wood per ring as the 4 mm dowel from a 6 mm corer. The decision was made early on to use latewood only (where possible) extracted to α-cellulose, for this reason to retrieve enough material to measure both the $\delta^{13}C$ and $\delta^{18}O$ of individual rings the larger core diameter was necessary for rings with a width of <1 mm, which is typical for the older trees in this area. Dendrochronologists will typically oil their corers in cleaning and maintenance and as a lubricant to aid coring, this of course was avoided as contamination from hydrocarbons can seriously compromise isotope results.

It was felt desirable to select trees of mixed ages for each period so the chronology does not proceed back in time in cohorts, but has a mixed age structure throughout. Cohorts being where one group or cohort of similar aged trees are used (e.g. AD 1700-2001), which are then replaced by a cohort of similar aged fossil sub-fossil trees (e.g. AD 1450-1750). Aviding cohorts has the twin advantage of preventing offsets in the mean isotope

value when one cohort ends and the next begins (both carbon and oxygen isotopes often have an offset in absolute values between trees). A mixed age structure also allows for the *juvenile effect* in carbon isotope (discussed in Section 1.4.2) to be more easily recognisable.

Once a was is selected for coring a GPS location was taken, tree height estimated, girth, coring height and direction were noted. Slope angle was estimated and a general site description was made and photographs taken.

3.2 Sample Storage and Preparation

As was mentioned in Section 3.1.3 oil was not applied to corers used for extracting tree-cores for isotopes work. This is one of a number of simple precautions taken to avoid contamination of samples and thus compromising isotope results. Samples were not glued into mounts as is typical in ring-width studies. Once collected they were restrained in wooden mounts with string to prevent warping whilst drying. Cores were then left to dry at room temperature for at least one month before being further analysed. Once dry cores were machine and hand sanded, where appropriate, to prepare clean surfaces for accurate measurement and cutting. Chalk was not applied to these surfaces. For measuring and cutting it is useful to mark cores, once dated, at intervals of 10 calender years. This was done with a sharp metal point, rather than using the pen or pencil marks typical in dendrochronology. One hole was made at every decade, two every 50 years and three at every century. All possible precautions were taken in storage and preparation to avoid any contamination that might affect the isotope results.

3.3 Ring Width Measurement and Dating

Once dried and sanded the cores were dated against the master Forfjorddalen reference chronology (Kirchhefer, 2001, 2006). Ring-widths were measured using a microscope and

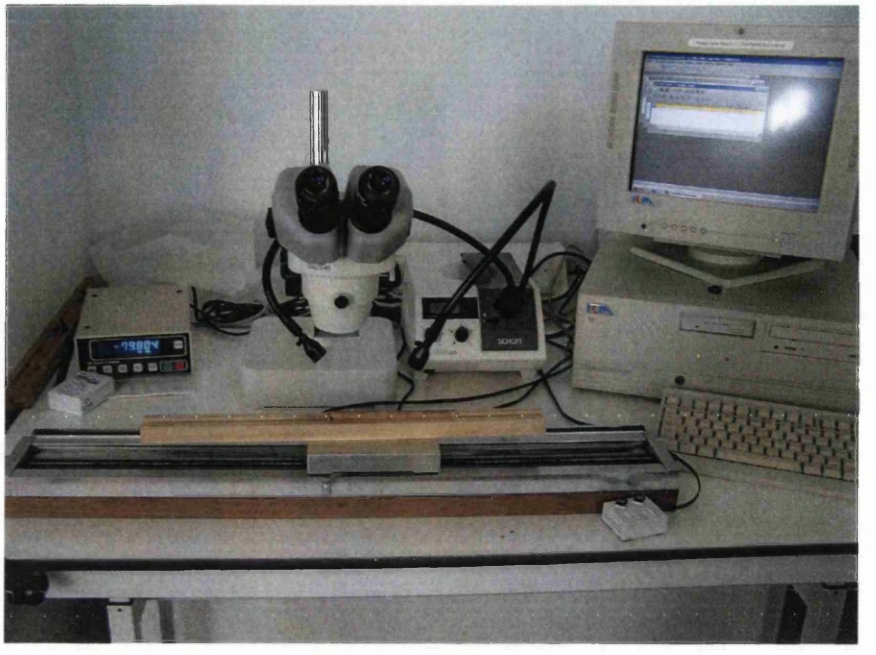

Figure 3.4: Tree-ring measuring Stage, with microscope and linked computer.

traveling stage linked to a computer running the Rinntech program TSAP (Time Series and Analysis Program) (Rinn, 1996), see Figure 3.4. Ring-widths were measured at a resolution of 0.001 mm and then cross-dated against the Forfjorddalen master chronology.

To cross-date using ring width measurements an undated sample is compared to a dated sequence (reference chronology) and an indication of how well they match must be determined. While visual matches are useful (and often extremely accurate) they lack the objectivity demanded by modern science (Pilcher, 1989) and so quantifiable methods must be used. The Student's t-value, although by no means the only or necessarily the best statistical indicator, has been widely and successfully used by European dendrochronologists, typically using algorithms derived from Baillie and Pilcher's CROS program (Baillie and Pilcher, 1973) and this statistic is included in the TSAP program.

Statistically t-values in excess of 3.5 should be considered significant (Baillie and Pilcher, 1973), but as it is not uncommon to find more than one match of greater than 3.5 between the same core and the reference chronology, ideally matches in excess of 5 or 6 should be sought, as an example of the level of t-values that may be expected Oak tree

in the Great Britain will often give t-values of around 10 from the same tree.

As a quality control for the TSAP dating and in order to identify any missing rings and measurement errors the results were fed into the COFECHA (an inveted Spainish word meaning "co-date" or "cross-date" (Grissino-Mayer, 2001)) program developed by Holmes (1983), see Grissino-Mayer (2001) for an evaluation and tutorial for this very useful program. As cross-dating in temperate areas is essentially concerned with 'high frequency' variations in ring-widths COFECHA uses segmented time series correlation techniques to asses the quality of cross-dating, in effect simulating mathematically human perception on visual examination of a tree-ring series (Grissino-Mayer, 2001). It analyses overlapping segments of the ring-width series against the reference chronology and 'slides' them backwards and forwards by typically 10 years (although this and the segment length can be user defined) to see if there is a better statistical fit, in effect checking for missing or false rings, much as an analyst would do by eye by sliding one graph over the other. It also checks measurement accuracy by flagging outlier ring measurements that lie in the outer distribution of all rings measured for that year (Grissino-Mayer, 2001). Once these results are obtained the analyst should return to the samples and graphs to check the voracity of the COFECHA results and make any adjustments in dating accordingly.

The trees sampled at Forfjorddalen in AD 2005 and AD 2006, in general, cross-dated very successfully with t-values in excess of 10 with the master chronology for all the trees used for isotope work. The cross-dating was also checked visually and using COFECHA, the results of this cross-dating exercise were further checked by an experienced dendrochronologistst (Kirchhefer, *pers. comm.*), who also dated all the cores collected in AD 2002.

3.4 Sample Preparation for Isotope Analysis

The first step once the tree cores have been dated and accurately pinned (as described in Sections 3.2 and 3.3) is to cut each core into individual annual rings, separating earlywood from latewood. This is done with a scalpel and a microscope. The fine wood

shavings produced are put into small glass vials with screw tops and each vial labeled with site location, tree number, calender year and contents (latewood (LW) or earlywood (EW)). With practice it is possible to accurately separate latewood from earlywood in rings of less than 0.5 mm. In many species including Scots pine cutting is aided by the difference in appearance and texture of the earlywood and latewood. In Scots pine the earlywood consists of large open cells, while latewood cells are much smaller and harder. The latewood is also much darker in colour than the earlywood. Working inwards from the bark latewood is shaved away until the latewood/earlywood boundary is reached. This boundary tends to be blurred and a judgment must be made based on texture and colour as to where to cease cutting. The consequences of incorporating the last few cells of earlywood into the latewood are not too great (McCarroll and Loader, 2006). The boundary between the earlywood of one year and the latewood of the previous year is typically an abrupt one. It is usually possible to scrape away the soft earlywood cells exposing the hard shiny latewood boundary.

There are instances where individual, and often groups of, rings are too narrow for latewood and earlywood to be accurately separated. Even were accurate cutting of LW possible, the few cells of latewood would not yield the 1 mg of cellulose required to measure both δ^{13}C and δ^{18}O. An experiment was therefore undertaken to decide whether it was advisable to incorporate some or all mof the earlywood into the sample or to have no result for one or both of the isotope proxies for that year.

Tree 129, a living tree cored in AD 2005, was selected. This tree had α-cellulose extracted from the EW for a 50 year period from 1929 to 1978 and δ^{13}C results from the unhomogenised cellulose were analysed. These results were compared to those for LW over the same period. This period was chosen firstly because there is climate data available with which to compare the results. Secondly, the rings widths of this period were wide enough for latewood to be separated with reasonable precision. Thirdly, fifty years was considered a long enough period for meaningful statistical comparison to be undertaken. δ^{13}C results were then corrected for the 'Suess effect' of the dilution of atmospheric carbon isotope ratios by the cumulative addition of 'light' carbon of organic

origin burned in fossil fuels, using the correction procedure of McCarroll and Loader (2004). A correction was also made for tree response to the effects of increased CO_2 in the atmosphere. This **pre-in**dustrial (PIN) correction is proposed by McCarroll et al. (2007), both of which corrections will be discussed at greater length in Chapter 3. The results of this comparison of LW and EW $\delta^{13}C$ can be seen in Figure 3.5 and Table 3.1, which compares the summary statistics for both $\delta^{13}C$ and $\delta^{13}C_{pin}$ of latewood and earlywood. Table 3.2 shows the mean squared error (MSE) between earlywood and latewood, calculated using Equation 3.2, where ew_t denotes the $\delta^{13}C$ value of earlywood at time t and lw_t denotes the $\delta^{13}C$ value of latewood at time t.

$$MSE = \frac{1}{N}\sum(ew_t - lw_t)^2 \tag{3.2}$$

The results in Tables 3.1 and 3.2 suggest that there is little difference between the latewood results and the earlywood results either before (MSE = 0.11) or post PIN correction (MSE = 0.14). While the visual comparison in Figure 3.5 would seem to confirm this, it should be noted that the *PIN* correction imparts slightly more variance to the data, which will be discussed briefly in Chapter 4.

Table 3.3 shows that the climate correlation for the $\delta^{13}C_{pin}$ of the LW are higher with August temperature ($r = 0.71$) than the EW ($r = 0.57$). The EW however correlates more strongly with July temperature ($r = 0.71$) than LW ($r = 0.63$). For mean July and August temperature there is little difference between the latewood ($r = 0.75$) and earlywood ($r = 0.72$). Some previous work has suggested that the use of stored photosynthates from the previous summer may compromise the earlywood signal and that if a truly annual resolution is required then latewood should be isolated (Switsur et al., 1995), although this research was carried out on oak trees rather than conifers. The results in Figure 3.5 and Table 3.3 suggest that the growing season for these trees covers some period contained in July and August and that the EW is laid down from photosynthates produced in July and the latewood from those produced in August. If there is any re-use of the previous years photosynthates, as has been demonstrated in *Larix gmelinii* saplings by Kagawa

et al. (2006b,a), there appears to be no more affect on the EW than the LW. Based on these results it seems that for Scots pine (at this location) there is little advantage to be gained from the separation of EW and LW. Indeed if a reconstruction of mean July and August temperature is sought it may be an advantageous to use the whole ring (EW and LW). In terms of this study it was decided, based on these results, that the incorporation of some earlywood into a sample was preferential to having too little or no sample for any particular year.

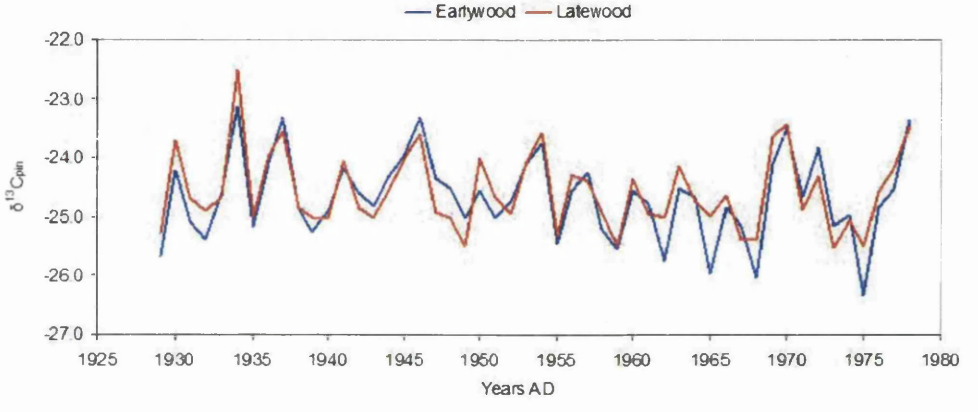

Figure 3.5: Comparison of $\delta^{13}C_{pin}$ (‰) results for cellulose from earlywood and latewood from Tree 129 (r = 0.87)

	Mean	Standard Dev.	Maximum	Minimum	Variance
LW	-24.94	0.66	-22.79	-26.13	0.44
EW	-25.03	0.71	-23.38	-26.85	0.45
LW_{pin}	-24.57	0.67	-22.51	-25.52	0.45
EW_{pin}	-24.66	0.72	-23.14	-26.32	0.52

Table 3.1: Summary statistics for earlywood (EW), latewood (LW) comparison ($\delta^{13}C_{pin}$ ‰)

	MSE
LW vs. EW	0.11
LW_{pin} vs. EW_{pin}	0.14

Table 3.2: Mean Square Error (MSE) for earlywood (EW), latewood (LW) comparison

	July Temperature	August Temperature	July & August Temperature
LW	0.59	0.71	0.72
LW_{pin}	0.63	0.71	0.75
EW	0.66	0.57	0.69
EW_{pin}	0.71	0.56	0.72

Table 3.3: *Pearson's r* values for $\delta^{13}C(‰)$ of latewood (LW) and earlywood (EW) against July, August and mean of July and August temperatures, with and without PIN correction

All samples were extracted to α-cellulose before isotopic analysis and while there is some evidence that that $\delta^{13}C$ results for wholewood, lignin and cellulose, although offset, remain generally in parallel with one another (Loader et al., 2003; Robertson et al., 2004b; Schulze et al., 2004) the position is much less clear for $\delta^{18}O$ (Borella et al., 2004). The little work that has been undertaken suggests that the $\delta^{18}O$ of cellulose correlates rather better with climate than that of wholewood (Borella et al., 1999). As $\delta^{18}O$ is to be used in this study and because some isotope results for trees at this location were already available, which had been obtained from α-cellulose, it was decided to extract all samples to α-cellulose.

A variety of techniques have been published for the extraction of cellulose from wholewood (Brendel et al., 2000; Loader et al., 1997, 2002; MacFarlane et al., 1999). The method chosen is based on the method of Loader et al. (1997), which has a proven track record of producing α-cellulose and is also a method with which the personnel at Swansea

University are familiar and for which the equipment is readily available. In essence the process involves the oxidisation of lignin with an acidified sodium chlorite solution followed by the removal of hemicelluloses with sodium hydroxide solutions and thorough rinsing. These procedures require the use of hazardous chemicals and so all work is done in a properly ventilated laboratory fume cupboard and suitable protective clothing was worn at all times (laboratory coat, gloves and safety spectacles).

First each sample is placed in an individual glass extraction tube (see Figure 3.6) which is labeled (in indelible pen) with the year of the ring, every third or fourth sample is placed in an extraction tube engraved with its unique number, this number and the sample year are noted down. These precautions are to guard against occasional mishaps in the laboratory which may lead to sample tubes becoming mixed up. The extraction tubes are then suspended on a specially constructed rack over a water bath filled with distilled water to a level where all the tubes are partially immersed in water without the samples being flooded. The design of the extraction tubes (Figure 3.6) allows for sample to be retained in the bowl by a glass sinter filter while liquids are removed through the hollow arm under suction. With the equipment available it is possible to process batches of up to 100 samples at a time. With the water bath heated to 80°C each sample is suspended in acidified sodium chlorite for 50 minutes, after which time each sampled is drained, this process is repeated six times. Each sample is then suspended in boiling water to reactivate any remaining sodium chlorite and then rinsed with distilled water five times. With the water bath heated to 70°C each sample is then suspended in a 10% solution of sodium hydroxide for 45 minutes, the samples are then drained and suspended in distilled water. The water bath is then cooled to room temperature and the samples suspended in a 17% solution of sodium hydroxide, again for 45 minutes and then drained. Each sample is then rinsed five time with distilled water. The water bath is reheated to 80°C and suspended twice more in acified sodium chlorite for 50 minutes. Finally each sample is rinsed five time with distilled water and hung on a drying rack. The samples are then dried at 60°C in a drying oven for a minimum of 48 hours. Meanwhile the labeled glass vials in which the wood samples were stored are individually blown out with an air gun,

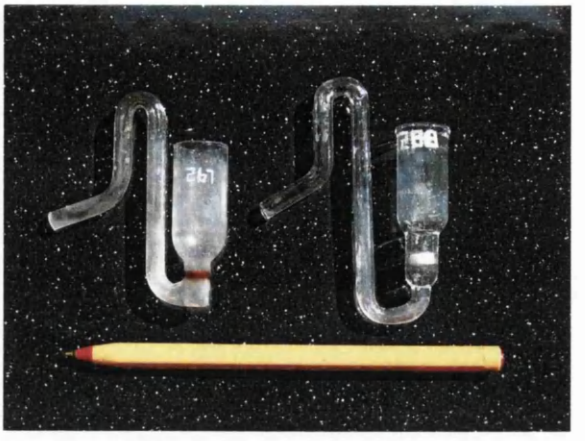

Figure 3.6: Examples of extraction tubes

Figure 3.7: Samples in extraction tubes suspended over a water bath

to remove any remaining wholewood pieces or dust. The dried samples are then replaced in their original glass tube and the cellulose is stored to await weighing out.

Samples for mass-spectrometry analysis are weighed out using a micro-balance. While samples with as little 50 μg of carbon can be routinely measured, with confidence, by a modern mass spectrometer it is not necessarily advantageous to use such small quantities in tree-ring analysis as the within-tree variability will not be averaged if only a few fibers

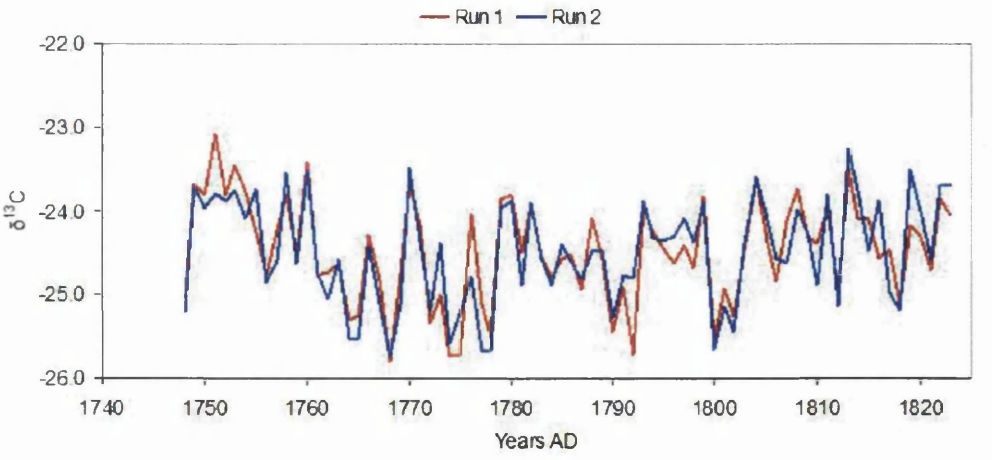

Figure 3.8: Comparison of δ^{13}C (‰) results for Tree 87, Runs 1 & 2 between 1748 and 1823 ($r = 0.87$).

	Mean	Standard Dev.	Maximum	Minimum	MSE
Run 1	-24.47	0.62	-23.07	-25.81	0.10
Run 2	-24.49	0.64	-23.26	-25.73	

Table 3.4: Summary statistics for Runs 1 and 2 of δ^{13}C (‰) for Tree 87 between 1748 and 1823, and the MSE between the two runs.

are used (McCarroll and Loader, 2006). For analysis in the Swansea mass spectrometry laboratory samples of between 0.30 mg and 0.35 mg are weighed out for both δ^{13}C and δ^{18}O analysis. Single samples of cellulose are weighed out for each year for δ^{13}C analysis and duplicates for δ^{18}O because of the lower precision of the results. Ideally multiple samples would have been run for both δ^{13}C and δ^{18}O , however this was not possible. However, the advantage of doing multiple trees for each individual year are manifold, among which is the possibly to cross check annual values for anomalous results which may need to be re-measured. While there may be considerable within-tree variability, the variability between trees within even a few metres of one other is usually much greater and so it is may be advisable utilising scarce resources in analysing more trees, rather than carrying out more measurement on one tree (McCarroll and Loader, 2004).

In light of the above discussion it was considered advisable to carry out a comparison of replicate analyses or $\delta^{13}C$ from one tree. Tree 87 was selected at random for a period from 1748 to 1823. The results were not run in tandem, as duplicates usually are, but on separate occasions, which may have increased the variability slightly. The results for this comparison can be seen in Figure 3.8 and Table 3.4, MSE of only 0.10 between the two runs (Pearson's r *of 0.87)* between the two runs. Over such a long period (76 years) this was considered an encouraging result and reasonable justification for running $\delta^{13}C$ results as singly. Interestingly the correlation between these two runs (r = 0.87) is the same as for the latewood earlywood comparison for Tree 129 (see Figure 3.1) which makes the latewood/ earlywood comparison results seem the more impressive.

3.5 Choice of Proxies

This study aims to use a multi-proxy approach to climatic reconstruction from tree rings as suggested by McCarroll and Loader (2004, 2006). The proxies chosen with their relationships to climate are outlined below (sections 3.5.1, 3.5.2 and 3.5.3). They consists of two chemical properties, $\delta^{13}C$ and $\delta^{18}O$ ratios and one physical, tree-ring widths.

3.5.1 $\delta^{13}C$ ratios in tree-rings

The $\delta^{13}C$ ratio of cellulose in tree rings has been demonstrated to show a high correlation with summer temperature and antecedent precipitation (McCarroll et al., 2003; Gagen et al., 2004). Stable carbon isotope fractionation in trees is a function of internal to external CO_2 concentrations and thus the balance between stomatal conductance and photosynthetic rate. Stomatal conductance will tend to dominate where moisture is the limiting factor and where there is little or no moisture stress photosynthetic rate is likely to be the controlling factor (McCarroll and Loader, 2004).

As carbon dioxide diffuses through the stomata into the intercellular spaces within the leaves there is a fractionation of around -4.4‰, this fractionation is due to the differ-

ence in mass between ^{13}C and ^{12}C , as these molecule bounce around the lighter ones bounce furthest and are more likely to pass through the stomatal openings (McCarroll and Loader, 2004). At the site of the ribulose bisphosphate carboxylase (rubisco) enzyme, where photosynthesis produces sugars by combining leaf water with intercellular CO_2 a fractionation of both water and carbon isotopes occurs (Farquhar et al., 1982; Frencey and Farquhar, 1982; Farquhar et al., 1989). The discrimination against the heavier ^{13}C is about -27‰ as the lighter ^{12}C is preferentially used in photosynthesis. If the photosynthetic rate of CO_2 usage is greater than the supply of CO_2 from stomatal conductance the intercellular concentration of CO_2 falls and becomes enriched in the heavier ^{13}C and although fractionation remains nearly constant at -27‰, the ratio of ^{13}C in the leaf sugars will increase as the ratio of its intercellular source rises (McCarroll and Loader, 2004). The factors involved in carbon isotope fractionation have been expressed in equation 3.3 (Farquhar et al., 1982). Here $\delta^{13}C_{plant}$ is the stable carbon isotope ratio fixed by the tree; $\delta^{13}C_{air}$ is the isotope ratio of the carbon dioxide in the atmosphere; *a* is the fractionation as CO_2 diffuses through the stomata into the intercellular spaces (around -4.4‰); *b* is the fractionation during photosynthesis (around -27‰); c_i/c_a is the ratio of the CO_2 pressure in the intercellular spaces (c_i) to that in the atmosphere (c_a).

$$\delta^{13}C_{plant} = \delta^{13}C_{air} - a + (b - a) \cdot \frac{c_i}{c_a} \tag{3.3}$$

The dominant controls on the intercellular concentration of CO_2 in terms of climate are moisture stress and relative humidity for stomatal conductance and sunlight and temperature for photosynthetic rate. When a tree becomes moisture stressed it restricts its stomata to prevent water loss and so intercellular CO_2 concentration fall and the ratio of ^{13}C in the leaf sugars produced rises. If atmospheric relative humidity is high fewer water molecules evaporate through the stomata and moisture stress is reduced, stomata remain open and intercellular CO_2 concentrations rise. Photosynthetic rate is primarily

controlled by temperature and irradiance, during warm and sunny periods photosynthetic rate is high and photosynthetic rate may outpace stomatal conductance, again leading to a fall in intercellular concentrations of CO_2 and a rise in ^{13}C in the sugars produced.

For $\delta^{13}C$ ratios there are then at least two climatic conditions that can produce elevated $\delta^{13}C$ ratios: hot and sunny, or dry. While there is a general negative correlation between temperature and precipitation (Madden and Williams, 1978; Trenberth and Shea, 2005), hot summers tending to be dry and wet summers cool, this is not always the case and warm and wet or cool and dry summers are not unknown events in northern Norway. In these situations it may become difficult to interpret the climatic signal from $\delta^{13}C$ on its own, especially beyond the period for which reliable climate data are available. At Forfjorddalen, near the latitudinal tree line for Scots pine, with its high annual precipitation, it might seem reasonable to expect little problem with moisture stress however there have been changes in mean annual precipitation over the period for which records are available, with some rather dry summers. This combined with the relatively free draining nature of the substrate and the sensitivity of $\delta^{13}C$ to even mild drought conditions makes the inclusion of other proxies seem wise.

3.5.2 $\delta^{18}O$ ratios in tree-rings

The $\delta^{18}O$ ratio in tree-rings is controlled by several factors. Firstly there is the $\delta^{18}O$ of the source water which is ultimately the $\delta^{18}O$ of precipitation, however there is potential for fractionation and mixing of the isotopic signal before it reaches the tree (Darling, 2004). The $\delta^{18}O$ ratio of precipitation varies seasonally and so water at differing depths and with different residence times can have different isotopic ratios (Darling, 2004) and so the seasonality of precipitation combined with the growing season of the trees and their access to groundwater are the critical factors here (McCarroll and Loader, 2006). The trees at Forfjorddalen, on such a free draining ridge, should reflect summer precipitation $\delta^{18}O$ values. There is also potential for fractionation within the soil as water evaporates preferentially losing molecules containing the lighter oxygen isotopes, this should be lim-

ited to near the ground surface and so should not normally affect the water taken in by the roots (McCarroll and Loader, 2006). Water enters the tree from the ground through its roots, there is no fractionation at this point, so the water which moves up through the xylem to the leaves should have the same isotopic signature as the source (McCarroll and Loader, 2006). However there are processes within the tree that can lead to fractionation of oxygen isotopes within water before they become fixed in tree-rings. In the leaf there is a potential for fractionation prior to photosynthesis. As water molecules (H_2O) are smaller than those of carbon dioxide (CO_2), when stomata are open to allow in CO_2 molecules they lose H_2O molecules through evaporation. The H_2O molecules with the lighter oxygen and hydrogen isotopes are preferentially evaporated leading to an enrichment of the ^{18}O oxygen isotope in the leaf water. The enrichment of ^{18}O of leaf water over xylem water at the sites of evaporation can be expressed by equation 3.4.

$$\delta^{18}O_e = \varepsilon^* + \varepsilon_k + \left(\delta^{18}O_v - \varepsilon_k\right) \cdot \frac{e_a}{e_i} \tag{3.4}$$

Where ε* is the proportional depression of water vapour pressure by the heavier water molecules, ε_k is the fractionation as water diffuses through the stomata, $\delta^{18}O_u$ the isotopic composition of water vapour in the atmosphere and e_i and e_a are the ambient and intercellular vapour pressures (Barbour et al., 2001, 2002; McCarroll and Loader, 2004). At constant temperature and where the isotopic ratio of the atmospheric and source water are the same the enrichment due to evaporation is linearly dependent on 1 - $\varepsilon_a/\varepsilon_i$ (Barbour et al., 2001). Equation 3.4 over-estimates the enrichment of leaf water because as H_2O enriched in ^{18}O diffuses backwards, it is opposed by the convection of lighter xylem water (Barbour and Farquhar, 2000; Barbour et al., 2001).

There is further generally constant fractionation of 27‰ when sucrose is formed by photosynthesis (Sternberg et al., 1986). So leaf sugars reflect the isotopic signature of leaf waters but with a 27‰ offset. Cellulose is formed by sugars transported down through the trunk, as it moves downwards there is exchange with xylem water (source

water). Current understanding suggests that an average of 42% of oxygen atoms in these sugars exchange with xylem water (Roden et al., 2000) and while the figure for Scots pine is not known, it seems likely that exchange of this nature will occur before the δ^{18}O signal becomes fixed. Research is currently underway to isolate the isotope signal from both the leaf and source water from cellulose as it is suggested that not all oxygen bearing compounds exchange in this way and that it may be possible to isolate these (Sternberg et al., 2003).

The δ^{18}Ovalues derived from tree ring cellulose, should then be partially a reflection of the source water signal and partially that of evaporation in the leaf, confused to some degree by exchanges with xylem water in the trunk. If the signal from the source water is consistent the climatic variable that δ^{18}Oreflects should be air relative humidity. If there is high atmospheric relative humidity then there will be less evaporation of the lighter H_2O molecules and once again δ^{18}Oleading to more negative values. Provided that the isotopic signal is not too corrupted by xylem water exchange this should allow us to better interpret the δ^{18}C signal (see Section 3.5.1).

3.5.3 Tree-ring widths

A third proxy available from tree-rings is their width measurements which have already been used for cross-dating the samples collected for isotope analysis (see Section 3.3). Tree-ring widths have been widely used as tool for climatic reconstruction in studies too numerous to mention. One of the major drawbacks with tree-ring widths as a means of reconstructing climate is the need to remove the growth trend by statistically de-trending the ring-width series which can lead to the removal of any climatic signal longer than the age of the trees, known as the 'segment length curse' (Cook et al., 1995). Large scale climatic reconstructions have been based largely on tree rings (Mann et al., 1999; Briffa, 2000; Moberg et al., 2005; Crowley, 2000) and much debate has ensued as to the best way to detrend tree-ring series to retain low-frequency climatic variability (Briffa and Osborn, 2002; Esper et al., 2002; Esper and Frank, 2004; Mann and Hughes, 2002).

At Forfjorddalen a reconstruction based on ring-widths has been undertaken by Kirchhefer (2001). This study demonstrated a significant positive correlation between ring-width and mean July and August temperatures recorded at the local climate station at Andenes, although winter temperatures also seem to strongly modify the low-frequency growth trends (Kirchhefer, 2001).

The use of the these ring-widths, which have reasonable correlation with mean July and August temperature (Kirchhefer, 2001), in conjunction with the carbon and oxygen isotope ratios should resolve still further any ambiguities regarding temperature and precipitation signal contained within the δ^{18}C record.

3.6 Mass Spectrometry

Samples were analysed in a mass spectrometry laboratory at Swansea University. The system in operation uses an on-line (continuous flow) method of isotope analysis where an elemental analyser is harnessed to an isotope mass spectrometer (Preston and Owens, 1985), which has proved to be a considerable advance for isotope-dendroclimatology over traditional off-line techniques where each sample had to be prepared for analysis individually and perhaps 20 or 30 samples could be analysed in a batch. In the on-line method around 200 samples can be analysed over a 24 hour period (Switsur and Waterhouse, 1998).

3.6.1 On-line carbon isotope analysis

Once the cellulose samples have been weighed out in tin capsules these are loaded into a computer controlled carousel which drops individual samples into a furnace contained within the elemental analyser, which is heated to between 1000 and 1100°C. A pulse of oxygen is admitted with the sample to aid combustion and the products carried in a stream of helium through a silica column packed with reagents, which are typically chromium oxide and copper oxide. These act as further oxygen sources ensuring total

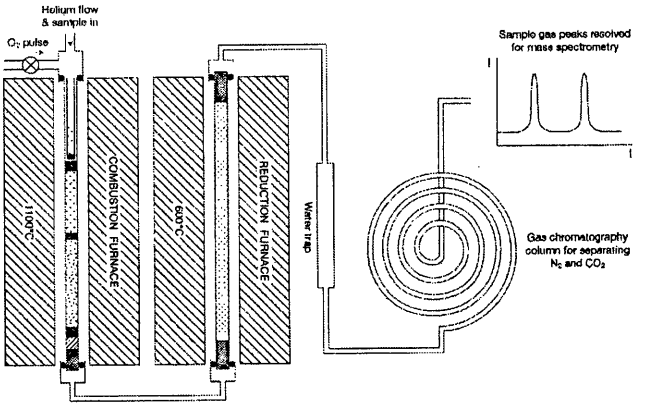

Figure 3.9: Schematic of elemental analyser setup for online $\delta^{13}C$ analysis (McCarroll and Loader, 2006)

combustion so that the carbon in the sample is completely oxidised to CO_2. The sample gas now consists of CO_2, nitrogen oxides and water vapour. Some of the oxides of nitrogen (N_2O and NO_2) could potentially corrupt the precise measurement of the stable carbon isotope ratios contained within the CO_2 and so they are reduced to nitrogen gas in a second furnace heated to 600° over copper. The water vapour is then removed in a chemical water trap containing magnesium perchlorate. The sample is then separated into CO_2 and N_2 in a gas chromatography column (see Figure 3.9).

The sample gas then enters the mass spectrometer to determine its $\delta^{13}C$ ratio. From entering the elemental analyser to producing an isotope result takes between 8 and 12 minutes, depending on current machine settings.

3.6.2 On-line oxygen isotope analysis

Methods for on-line oxygen isotope analysis of organic matter have been under development for some years (Santrock and Hayes, 1987; Werner et al., 1996; Werner, 2003;

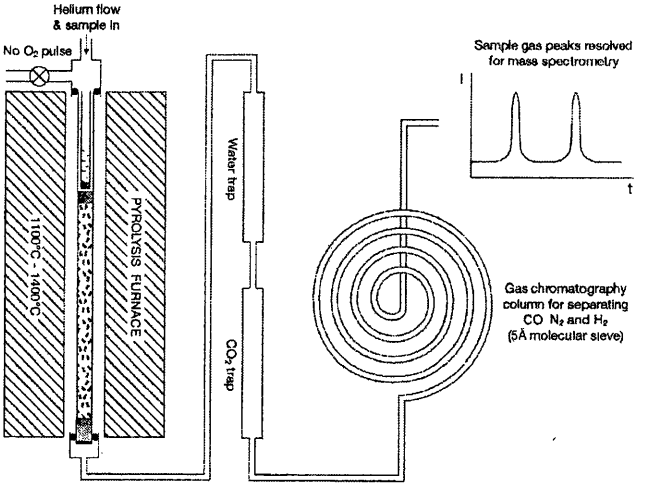

Figure 3.10: Schematic of elemental analyser setup for 'online' $\delta^{18}O$ analysis (McCarroll and Loader, 2006)

Saurer et al., 1998b; Loader and Buhay, 1999; Farquhar et al., 1997) with Santrock and Hayes (1987) probably being the first to measure $\delta^{18}O$ using a continuous-flow method (Saurer and Siegwolf, 2004). Samples are weighed out into silver capsules at between 0.3 and 0.35 mg. Once loaded into a carousel which delivers the samples into a quartz, ceramic or glassy carbon reaction tube heated to around 1000°C, the samples are pyrolised over glassy or nickelised carbon (McCarroll and Loader, 2006). The product gases of this combustion, which are carried on a flow of dry helium, are for cellulose CO and H_2 along with traces of CO_2 and water vapour which are removed in chemical traps containing magnesium perchlorate and ascarite (see Figure 3.10). The CO and N_2 gases are resolved into separate peaks in the gas chromatography column using a 5Å molecular sieve (Figure 3.10). The sample gases then pass into the mass spectrometer for isotopic analysis. On-line $\delta^{18}O$ measurement is generally considered rather more problematic than on-line $\delta^{13}C$ measurement and there are a number of problems which must be considered. The 'blank problem' or 'background problem' occurs where the introduced carbon can react with the reaction tube walls, resulting in the production of non-sample derived CO (Saurer and Siegwolf, 2004). The 'memory effect', involves the contamination of a sample with oxygen from the previous run, caused by the incomplete conversion of the

previous sample's oxygen to CO. However, these problems are generally resolvable with care (Saurer and Siegwolf, 2004). Recently work by Leuenberger and Filot (2007) suggests that lower temperature systems, such as the one currently in operation at Swansea University at around 1000°C may not be hot enough for quantitative conversion into CO, leading to further fractionation and although this can be accounted for by reference to the standard material, temperatures of around 1450°C should ideally be used to come as close as possible to the theoretical conversion rate and minimise fractionation during the reaction.

4

Data Sets and Analytical Stratergy

4.1 Data Sets

This chapter introduces the full stable isotope and climate data sets used for climate reconstruction in this thesis. It also outlines the analytical strategy used to produce climate reconstruction.

4.1.1 δ^{13}C Data Set

δ^{13}C data are available back as far as AD 1300, but only after AD 1394 are results for four simultaneous trees available. This number has been found to be sufficient for climate reconstruction (Robertson et al., 1997b; McCarroll and Pawellek, 1998), and is the minimum number considered for climatic reconstruction in this thesis. The δ^{13}C data set used in this thesis dates from AD 1394 to 2001. Raw $\delta^{13}C_{raw}$ results for individual trees can be seen in Figure 4.1. While, Figure 4.2 shows the mean $\delta^{13}C_{raw}$ for each year value with 95% confidence intervals.

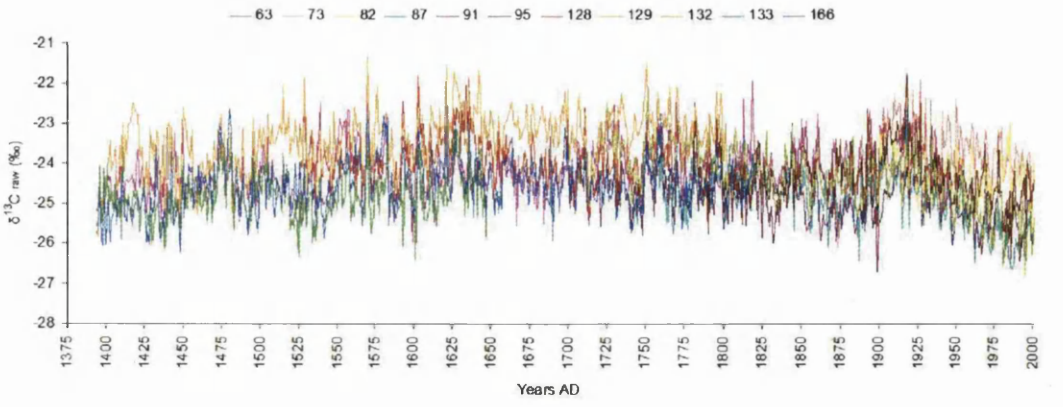

Figure 4.1: Raw $\delta^{13}C_{raw}(‰)$ results from AD 1394 to 2001. Individual trees shown in different colours and numbered.

The procedures for analyzing these data (Figures 4.1 and 4.2) are outlined in Section 4.2. Raw $\delta^{13}C_{raw}$ data are available in tabulated form in Appendix A.6.

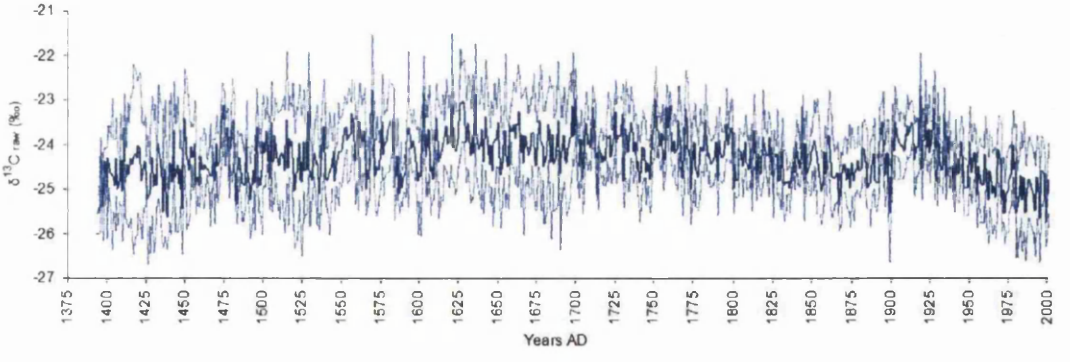

Figure 4.2: Raw mean $\delta^{13}C_{raw}(‰)$ values from AD 1394-2001 with 95% confidence limits around the mean value.

4.1.2 δ^{18}O Data Set

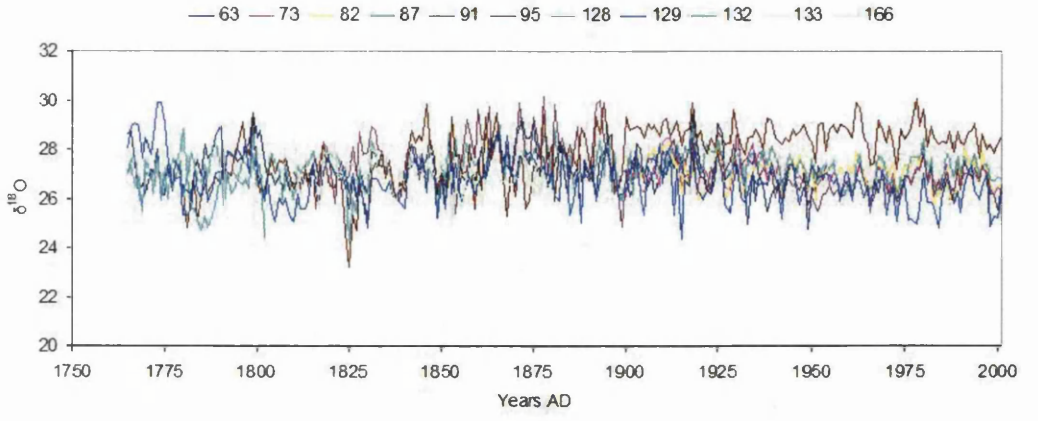

Figure 4.3: Raw δ^{18}O(‰) results from AD 1765 to 2001. Individual trees shown in different colours and numbered.

At the time of writing the δ^{18}O data available extends as far back as AD 1700, but only after AD 1765 are four simultaneous trees available in the time series. As mentioned in Section 4.1.1, this is the minimum number considered sufficient for climatic reconstruction in this thesis. Figure 4.3 shows the δ^{18}O values for individual trees and figure 4.4 shows the mean δ^{18}O value with 95% confidence intervals. The procedures for analysing these data are outlined in Section 4.2. Raw δ^{18}O data are available in tabulated form in Appendix A.7.

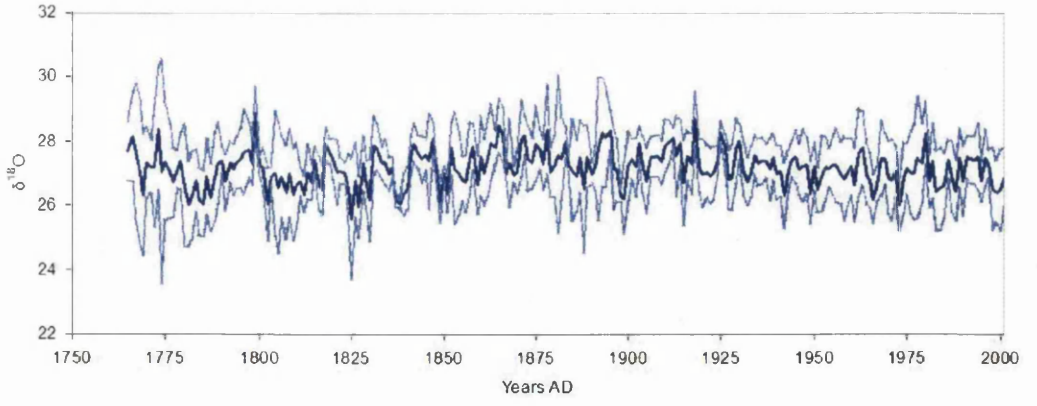

Figure 4.4: Mean $\delta^{18}O(‰)$ values from AD 1765-2001 with 95% confidence limits around the mean value.

4.1.3 Climate data sets

Three climate data sets are used for climate calibration in this thesis.

4.1.3.1 Andenes

The nearest meterological station to the field site at Forfjorddalen is Andenes. Andenes (Figure 2.1) lies at the northern tip of the Vesterålen archipelago (69°18'N and 16°09'E), ~60 km north-east of Forfjorddalen. Monthly mean temperatures from this station are available back to AD 1868 (Appendix A.1). Monthly mean precipitation data are available from AD 1910 (Appendix A.2).

4.1.3.2 Northern coastal composite

This composite standardised record of meteorological data for selected stations between the Polar Circle and Northern Cape are also be used for calibration. Data for the Andenes station are not included in this record. Monthly mean data are available for temperature from AD 1875-1997 (Hanssen-Bauer and Nordli, 1998) and precipitation from AD 1873-1997 (Hanssen-Bauer and Føland, 1998). Monthly values for temperature can be found in Appendix A.4 and for precipitation in Appendix A.5.

4.1.3.3 Tornedalen

One of the longest meteorological temperature records for Fennoscandia is the composite record from the Tornedalen area of subarctic Sweden (around 66°N, 24°E) published by Klingbjer and Moberg (2003). The Tornedalen area is ~450 km distant from Forfjord-dalen and on the other side of the Scandes mountain range. Stretching back to AD 1802 the Tornedalen record is a combination of continuous meteorological data from the Haparanda synoptic weather station from August AD 1859 combined with observational data from AD 1802 to 1862, the overlapping period being used to adjust the observational data to the Haparanda data (Klingbjer and Moberg, 2003). Klingbjer and Moberg (2003) believe the data to be reliable back to AD 1832, prior to which especially summer temperatures (June to August) are considered less reliable. Mean annual temperature are considered realistic to the beginning of the series. Monthly mean temperature data for Tornedalen can be found in Appendix A.3.

4.2 Analytical Strategy

4.2.1 Data correction

In Chapter 5 raw $\delta^{13}C$ values are corrected for increases in atmospheric ^{12}C ($\delta^{13}C_{cor}$) and CO_2 ($\delta^{13}C_{pin}$). Increases in atmospheric ^{12}C during the industrial period (since *c.* AD 1850) have led directly to a decline in $\delta^{13}C$ in tree rings (McCarroll and Loader, 2004). As this decline is not related to climate it must be corrected prior to climate calibration. Increases in atmospheric CO_2 have also been linked to a decline in $\delta^{13}C$ in tree rings (Treydte et al., 2001) . A new logically constrained correction procedure proposed by McCarroll et al. (2007) is used to correct this decline in $\delta^{13}C$. $\delta^{18}O$ values from tree rings require no correction prior to climate calibration (McCarroll and Loader, 2004).

The $\delta^{13}C_{pin}$ and $\delta^{18}O$ results seen in Figures 4.1 and 4.3 exhibit considerable between tree variability. To prevent offsets in the mean value, as trees drop out or are introduced into

the sequence, an adjustments or shift towards the mean value are made. This procedure is carried out on the individual trees using common periods (Chapter 5).

4.2.2 Climate Calibration

The relationship between both mean $\delta^{13}C_{pin}$ and $\delta^{18}O$ and available climatic variables are explored using correlation techniques. The climatic variables and temporal periods most strongly statistically linked with each stable isotope are then calibrated. This calibration procedure employs a split data set technique and are verified using reduction of error (RE) and co-efficient of efficiency (CE) statistics. Climate data from Andenes, Tornedalen and the regional Northern Coastal data sets are used for these calibrations. Climate calibration are is also guided by stable isotope theory. Therefore, calibration and climate reconstruction is only undertaken where there is a sound theoretical understanding of the climate/stable isotope relationship.

4.2.3 Multiproxy Dendroclimatology

A conceptual model exploring the relationships between stable isotopes ($\delta^{13}C_{pin}$ and $\delta^{18}O$) and the available climatic variables (temperature and precipitation) is presented in Chapter 8. The models purpose is to aid in understanding of the complex relationship between stable isotopes in tree rings and climate. It also offers an explanation for a period of low correlation in between $\delta^{13}C_{pin}$ and temperature ($\sim$AD 1880-1926) and form the basis for the exclusion of this period from the calibration of $\delta^{13}C_{pin}$ and temperatureused used for climate reconstruction.

Multiple regression models are employed to determine whether two or more of the tree ring proxies available can improve upon models using single proxies. The available proxies are, ring widths, $\delta^{13}C$ and $\delta^{18}O$. All calibrations are made using split data set technique and verified using RE and CE statistics.

4.2.4 Climate reconstruction

In Chapter 9 the stable isotope/climate calibrations from Chapter 8 are used to reconstruct climate using linear regression. Due to data availability reconstructions based upon $\delta^{13}C_{pin}$ extend from AD 1394 to 2001, while those based on $\delta^{18}O$ extend from AD 1765 to 2001. Error estimates will be calculated using 2 standard errors of prediction.

Temperature reconstructions are compared too: the long temperature record from Uppsala (Moberg and Bergström, 1997), beginning AD 1722; a recent tree ring density based reconstruction from Torneträsk (Grudd, 2008); and the existing ring width based reconstruction from Forfjorddalen (Kirchhefer, 2001).

The regional temperature and precipitation signals contained within the Forfjorddalen data are explored, using correlation maps (KNMI, 2008) produced with gridded climate data (CRU, 2008).

5

δ^{13}C Corrections

5.1 Introduction

Prior to calibration with climate two corrections will be made to the δ^{13}C data over the industrial period (from AD 1850). The first in section 5.2 is a correction for changes in $\delta^{13}C_{air}$ caused by the burning of fossil carbon of organic origin. The second in section 5.3 is a correction proposed by McCarroll et al. (2007) to account for the response of trees to increased concentration of CO_2 in the atmosphere. Once these corrections have been made variability in the isotope data will be discussed and standardised in section 5.4. Finally a measure of the common signal between the trees in the calibration data set will be made in Section 5.5. Raw δ^{13}C data for all trees can be seen in Figures 5.1 and 5.2.

5.2 Correction for Atmospheric Decline in the Ratio of δ^{13}C

The burning of fossil fuels associated with with rise of industrialisation since the nineteenth century has released increasingly large amounts of isotopically light CO_2 in to the

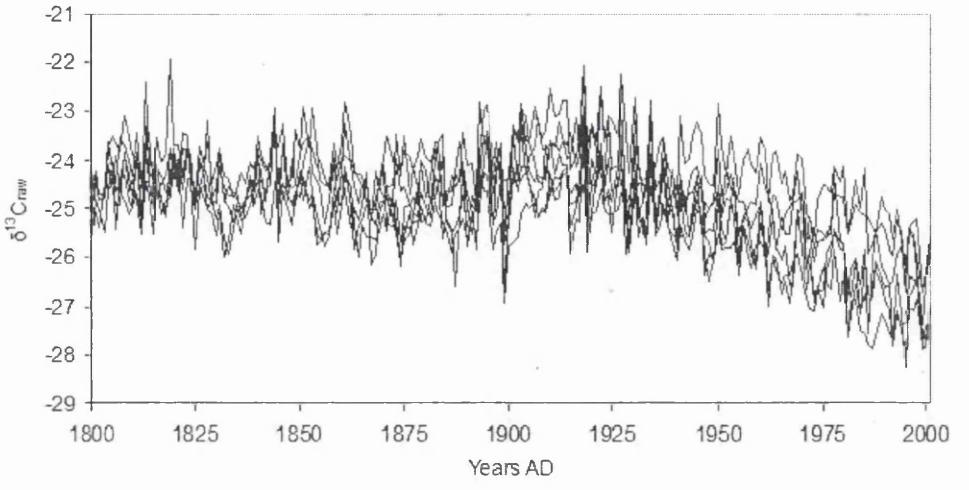

Figure 5.1: Raw $\delta^{13}C_{raw}$ (‰) results for all trees from AD 1800-2001

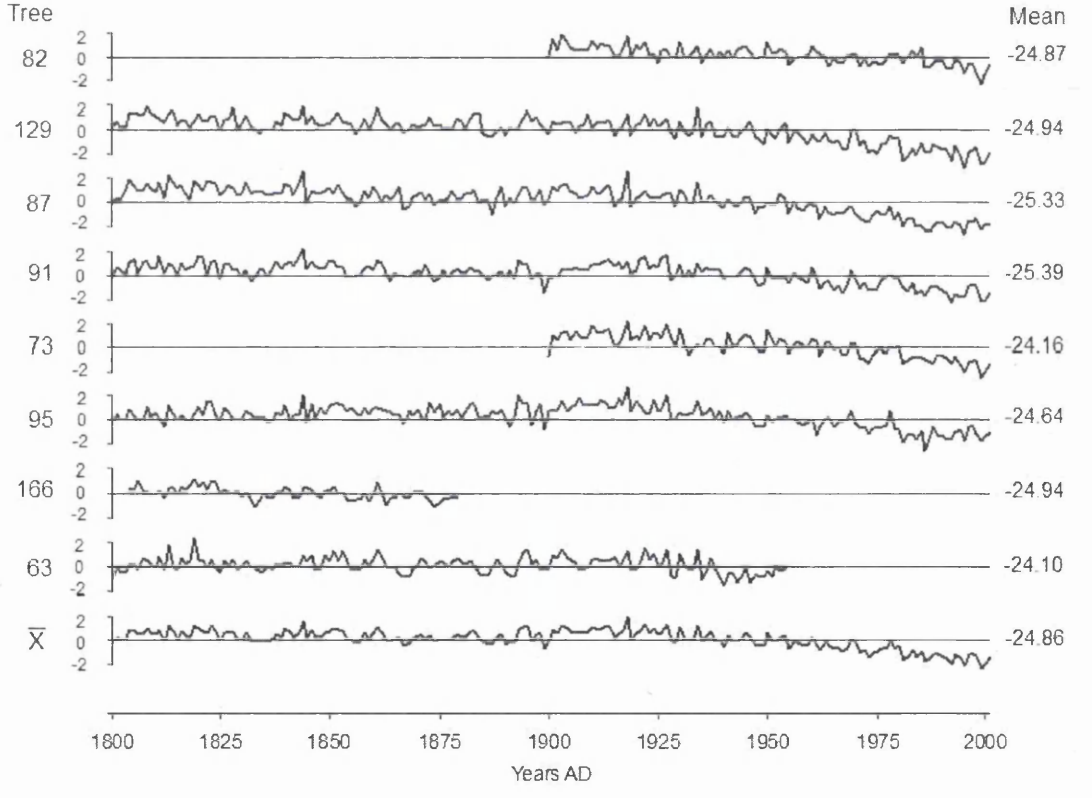

Figure 5.2: Uncorrected $\delta^{13}C_{raw}$ (‰) for individual trees and for the mean of all trees from Forfjorddalen.

atmosphere. As these fossil fuels have an organic origin the carbon captured in them has already been through the fractionation processes described in Section 3.5.1 and so are depleted in the heavier ^{13}C isotope. Since the onset of industrialisation the δ^{13}C value of atmospheric CO_2 has declined by more than 1.5‰. This decline can be seen in the raw δ^{13}C values from the tree-rings at Forfjorddalen in Figure 5.1 and is especially pronounced in the second half of the twentieth century. This atmospheric decline (Suess effect) must be removed before any comparison with climate data can be made (McCarroll and Loader, 2004, 2006).

Removal of this decline in δ^{13}C values can be approached in a number of ways. One simple method would be to statistically de-trend the data series by fitting a line or curve and adding or subtracting the individual years isotope values from this line, much as is done in tree-ring width studies to remove growth trends. This is however a most unsatisfactory way to proceed (McCarroll and Loader, 2006). This method would indeed remove the industrial decline in the δ^{13}C values but it would also remove other long term trends that might be present in these data, keeping only the trends at around the decadal scale. This may lead to the removal any low frequency signals such as: changes in tree response to such elevated levels of CO_2; and any evidence for global warming. As this period will also be used as the calibration period for past climatic reconstruction removing any low frequency trends in the calibration set would have a severely detrimental effect on past low frequency climate reconstruction. Statistical de-trending should therefore be avoided.

To remove this industrial decline, without recourse to statistical de-trending an annually resolved record of the δ^{13}C ratio in the atmosphere is required. Ice cores contain a long record of atmospheric CO_2 and in recent years these have been supplemented by air samples. The data is, however, incomplete and subject to considerable scatter (Keeling et al., 1979; Mook et al., 1983). In terms of palaeoclimatic research it is helpful to compare results from different studies, and desirable to combine such results to reconstruct larger scale and even hemispheric and global changes. To achieve this results should be comparable and so it would useful if a common data set, and method, were used.

McCarroll and Loader (2004) propose such a common data set based on an extrapolation of a high-precision ice-core record from the Antarctic (Francey et al., 1999).

The correction method, proposed by McCarroll and Loader (2004), corrects the data mathematically to a pre-industrial standard value. This is simply achieved by adding the difference between the atmospheric value and the standard value for each year to that years δ^{13}C value. McCarroll and Loader (2004) propose standard pre-industrial value for the δ^{13}Cof the atmosphere of -6.4‰, which is close to values at AD 1850 and prior to the Little Ice Age (Francey et al., 1999). The correction is made using Equation 5.1, tabulated values for $\delta^{13}C_{air}$ are available in McCarroll and Loader (2004, 2006). This is the method employed in this thesis, with this additive correction being made for every year from AD 1850 using the correction factors in McCarroll and Loader (2004). The correction for each tree is carried out individually (see Figure 5.7a), the mean of these corrected δ^{13}C results can be seen in Figure 5.3 which shows δ^{13}C corrected for the atmospheric decline in ^{13}C ($\delta^{13}C_{cor}$).

$$\delta^{13}C_{cor} = \delta^{13}C_{plant} - (\delta^{13}C_{air} + 6.4) \tag{5.1}$$

Comparing Figures 5.1 and 5.3 it can be seen that a considerable proportion of the decline in δ^{13}C values throughout the twentieth century has been removed. However, there remains a declining trend in δ^{13}C values over much of the twentieth century. This trend is not uncommon in δ^{13}C values from tree-ring series (Treydte et al., 2001), and will be discussed and corrected for in Section 5.3.

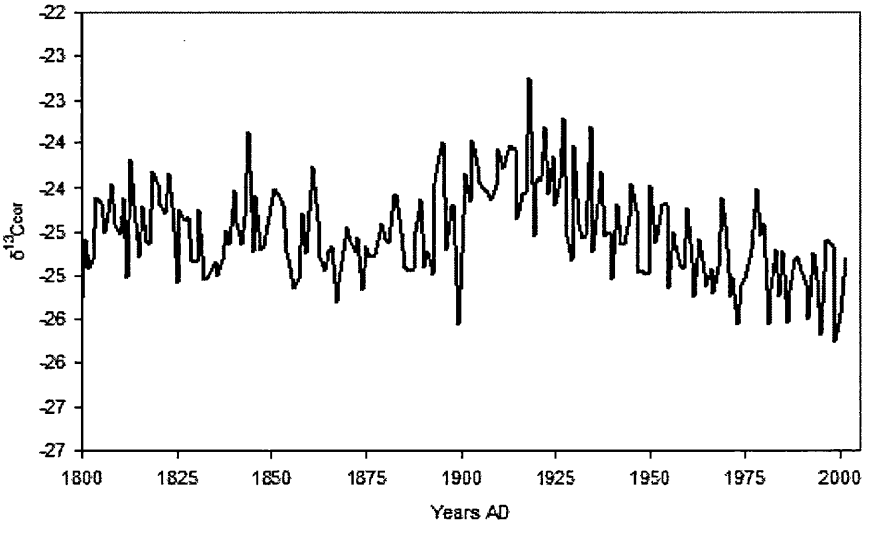

Figure 5.3: Mean Forfjorddalen δ^{13}C(‰) ratios corrected for the atmospheric decline in δ^{13}C(‰) ratios of atmospheric CO_2.

5.3 Correction for Changes in the CO_2 Content of the Atmosphere

Once a correction for the Suess effect has been applied many trees still exhibit a decline in δ^{13}C values during the industrial period which seems unrelated to climate causes (Treydte et al., 2001) and may be attributable to changes in the CO_2 content of the atmosphere (McCarroll et al., 2007). The δ^{13}C values from Forfjorddalen also exhibit this continued decline after the correction for the atmospheric decline in the ratio of ^{13}C outlined in Section 5.2 has been made (see Figure 5.3). There is at Forfjorddalen, however, a climatic mechanism which could be responsible for this decline in $\delta^{13}C_{cor}$ values and this is the apparent increase in precipitation during the twentieth century (see Figure 5.4), which may be part of a more general trend of increasing wetness over recent decades in Scandinavia (Hanssen-Bauer and Føland, 1998; Tuomenvirta et al., 2000; Busuioc et al., 2001; Linderholm and Chen, 2005). It is then possible that the decline in $\delta^{13}C_{cor}$ values could be as a result of this increase in precipitation and/or the increase in atmospheric CO_2 concentrations. This is a question which will be addressed

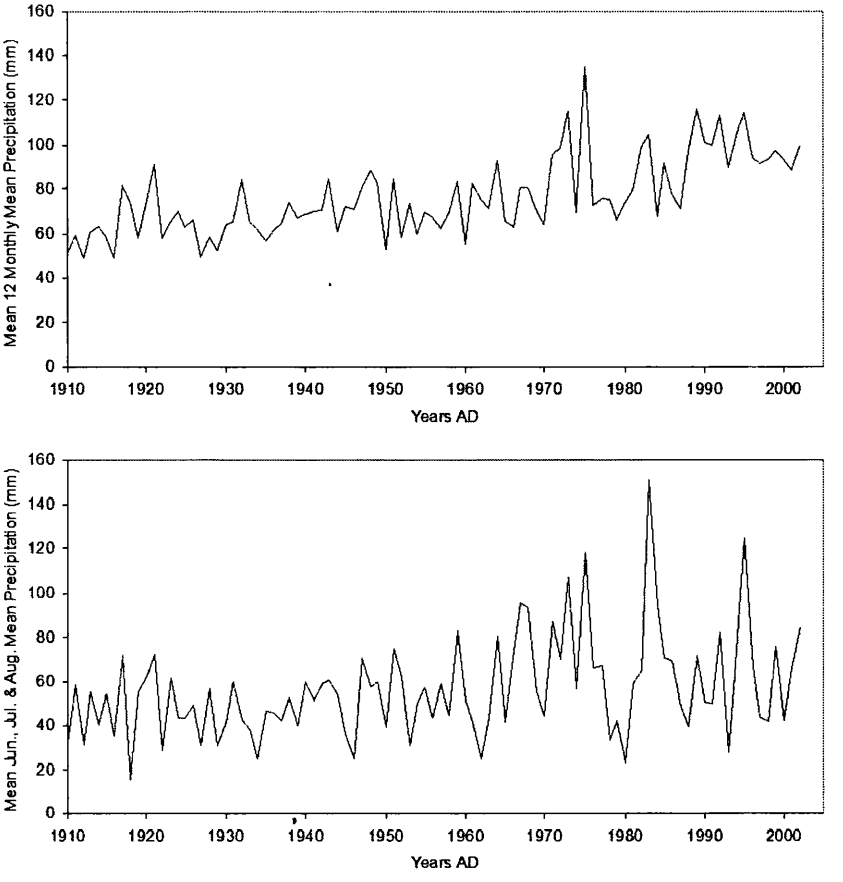

Figure 5.4: Precipitation from Andenes. Mean annual (top) and mean of June, July and August (bottom).

as the correction procedure unfolds.

There is a growing body of work on changes in trees' physiological response to increased CO_2 concentrations in the atmosphere (Feng and Epstein, 1995a; Marshall and Monserud, 1996; Feng, 1998, 1999; Krishnamurthy and Machavaram, 2000; Waterhouse et al., 2004). It has therefore been suggested that a correction should be made that accounts for the response of trees to increasing atmospheric CO_2 concentrations (Treydte et al., 2001; McCarroll et al., 2007). The approach that is usually taken is to add a standard value to δ^{13}C per unit increase in the CO_2 concentration of the atmosphere (*ca*). Values

ranging from 0.007‰ to 0.02‰ have been proposed (Feng and Epstein, 1995a; Treydte et al., 2001), these figures are rather subjective and lead to very different corrections (Loader et al., 2007). This approach assumes that tree response to increasing CO_2 levels is both uniform and linear, unfortunately the opposite is often true with changes of δ^{13}C fractionation in trees as a result of increasing CO_2 being both non-linear and non-uniform (Waterhouse et al., 2004). An alternative approach proposed by McCarroll et al. (2007) is to use an objective correction based on the physiological response of trees to increased atmospheric CO_2 concentrations.

The fractionation (Δ) of carbon isotopes by trees can be described in Equation 5.2 (Farquhar et al., 1982). Here *a* and *b* are constants that represent the fractionation due to diffusion through the stomata of around 4.4‰(*a*) and carboxylation of around 27‰(*b*), c_i and c_a are intercellular and ambient CO_2 concentrations.

$$\Delta = a + (b - a) \cdot \frac{c_i}{c_a} \tag{5.2}$$

This model represents fractionation as an additive process, acting on the isotopic ratio of the source gas, so the isotopic ratio of the plant ($\delta^{13}C_{plant}$) can be expressed in Equation 5.3, using the fractionation (Δ) value obtained from Equation 5.2.

$$\delta^{13}C_{plant} = \delta^{13}C_{air} - \Delta \tag{5.3}$$

As a result of the burning of fossil fuels since industrialisation the isotopic composition of atmospheric CO_2 ($\delta^{13}C_{air}$) has changed and the isotopic ratios of tree rings ($\delta^{13}C_{plant}$) has declined. However as described in Section 5.2, a correction for this decline can be made using available $\delta^{13}C_{air}$ records of CO_2 to the pre-industrial standard value of -6.4‰($\delta^{13}C_{cor}$) using Equation 5.4 (McCarroll and Loader, 2004).

$$\delta^{13}C_{cor} = \delta^{13}C_{plant} - (\delta^{13}C_{ait} + 6.4) \tag{5.4}$$

The only non-constant factors in Equation 5.2 are c_i and c_a, intercellular and ambient

CO_2 concentrations. For most of the pre-industrial Holocene $\delta^{13}C_{air}$ has changed rather slowly (rising from 260ppm at 8K BP to 285ppm at around AD 1850), which would suggest that in terms of palaeoclimate δ^{13}C values in tree rings are a record of the internal concentrations of CO_2 or the c_i of Equation 5.2. Which, as discussed in Section 3.5.1, is controlled by the balance between stomatal conductance and photosynthetic rate. If we assume that the values available for $\delta^{13}C_{air}$ are reasonable and that changes in environmental conditions are not sufficient some or all of the remaining decline in $\delta^{13}C_{cor}$ may represent a direct response to increasing CO_2 concentrations in the atmosphere (McCarroll et al., 2007), represented by the c_a of Equation 5.2.

Two potential responses by trees to increasing c_a are possible, one passive the other active (McCarroll et al., 2007). If trees display a passive responses to increasing CO_2 concentrations (c_a), the greatest decline in $\delta^{13}C_{cor}$ will occur, as trees do not alter either their stomatal conductance or photosynthetic rate. In this situation for every incremental increase in c_a there will be an equal increase in c_i. Such a passive response to increases in c_a would then bring about the maximum increase in c_i that could be reasonably attributed to increased atmospheric CO_2 concentrations, see Figure 5.5. The example in figure 5.5 of a passive response ($c_i - c_a$) shows a tree with a pre-industrial δ^{13}C value of -23‰, which equates to a pre-industrial c_i of 154ppm given that pre-industrial values for c_a and $\delta^{13}C_{air}$ of 285ppm and -6.4‰. Such a tree would have c_i of 237ppm by AD 2000 and a δ^{13}C value of -25.35‰, assuming no influence from climatic fluctuations (McCarroll et al., 2007).

From many of the published δ^{13}C studies of tree-rings it seems clear that the decline in δ^{13}C values though the industrial period is too small to have been produced by such a passive response. In some cases the increase in c_a-c_i is sufficient to maintain an almost constant c_i/c_a, in which case the decline in the $\delta^{13}C_{plant}$ ratios can be explained by the changes in $\delta^{13}C_{air}$ and so the final $\delta^{13}C_{cor}$ exhibits no declining trend (McCarroll et al., 2007). An active response to rising atmospheric CO_2 concentrations that gives rise to

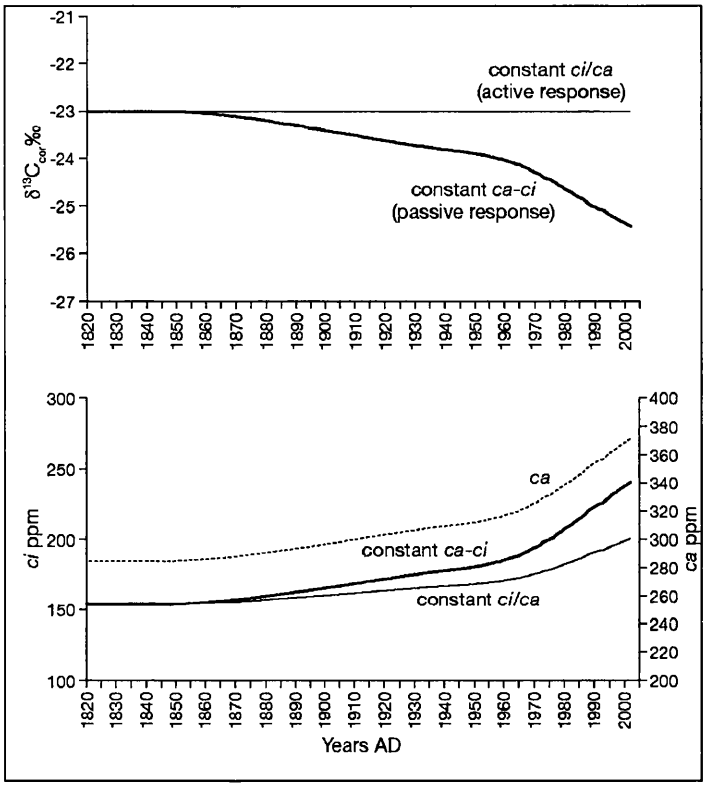

Figure 5.5: Possible tree responses to increased CO_2 concentrations (McCarroll et al., 2007)

an increase in c_i/c_a may be explicable by an improvement in a tree's water use efficiency. Water use efficiency is a measure of the water loss per unit of carbon gained (Saurer et al., 2004), which at the plant level includes respiratory losses (McCarroll et al., 2007). At the leaf level however, the potential or intrinsic water use efficiency (W_i) is proportional to c_a-c_i (Ehleringer and Cerling, 1995; Saurer et al., 2004), and can be summarised in Equation 5.5, where 1.6 represents the conductance ratio of water to CO_2.

$$W_i = \frac{(c_a - c_i)}{1.6} \tag{5.5}$$

Increased intrinsic water use efficiency may occur if there is a decrease in stomatal conductance and/or an increase in assimilation rate, both of which have been observed in experiments on plants using elevated CO_2 levels, although whether these experimental results are applicable to trees in the real world is a matter of some debate (Körner, 2003,

2006). While some trees maintain a near constant c_i/c_a through the industrial period others show a marked non-linear response to increased c_a, displaying a switch from a near constant c_i/c_a (active response) to a near constant c_a-c_i (passive response), and thus a marked decline in $\delta^{13}C_{cor}$ over recent decades (Waterhouse et al., 2004). The method proposed by McCarroll et al. (2007) to correct for this is outlined below in Section 5.3.1.

5.3.1 Correction Procedure

The aim of this correction procedure is to remove the part of any increase in c_i and therefore any decline in $\delta^{13}C_{cor}$ that is directly due to an increase in c_a, without removing any trend that may be due to climate. There are seven steps to the procedure and while a script is available to run the correction in the open source statistical program R (R.Development.Core.Team, 2006), the full correction procedure will be briefly outlined below. It includes two logical constraints to enable low-frequency climatic information to be retained while trends imparted by increasing CO_2 are removed, these can be found in Sections 5.3.1.4 and 5.3.1.5.

5.3.1.1 Calculate annual values of c_i

The annual atmospheric CO_2 concentrations for every year AD used are a composite of those provided by Robertson et al. (2001a) prior to AD 1994 and those measured at Mauna Loa for the period from AD 1994-2005. As the concern here is for annual incremental increases inCO_2 the sequence is smoothed using a locally weighted scatterplot smoother (lowess) regression line fitted with a span of 0.5, to remove any high frequency signal that may impart spurious common signal to the corrected tree-ring series (McCarroll et al., 2007).

5.3.1.2 Convert $\delta^{13}C_{cor}$ into c_i values

Tree-ring $\delta^{13}C_{cor}$ are converted to a corrected fractionation value (Δ_{cor}) and then into c_i values using Equations 5.6, 5.7 and 5.8.

$$\Delta_{cor} = -6.4 - \delta^{13}C_{cor} \tag{5.6}$$

$$c_i/c_a = \frac{(\Delta_{cor} - a)}{(b - a)} = \frac{(\Delta_{cor} - 4.4)}{22.6} \tag{5.7}$$

$$c_i = c_a \cdot \left(\frac{c_i}{c_a}\right) \tag{5.8}$$

Equations 5.6, 5.7 and 5.8 can be summarised in Equation 5.9

$$c_i = c_a \cdot \left(\frac{(-10.8 - \delta^{13}C_{cor})}{22.6}\right) \tag{5.9}$$

The values for c_i calculated in Equation 5.9 are those for tree ring wood or in this case α-cellulose, which is isotopically offset from leaf sugars (Loader et al., 2003), they are not then the true values that would have occurred in the leaf, however for the the purposes of this correction it is the trends in c_i that are important, rather than the absolute values. At the end of the correction the c_i values are re-converted to δ^{13}C values and so any offset has no effect on the correction (McCarroll et al., 2007).

5.3.1.3 Define low frequency trends in c_i as a function of c_a

Year to year high-frequency variation in c_i should be as a result of climatic variability. Low frequency trends since the on-set of the industrial period (here defined as AD 1850), can be as a result of either changes in c_a or as a result of climatic variability. Since these low-frequency trends in c_i may be non-linear a non-linear lowess regression would seem a suitable way of defining the relationship between c_i and c_a. This can be run using the R free source statistical package (R.Development.Core.Team, 2006), a span of 0.9 was found to be suitably rigid, however the correction is not sensitive to the choice of lowess span (McCarroll et al., 2007).

5.3.1.4 (First logical constraint) Define the low-frequency trends in c_i that would have occurred had c_a-c_i remained constant.

If the lowess regression line is simply used to de-trend the δ^{13}C series, it will remove any trend imparted by increasing c_a but also any trends in c_i that result from low-frequency climatic change. To avoid this two logical constraints are applied to the correction procedure. The first is that if a tree response is entirely passive then c_a-c_i will remain constant, as discussed above. It is hard to conceive a scenario, under present conditions, where water use efficiency might decline as a result of increasing atmospheric CO_2. The smoothed annual increase in c_a can be used as a logical constraint on the correction. Any increase in c_i that is equal to or less than the increase in c_a could be as a result of increased atmospheric CO_2 levels and can therefore be removed. However any increase in c_i that is greater than the annual increase in c_a cannot be as a direct result of increasing atmospheric CO_2 and should be retained. This should allow any decline in δ^{13}C values that may be as a result of cooling or a reduction in moisture stress to be retained. The annual c_a increment for year *n* is merely the smoothed value of c_a for year *n* minus the smoothed value for *n*-1 (McCarroll et al., 2007).

5.3.1.5 (Second logical constraint) Define low-frequency c_i trends that would have occurred had c_i/c_a remained constant

It is possible to calculate the incremental increases in c_i that would be required to maintain a constant c_i/c_a and therefore display no trend in $\delta^{13}C_{cor}$ values by using an average pre-industrial value for δ^{13}C. A pre-industrial mean value for δ^{13}C of -23‰, with c_a values at 285ppm, would yield a pre-industrial c_i/c_a ratio of 0.54. Equation 5.7 can be used to calculate the changes in c_i that would bring about no declining trend in $\delta^{13}C_{cor}$. If we then make the assumption that the maximum improvement in water use efficiency that a tree will make to increasing c_a is one that maintains a constant c_i/c_a, the result is that an increase in c_a can only lead to a decline in $\delta^{13}C_{cor}$ and not an increase (McCarroll et al., 2007). This seems to be a reasonable assumption, for northern Europe at least

(Saurer et al., 2004). In short this logical constraint means that an increase in c_i as a result of an increase in c_a cannot be less that that required to maintain a constant c_i/c_a, effectively preventing the removal of any long-term increase in $\delta^{13}C_{cor}$.

5.3.1.6 Correct long term-trends in c_i as a function of c_a

If the annual increments in the long-term trend of c_i as a function of c_a falls between these two logical constraints it is added to the correction (C_{pin}). If the annual increments in the long-term trend of c_i as a function of c_a falls outside either of these constraints, the excess is not added to the correction (McCarroll et al., 2007).

5.3.1.7 Calculate the pre-industrial corrected isotope ratios ($\delta^{13}C_{pin}$)

Pre-industrial corrected values for c_i ($c_{i(pin)}$) can be calculated using the difference between annual c_i values and the correction (C_{pin}). These can be converted into pre-industrial corrected fractionation (Δ_{pin}) and thus into pre-industrial corrected isotopes ratios ($\delta^{13}C_{pin}$). Assuming pre-industrial values for $\delta^{13}C_{atmos}$ of -6.4‰ and C_i values of 285ppm, the correction can be calculated using Equations 5.10, 5.11 and 5.12 (McCarroll et al., 2007).

$$c_{i(pin)} = c_i - C_{pin} \tag{5.10}$$

$$\Delta_{pin} = a + (b - a) \cdot \left(\frac{c_{i(pin)}}{285}\right) = 4.4 + 22.6 \cdot \left(\frac{c_{i(pin)}}{285}\right) \tag{5.11}$$

$$\delta^{13}C_{pin} = -6.4 - \Delta_{pin} \tag{5.12}$$

Equations 5.10, 5.11 and 5.12 can be summarised in Equation 5.13.

$$\delta^{13}C_{pin} = -10.8 - \left(22.6 \cdot \frac{(c_i - C_{pin})}{285}\right) \tag{5.13}$$

The results of Equation 5.13, in theory, should be $\delta^{13}C_{pin}$ values which would be equivalent to those obtained under pre-industrial conditions with $\delta^{13}C_{atmos}$ values at around -6.4‰ and C_i values of 285ppm. Any trends in $\delta^{13}C_{cor}$ values imparted by increases in atmospheric CO_2 (C_a) should have been removed leaving any trends that may be accounted for by changes in climate.

If the first logical constraint (Section 5.3.1.4) is regularly applied a declining trend in δ^{13}C values will endure, which can be accounted for by an increase in internal CO_2 concentrations, brought about by either an increase in stomatal conductance or a decline in photosynthetic rate, which are often associated with increasing moisture availability and/or a decline in growing season temperature. Where the second logical constraint (Section 5.3.1.5) is predominant δ^{13}C values will tend to rise suggesting a move to warmer and/or dryer conditions.

5.3.2 Application of the 'pre-industrial correction'

McCarroll et al. (2007) apply this 'pre-industrial correction' (pin correction) to three northern European δ^{13}C isotope series, including the Forfjorddalen series. At Laanila in northern Finland, where there has been no significant trend in summer temperature, relative humidity or precipitation in recent decades the pre-industrial correction was applied to seven Scots pines which had previously shown a decline, even post Suess correction, in $\delta^{13}C_{cor}$ values. However after applying the 'pre-industrial correction' this trend was removed, see Figure 5.6.

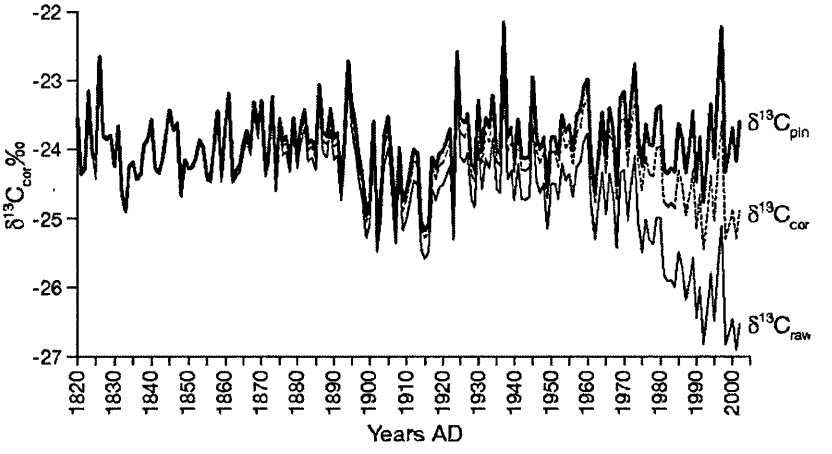

Figure 5.6: Comparison of the mean $\delta^{13}C_{raw}(‰)$, mean $\delta^{13}C_{cor}(‰)$ and mean $\delta^{13}C_{pin}(‰)$ values for seven Scots pine from Laanila in northern Finland (McCarroll et al., 2007)

As can be seen from Figure 5.6 the correction has very little effect early in the series with the majority of the decline occurring post AD 1970, (McCarroll et al., 2007) suggest that this is due to trees switching from a more active response by increasing water use efficiency up to the middle of the twentieth century (maintaining near constant c_i/c_a) to a more passive response (maintaining a constant $c_i - c_a$). The data with and without the correction applied ($\delta^{13}C_{pin}$ and $\delta^{13}C_{cor}$) were then compared to data from the local meteorological station. The correlations improved for: mean July and August temperature from r = 0.54 ($\delta^{13}C_{cor}$) to r = 0.71 ($\delta^{13}C_{pin}$); mean July and August sunshine hours from r = 0.61 to r = 0.76; and mean June to August relative humidity from r = -0.53 to r = -0.61 (McCarroll et al., 2007; Gagen et al., 2007). A test of the pin correction at this site was further undertaken by Gagen et al. (2007) who ran a calibration using the $\delta^{13}C_{pin}$ both with and without the post AD 1950 period, the results were nearly identical, demonstrating that no bias was imparted by the pin correction.

At Rovaniemi in northern Finland when the pin correction was applied to $\delta^{13}C_{cor}$ from six Scots pines it removed the declining trend from some trees but not a rising trend from others. The inter-correlation of the trees was improved, with the EPS rising from 0.84

to 0.88, and the correlation with summer relative humidity, the only significant climate parameter, rose from r = 0.57 ($\delta^{13}C_{cor}$) to r = 0.63 ($\delta^{13}C_{cor}$) (McCarroll et al., 2007).

5.3.2.1 Pre-industrial correction applied at Forfjorddalen

The uncorrected $\delta^{13}C_{raw}$ data can be seen in Figure 5.1, while Suess corrected values can be seen in Figure 5.3. The Suess correction removes much of the declining trend from the $\delta^{13}C_{raw}$ values but the $\delta^{13}C_{cor}$ values still exhibit a decline through the twentieth century. This decline may in part be linked to the increase in precipitation sshown in Figure 5.4. However, in light of the discussion above (Section 5.3) it seems likely that this decline may in part be due directly to incremental increases in c_a over the industrial period. The trend may also be linked to changes in water use efficiency and as trees move from an active to a passive response to increasing atmospheric CO_2. The correction procedure used is as outlined in Section 5.3.1 and was calculated for each tree included in the period AD 1820-2001, whether wholly or partially. The correction was calculated using the PIN package written for the free source statistical program R (R.Development.Core.Team, 2006). Figure 5.7 shows the results for individual trees and also the mean value plotted on individual axes for both the correction for changes in the isotopic ratios of CO_2 in the atmosphere (Suess correction) (a) , and the pre-industrial correction (PIN correction) (b). The mean over the period AD 1800-2001 for $\delta^{13}C_{raw}$, $\delta^{13}C_{cor}$ and $\delta^{13}C_{pin}$ can be seen in Figure 5.9 and the $\delta^{13}C_{raw}$, $\delta^{13}C_{cor}$ and $\delta^{13}C_{pin}$ for individual trees can be seen in Figure 5.8. Values are shown from AD 1800 onwards, prior to AD 1850 there is no need for any corrections and raw δ^{13}C values are used.

It is clear from both Figures 5.8 and 5.9 that the pin correction has removed most (but not all) of the decline that remained in the $\delta^{13}C_{cor}$ values. The effect of the pin correction on the δ^{13}C data can be seen in Figures 5.10 and 5.11. Figure 5.10 shows a weighted and centred 11 year running mean for $\delta^{13}C_{raw}$, $\delta^{13}C_{cor}$ and $\delta^{13}C_{pin}$ while Figure 5.11 shows the difference between the $\delta^{13}C_{cor}$ and $\delta^{13}C_{pin}$ data, by simply subtracting one

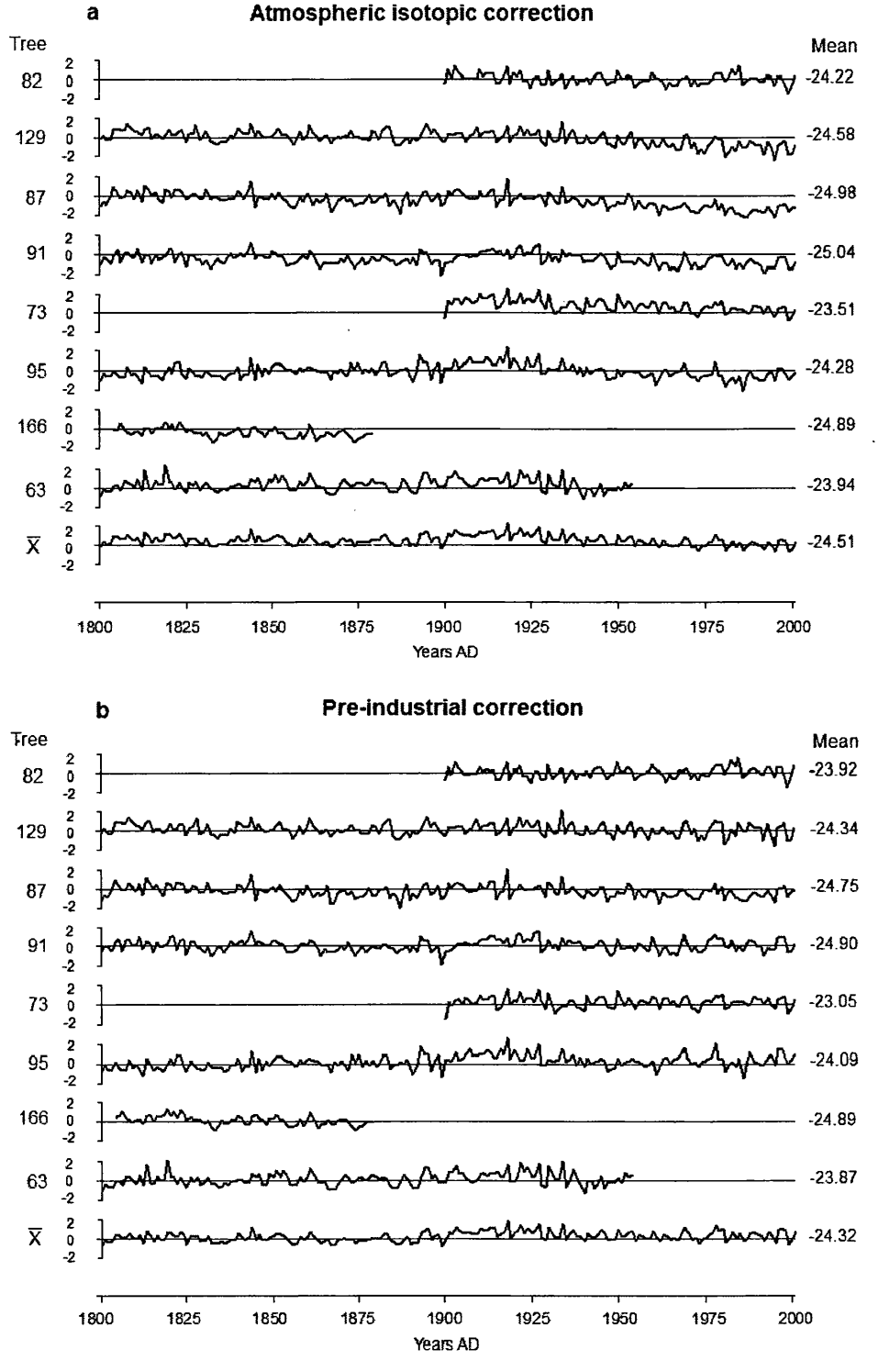

Figure 5.7: Stable carbon isotope ratios for individual trees and for the mean of all trees shown (a) after correction for changes in the isotopic ratios of CO_2 in the atmosphere (cor) , and (b) after the pre-industrial correction (pin).

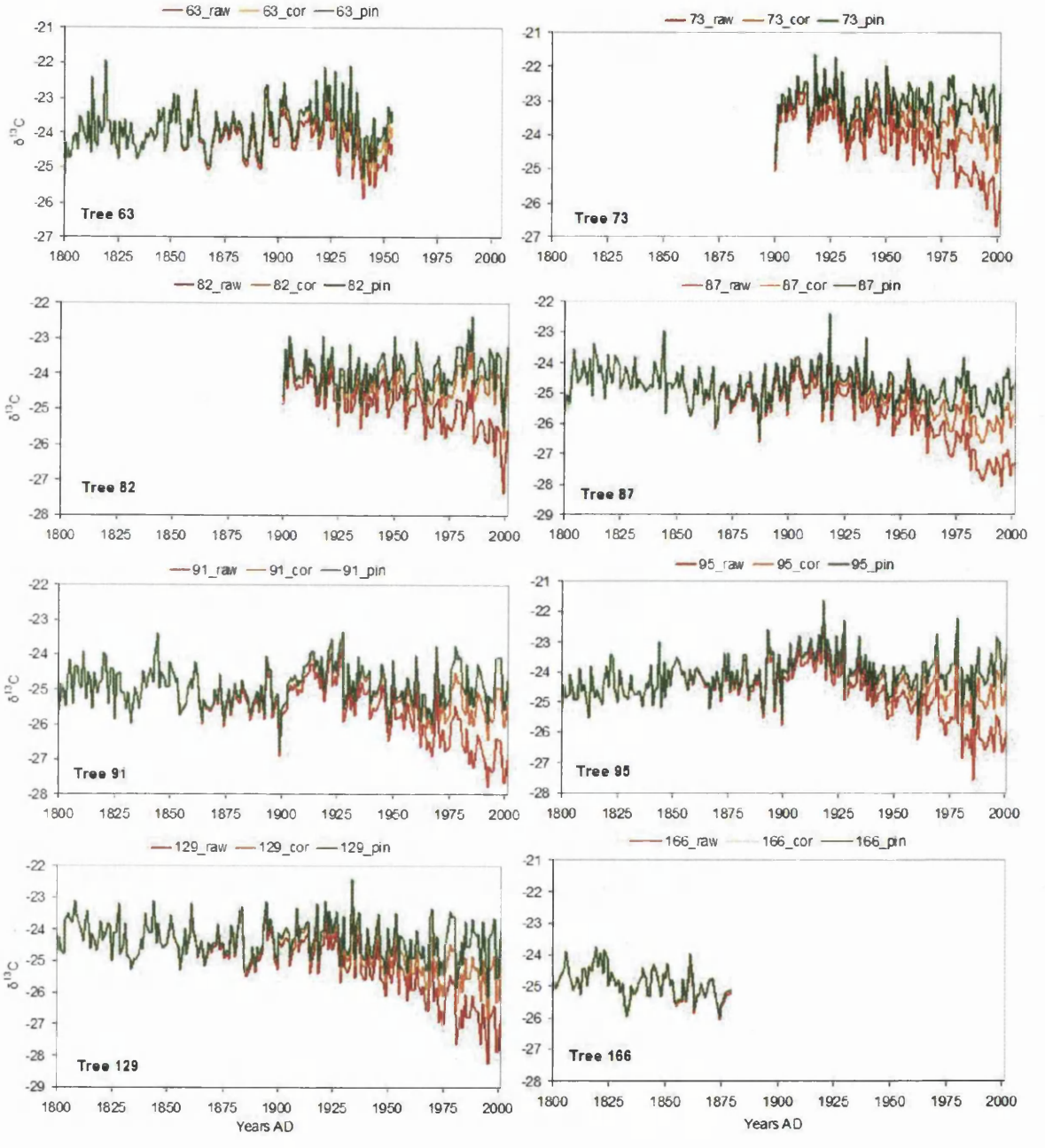

Figure 5.8: $\delta^{13}C_{raw}$, $\delta^{13}C_{cor}$ and $\delta^{13}C_{pin}$ for each individual corrected tree, for the calibration period.

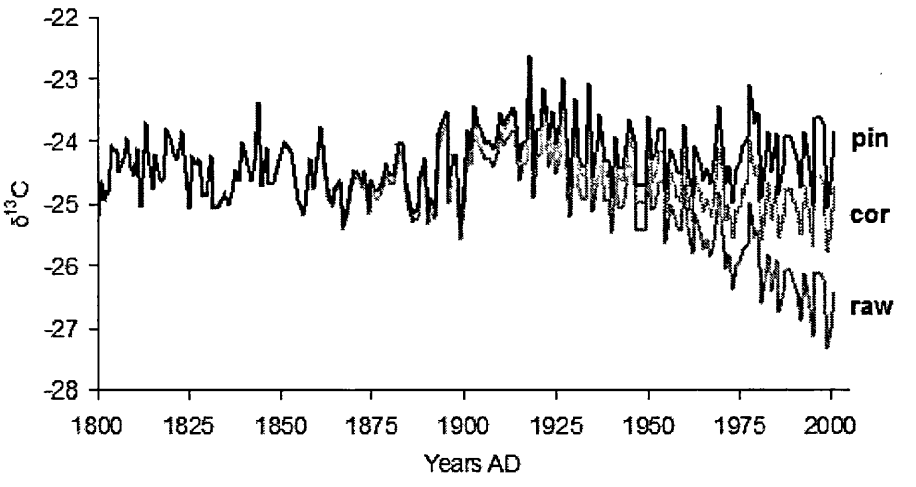

Figure 5.9: Mean of all corrected trees from AD 1800 to 2001, showing $\delta^{13}C_{raw}$, $\delta^{13}C_{cor}$ and $\delta^{13}C_{pin}$.

from the other. The PIN correction to take effect at $\sim$ AD 1900 and by the end of the sequence in 2001 the total mean divergence is just under 1.0‰. As can bee seen from Figure 5.11 nearly one third of the correction occurs up to AD 1950 two thirds between AD 1950 and 2001. Figure 5.10 shows that after a rapid rise up to about AD 1925 both the $\delta^{13}C_{cor}$ and $\delta^{13}C_{pin}$ values decline. However the $\delta^{13}C_{pin}$ values cease declining at around AD 1940, maintaining a mean δ^{13}C value of -24.25 between AD 1940 and 2001, with the maximum mean for any running 10 year period for this period of -24.03 and a minimum of -24.42. The $\delta^{13}C_{cor}$ continue to decline over this period, the mean value for the whole period being -24.83, with 10 year mean values ranging from -24.45 in the AD 1940s and -25.10 in the AD 1990s.

If the PIN correction is successful and the difference between the $\delta^{13}C_{cor}$ and $\delta^{13}C_{pin}$ values seen in Figure 5.11 are as a result of increasing atmospheric CO_2 concentrations, the remaining trends in the $\delta^{13}C_{pin}$ values should be explicable by changes in temperature and/or precipitation, this will be discussed in Chapter 6. Suffice it to say at present that there is a significant improvement in the correlation between mean July and August temperature and the $\delta^{13}C_{pin}$ values ($r = 0.47$) as opposed to the $\delta^{13}C_{cor}$ values ($r = 0.26$) for the entire period for which temperature and δ^{13}C data are both available (AD

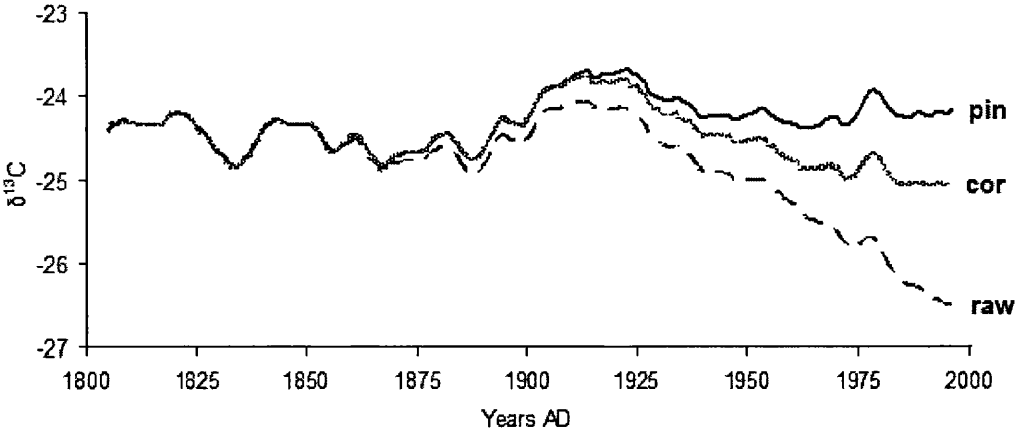

Figure 5.10: Weighted centred running 11 means of $\delta^{13}C_{raw}$, $\delta^{13}C_{cor}$ and $\delta^{13}C_{pin}$ (weighted at 1,2,3,4,5,6,5,4,3,2,1).

1867 to 2001).

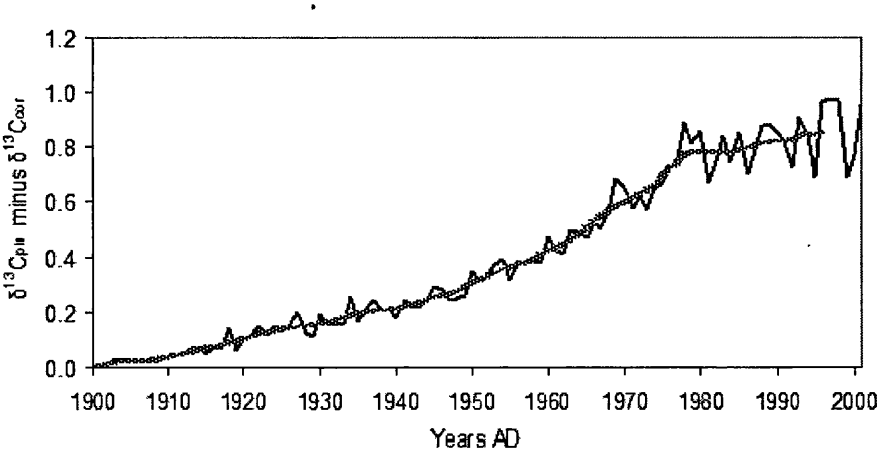

Figure 5.11: $\delta^{13}C_{pin}$ minus $\delta^{13}C_{cor}$ with a weighted centred 11 year running mean (as Figure 5.10).

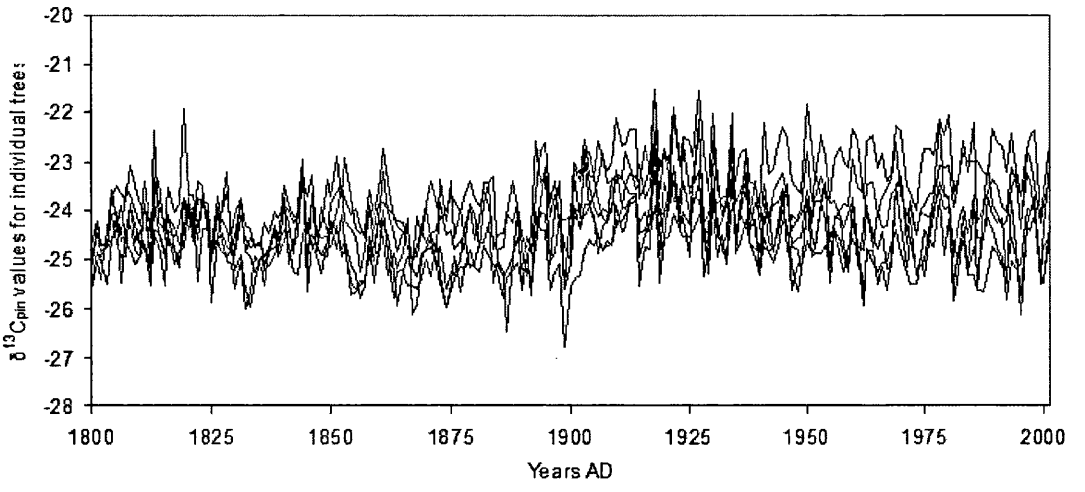

Figure 5.12: Individual $\delta^{13}C_{pin}$values from AD 1800-2001, no individual labels given as this is to indicate spread of values.

5.4 Between Tree Variability

Prior to calibrations with climate data can be undertaken the range in δ^{13}C values must be dealt with. This between tree variability in δ^{13}C is apparent Figures 5.12 and 7.9. It is important to estimate the 'true' mean value of the population of trees from the sample n, throughout the time series. This is especially important as trees enter or leave the time series, as the introduction or removal of a tree with a high or low δ^{13}C value will produce an offset in the mean series value, that has no climatic cause.

A comparison of the absolute range of values between the $\delta^{13}C_{pin}$ and $\delta^{13}C_{raw}$ was made to see if the apparent rise in the isotope variability seen in Figure 7.9 were some artifact of the PIN correction, a graph showing this comparison can be seen in Figure 5.14. The ranges are slightly diferent, so it does seem that the PIN correction increase the interannual variability between trees, especially post AD 1950 when the majority of the correction takes effect. The mean range of values for $\delta^{13}C_{pin}$ is 1.72 (and 2.16 post AD 1950), while for $\delta^{13}C_{raw}$ it is 1.68 (2.10 post AD 1950). But this only explains a small proportion of the increase in range through the series seen in Figures 7.9 and 5.14.

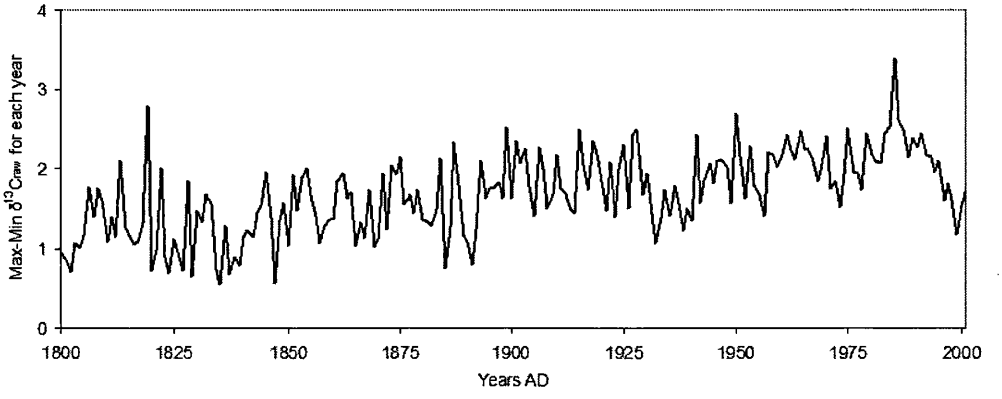

Figure 5.13: Range of values in $\delta^{13}C_{pin}$ values from AD 1800-2001, here the minimum $\delta^{13}C_{pin}$ each year is subtracted from the maximum $\delta^{13}C_{pin}$ for that year.

The phenomena off-sets in isotope ratios from tree growing at the same site under seemingly similar conditions has been noted previously for Scots pine and other tree species (McCarroll and Loader, 2004, 2006), the reasons behind it are far from clear. However it is an issue that needs to be addressed. The evidence available would seem to suggest that the offset between trees remains stable over time (McCarroll and Pawellek, 1998), beyond the juvenile phase, and this would seem to be the case at Forfjorddalen, where tree δ^{13}C values generally maintain their position relative to those of other series.

To investigate the variability of the mean values for the $\delta^{13}C_{pin}$ values 95% confidence intervals were calculated for the mean value using Equation 5.14, where σ is the sample standard deviation and n is the sample size and t is a correction factor taken from the t distribution, which is a more suitable correction for small sample sizes (< 30) than the z-score of 1.96 (for 95% confidence intervals) (McCarroll and Loader, 2006).

$$t \cdot \left(\frac{\sigma}{\sqrt{n}} \right) \tag{5.14}$$

The mean $\delta^{13}C_{pin}$ value from AD 1800 to 2001 with 95% confidence intervals plottedis

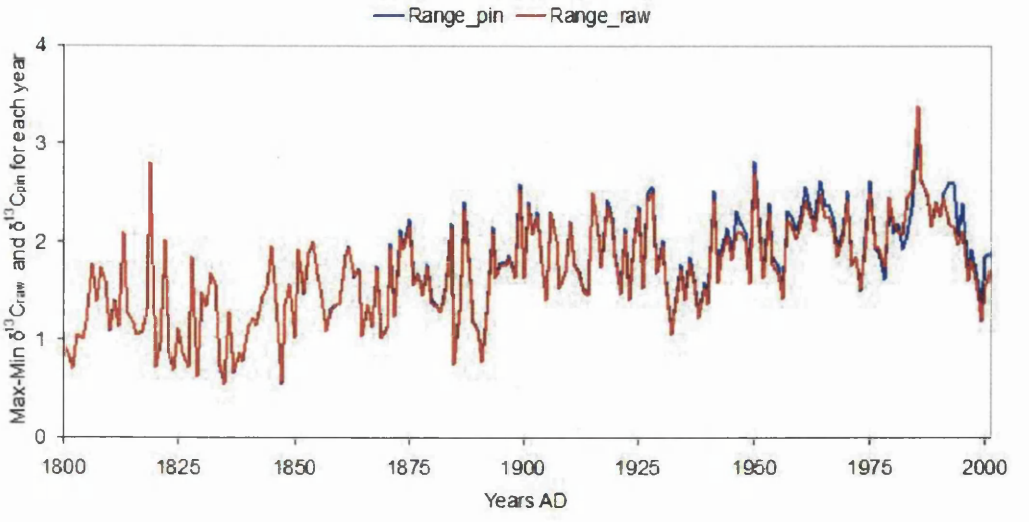

Figure 5.14: Range of values in $\delta^{13}C_{raw}$ and $\delta^{13}C_{pin}$ values from AD 1800-2001 (calculated as for Figure 5.14).

shown in Figure 5.15. Figure 7.8 shows the 95% confidence interval plotted on it own through time. It is apparent from these two figures that not only is there a degree of uncertainty surrounding the mean value but also that this uncertainly increases nearer to the present. The 95% confidence intervals start at $\sim\pm0.5‰$ in the early nineteenth century (when there are only 5 trees in the series) rising to in excess of ±0.75 at the end of the twentieth century (where there are six trees in the series). This increase in uncertainty appears to be as a result of the introduction of two trees with relatively high mean values at the strart of the twentieth century, which were not included earlier in the series (Trees 73 and 82, see Figure 5.8). It is slightly concerning that the inclusion of more trees in the mean value does not reduce the 95% confidence interval, there are in fact 7 trees in the series from AD 1900 to 1950 and the uncertainty is still higher for this period than for the early nineteenth century where there are only 5 trees for this period (see Figure 7.8). This does however illustrate the importance of removing this between tree variability so that non-climatic offsets in the mean do not occur as new trees are introduced earlier in the sequence. As the absolute values for δ^{13}C are not vital for the purposes of climatic reconstructions, shifting the isotope values should be beneficial to any climate reconstruction.

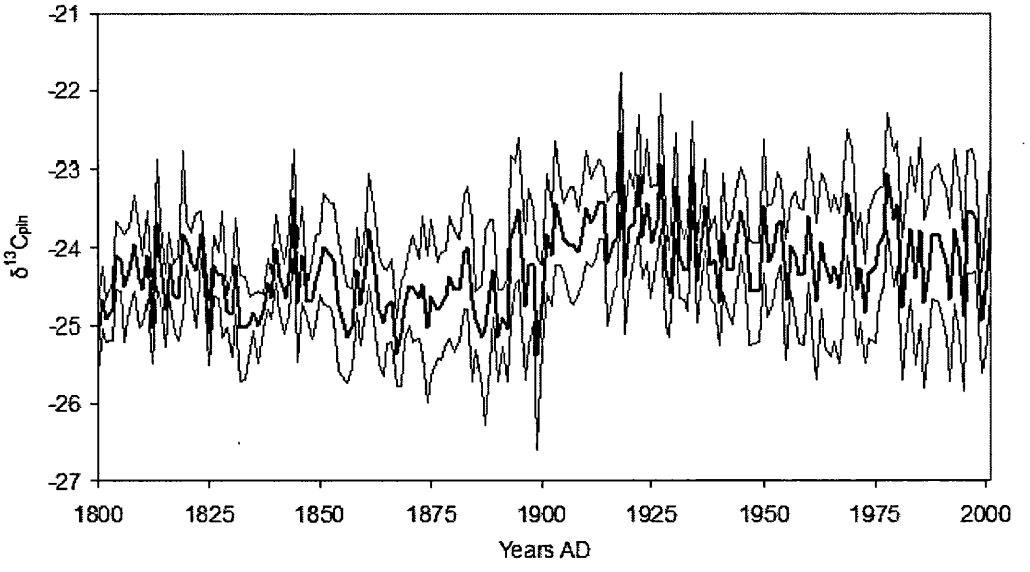

Figure 5.15: Mean $\delta^{13}C_{pin}$‰ with 95% confidence intervals

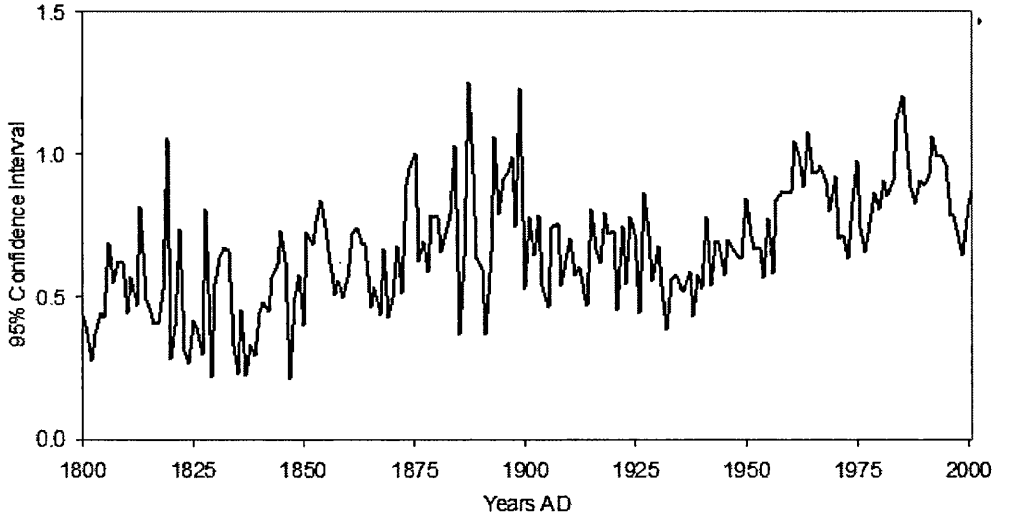

Figure 5.16: 95% confidence interval trend for $\delta^{13}C_{pin}$ (‰)

It would be a relatively simple matter to standardise all the δ^{13}C values so that they have mean of zero and a standard deviation of one. This would however have the

potentially negative effect of removing long term variations in the isotope values as trees are introduced, in effect losing the desired low-frequency climatic signals that have proved so elusive in tree-ring reconstructions (Cook et al., 1995). The method proposed here is to use the $\delta^{13}C_{pin}$ results over a common period shifted towards the mean to calibrate the entire data sets. This calculation is made using Equation 9.1, where $\bar{x}$ is the mean $\delta^{13}C_{pin}$ value for the common period $\bar{n}$ is the mean $\delta^{13}C_{pin}$ of the tree to be shifted over the common period and n is the individual $\delta^{13}C_{pin}$ value.

$$\delta^{13}C_{shift} = n - (\bar{n} - \bar{x}) \tag{5.15}$$

To determine which common period(s) to use, all the trees covering the calibration period were plotted showing their temporal overlaps in Figure 5.17. It is clear from this figure that it is not possible to use the whole period as two of the trees (73 and 82) do not begin until AD 1900 and two of the trees (166 and 63) finish before the end of the sequence. An initial common period from AD 1800 to 1879 was chosen for two reasons: firstly it is the longest sequence of continuous overlap of trees; and secondly it is very early in the industrial period and so only minor corrections have been made to the data (Figure 5.17). To correct the final two trees which do not fall into the first common period (trees 73 and 82) a second common period was chosen (see Figure 5.17) from AD 1900-1954, the choice of which was fairly straightforward as it is the longest continuous period of overlap containing both these trees. These tree were shifted by using the mean $\delta^{13}C_{shift}$ value of the tree shifted in the first common period as $\overline{x}$ value in equation 9.1 to shift the trees in the second in the second common period.

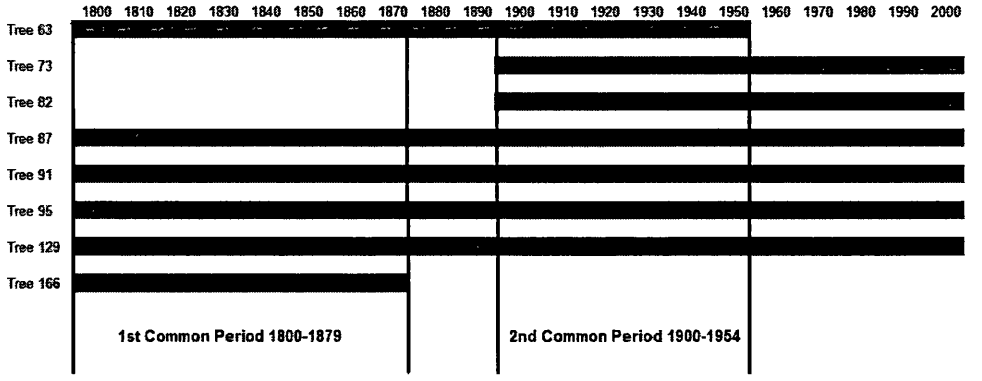

Figure 5.17: Temporal ranges of all trees for the calibration period, showing the two common periods used to shift the data.

The results of this shifting of the $\delta^{13}C_{pin}$ data can be seen in Figures 5.18 and 5.19. Figure 5.18 shows a comparison of the mean curves for $\delta^{13}C_{pin}$ and the $\delta^{13}C_{pin}$ shifted results. The overall difference to the means is relatively small ($\delta^{13}C_{pin}$, -24.26 and $\delta^{13}C_{pin}$ shifted, -24.39), with mean values for the nineteenth century almost identical and those for the twentieth century slightly depressed ($\delta^{13}C_{pin}$, -24.00 and $\delta^{13}C_{pin}$ shifted, -24.25).

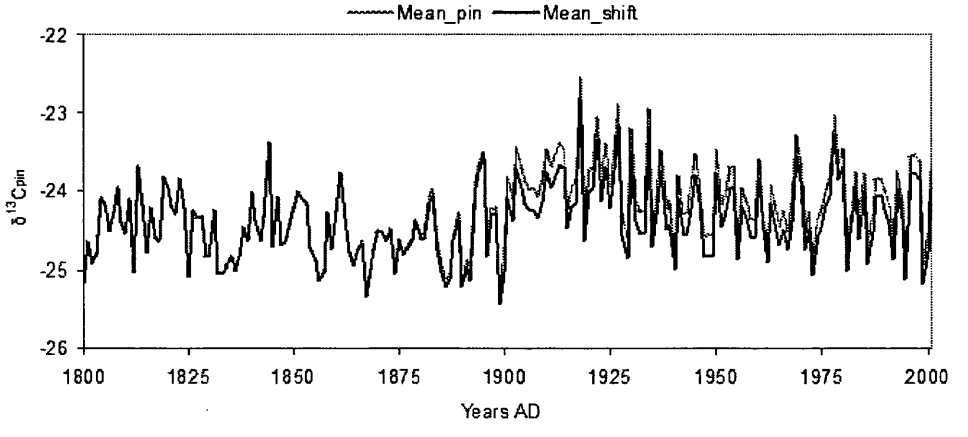

Figure 5.18: Mean results for $\delta^{13}C_{pin}$(‰) and $\delta^{13}C_{shift}$(‰) . The $\delta^{13}C_{shift}$(‰) results have been shifted towards the mean value using two common periods (AD 1800-1879 and AD 1900-1954) using Equation 9.1

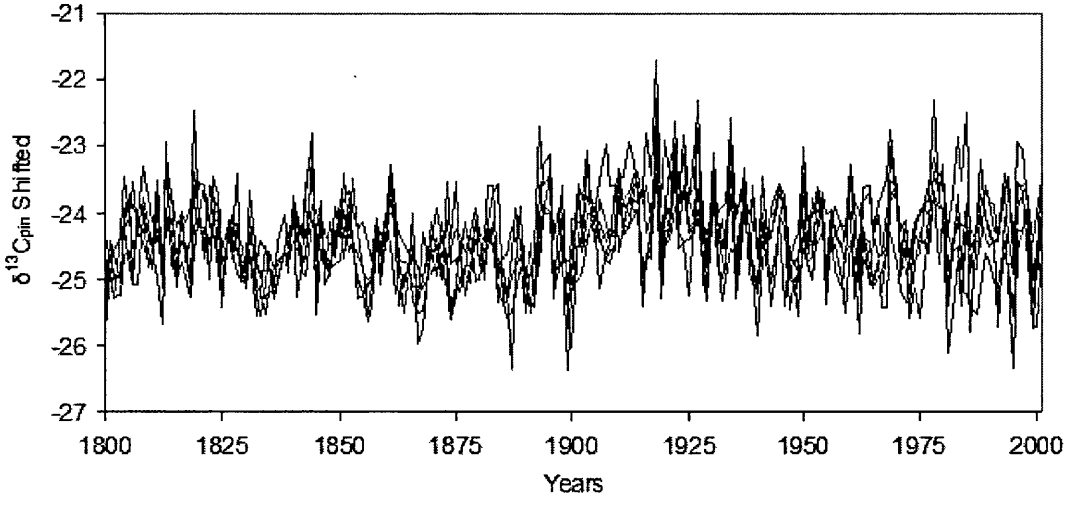

Figure 5.19: $\delta^{13}C_{pin}(‰)$ shifted results for individual trees.

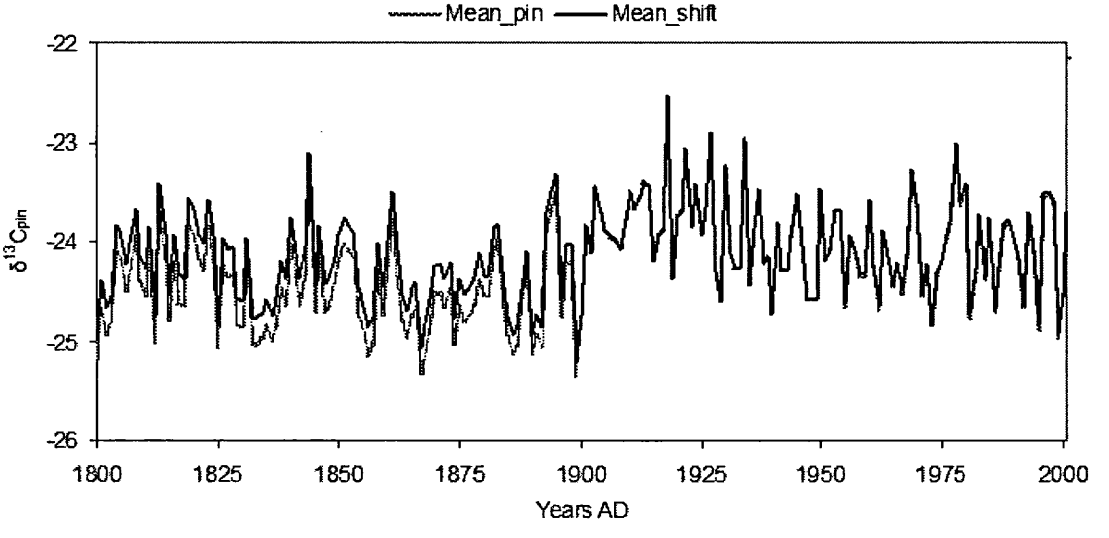

Figure 5.20: Mean results for $\delta^{13}C_{pin}(‰)$ and $\delta^{13}C_{shift}(‰)$. The $\delta^{13}C_{shift}(‰)$ results have been shifted towards the mean value using two common periods (AD 1900-1954 and AD 1800-1879) using Equation 9.1 using AD 1900-1954 as the initial common period.

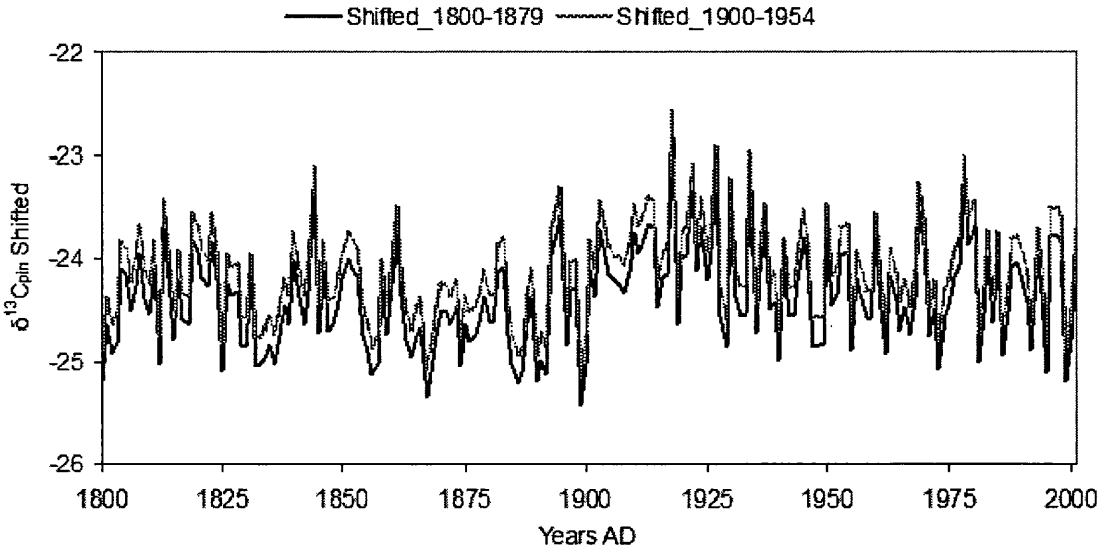

Figure 5.21: Comparison of the two $\delta^{13}C_{pin}$(‰) data shifts

To ensure that the choice of the initial common period did not bias the shifted results in some way the process was then carried out in reverse, using the original second common period (AD 1900-1954) as the initial common period and then using the period from AD 1800-1879 to shift Tree 166, the only tree not common to period AD 1900-1954 (see Figure 5.17). The results of this can be seen compared to the $\delta^{13}C_{pin}$ data in Figure 5.20 and compared to the original shift, carried out above in, Figure 5.21. This common period has produced slightly different results, there is a slight rise in the values for the nineteenth century while those for the twentieth century remain almost identical. Figure 5.21, which compares the two sets of results, shows that both initial common produce the same curve except with a constant offset of of 0.27‰ (actually 0.27 from AD 1800-1953 and 0.264 from AD 1954-2001). This difference between the two curves is probably due to the presence of two tree in the twentieth century which both have isotope values higher than the mean (Trees 73 and 82), which are not present in the nineteenth century, thus leading to a slightly higher mean figure for the period AD 1900-1944 than for AD 1800-1879. However, as mentioned above, the absolute values for $\delta^{13}C_{pin}$ are not important

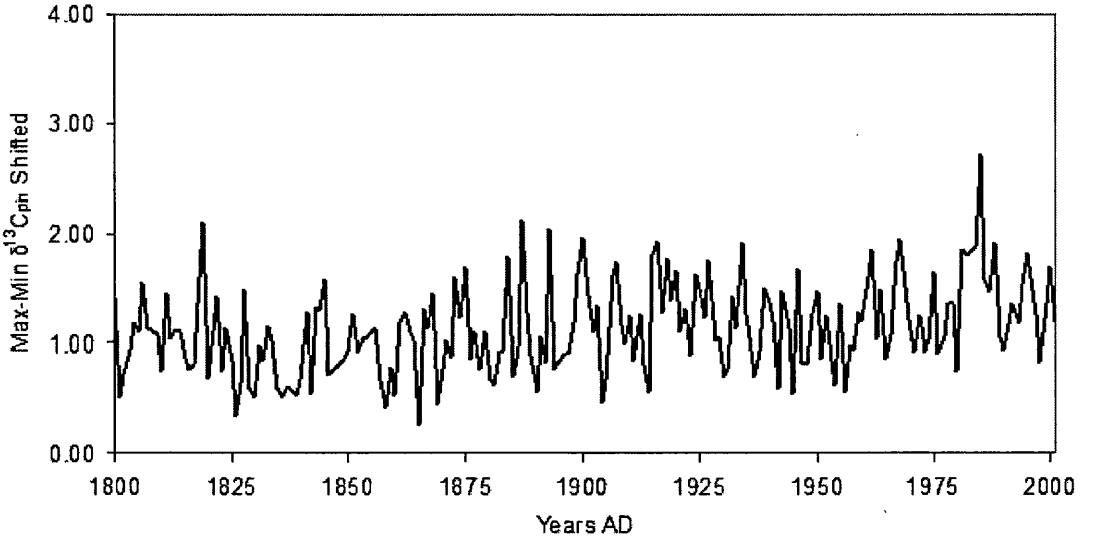

Figure 5.22: Range of $\delta^{13}C_{pin}(‰)$ shifted results (maximum $\delta^{13}C_{pin}(‰)$ for each year minus minimum)

for climatic reconstructions and so either would be suitable to use for climatic calibration, $\delta^{13}C_{pin}$ data shifted using the period AD 1800-1879 will be used (Figure 5.18).

The range in isotope values for $\delta^{13}C_{pin}$ shifted can be seen in Figure 5.22 and the data plotted with 95% confidence intervals in Figure 5.23. The 95% confidence interval plotted on its own can be seen in Figure 5.24. These figures show that shifting the data has produced a marked improvement in the range and the 95% confidence interval (compare Figures 5.22, 5.23 and 5.24 with Figures 7.9, 5.15 and 7.8). Note that the 95% confidence interval is at its widest between about AD 1875 and 1900, this is a period which we will return to in Section 5.5 and also in Chapter 5 on climate calibration. The rest of the data series (pre AD 1800) will be treated in the same manner as the period AD 1800 to 2001 and all isotope results for new trees which are introduced prior to AD 1800 will be shifted to the AD 1800-1879 period mean value using further common periods as required.

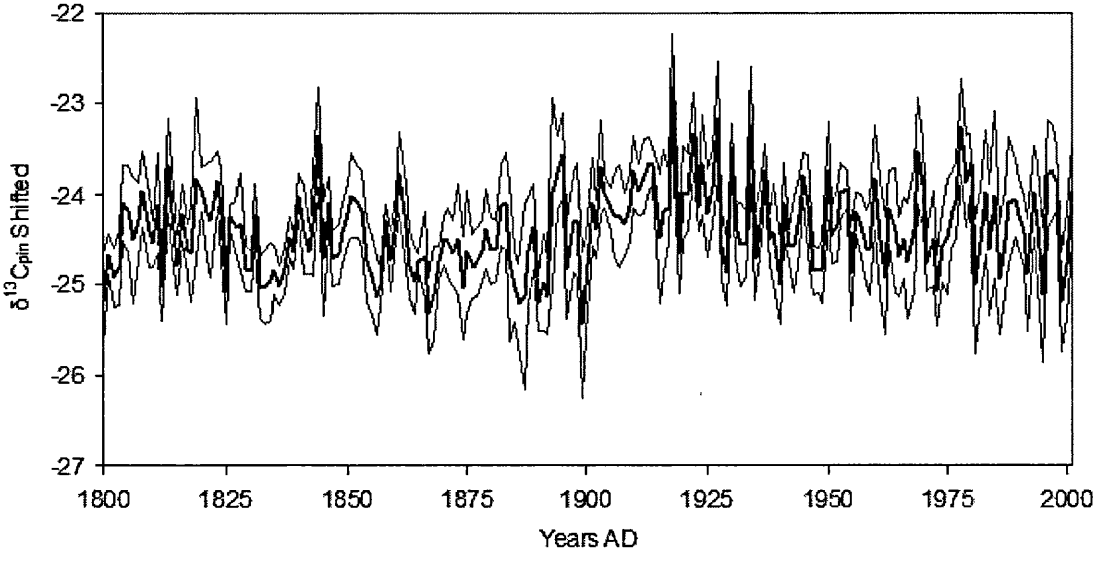

Figure 5.23: $\delta^{13}C_{pin}(‰)$ results shifted to the AD 1800-1879 common period with 95% confidence intervals

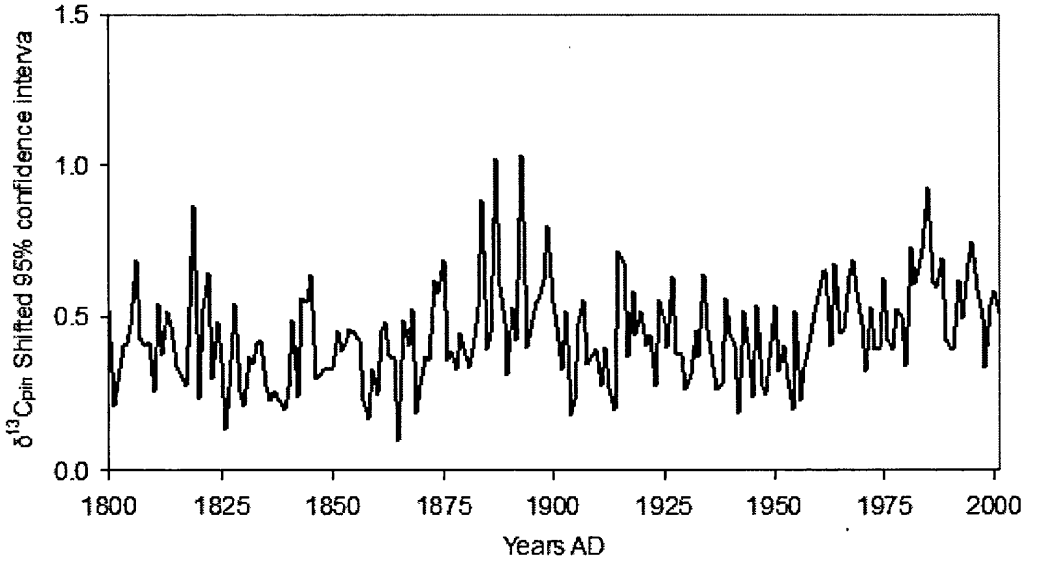

Figure 5.24: 95% confidence interval for $\delta^{13}C_{pin}(‰)$ shifted to the AD 1800-1879 common period

	Tree 63	Tree 73	Tree 82	Tree 87	Tree 91	Tree 95	Tree 129
Tree 73	0.45						
Tree 82	0.45	0.57					
Tree 87	0.54	0.61	0.42				
Tree 91	0.54	0.61	0.39	0.53			
Tree 95	0.54	0.44	0.30	0.43	0.57		
Tree 129	0.56	0.66	0.49	0.62	0.58	0.42	
Tree 166	0.44	NA	NA	0.48	0.56	0.07	0.48

Table 5.1: Inter-correlation between all trees from AD 1800-2001. Mean $r = 0.49$.

5.5 Signal Strength

It is desirable to obtain some measure of how much tree-ring proxies (including δ^{13}C) co-vary from year to year, to enable some measure of common signal strength to be calculated. A simple approach to this is to look at the inter-correlation (*Pearson's r* value) between all the trees, the results of which can be seen in table 5.1. In tree-ring studies it is considered desirable to see how stable this covariance is over time and so running correlation can be made over a suitably long interval > 30 years is normally considered sufficient. In this case a running 31 year value has been calculated. The results of which can be seen in Figure 7.4.

The data in Table 5.1 shows that the mean correlation between all the trees is $r = 0.49$. The highest value is 0.66 between Trees 129 and 73 and the lowest 0.07 between Trees 95 and 166, the next lowest being r $= 0.3$. Such a low value between two trees may indicate some dating problem, however, the dating has been checked and as both trees correlate well with other trees this correlation seems real and may simply indicate that these two trees are responding to different forcing mechanisms, also as correlations with climatic parameters in excess of $r = 0.71$ (explaining half the total variance) are fairly uncommon it is possible that two trees could both be responding to say temperature and still not correlate well with one another. The running 31 year correlation shown in Figure

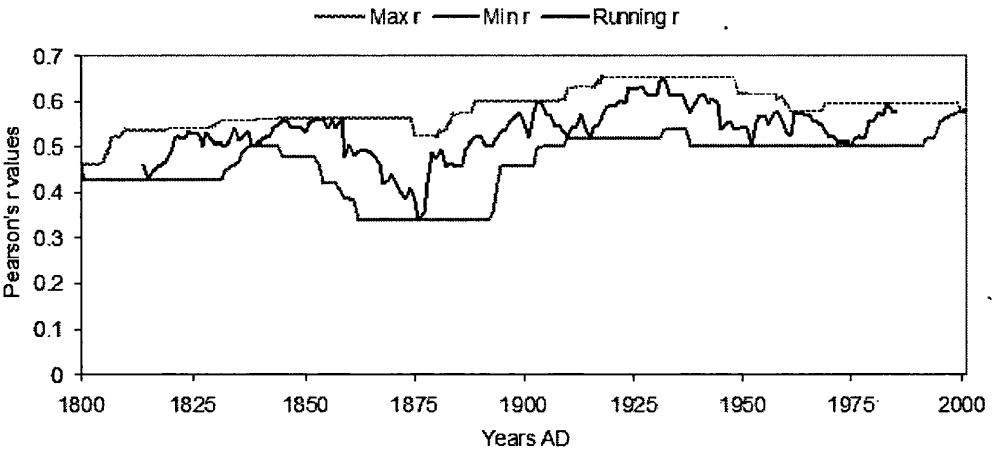

Figure 5.25: Inter-correlation between between all trees for a 31 year running period from AD 1800-2001. Showing the 31 year running correlation and also the maximum and minimum correlation in any 30 year window.

7.4 shows that the mean r value of 0.49 in table 5.1 is not stable over the period AD 1800 to 2001. The correlation remains above $r = 0.5$ for much of the series, especially the AD 1900s, but dips dramatically at around AD 1875 to $r = 0.34$, rapidly recovering on both sides of this. One reason for this may be some dating inaccuracy during this period, but this has been carefully checked and the dating seems to be correct. As with the low inter-correlation between Trees 95 and 166, this may reflect real phenomena which may prove explicable.

In dendroclimatology various techniques such as analysis of variance (ANOVA) have been used to estimate signal to noise ratio (Fritts, 1976). However, ANOVA requires that all data series be of an equal length which limits analysis to to the length of the shortest time series. As a result of this an alternative method known as the mean correlation technique (Wigley et al., 1984; Briffa and Jones, 1989), which has no such limitation, is now widely used by dendroclimatologists as a method to estimate common signal strength between trees. The result of a mean correlation technique is termed the expressed population signal (EPS), which is the degree to which the sample (presumed un-biased) portrays the hypothetical 'perfect chronology'. This can be calculated using Equation 7.1. The signal or EPS is defined as the mean correlation calculated between all possible pairs of trees

($\overline{r}_{bt}$), which is equivalent to the fractional variance component in ANOVA. The 'noise' or variance not common between trees is canceled in direct proportion to the number of trees (t).

$$\text{EPS}(t) = \frac{(t \cdot \overline{r}_{bt})}{(t \cdot \overline{r}_{bt} + (1 - \overline{r}_{bt}))} \tag{5.16}$$

Values for EPS are very sensitive to the number of trees (t) used in the chronology and typically increases rapidly as additional trees are added up to around 10 trees, from then onwards the incremental advantage of adding extra trees rapidly decreases (Briffa and Jones, 1989). While there is no formal minimum limit for EPS that can be used for climatic reconstruction, a figure of EPS = 0.85 has been suggested as a reasonable value by Wigley et al. (1984) and is typically used. A figure in excess of 0.85 does not necessarily mean that a chronology is suitable for climatic reconstruction as, especially in ring-widths, this common signal may be something other than climatic (pests, pollution or forest management). However reference to isotope theory and comparisons with meteorological data should, combined with an estimate of common signal strength, enable us to draw some conclusions as to the suitability of δ^{13}C at this location to reconstruct past climate. A graph showing the running 30 year EPS for the $\delta^{13}C_{pin}$ values at Forfjorddalen from AD 1800 to 2001 can be seen in Figure 5.26 and the maximum EPS in a running 31 year window in Figure 5.27 and the mean for the same 31 year running window in Figure 5.28

Figure 5.26, which shows the running 31 year EPS shows that after an initial drop below 0.85 in the early nineteenth century, the EPS remains above this threshold for most of the nineteenth and twentieth century. As was also apparent in Figure 7.4 there is a decline in the EPS towards the end of the nineteenth century, remaining below 0.85 from AD 1866 to 1895, with a minimum of only 0.72 in AD 1876. This represents a mean inter-correlation between the 5 trees of $r = 0.33$, considerably lower than for rest of the series. The highest EPS in a running window (Figure 5.27) shows that the EPS is only below 0.85 in the early AD 1800s. In the late nineteenth century the EPS does not fall

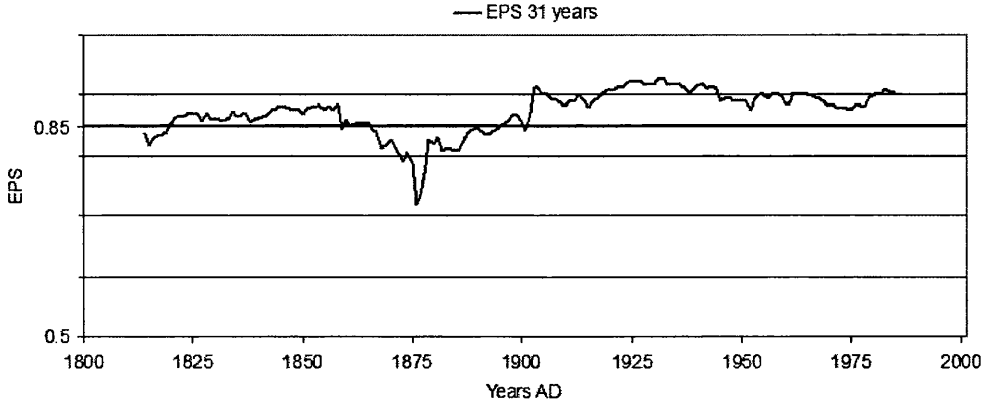

Figure 5.26: A 31 running EPS for $\delta^{13}C_{pin}(‰)$ from AD 1800 to 2001

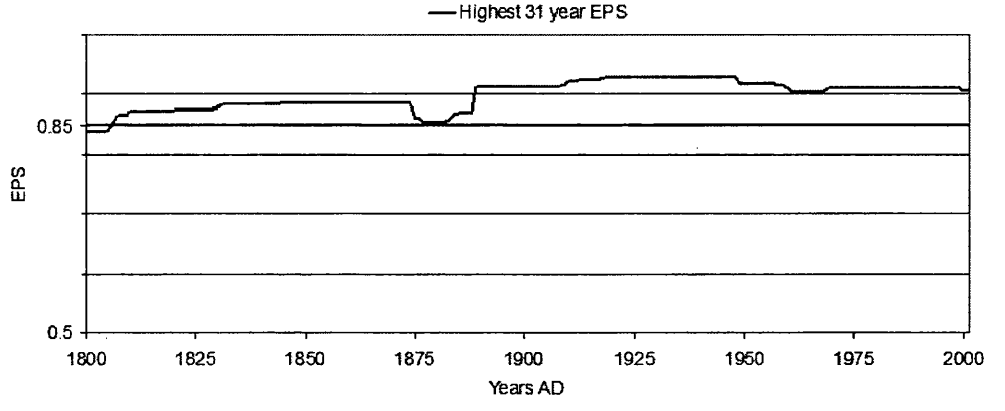

Figure 5.27: Highest EPS in a 31 year running window for $\delta^{13}C_{pin}(‰)$ from AD 1800 to 2001

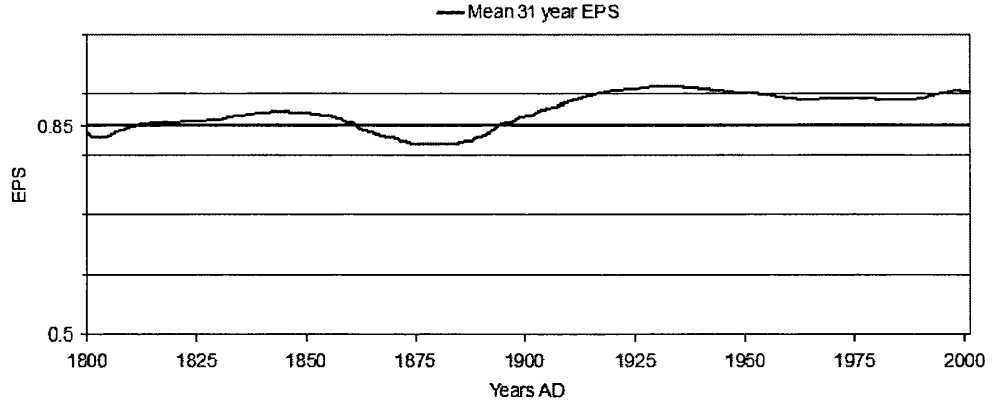

Figure 5.28: Mean EPS in a 31 year running window for $\delta^{13}C_{pin}(‰)$ from AD 1800 to 2001

below 0.85, however a dip at this point is apparent. For the mean 31 year EPS in Figure 5.28 the same pattern is apparent. Improving the EPS to in excess of 0.85 should be possible by adding extra data to areas of low EPS, it is estimated that (providing any δ^{13}C series added did not correlate any worse than existing series) the addition of 3 extra data sets (a total of 8 trees) to the late nineteenth century would give an EPS >0.85. However, the limitations of a PhD thesis, in terms of time and money, mean that this is not possible for this study.

Also Simply adding trees to the series may only mask a phenomena which in itself may prove to be highly informative. Periods when there is a high common signal may be indicative of periods of strong common climatic forcing, for example sharply decreasing temperatures or indeed precipitation may be expected to lead to strong common changes in the isotope ratios of trees as they become more stressed. On the other hand a weak common signal between trees may indicate that the trees are not suffering much climate stress and they therefore may be reacting more to individual site conditions.

5.6 Chapter Conclusion

In this chapter the δ^{13}C series from AD 1800-2001 has been corrected for both the changes in atmospheric isotope ratios (Section 5.2) and also for for increasing CO_2 concentrations in the atmosphere (Section 5.3). Individual δ^{13}C series have been shifted towards the mean of a common period. To prevent any problems of offsets in the mean δ^{13}C value as trees enter or leave the time series. Finally in Section 5.5 a measure of the common signal in the δ^{13}C series was made and while there appears to be a very interesting drops in the common signal towards the end of the nineteenth century, which will receive more detailed attention in the following chapters, most of the δ^{13}C series seems eminently suitable for use in climatic reconstruction.

As one of the principle aims of this thesis is to attempt to reconstruct low-frequency climatic change avoiding statistical de-trending, which has proved so problematic for reconstructing low-frequency climate using ring-widths (Cook et al., 1995), was con-

sidered desirable. So while various steps, outlined in this chapter, have been taken to enable the final $\delta^{13}C_{pin}$ series to be optimally compared with climate the use of statistical de-trending has been limited to a logically constrained lowess regression during the pre-industrial (PIN) correction procedure (see Section 5.3.1). As a result it is expected that any low-frequency climatic signals which were present in the original $\delta^{13}C_{raw}$ data should still be present in the final $\delta^{13}C_{pin}$ shifted data, as indeed should high frequency signals. The object of the next chapter will be to determine if and to what degree the $\delta^{13}C_{pin}$ series at Forfjorddalen can be explained by climatic parameters and how useful it may prove in reconstructing past climate.

6

δ^{13}C Calibration with Climate

6.1 Introduction

Data from the meteorological station at Andenes (Figure 2.1) stretches as far back as AD 1868 for temperature and AD 1910 for precipitation. $\delta^{13}C_{pin}$ shifted data will be initially compared to climate over these two periods. There are other climate data sets available for this region including combined and standardised temperature (AD 1875-1997) and precipitation (AD 1873-1997) data sets for selected meteorological stations between the Polar Circle and Northern Cape (Hanssen-Bauer and Føland, 1998; Hanssen-Bauer and Nordli, 1998), which do not include the Andenes data. There is also a composite temperature record from Tornedalen in northern Sweden stretching from AD 1802-2002. This is made up of meteorological data which started in AD 1859 and observational data stretching back to AD 1802 (Klingbjer and Moberg, 2003). While Tornedalen is approximately 450 km away on the other side of the Scandes mountain range it may prove useful for comparing the low frequency signal contained within the isotope record. Daily temperature data is available for Tromsø from AD 1931, with a break in the data set from AD 1941 to 1945, this meteorological station is some 175 km northeast of Forfjorddalen. These data may prove useful in attempting to define the critical length of growing season for the production of sugars for latewood cellulose.

6.2 The relationship between temperature and $\delta^{13}C_{pin}$

6.2.1 Andenes Temperature Data and $\delta^{13}C_{pin}$

There are mean monthly temperature data available from the Andenes meteorological station for every month from the year AD 1868. Located at the northern tip of the Vesterålen archipelago at 69°18'N and 16°9'E (Figure 2.1) this meteorological station is approximately 60 km north-east of Forfjorddalen and so should reflect mean monthly temperature at the field site. To explore the relationship between δ^{13}C and growing season temperature the mean $\delta^{13}C_{pin}$ values for each year were compared using correlation with the mean temperature from Andenes for each month from January of the previous year to September of the current year for the period from AD 1868 to 2001. This was carried out using the program DENDROCLIM2002 (DendroClim) (Biondi and Waikul, 2004). The results of this can be seen in Figure 6.1, which shows all correlation values, and Figure 6.2 showing only those those correlation with a significance of p <0.05.

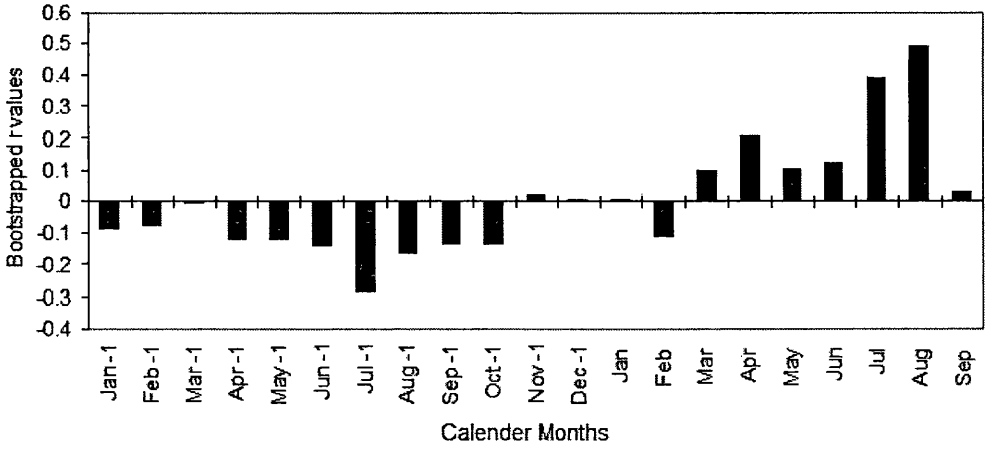

Figure 6.1: Bootstrapped correlation values for $\delta^{13}C_{pin}$(‰) shifted data and mean monthly temperatures from Andenes from AD 1869 to 2001. Using the whole of the previous calender year and the current year to September to encompass the whole potential growing season and any possible correlations with earlier season's temperatures.

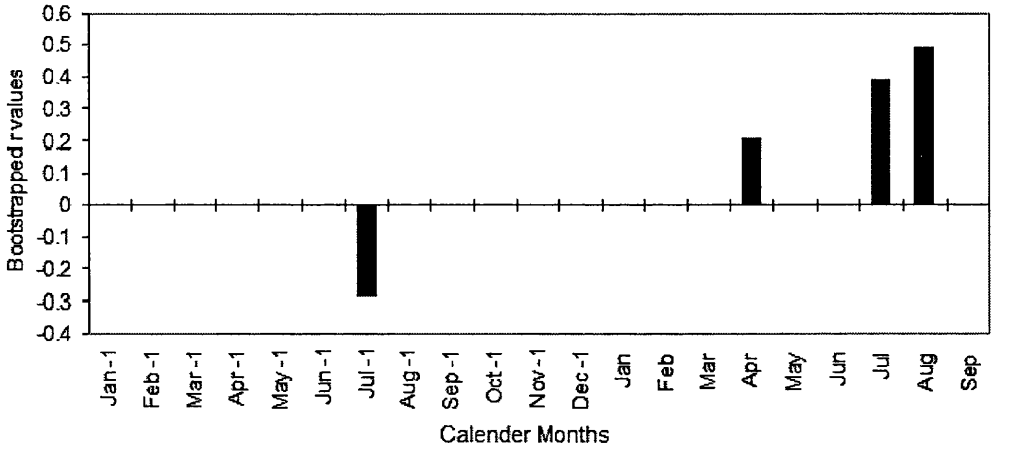

Figure 6.2: Bootstrapped correlation values for $\delta^{13}C_{pin}$(‰) shifted and mean monthly temperatures as Figure 6.1 showing only correlations with a significance of p <0.05.

Figure 6.2 shows that there are significant positive correlations between the current years summer temperatures and the $\delta^{13}C_{pin}$ of the tree-ring latewood, the correlation with July mean temperature is $r = 0.39$ and for August $r = 0.49$. There are also weaker, but still statistically significant, correlations with mean April temperature of the current year ($r = 0.20$) and a significant negative correlation with the July temperature of the previous year (r = -0.29). As there is no obvious reason why these two months should affect the δ^{13}C of latewood cellulose, and as the correlation values are relatively low they will, for the time being, be disregarded, although the negative correlation with the previous summer will be discussed briefly later in this chapter.

As there are significant correlations with both July and August temperature it seems reasonable to combine these two months temperatures. When mean of July and August temperatures is compared to the isotope values there is some small improvement but only to $r = 0.51$, suggesting that the key month for the production of sugars for latewood is August.

6.2.2 Tornedalen Temperature Data and $\delta^{13}C_{pin}$

One of the longest meteorological temperature records for Fennoscandia is the composite record from the Tornedalen area of subarctic Sweden (around 66°N, 24°E) published by Klingbjer and Moberg (2003). While this site is some 450 km distant from Forfjorddalen and on the other side of the Scandes mountain range, it may still prove a useful comparison data set. Stretching back as far as AD 1802 the Tornedalen record is a combination of continuous meteorological data from the Haparanda synoptic weather station from August AD 1859 combined with observational data from AD 1802 to 1862, the overlapping period being used to adjust the observational data to the Haparanda data (Klingbjer and Moberg, 2003). Klingbjer and Moberg (2003) believe the data to be reliable back to AD 1832, prior to which especially summer temperatures (June to August) are thought to be less reliable. Mean annual temperature are considered realistic as far back as the beginning of the series.

The procedure for comparing the annual $\delta^{13}C_{pin}$ values and the Tornedalen temperature data is the same as was used for the Andenes data described in section 6.2.1. Figure 6.3 shows the monthly correlation values, while Figure 6.4 shows those which are significant at the 95% level (p=<0.05). More months temperatures from Tornedalen are significantly correlated with the $\delta^{13}C_{pin}$ data. August of the current year correlates highest at $r = 0.30$, followed by July with $r = 0.26$. The length of the record at 200 years is the key factor in making relatively low correlations such as the $r = 0.13$ for March of the current year significant at the 95% level (p=<0.05).

May ($r = 0.25$) and June ($r = 0.22$) are more strongly correlated with the Tornedalen record than the Andenes record. The reason for their increased importance can be seen in Figure 6.5. This shows 40 year running correlation values for the four most highly correlated months (May, June, July and August). For some reason(s) not yet fully understood both May and June become more highly correlated with $\delta^{13}C_{pin}$ than either July or August for a period in the nineteenth century, especially from AD 1850 to 1900 when July and August correlation fall away. Indeed July correlates very poorly

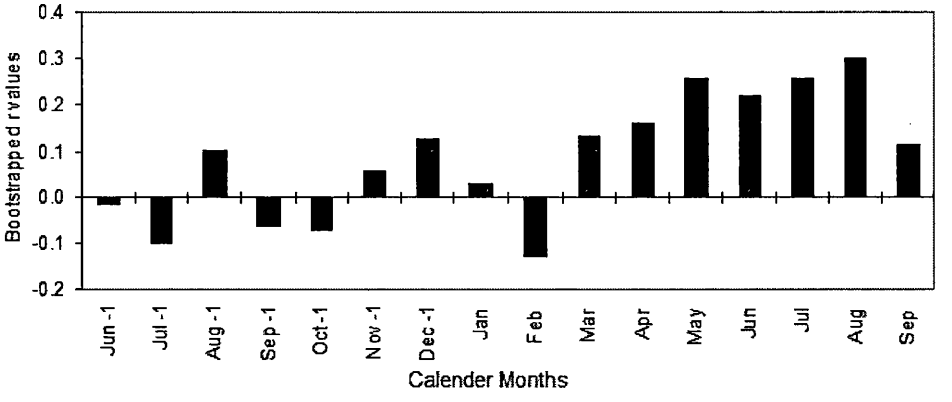

Figure 6.3: Bootstrapped Correlations between Tornedalen monthly mean temperature and δ^{13}C (‰), using DendroClim (Biondi and Waikul, 2004)

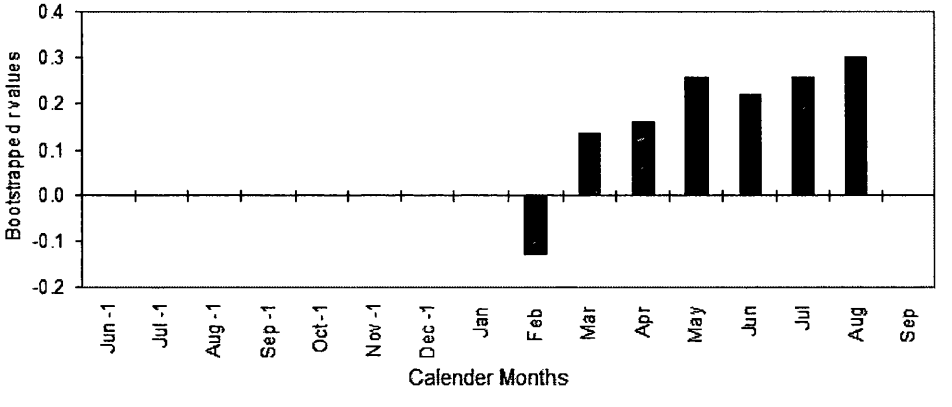

Figure 6.4: Bootstrapped Significant Correlations (p=<0.05) with Tornedalen monthly mean temperature and δ^{13}C(‰), using DendroClim (Biondi and Waikul, 2004)

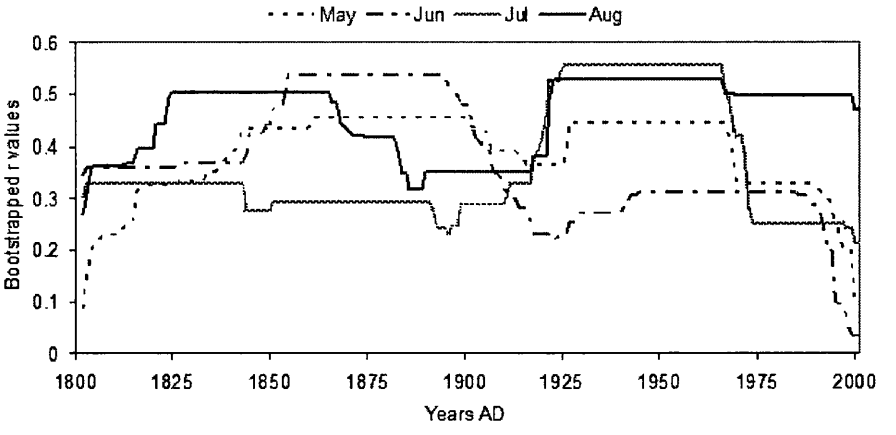

Figure 6.5: Maximum 40 year bootstrapped correlations between δ^{13}C(‰) and Tornedalen temperature for May, June, July and August

with this part of the Tornedalen record and as this appears to be the coldest part of the summer temperature record, may represent a contraction of the growing season into August. This does not, however, explain why May and June should correlate so highly, June has a correlation with $\delta^{13}C_{pin}$ in excess of $r = 0.50$ form AD 1854 to 1900 (with a maximum of $r = 0.54$). Whether this is some artifact or the data set or there is some genuine reason why in this cool period May and June temperatures play an important role in δ^{13}C fractionation for latewood production is not entirely clear. This interesting phenomenon will however be laid aside and anlysis will proceed with later summer season temperatures. One other noteworthy thing from Figures 6.3 and 6.4 is that the negative correlation with the previous July temperature seen in the Andenes record (Figure 6.2) is not apparent in the full Tornedalen data set. If however only the twentieth century of the Tornedalen record is used the negative correlation for the previous July once again rises to significant levels ($> 95\%$) but this correlation is not apparent in the nineteenth century.

6.2.3 Tromsø Daily Temperature Record

The daily temperature record for Tromsø stretches back to AD 1931 with a break between AD 1941 and 1945, at approximately 175 km northwest of Forfjorddalen it seems

reasonable to expect that it may correlate well with the $\delta^{13}C_{pin}$. While the record is much shorter than either the Andenes or Tornedalen record and has a break, it has the major advantage of having daily data available. This data set will be used primarily in an attempt to fix the position of the critical part of the growing season for latewood sugar production. The monthly data sets from Andenes and Tornedalen suggest that this should be some period contained within the calender months of July and August. This period may not be entirely stable but an estimate based on the data available from Tromsø may prove useful in understanding the relationship between $\delta^{13}C_{pin}$ and mean monthly temperatures.

Figure 6.6 shows a comparison of the temperature record from Andenes and the daily temperature data from Tromsø (r = 0.97), with no obvious divergence between the two data sets. Figure 6.7 shows the maximum correlation between $\delta^{13}C_{pin}$ and the Tromsø daily temperature records for a 30 day moving window starting at the beginning of July and finishing at the end of August. The peak correlation is $r = 0.69$ achieved for 30 day periods between the 23rd of July and the 23rd of August, with a maximum correlation for any period of $r = 0.70$ from the 19th of July to the 23rd of August. This would seem to suggest that the key period for the formation of sugars for latewood at this location is a period of just over one month encompassing the end of July and most of August.

6.3 Stability of the Relationship Between $\delta^{13}C_{pin}$ and Temperature

6.3.1 Andenes Temperature and $\delta^{13}C_{pin}$

Figure 6.8 shows mean July and August temperature from Andenes plotted alongside $\delta^{13}C_{pin}$ and again in Figure 6.9, where both data sets have been normalised to a mean of zero and a standard deviation of one. Two things are apparent from these figures: firstly that there seems to be a very strong association between $\delta^{13}C_{pin}$ and mean July and August temperature from approximately the mid AD 1920s to the end of the series;

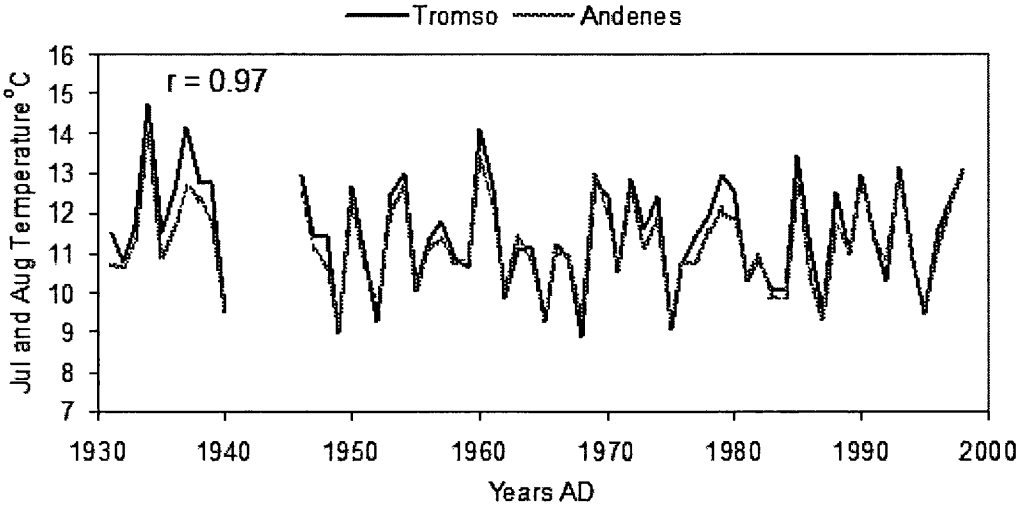

Figure 6.6: A comparison of mean July and August temperature from Andenes and Tromsø.

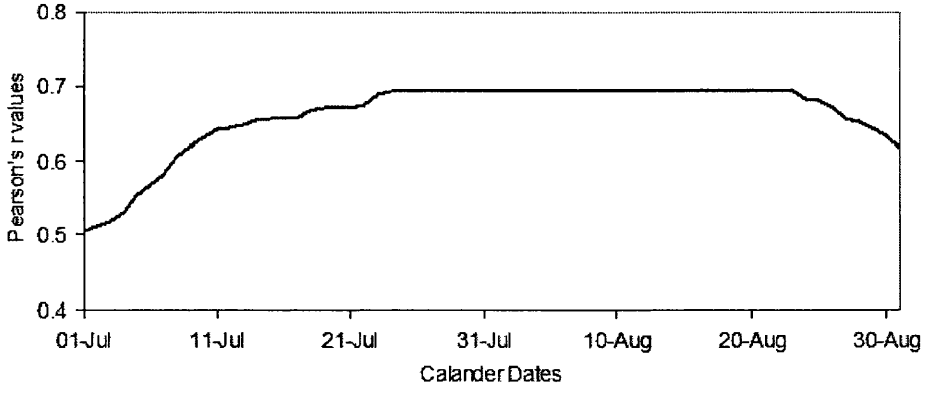

Figure 6.7: Maximum 31 day running correlation between $\delta^{13}C_{pin}(‰)$ and daily Tromsø temperature data for July and August, for the period from AD 1931 to 1998 (no data for the years AD 1941-45). The correlation between temperature and $\delta^{13}C_{pin}(‰)$ has been calculated for each 31 day period from the 1st of July to the 31st of August and then a moving 31 window has been applied to these correlations. The graph shows the maximum correlation in this widow, the first point represents the maximum correlation for the period form the 1st of July to the 31st of August, with the highest correlation (r = 0.69) for the 31 day windows from the 23rd of July to the 22nd of August and the 24th of July to the 23rd of August.

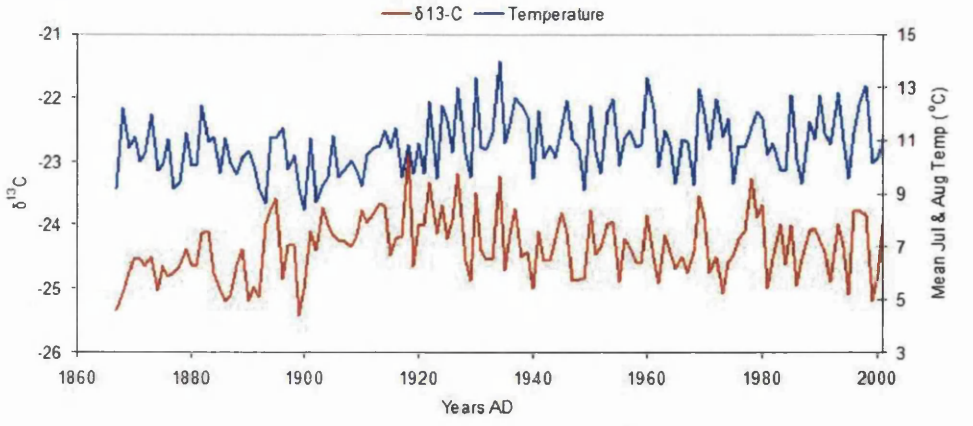

Figure 6.8: Mean July and August temperature from Andenes plotted alongside $\delta^{13}C_{pin}$(‰) from AD 1869-2001.

and secondly that this this association seems to break down before ~AD 1920, although the relationship appears to re-establish itself in the earliest part of the record. This is especially interesting considering the low common signal between the trees (EPS) noted in Section 4.5, although the timing does not appear to be exact. The EPS between the trees recovers quite quickly after AD 1900 (the first 31 year period with an EPS of > 0.85 is AD AD 1881 to 1911) while temperature and $\delta^{13}C_{pin}$ begin to diverge after AD 1901. Figure 6.9, where both data sets have been normalised, shows this clearly.

To investigate the temporal relationship between between $\delta^{13}C_{pin}$ and temperature a running correlation is applied to the data, again using the program DendroClim (Biondi and Waikul, 2004). The results of this using a running 40 year bootstrapped correlation window can be seen in Figure 6.10 for July and August temperatures separately and Figure 6.11 which shows mean July and August temperature, the lines in both these graphs show the maximum bootstrapped correlation coefficient in a 40 year moving window.

Figure 6.10 shows the temporal changes of the relationship between $\delta^{13}C_{pin}$ and July and August temperature, which are stable over this period. Correlation values with both July and August temperature start low. The maximum correlation for August for the period up to AD 1912 is r =0.254 and for July the maximum correlation is r = 0.035. The correlation coefficients for both July and August then begin to increase. The correlation

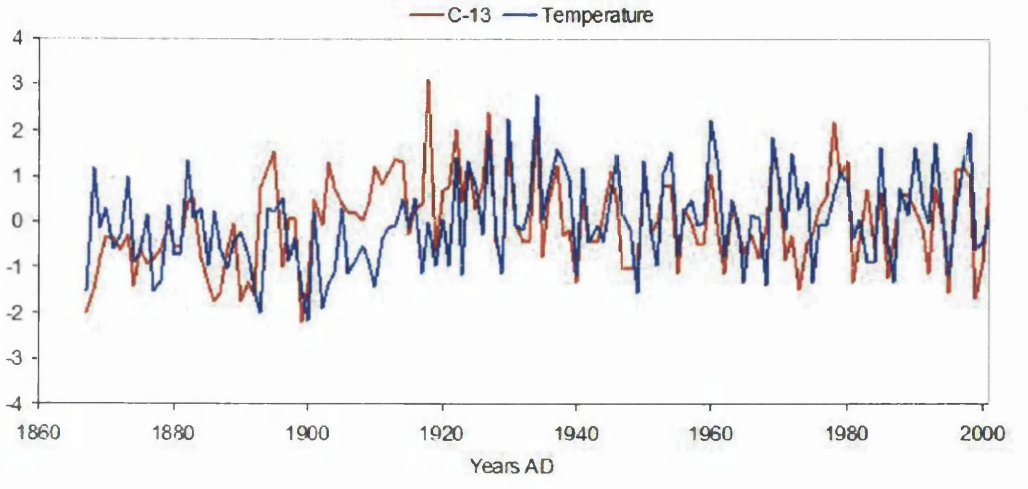

Figure 6.9: Mean July and August mean temperature from Andenes plotted against $\delta^{13}C_{pin}(‰)$ from AD 1869-2001, both data set have been normalised (to a mean of 0 and a standard deviation of 1), for ease of comparison.

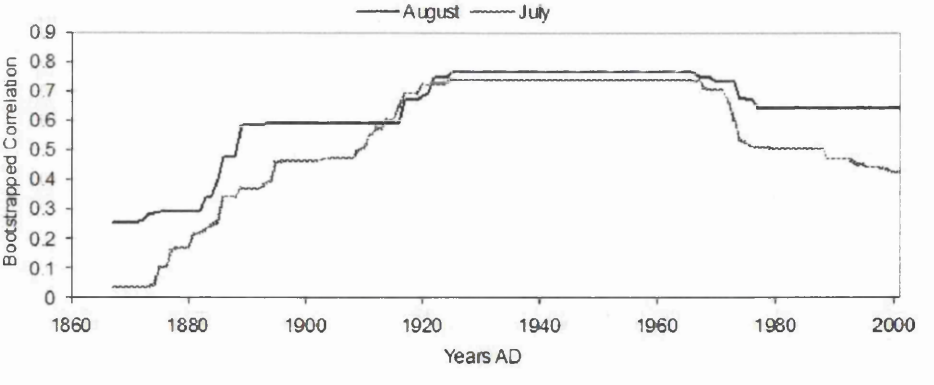

Figure 6.10: Running 40 year correlation between $\delta^{13}C_{pin}(‰)$ and July and August temperatures. Graph shows the maximum correlation in any given 40 year running window.

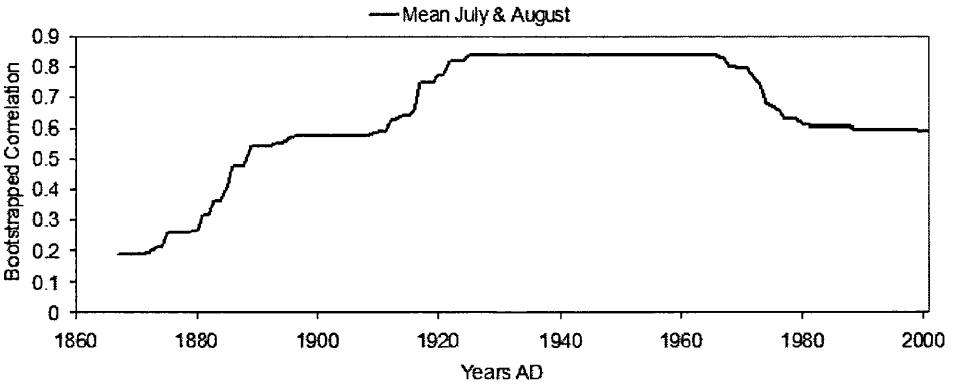

Figure 6.11: Running 40 year correlation between $\delta^{13}C_{pin}$(‰) and mean July and August temperature. Graph shows maximum correlation in any given 40 year running window.

for August reaches $r = >0.50$ for the 40 year period ending in AD 1930 (AD 1891-1930) and $r = >0.70$ for the period ending in AD 1962 (reaching a maximum in any 40 year period of $r = 0.77$), thereafter there is some decline with a final value of $r = 0.64$ for the 40 year correlation window ending in 2001. For July the increase is even more dramatic reaching $r = >0.5$ for the 40 year period ending in AD 1950 and $r = >0.70$ by AD 1961 (with a maximum of $r = 0.74$), and then declines more than the August correlation with a final $r = 0.43$ in 2001.

Figure 6.10 shows that while, for a large part of the record, there are strong correlations between $\delta^{13}C_{pin}$ and both July and August temperature, this is not so early in the record. Correlations do not reach $r = > 0.6$ for either month until 40 year period starting after AD 1913. The difference between the two months is interesting and would seem to suggest that there have been some changes in the growing season for the Scots pine at Forfjorddalen. When correlations of $r = > 0.5$ occur early in the twentieth century August appears more important than July in the production of sugars for latewood. However in the middle part of the series July becomes increasingly important and although generally below August (it does at one point overtake August) the levels for both are quite similar for much of the middle of the AD 1900s. However, while August correlations with $\delta^{13}C_{pin}$ remain robust until the end of the series, the correlations with July temperature decline (Figure 6.10). This may suggest that a lengthening of the growing season occurred at

this location from perhaps the mid AD 1920s until the AD 1970s. During this period the production of sugars for latewood cellulose may move earlier into July but after ~AD 1970 they may become restricted more to August.

Figure 6.11 shows the moving correlation for 40 year period, using a mean of July and August mean temperatures. Figure 6.11 shows why combining July and August temperatures made only a small improvement to correlation with $\delta^{13}C_{pin}$ ($r = 0.51$) over those for August alone ($r = 0.49$), for the period from AD 1869 to 2001. In the middle of the twentieth century when both July and August temperature correlate well with $\delta^{13}C_{pin}$ the correlation for mean July and August temperatures reach their maximum (r = >0.80 from AD 1923 to 1969). The maximum correlation of $r = 0.84$ is for the period AD 1927 to 1966, which equates to r^2= 0.70, explaining greater than 70% of the variance in $\delta^{13}C_{pin}$. However, when correlations with July temperature decline the mean July and August correlation with $\delta^{13}C_{pin}$ also falls to below the level of that for August alone. The correlation with August also falls and so the mean correlation for the whole period is affected.

The period for which temperature data exist from Andenes can be divided into two periods (Figure 6.12). For the period AD 1869 to 1926 there is a poor correlation with summer temperature (r = 0.27) (Figure 6.12, left-hand panel) and for the period from AD 1927 to 2001 there is a strong correlation with climate of (r = 0.71) (Figure 6.12, right-hand panel). There are a number of possible explanations for this breakdown in the correlation between temperature and $\delta^{13}C_{pin}$. Firstly there may be some tree-ring dating problems within this 50 year period; secondly there may be inaccuracies in the temperature records from Andenes during this period; and thirdly there may be some climatic (or indeed not climatic) reasons for the low correlation between $\delta^{13}C_{pin}$ and temperature.

The tree-ring cross dating has been thoroughly checked (Kirchhefer, *pers. comm.*), however even if some cutting or dating errors have gone unnoticed during this period it seems very unlikely that the resulting series would take on the form seen in Figures 6.8 and 6.9. If some problems with dating or cutting had occurred one would expect there to be an offset between adjacent peaks and troughs in the $\delta^{13}C_{pin}$ and temperature series,

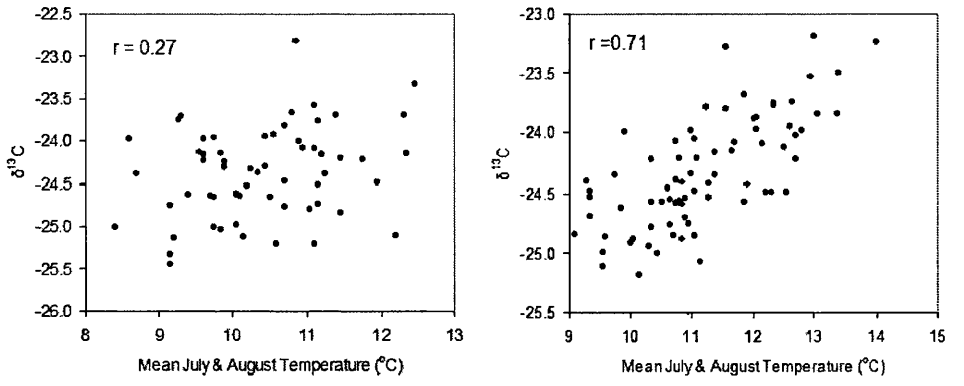

Figure 6.12: Scatter plots of δ^{13}C (‰) against mean July and August temperature for the period AD 1869-1926 (left) and AD 1927-2001 (right)

which should be relatively easy to spot by eye or using a computer program such as COFECHA. This could then be rectified by adding or removing ring(s) at the appropriate point(s). For the period with the lowest EPS (AD 1870s and 1880s) no such offset occurs for either the mean series or the individual tree-ring series. As the EPS recovers in the early AD 1900s (suggesting a stronger common signal between trees, and so unlikely to include any major dating errors) there is a divergence between the temperature record and the $\delta^{13}C_{pin}$ series (Figure 6.9) associated with very low correlations with summer temperature, this again seems inconsistent with dating errors.

The second possible explanation for the breakdown in the association between the $\delta^{13}C_{pin}$ data and temperature is that a problem exists with the climate data from the Andenes meteorological station during this period. To test this there are alternative temperature data available for the same period with which the Andenes temperature record can be compared. Perhaps the most suitable for this is the temperature data set compiled by Hanssen-Bauer and Nordli (1998). This is a composite of data from a number of stations from the polar circle to Northern Cape. As this data set does not include data from the Andenes station it seems highly suitable for comparison. As this northern coast data set is compiled from a number of disparate stations the results are indexed rather than in °C and so for comparison both this data set and the Andenes data were first normalised (to a mean of zero and a standard deviation of one). The results of this comparison can be

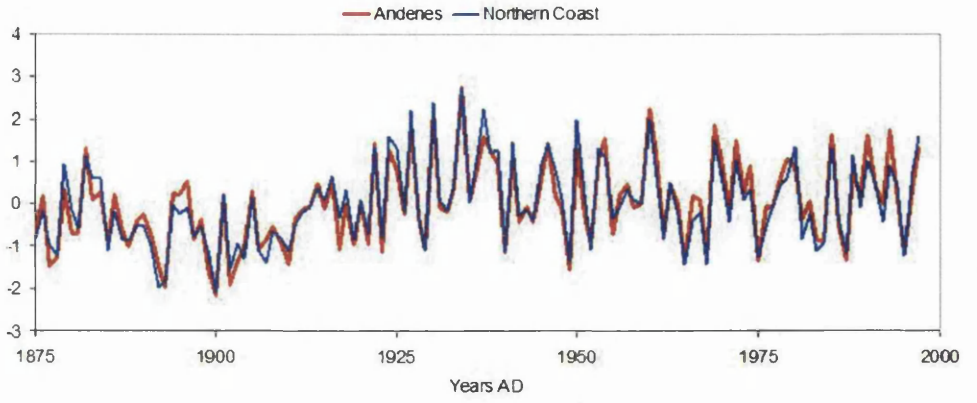

Figure 6.13: Comparison of mean normalised July and August temperature data from AD 1875-1997 for Andenes and the composite data set of northern stations (northern coast) produced by Hanssen-Bauer and Nordli (1998).

seen in Figure 6.13 and also as scatter plots in Figure 6.14, which compares the entire common period for both series (AD 1875 to 1997) and also the period under discussion here (AD 1875 to 1926).

This comparison suggests that the Andenes temperature record is reliable. In its entirety it correlates with the northern coast record at $r = 0.95$ and for the period in question (AD 1875-1926) at $r = 0.93$ (Figure 6.14), while Figure 6.13 shows that the two data series maintain a consistent relationship through time. These results are not consistent with measurement or recording errors that are likely to lead to the breakdown in the relationship between $\delta^{13}C_{pin}$ and mean July and August temperature described above. If then there are no major problems with the $\delta^{13}C_{pin}$ record or the temperature record for the period between AD 1869 and 1926 it seems likely that there is some other, potentially climatic, reason for this decline in correlation. It is possible that the $\delta^{13}C_{pin}$ fractionation is predominantly controlled by some factor other than temperature, but which normally co-linear with temperature, but which diverges during this period. Moisture availability would seem a possible candidate for this as temperature and precipitation are often negatively correlated (Trenberth and Shea, 2005). Alternatively as δ^{13}C can be controlled by both sunshine and moisture availability (Edwards et al., 2000; McCarroll and Loader, 2004) and although precipitation in this area is normally high there may be periods for

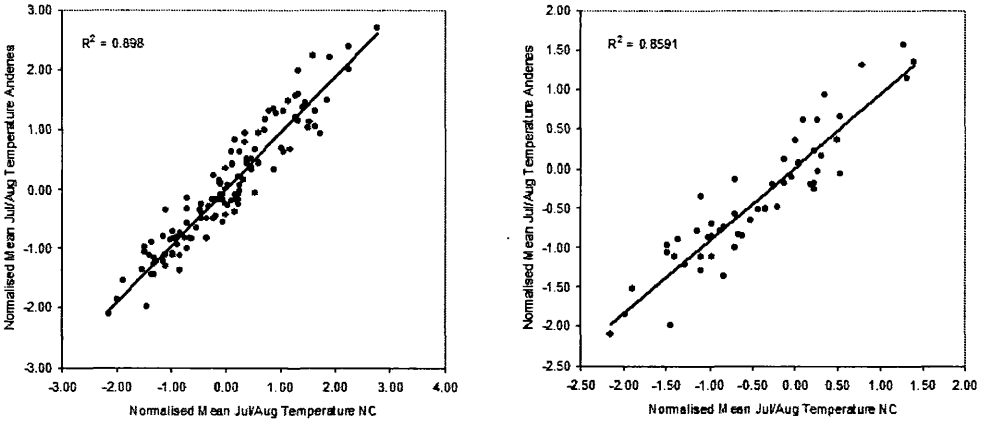

Figure 6.14: Scatter plot of Andenes and Northern Coast temperatures. Right hand panel AD 1875-1997 and left hand panel AD 1875-1926.

which moisture stress rather than temperature may be the major control over $\delta^{13}C_{pin}$ here. These and other possibilities for this non-linear response will be discussed later Chapter 8.

Another factor which may have some bearing on the low correlation during the period from the AD 1870s to the AD 1920s, is the relationship between July and August temperatures over this period. As has already been discussed there appear to have been changes in the timing of the key period for the production of sugars for latewood cellulose at this location. Expanding further into July during the middle years of the AD 1900s and contracting more into August at both ends of the record. The relationship between July and August temperatures also appears not to have been stable. For much of the record there is quite a strong positive relationship between July and August temperature, typically when August is warm (cool) July is also warm (cool). However, in the early part of the record, this was not the case as can be seen in Figure 6.15. This shows a 30 year running correlation between July and August temperatures and shows the highest correlation in any 30 year running window.

Interestingly Figure 6.15 follows a very similar pattern to those seen in Figures 6.10 and 6.11 (which show the running correlation between $\delta^{13}C_{pin}$ and temperature). Correlation start low rising to a peak in the middle of the twentieth century and then decline. To

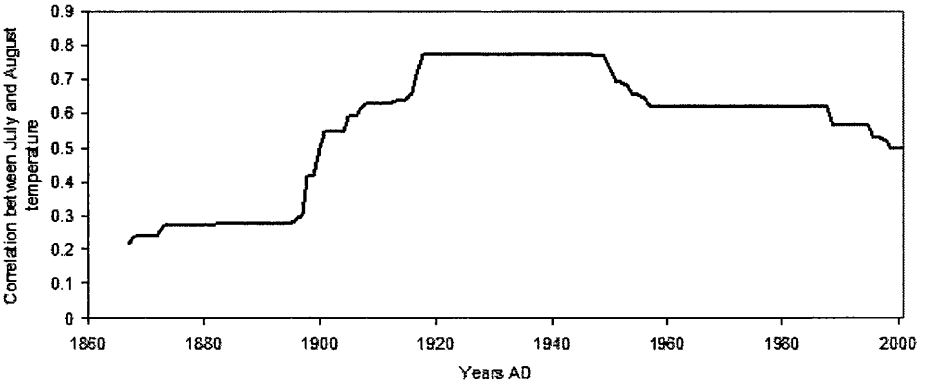

Figure 6.15: Relationship between July and August temperature from AD 1867 to 2001

establish that there are no systematic error in the temperature record for either month each month was checked individually against the equivalent month from the northern coast series. Both months appear to be as robust as the mean of both shown in Figure 6.14.

By taking a mean of July and August temperature when both are either warm or cool, as happens in the middle of the series the figure is likely to correlate rather better with $\delta^{13}C_{pin}$ than when one is cool and the other is warm, or vice versa. While this does not seem to be at the root or the problem of the low correlations between $\delta^{13}C_{pin}$ and mean July and August temperature, it may contribute to lower correlation values and suggests that August temperatures on their own may be more suitable than a mean July and August. However, correlations do no significantly improve when August is taken on its own or even when the warmest month for each year is chosen. It also likely that the temperatures of July and August may in themselves not be homogeneous, were daily data available to check them. It does suggest however, that the period at the end of the AD 1800s and the early AD 1900s is climatically unusual. It starts cool (Figure 6.8) and rapidly warms to the middle of the AD 1920s, it also now seems that summer temperature during this period may have been more variable than for the rest of the twentieth century (Figure 6.15) , it was also a relatively dry period for this area (in comparison with the rest of the twentieth century).

The data presented in Figures 6.10 and 6.11 raise some questions as to how to approach a temperature calibration and palaeotemperature reconstruction at this location over the past 600 years. Most importantly, it must ascertained which part of the calibration record may most accurately reflect the relationship between $\delta^{13}C_{pin}$ and temperature over the past millennium: the latter part of the record which has high correlations with climate, but which is also the period most effected by anthropogenic CO_2 emissions: or the early part of the record where the relationship between summer temperature and $\delta^{13}C_{pin}$ is almost non-existent? Secondly as the growing season appears not to be especially stable, which of the summer months should be used for calibration with climate? A mean of July and August yields marginally the highest correlation for the whole period, however the correlation with August appears the more stable and if, as much of the literature on the subject would suggest (e.g. Lamb (1995)), climate over the last few hundred years has been somewhat cooler than that of the twentieth century perhaps August temperature would be more appropriate. Some of these questions may be resolved with reference to one of the longer Fennoscandian temperature records, to determine how typical or atypical the period from AD 1869 to 1926 is.

6.3.2 Tornedalen Temperature and $\delta^{13}C_{pin}$

A discussed in Section 6.2.2 mean July and August temperatures and $\delta^{13}C_{pin}$ provides the highest significant correlation for the whole series from Tornedalen of $r = 0.36$, which is considered quite impressive for such a distant climate station. Figure 6.16 shows a running 40 year correlation between mean July and August temperature from Tornedalen and $\delta^{13}C_{pin}$, showing the maximum, minimum and mean correlation for each 30 year running period. What is apparent from this is that the dramatic dip in the association between summer temperature and $\delta^{13}C_{pin}$ is once again present, with negative correlation for a the 40 year period ending in AD 1912 (minimum r = -0.005). What is also clear is that not only do the correlations with summer climate recover in the twentieth century but also importantly in the earlier part of the nineteenth century, with correlation reaching in excess of $r = 0.50$ (maximum $r = 0.52$), which considering that this record consists of

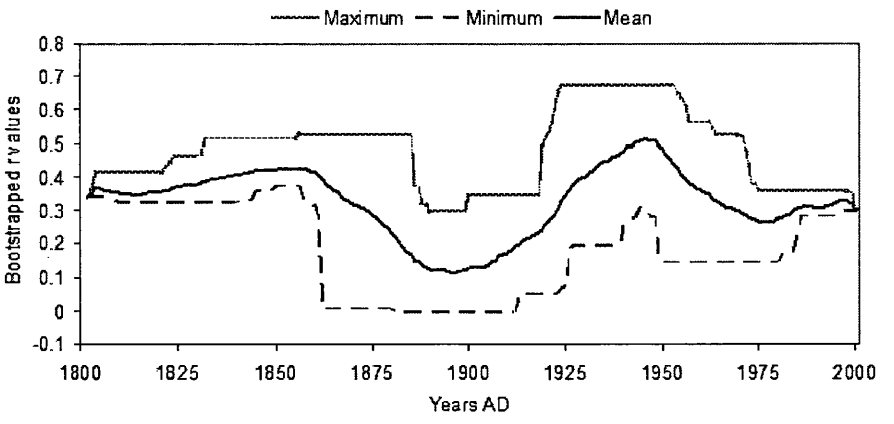

Figure 6.16: Running 30 year correlation between $\delta^{13}C_{pin}$(‰) and a mean of July and August mean temperature for the Tornedalen record.

observational rather than true meteorological data prior to AD 1859 and that the authors do not consider the summer temperature record as reliable prior to AD 1832 (Klingbjer and Moberg, 2003), seems impressive. Indeed if the problematic period from around AD 1885 to 1926 is removed from the record the overall correlation between $\delta^{13}C_{pin}$ and July and August temperatures rises from $r = 0.36$ to $r = 0.48$ and if part of this period of unreliable summer temperatures (AD 1802 to 1828) is removed the correlation for the remaining years rises to $r = 0.52$.

Evidence from Figure 6.16 is encouraging for a temperature reconstruction based on $\delta^{13}C_{pin}$. It suggests that apart from the period identified (from approximately AD 1880 to 1925), the $\delta^{13}C_{pin}$ record from Forfjorddalen matches especially the high frequency of the temperature records available quite well. What is more important, in terms of this study, is that the $\delta^{13}C_{pin}$ record captures the low-frequency temperature variability, an indication of which can be seen in Figures 6.17 and 6.18. Here the full $\delta^{13}C_{pin}$ record is compared to the Tornedalen mean July and August temperature record: in Figure 6.17 the data are presented on separate axis; while in Figure 6.18 the data have been normalised for ease of comparison. Centered running 11 year means have been added to both temperature and isotope data to give an indication of the low-frequency association.

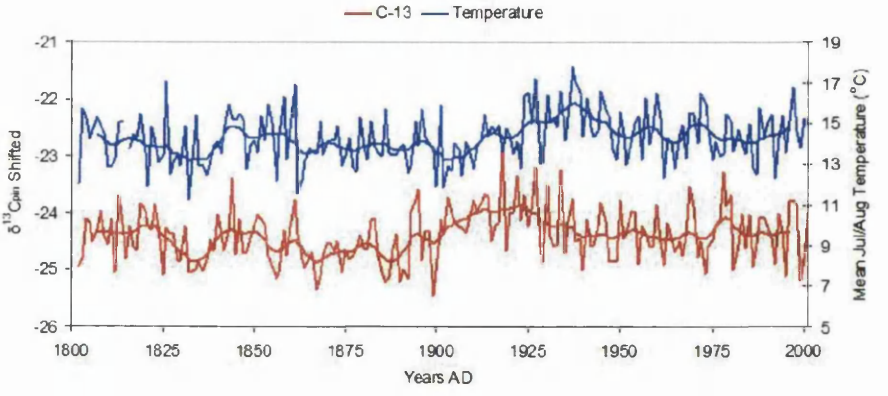

Figure 6.17: $\delta^{13}C_{pin}(‰)$ shifted data compared to mean July and August Tornedalen temperature from AD 1802-2001.

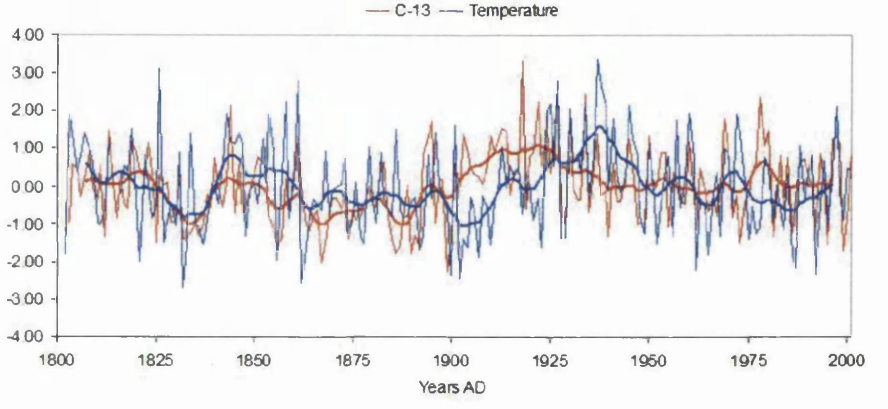

Figure 6.18: $\delta^{13}C_{pin}(‰)$ shifted data compared to mean July and August Tornedalen temperature from AD 1802-2001. Here both data sets have been normalised so the data has a mean of zero and a standard deviation of one.

It is apparent from Figures 6.17 and 6.18 that there is a divergence between the mean $\delta^{13}C_{pin}$ and the July and August mean temperature data in the early twentieth century. Values for $\delta^{13}C_{pin}$ begin to rise sharply from around AD 1898, peaking at about AD 1925 while the increase in temperature lags behind this rise in $\delta^{13}C_{pin}$ beginning to increase from $\sim$AD 1907 and peaking in AD 1937. That the rise in $\delta^{13}C_{pin}$, at least initially, precedes any rise in summer temperature would suggest that for this period, at least, other factors must be controlling $\delta^{13}C_{pin}$ ratios, a decline in precipitation would seem an obvious candidate and this will be discussed later. The correlation between the two

series begins to deteriorate rapidly after about AD 1875, as can be seen in Figure 6.16. It is also clear that prior to AD 1900 the low frequency signal contained in the $\delta^{13}C_{pin}$ begins to match very well with that of the Tornedalen temperature record all the way back to AD 1802 when the record begins. The high frequency association between the $\delta^{13}C_{pin}$ and the mean July and August Tornedalen temperature record improves rapidly before AD 1875 (Figure 6.16) reaching much the same levels as in the last 75 years of the twentieth century.

Returning to the questions posed at the end of section 6.2.1 the temperature data from Tornedalen would then seem to suggest that the $\delta^{13}C_{pin}$ data from Forfjorddalen reflect both the high and low frequency temperature, except for a period of approximately 50 years in length (around AD 1875-1926) when both the low and high frequency $\delta^{13}C_{pin}$ seem to be predominantly controlled by factors other than temperature. This period, although covering around one quarter of the meteorological data discussed so far, would appear to be the exception rather than the rule and possible reasons for this non-linear response will be discussed in Chapter 7, on a multiproxy approach to climatic reconstruction. The choice of which period of the summer to use for calibration has also to some extent been clarified by comparison with the Tornedalen record and while August appears to be the most consistently important month for δ^{13}C ratios in latewood over the entire period of AD 1802-2001 ($r = 0.31$) the correlation with July temperature while lower ($r = 0.26$) is still significant (at the 99.8% confidence interval) and the combined July and August temperature yields a correlation of $r = 0.37$ with $\delta^{13}C_{pin}$. There are also significant positive correlation with both May ($r = 0.25$) and June ($r = 0.20$) and indeed a mean of May, June , July and August temperatures returns the highest correlation with $\delta^{13}C_{pin}$ of $r = 0.39$, however the importance of these months is not apparent in the closer Andenes temperature record and for the Tornedalen record their significance seems restricted to the anomalous period at the end of the nineteenth century (Figure 6.5).

Calibration of the $\delta^{13}C_{pin}$ data set with temperature will be undertaken in Section 6.5. It is proposed to calibrate the $\delta^{13}C_{pin}$ shifted data set with the Andenes temperature

record for the entire series and also for the series excluding the early part of the record from AD 1868 to 1926, which has a low common carbon isotope signal between the trees and a poor correlation with temperature. Calibration will also be undertaken using the more distant Tornedalen record again using firstly the entire record form AD 1802 to 2001 and then removing the problematic period of AD 1880 to 1927 and the earliest part of the record which Klingbjer and Moberg (2003) consider unreliable. A mean of July and August temperatures consistently returns the highest correlation with both the Andenes and the Tornedalen meteorological data and so these will be used for calibration purposes.

6.4 Relationship Between Precipitation and $\delta^{13}C_{pin}$

Two approaches will be made examining the relationship between monthly precipitation and $\delta^{13}C_{pin}$. Firstly we will examine the mean monthly precipitation data available from the Andenes meteorological station for every month from AD 1910. Secondly as an alternative to using mean monthly precipitation data the Standardised Precipitation Index (SPI) developed by McKee et al. (1993) will be calculated from the mean monthly Andenes precipitation data set using the computer program *SPI_SL_6* (Hayes, 2006).

6.4.1 Mean monthly precipitation from Andenes and $\delta^{13}C_{pin}$

Isotope theory would suggest that moisture availability, as well as temperature, can be a key controlling environmental factor in δ^{13}C fractionation (Switsur and Waterhouse, 1998; McCarroll and Loader, 2004, 2006). The relationship between $\delta^{13}C_{pin}$ and precipitation will be examined in same manner as with temperature (described in Section 6.2). Figure 6.19 shows the bootstrapped correlation values between mean monthly precipitation and $\delta^{13}C_{pin}$ from January of the previous year to September of the current year. Only those months with correlations significant at the 95% confidence interval can be seen in Figure 6.20.

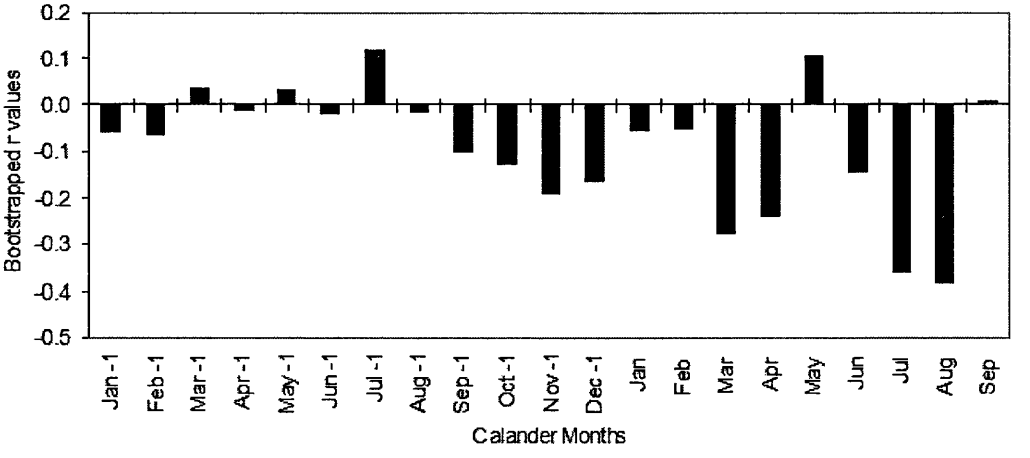

Figure 6.19: Bootstrapped correlation values for $\delta^{13}C_{pin}(‰)$ shifted data and mean monthly precipitation from Andenes from AD 1910 to 2001. Using the whole of the previous calender year and the current year to September to encompass the whole potential growing season and any possible correlations with earlier season's temperatures.

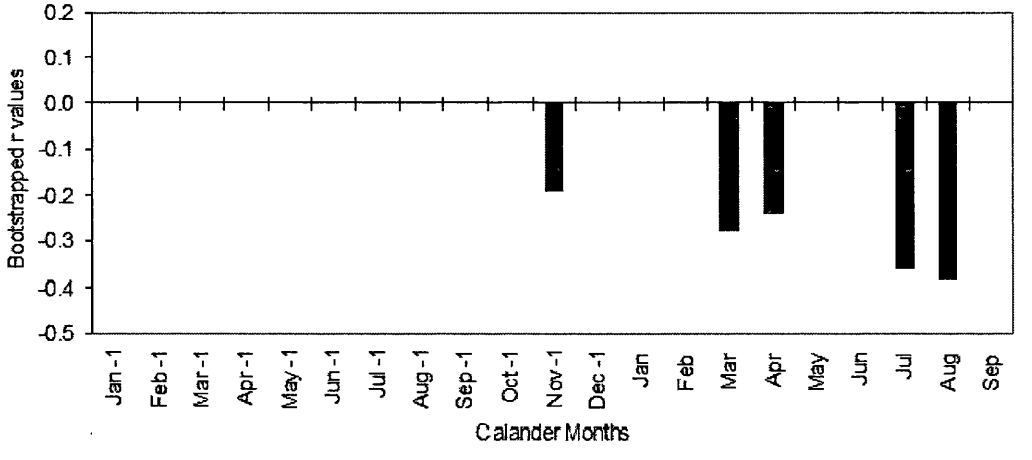

Figure 6.20: Bootstrapped correlation values for $\delta^{13}C_{pin}(‰)$ shifted and mean monthly precipitation as Figure 6.19 but showing only correlations which fall within the 95% confidence limits.

Figure 6.20 shows that a number of months have significant negative correlations with $\delta^{13}C_{pin}$. The correlation with the previous Novembers precipitation is relatively low and it is hard to envisage how it could directly affect the δ^{13}C of latewood cellulose and so this will be disregarded. The positive correlations with March and April precipitation are more negative and may suggest that precipitation throughout the spring and summer months can affect moisture availability, possibly more so if these periods are exceptionally dry or wet. The highest negative correlations are for July (r = -0.36) and August (r = -0.39) of the current year. As with temperature it seems reasonable to expect a mean of July and August precipitation to correlate better with $\delta^{13}C_{pin}$ than either month alone, and indeed this is the case with the mean of July and August precipitation correlating at r = 0.47 with $\delta^{13}C_{pin}$, a graph showing these two variables plotted alongside one another can be seen in Figure 6.21 and and these data normalised can be seen in Figure 6.22. Note that the precipitation axes have been inverted for ease of comparison. It seems from Figures 6.21 and 6.22 that not only do many of the peaks and troughs match, but also the trend in the precipitation data is also present in the $\delta^{13}C_{pin}$ data. This is important as it not only suggests an association between precipitation and $\delta^{13}C_{pin}$, but also in testing the veracity of the PIN correction described in the previous chapter, this will be discussed in Section 6.4.3. Note the two extreme precipitation events in the late twentieth century AD 1983 and 1995, the two wettest summers for the Andenes record.

As was pointed out in Chapter 2, it is possible to see from Figure 6.21 that there is a noticeable increase not only in the amount of precipitation, but also the variability from around the mid AD 1950s onwards. While, as will be seen in Section 6.4.3, the trends in the precipitation and $\delta^{13}C_{pin}$ data are very similar the change in variability in precipitation is not reflected in the $\delta^{13}C_{pin}$ data. This may be because the relationship between precipitation and $\delta^{13}C_{pin}$ is a non-linear one, with wet and extremely wet conditions having the same affect on $\delta^{13}C_{pin}$, while dry conditions may have more affect on $\delta^{13}C_{pin}$ values. This change in precipitation variability may also not be real and simply be as

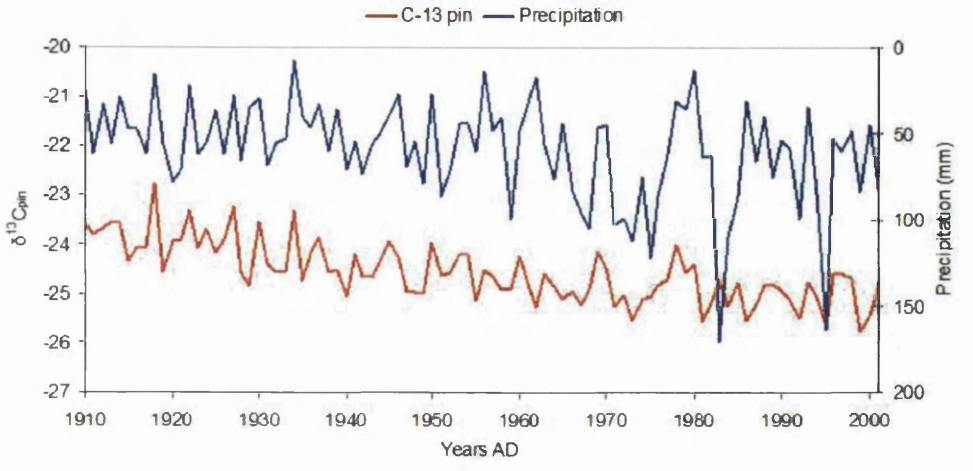

Figure 6.21: $\delta^{13}C_{pin}(‰)$ plotted against mean July and August precipitation from Andenes. Note that the precipitation axis has been inverted.

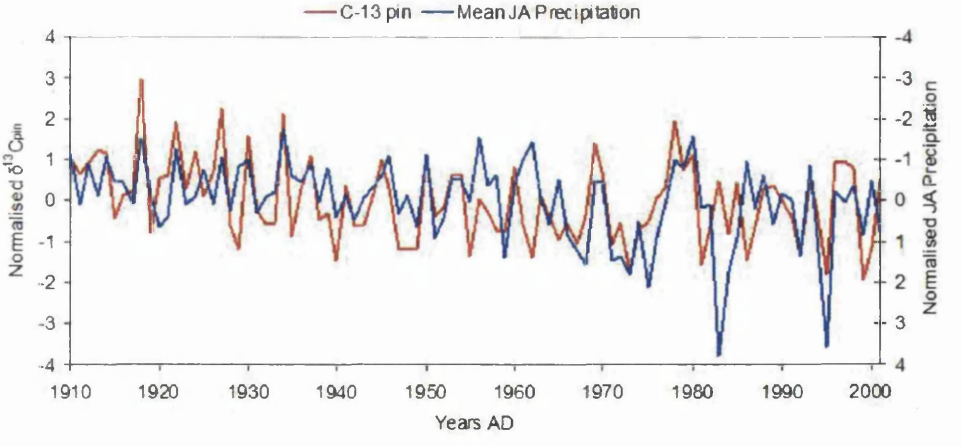

Figure 6.22: $\delta^{13}C_{pin}(‰)$ plotted against mean July and August precipitation from Andenes, with both data sets normalised to a mean of zero and a standard deviation of one. Note that the precipitation axis has been inverted.

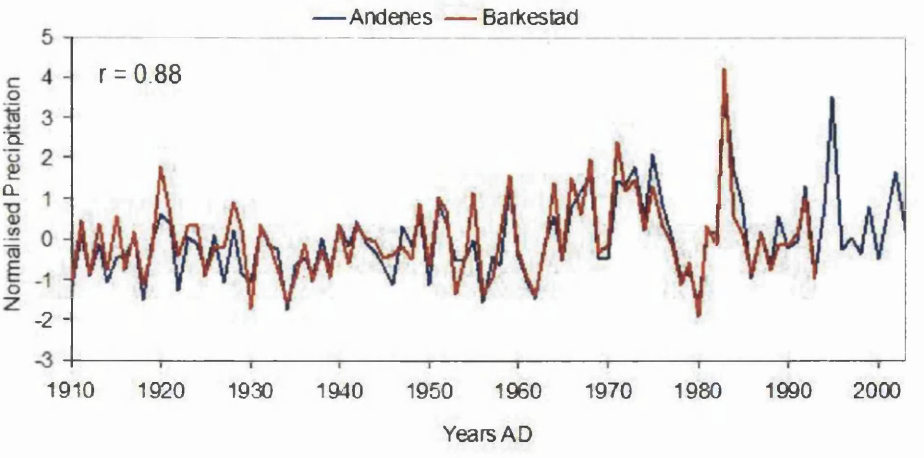

Figure 6.23: Comparison between mean July and August Andenes and Barkestad precipitation, both data sets have been normalised (to a mean of 0 and standard deviation of 1) for ease of comparison.

a result of some artifact in the way data at Andenes is collected, if so this obviously has important implications on the calibration of precipitation data from Andenes with proxy climate data and so to check this the record from Andenes was compared with the nearest climate station at Barkestad, some 60 km distant on the western edge of the Vesterålen archipelago and also with the regional precipitation data set compiled by Hanssen-Bauer and Føland (1998), these comparisons can be seen in Figures 6.23 and 6.24. As can be clearly seen from these figures both the general increase in precipitation and the change in variability are present in both of these records and so the precipitation data from Andenes would seem to be a reliable record.

A thirty year running correlation between $\delta^{13}C_{pin}$ and July, August and mean July and August precipitation can be seen in Figure 6.25. Figure 6.25 shows that the relationship between $\delta^{13}C_{pin}$ and precipitation is not stable through time, the pattern here is similar to the relationship between $\delta^{13}C_{pin}$ and temperature seen in Figures 6.10 and 6.11. The

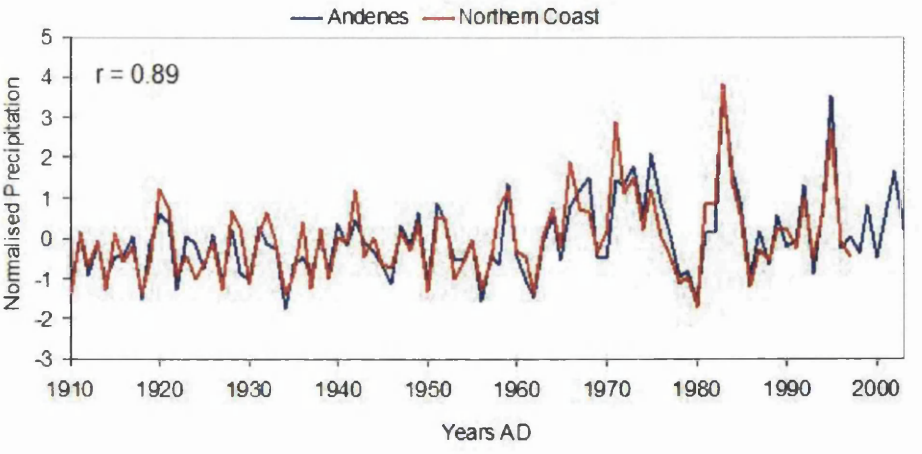

Figure 6.24: Comparison between mean July and August Andenes precipitation and the composite Northern Coastal record (Hanssen-Bauer and Føland, 1998) of which Andenes does not form a part, both data sets have been normalised (to a mean of 0 and standard deviation of 1) for ease of comparison.

most negative correlations between $\delta^{13}C_{pin}$ and precipitation occur in the middle years of the twentieth century with less negative correlations at the beginning and end of the sequence. However, the decline in the correlations is not so great at the begging of the sequence and the decline towards the end of the twentieth century can be explained by the excluding of the two largest residual years (AD 1962 and 1995). Figure 6.26 shows the 30 year maximum, minimum and mean correlations between July and August precipitation and $\delta^{13}C_{pin}$ with these two years removed, in this figure the correlation between precipitation and $\delta^{13}C_{pin}$ are more stable. Although the precipitation data are not as long as the temperature data, the decline in the correlation between mean July and August temperature and $\delta^{13}C_{pin}$ was already present by AD 1910 (see Figure 6.11). The correlation between precipitation and $\delta^{13}C_{pin}$ does not decline in the same manner. Which would appear to support the idea that the decline in correlation between temperature and $\delta^{13}C_{pin}$ is not as a result of dating or cutting errors.

A scatter plot of $\delta^{13}C_{pin}$ and mean July and August precipitation can be seen in Figure 6.27, this highlights an interesting aspect to the relationship between these two variables.

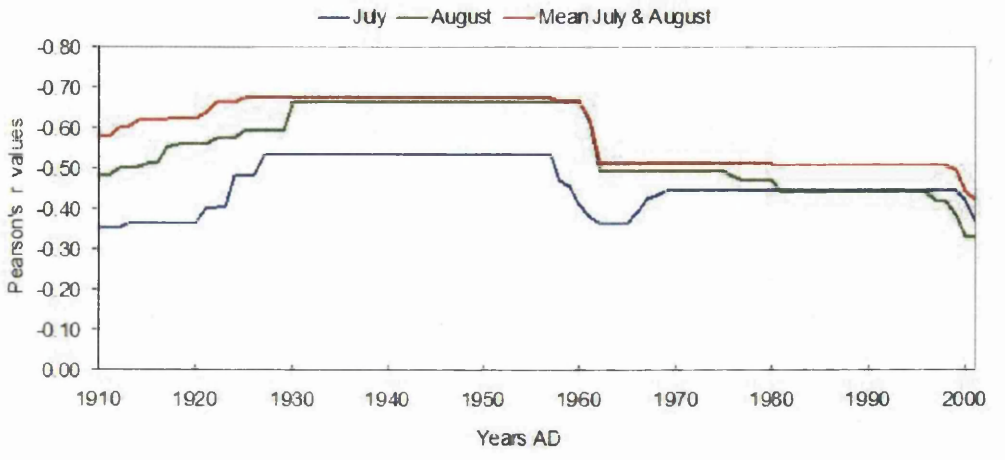

Figure 6.25: Thirty year maximum running correlations between $\delta^{13}C_{pin}(‰)$ and July, August and mean July and August precipitation from Andenes.

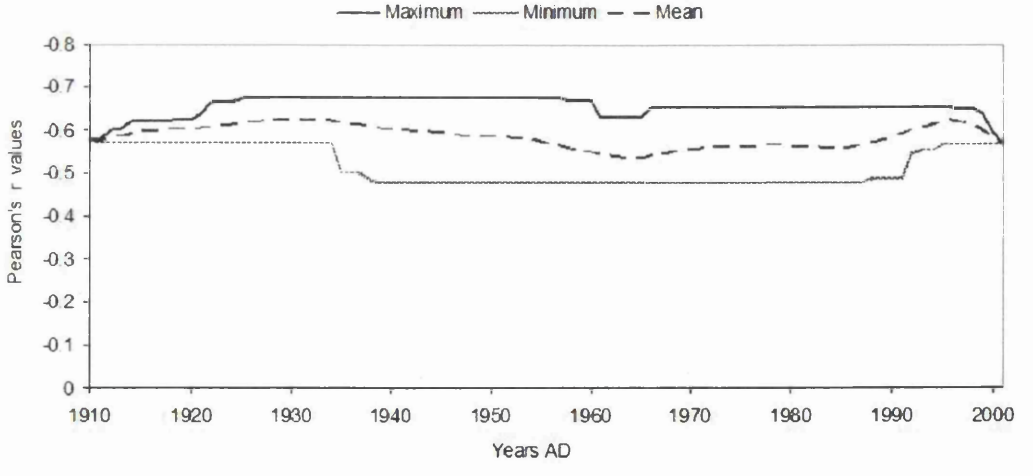

Figure 6.26: Thirty year running maximum, minimum and mean correlations between mean July and August precipitation and $\delta^{13}C_{pin}(‰)$. The largest residual years AD 1962 and 1983 have been removed.

It appears that, except for the year AD 1983, all the variability between $\delta^{13}C_{pin}$ and mean July and August precipitation falls under the line added to the graph. This seems to suggest that precipitation may limit isotope fractionation in one direction so that any value of $\delta^{13}C_{pin}$ can have a maximum level of precipitation assigned to it (except for the outlier year of AD 1983). So that while a mean July and August precipitation of say 75mm can encompass a range of isotope values from -25.00 to -23.75 an isotope value of -23.75 may only occur for a precipitation value of less than 75 mm. If correct this would seem to suggest that precipitation may control $\delta^{13}C_{pin}$ fractionation in a fairly general way by defining the maximum isotope value, while temperature may be responsible for much of the variation beneath the line. While this is not especially useful for reconstructing precipitation, as it can only give a maximum precipitation for any isotope values, it may prove useful when combining proxies and when trying to define thresholds. It should prove especially helpful in identifying very dry summers as the most positive $\delta^{13}C_{pin}$ results occur only in dry summers, Figure 6.27 shows that the seven most positive isotope values all occurred in summers with a mean July and August precipitation of less than 50 mm. While at higher levels of precipitation it is possible to have a much larger range of isotope results. This would seem to suggest that precipitation is a more important factor in isotope fractionation in dry years than wet years, although of course the timing of wet or dry periods is critical, as a dry or wet period may have a large effect on mean monthly precipitation values but miss the period critical for latewood formation and so have little effect on isotope values.

Much of the pattern seen in Figure 6.27 may be due to a negative relationship between temperature and precipitation, as low values for precipitation are likely to be associated with warmer than average temperature and visa versa and as we have already seen there is a fairly strong relationship between $\delta^{13}C_{pin}$ and summer temperatures. Figure 6.28 shows that there is a negative relationship between mean July and August temperature and precipitation (r = -0.41) and that again most of the points fall below the line added. There is however more spread than in Figure 6.27, especially for mid range temperatures and levels of precipitation and so, to some degree, precipitation may play a role in capping

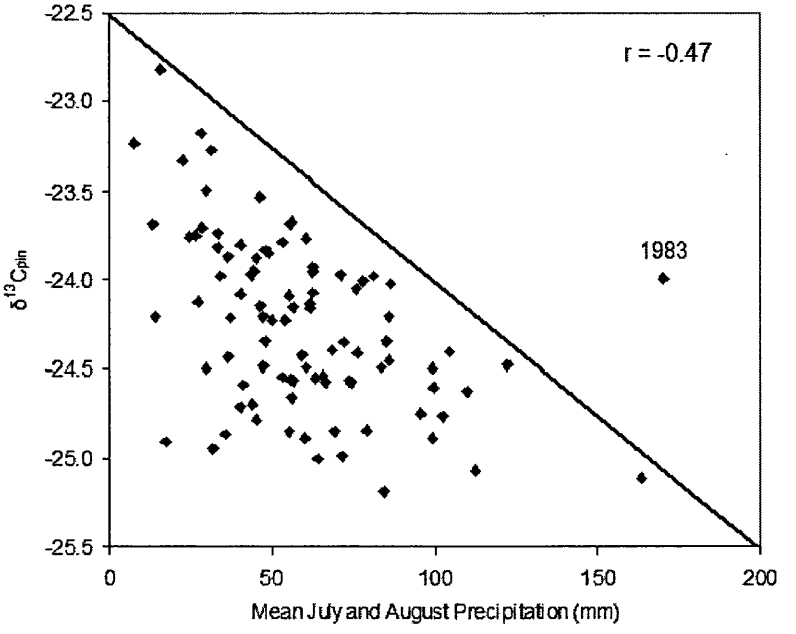

Figure 6.27: Scatter plot of Mean July and August precipitation and $\delta^{13}C_{pin}(‰)$, outlier year AD 1983 identified. A line suggesting the possible maximum $\delta^{13}C_{pin}(‰)$ for any given level of precipitation has been added.

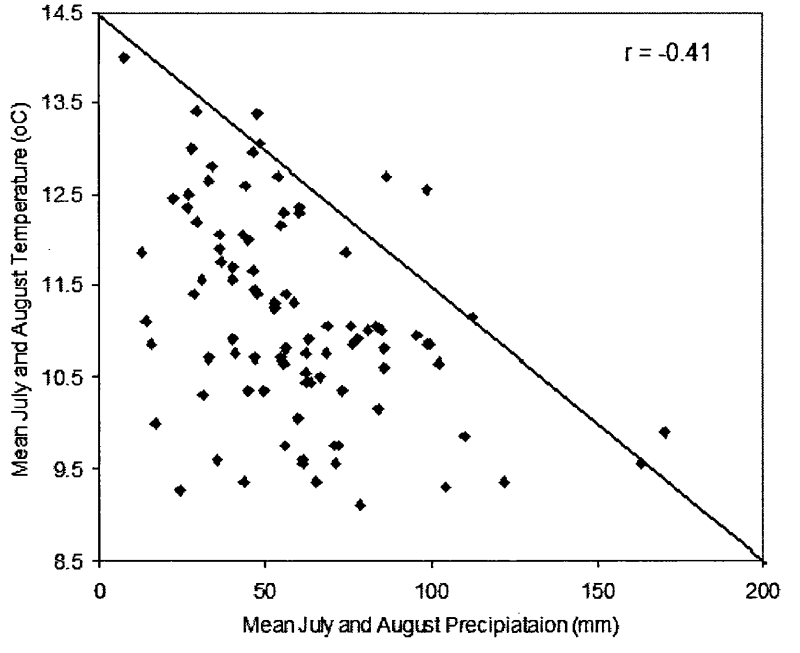

Figure 6.28: Scatter plot of Mean July and August precipitation and mean July and August temperature. A line similar to that in Figure 6.27 has been added, suggesting there may be a general maximum precipitation for any given temperature, and visa versa.

$\delta^{13}C_{pin}$ values.

In conclusion, there is a statistically significant relationship between $\delta^{13}C_{pin}$ and precipitation with mean July and August demonstrating the strongest and most consistent relationship. It is this data that will then be used in Section 6.6.1 to make a calibration of $\delta^{13}C_{pin}$ with precipitation.

6.4.2 Standardised Precipitation Index (SPI) and $\delta^{13}C_{pin}$

SPI is calculated by fitting a a probability density function to a precipitation frequency distribution summed over over the time scale of interest. The calculation is performed separately for each month. Every probability density function is then transformed to a standardised normal distribution to give the SPI. The values for SPI are laid out in Table 6.1, from extremely wet (2 or greater) to extreme drought (-2 or less), with their corresponding event probabilities. Figure 6.29 illustrates this process of transformation. The left hand panel shows the empirical cumulative probability distribution of the fitted gamma distribution for precipitation from 1901-99 over south east England (December, January and February three month average). The theoretical cumulative gamma distribution is fitted over the this (red line). The right hand panel shows a graph of standard normal cumulative probability. The conversion is made by by locating a given precipitation level (77 mm in this example) on the left hand graph and drawing a perpendicular to locate the intersection point on the theoretical distribution. Then project this point horizontally to the intersection of the graph of standard normal cumulative probability (right hand panel). The intersection between this point and a and a line drawn vertically down to the x axis determines the SPI (Lloyd-Hughes and Saunders, 2002). This is illustrated by the example from Lloyd-Hughes and Saunders (2002) in Figure 6.29. A more complete description and analysis of SPI can be found in Lloyd-Hughes and Saunders (2002). This includes the equations necessary for it's calculation.

SPI has three key advantages over alternative drought indices. The first advantage is simplicity requiring only precipitation for it's calculation. The more commonly used Palmer

SPI value	Category	Probability %
2.00 or more	Extremely wet	2.3
1.50 to 1.99	Severely wet	4.4
1.00 to 1.49	Moderately wet	9.2
0.00 to 0.99	Mildly wet	34.1
0.00 to -0.99	Mildly dry	34.1
-1.00 to -1.49	Moderate drought	9.2
-1.50 to -1.99	Severe drought	4.4
-2.00 or less	Extreme drought	2.3

Table 6.1: Classification of drought by SPI and the corresponding event probabilities (Lloyd-Hughes and Saunders, 2002)

Drought Severity Index (PDSI) requires an estimate of soil water holding capacity. SPI requires the calculation of only two parameters compared to the 68 for PDSI (Lloyd-Hughes and Saunders, 2002). By avoiding a dependence on soil moisture conditions SPI can be used effectively over all seasons and is not adversely affected by topography. The second advantage of SPI is that it can be calculated over a variety of timescales to take into account preceding precipitation by using a sum of between 1 to 48 months precipitation. The third advantage come from standardisation which ensures that the frequency of extreme events at a location on any timescale are consistent. There are also some potential disadvantages with SPI. Firstly the assumption that a suitable theoretical probability distribution can be found to model the precipitation data. A second related from is that reliable monthly precipitation data are required with a recommended minimum of 30 years of data (McKee et al., 1993). A third problem arises from standardisation. This means that severe droughts (wetness) will occur at the same frequency at all locations, when considered over a long enough time period. Thus, SPI is unable to identify area that are more drought prone than others. A forth problem comes when applying short time scales (1-3 months) in areas with low seasonal precipitation. In such cases, misleadingly large positive or negative SPI values may be produced (Lloyd-Hughes and Saunders, 2002). None of these disadvantages seems likely to affect Forfjorddalen. While developed for drought analysis in the United States it is becoming more widely used in Europe (Lloyd-Hughes and Saunders, 2002) and in European dendroclimatology (Linderholm and Molin, 2005; Touchan et al., 2005).

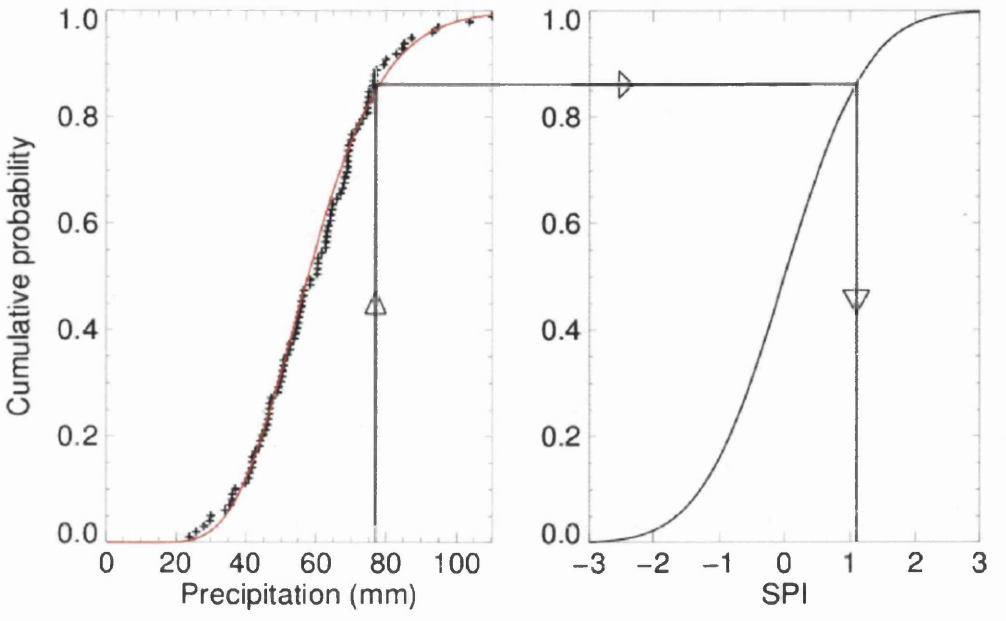

Figure 6.29: Example of transformation form a gamma distribution to the standard normal distribution. Data are from the the south east of England for the three month average precipitation (DJF) (Lloyd-Hughes and Saunders, 2002). (After Edwards and McKee (1997))

As discussed above a major advantage of the SPI is that it can be run over a number of timescales so that the precipitation of previous months can be taken into account. As has already been established, in Section 6.4.1, August appears to be the single most important month for $\delta^{13}C_{pin}$ fractionation and so the SPI was run for August with a variety of lags in an attempt to determine which demonstrates the best relationship with $\delta^{13}C_{pin}$. The results of this can be seen below in Figure 6.30, with lags at 1, 2, 3, 4, 5, 6, 12, 24 and 48 months. This shows that, as one might expect for tree growth it is the lags of less that 6 months which demonstrate the best relationship with $\delta^{13}C_{pin}$, with the best correlations for August SPI lagged by 3 months ($r = 0.50$) and 6 months ($r = 0.49$), this seems reasonable when considering which months precipitation demonstrated a relationship with $\delta^{13}C_{pin}$ (see Figure 6.19). Figure 6.31 shows the relationship between both 3 and 6 month August SPI and $\delta^{13}C_{pin}$ through time, using a 30 year running correlation, the pattern for both is similar with perhaps the 3 month SPI more stable

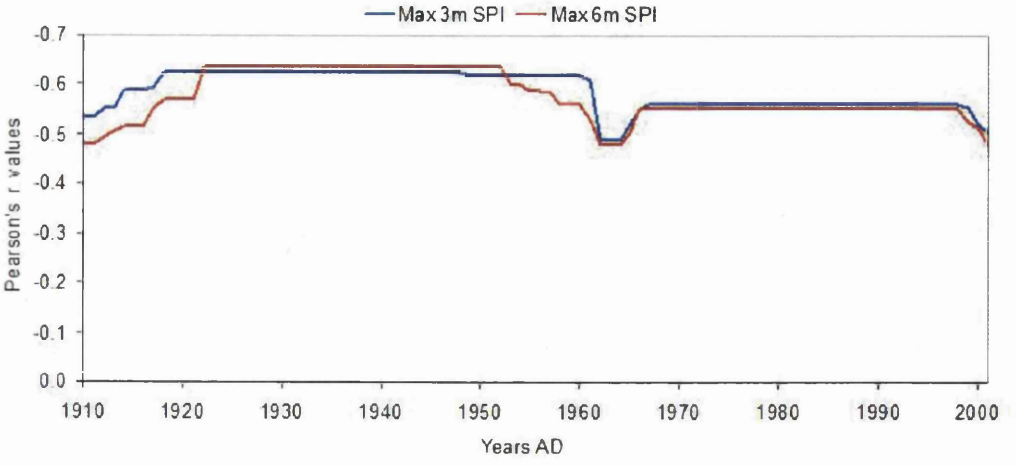

Figure 6.31: Maximum 30 year running correlations between 3 and 6 month August SPI and $\delta^{13}C_{pin}$.

through time.

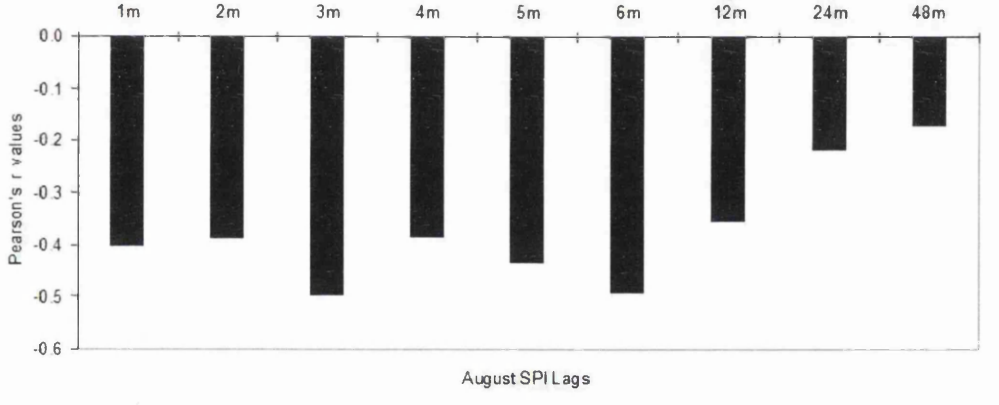

Figure 6.30: Bar chart showing the correlation between $\delta^{13}C_{pin}$(‰) and the calculated Standardised Precipitation Index (SPI), lagged by 1, 2, 3, 4, 5, 6, 12, 24 and 48 months.

When the two largest residual years are removed (AD 1962 and 1983), the August 3 month SPI ($r = 0.59$) establishes a rather stronger relationship with $\delta^{13}C_{pin}$ than the 6 month SPI ($r = 0.55$), although all correlations improved (24 and 48 month only marginally). The maximum 30 year running correlation without these residual years can be seen in Figure 6.33, this shows that now the correlation between the August 3 month SPI and $\delta^{13}C_{pin}$ is consistently the strongest and actually increases towards the end of the

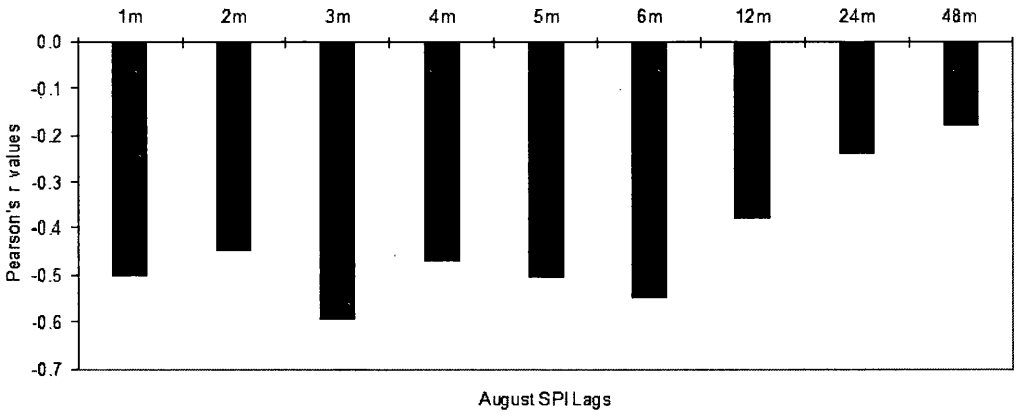

Figure 6.32: Bar chart showing the correlation between $\delta^{13}C_{pin}$(‰) and the calculated Standardised Precipitation Index (SPI) excluding AD 1962 and 1983, lagged by 1, 2, 3, 4, 5, 6, 12, 24 and 48 months, excluding AD 1962 and 1983.

twentieth century. It seems that the 6 is less sensitive to the effect of these two residual years than does the shorter term 3 month model, however the 3 month SPI (including data for June, July and August precipitation) has the strongest relationship with $\delta^{13}C_{pin}$. It seems reasonable, in an area with a short growing season combined with the high levels of precipitation and the rather free draining nature of the substrate, that $\delta^{13}C_{pin}$ is likely to be most strongly effected by fluctuations in summer precipitation.

It would appear that the August SPI lagged by 3 months demonstrates a better relationship with $\delta^{13}C_{pin}$ than does mean July and August precipitation and so this will also be used for calibrating the $\delta^{13}C_{pin}$ later in this chapter in Section 6.6.2 to see if it is a more suitable variable to reconstruct using $\delta^{13}C_{pin}$ than mean July and August precipitation.

6.4.3 A test of the pre-industrial CO_2 correction

A potential problem with the PIN correction as applied to the Forfjorddalen data is that there is an environmental variable (increased precipitation) which may explain the continued decline in $\delta^{13}C_{cor}$ data the Seuss correction for the increasing proportion of ^{12}C in the atmosphere, without further recourse to correcting for increased CO_2 in the atmosphere. If the decline in $\delta^{13}C_{cor}$ values were explicable by increased precipitation

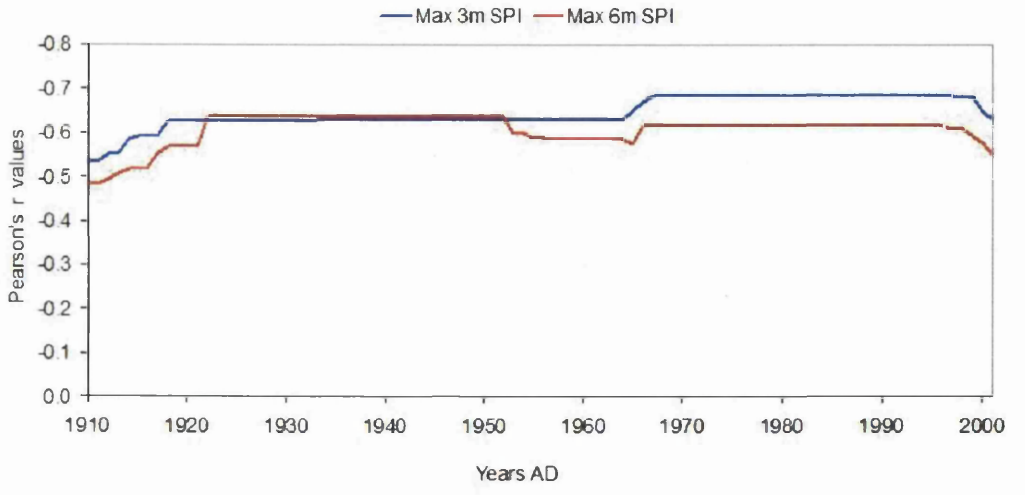

Figure 6.33: Maximum 30 year running correlations between 3 and 6 month August SPI and $\delta^{13}C_{pin}$(‰) , excluding AD 1962 and 1983.

it would seem reasonable to expect the trend in precipitation to be similar to that in the $\delta^{13}C_{cor}$ data. Figure 6.34 compares normalised $\delta^{13}C_{cor}$ and mean July and August precipitation, while Figure 6.35 compares normalised precipitation with $\delta^{13}C_{pin}$. The data have been normalised (mean of 0 and standard deviation of 1) to ease comparison and linear best fit trend lines have been added to each variable to determine any trends, in both graphs the precipitation axis has been inverted.

Figures 6.34 and 6.35 would both seem to suggest that the trend, represented by the best fit line, in the pin corrected data ($\delta^{13}C_{pin}$) matches the trend in the mean July and August precipitation data much better than does the trend in the $\delta^{13}C_{cor}$ data. The slope of the best fit line for mean July and August precipitation is 0.0136 in both figures, while the figure for the $\delta^{13}C_{pin}$ data at -0.0112 (the sign is opposite as the relationship between δ^{13}C and moisture availability is a negative one) is much closer to the precipitation trend than that for the $\delta^{13}C_{cor}$ data at -0.0266. Although interestingly the overall correlation between mean July and August precipitation is better than for the $\delta^{13}C_{cor}$ data (r = -0.53) than for the $\delta^{13}C_{pin}$ (r = 0.47), although this appears to have much to do with the way in which the model based on $\delta^{13}C_{cor}$ deals with the largest outliers (AD 1928, AD 1962 and AD 1983). It would then seem that the pin correction not only improves

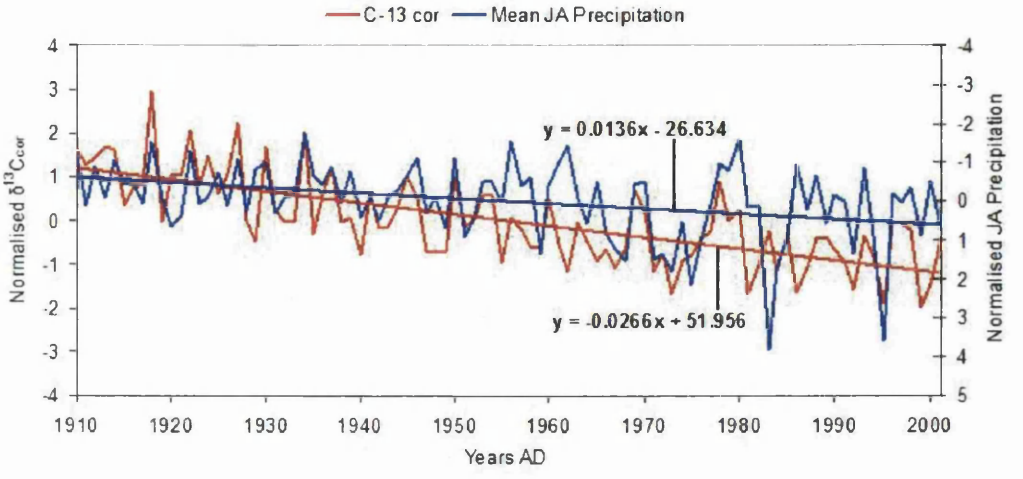

Figure 6.34: Mean July and August precipitation compared to $\delta^{13}C_{cor}(‰)$. Linear best fit trend lines have been added to each data series and the equation for each added to the chart, showing the slope and intercept of each line. The precipitation axis has been inverted to ease comparison.

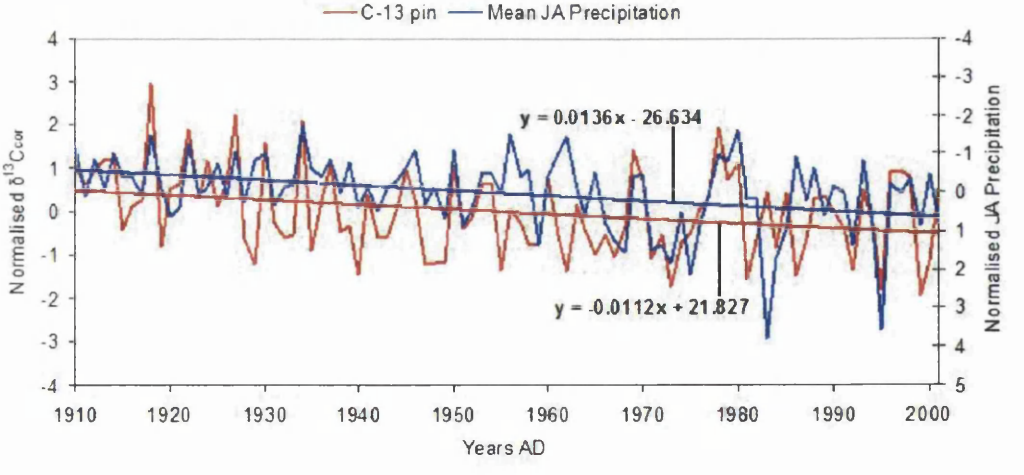

Figure 6.35: Mean July and August precipitation compared to $\delta^{13}C_{pin}(‰)$. Linear best fit trend lines have been added to each data series and the equation for each added to the chart, showing the slope and intercept of each line. The precipitation axis has been inverted to ease comparison.

the fit of temperature with the δ^{13}C data, but also brings the trend of the $\delta^{13}C_{pin}$ data into a better agreement with mean July and August precipitation data than the $\delta^{13}C_{cor}$ data. This suggests that the pin correction is justifiable and that the trend removed is likely to be due to increased atmospheric CO_2.

6.5 Calibration of $\delta^{13}C_{pin}$ and Temperature

6.5.1 Calibration procedure and statistics

For calibration purposes meteorological data sets will be split in two with a calibration period and a verification period, the process will then be reversed with the initial verification period being used as the calibration period. A calibration and verification will then be carried out on the complete data sets. Calibration will be undertaken using the best fit regression equation shown in equation 6.1 between temperature (on the *y* axis) and $\delta^{13}C_{pin}$ (on the *x* axis) so that $\delta^{13}C_{pin}$ predicts temperature for the calibration period, this will then be used to predict temperature for both the calibration and the verification period by applying the regression equation to the $\delta^{13}C_{pin}$ for both periods.

$$y = c + bx \tag{6.1}$$

In equation 6.1 *y* is the predicted value (temperature in this case) and *x* is the predictor ($\delta^{13}C_{pin}$), *b* is the slope of the regression line and can be calculated with equation 6.2 and *a* is the intercept which can be calculated using equation 6.3.

$$b = \frac{\sum(x - \bar{x})(y - \bar{y})}{\sum(x - \bar{x})^2} \tag{6.2}$$

$$a = \bar{y} - b\bar{x} \tag{6.3}$$

To test the predictive skill of the resulting reconstructions four statistical tests, which are

commonly used in statistics and geosciences will be used (NRC, 2006): mean squared error (MSE); reduction of error (RE); coefficient of efficiency (CE); and the squared correlation (r^2). MSE is a measure of how close a set of predictions are to the actual values, the formula for calculating this can be seen in equation 6.4, where y_t denotes temperature at time t and $\hat{y}_t$ denotes temperature at time t predicted by $\delta^{13}C_{pin}$.

$$MSE = \frac{1}{N}\sum (y_t - \hat{y}_t)^2 \tag{6.4}$$

The RE statistic (Fritts, 1976) tests how well the MSE of the reconstruction over the verification period ($\hat{y}_t$) perform when compared to the MSE of the mean temperature of the calibration period ($\bar{y}_c$). The theoretical range of the RE statistic is from $+1$, which indicates perfect agreement, to minus infinity, minus values in practice are treated as zero and indicate no agreement (Fritts, 1976). One problem with the RE (and indeed the CE) statistic is that one very bad estimate can offset the effect of several very good estimates (Fritts, 1976). If a reconstruction is then to have any predictive power it should do better than the mean the calibration period and have a RE of greater than zero (NRC, 2006)

$$RE = 1 - \frac{MSE\left(\hat{y}_t\right)}{MSE\left(\bar{y}_c\right)} \tag{6.5}$$

A more demanding test of the performance of a reconstruction is the CE statistic shown in equation 6.6. Here rather than comparing the MSE $(\hat{y}_t)$ to that of the mean of the calibration period MSE($\bar{y}_c$) it is compared with the mean temperature over which the reconstruction is being made (MSE($\bar{y}_i$). It is a more demanding statistic than the RE and its value (although on the same scale) and will in practice always be lower and the difference between it and the CE statistic will become greater as the difference between sample means of the calibration and verification periods increases (NRC, 2006).

$$CE = 1 - \frac{MSE\left(\hat{y}\right)}{MSE\left(\bar{y}_i\right)} \tag{6.6}$$

The measure of association between two variables that is normally used is the squared

correlation (r^2), which represents the proportion of the total variance explained by the predicted values. It measures the strength of the linear relationship between two variables and can be calculated using equation 6.7. Its range is from -1 (perfect negative correlation) to +1 (perfect positive correlation), while figure around 0 would indicate little or no relationship.

$$r^2 = \frac{\left[\sum (y_t - \bar{y}_i)\left(\hat{y}_t - \bar{\hat{y}}\right)\right]^2}{\sum (y_t - \bar{y}_i)^2 \left(\hat{y}_t - \bar{\hat{y}}\right)^2} \tag{6.7}$$

The combination of these four statistics is very useful as they all have slightly different things to say about the comparison of two variables. For example a high r^2 value may be indicative of an extremely good linear relationship between two variables, but it is quite possible for these two variable to have minus RE and CE. An example of this can be seen in Figure 6.36 (NRC, 2006). The blue line in Figure 6.36 shows a hypothetical temperature series, the red line represents a reconstruction of this which has a perfect r^2 of +1 but a CE of -18.09 and so is perfectly correlated but has no predictive skill. The dashed blue line is the mean of the temperature series and has a r^2 and a CE of zero. The blue and green lines both have a CE of 0.50, while the green line has an r^2 value of 0.51 and the blue line of 0.68. Obviously despite having the same CE they both match temperatures in different ways, the blue line correlates with the high and low frequency fluctuation while the green line captures only the low frequency variation (NRC, 2006). This example illustrates that neither r^2 nor CE contain all the information required to test reconstruction error on their own.

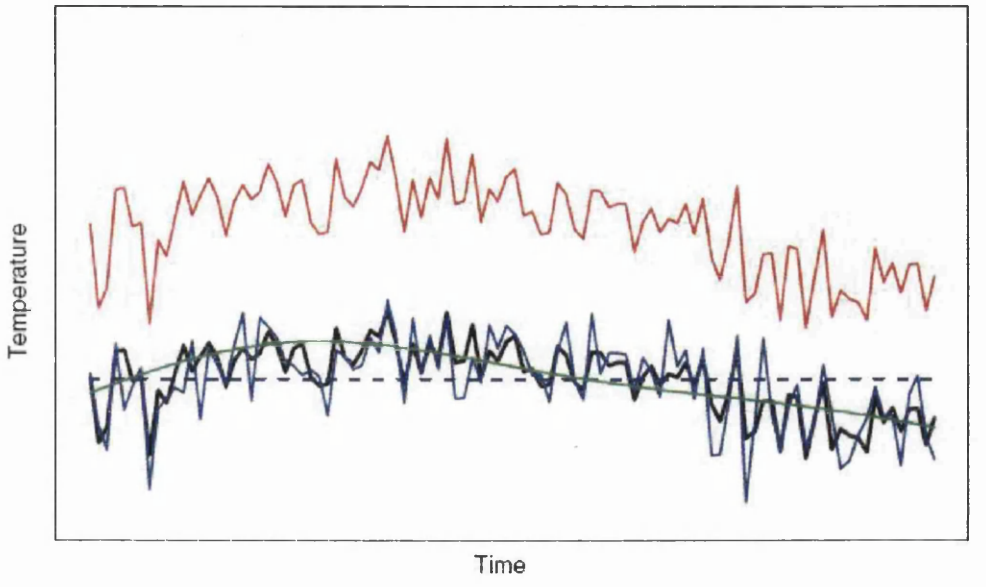

Figure 6.36: A hypothetical temperature series (black line) and four possible reconstructions (NRC, 2006)

6.5.2 Andenes Calibration

Calibration will initially be carried out using $\delta^{13}C_{pin}$ and mean July and August temperature from Andenes for the period AD 1869 to 2001. Figure 6.37A shows the reconstructed mean July and August temperature compared to the actual mean temperature for the calibration period from AD 1869-1934 and the verification period from AD 1935-2001, while Table 6.2 shows the statistics for both the calibration and verification period. While a calibration based on this period (AD 1869-1934) is able to outperform the mean temperature of the calibration period (RE statistic) with an RE of 0.22 for the verification period of AD 1935-2001 it is unable to outperform the mean of the verification period (CE statistic) with a CE of -0.04, although the r^2 is high at 0.40, demonstrating again the point made in Figure 6.36, that a high correlation does not guarantee good predictive skill. The reason for this can be better understood with reference to Figure 6.37A which shows that the temperatures for the period AD 1935 to 2001 are mostly under predicted by the calibration based on the period AD 1869-2001. The variance of the reconstructed

time series is also much smaller than the actual temperature.

This calibration performed in reverse, calibrated on the period AD 1935 to 2001 and verified for the period AD 1869 to 1935, can be seen in Figure 6.37B with the statistics for this calibration in Table 6.2. The statistics for the calibration period are positive and Figure 6.37B confirms that the $\delta^{13}C_{pin}$ of the period AD 1935-2001 is able to reconstruct its temperature ($r^2 = 0.40$). The statistics for the verification period (AD 1869-1934) are, however, poor with an RE of only 0.04 and a negative CE statistic of -0.26. Figure 6.37B shows that while the reconstruction for this period appears to be good after the mid AD 1920s and before about AD 1880 it is very poor for the intervening period, which has already been discussed at some length and highlighted as potentially problematic for any temperature reconstruction based on $\delta^{13}C_{pin}$ (see Sections 6.2.1 and 6.2.2). The same divergence between actual and predicted temperatures can also be seen in Figure 6.37A, to a lesser degree suggesting that even a calibration based on $\delta^{13}C_{pin}$ using this problematic period is unable to successfully reconstruct temperature.

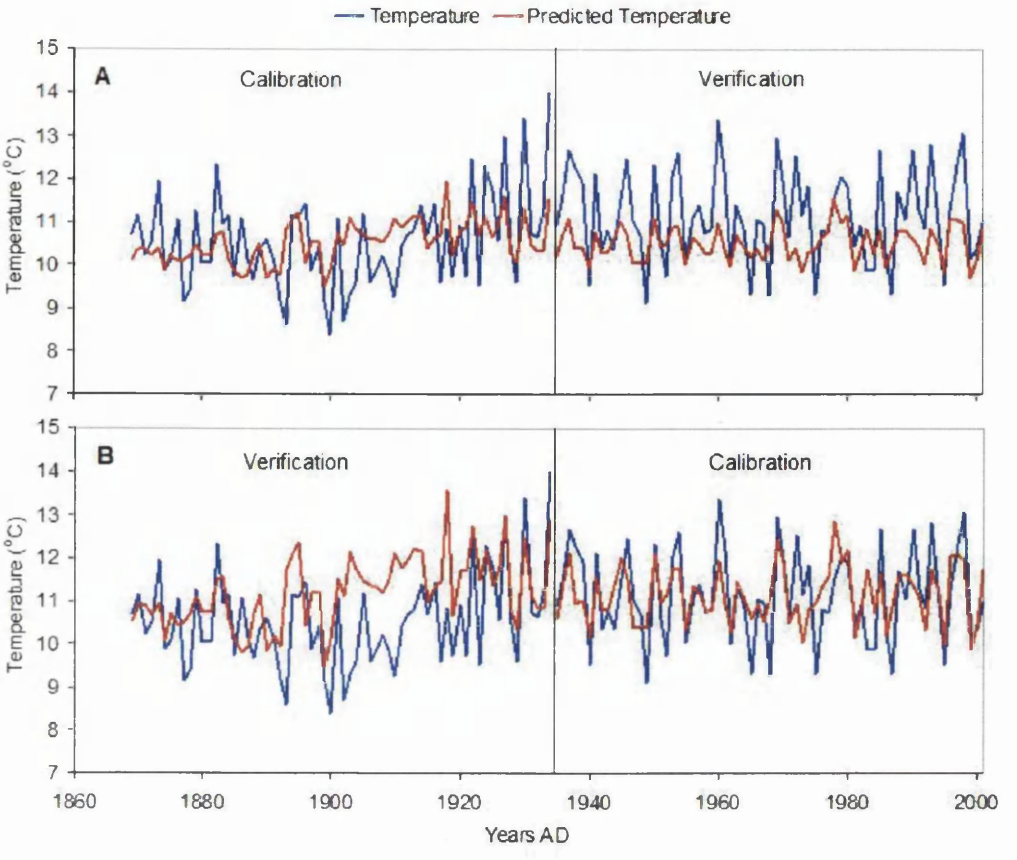

Figure 6.37: Reconstructed mean July and August temperatures using (A) AD 1869-1934 as the calibration period and AD 1935-2001 as the verification period and (B) AD 1935-2001 as the calibration period and AD 1869-1934 as the verification period. In both cases compared to actual mean July and August temperature.

	Calibration AD AD 1869-1934	Verification AD 1935-2001	Calibration AD 1935-2001	Verification AD 1869-1934
MSE	0.94	1.16	0.67	1.50
RE	0.21	0.22	0.40	0.04
CE	NA	-0.04	NA	-0.26
r^2	0.21	0.40	0.40	0.21

Table 6.2: Verification statistics for the mean July and August temperature reconstruction using the (on the left) AD 1869-1934 for calibration and AD 1935-2001 for verification an (on the right) AD 1935-2001 for calibration and AD 1869-1934 for verification.

The results of this calibration and reconstruction procedure carried out using the entire period (AD 1869 to 2001) can be seen compared to actual mean July and August temper-

atures in Figure 6.38. The statistics (without the CE statistic which is not appropriate here) can be seen in Table 6.3, the r^2here is 0.25. Figure 6.38 shows the divergence between the actual and predicted temperatures from the late nineteenth century to the mid AD 1920s.

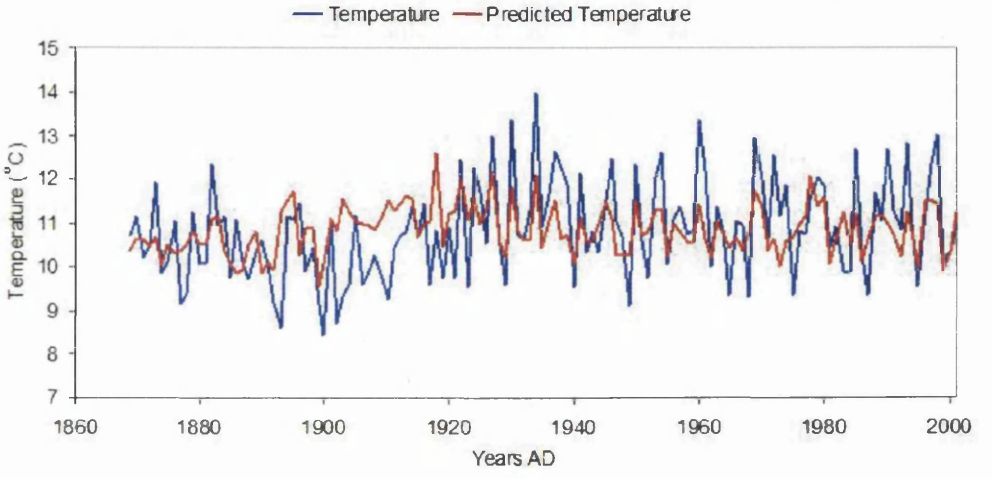

Figure 6.38: Reconstructed mean July and August temperatures from AD 1869-2001 using the same period for calibration, compared to actual temperature.

	Calibration AD 1869-2001
MSE	0.93
RE	0.25
CE	NA
r^2	0.25

Table 6.3: Statistics for the mean July and August temperature reconstruction AD 1869-2001, using the same period for calibration.

It is clear from Figure 6.37 and Table 6.2 that $\delta^{13}C_{pin}$ does not reconstruct temperature successfully for the period AD 1869 to 2001. CE statistics for both verification periods are negative, demonstrating that there is lower error in predictions based on the mean temperature of the period being reconstructed than of the reconstruction based on $\delta^{13}C_{pin}$ of the calibration period. Although, again in both cases, the reconstructed temperature is able to outperform the mean of the calibration period (RE statistic) although this is only just the case for the calibration period AD 1969-1934 (RE = 0.04).

The period ~AD 1880s to 1920s appears problematic in terms of the $\delta^{13}C_{pin}$ from Forfjorddalen. Not only is there a low correlation with temperature during this period but also, more importantly, there is an extremely low between-tree correlation for the $\delta^{13}C_{pin}$ during the period ~AD 1880 and 1910, and also a large divergence in trend between $\delta^{13}C_{pin}$ and temperature in the early years of the twentieth century. It is proposed that during this period a climatic regime persists which makes δ^{13}C unreliable for reconstructing summer temperature. Carbon isotope fractionation can be controlled by both temperature and moisture availability, which to some degree appears the case at Forfjorddalen. The effect of temperature and precipitation on carbon isotope fractionation will be in the same direction (positive or negative) when a negative relationship exists between temperature and precipitation (warm/dry or cold/wet). If however it is both wet and warm or cool and dry (which is probably the most important here as moisture is likely to become more important in δ^{13}C fractionation in very dry years) these two climatic variable will be pulling the carbon isotope fractionation in opposite directions (cool = negative & dry = positive), this climatic regime seems to be typical of the late nineteenth century and early twentieth century and would seem likely to affect the normally strong positive relationship between $\delta^{13}C_{pin}$ and summer temperature. This will be discussed at greater length in Chapter 7 and a model carbon isotope fractionation in relation to both temperature and precipitation will be presented. Climate calibration will proceed excluding this part of the $\delta^{13}C_{pin}$ record, which has a poor inter-correlation between trees.

It must be stressed that it not proposed to exclude the period from AD 1869 to 1927 simply because it does not correlate well with temperature and so does not fit a preconceived model of δ^{13}C and temperature; this would not be justifiable. This period is considered worth excluding from the calibration model for the following reasons: a) it has a very poor between-tree signal (EPS considerably less than 0.85) and so the data from this period would not normally be considered reliable enough to reconstruct climate; and b) because it is believed that the reasons for the breakdown between the common signal between the tree and therefore the correlation with climate can be explained by recourse

to isotope theory. In addition, it will be excluded only if it can be established that this period is anomalous (in the available records) and that summer temperatures prior to this can be reconstructed as reliably as those after it. Indeed, this period is perhaps of greater interest that the rest of the period for which climate data are available as it has potentially important lessons to teach us about how to go about effective climatic reconstructions using isotopes from tree rings and the dangers of relying on one proxy record which may be affected by more than one climatic variable. Thorough analysis of the period has allowed for the development of a conceptual model of carbon isotope fractionation and an approach to multiproxy dendroclimatology which may lead to a fuller understanding of past climate; this will be discussed in Chapter 7.

A reconstruction of mean July and August temperature using only the period from AD 1927 to 2001 can be seen in Figure 6.39 and Table 6.4, the same calibration and verification method will be used except with the more restricted data set. Figure 6.39B shows the reconstructed mean July and August temperature compared to the actual mean temperature for the verification period from AD 1927 to 1963 for the reconstruction calibrated on the period AD 1964 to 2001, while Table 6.4 shows the verification statistics for both the calibration and verification period. Both these would seem to demonstrate that the calibration based on the period from AD 1964 to 2001 successfully reconstructs mean July and August temperatures for the period from AD 1927 to 2001, with a high r^2 of 0.70 and high positive RE (0.58) and CE (0.56) statistics, demonstrating that the reconstruction considerably out performs the mean of both calibration period (AD 1927-2001) and the verification period (AD 1927-1963) from which the values are withheld from the calibration. The statistics for the calibration period are lower with an r^2 of 0.33.

The results for the calibration and verification periods reversed (calibration, AD 1927-1963 and verification AD 1964-2001) can be seen in Figure 6.39A and Table 6.4. The reconstruction for the verification period here is not as good as the above reconstruction with an r^2 of 0.33, an RE of 0.21 and a CE of 0.18. The reconstruction of the calibration period works well with a high r^2 of 0.70. A likely reason for the generally lower figures for the period AD 1964 to 2001 can be seen in Figures 6.10 and 6.11 which show that the

correlation between $\delta^{13}C_{pin}$ and mean July and August temperature and more especially mean July temperature falls away during this period. The ability of the reconstruction based on this period to reconstruct mean July and August temperatures for the period from AD 1927 to 1963 so well (Figure 6.39A and Table 6.4) demonstrates that the reconstruction is robust, performing well on data withheld from the calibration.

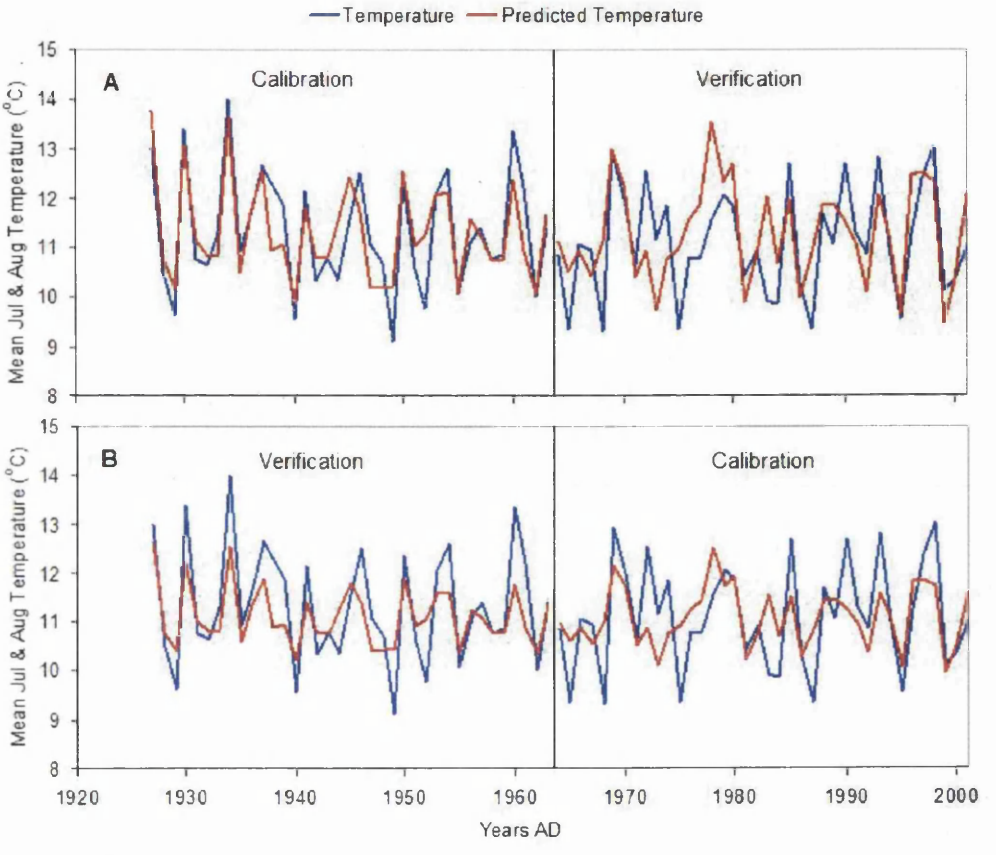

Figure 6.39: Reconstructed mean July and August temperatures using (A) AD 1927-1963 as the calibration period and AD 1964-2001 as the verification period and (B) AD 1964-2001 as the calibration period and AD 1927-1963 as the verification period. In both cases compared to actual mean July and August temperature.

	Calibration AD 1927-1963	Verification AD 1964-2001	Calibration AD 1964-2001	Verification AD 1927-1963
MSE	0.41	0.94	0.76	0.59
RE	0.70	0.22	0.33	0.58
CE	NA	0.18	NA	0.56
r^2	0.70	0.33	0.33	0.70

Table 6.4: Verification statistics for the mean July and August temperature reconstruction using the (on the left) AD 1927-1963 for calibration and AD 1964-2001 for verification an (on the right) AD 1964-2001 for calibration and AD 1927-1963 for verification.

When the period AD 1927 to 2001 is taken in its entirety, the reconstructed July and August temperatures plotted against the actual mean July and August temperatures can be seen in Figure 6.40 with statistics shown in Table 6.5. The model again performs well with a high r^2/RE of 0.50.

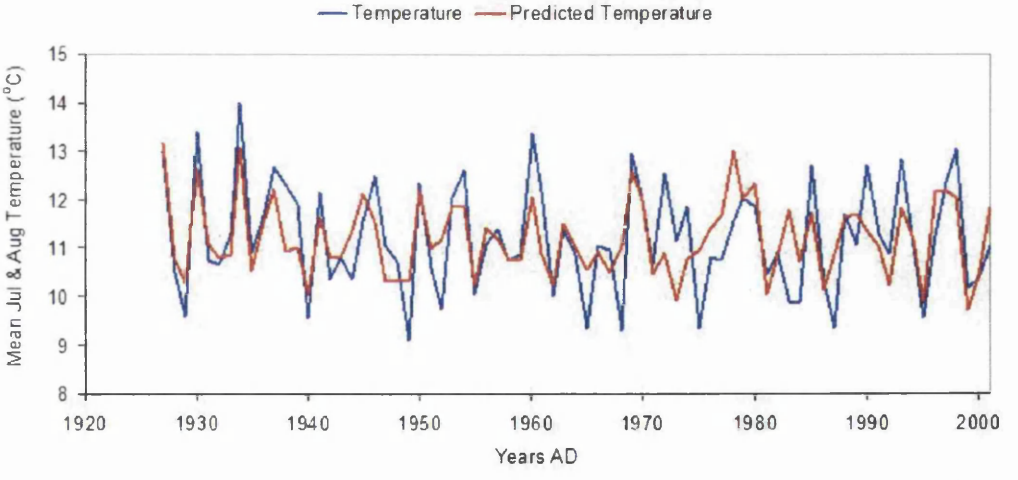

Figure 6.40: Reconstructed mean July and August temperatures from AD 1927-2001 using the same period for calibration, compared to actual temperature.

	Calibration AD 1927-2001
MSE	0.63
RE	0.50
CE	NA
r^2	0.50

Table 6.5: Verification statistics for the mean July and August temperature reconstruction AD 1927-2001, using the same period for calibration.

These data suggest that the $\delta^{13}C_{pin}$ for the period AD 1927 to 2001 are able to reconstruct mean July and August temperature in this area successfully. By tuning to the longer, more distant, Tornedalen temperature record it may be possible to determine how well the $\delta^{13}C_{pin}$ from Forfjorddalen can reconstruct regional temperature. This longer record may also establish whether $\delta^{13}C_{pin}$ can reconstruct temperatures in the earlier part of the nineteenth century, or whether weak relationship between $\delta^{13}C_{pin}$ and temperatures (~AD 1880-1920) persists throughout the AD 1900s.

6.5.3 Tornedalen Calibration

As discussed in Section 6.2.2 the composite temperature record from the Tornedalen area of subarctic Sweden (Klingbjer and Moberg, 2003) is a useful comparison record for the Forfjorddalen data. It can help to determine whether $\delta^{13}C_{pin}$ re-establishes the strong positive relationship with summer temperature found through most of the twentieth century in the period between AD 1802-1868. To determine this the same calibration/verification procedure as was used with the Andenes temperature record was undertaken.

As demonstrated in Section 6.2.2 mean July and August temperatures from Tornedalen consistently exhibit the strongest relationship with $\delta^{13}C_{pin}$ and so a mean of these two months will be used for calibration and verification. The initial calibration and verification procedure described in Section 6.5.1 was undertaken for the entire period AD 1802 to 2001, including the problematic period from AD 1880 to 1926 and the early period for which July and August temperatures are considered unreliable (around pre AD 1830) (Klingbjer and Moberg, 2003). This data set was split in two, AD 1902 to 2001 and AD 1802 to 1901. The results can be seen in Table 6.6 with the reconstructed temperature of the verification period compared to actual temperatures in Figure 6.41B. At a distance of around 450 km one would not expect the Tornedalen reconstruction to be as good as for Andenes, but despite this distance and problems with two periods of the data set (mentioned above) both the RE and CE statistics show that this reconstruction has a certain amount of predictive power, although the r^2 values are relatively low.

The verification statistics for this calibration in reverse can be seen again in Table 6.6 and the reconstruction for the verification data set (AD 1902-2001) compared to actual temperatures in Figure 6.41A. Once again the verification statistics are greater than zero and so out-perform the mean in terms of predictive power, with again fairly high values for the RE statistics and rather more modest but still positive values for the CE statistic. This is despite the divergence between the reconstruction and the actual temperatures in the early twentieth century (Figure 6.41). This departure can also be seen in Figure 6.42, which shows the temperatures reconstructed over the entire period compared to the Tornedalen record. The statistics for this can be seen in Table 6.7. These statistics suggest that once again this model has some reconstructive power, although with a rather reduced magnitude of variability.

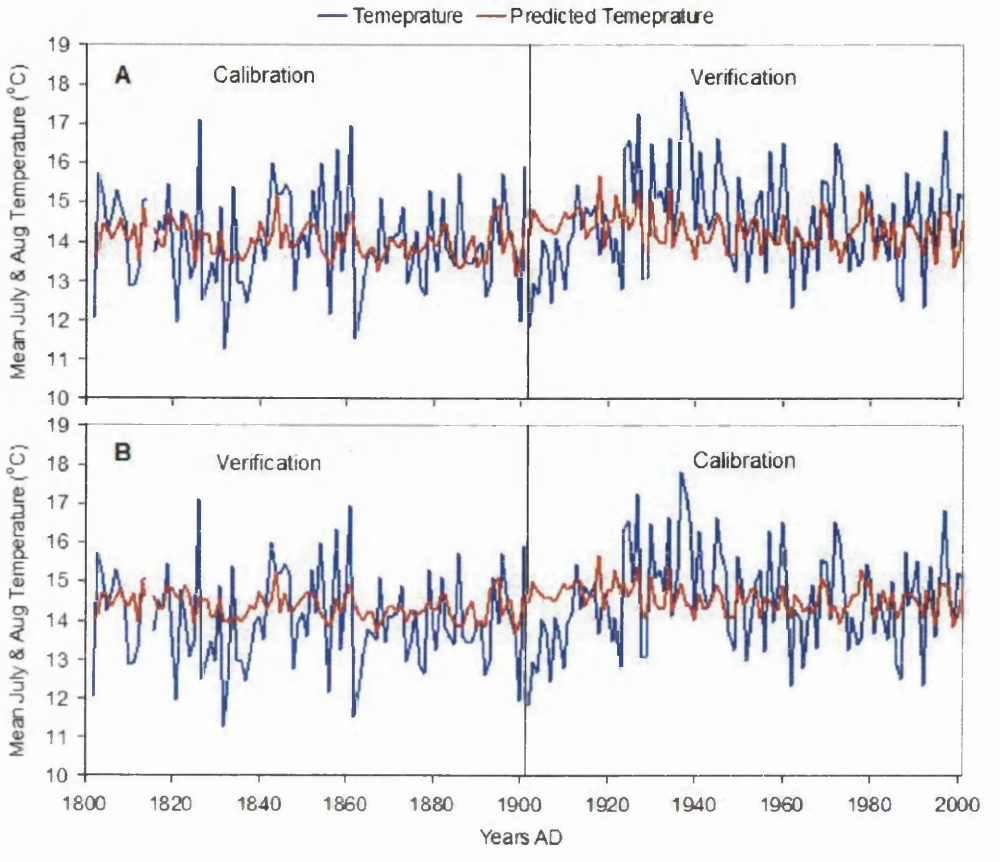

Figure 6.41: Reconstructed mean July and August temperatures using (A) AD 1802-1901 as the calibration period and AD 1902-2001 as the verification period and (B) AD 1902-2001 as the calibration period and AD 1802-1901 as the verification period. In both cases compared to actual mean July and August temperature from the Tornedalen record (Klingbjer and Moberg, 2003).

	Calibration AD 1802-1901	Verification AD 1902-2001	Calibration AD 1902-2001	Verification AD 1802-1901
MSE	1.21	1.52	1.43	1.33
RE	0.12	0.19	0.08	0.21
CE	NA	0.03	NA	0.03
r^2	0.12	0.08	0.08	0.12

Table 6.6: Verification statistics for the mean July and August temperature reconstruction using the (on the left) AD 1802-1901 for calibration and AD 1902-2001 for verification an (on the right) AD 1902-2001 for calibration and AD 1802-1901 for verification.

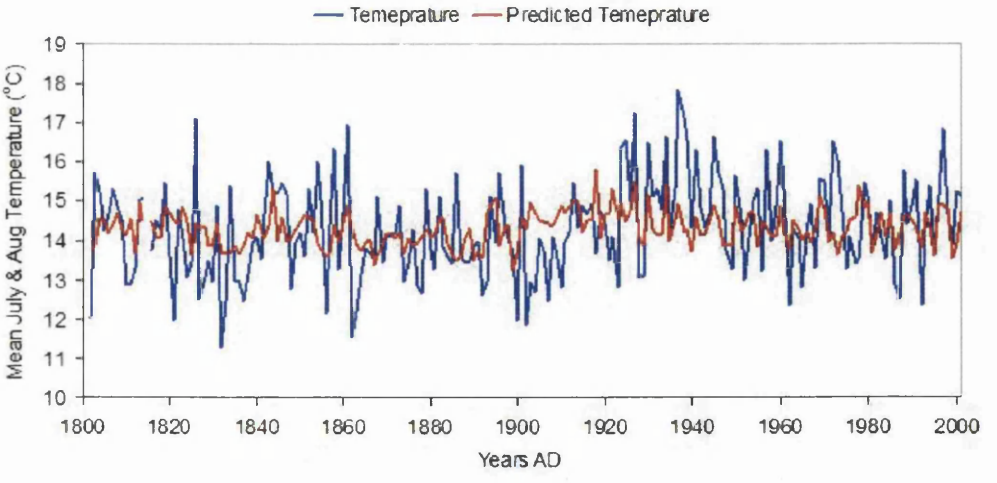

Figure 6.42: Reconstructed mean July and August Tornedalen temperatures from AD 1802-2001 using the same period for calibration, compared to actual temperature.

	Calibration AD 1802-2001
MSE	1.34
RE	0.13
CE	NA
r^2	0.13

Table 6.7: Verification statistics for the mean July and August Tornedalen temperature reconstruction AD 1802-2001, using the same period for calibration.

To test how well nineteenth and twentieth century $\delta^{13}C_{pin}$ reconstruct each temperatures it seems reasonable to carry out a calibration and verification exercise excluding the years which have been highlighted as problematic. The early part of the nineteenth century is excluded as Klingbjer and Moberg (2003) suggest the summer temperature data from Tornedalen are suspect. The period from AD 1881 to 1926 is also excluded as these data have a low inter-tree EPS. Table 6.8 shows the verification statistics for a calibration carried out over the period AD 1927 to 2001 and verified over the period AD 1829 to 1880, while Figure 6.43B shows the reconstructed temperatures of the verification period against mean July and August Tornedalen temperature. Despite the distance

from Tornedalen the reconstruction seems fairly sound with an r^2 of 0.21, an RE of 0.36 and a CE of 0.10 for the verification period.

The reverse calibration/verification procedure using AD 1829 to 1880 for calibration and AD 1927 to 2001 for verification can be seen in Figure 6.44A and Table 6.8. Once again the reconstruction seems impressive for so distant a climate station with a r^2 of 0.24, an RE of 0.39 and a CE of 0.15 for the verification period. That both periods are able to reconstruct the other's temperature to the degree shown here is highly promising and suggests that temperatures prior to AD 1881 and post AD 1927 have a similar relationship with $\delta^{13}C_{pin}$. Also from Figure 6.43 it can see that the mean temperatures of the two periods are rather different (AD 1829-1879, 13.99°C and AD 1927-2001, 14.76°C). This suggests that the success of the $\delta^{13}C_{pin}$ of one period in reconstructing the temperature of the other means that the isotopes are capturing the low frequency temperature signal quite successfully. It seems likely that the intervening period is anomalous (although it may not be unique, this will be discussed later). On this basis, it seems reasonable to expect a model, based on Andenes temperatures post AD 1927, to have some predictive powers in earlier centuries.

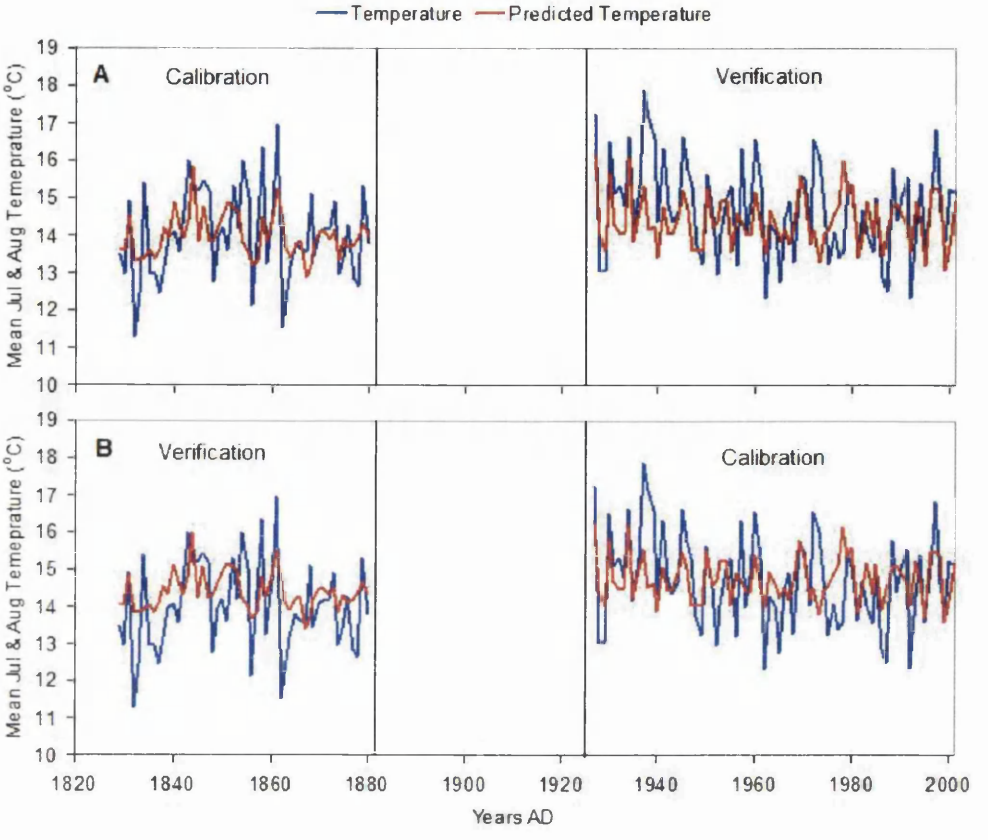

Figure 6.43: Reconstructed mean Tornedalen July and August temperatures using (A) AD 1829-1880 as the calibration period and AD 1927-2001 as the verification period and (B) AD 1927-2001 as the calibration period and AD 1829-1880 as the verification period. In both cases compared to actual mean July and August temperature from the Tornedalen record (Klingbjer and Moberg, 2003).

	Calibration AD 1829-1880	Verification AD 1927-2001	Calibration AD 1927-2001	Verification AD 1829-1880
MSE	1.16	1.31	1.18	1.34
RE	0.21	0.39	0.24	0.36
CE	NA	0.15	NA	0.10
r^2	0.21	0.24	0.24	0.21

Table 6.8: Statistics for the mean July and August temperature reconstruction using the (on the left) AD 1929-1880 for calibration and AD 1927-2001 for verification and (on the right) AD 1927-2001 for calibration and AD 1829-1880 for verification.

Finally a reconstruction was made for both periods (AD 1829-1880 and AD 1927-2001)

using the combined data set. The results of this can be seen in Figure 6.44 and Table 6.9. Based on these statistics and the visual evidence shown in Figure 6.44, this reconstruction appears useful with a high r^2 of 0.27. To establish whether the reconstructed data in the nineteenth century are as robust as those for the twentieth century verification statistics based on this reconstruction were produced for each period separately (Table 6.10). A CE statistic would not normally be presented here as it is usually used where a data set is split into calibration and verification periods. The statistic presented in Table 6.10 is calculated in the same manner as a CE statistic (see Equation 6.6), but unlike a normal CE statistic, the mean temperature data used in this statistic forms part of the reconstruction data set, which would not normally be the case. It is considered worth presenting as it is still represents a more challenging test of the reconstructions than the mean of the whole series (RE statistic), although not as tough a test as a normal CE statistic, to avoid confusion this will be called a split data efficiency test (SDET), the calculation of which can be seen in Equation 6.8. Here $\hat{y}_s$ is the temporally separate (split) part of the reconstruction under consideration and $\bar{y}_s$ is the mean temperature of the same period.

$$SDET = 1 - \frac{MSE(\hat{y}_s)}{MSE(\bar{y}_s)} \tag{6.8}$$

Table 6.10 shows that the reconstruction of nineteenth century temperates is only slightly inferior in terms of r^2 (0.21 as opposed 0.24) and SDET statistic (0.18 compared to 0.22) and the differences are relatively small. Indeed the RE statistic for this period is slightly higher than for twentieth century reconstructed temperatures (0.28 and 0.27). Considering that temperature records in the nineteenth century are unlikely to be better than those in the twentieth century and that the Tornedalen data prior to AD 1859 is not considered as accurate as later data (Klingbjer and Moberg, 2003) this would seem to confirm that a reconstruction model based upon twentieth century temperates should be applicable to earlier periods. Note that this reconstruction (Figure 6.44), due to the higher correlation, retains more of the annual variability that the one presented in Figure

6.42, reconstructed over the entire period of AD 1802 to 2001.

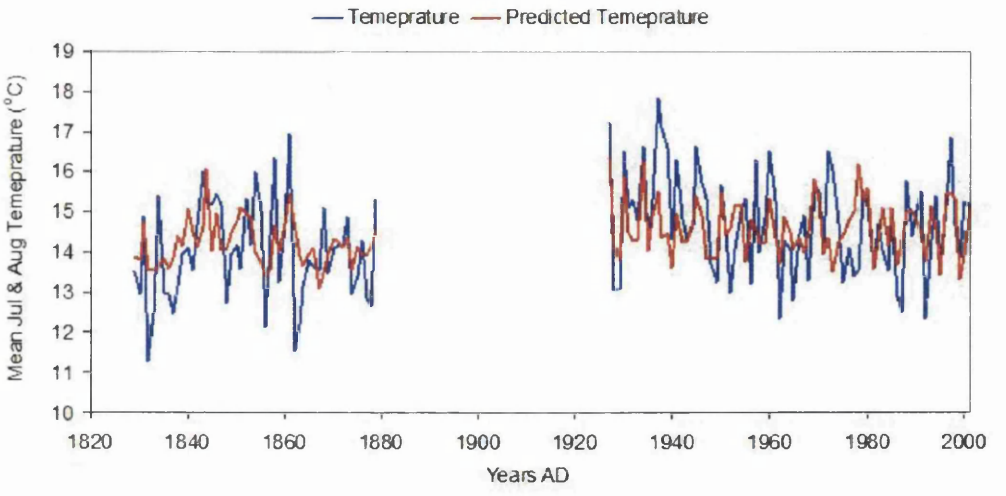

Figure 6.44: Reconstructed mean July and August Tornedalen temperatures from AD 1802-2001 and AD 1927-2001 using the same periods for calibration, compared to actual temperature.

	Calibration AD 1829-1880 & AD 1927-2001
MSE	1.22
RE	0.27
CE	NA
r^2	0.27

Table 6.9: Verification statistics for the mean July and August Tornedalen temperature reconstruction AD 1829-1880 & AD 1927-2001, using the same periods for calibration.

	AD 1829-1880	AD 1927-2001
MSE	1.23	1.21
RE	0.28	0.27
SDET	0.18	0.22
r^2	0.21	0.24

Table 6.10: Two periods of reconstruction for AD 1829-1880 & AD 1927-2001 analysed separately. The RE statistic here is derived from the mean of both periods, while the SDET statistic (which is similar to a CE statistic) is derived from the MSE of the mean temperature of each of the two periods compared to the MSE of each periods reconstruction (see Equation 6.8).

6.5.4 $\delta^{13}C_{pin}$ Temperature Calibration Conclusion

The mean $\delta^{13}C_{pin}$ data series compared to the full Andenes temperature record from AD 1869 to 2001 does not reconstruct temperature very effectively (See Figure 6.37 and Table 6.2). The reason for this would appear to be that the early part of the record matches the temperature record rather poorly, there is also a rather weak between-tree $\delta^{13}C_{pin}$ signal for this part of the series, which would normally suggest that it was not suitable for climatic reconstruction.

When the early part of the series is removed and a calibration is performed using only the period AD 1927 to 2001 the $\delta^{13}C_{pin}$ reconstructs mean July and August temperature (Figure 6.39 and Table 6.4) quite satisfactorily. The $\delta^{13}C_{pin}$ record is also able to reconstruct temperatures from the distant Tornedalen record quite effectively, albeit with rather low correlation values for the entire series (Figure 6.41 and Table 6.6). The problematic period spanning the end of the nineteenth and early twentieth centuries is also apparent in the Tornedalen record. When this period (and the early part of the Tornedalen record which the authors do not have confidence in (Klingbjer and Moberg, 2003)) are removed, the $\delta^{13}C_{pin}$ from Forfjorddalen are able to reconstruct temperatures for the period AD 1927 to 2001 and more importantly the period from AD 1829 to 1880 quite effectively and almost equally well (Figure 6.44 and Tables 6.9 and 6.10). This suggests that, for the period for which records are available, the period from around AD 1880 to 1928 is an anomalous one. It is however an important period as it demonstrates that a breakdown in the statistical relationship between $\delta^{13}C_{pin}$ and summer temperature is possible even towards the limits of Scots pine growth in an area with high precipitation and a more thorough interpretation of this period will be presented in Chapter 7. The success of the $\delta^{13}C_{pin}$ data from Forfjorddalen in reconstructing temperature from a station some 450 km away on the other side of the Scandes mountain range suggests that a temperature reconstruction based on the Forfjorddalen data may contain important information about regional temperature changes over past centuries.

6.6 $\delta^{13}C_{pin}$ and Precipitation Calibration

Calibration between $\delta^{13}C_{pin}$ and precipitation and SPI was carried out in the same manner as the calibration between $\delta^{13}C_{pin}$ and temperature outlined in Section 6.5.1. As the precipitation record from Andenes stretches back to AD 1910 is over this period that calibration will be undertaken, split again into two period for the purposes of calibration and verification (AD 1910 to 1955 and AD 1956 to 2001). The SPI has been calculated from the Andenes precipitation record using August lagged by 3 months (3 month August SPI).

6.6.1 Calibration with Mean July and August Mean Precipitation

Figure 6.45A shows reconstructed mean July and August precipitation compared to actual precipitation using AD 1910 to 1955 for calibration and AD 1956 to 2001 for verification, while 6.45B shows this calibration procedure in reverse. The verification statistics for both 6.45A and B can be seen in Table 6.11. Figure 6.46 and Table 6.12 show the results of the calibration and verification process using the entire period (AD 1910-2001).

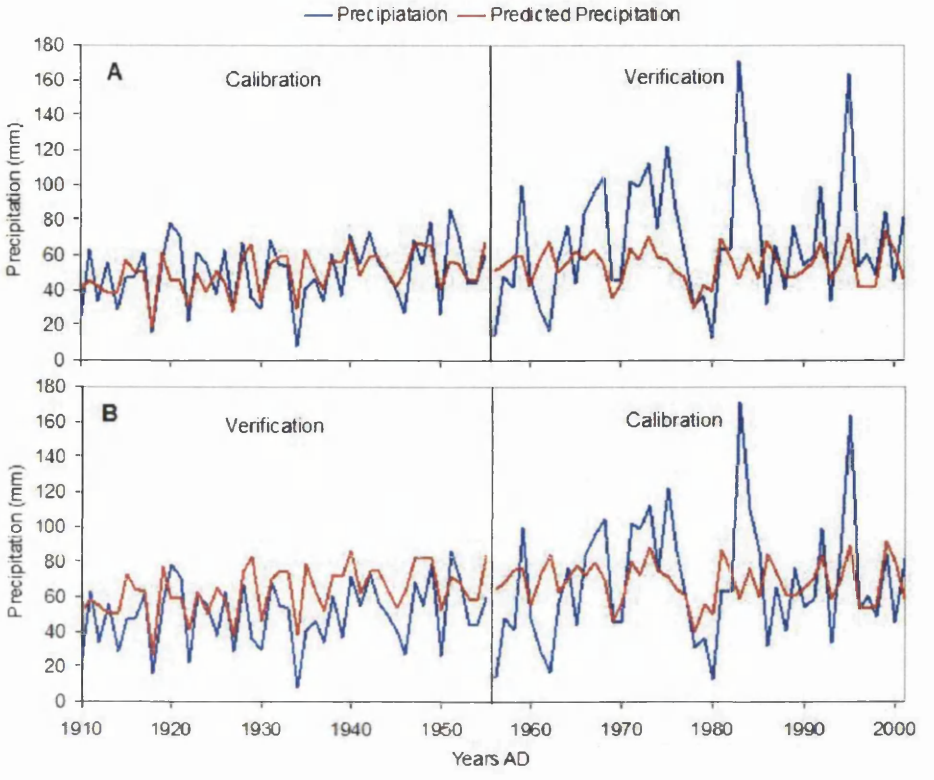

Figure 6.45: Reconstructed mean July and August precipitation using (A) AD 1910-1955 as the calibration period and AD 1956-2001 as the verification period and (B) AD 1956-2001 as the calibration period and AD 1910-1955 as the verification period. In both cases compared to actual mean July and August precipitation from Andenes.

	Calibration AD 1910-1955	Verification AD 1956-2001	Calibration AD 1956-2001	Verification AD 1910-1955
MSE	198.29	1259.97	1042.40	393.16
RE	0.40	0.19	0.12	0.43
CE	NA	-0.06	NA	-0.20
r^2	0.40	0.12	0.12	0.40

Table 6.11: Verification statistics for the mean July and August precipitation reconstruction using the (on the left) AD 1910-1955 for calibration and AD 1956-2001 for verification an (on the right) AD 1956-2001 for calibration and AD 1910-1955 for verification.

Despite having a good r^2 value of 0.40 for the period from AD 1910 to 1955 and a lower r^2 value of 0.12 for the period from AD 1956 to 2001 the calibration based on either period is able to outperform the predictive power of the mean value of the calibration period (CE

statistic). However the RE statistic for both periods are considerably better than zero suggesting that the models have a certain amount of predictive power. The problem for both reconstructions would appear to lie in the period AD 1956 to 2001 (Figure 6.45). Here the $\delta^{13}C_{pin}$ consistently fails to predict the larger precipitation events (such as AD 1978, AD 1983 and AD 1995) and while dry years such as AD 1929 and AD 1962 also come out as large residuals the $\delta^{13}C_{pin}$ seems to generally capture dry years rather better than wet years, the best example of this being AD 1918 which had the driest summer on record (although not especially warm). It seems reasonable near the northern tree line for Scots pine in a an area of high precipitation, that moisture availability would become more important in δ^{13}C fractionation during unusually dry periods. As was seen in Figure 6.27 the most positive $\delta^{13}C_{pin}$ values only occurred at mean July and August precipitation levels of less than about 50 mm, while a wide range of $\delta^{13}C_{pin}$ values occurred at higher precipitation levels.

Figure 6.46 shows $\delta^{13}C_{pin}$ calibrated with mean July and August precipitation for the entire period of AD 1910 to 2001, with the verification statistics in Table 6.12, again the earlier (dryer) part of the record appears to match precipitation better than the second half of the series with its large precipitation events.

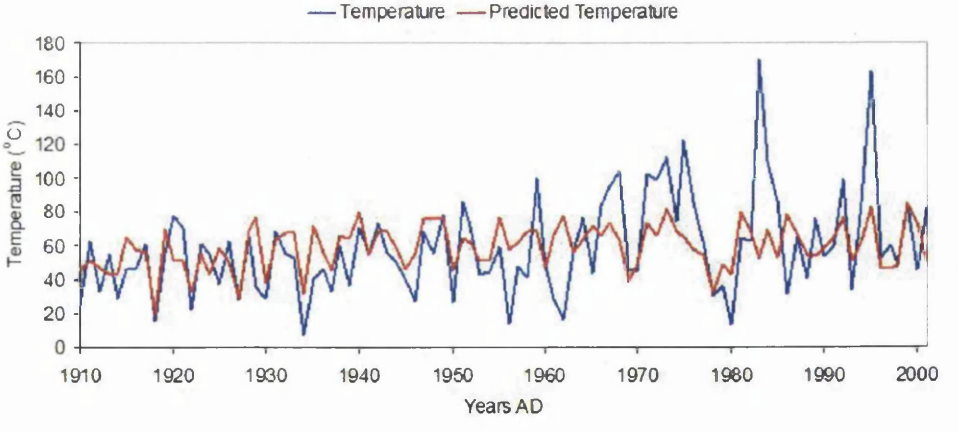

Figure 6.46: Reconstructed mean July and August precipitation from AD 1910-2001 using the same period for calibration, compared to actual precipitation.

	Calibration AD 1910-2001
MSE	670
RE	0.21
CE	NA
r^2	0.21

Table 6.12: Verification statistics for the mean July and August precipitation reconstructed for AD 1910-2001, using the same period for calibration.

It is possible to achieve a better calibration with mean July and August by removing the most extreme residual years from the calculation, in this case AD 1929, AD 1962 and AD 1983. The statistics for this can be seen in Table 6.13. This shows an improvement in the statistics especially for the period AD 1956 to 2001 with an improvement in the r^2 from 0.12 to 0.27 and now marginally positive CE vales for both verification periods (0.08 for AD 1956 to 2001 and 0.05 for AD 1910-2001). This demonstrates that the problem for $\delta^{13}C_{pin}$ in successfully reconstructing precipitation is partially the large residual years as it would appear that $\delta^{13}C_{pin}$ is not especially sensitive to large precipitation events and despite high correlations and RE statistics the CE statistics are rather low, much lower than those for the equivalent reconstructions of temperature (Figure 6.39).

	Calibration AD 1910-1955	Verification AD 1956-2001	Calibration AD 1956-2001	Verification AD 1910-1955	Calibration AD 1910-2001
MSE	180.38	869.12	687.99	315.91	469.80
RE	0.46	0.31	0.27	0.51	0.34
CE	NA	0.08	NA	0.05	NA
r^2	0.46	0.27	0.27	0.46	0.34

Table 6.13: Verification statistics for the mean July and August precipitation reconstruction using the (on the left) AD 1910-1955 for calibration and AD 1956-2001 for verification, (in the middle) AD 1956-2001 for calibration and AD 1910-1955 for verification and (on the right) AD 1910-2001 for calibration and verification.

6.6.2 Calibration with 3 Month August SPI

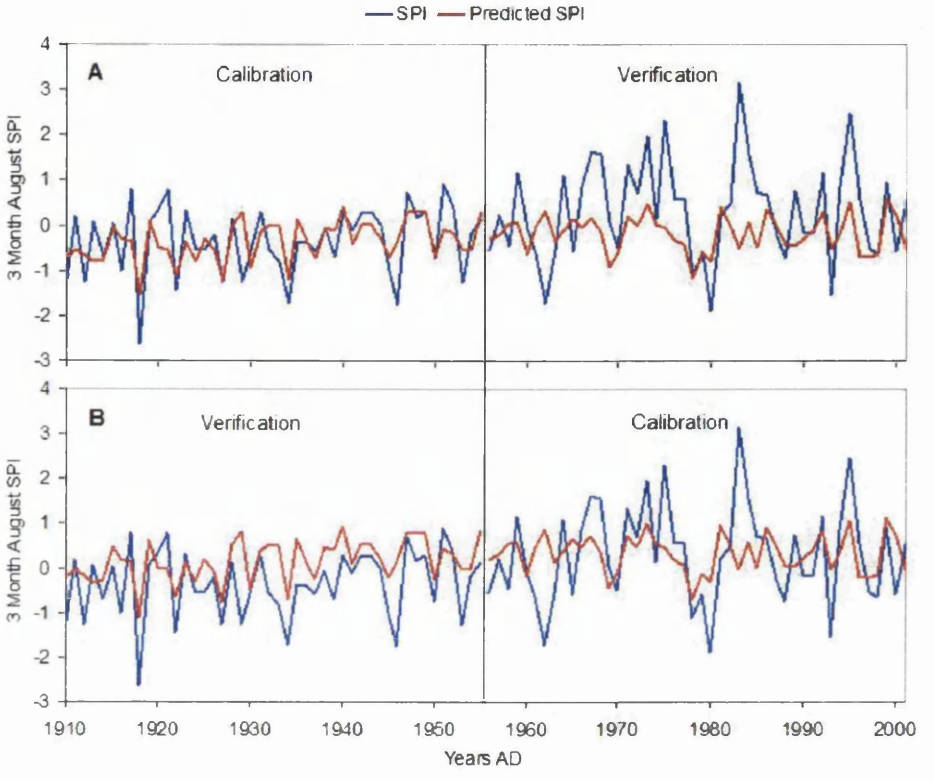

Figure 6.47: Reconstructed 3 month August SPI using (A) AD 1910-1955 as the calibration period and AD 1956-2001 as the verification period and (B) AD 1956-2001 as the calibration period and AD 1910-1955 as the verification period. In both cases compared to the actual calculated 3 month August SPI.

	Calibration AD 1910-1955	Verification AD 1956-2001	Calibration AD 1956-2001	Verification AD 1910-1955
MSE	0.38	1.26	0.99	0.63
RE	0.35	0.23	0.15	0.40
CE	NA	-0.08	NA	-0.10
r^2	0.35	0.15	0.15	0.35

Table 6.14: Verification statistics 3 month August SPI reconstructed using the (on the left) AD 1910-1955 for calibration and AD 1956-2001 for verification an (on the right) AD 1956-2001 for calibration and AD 1910-1955 for verification.

The same calibration and verification procedure using the 3 month August SPI can be seen in Figure 6.47. Figure 6.47A shows reconstructed mean 3 month August SPI using AD 1910 to 1955 for calibration and AD 1956 to 2001 for calibration, while 6.47B shows this calibration procedure in reverse. The verification statistics for both 6.45A and B can be seen in Table 6.14. Figure 6.48 and Table 6.15 show the results of the calibration process using the entire period (AD 1910-2001).

As the data for the 3 month August PSI is derived from the same Andenes data set as the Mean July and August precipitation calibrated in the previous section, the results look very similar. However while the SPI calibration still fails to capture the extreme years such as AD 1983, the 3 month lag in the SPI data seems better able deal with the extremes of the period AD 1956 to 2001 and hence has a higher RE and r^2 value of 0.15 for this as a calibration period and when this calibration is verified on the period AD 1910 to 1955. While there is a small fall in the RE statistic when compared to mean July and August precipitation (0.40 compared to 0.43), there is quite a large improvement in the CE statistic from -0.20 to -0.10, although still negative. The verification statistics for the calibration based on the period AD 1910 to 1955 are slightly lower using SPI instead of mean July and August precipitation (Tables 6.14 and 6.11). When a calibration is made using the entire period (see Figure 6.48 and Table 6.15) there is a small improvement over the RE and r^2 statistic from the equivalent reconstruction using mean July and August precipitation from 0.21 to 0.25 (see Table 6.12). This suggests a slightly better fit to the data for the period AD 1956 to 2001.

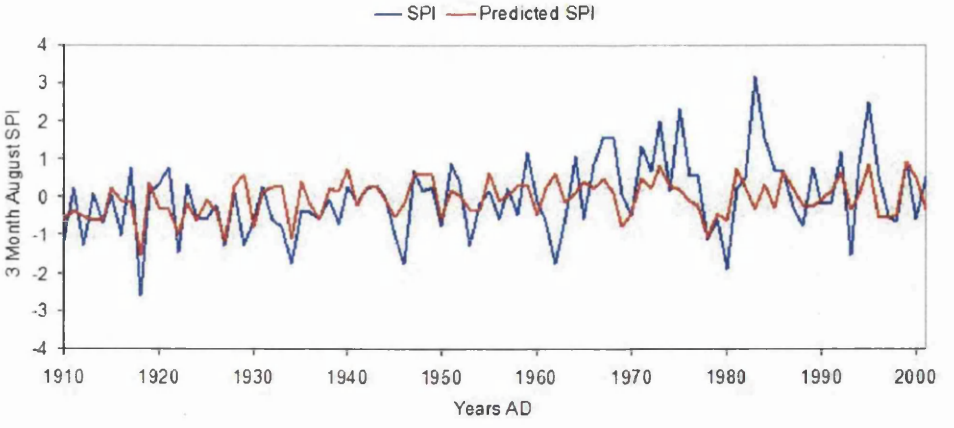

Figure 6.48: Reconstructed 3 month August SPI for AD 1910-2001 using the same period for calibration, compared to the calculated 3 month August SPI.

	Calibration AD 1910-2001
MSE	0.75
RE	0.25
CE	NA
r^2	0.25

Table 6.15: Verification statistics for 3 month August SPI reconstructed from AD 1910-2001, using the same period for calibration.

Removing the same three residuals from the calibration for SPI as were removed for precipitation (see Table 6.13) yields the results in Table 6.16. There is an improvement in the CE statistics for both verification periods compared to those in Table 6.13, both now at least 0.10 and also an improvement for the calibration taken over the whole period with RE and r^2 of 0.39 compared to 0.34 for mean July and August precipitation.

	Calibration AD 1910-1955	Verification AD 1956-2001	Calibration AD 1956-2001	Verification AD 1910-1955	Calibration AD 1910-2001
MSE	0.33	0.85	0.64	0.50	0.53
RE	0.43	0.38	0.32	0.50	0.39
CE	NA	0.10	NA	0.13	NA
r^2	0.43	0.32	0.32	0.43	0.39

Table 6.16: Verification statistics for the 3 month August SPI reconstruction using the (on the left) AD 1910-1955 for calibration and AD 1956-2001 for verification, (in the middle) AD 1956-2001 for calibration and AD 1910-1955 for verification and (on the right) AD 1910-2001 for calibration and verification.

6.6.3 Precipitation Calibration Conclusion

$\delta^{13}C_{pin}$ calibrated with mean July and August over the period AD 1910 to 2001 has some predictive ability as the RE statistics for both calibration and verification are positive at 0.19 and 0.43 (see Table 6.11). However, as can be seen in the same table the more demanding CE statistic in both cases is negative showing that neither calibration can outperform the mean of the verification periods, which would seem to limit the effectiveness of $\delta^{13}C_{pin}$ as a tool for reconstructing precipitation. The period which seems especially problematic is the latter part of the series where precipitation is increasing and there are some years with extremely heavy summer rainfall which the $\delta^{13}C_{pin}$ fails to pick up (especially AD 1983). Although it should also be noted that of the three largest residual years (AD 1929, AD 1962 and AD 1983) both AD 1929 and AD 1962 are dry summers which the $\delta^{13}C_{pin}$ fails to pick up. The removal of these residual years improves all the verification statistics with the CE statistics now slightly positive (see Table 6.13).

When the 3 month SPI is used instead of mean July and August precipitation correlations in the more problematic period from AD 1956 to 2001 improve slightly, although for the period AD 1910 to 1955 the figures deteriorate slightly (see Tables 6.47), suggesting that the smoothing effect of the SPI helps deal better with the more extreme precipitation events in second half of the twentieth century. When the same three residuals (AD 1929, AD 1962 and AD 1929) are removed from the SPI calibration the statistics once again

improve (Table 6.16) and now the CE statistics are both positive and, while modest, are both in excess of 0.10. Suggesting that the SPI. with its lags, may prove better for reconstruction purposes than actual precipitation levels.

In general it seems that δ^{13}C fractionation at Forfjorddalen can be affected by precipitation but that this may be rather more important in extremely dry years than in wetter years. As we have already seen in Figure 6.27, $\delta^{13}C_{pin}$ values are always very positive in extremely dry years (even when as in AD 1918 these years are not especially hot) but can have a wide range of values in extremely wet years. It seems then that except in rather dry years $\delta^{13}C_{pin}$ is controlled more by summer temperature and that much of the apparent correlation between $\delta^{13}C_{pin}$ and precipitation may be due to the generally negative relationship between temperature and precipitation. To reconstruct precipitation independently of temperature, which is highly desirable to fully understanding the climate signal contained in the $\delta^{13}C_{pin}$ data, it may be more useful to use another proxy such as δ^{18}O and this will be addressed in the next chapter.

6.7 Conclusion

$\delta^{13}C_{pin}$ has a statistically significant relationship with the summer temperature data from Andenes with a correlation of $r = 0.51$ for the entire length of the climate record from AD 1869 to 2001. However this relationship with temperature is much weaker for the initial approximately 50 years of the series (for the period AD 1869 to 1926 $r = 0.27$) than for the remaining 75 years ($r = 0.71$ for the period AD 1927 to 2001). Comparison of the climate data to other available temperature records would suggest that there is likely to be little problem with the Andenes temperature record (see Figure 6.13). Analysis of the tree ring cross dating and the nature of the breakdown in the relationship between $\delta^{13}C_{pin}$ and temperature suggest that dating and cutting were accurate. It would appear then that this breakdown in the relationship between $\delta^{13}C_{pin}$ and temperature is a genuine environmental phenomena which requires explanation.

When the longer (and more distant) Tornedalen temperature series in compared to

$\delta^{13}C_{pin}$ the same pattern emerges (albeit with lower correlation values). However, as the Tornedalen record stretches back to AD 1802 and summer monthly temperature are considered reliable back to around AD 1830 (Klingbjer and Moberg, 2003) it is possible to determine whether or not the strong correlation with temperature existed prior to the beginning of the Andenes temperature record, and indeed this would appear to be the case with correlation with mean July and August temperatures at much the same level for the period AD 1829 to 1880 as for AD 1927 to 2001 (see Figure 6.16). Also importantly for long term temperature reconstruction the low frequency variations between the $\delta^{13}C_{pin}$ and the Tornedalen temperature series seem to match rather well prior to AD 1880.

When $\delta^{13}C_{pin}$ was calibrated against temperature using the full Andenes data set (AD 1869 to 2001) it was unable to satisfactorily reconstruct temperature successfully in terms of the calibration tests used (see Section 6.5.1 and Table 6.2). When the period AD 1869 to 1926 was removed from the calibration $\delta^{13}C_{pin}$ was able to reconstruct temperature rather well (see Table 6.4). Calibration of $\delta^{13}C_{pin}$ against the Tornedalen record was able to produce positive verification statistics over the entire length (see Table 6.6) perhaps because the problem period (AD 1880 to 1926) made up a much smaller part of the record. When this section was removed form the calibration the $\delta^{13}C_{pin}$ values of the two remaining periods (AD 1929 to 1880 and AD 1927 to 2001) were able to reconstruct temperature of the other period surprisingly well for a composite climate record at a distance of some 450 km.

Removal of the period AD 1869 to 1926 from the final calibration data set to reconstruct climate for previous centuries was a difficult decision and one justified for two major reasons. Firstly this period is one of rather low common signal between the $\delta^{13}C_{pin}$ values of the trees, which would normally be taken to indicate that these data were not suitable for climate reconstruction. Secondly because it is believed that the breakdown in the common isotope signal between the trees and the low correlation with temperature is explicable in terms of the relationship of δ^{13}C fractionation with temperature and precipitation, which will be further discusses in Chapter 8.

As was inferred from Figure 6.7 the key part of the growing season for the fixation of sugars for latewood cellulose appears to be from around the 20th of July to the 20th of August. This means that both mean July and mean July and August had similarly strong relationships with $\delta^{13}C_{pin}$from Andenes. However mean July and August temperature yielded consistently the strongest relationship with $\delta^{13}C_{pin}$ from Andenes and Tornedalen and so it was decided to use this calender period for calibration. It should be noted that as the experiment using isotopes from early wood showed (Chapter 3) there was probably no need for this study to isolate cellulose from latewood alone and that using the whole ring may have given a stronger mean July and August signal and saved many hours of cutting in the laboratory.

The relationship between $\delta^{13}C_{pin}$ and precipitation, although not as strong as with temperature, seems fairly robust with a correlation of $r = 0.47$ for July and August precipitation and $r = 0.50$ for 3 month August SPI for the period AD 1920 to 2001. This relationship is rather more stable through time than that of temperature, although poorer in the late twentieth century which seems to be due to some extreme rainfall events which the $\delta^{13}C_{pin}$ fails to pick up. In general it appears that precipitation is more important in δ^{13}C fractionation when summers are dry as Figure 6.27 demonstrates and would seem to dominate carbon isotope fractionation in extremely dry years such as AD 1918.

Using $\delta^{13}C_{pin}$ to calibrate mean July and August precipitation meets with mixed success and is unable to meet fully the calibration tests set in this chapter. By removing several residual years and using a precipitation index (SPI) rather than mean July and August precipitation (Table 6.16) it was possible to achieve positive, but rather low CE statistics (Table 6.16).

The relationship between δ^{13}C and temperature and moisture availability even near the tree line seems to be a complex one. What appears likely from the data presented here is that a reconstruction of precipitation based on $\delta^{13}C_{pin}$ may only successfully pick up dry years and that much of its success in predicting the precipitation of other years may be due largely to precipitation having negative relationship with temperature in this area (see Figure 6.28). $\delta^{13}C_{pin}$ should however be very useful in identifying very dry years and

may prove useful in conjunction with δ^{18}O in reconstructing precipitation more fully.

Provided the period at the end of the nineteenth century and at the start of the twentieth century are removed , $\delta^{13}C_{pin}$ has fairly good reconstructive power for summer temperatures at Forfjorddalen. The failure of the correlation observed at other times makes this period potentially very interesting, and it is analysed in greater depth later in this thesis.

7

δ^{18}O Calibration with Climate

7.1 Introduction

Unlike δ^{13}C, there is no need to correct the raw δ^{18}O values from tree rings for any atmospheric changes. However it is desirable to shift the δ^{18}O towards the mean value (data shifting), as was carried out on the δ^{13}C series to circumvent the potential problem of off-sets in the mean value as trees are introduced and leave the time series.

Calibration with climate will be undertaken using the climate data from Andenes, for which monthly mean precipitation data are available from AD 1910, and also using a longer composite precipitation data set for selected stations between the Arctic Circle and Northern Cape compiled by Hanssen-Bauer and Føland (1998), which has mean monthly precipitation values for the period AD 1873 to 1997.

At the time of writing, not all the possible δ^{18}O results are available and so the δ^{18}O record is somewhat less complete than the δ^{13}C series. Figure 7.2 shows the results currently available over the same period as the δ^{13}C series was calibrated (AD 1800-2001). Too little data is available at the beginning of the series (AD 1800-1810) and so calculation of common signal strength and the shifting of the data will be carried out from AD 1810 onwards. There are also data missing for Tree 63 in the early part of the series which may have a detrimental affect on the EPS. As we will see in Section 7.4, the most convincing variable available controlling δ^{18}O fractionation is precipitation and as the available precipitation records are rather shorter than those for temperature these problems with the isotope data in the nineteenth century do not impinge upon calibrating

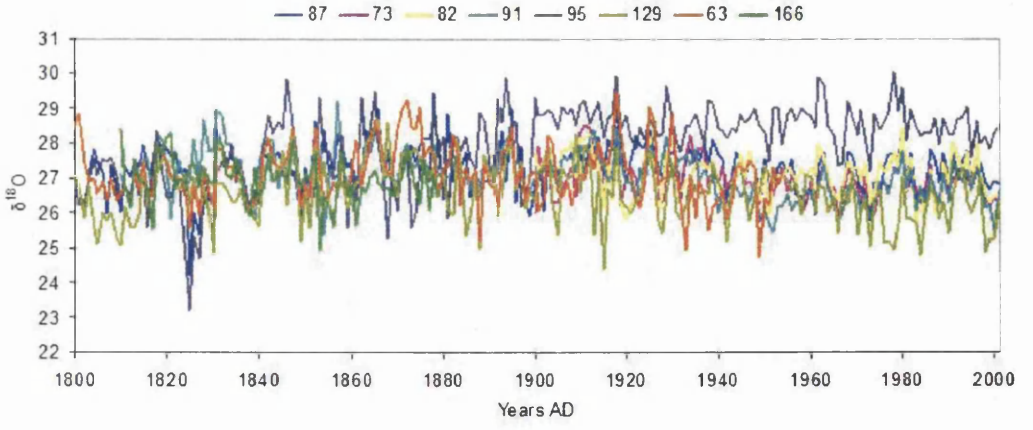

Figure 7.1: δ^{18}O(‰) results for all trees from AD 1800-2001.

the δ^{18}O series with climate.

Raw δ^{18}O data for all the available trees can be seen in Figure 7.1 (with all trees on the same axis) and in Figure 7.2 (with each tree on an individual axis). With the exception of Tree 87 the mean isotope values for all the trees are similar. The values for Tree 87 are close to the mean value of the other trees during the early AD 1800s but during the AD 1900s they rise noticeably above the values for the other trees. This variability in isotope value is not what one would normally expect in tree rings (McCarroll and Loader, 2004), as they usually hold their positions relative to one another. There is however, no reason to suspect that the trend in this tree is not a response to external forcing, indeed the δ^{13}C results for this tree appear perfectly normal. This variability in Tree 87 causes some problems in shifting the isotope data towards the mean, as we will see in Section 7.3. Despite this the data is retained in the series as the trend may well have a genuine climatic reason specific to the site of this tree.

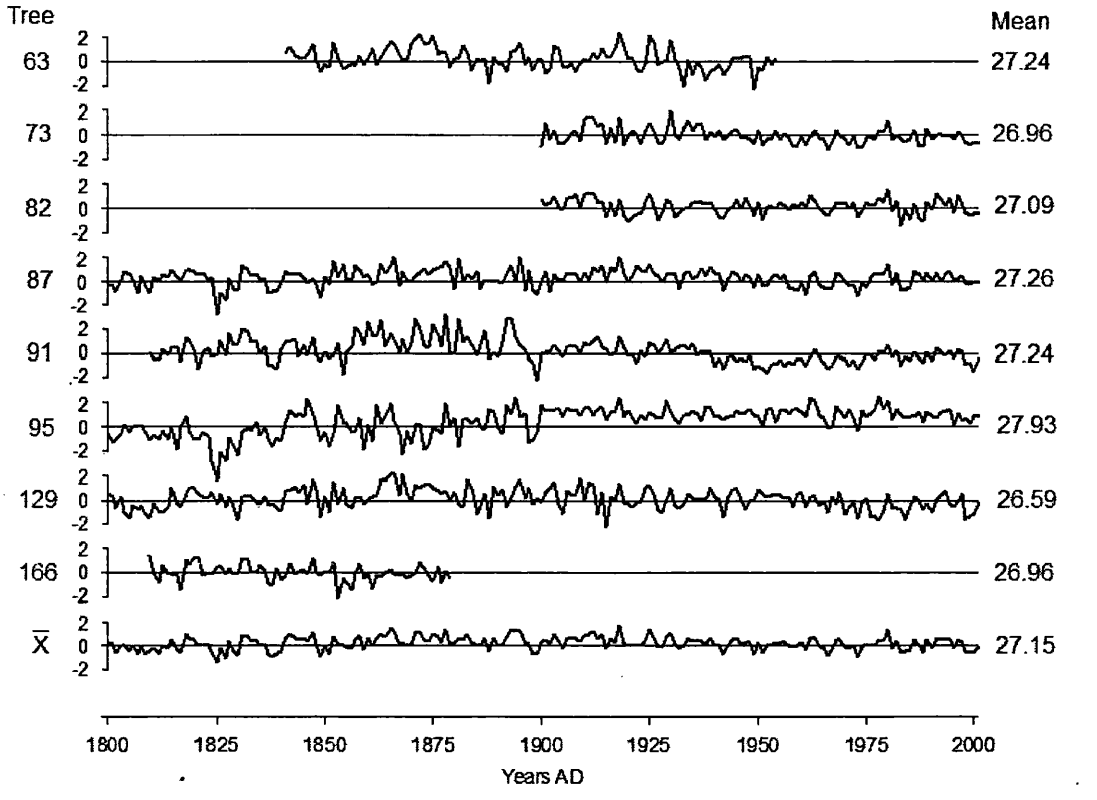

Figure 7.2: δ^{18}O(‰) ratios for individual trees and for the mean of all trees from Forfjorddalen for the period AD 1800-2001.

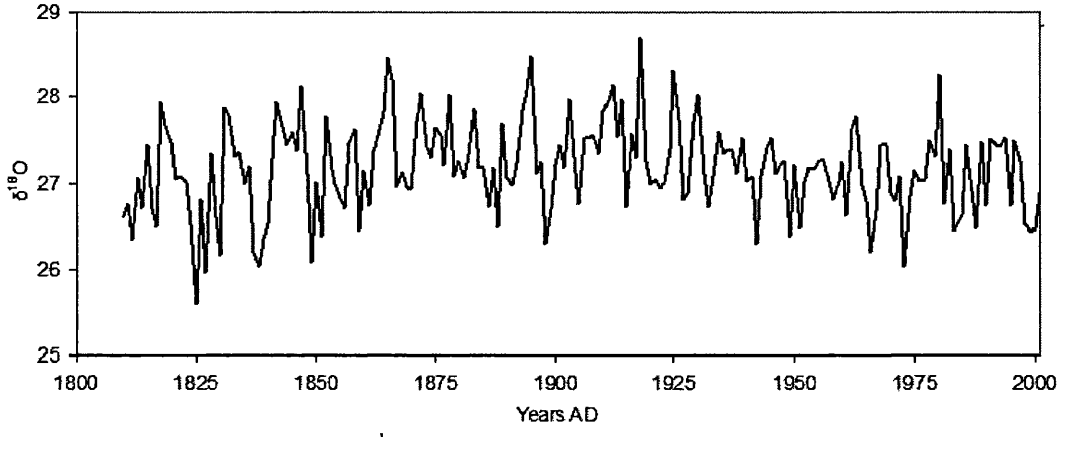

Figure 7.3: Mean δ^{18}O (‰) values from AD 1810-2001

	Tree 63	Tree 73	Tree 82	Tree 87	Tree 91	Tree 95	Tree 129
Tree 73	0.31						
Tree 82	0.25	0.59					
Tree 87	0.38	0.67	0.47				
Tree 91	0.41	0.58	0.53	0.46			
Tree 95	-0.04	0.37	0.60	0.32	-0.01		
Tree 129	0.44	0.50	0.47	0.45	0.36	0.10	
Tree 166	0.33			0.16	0.16	0.02	0.22

Table 7.1: Inter-correlation of δ^{18}O(‰) values between all trees from AD 1800-2001. Mean $r = 0.35$.

Figure 7.3 shows the mean δ^{18}O values of the tree in Figure 7.1. δ^{18}O values increase through the nineteenth century peaking in the early twentieth century (as do the δ^{13}C values). There is decline through the middle years of the twentieth after which δ^{18}O values become more stable (post ~AD 1960).

7.2 Signal Strength

Table 7.1 shows the inter correlation between the δ^{18}O values of all the available trees from AD 1810 to 2001, with a mean inter correlation of $r = 0.35$ (rather lower than the 0.49 for δ^{13}C for the period AD 1800-2001). The between tree correlation is rather variable with two instances of negative correlation between trees (Tree 95 and 63 $r =$ -0.04 and Trees 95 and 91 $r =$ -0.01). Indeed Tree 95 would seem to be a slightly problematic tree in terms of its δ^{18}O record, especially in the twentieth century. It correlates best with Trees 73 and 82 whose records only begin in AD 1900. In general it seems that the common signal for δ^{18}O is rather weaker than for δ^{13}C and also more variable.

The running 31 year correlation between trees from AD 1810 to 2001 can be seen in Figure 7.4, which shows the maximum, minimum, and actual 31 year mean inter correlation between all trees. A similar pattern emerges to the inter correlation of the δ^{13}C results,

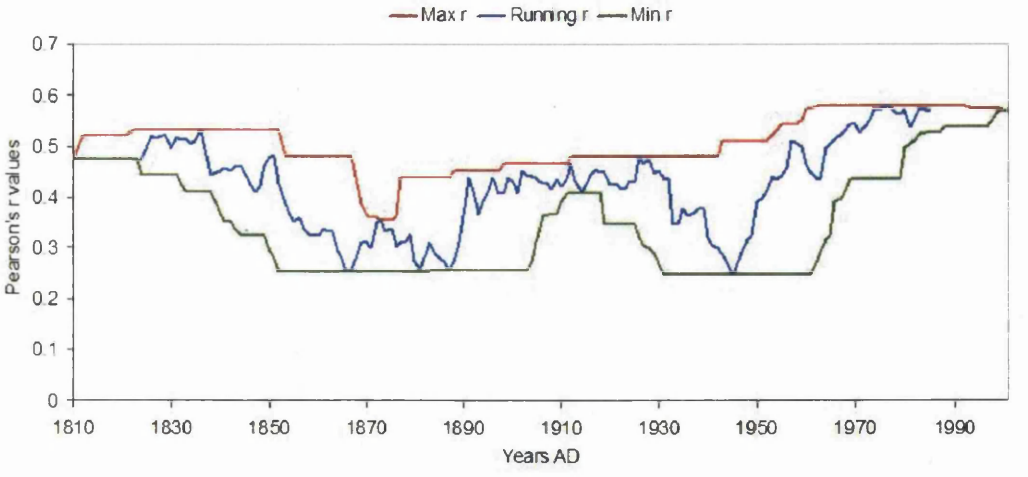

Figure 7.4: Inter-correlation of δ^{18}O(‰) values between all trees for a 31 year running period from AD 1810-2001. Showing the 31 year running correlation and also the maximum and minimum correlation in any 30 year window.

with a decline towards the end of the AD 1800s. The dip in correlation between trees for δ^{18}O (~AD 1860-1890) begins earlier than between trees for δ^{13}C(~AD 1870-1900). Unlike δ^{13}C, there is also a decline in the inter correlation between trees for a brief period in the middle of the twentieth century. As the δ^{13}C and δ^{18}O results are obtained from the same cellulose, this cannot be as a result of errors in cutting or dating, as the inter correlation between δ^{13}C for this period is very good.

The expressed population signal (EPS) was again calculated using the equation 7.1, where $\overline{r}_{bt}$ is the mean correlation calculated between all possible pairs of trees and t is the number of trees.

$$\text{EPS}(t) = \frac{(t \cdot \overline{r}_{bt})}{(t \cdot \overline{r}_{bt} + (1 - \overline{r}_{bt}))} \tag{7.1}$$

Figure 7.5 shows the running 31 year EPS for the δ^{18}O series from AD 1810 to 2001. A line has been added to this graph at EPS = 0.85 which is typically considered a reasonable value (Wigley et al., 1984). While the maximum running EPS remains above this 0.85

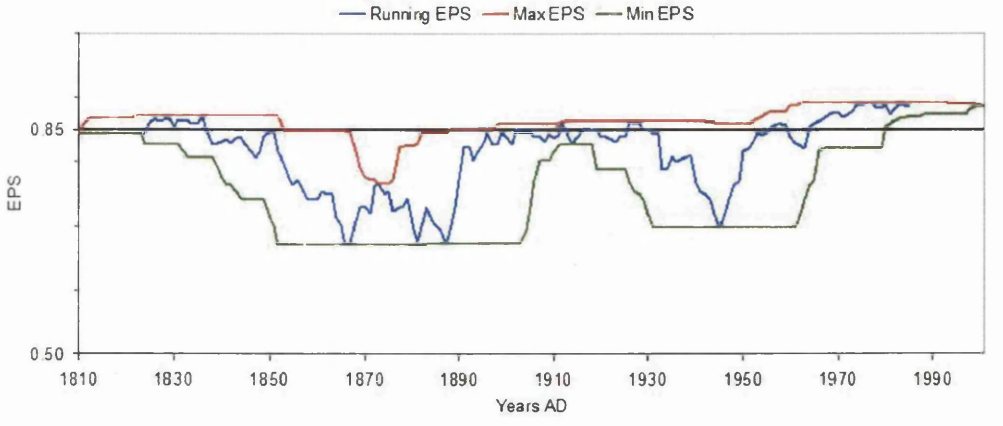

Figure 7.5: 31 year running EPS between δ^{18}O(‰) values between all trees for period the AD 1810-2001. This graph shows the actual 31 year running EPS (in blue), and the maximum (red line) and minimum (green line) EPS in a 30 year moving window.

threshold for all but a short period in the AD 1870s and AD 1880s, the actual running EPS remains below 0.85 for long periods, including the decline in the mid AD 1900s. This suggests that rather more trees need to be included in the series to maintain an EPS above 0.85. However, as was pointed out earlier simply adding trees to the series to achieve an EPS $>$0.85 may only mask underlying reasons why the common signal between isotopes in tree rings is poor during certain periods, notably the late AD 1800s in this area. The lower precision of the δ^{18}O measurements may also have some bearing on the relatively poor common signal, as does the lower number of trees in the early part of the series. Despite these problems the fact that the maximum EPS remains high for much of the series suggests that δ^{18}O may be useful in reconstructing climate especially as it may yield an independent estimate of precipitation, which may prove helpful in interpreting the δ^{13}C signal. Caution will however be exercised in interpreting the results of a reconstruction based on δ^{18}O, especially during periods where the EPS is low.

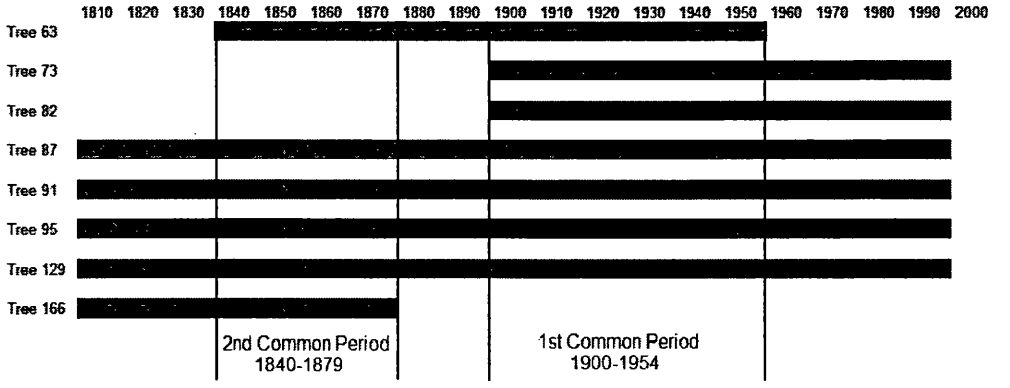

Figure 7.6: Temporal ranges of all trees for the calibration period, showing the two common periods used to shift the data.

7.3 Data Adjustment

As was mentioned in Section 8.1, it is desirable to shift the δ^{18}O values towards the mean value (as was carried out on the δ^{13}C series) to prevent problems associated with offsets in the mean which are not due to external forcing but which may arise when new trees are added further back in the series. Again as with δ^{13}C common periods are used to shift the δ^{18}O values and these are identified in Figure 7.6. Two suitable periods over which to shift the data were identified, the longest common period AD 1900 to 1954 and a secondary common period of AD 1840 to 1879 which was used to shift the isotope values of the one tree not common to the first common period (Tree 166).

The mean δ^{18}O series prior to shifting with 95% confidence limits can be seen in Figure 7.7, with the 95% confidence interval plotted on its own in Figure 7.8. A graph showing the range of δ^{18}O values can be seen in Figure 7.9. These figures show that the spread of isotope values is fairly consistent throughout the series, with a slight increase through the twentieth century, no doubt a result of the rather positive values for Tree 95 in AD 1900s (see Figure 7.1). Note also that the 95% confidence interval is wide at the end of the AD 1800s, where the EPS is low (Figures 7.5 and 7.8), although the range of values at this point is not especially great (Figure 7.9).

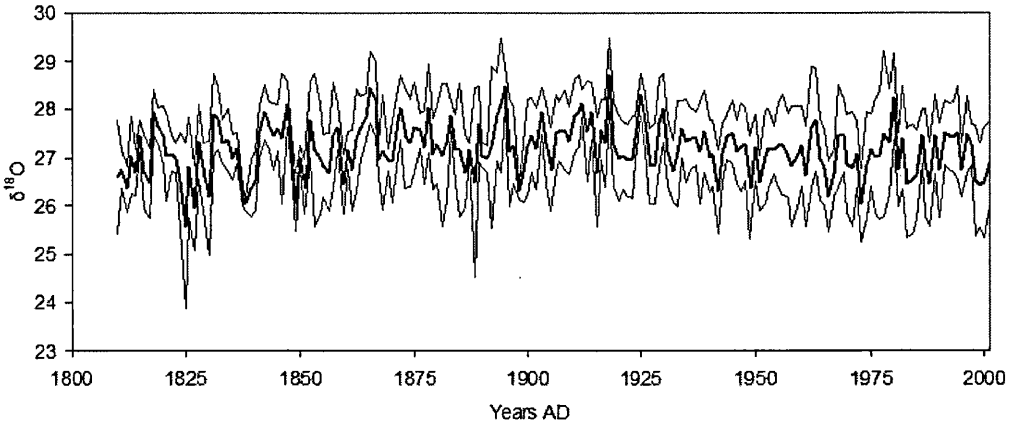

Figure 7.7: Mean δ^{18}O(‰) from AD 1810-2001 with 95% confidence intervals

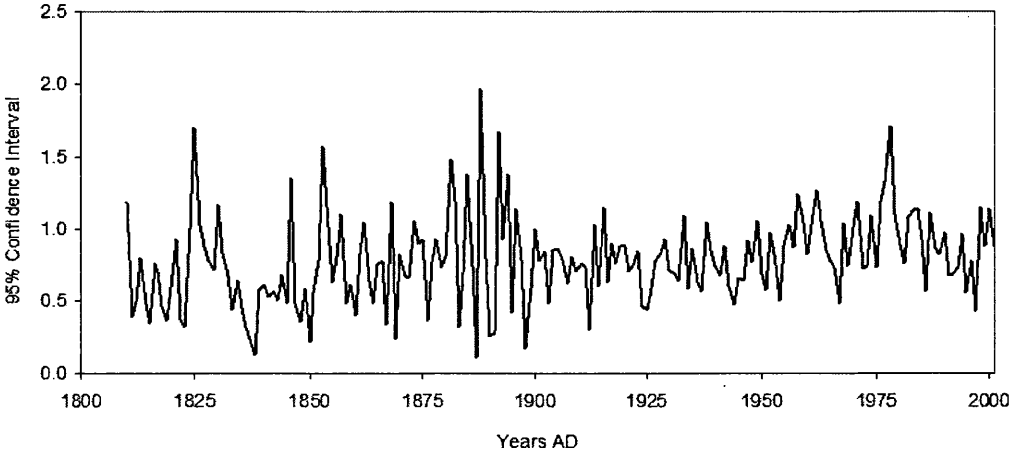

Figure 7.8: 95% (‰) confidence interval for mean δ^{18}O from AD 1810-2001.

The δ^{18}O values were shifted towards the mean using equation 7.2 (the same as was used for shifting the δ^{13}C results), where $\bar{x}$ is the mean δ^{18}O value for the common period $\bar{n}$ is the mean δ^{18}O of the tree to be shifted over the common period and n is the individual δ^{18}O value. This data shift was carried out using the two common period identified in Figure 7.6.

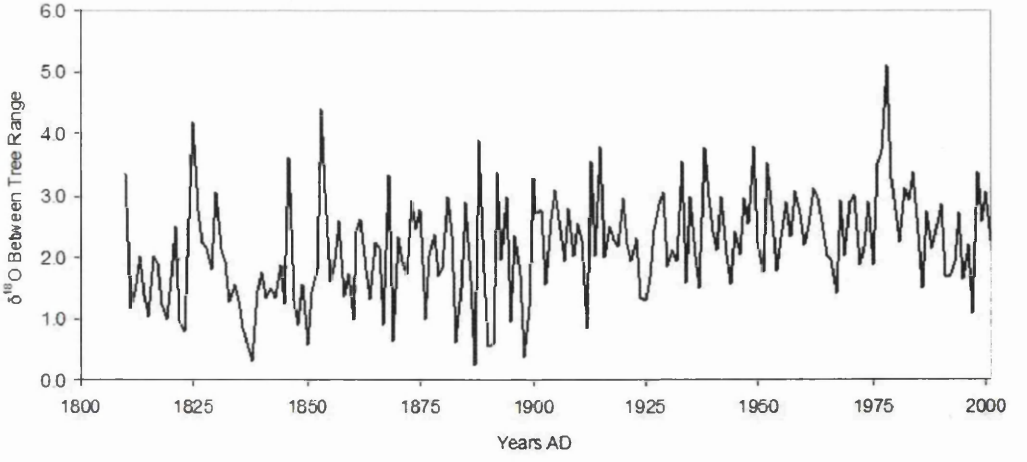

Figure 7.9: Range of values in δ^{18}O (‰) values from AD 1810-2001. Here the minimum δ^{18}O (‰) each year is subtracted from the maximum δ^{18}O (‰) for that year.

$$\delta^{13}C_{shift} = n - (\bar{n} - \bar{x}) \tag{7.2}$$

Figure 7.10 shows the δ^{18}O results for each individual tree, post shifting, while Figure 7.11 shows the mean shifted δ^{18}O with 95% confidence intervals. Figures 7.12 and 7.13 show the 95% confidence interval and the range of shifted values.

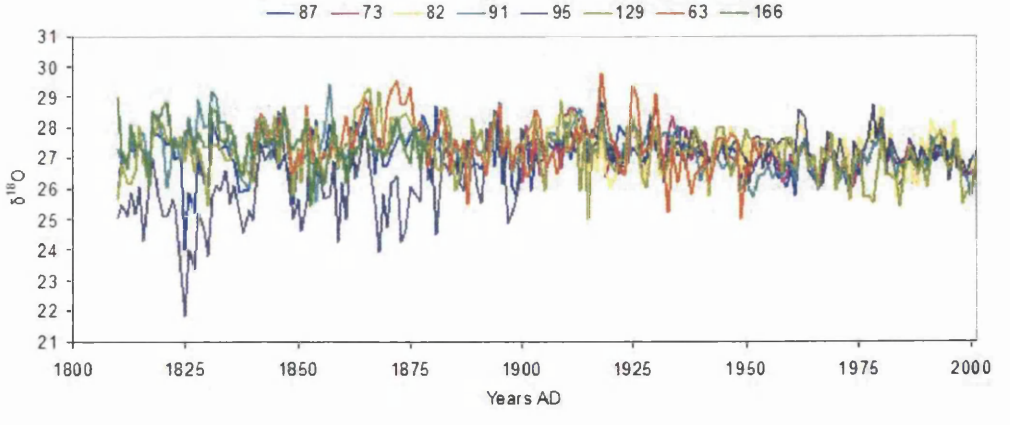

Figure 7.10: δ^{18}O (‰) shifted results for individual trees from AD 1810-2001.

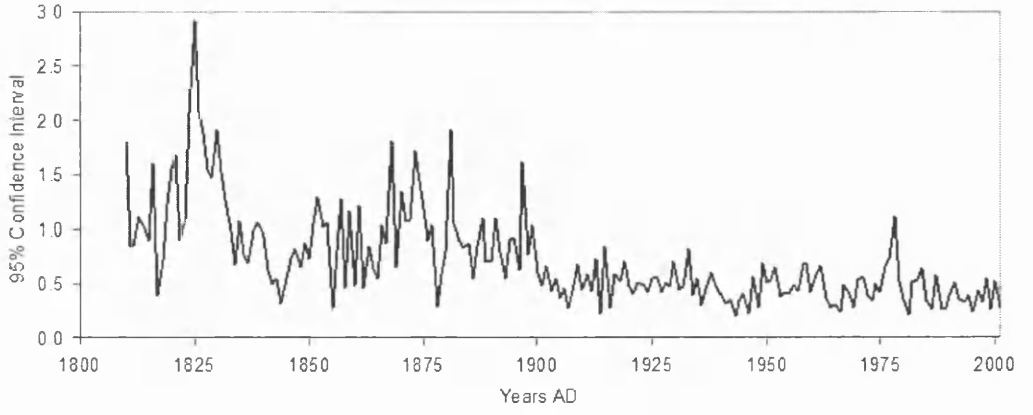

Figure 7.12: 95% confidence interval for the mean δ^{18}O (‰) values shifted to the AD 1900-1954 common period.

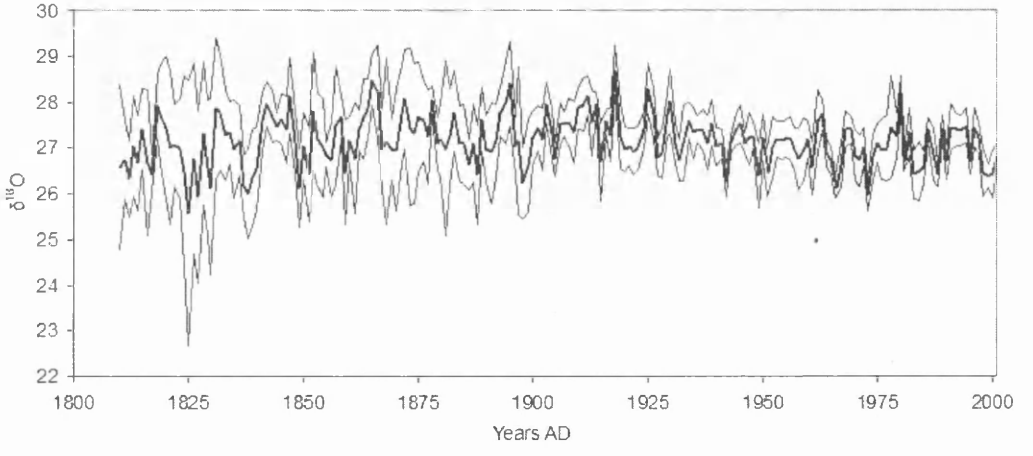

Figure 7.11: Mean δ^{18}O(‰) results shifted to the AD 1900-1954 common period with 95% confidence intervals

For the δ^{18}O shifted data post AD 1900 both the 95% confidence interval (Figures 7.11 and 7.12) and the range of values (Figure 7.13) are narrow (mean range = 1.35 and mean 95% confidence interval = 0.47), however from AD 1810 to 1900 the 95% confidence interval and range widen (mean range = 2.35, mean 95% confidence interval = 1.06). A comparison of these results with those of the unshifted data can be seen in Table 7.2. This problem of increase variance in the nineteenth century is largely due to Tree 87.

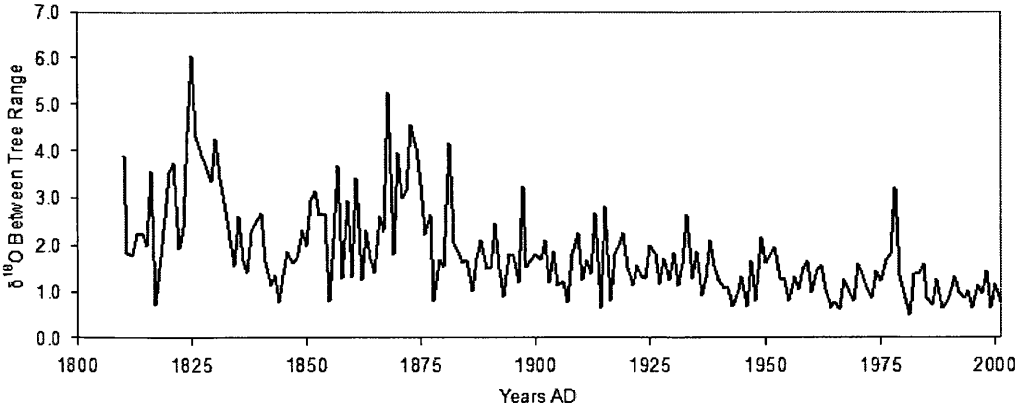

Figure 7.13: Range of δ^{18}O(‰) shifted results (maximum δ^{18}O (‰) for each year minus minimum)

	AD 1810-1899	AD 1900-2001
Range Raw	1.83	2.47
Range Shifted	2.35	1.35
95% Raw	0.80	0.84
95% Shifted	1.06	0.47

Table 7.2: Comparison of the range and 95% confidence intervals of the unshifted and shifted δ^{18}O(‰) over the nineteenth and twentieth centuries.

This tree, as has already discussed, is rather more variable than the rest of the trees throughout the series (see Figure 7.1). When its values are brought towards the mean of the values for AD 1900 to 1954 its values for the nineteenth century are rather lower than those for the other trees (see Figure 7.10) leading to an increase in range and the 95% confidence interval over this period. However, despite problems with this tree, the overall mean range and 95% confidence interval are significantly reduced by the shifting process as can be seen in Table 7.3 and are better than when the period AD 1840 to 1879 is used as the first common period, details of which are also shown in this figure.

	Raw data	Shifted AD 1840-1879	Shifted AD 1900-1954
Range	2.17	2.01	1.82
95% confidence interval	0.82	0.77	0.75

Table 7.3: Comparison of the range and 95% confidence intervals for the raw δ^{18}O (‰) values and values shifted over the periods AD 1840-1879 and AD 1900-1954.

	MSE
$\delta^{18}O_{raw}$ & $\delta^{18}O_{shift}$ C19th	0.0016
$\delta^{18}O_{raw}$ & $\delta^{18}O_{shift}$ C20th	0.0015
$\delta^{18}O_{shift}$C19th & $\delta^{18}O_{shift}$ C20th	0.0020

Table 7.4: Mean squared error (MSE) between raw mean δ^{18}O(‰) values and mean values shifted over the periods AD 1840-1879 (C19th) and AD 1900-1954 (C20th).

Table 7.4 shows the MSE between the mean $\delta^{18}O_{raw}$ unshifted (raw) values and those shifted using the period AD 1840 to 1879 and then AD 1900 to 1954 as the first common period. It is clear from this table that the error between these three data sets are so low that they are virtually identical. A graph showing the three data is relativly uninformative as it shows three nearly identical overlaid lines and so is not shown. The choice of correction periods, or indeed using the uncorrected data, would therefore have a negligible affect on any calibration or climatic reconstruction. However, as discussed earlier, using the shifted data set will negate potential problems of non climate related offsets in the mean value as new trees are introduced earlier in the sequence. The comparisons and calibration verification procedure with climatic data will therefore proceed using the mean δ^{18}O data shifted over the period AD 1900 to 1954 ($\delta^{18}O_{shift}$).

7.4 δ^{18}O and Climate

In this section the mean $\delta^{18}O_{shift}$ data will be compared to the temperature and precipitation records from the Andenes meteorological climate station and also from the northern coast composite precipitation record compiled by Hanssen-Bauer and Føland (1998).

7.4.1 δ^{18}O and Temperature

The correlation coefficients between $\delta^{18}O_{shift}$ and mean monthly temperature from Andenes for the previous and current year can be seen in Figure 7.14, while only those months significant at the 95% level can be seen in Figure 7.15. In general the cor-

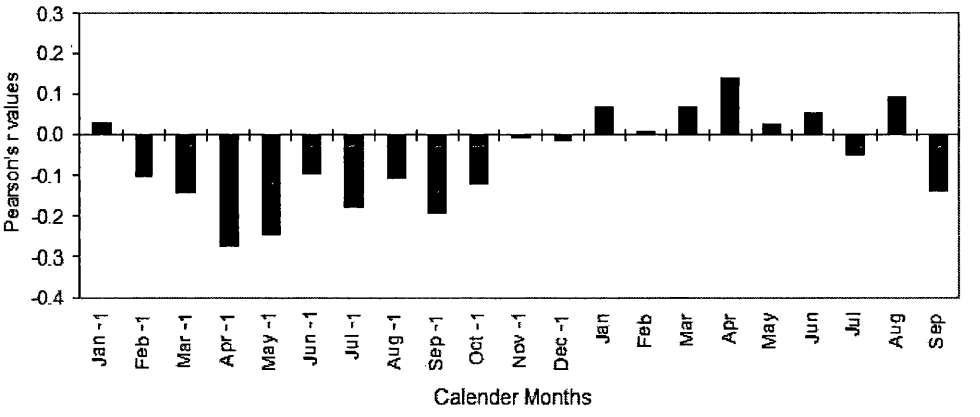

Figure 7.14: Bootstrapped correlation values for $\delta^{18}O_{shift}(‰)$ data and mean monthly temperatures for Andenes from AD 1869 to 2001. Using the whole of the previous calender year and the current year to September to encompass the whole potential growing season and any possible correlations with earlier seasons temperatures.

relations between $\delta^{18}O_{shift}$ and temperature are low, with significant correlations only occurring for the previous years April, May and September temperature. As these correlation are rather low and there seems to be no obvious causal relationship between the previous years spring or autumn temperature and the fractionation of δ^{18}O, these will be disregarded. As there seems to be no obvious relationship between temperature and δ^{18}O fractionation at this location, we will move on to consider the relationship between δ^{18}O and precipitation.

7.4.2 δ^{18}O and Precipitation

Figure 7.16 shows mean monthly correlation between $\delta^{18}O_{shift}$ and mean monthly precipitation from the Andenes meteorological station from AD 1910 to 2001, while Figure 7.17 shows only those months significant at the 95% level. The highest significant correlation is with the current years August precipitation at r = -0.51, while there are also significant correlation with the current year's March and July precipitation both at r = -0.25. Mean July and August precipitation yields a correlation very slightly lower than August alone at r = -0.50.

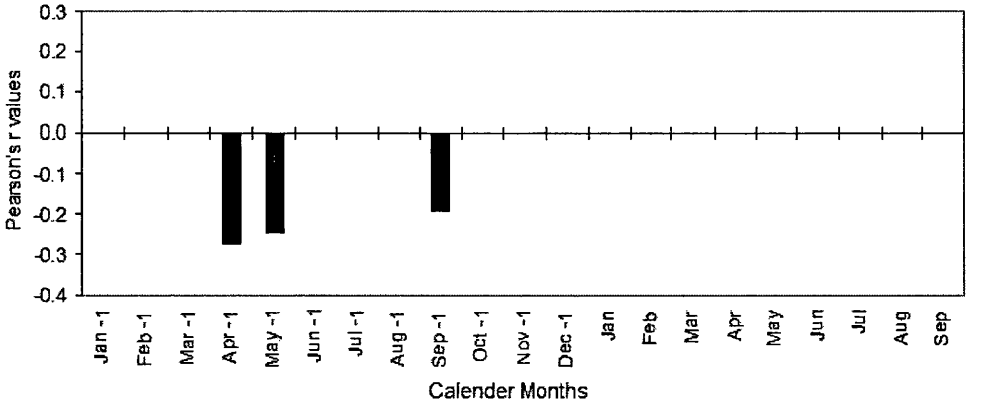

Figure 7.15: Bootstrapped correlation values for $\delta^{18}O_{shift}(‰)$ and mean monthly temperatures as figure 7.14 showing only correlation within the 95% confidence limits.

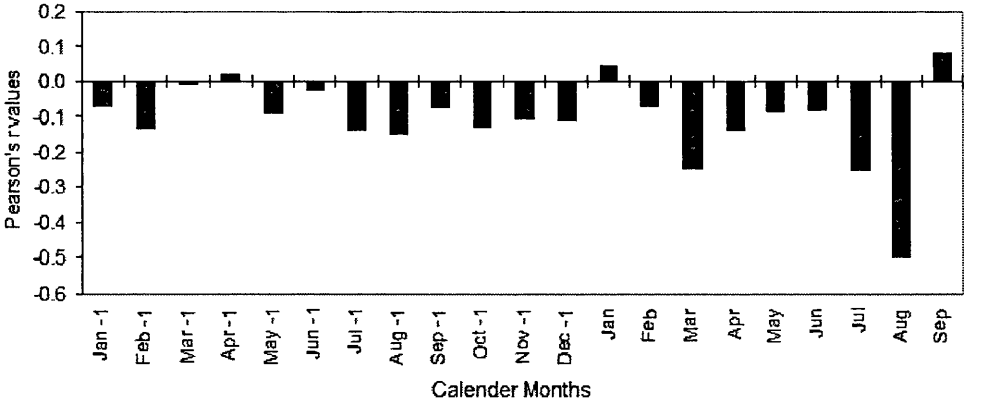

Figure 7.16: Bootstrapped correlation values for $\delta^{18}O_{shift}(‰)$ data and mean monthly precipitation from Andenes from AD 1910 to 2001. Using the whole of the previous calender year and the current year to September to encompass the whole potential growing season and any possible correlations with earlier seasons precipitation.

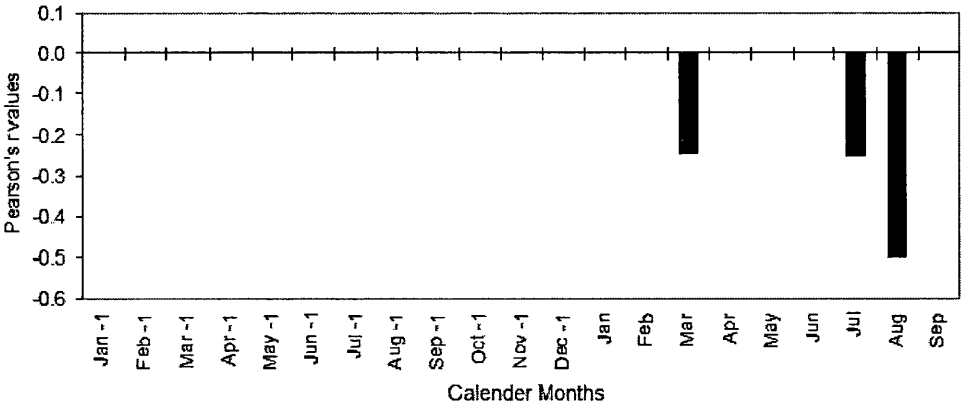

Figure 7.17: Bootstrapped correlation values for $\delta^{18}O_{shift}$(‰) shifted and mean monthly precipitation as Figure 7.16 but showing only correlation within the 95% confidence limits

.

The monthly correlation between $\delta^{18}O_{shift}$ and the precipitation data for selected stations from the arctic circle to northern cape compiled by Hanssen-Bauer and Føland (1998) can be seen in Figure 7.18. There are significant correlations with July (r = -0.36), August (r = -0.43) and mean July and August (r = -0.49). This record is much longer (starting at AD 1873) than than the Andenes record and so includes much of the period where the EPS is low (Figure 7.5). It is also a composite of a number of widely spread climate stations. This makes the mean July and August correlation of r = -0.49 seem rather impressive when compared to the correlation for the more local Andenes station for July and August of r = -0.49 for the period AD 1910 to 2001. Indeed if the two mean July and August precipitation records are compared over the same period (AD 1910 to 1997), the correlation with the northern coast record is rather better (r = -0.57) than the Andenes record (r = -0.51).

It would seem that, in the absence of data for other potential controlling factors such as relative humidity, August mean or mean July and August mean precipitation is the environmental variable that is linked most strongly with δ^{18}O fractionation. Moisture availability is, in reality, unlikely to be the major controlling factor of δ^{18}O fractionation at this location with its relatively high annual rainfall. Vapour pressure deficit (VPD)

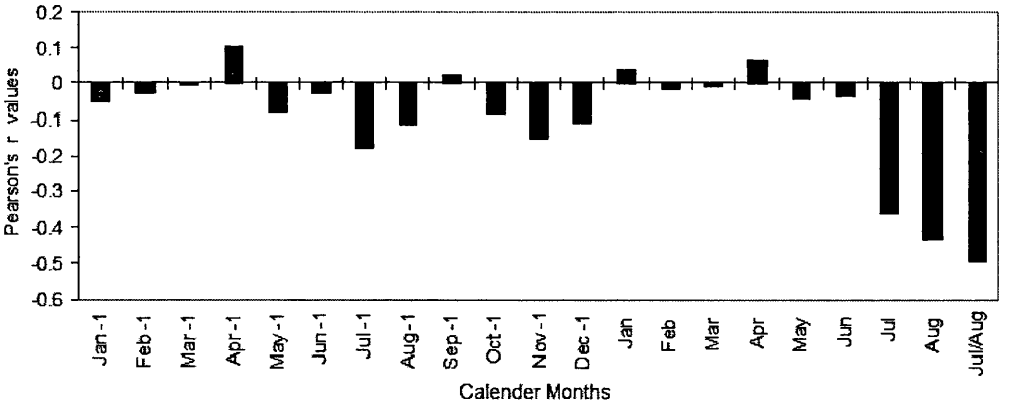

Figure 7.18: Bootstrapped correlation values for $\delta^{18}O_{shift}$(‰) data and mean monthly northern coast precipitation (Hanssen-Bauer and Føland, 1998)from AD 1873 to 2001. Using the whole of the previous calender year and the current year to September.

would seem likely to have an important role in controlling the evaporation of H_2O through the stomata and hence the preferential loss of water molecules containing the lighter ^{16}O atom. While there may be a relationship between relative air humidity and precipitation at this coastal location, high relative air humidity may occur from factors such as mist which is not be associated with precipitation. Indeed this phenomena was observed on more than one occasion during summer fieldwork (2 weeks over 2 years). Several sea mists enveloped most, but not always all of the forest, as there was often an altitudinal limit, for much of the day. Despite this, if $\delta^{18}O$ is capable of reconstructing growing season precipitation to some degree, this should prove extremely useful in interpreting the $\delta^{13}C$ results which have a potentially mixed signal from temperature, moisture availability, and relative air humidity.

Before proceeding with the calibration procedure, the relationship between $\delta^{18}O$ and precipitation through time will be briefly examined. Figure 7.19 shows the maximum 30 year running correlation between $\delta^{18}O_{shift}$ and mean July, August, and July and August precipitation from the Andenes meteorological station (AD 1910 to 2001). Figure 7.20 shows the same running correlation for mean July and August precipitation for the Norwegian northern coastal stations (Hanssen-Bauer and Føland, 1998). As with $\delta^{13}C$ and temperature, Figure 7.19 shows that the correlation between $\delta^{18}O_{shift}$ and Andenes

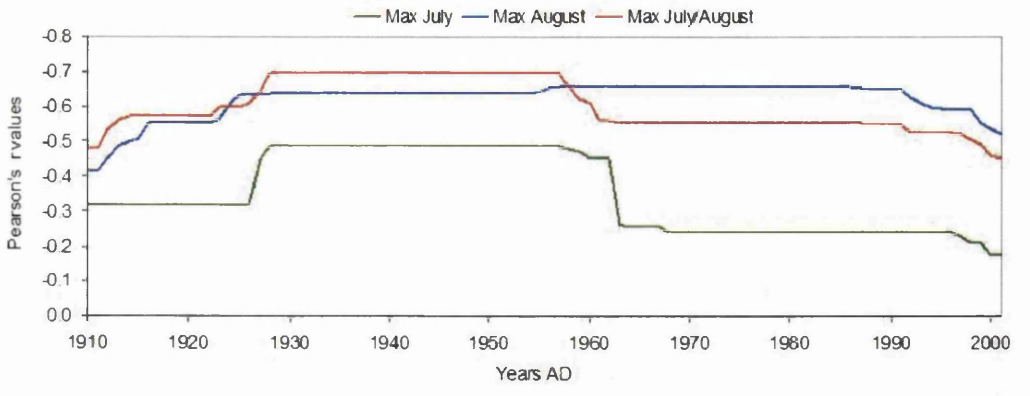

Figure 7.19: Running 30 maximum correlations between $\delta^{18}O_{shift}(‰)$ and mean July, August and July and August precipitation from Andenes

precipitation are strongest in middle years of the twentieth century and fall away a little at both ends of the time series. This is especially evident for July precipitation, but mean July and August correlates better than August precipitation in the mid AD 1900s. This may again be suggestive of an expansion of the critical period for latewood formation in the middle years of the twentieth century. The signal for August temperature is rather more stable than mean July and August, but again the correlations tail off rather early in the series, perhaps as the common signal strength declines.

The relationship between northern coastal mean July and August precipitation and $\delta^{18}O_{shift}$ is more consistent through time than the relationship with Andenes precipitation, with a maximum 30 year running correlation of $r = 0.59$ for 30 year blocks starting from AD 1892. Prior to this point in time, correlations decline as the common signal strength among trees declines (Figures 7.4 and 7.5).

A comparison between mean July and August precipitation from Andenes and the northern coastal stations can be seen in Figure 7.21. With an r value of 0.89 and no obvious offsets between them, the two records appear fairly homogeneous. However, Figure 7.22 which shows a running 30-year correlation between the two records, demonstrates that, while still fairly high, the correlations in the early part of the record are somewhat weaker than at the end. This perhaps explains why the correlations between the $\delta^{18}O_{shift}$ and mean July and August precipitation from the northern coastal record are rather bet-

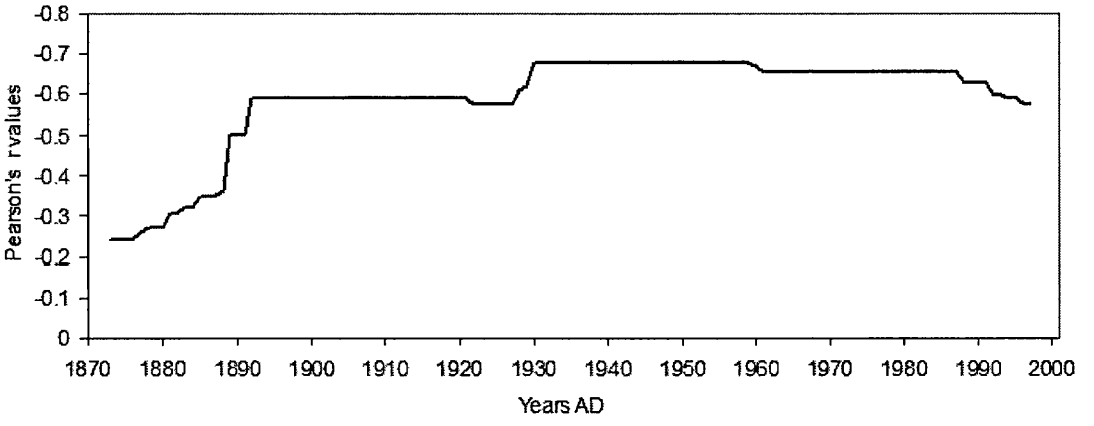

Figure 7.20: Running 30 maximum correlations between $\delta^{18}O_{shift}$(‰) and mean July and August precipitation for the Norwegian northern coastal stations (Hanssen-Bauer and Føland, 1998)

ter than with the Andenes record early in the series. It is slightly surprising that this composite of various coastal stations correlates better with the $\delta^{18}O_{shift}$ record from Forfjorddalen than the nearest climate station, but perhaps this demonstrates that precipitation is rather variable in this mountainous coastal area, and that the regional trend gives a better match than simply the nearest station, which is some 60 km away and in a somewhat different geographical setting.

7.5 δ^{18}O Calibration with Precipitation

Both the Andenes and the longer northern coastal record (Hanssen-Bauer and Føland, 1998) will be used for calibrating the $\delta^{18}O_{shift}$ isotope data. These data will also be converted into the Standardised Precipitation Index (SPI) developed by McKee et al. (1993). The calibration procedure is the same as that carried out for δ^{13}C and temperature in the preceding chapter, with the data sets being split into calibration and verification periods and the results analysed using the same verification statistics.

Figure 7.23 shows reconstructed August precipitation from Andenes for the full period for which mean monthly precipitation data are available (from AD 1910). Figure 7.23a uses

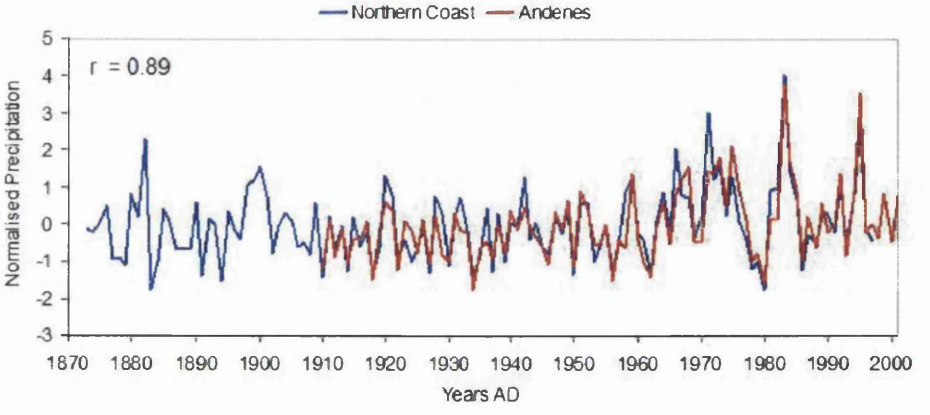

Figure 7.21: A comparison between mean July and August precipitation from Andenes and for the combined northern coastal station. Both data sets have been normalised, as the northern coast data set is indexed rather than in mm.

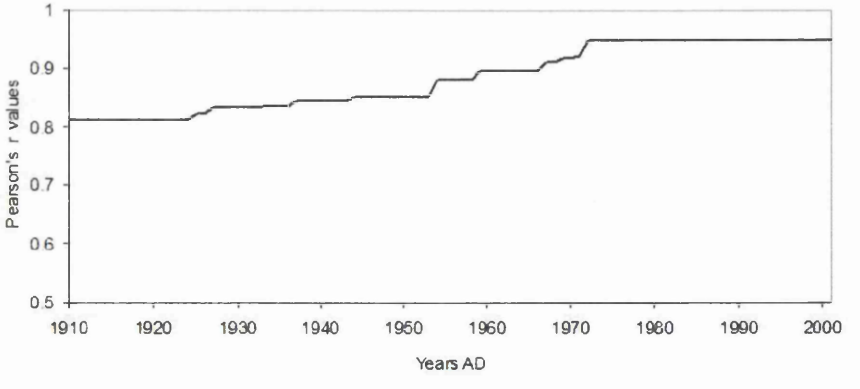

Figure 7.22: Running 30 year correlation between the northern coast and Andenes mean July and August precipitation

the period AD 1910 to 1955 for calibration and AD 1956 to 2001 for verification while 7.23b reverses the calibration and verification periods. The statistics for both 7.23a and b can be seen in Table 7.5. Both periods display positive RE and CE statistics, demonstrating that both reconstructions are able to outperform the mean of both period used for calibration (RE) and (more demanding) verification (CE). The CE statistics are fairly modest, especially when AD 1956 to 2001 is used to reconstruct AD 1910 to 1955 (CE = 0.07). This would appear to be partially due to the extreme precipitation years in the second half of the twentieth century, whose magnitude the $\delta^{18}O_{shift}$ results do not capture very well. However, as we have already seen, the correlations are fairly consistent for both periods (Table 7.5).

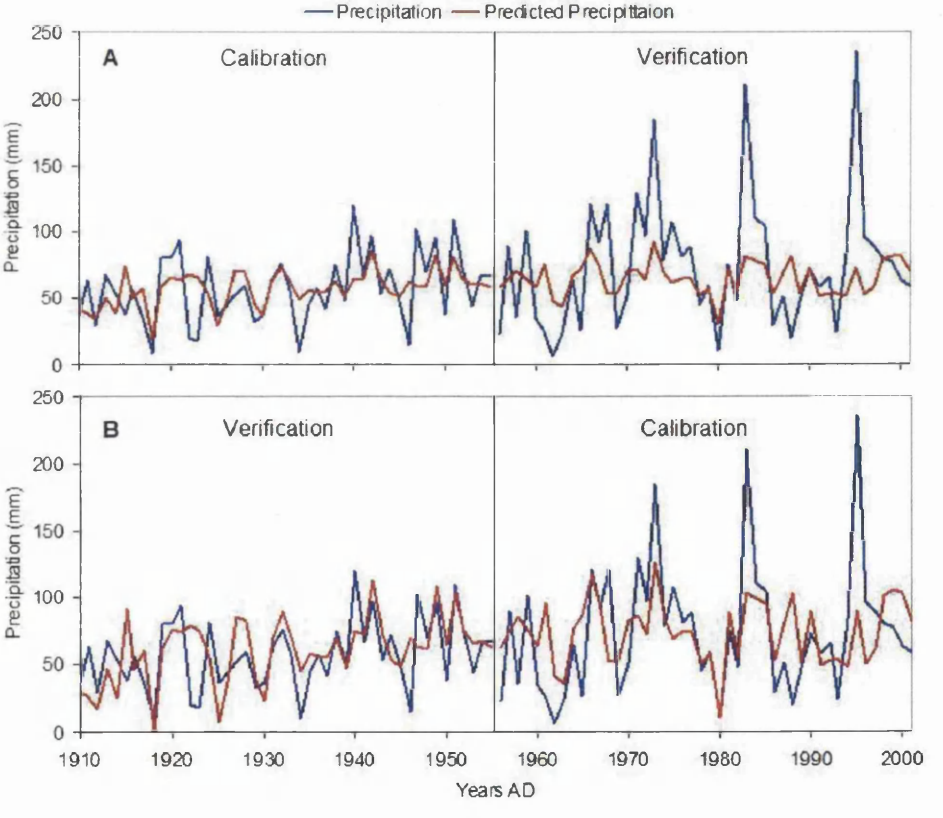

Figure 7.23: Reconstructed mean August Andenes precipitation using (A) AD 1910-1955 as the calibration period and AD 1956-2001 as the verification period and (B) AD 1956-2001 as the calibration period and AD 1910-1955 as the verification period. In both cases compared to actual mean August precipitation.

	Calibration AD 1910-1955	Verification AD 1956-2001	Calibration AD 1956-2001	Verification AD 1910-1955
MSE	486.97	1968.11	1758.80	622.40
RE	0.27	0.24	0.24	0.35
CE	NA	0.15	NA	0.07
r^2	0.27	0.24	0.24	0.27

Table 7.5: Verification statistics for the mean August precipitation reconstruction using the (on the left) AD 1910-1955 for calibration and AD 1956-2001 for verification and (on the right) AD 1956-2001 for calibration and AD 1910-1955 for verification.

A graph showing the calibration made over the entire period can be seen in Figure 7.24, with accompanying statistics in Table 7.6. Again the reconstruction appears to be a reasonable one with an $r^2$and RE of 0.50, although again the magnitude of the more extreme late twentieth century precipitation events (especially AD 1983 and AD 1995) is not captured. Given the fairly moderate correlations between $\delta^{18}O_{shift}$ and August precipitation the reconstruction appears to be a useful one, although not for predicting large August rainfall events in excess of around 100 mm.

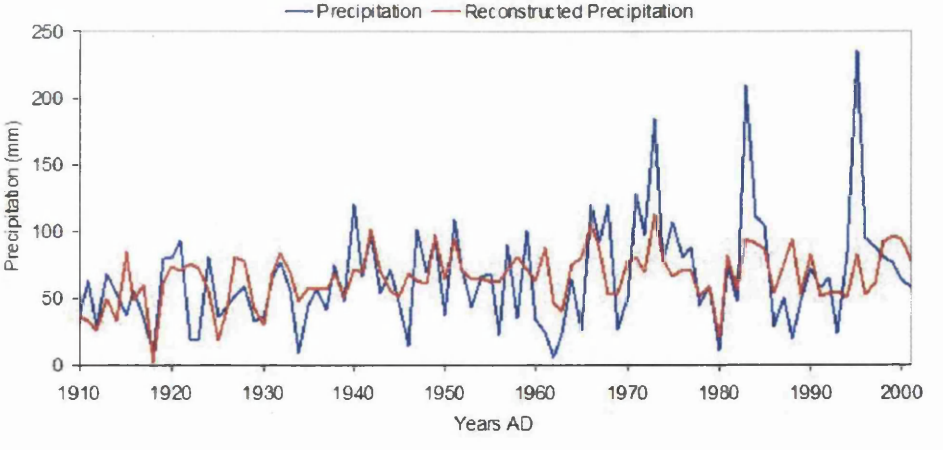

Figure 7.24: Reconstructed mean August precipitation from AD 1910-2001 using the same period for calibration, compared to actual precipitation.

	Calibration AD 1910-2001
MSE	1164.01
RE	0.25
CE	NA
r^2	0.25

Table 7.6: Statistics for the mean August precipitation reconstructed for AD 1910-2001, using the same period for calibration.

When the August precipitation data are converted in a SPI (in this case 1 month August SPI), the results of the same calibration and verification process can be seen in Figures 7.25 and 7.26 and Tables 7.7 and 7.8. Although the overall correlation are quite similar to those using August precipitation (the data used is in effect the same), the slight smoothing effect that the SPI has on the precipitation data has quite a noticeable affect on the CE statistics which improve for both verification periods (AD 1956-2001: 0.15 to 0.23 and AD 1910-1955: 0.07 to 0.17). A comparison of the calibration carried out over the whole period in Figures 7.24 and 7.26 and supported by the statistics in Tables 7.6 and 7.8 suggests that a reconstruction of August SPI using $\delta^{18}O_{shift}$ is slightly more effective than that for precipitation alone.

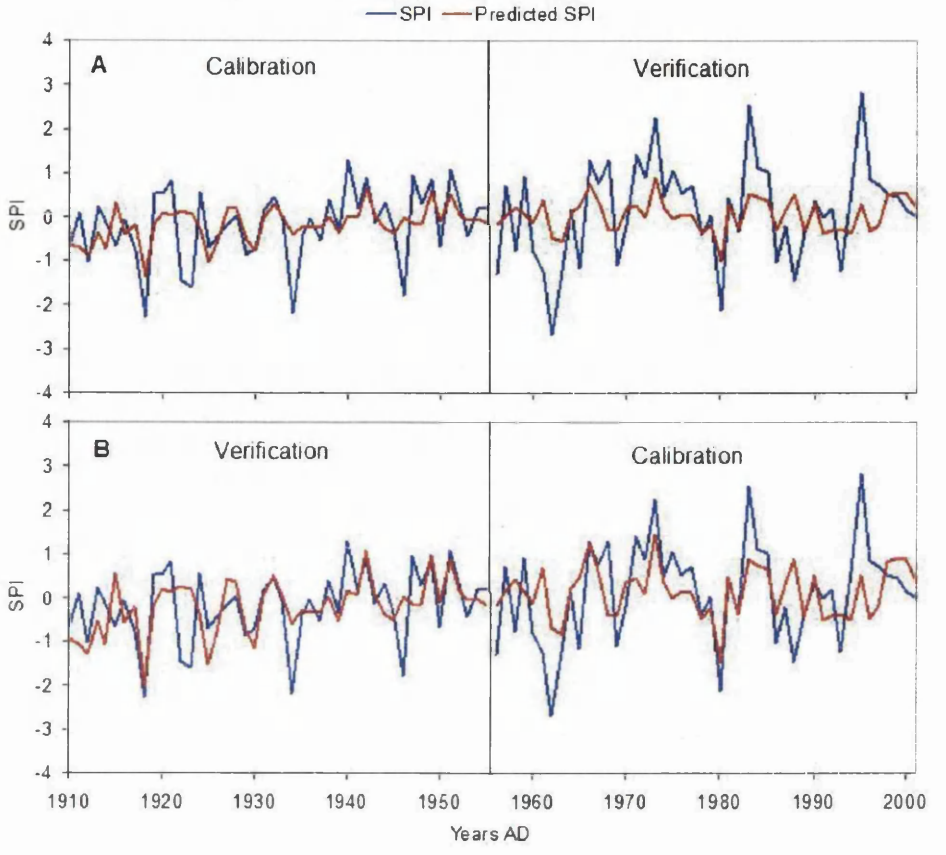

Figure 7.25: Reconstructed August SPI using (A) AD 1910-1955 as the calibration period and AD 1956-2001 as the verification period and (B) AD 1956-2001 as the calibration period and AD 1910-1955 as the verification period. In both cases compared to actual calculated SPI.

	Calibration AD 1910-1955	Verification AD 1956-2001	Calibration AD 1956-2001	Verification AD 1910-1955
MSE	0.49	1.00	0.94	0.54
RE	0.25	0.28	0.27	0.28
CE	NA	0.23	NA	0.17
r^2	0.25	0.27	0.27	0.25

Table 7.7: Verification statistics for the Andenes August SPI reconstruction using the (on the left) AD 1910-1955 for calibration and AD 1956-2001 for verification and (on the right) AD 1956-2001 for calibration and AD 1910-1955 for verification.

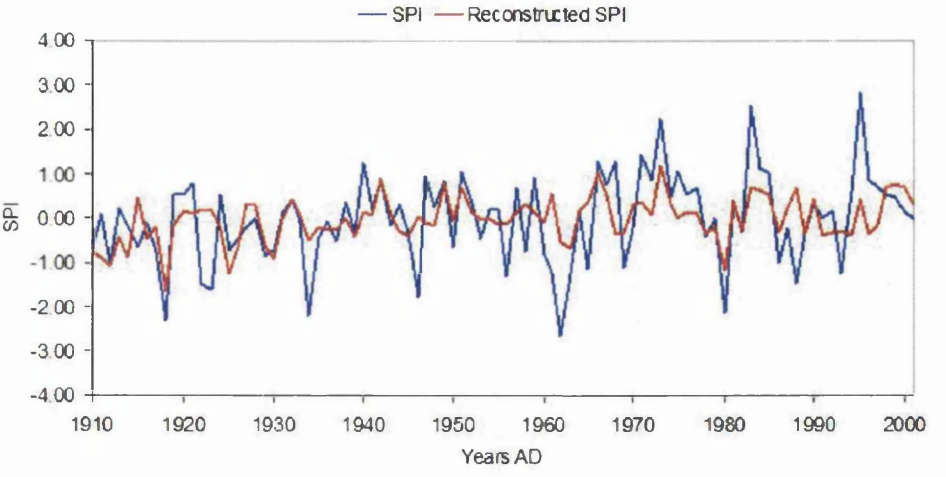

Figure 7.26: Reconstructed August SPI from AD 1910-2001 using the same period for calibration, compared to actual calculated SPI.

	Calibration AD 1910-2001
MSE	0.73
RE	0.27
CE	NA
r^2	0.27

Table 7.8: Verification statistics for Andenes August SPI reconstructed for AD 1910-2001, using the same period for calibration.

The longer composite record for the northern coastal stations (not including Andenes) covers the period from AD 1873 to 1997 (Hanssen-Bauer and Føland, 1998). These data come from a number of stations and so the precipitation values are indexed rather than being in millimeters. The record also covers the period of the $\delta^{18}O_{shift}$ record which has poor common signal strength between the trees (Figures 7.4 and 7.5), from $\sim$ AD 1865 to 1890.

Figure 7.27 shows these data reconstructed using $\delta^{18}O_{shift}$, with the period AD 1873 to 1934 used for calibration, and AD 1935 to 1997 used for verification Figure 7.27A. These periods are reversed in Figure 7.27B, and the statistics for both of these can be seen in Table 7.9. It has already been shown that there is a decline in the correlation between $\delta^{18}O_{shift}$ and mean July and August precipitation in the early part of this record

(before ~AD 1895, see Figure 7.20). This is reflected in the low correlation values for the period AD 1873 to 1934 (r^2= 0.13 compared to r^2= 0.34 for the period AD 1935 to 1997), which has a detrimental affect on the reconstruction. Figure 7.27A shows the reconstruction based on the calibration period AD 1873 to 1934. This captures the high frequency fairly poorly (due to the low correlation), the CE figure is however positive at 0.19. Figure 7.27B appears to capture more high frequency variation, it has however a very poor CE figure for the verification period (-0.17) and an RE of only 0.02. This is due to the reconstruction failing to match actual precipitation at all well prior to about AD 1895. That the calibration based on this period is able to reconstruct precipitation for the period AD 1935 to 1997 suggests that the model has some merit.

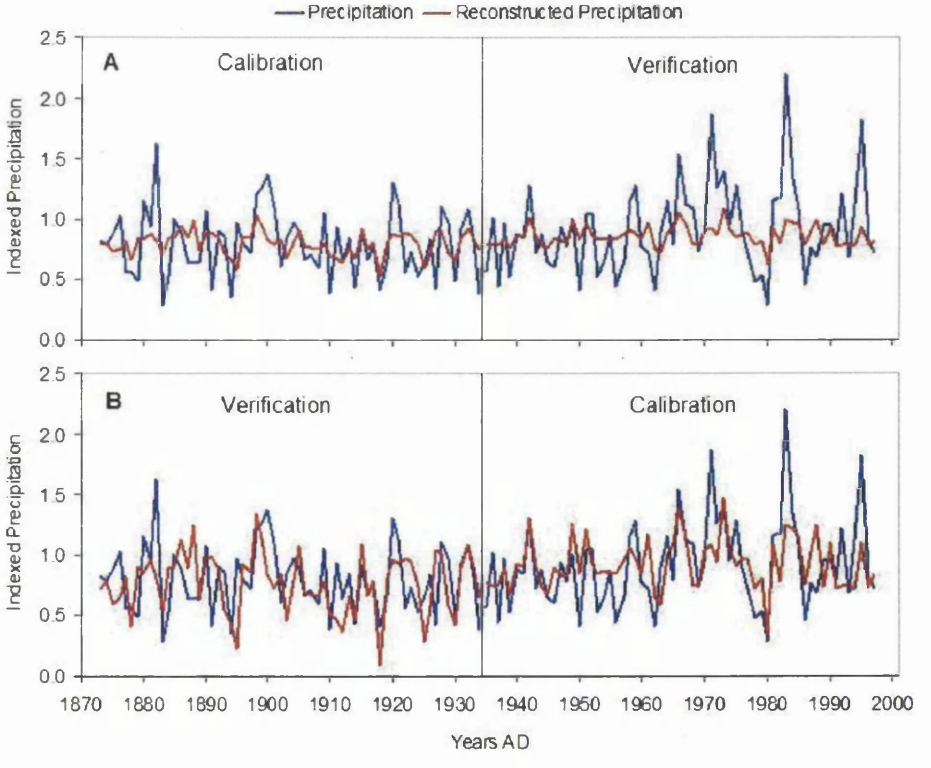

Figure 7.27: Reconstructed mean July and August northern coastal precipitation using (A) AD 1873-1934 as the calibration period and AD 1935-1997 as the verification period and (B) AD 1935-1997 as the calibration period and AD 1873-1934 as the verification period. In both cases compared to actual precipitation.

	Calibration AD 1873-1934	Verification AD 1935-1997	Calibration AD 1935-1997	Verification AD 1873-1934
MSE	0.07	0.11	0.09	0.09
RE	0.13	0.27	0.34	0.02
CE	NA	0.19	NA	-0.17
r^2	0.13	0.34	0.34	0.13

Table 7.9: Statistics for the northern coastal mean July and August precipitation reconstruction using the (on the left) AD 1873-1934 for calibration and AD 1935-1997 for verification and (on the right) AD 1935-1997 for calibration and AD 1873-1934 for verification.

Figure 7.28 shows a reconstruction based on the entire period compared to actual precipitation, with statistics in Table 7.10. Again this appears to be a good reconstruction of precipitation, although it is again possible to see that prior to ~AD 1895 the inter annual variability matches quite poorly. However, the overall r^2 of 0.24 appears is quite high.

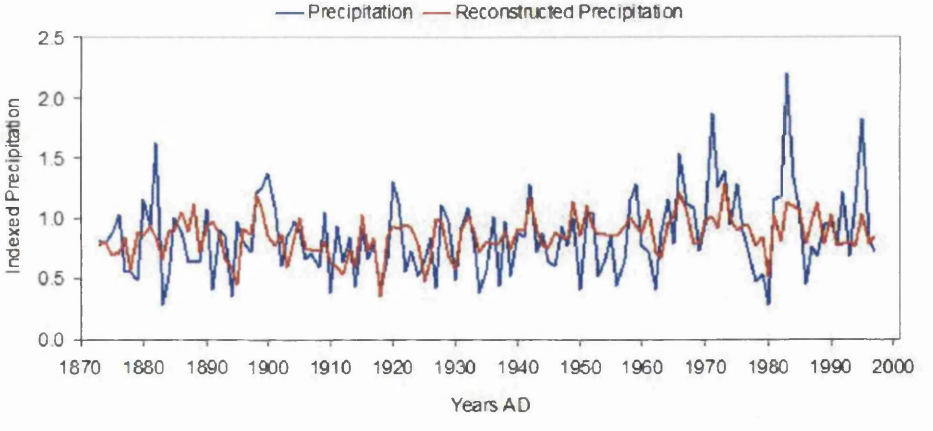

Figure 7.28: Reconstructed mean July and August northern coastal precipitation from AD 1873-1997 using the same period for calibration, compared to actual precipitation.

	Calibration AD 1873-1997
MSE	0.08
RE	0.24
CE	NA
r^2	0.24

Table 7.10: Statistics for northern coastal mean July and August precipitation reconstructed for AD 1873-1997, using the same period for calibration.

When the early period of the record is removed from AD 1873 to 1895 the time series, due to it's poor common signal, the reconstruction improves (Figures 7.11 and 7.12 and Tables 7.11 and 7.12). The reconstructions now have positive CE values for both verification periods (0.22 and 0.14) and also a higher overall r^2 of 0.31 (Table 7.12). As was the case for δ^{13}C and temperature, the period at the end of the nineteenth century has a low common final strength between trees and also a poor correlation with climate.

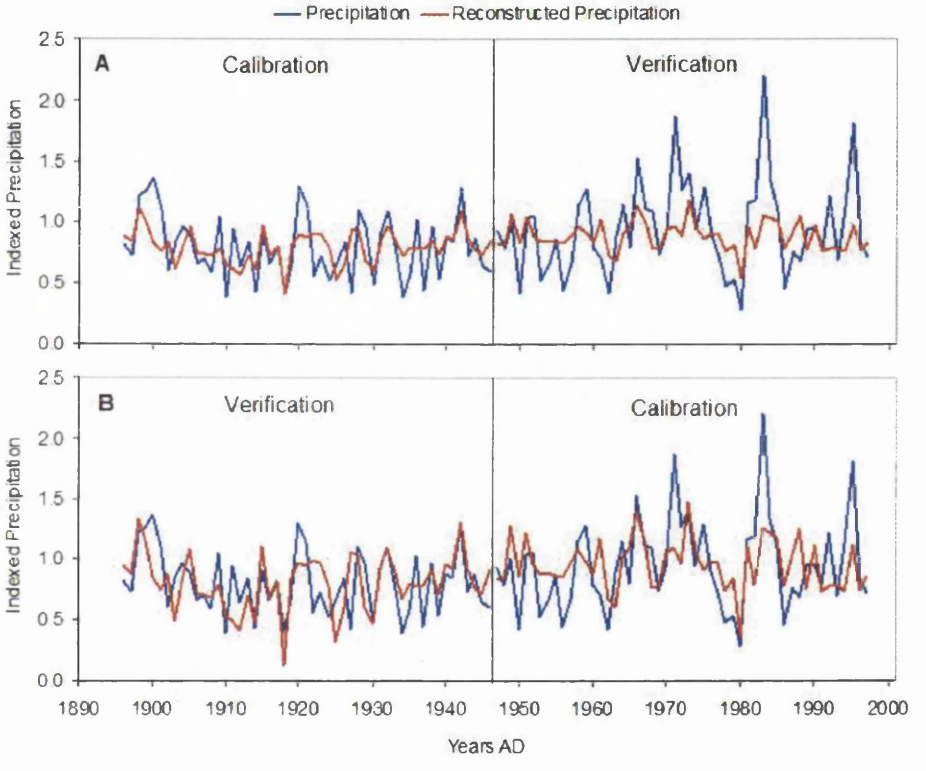

Figure 7.29: Reconstructed mean July and August northern coastal precipitation using (A) AD 1896-1946 as the calibration period and AD 1947-1997 as the verification period and (B) AD 1947-1997 as the calibration period and AD 1896-1946 as the verification period. In both cases compared to actual precipitation.

	Calibration AD 1896-1946	Verification AD 1947-1997	Calibration AD 1947-1997	Verification AD 1896-1946
MSE	0.05	0.11	0.10	0.06
RE	0.28	0.33	0.31	0.36
CE	NA	0.22	NA	0.14
r^2	0.28	0.31	0.31	0.28

Table 7.11: Statistics for the northern coastal mean July and August precipitation reconstruction using the (on the left) AD 1896-1946 for calibration and AD 1947-1997 for verification, and (on the right) AD 1947-1997 for calibration and AD 1896-1946 for verification.

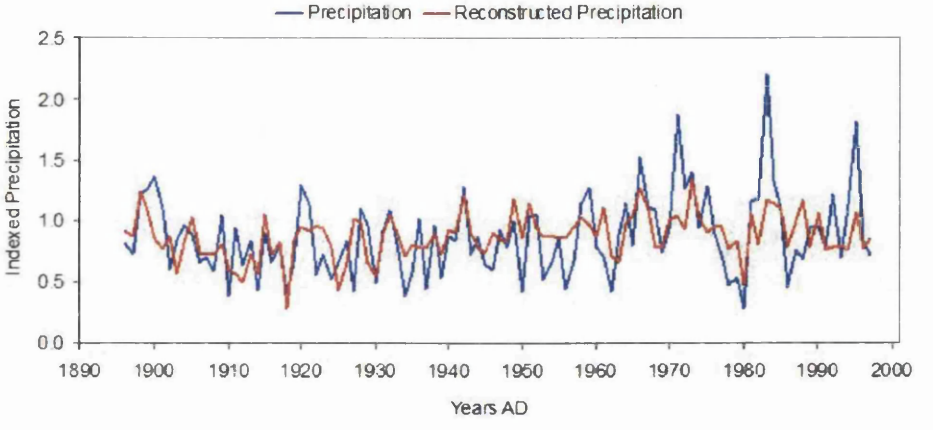

Figure 7.30: Reconstructed mean July and August northern coastal precipitation from AD 1896-1997 using the same period for calibration, compared to actual precipitation.

	Calibration AD 1896-1997
MSE	0.08
RE	0.31
CE	NA
r^2	0.31

Table 7.12: Statistics for northern coastal mean July and August precipitation reconstructed for AD 1896-1997, using the same period for calibration.

Finally SPI was calculated for the northern coastal precipitation record (this time a 2 month August SPI) and calibrated with precipitation. While this was unable to improve on the full record from AD 1873 to 1997 (details not shown here), when compared to the $\delta^{18}O_{shift}$ record from AD 1896 to 1997 it was able to provide a better reconstruction than

using precipitation alone (Figures 7.31 and 7.32 and Tables 7.13 and 7.14). Returning quite satisfactory RE (0.37 and 0.34) and CE (0.27 and 0.18) figures for both verification periods. Again, this suggests that $\delta^{18}O_{shift}$ is better suited to reconstructing SPI than precipitation alone, largely because the SPI ameliorates the more extreme precipitation events which $\delta^{18}O_{shift}$ seems unable to satisfactorily capture.

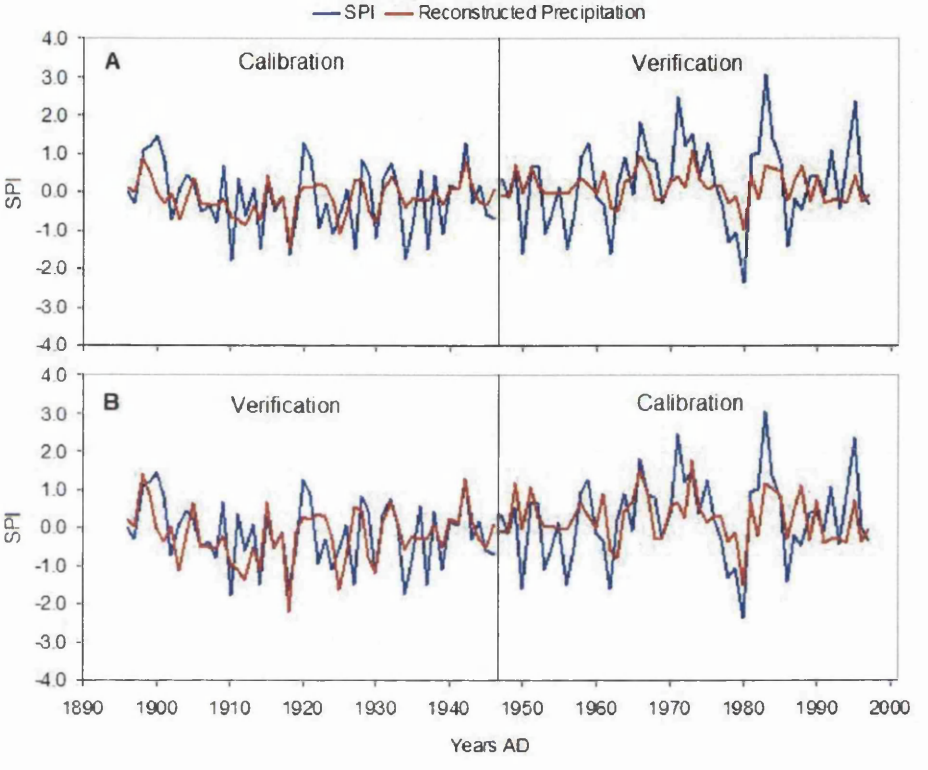

Figure 7.31: Reconstructed northern coastal August 2-month SPI using (A) AD 1896-1946 as the calibration period and AD 1947-1997 as the verification period, and (B) AD 1947-1997 as the calibration period and AD 1896-1946 as the verification period. In both cases compared to the actual calculated SPI.

	Calibration AD 1896-1946	Verification AD 1947-1997	Calibration AD 1947-1997	Verification AD 1896-1946
MSE	0.52	0.85	0.78	0.59
RE	0.27	0.37	0.33	0.34
CE	NA	0.27	NA	0.18
r^2	0.27	0.33	0.33	0.27

Table 7.13: Statistics for the northern coastal 2- month August SPI reconstruction using the (on the left) AD 1896-1946 for calibration and AD 1947-1997 for verification and (on the right) AD 1947-1997 for calibration and AD 1896-1946 for verification.

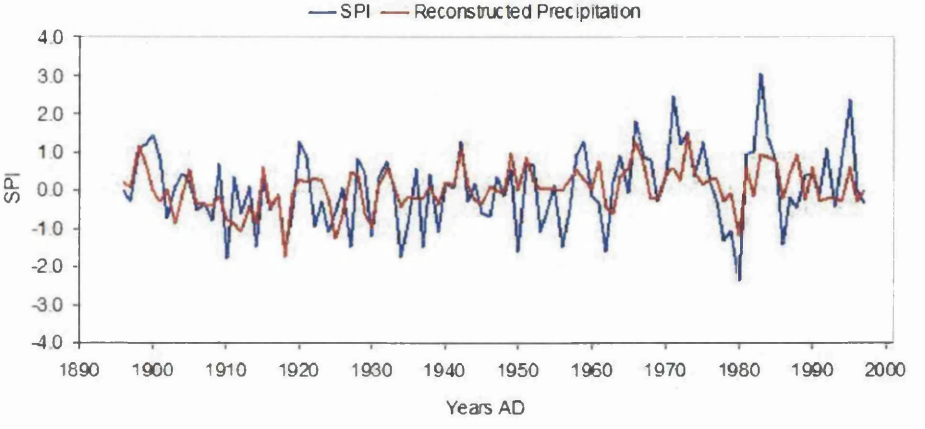

Figure 7.32: Reconstructed northern coastal August 2-month SPI from AD 1896-1997 using the same period for calibration, compared to the actual calculated SPI.

	Calibration AD 1896-1997
MSE	0.67
RE	0.33
CE	NA
r^2	0.33

Table 7.14: Statistics for the northern coastal 2 month August SPI reconstructed for AD 1896-1997, using the same period for calibration.

7.6 Chapter Conclusion

The common signal for the δ^{18}O record from Forfjorddalen is not as strong as that for δ^{13}C and suffers a decline during much the same period as the δ^{13}C record, at the end of

the nineteenth century. There is also a dip in the record in the middle of the twentieth century which is not reflected in the δ^{13}C signal strength. While there are some problems with common signal strength the maximum EPS for the entire record is greater than 0.85 for all but a short period (Figure 7.5) and so seems generally suitable for climatic reconstruction. As was the case for the $\delta^{13}C_{pin}$ record the δ^{18}O values have been shifted towards the mean value using a common period, to prevent offsets in the mean as new trees are added to the series.

The fractionation of δ^{18}O from α-cellulose extracted from the latewood of Scots pine at Forfjorddalen appears to be linked fairly strongly to late summer precipitation (July to August). As we have already seen, evidence from the δ^{13}C record would seem to suggest that the key period in the production of sugars for latewood cellulose stretches from around the 20th of July to the 20th of August, and the δ^{18}O would seem to support this.

Correlation with the local precipitation record from Andenes between AD 1810 and 2001 is $r = 0.51$ for August precipitation and $r = 0.49$ for mean July and August. The composite northern coastal record (Hanssen-Bauer and Føland, 1998) also correlates reasonably well with the δ^{18}O record ($r = 0.49$), suggesting that as with δ^{13}C and temperature, the isotopes from Forfjorddalen may reflect more than a purely local signal.

The calibration of δ^{18}O with mean August precipitation from Andenes is generally successful, with positive RE and CE statistics (Figure 7.23 and Table 7.5). These statistics improve when the precipitation data are converted into the SPI (Table 7.7). When the northern coastal record is used for calibration the period at the end of the nineteenth century with low common signal strength is included and the reconstruction suffers accordingly with a negative CE and low RE figure for the verification period AD 1873-1934 (7.9). When the early part of the record is excluded from the calibration and only the period from AD 1896 to 1997 is used, the calibration is much more successful, especially when the precipitation data are converted into SPI (Figure 7.31 and Table 7.13). Unfortunately, unlike temperature, there are no longer precipitation records available to check whether the correlation between δ^{18}O and precipitation reestablishes itself in the early part of the nineteenth century, as the relationship between $\delta^{13}C_{pin}$ and temperature

does. It does seem reasonable to expect this to occur as the inter-correlation between trees improves in the first half of the AD 1800s.

The ability of δ^{18}O to explain around one third of the variance in precipitation makes it an extremely useful addition to the tools available to reconstruct past climate at Forfjorddalen. As has been demonstrated in the previous chapter, $\delta^{13}C_{pin}$ is (if the period of low common signal between trees is excluded) able to reconstruct temperature rather successfully. However, as $\delta^{13}C_{pin}$ is potentially controlled by both photon flux (correlating strongly with temperature) and moisture availability it is important to have some independent estimate of moisture availability (precipitation) to be able to interpret the $\delta^{13}C_{pin}$ with confidence. Aside from this a reconstruction of past precipitation in this region is also of great interest, as in this area there are no obvious recent increases in mean summer temperature, but rather an increase in summer precipitation, which may in itself be linked to larger scale climatic changes.

In the next chapter δ^{18}O and $\delta^{13}C_{pin}$ records will be used in conjunction to yield a potentially more comprehensive understanding of past climatic changes; especially for periods of non-corelative behavior in the relationships between stable isotopes from tree rings, and climate, such as appears to have occurred the end of the nineteenth century and how periods such as this may be identified further back in time where no climate records are available.

8

Multiproxy Dendroclimatology

8.1 Introduction

Thus far this thesis has concentrated on identifying links between individual tree-ring proxies and climate parameters and then using this relationship to reconstruct climate. In this chapter all the available tree ring proxy evidence from Forfjorddalen will be combined in an attempt to gain a fuller understanding of the links between climate, $\delta^{13}C$, $\delta^{18}O$ and ring width series and to explore the possibilities of multiproxy climate reconstructions.

Initially a model will be presented to help understand the relationship between climate, $\delta^{13}C$ and $\delta^{18}O$. Subsequently multiple regression models will be employed to establish whether better climatic reconstructions can be made by using more than one proxy to reconstruct a single climatic variable.

8.2 Conceptual Model

To aid in understanding the inter-relationship between temperature and precipitation an $\delta^{13}C$ and $\delta^{18}O$ fractionation a simple conceptual model has been developed (see Figure 8.1). In this model only temperature and precipitation (moisture availability) are considered, although it is appreciated that vapour pressure deficit (VPD) plays an important role in the fractionation of both $\delta^{13}C$ and $\delta^{18}O$, but as there are no suitable data available (relative humidity) it will not be included at this time. Figure 8.1 shows what may be expect to happen to $\delta^{13}C$ and $\delta^{18}O$ fractionation as precipitation and

temperature rise and fall. As we have already seen, there would appear to be a strong relationship between temperature and $\delta^{13}C$ fractionation with values becoming more positive as temperature rises and more negative as temperature declines (represented by directional arrows). As was demonstrated in the previous chapter there appears to be no direct relationship between temperature and $\delta^{18}O$ at this location (shown as crosses in Figure 8.1). For precipitation the situation is a little more complex as it potentially affects both $\delta^{13}C$ and $\delta^{18}O$ fractionation. Results from the previous chapter would seem to suggest a clear negative relationship between precipitation and $\delta^{18}O$, as precipitation increases $\delta^{18}O$ values decline and visa versa.

The relationship between precipitation and $\delta^{13}C$ fractionation at Forfjorddalen is less clear, although there is a well documented theoretical relationship (McCarroll and Loader, 2004). Precipitation is clearly important for $\delta^{13}C$ fractionation at Forfjorddalen in years with dry summers (for example AD 1918) and there is a reasonably strong correlation between $\delta^{13}C$ and summer precipitation, although as was shown in Chapter 5, much of this may be as a result of the inter-correlation between temperature and precipitation, although the overall trend in $\delta^{13}C$ through the twentieth century does seem to mirror the long term trend in precipitation.The theoretical relationship between $\delta^{13}C$ and precipitation is shown in Figure 8.1. It seems likely, in light of the evidence available that the relationship between $\delta^{13}C$ and precipitation at this location is non linear and possibly threshold related, with low levels of precipitation being much more important than higher levels.

Figure 8.2 shows the nine possible basic year to year climate scenarios (in five groups) and the theoretical reaction of $\delta^{13}C$ and $\delta^{18}O$ fractionation to these changes based on the model presented in Figure 8.1.

Scenario 1: No change in temperature and precipitation which should lead to no change in isotope values for either $\delta^{13}C$ and $\delta^{18}O$ from the previous year. This is admittedly a highly simplistic way of looking at the relationship between isotope fractionation and climate. The climate for two consecutive years will never be identical and even if mean figures for precipitation and temperature are the same or very similar the day to day climate may be

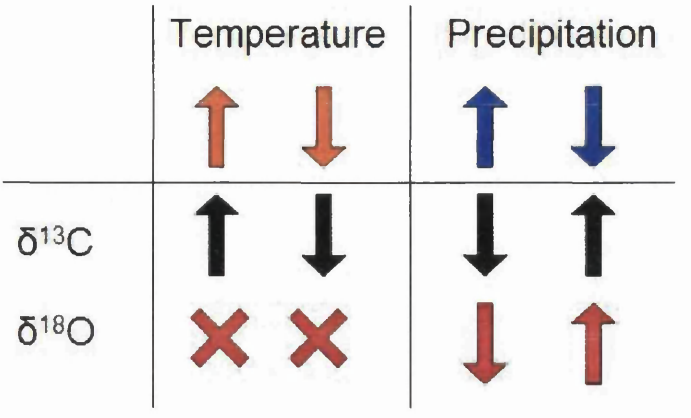

Figure 8.1: Conceptual model of the relationship between δ^{13}C(‰) and δ^{18}O(‰) fractionation and temperature and precipitation. At the top arrows represent increasing or decreasing precipitation and under these the theoretical response of the isotopes, with a cross indicating no relationship.

quite different for the two years and lead to quite different isotope fractionation. However, this model is considered a useful tool in helping interpret changes in isotope fractionation and as only monthly climate data are available we will proceed at this relatively simplistic level.

Scenario 2: Precipitation remains constant while temperature either (a) increases or (b) decreases. As already discussed the strong positive relationship between δ^{13}C fractionation and summer temperature would suggest that while precipitation remains constant an increase in temperature would lead to more positive δ^{13}C values while a decline would lead to more negative values. As δ^{18}O has no obvious relationship with summer temperatures one would expect no change for either scenario 2a or 2b.

Scenario 3: Temperature remains constant while precipitation (a) increases or (b) declines. While the relationship between precipitation δ^{13}C is less clear and almost certainly non linear, changes in precipitation accompanied by no change in temperature would seem likely to affect δ^{13}C fractionation. In scenario 3a an increase in precipitation would then lead to a decline in δ^{13}C values, although the magnitude of this change may well depend on the base level with an increase in precipitation from a low level (dry year) to a more normal or wet year having a larger affect than from an average year to a somewhat wetter

year. In scenario 3b a decline in precipitation would seem likely to lead to increased $\delta^{13}C$ values, but again the absolute values may be critical here and if precipitation falls below a threshold that causes moisture stress to the tree this increase may be sharp. For $\delta^{18}O$ one would expect the same pattern with a negative relationship between precipitation and $\delta^{18}O$.

Scenario 4: This is perhaps the most likely of all the scenarios for any given year due to the general negative relationship between temperature and precipitation (dry/warm and wet/cool). Under this scenario both temperature and precipitation force $\delta^{13}C$ fractionation in the same direction, warmer and dryer (scenario 4a) both should lead to more positive values and cooler and wetter (scenario 4b) to more negative values. Under this scenario $\delta^{18}O$, unaffected by temperature should be negatively related to precipitation, dryer (4a) more negative, wetter (4b) more positive. Under these (what we may call normal) conditions when there is a strong negative correlation between temperature and precipitation one would expect a strong positive correlation between temperature and $\delta^{13}C$ and a negative correlation between $\delta^{13}C$ and precipitation.

Scenario 5: Under this scenario both temperature and precipitation are either (5a) increasing or (5b) decreasing. If $\delta^{13}C$ fractionation is affected by both temperature and precipitation, as would appear to be the case at Forfjorddalen (albeit more when precipitation levels are low) this scenario could result in an ambiguous response between climate and $\delta^{13}C$ fractionation. As temperature and precipitation either both (5a) increase or (5b) decrease their effect on $\delta^{13}C$ fractionation will be in opposite directions (decreasing temperature should lead to more negative $\delta^{13}C$, while decreasing precipitation should lead to more positive $\delta^{13}C$ and visa versa). Under scenarios 5a and 5b it may then be hard to predict what will happen to $\delta^{13}C$ fractionation. This may be strongly controlled by the timing and magnitude of warm/cool and wet/dry events during the growing season and also the absolute level or precipitation compared to the previous year. Again one would expect $\delta^{18}O$ fractionation to be negatively related to precipitation. Under these (what we may term abnormal) conditions where there is a weak (or no) negative correlation between temperature and precipitation one would expect a weak correlation between $\delta^{13}C$

and both temperature and precipitation.

8.2.0.1 Testing the conceptual model

If the conceptual model set out in Figure 8.1 and the scenarios in Figure 8.2 are of any utility in understanding the relationship between climate and isotope fractionation they should make predictions which are testable using real world data. The major prediction this model makes is that as any negative correlation between temperature and precipitation becomes stronger so should the positive correlation between temperature and $\delta^{13}C$ and the negative correlation between precipitation and $\delta^{13}C$ and visa versa. This is relatively simple to test using the isotope data available from Forfjorddalen and the available climate data. A moving correlation window is applied to temperature and precipitation and to $\delta^{13}C_{pin}$ and temperature and also $\delta^{13}C_{pin}$ and precipitation and these correlations are then compared to see if any pattern emerges. To encompass as much the $\delta^{13}C_{pin}$ record as possible the composite northern coastal temperature (Hanssen-Bauer and Nordli, 1998) and precipitation (Hanssen-Bauer and Føland, 1998) were used for this comparison.

Figure 8.3 shows the maximum correlation in a 30 year running window between $\delta^{13}C_{pin}$ and mean July and August temperature compared to that between mean July and August temperature and precipitation (this axis has been inverted for ease of comparison), while Figure 8.4 shows the actual running 30 year correlations for the same data. It is clear for these two figures that the prediction made by the conceptual model that $\delta^{13}C_{pin}$ and temperature should be strongly positively correlated when there is a strong negative relationship between temperature and precipitation seem to match the results from Forfjorddalen well. Both sets of correlations (Figure 8.3 and 8.4) begin low and climb rapidly both reaching a peak for the period from the AD 1920s to the AD 1960s and then decline again towards the end of the series, with the decline in the correlation between temperature and precipitation being rather more sharp than that between $\delta^{13}C_{pin}$ and temperature. In both Figures 8.3 and 8.4 the lines are not by any means identical but the fit seems too good to be merely coincidental indeed the correlation between the two

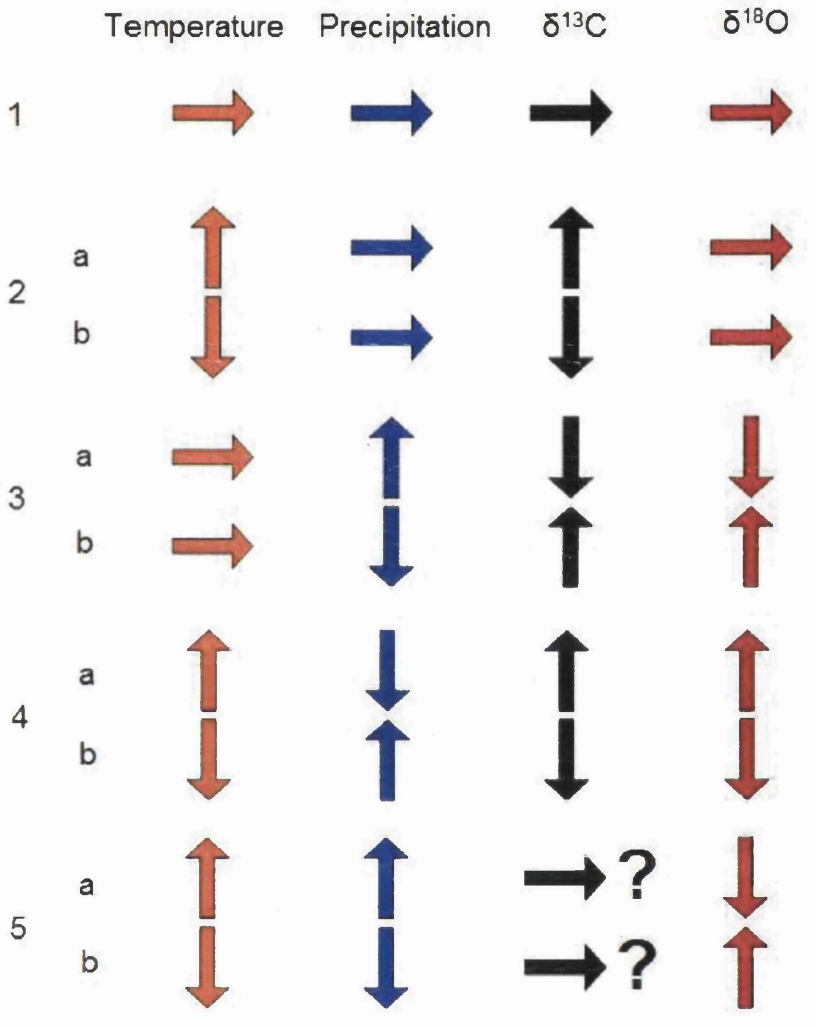

Figure 8.2: Nine basic climate scenarios (in five groups) and the resulting $\delta^{13}C(‰)$ and $\delta^{18}O(‰)$ fractionation. On the left arrows represent changes in temperature and precipitation and on the right arrows show changes in isotope fractionation based on the model in Figure 8.1.

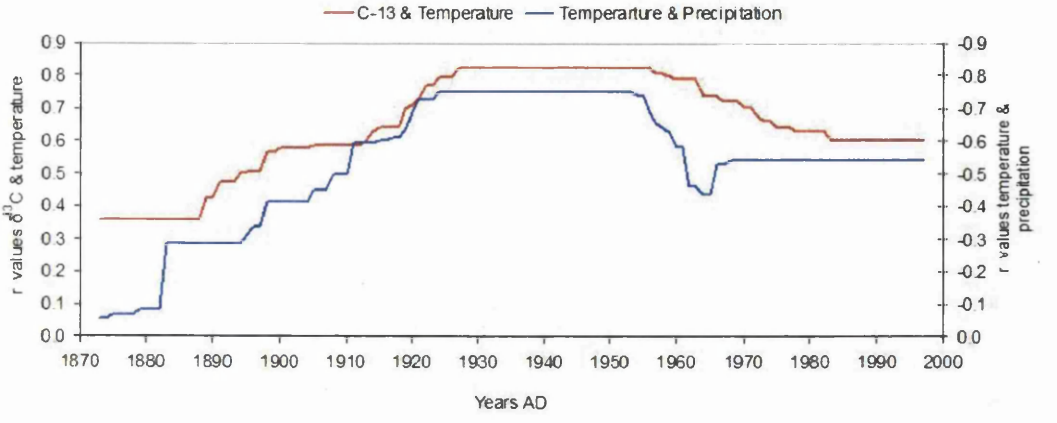

Figure 8.3: Maximum correlation in a 30 year running window between: (in red) $\delta^{13}C_{pin}(‰)$ and mean July and August temperature for the northern coastal stations; and (in blue) mean July and August temperature and mean July and August precipitation (this axis has been inverted for ease of comparison), between AD 1875 and 1997

lines in Figure 8.4 is $r = 0.85$.

The model in Figure 8.1 also predicts that there should be a strong negative correlations between $\delta^{13}C_{pin}$ and precipitation when the negative relationship between temperature and precipitation is strong. Figures 8.5 and 8.6 show the running 30 year correlations between $\delta^{13}C_{pin}$ and precipitation compared to those for temperature and precipitation, with the the maximum in a 30 year running window in Figure 8.5 and the actual 30 year running correlation in Figure 8.6. The fit between the two curves in both these Figures is, if anything, better than that in Figures 8.3 and 8.4 (for $\delta^{13}C_{pin}$ and temperature), although the correlation between the two line in Figure 8.6 is similar to that in 8.4 at $r = 0.86$. Again the fit between the two running correlations would seem too strong to be coincidental suggesting that the proposed model has a certain predictive ability.

The strong relationship between correlations between $\delta^{13}C_{pin}$ and precipitation and temperature and precipitation may also support the idea that much of the correlation between $\delta^{13}C_{pin}$ and precipitation may be due to the relationship between temperature and precipitation. If $\delta^{13}C_{pin}$ correlates well with temperature when temperature correlates well with precipitation, then $\delta^{13}C_{pin}$ is also likely to correlate well with precipitation, although there may be no direct causal link for this correlation between $\delta^{13}C_{pin}$ and precipitation.

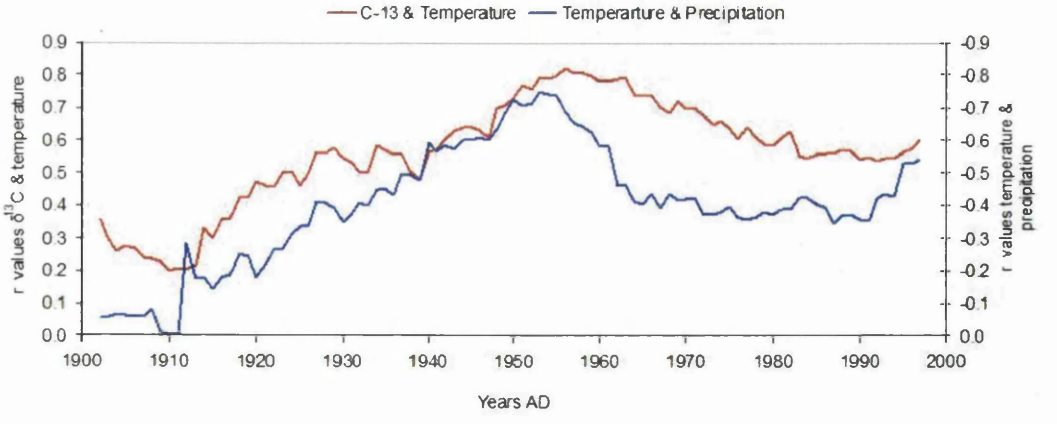

Figure 8.4: Running 30 year correlation between: (in red) $\delta^{13}C_{pin}(‰)$ and mean July and August temperature for the northern coastal stations; and (in blue) mean July and August temperature and mean July and August precipitation (axis inverted), between AD 1875 and 1997. In this graph the first point is the 30 year correlation starting in AD 1875 and ending in AD 1904, so each point represents the final year of a 30 year window.

This is, however, to some extent a circular argument, as it could equally work the other way round, with $\delta^{13}C_{pin}$ fractionation being driven by precipitation and only correlating well with temperature when temperature and precipitation correlate well. Most of the data presented so far would suggest however that $\delta^{13}C_{pin}$ fractionation at this location is controlled generally by temperature with precipitation more important in dryer years.

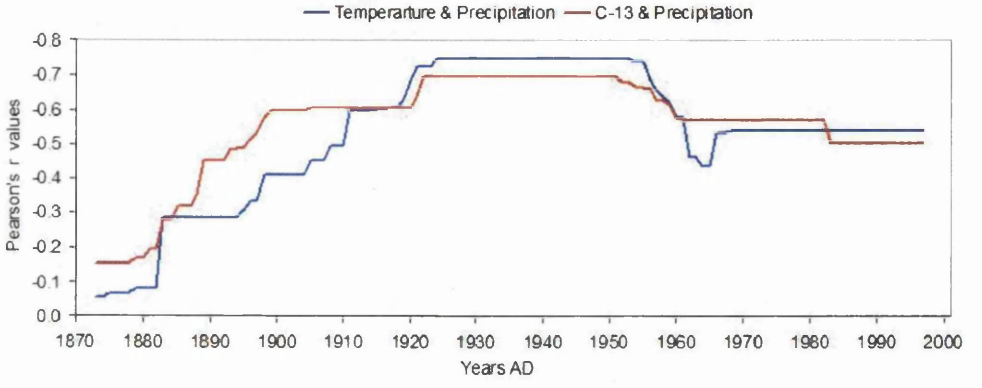

Figure 8.5: Maximum correlation in a 30 year running window between: (in red) $\delta^{13}C_{pin}(‰)$ and mean July and August precipitation for the northern coastal stations; and (in blue) mean July and August temperature and mean July and August precipitation (the y axis has been inverted), between AD 1875 and 1997

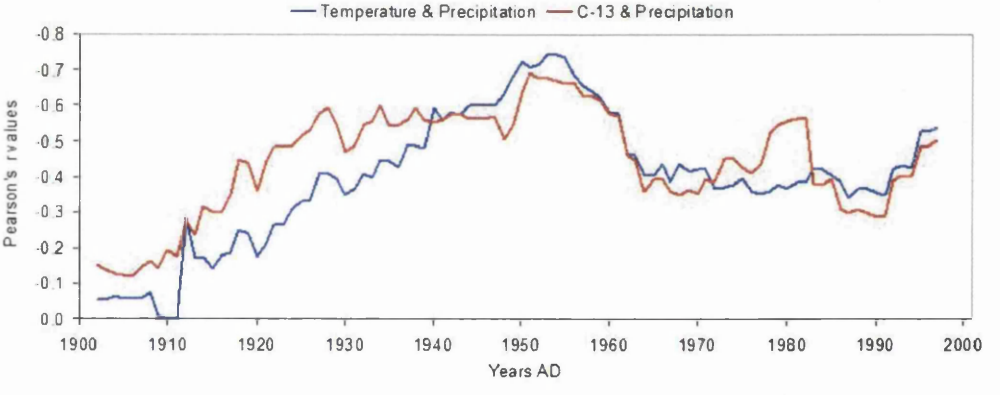

Figure 8.6: Running 30 year correlation between: (in red) $\delta^{13}C_{pin}(‰)$ and mean July and August precipitation for the northern coastal stations; and (in blue) mean July and August temperature and mean July and August precipitation (the y axis has been inverted), between AD 1875 and 1997. In this graph the first point is the 30 year correlation starting in AD 1875 and ending in AD 1904, so each point represents the final year of a 30 year window.

Returning to the period from the AD 1870s to the mid AD 1920s, when the relationship between $\delta^{13}C_{pin}$ and temperature breaks down, with the help of the conceptual model presented in Figures 8.1 and 8.2 reasons for this breakdown in correlation may become more explicable. Figure 8.7 shows $\delta^{13}C_{pin}$ (black) plotted alongside mean July and August temperature (red) and precipitation (blue, axis inverted). From the the mid AD 1920s

onwards all three line appear to match well and follow a similar slightly declining trend (with a few notable exceptions such as AD 1983) with strong correlations between all three variable (Figures8.3 and 8.5). During this period correlations between $\delta^{13}C_{pin}$ and temperature are generally in excess of $r = 0.70$ and that the reconstruction of temperature based on $\delta^{13}C_{pin}$ produced satisfactory verification statistics.

In the period prior to AD 1920 the situation is totally different, the correlation between temperature and precipitation declines towards zero, while the correlations between $\delta^{13}C_{pin}$ and temperature and $\delta^{13}C_{pin}$ and precipitation also decline (Figures 8.3, 8.4, 8.5 and 8.6). From Figure 8.7 it is not clear which of the two climate variables (if either) $\delta^{13}C_{pin}$ is reacting to during this period, from ~AD 1900 to 1925 when the $\delta^{13}C_{pin}$ and the temperature lines diverge $\delta^{13}C_{pin}$ would appear to be following the precipitation trend as it gets dryer, although not the year to year variations. Prior to AD 1900 $\delta^{13}C_{pin}$ does not appear to be linked especially strongly to either climate parameter, or either of the two to each other.

In light of the model presented (Figures 8.1 and 8.2) this is not surprising. If indeed $\delta^{13}C$ fractionation is linked to both temperature and precipitation under climate scenario 5 (Figure 8.2), when both precipitation and temperature are either rising or falling, the $\delta^{13}C$ fractionation will be, in effect, pulled in opposite directions by the two climate parameters leading to a weak and confused relationship between $\delta^{13}C$ and either parameter. It may be especially important that during this period northwest Norway appears to have been cool and rather dry, which of the two possible non linear scenarios (warm and wet or cool and dry) seems the most likely to affect $\delta^{13}C$in this way.

8.2.0.2 Recognising Periods of Non-linearity

Were it not for the availability of climate data for this period (AD 1875 to 1925) this breakdown in the relationship between $\delta^{13}C_{pin}$ and temperature and precipitation would probably not have been recognised, with only a short period of low common signal

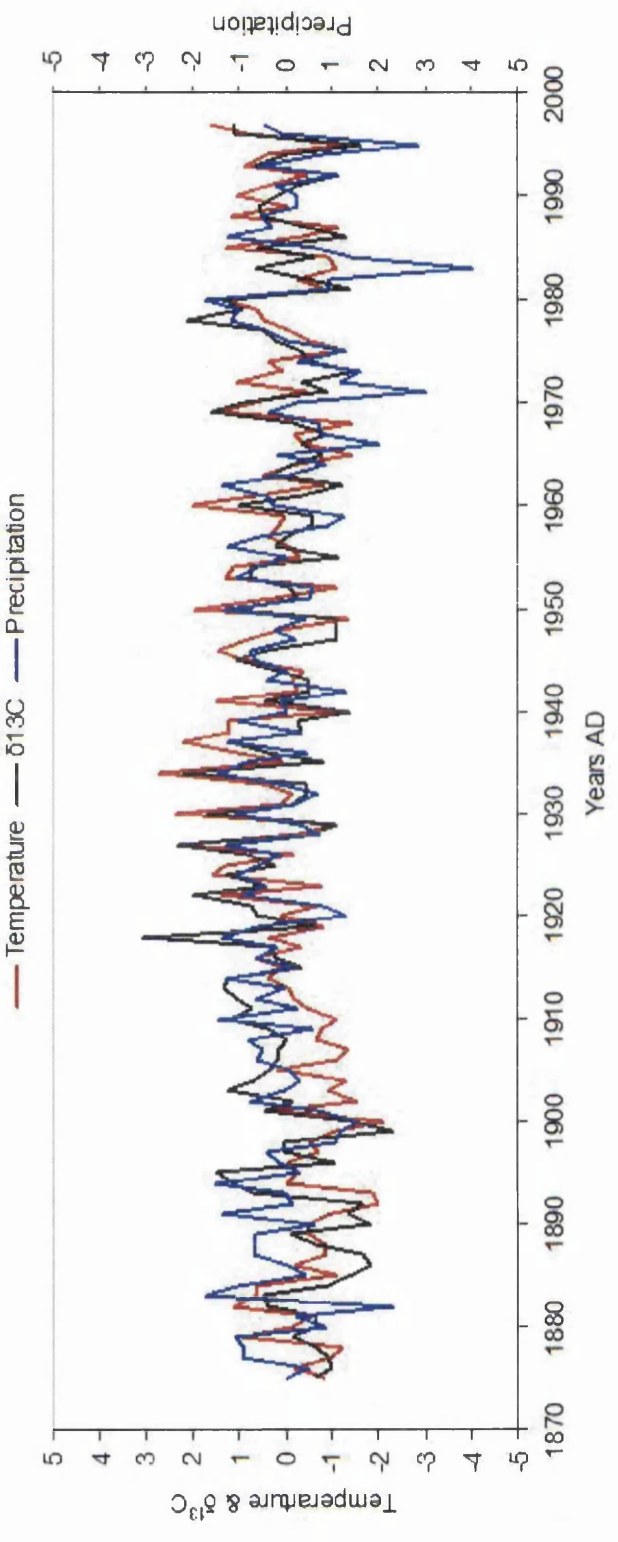

Figure 8.7: $\delta^{13}C_{pin}(‰)$ (black) and mean July and August temperature (red) and precipitation (blue) from the northern coastal stations (Hanssen-Bauer and Føland, 1998; Hanssen-Bauer and Nordli, 1998) from AD 1875 to 1997 all data has been normalised (mean of 0, standard deviation 1) and the precipitation axis has been inverted for ease of comparison.

strength between trees as evidence. This raises the question of how other potential periods of low correlation can be recognised further back in time where no climate data are available? This is perhaps an example of the great strength of a multi-proxy approach to climate reconstruction. Potentially we must identify periods when temperature and precipitation do not negatively correlate well together (Figure 8.2, scenario 5).

At present the proxies we have available to identify this are, $\delta^{13}C_{pin}$, $\delta^{18}O$ and ring-width measurements (in due course maximum latewood density will be available, which as a good proxy for summer temperature may prove very useful). As already demonstrated $\delta^{13}C_{pin}$ is, under normal circumstances (Figure 8.2, scenarios 1-4), a good proxy for summer temperature, however it also has somewhat more ambiguous relationship with summer precipitation. $\delta^{18}O$ appears to have a reasonably strong relationship with summer precipitation, although it must be borne in mind that other factors such a source water and vapor pressure deficit may be important. At this location Kirchhefer (2001) has demonstrated that tree ring widths have a good relationship with summer temperature. So we potentially have one proxy which reflects temperature (ring-widths), one which reflects precipitation ($\delta^{18}O$) and one with a somewhat mixed temperature and precipitation signal ($\delta^{13}C_{pin}$).

To estimate the strength of the negative co-linearity between temperature and precipitation a comparison between $\delta^{18}O$ (precipitation proxy) and ring widths (temperature proxy) would seem an obvious choice and the results of a running 30 year correlation between these two proxies can be seen in Figure 8.8. Unfortunately the relationship between $\delta^{18}O$ and precipitation also breakdown prior to around AD 1900, which makes the obvious comparison of ring widths (temperature) and $\delta^{18}O$ (precipitation) problematic, indeed this comparison gives little useful information.

A more useful comparison is between $\delta^{18}O$ and $\delta^{13}C_{pin}$, which can be seen plotted in Figure 8.9. Two things are apparent for this figure: firstly that for much of this 200 year sequence $\delta^{13}C_{pin}$ and $\delta^{18}O$ appear to follow each other quite well ($r = 0.44$); secondly there is a divergence between the two line from AD 1860 to about AD 1900. As already seen in Figure 8.7 the prevailing regional conditions during this period appear to be dry

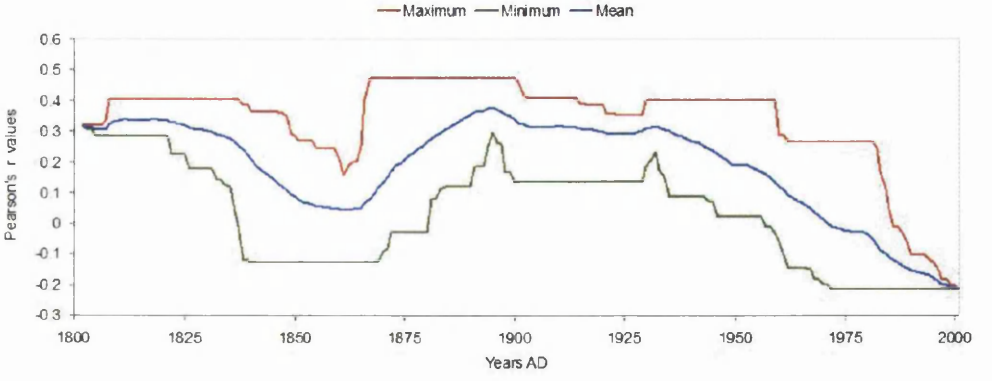

Figure 8.8: Maximum, minimum and mean correlation between ring widths (residual chronology) and δ^{18}O(‰) from AD 1802-2001

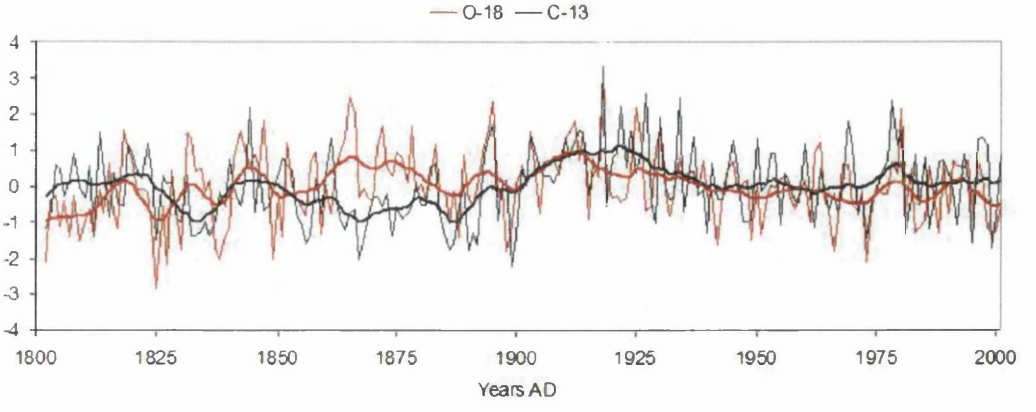

Figure 8.9: $\delta^{13}C_{pin}$(‰) plotted alongside δ^{18}O(‰) from AD 1802-2001, both data sets have been normalised (to a mean of 0 and a standard deviation of 1) to ease comparison. An 11 years centered running mean has been added to both time series.

and rather cool, which (although the correlations between $\delta^{13}C_{pin}$ and temperature and δ^{18}O and precipitation during this period are rather weak) is what the isotope records point to. This is exactly the scenario (5) in Figure 8.2 which would be expected to disrupt δ^{13}C the most. A third thing to note from Figure 8.9 is that from AD 1900 to the early AD 1920s when the $\delta^{13}C_{pin}$ trend and temperature diverge (Figure 8.7) the $\delta^{13}C_{pin}$ and δ^{18}O lines appear to match the best.

A running 30 year correlation between $\delta^{13}C_{pin}$ and δ^{18}O (Figure 8.10) would seem to

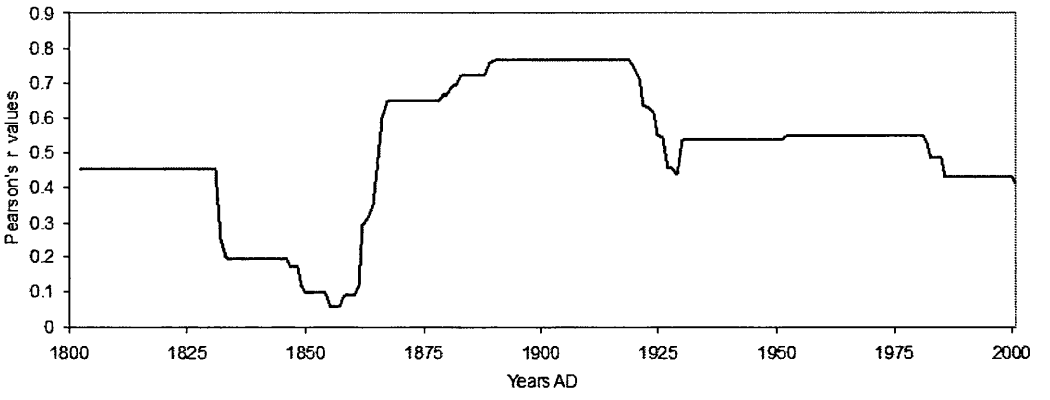

Figure 8.10: Maximum correlation in a 30 year running window between $\delta^{13}C_{pin}(‰)$ and $\delta^{18}O(‰)$ from AD 1802-2001

confirm this with the relationship between these two proxies at its strongest for the period when the correlation between $\delta^{13}C_{pin}$ and temperature and $\delta^{18}O$ and precipitation and temperature and precipitation are at their weakest, and also when the common signal between trees is rather weak. For the entire period (AD 1802 to 2001) there is a modest but significant (at 99.98%) correlation between $\delta^{13}C_{pin}$ and $\delta^{18}O$ of $r = 0.29$, however, over the period AD 1880 to 1920 the correlation between these two variable is at $r = 0.75$.

It is possible that this strong correlation between $\delta^{13}C_{pin}$ and $\delta^{18}O$ may be in part due to both proxies having the same trend during this period (Figure 8.7) . To determine to what extent this affects the correlation the same running correlation exercise was carried out on the first differences between both $\delta^{13}C_{pin}$ and $\delta^{18}O$, to determine only the inter-annual correlation (by subtracting the value for *n* from *n -1*). The results of this can be seen in Figure 8.11 compared to the actual running correlation from Figure 8.10. While there is a reduction in the correlation between AD 1866 and 1888, from AD 1889 to 1925 the maximum correlation is still greater than $r = 0.70$ and considerably higher than during any other period. This would seem to confirm that this unusually high correlation between $\delta^{13}C_{pin}$ and $\delta^{18}O$ is operating at low and high frequency, suggesting

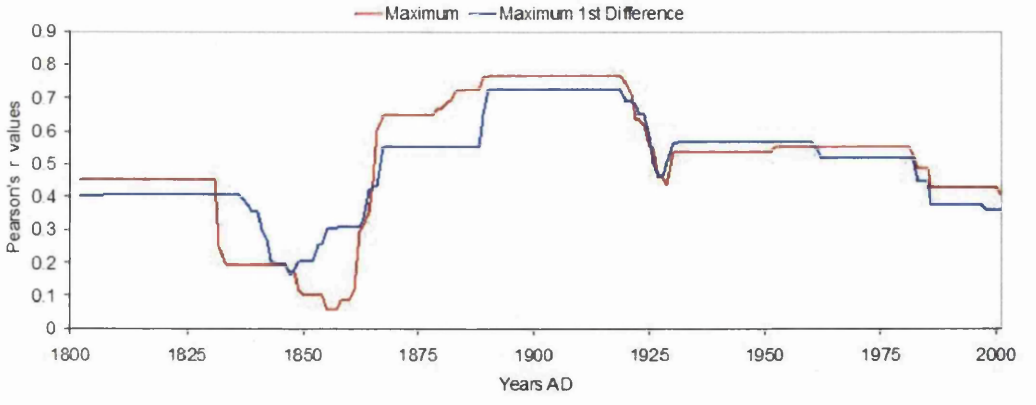

Figure 8.11: Maximum correlation in a 30 year running window between $\delta^{13}C_{pin}(‰)$ and $\delta^{18}O(‰)$ from AD 1802-2001, using the first difference for both $\delta^{13}C_{pin}(‰)$ and $\delta^{18}O(‰)$.

some common forcing.

This presents an intriguing scenario that over this brief period (AD 1890 to 1925), while $\delta^{13}C_{pin}$ does not correlate well with temperature or precipitation and $\delta^{18}O$ does not correlate especially well with precipitation, they both correlate extremely well with each other. Which would appear to suggest that there is some other variable which is driving the fractionation of both these isotopes during this period. Indeed it seems likely that some other factor may be involved as, if the conceptual model set out in Figure8.1 and the climate scenarios in Figure 8.2 are correct, they would predict a breakdown in the correlation between $\delta^{13}C_{pin}$ and both temperature and precipitation but not between $\delta^{18}O$ and precipitation, as $\delta^{18}O$ should be largely unaffected by temperature and so should continue to correlate reasonably well with precipitation, which is not the case.

One factor which can affect the fractionation of both $\delta^{13}C$ and $\delta^{18}O$ but which may be independent of temperature and precipitation to some degree is relative air humidity. High relative air humidity reduces evaporation at the stomata and so the preferential loss of water molecules containing the ^{16}O isotope, it also affects $\delta^{13}C$ because when relative humidity is high the stomata can remain open more as there is less evaporation and so

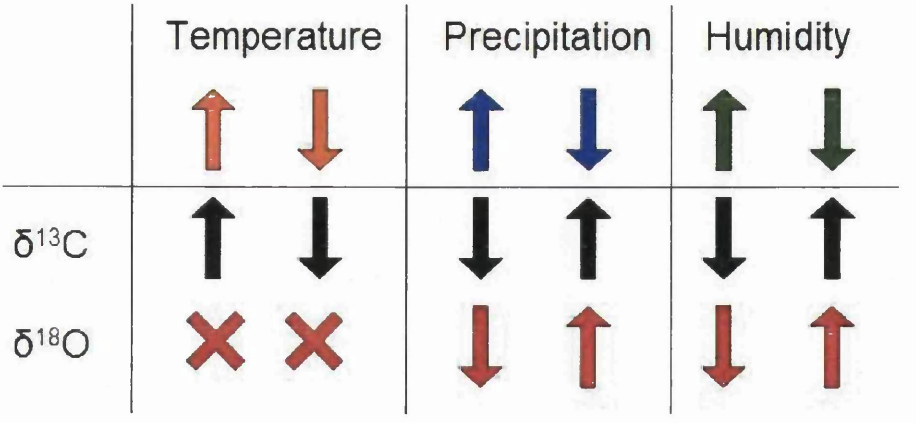

Figure 8.12: Conceptual model of the relationship between $\delta^{13}C(‰)$ and $\delta^{18}O(‰)$ fractionation and temperature, precipitation and relative humidity. At the top arrows represent increasing or decreasing precipitation and under these the theoretical response of the isotopes, with a cross indicating no relationship.

less potential moisture stress. High relative humidity should then lead to more negative $\delta^{13}C_{pin}$ and $\delta^{18}O$, while low relative humidity would have the opposite affect. During a relatively dry, cool period relative humidity could have an important affect on isotope fractionation. A revision of the model in 8.1 including relative humidity can be seen in Figure 8.12, while an adaption of Figure 8.2, scenarios 5 and 6 (here labeled scenarios 7 and 8), to include relative humidity can be seen in Figure 8.13.

Figure 8.12 shows that humidity should act on isotope fractionation in the same direction as precipitation, increasing humidity should lead to more negative isotope values and visa versa. While there is no local relative humidity data with which to compare with the isotope records or climate records it seems reasonable to expect a relationship between relative humidity and precipitation as the closer dewpoint and air temperature are, the more likelihood there is for precipitation. Figure 8.13 shows that when such a positive relationship between relative humidity and precipitation is in operation (Figure 8.13, scenario 7a and 7b) humidity will act in the same direction on isotope fractionation and

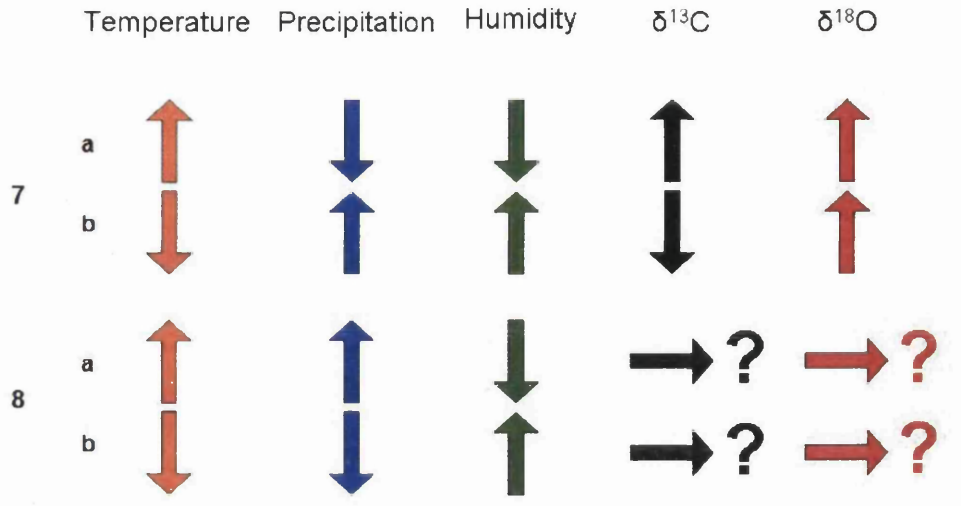

Figure 8.13: Scenarios 5 and 6 (here labeled 7 and 8) from figure 8.2 with relative humidity added to the conceptual model of $\delta^{13}C(‰)$ and $\delta^{18}O(‰)$ fractionation. On the left arrows represent changes in temperature and precipitation and on the right arrows show changes in isotope fractionation based on the model in Figure 8.12.

if (as is shown in this scenario) temperature is also negatively correlated with temperature $\delta^{13}C_{pin}$ and $\delta^{18}O$ should correlate well with temperature. Figure 8.13, scenario 8a and 8b show two possible climatic situations where both $\delta^{13}C_{pin}$ and $\delta^{18}O$ may be disrupted so that the normal linear relationship between $\delta^{13}C_{pin}$ and temperature and $\delta^{18}O$ and precipitation both break down. Here, not only do temperature and precipitation not correlate, but neither does precipitation and relative humidity, while allowing for $\delta^{13}C_{pin}$ and $\delta^{18}O$ and to correlate well with each other if the dominating factor at this time is humidity. As we have no humidity data available to test this hypothesis, it remains speculation. It does however demonstrate that it is possible to explain the failure of the correlation between isotopes and climate while still maintaining a correlation with each other. The coastal location of these trees may help to create a situation where relative humidity is high but precipitation is low more likely. With sea mists persisting over the forest often, as was observed, for much of the day. In the late nineteenth and early twentieth century when it appears to have been cool and dry in this area such an occurrence may well have been frequent.

While there may be no absolutely definitive way of identifying such periods when no

climate data exists. The following situations may be indicative of such a situation:

1. A poor common signal between trees (periods of less than EPS = 0.85 for both δ^{13}C and δ^{18}O).

2. A divergence between δ^{13}C and δ^{18}O, suggestive of cool and dry or perhaps warm and wet conditions.

3. A breakdown in the relationship between ring widths and δ^{18}O, although this relationship does not appear especially stable at Forfjorddalen and should be viewed with some skepticism.

4. A higher than normal correlation between δ^{13}C and δ^{18}O, which may indicate that some factor other than temperature and precipitation is driving fractionation of both these isotopes.

5. A combination of most or all of the above occurring at the same time, as appears to have happened in the late nineteenth and early twentieth centuries at Forfjorddalen, should indicate that caution should be exercised when attempting to reconstruct climate. Indeed it may be more appropriate to use proxies such as ring widths or density which appear to be almost entirely controlled by temperature in the boreal forest of Scandinavia during any such interludes.

8.3 Multiple Regression Models

So far the focus has been on using one proxy to reconstruct a single climatic parameter. It may be possible to use more than one of the proxies available in a multiple regression model for a better climatic reconstruction. As discussed above we have three proxies available which appear to be linked to climate. δ^{13}C which has a mixture of temperature and precipitation signal, although predominantly temperature; δ^{18}Owhich is fairly strongly linked to precipitation; and ring widths, which are predominantly controlled by summer

temperature. In the following sections various combinations of these proxies have been used to determine whether a better reconstruction of climate can be made than by using a single proxy alone.

The ring widths of all the trees in the Forfjorddalen chronology have been detrended to remove the growth trend by the normal dendrochronological methods (Kirchhefer, 2006) producing three separate chronologies the residual, standard and arstan chronologies, which comprise the same data treated statistically slightly differently. Initially all three chronologies were used in turn in each regression model to determine which performed the best overall.

8.3.1 Temperature

8.3.1.1 Andenes

Table 8.1 shows the statistics for reconstructed mean July and August temperature from Andenes from AD 1869 to 2001 using multiple regression models combining $\delta^{13}C_{pin}$, $\delta^{18}O$ and ring widths in various combinations (Table 8.1a to h). The initial model combines $\delta^{13}C_{pin}$, $\delta^{18}O$ and the three combinations of ring widths chronologies (Table 8.1a, b and c). Next $\delta^{18}O$ is dropped from the model, as the least likely to reconstruct temperature and the combination of $\delta^{13}C_{pin}$ and the three ring width chronologies are used (8.1d, e and f). Finally in 8.1g ($\delta^{13}C_{pin}$) and h (ring width residual chronology) are dealt with separately. The residual chronology is used, and will be used from now on, as it constantly returns the best results (both in terms of correlation and RE and CE statistics) when compared to climate.

What is apparent from Table 8.1 is that none of the combinations used, or indeed, $\delta^{13}C_{pin}$ (as we have already seen) or ring widths on their own are able to reconstruct temperature to the extent that they can outperform the predictive power of the mean temperature of the verification periods (CE statistic). The combination of $\delta^{13}C_{pin}$, $\delta^{18}O$ and the residual chronology gives the highest overall correlation with mean July and August temperature r^2= 0.40 (r= 0.63) but the CE statistics for this reconstruction are little better than for

the much lower correlation from $\delta^{13}C_{pin}$ on it's own (r^2= 0.25), which demonstrates that a high correlation with temperature does not necessarily produce a good reconstruction.

The reconstructions in Table 8.1 all include the problematic period from around AD 1880 to 1925, during which there now seem to be convincing reasons (Section 8.2) why especially $\delta^{13}C_{pin}$ is unable to successfully reconstruct temperature. Interestingly ring widths are also unable to reconstruct temperature successfully during this period considering that they should have a very strong link to summer temperature at this location. The problem with the ring width chronologies would appear to be that they capture the high frequency variations quite well but low frequency changes more poorly.

There is good evidence from this site (discussed earlier in this chapter and in previous chapters) that there is an explicable failure in correlation between $\delta^{13}C_{pin}$ and temperature during the period from around AD 1880 to 1926. Having already proposed to use the period from AD 1927 to 2001 to calibrate for climatic reconstruction and discussed the reasons for this, it will now be determined whether this calibration can be improved by using multiple regression models.

Table 8.2 shows the statistics for the temperature reconstruction over the period AD 1927 to 2001 using combinations of $\delta^{13}C_{pin}$, $\delta^{18}O$ and the ring width residual chronology and also the $\delta^{13}C_{pin}$ and the ring width residual chronology on their own. All of the combinations used are able to reconstruct climate satisfactorily over this period (Table 8.2a-d. The combination of $\delta^{13}C_{pin}$, $\delta^{18}O$ and the ring-width residual chronology (Table 8.2a) yields the marginally highest correlation value (r^2 = 0.55 from AD 1927-2001) but the calibration statistics are poorer than the combination of $\delta^{13}C_{pin}$ and the ring width residual chronology (Table 8.2b) suggesting that $\delta^{18}O$ is of little use in reconstructing temperature here. However, using $\delta^{13}C_{pin}$ on its own produces only slightly lower correlations and RE and CE statistics than the multiple regressions (Table 8.2c). Ring widths (Table 8.2d) on their own give the lowest correlations and statistics. This would seem to suggest that while some small advantage may be gained by adding ring widths to $\delta^{13}C_{pin}$

	Period	MSE	RE	CE	r^2
a. $\delta^{13}C_{pin}$, $\delta^{18}O$ and RW residual	AD 1869-2001	0.75	0.40	NA	0.40
	AD 1869-1934	1.37	0.12	-0.15	0.33
	AD 1935-2001	1.15	0.22	-0.04	0.28
b. $\delta^{13}C_{pin}$, $\delta^{18}O$ and RW standard	AD 1869-2001	0.78	0.38	NA	0.38
	AD 1869-1934	1.44	0.08	-0.21	0.32
	AD 1935-2001	1.16	0.22	-0.04	0.28
c. $\delta^{13}C_{pin}$, $\delta^{18}O$ and RW arstan	AD 1869-2001	0.77	0.38	NA	0.38
	AD 1869-1934	1.47	0.06	-0.23	0.32
	AD 1935-2001	1.14	0.24	-0.02	0.30
d. $\delta^{13}C_{pin}$ and RW residual	AD 1869-2001	0.79	0.36	NA	0.36
	AD 1869-1934	1.32	0.16	-0.10	0.33
	AD 1935-2001	1.25	0.16	-0.12	0.34
e. $\delta^{13}C_{pin}$ and RW standard	AD 1869-2001	0.82	0.34	NA	0.34
	AD 1869-1934	1.39	0.11	-0.16	0.33
	AD 1935-2001	1.28	0.14	-0.15	0.32
f. $\delta^{13}C_{pin}$ and RW arstan	AD 1869-2001	0.81	0.34	NA	0.34
	AD 1869-1934	1.39	0.12	-0.16	0.33
	AD 1935-2001	1.26	0.16	-0.13	0.36
g. $\delta^{13}C_{pin}$	AD 1869-2001	0.93	0.25	NA	0.25
	AD 1869-1934	1.50	0.04	-0.26	0.21
	AD 1935-2001	1.16	0.22	-0.04	0.40
h. RW residual	AD 1869-2001	0.87	0.30	NA	0.30
	AD 1869-1934	1.18	0.25	0.01	0.44
	AD 1935-2001	1.35	0.08	-0.21	0.28

Table 8.1: Statistics for reconstructed mean July and August Andenes temperature from AD 1869-2001 using multiple regression models combining $\delta^{13}C_{pin}$(‰), $\delta^{18}O$(‰) and the three ring width chronologies (residual, standard and arstan).

the benefit is relatively small and may be outweighed by the advantages of using simple model containing one variable, especially as it is problematic to retain low frequency climate information in rings widths series (Cook et al., 1995). Prior to deciding whether or not to use a multiple regression model to reconstruct summer temperature it will be examined how well these models perform against the longer Tornedalen temperature record of Klingbjer and Moberg (2003).

		Period	MSE	RE	CE	r^2
a. $\delta^{13}C_{pin}$, $\delta^{18}O$ and RW residual		AD 1927-2001	0.57	0.55	NA	0.55
	cal	AD 1927-1963	0.40	0.71	NA	0.71
	ver		0.55	0.61	**0.59**	0.64
	cal	AD 1964-2001	0.65	0.43	NA	0.43
	ver		0.88	0.26	**0.22**	0.35
b. $\delta^{13}C_{pin}$ and RW residual		AD 1927-2001	0.57	0.54	NA	0.54
	cal	AD 1927-1963	0.40	0.70	NA	0.70
	ver		0.55	0.61	**0.59**	0.64
	cal	AD 1964-2001	0.66	0.43	NA	0.43
	ver		0.86	0.28	**0.25**	0.37
c. $\delta^{13}C_{pin}$		AD 1927-2001	0.63	0.50	NA	0.50
	cal	AD 1927-1963	0.41	0.70	NA	0.70
	ver		0.59	0.58	**0.56**	0.70
	cal	AD 1964-2001	0.76	0.33	NA	0.33
	ver		0.94	0.22	**0.18**	0.33
d. RW residual		AD 1927-2001	0.61	0.37	NA	0.37
	cal	AD 1927-1963	0.79	0.42	NA	0.42
	ver		0.84	0.41	**0.38**	0.42
	cal	AD 1964-2001	0.78	0.31	NA	0.31
	ver		0.83	0.31	**0.28**	0.31

Table 8.2: Statistics for reconstructed mean July and August Andenes temperature from AD 1927-2001 using multiple regression models combining $\delta^{13}C_{pin}$(‰), $\delta^{18}O$(‰) and the ring width residual chronology.

8.3.1.2 Tornedalen

The statistics for the entire Tornedalen record (AD 1802-2001) can be seen in Table 8.3. The only two reconstructions which give constantly positive CE statistics here are for $\delta^{13}C_{pin}$ and the ring width chronology combined (8.3b) and $\delta^{13}C_{pin}$ on its own (8.3c). Although $\delta^{13}C_{pin}$ has the lowest overall correlation with temperature (r^2= 0.13) (which has much to do with the much discussed problems which $\delta^{13}C_{pin}$ has in capturing temperature at the end of the nineteenth century) it still performs better in terms of RE and CE statistics than do ring widths (8.3c and d).

Finally in Table 8.4 the Tornedalen record split into two sections (as in the $\delta^{13}C_{pin}$ calibration chapter) is examined by excluding the problematic period from AD 1880 to 1926 and the early part of the record, in which Klingbjer and Moberg (2003) have less

		Period	MSE	RE	CE	r^2
a. $\delta^{13}C_{pin}$, $\delta^{18}O$ and RW residual		AD 1802-2001	1.26	0.19	NA	0.19
	cal	AD 1802-1901	1.14	0.17	NA	0.17
	ver		1.38	0.19	**0.00**	0.13
	cal	AD 1902-2001	1.28	0.18	NA	0.18
	ver		1.46	0.22	**0.06**	0.15
b. $\delta^{13}C_{pin}$ and RW residual		AD 1802-2001	1.27	0.19	NA	0.19
	cal	AD 1802-1901	1.15	0.16	NA	0.16
	ver		1.37	0.19	**0.01**	0.16
	cal	AD 1902-2001	1.29	0.17	NA	0.17
	ver		1.45	0.28	**0.08**	0.16
c. $\delta^{13}C_{pin}$		AD 1802-2001	1.34	0.13	NA	0.13
	cal	AD 1802-1901	1.21	0.12	NA	0.12
	ver		1.33	0.21	**0.03**	0.12
	cal	AD 1902-2001	1.43	0.08	NA	0.08
	ver		1.52	0.19	**0.03**	0.08
d. RW residual		AD 1802-2001	1.31	0.16	NA	0.16
	cal	AD 1802-1901	1.18	0.14	NA	0.14
	ver		1.45	0.15	**-0.05**	0.14
	cal	AD 1902-2001	1.13	0.17	NA	0.17
	ver		0.83	0.17	**0.01**	0.17

Table 8.3: Statistics for reconstructed mean July and August Tornedalen temperature from AD 1802-2001 using multiple regression models combining $\delta^{13}C_{pin}$(‰), $\delta^{18}O$(‰) and the ring width residual chronology.

confidence. Here only reconstructions based on a multiple regression $\delta^{13}C_{pin}$ and the RW residual chronology and $\delta^{13}C_{pin}$ alone are presented. Again the multiple regression model (8.4a) gives the highest correlation with climate (r^2= 0.30), but this is only slightly better than the reconstruction based on $\delta^{13}C_{pin}$ alone (r^2= 0.27) (8.4b), while both the RE and CE statistics for the $\delta^{13}C_{pin}$ model are better than those for the multiple regression model.

		Period	MSE	RE	CE	r^2
a. $\delta^{13}C_{pin}$ and RW residual		AD 1829-//-2001	1.17	0.30	NA	0.30
	cal	AD 1829-1880	1.14	0.24	NA	0.24
	ver		1.42	0.32	**0.06**	0.24
	cal	AD 1927-2001	1.11	0.28	NA	0.28
	ver		1.33	0.38	**0.14**	0.28
b. $\delta^{13}C_{pin}$		AD 1829-//-2001	1.22	0.27	NA	0.27
	cal	AD 1829-1880	1.16	0.21	NA	0.21
	ver		1.34	0.36	**0.10**	0.21
	cal	AD 1927-2001	1.18	0.24	NA	0.24
	ver		1.31	0.39	**0.15**	0.24

Table 8.4: Statistics for reconstructed mean July and August Tornedalen temperature from AD 1802-2001 using a multiple regression models combining $\delta^{13}C_{pin}$(‰) and the ring width residual chronology and $\delta^{13}C_{pin}$ (‰) alone.

Based on the data presented in this section it would seem that while some small increases in correlation can be achieved by combining $\delta^{13}C_{pin}$ with $\delta^{18}O$ and the ring width residual chronology, there is little, if anything, to be gained in terms of RE and CE statistics by adding to the complexity of the model, especially when the longer Tornedalen record is used. It would appear that a temperature reconstruction based upon $\delta^{13}C_{pin}$ alone best captures lower frequency temperature changes at this location and so it is on this proxy that such a reconstruction will be based.

8.3.2 Precipitation

This section will attempt to determine whether there is any advantage in using a multiple regression model to reconstruct precipitation or the Standardised Precipitation Index (SPI) (McKee et al., 1993; Edwards and McKee, 1997). Ring widths at this location are of little utility in reconstructing precipitation and so only the two stable isotope proxies of $\delta^{18}O$ and $\delta^{13}C_{pin}$ are used.

		Period	MSE	RE	CE	r^2
a. $\delta^{13}C_{pin}$ and $\delta^{18}O$		AD 1910-2001	1111	0.29	NA	0.29
	cal	AD 1910-1955	404	0.39	NA	0.39
	ver		570	0.41	**0.14**	0.34
	cal	AD 1956-2001	1747	0.25	NA	0.25
	ver		1955	0.25	**0.15**	0.21
b. $\delta^{18}O$		AD 1910-2001	1164	0.25	NA	0.25
	cal	AD 1910-1955	487	0.27	NA	0.27
	ver		622	0.35	**0.07**	0.26
	cal	AD 1956-2001	1759	0.24	NA	0.24
	ver		1968	0.24	**0.15**	0.24

Table 8.5: Statistics for reconstructed mean August Andenes precipitation from AD 1910-2001 using (a) a multiple regression models combining $\delta^{13}C_{pin}$(‰) and $\delta^{18}O$(‰) and (b) a regression model using $\delta^{18}O$(‰) alone.

8.3.2.1 Andenes

Tables 8.5 and 8.6 show the statistics for reconstructed August precipitation (Table 8.5) and August SPI (Table 8.6) using both a multiple regression model including $\delta^{18}O$ and $\delta^{13}C_{pin}$, and also the reconstruction (previously presented), using $\delta^{18}O$ alone. In both cases there is a slight improvement in the r^2 values, but the improvement in the RE and CE statistics is small for precipitation, while for the SPI there is no obvious improvement. There seems little benefit in adding to the complexity of the regression model (by adding $\delta^{13}C_{pin}$) to reconstruct Andenes precipitation. In the precipitation calibration chapter it appeared that the $\delta^{18}O$ signal from Forfjorddalen was better reflected in the longer composite Northern Coastal record of Hanssen-Bauer and Føland (1998) and so this record is examined in the next section.

		Period	MSE	RE	CE	r^2
a. $\delta^{13}C_{pin}$ and $\delta^{18}O$		AD 1910-2001	0.69	0.30	NA	0.30
	cal	AD 1910-1955	0.39	0.40	NA	0.40
	ver		0.51	0.33	**0.22**	0.29
	cal	AD 1956-2001	0.94	0.27	NA	0.27
	ver		1.06	0.24	**0.18**	0.18
b. $\delta^{18}O$		AD 1910-2001	0.73	0.27	NA	0.27
	cal	AD 1910-1955	0.49	0.25	NA	0.25
	ver		0.54	0.28	**0.17**	0.25
	cal	AD 1956-2001	0.94	0.27	NA	0.27
	ver		1.00	0.28	**0.23**	0.27

Table 8.6: Statistics for reconstructed mean August SPI from AD 1910-2001 using (a) a multiple regression models combining $\delta^{13}C_{pin}$(‰) and $\delta^{18}O$(‰) and (b) a regression model using $\delta^{18}O$(‰) alone.

8.3.2.2 Northern Coast

The Northern Coastal record of Hanssen-Bauer and Føland (1998) stretches back further (AD 1873) than the Andenes precipitation record (AD 1910) and while a generally effective reconstruction can be made of the Andenes record using $\delta^{18}O$ alone or a combination of $\delta^{13}C_{pin}$ and $\delta^{18}O$ (Table 8.6). The longer Northern Coastal record shows the same problem of declining correlations between precipitation and both $\delta^{13}C_{pin}$ and $\delta^{18}O$ prior to AD 1900 as does the temperature record and $\delta^{13}C_{pin}$, a possible explanation for both of these was discussed in Section 8.2.

A multiple regression model using both $\delta^{18}O$ and $\delta^{13}C_{pin}$ to reconstruct precipitation was used to determine whether this could be improved, the results of which can be seen in Table 8.7a, and compared to the reconstruction using $\delta^{18}O$ alone in 8.7b. While the correlation improves slightly the reconstruction benefits only marginally and still fails to successfully reconstruct for the period AD 1873 to 1934 using the period AD 1935 to 1997 (CE = -0.17). The same procedure was carried out on August precipitation converted into SPI in Table 8.8b and while the results here are better than those for precipitation (Table 8.7) they only slightly improve on the reconstruction using only $\delta^{18}O$ (Table 8.8b), and still fail to satisfactorily reconstruct precipitation during the early period (AD 1873-1934).

		Period	MSE	RE	CE	r^2
a. $\delta^{13}C_{pin}$ and $\delta^{18}O$		AD 1873-1997	0.08	0.27	NA	0.27
	cal	AD 1873-1934	0.06	0.18	NA	0.18
	ver		0.09	0.02	**-0.17**	0.17
	cal	AD 1935-1997	0.08	0.38	NA	0.38
	ver		0.11	0.28	**0.20**	0.36
b. $\delta^{18}O$		AD 1873-1997	0.08	0.24	NA	0.24
	cal	AD 1873-1934	0.07	0.13	NA	0.13
	ver		0.09	0.02	**-0.17**	0.13
	cal	AD 1935-1997	0.09	0.34	NA	0.34
	ver		0.11	0.27	**0.19**	0.34

Table 8.7: Statistics for reconstructed mean July and August northern coastal precipitation from AD 1873-1997 using (a) a multiple regression models combining $\delta^{13}C_{pin}$(‰) and $\delta^{18}O$(‰) and (b) a regression model using $\delta^{18}O$(‰) alone.

When the very early part of the Northern Coastal precipitation record is removed (AD 1873-1895), where the common signal strength between trees for both $\delta^{18}O$ and $\delta^{13}C_{pin}$ is very low and, as we have already seen in Section 8.2, there may be very good reasons to expect non-linear behavior in both isotope series there is a considerable improvement in all the statistics. Table 8.9a shows the statistics for the reconstruction of precipitation based on both $\delta^{18}O$ and $\delta^{13}C_{pin}$, compared to that for $\delta^{18}O$ alone (Table 8.9b). In this case the addition of $\delta^{13}C_{pin}$ to the model would appear to make quite a positive improvement to, not only, the correlation (r^2= 0.38), but also to the CE and RE statistics.

When the Northern Coastal precipitation record is converted into the SPI index (Table 8.10) the improvement using the multiple regression model is even greater, with an overall r^2 of 0.41 and CE statistics in excess of 0.30 for both verification periods. These reconstructions can be seen graphically in Figures 8.14 (for the two calibration and verification periods) and 8.15 (for the calibration taken over the entire period from AD 1896 to 1997).

		Period	MSE	RE	CE	r^2
a. $\delta^{13}C_{pin}$ and $\delta^{18}O$		AD 1873-1997	0.71	0.29	NA	0.29
	cal	AD 1873-1934	0.68	0.19	NA	0.19
	ver		0.88	0.09	**-0.04**	0.18
	cal	AD 1935-1997	0.65	0.41	NA	0.41
	ver		0.82	0.25	**0.32**	0.25
b. $\delta^{18}O$		AD 1873-1997	0.75	0.25	NA	0.25
	cal	AD 1873-1934	0.73	0.14	NA	0.14
	ver		0.19	0.07	**-0.07**	0.14
	cal	AD 1935-1997	0.70	0.36	NA	0.36
	ver		0.83	0.44	**0.23**	0.36

Table 8.8: Statistics for reconstructed mean July and August northern coastal SPI from AD 1873-1997 using (a) a multiple regression models combining $\delta^{13}C_{pin}$(‰) and $\delta^{18}O$(‰) and (b) a regression model using $\delta^{18}O$ (‰) alone.

		Period	MSE	RE	CE	r^2
a. $\delta^{13}C_{pin}$ and $\delta^{18}O$		AD 1896-1997	0.07	0.38	NA	0.38
	cal	AD 1896-1946	0.04	0.40	NA	0.40
	ver		0.05	0.43	**0.23**	0.39
	cal	AD 1947-1997	0.09	0.36	NA	0.36
	ver		0.11	0.37	**0.27**	0.33
b. $\delta^{18}O$		AD 1896-1997	0.08	0.31	NA	0.31
	cal	AD 1896-1946	0.05	0.28	NA	0.28
	ver		0.06	0.36	**0.14**	0.28
	cal	AD 1947-1997	0.10	0.31	NA	0.31
	ver		0.11	0.33	**0.22**	0.31

Table 8.9: Statistics for reconstructed mean July and August northern coastal precipitation from AD 1896-1997 using (a) a multiple regression models combining $\delta^{13}C_{pin}$(‰) and $\delta^{18}O$(‰) and (b) a regression model using $\delta^{18}O$(‰) alone.

		Period	MSE	RE	CE	r^2
a. $\delta^{13}C_{pin}$ and $\delta^{18}O$		AD 1896-1997	0.58	0.41	NA	0.41
	cal	AD 1896-1946	0.41	0.42	NA	0.42
	ver		0.50	0.44	**0.31**	0.40
	cal	AD 1947-1997	0.71	0.39	NA	0.39
	ver		0.79	0.41	**0.32**	0.36
b. $\delta^{18}O$		AD 1896-1997	0.67	0.32	NA	0.32
	cal	AD 1896-1946	0.52	0.27	NA	0.27
	ver		0.59	0.34	**0.18**	0.27
	cal	AD 1947-1997	0.78	0.33	NA	0.33
	ver		0.85	0.37	**0.27**	0.33

Table 8.10: Statistics for reconstructed mean July and August northern coastal SPI from AD 1896-1997 using (a) a multiple regression models combining $\delta^{13}C_{pin}(‰)$ and $\delta^{18}O(‰)$ and (b) a regression model using $\delta^{18}O(‰)$ alone.

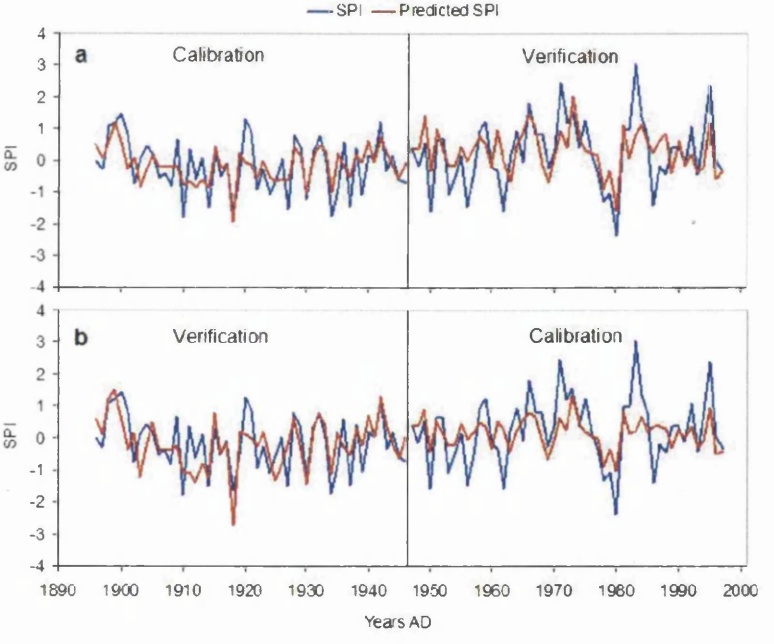

Figure 8.14: Reconstructed August Northern Coast SPI based on a multiple regression model using $\delta^{18}O(‰)$ and $\delta^{13}C_{pin}(‰)$, with (A) AD 1896-1946 as the calibration period and AD 1947-1997 as the verification period and (B) AD 1947-1997 as the calibration period and AD 1896-1946 as the verification period. In both cases compared to actual calculated August SPI.

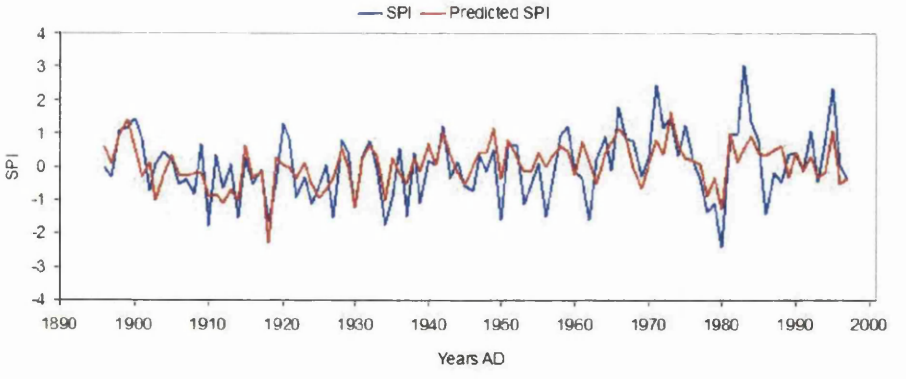

Figure 8.15: Reconstructed August Northern Coast SPI based on a multiple regression model using $\delta^{18}O(‰)$ and $\delta^{13}C_{pin}(‰)$ from AD 1896-1997 using the same period for calibration, compared to actual calculated SPI.

8.4 Chapter Conclusion

In Section 8.2 a conceptual model was introduced to explain the low correlation between $\delta^{13}C_{pin}$ and summer temperature from Andenes at the end of the nineteenth and in the early twentieth centuries (Figures 8.1 and 8.2). The predictions of this model would appear to fit the available data. The low correlation between $\delta^{18}O$ and precipitation at the end of the nineteenth century is a little more difficult to explain. However, the inclusion of relative humidity into the model (Figures 8.12 and 8.13) may possibly explain this, unfortunately there are no data available with which to test this extension of the model. One intriguing aspect of this period of low correlation between $\delta^{13}C_{pin}$ and $\delta^{18}O$ and climate is that it is during this period that these proxies correlate best with one another (Figure 8.10), despite relatively low common signal between trees during much of this period. This would seem to suggest that while $\delta^{13}C_{pin}$ and $\delta^{18}O$ are not being primarily controlled by temperature and precipitation during this period there is likely to be some factor controlling the fractionation of both these isotopes.

If such an episode of low correlation exists during the period for which instrumental data

are available it seems probable that such periods may also exist further back in time and so it is important to be able to recognise them. This was addressed in Section 8.2.0.2, with perhaps the most useful tool in recognising such periods being the low EPS between trees for both $\delta^{13}C_{pin}$ and $\delta^{18}O$.

In Section 8.3 attempts were made to improve the climatic reconstruction by using more than one of the proxies available in a multiple regression model. In general there seems to be little advantage in adding proxies to reconstruct temperature, with the simple linear model using $\delta^{13}C_{pin}$ performing well compared to multiple regression models, especially when using the longer Tornedalen record, which is perhaps the best available test of low frequency temperature reconstruction. There are two major advantages of using $\delta^{13}C_{pin}$ alone to reconstruct past temperature. Firstly one of model simplicity, based upon the principle of Occam's razor, and secondly that any model including tree-ring widths may have problems reconstructing lower frequency temperature variation (Cook et al., 1995), while no such problems are apparent with $\delta^{13}C$ (Gagen et al., 2007).

When attempting to reconstruct precipitation, or a precipitation index (SPI) there does appear to be some advantage in using both $\delta^{18}O$ and $\delta^{13}C_{pin}$ in a multiple regression model, especially when the longer Northern Coastal record of Hanssen-Bauer and Føland (1998) is used and when the period of non-linearity at the end of the nineteenth century is removed (Table 8.10 and Figures 8.14 and 8.15).

In the next chapter a reconstruction of temperature will be undertaken using $\delta^{13}C_{pin}$, calibrated on the mean July and August temperature record over the period AD 1927 to 2001 and a reconstruction of precipitation in the form of SPI calibrated on the Northern Coastal record from AD 1896 to 1997 using a multiple regression model based on $\delta^{18}O$ and $\delta^{13}C_{pin}$. A reconstruction of SPI will also be made using $\delta^{18}O$ alone to ensure that the inclusion of $\delta^{13}C_{pin}$ does not impart a temperature signal to the reconstruction as it is believed that a reasonably accurate precipitation reconstruction may be vital to the interpretation of a temperature reconstruction based on $\delta^{13}C_{pin}$.

9

Climate Reconstructions

9.1 Introduction

In this chapter a reconstruction of temperature from AD 1394 to 2001 will be undertaken using $\delta^{13}C_{pin}$ (Section 9.4) and a shorter reconstruction of precipitation (SPI) from AD 1765 to 2001 (Section 9.5). Prior to this, in Sections 9.2 and 9.3, both data sets will be examined over their full length and running between-tree correlations and EPS calculated. Both data sets will be shifted towards the mean (where necessary) using common periods. The temperature reconstruction will be compared with long regional climate records and other local climate reconstructions in an attempt to establish its veracity (Section 9.4.1). Finally, in Section 9.6, the potential for a more regional climate reconstruction will be explored.

9.2 $\delta^{13}C_{pin}$ Data Set

$\delta^{13}C$ results from Forfjorddalen are available back to AD 1300. However, prior to AD 1394 there are only three trees in the series (63, 133 and 166) and prior to AD 1330 only two trees (63 and 166). Prior to AD 1390 the correlation between tree 166 and the other two trees is poor (although the correlation between trees 63 and 133 remains good back to AD 1330), this small number of trees combined with the low inter-correlation with tree 166 combine to produce a low common signal between trees. Because of this

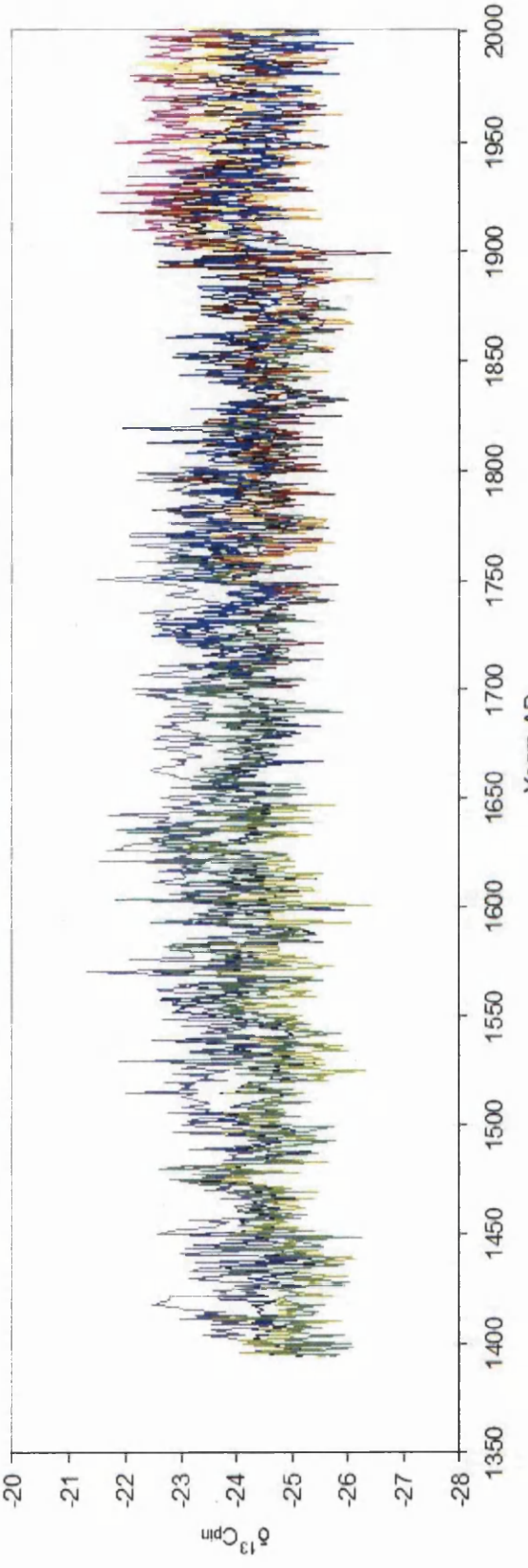

Figure 9.1: All $\delta^{13}C_{pin}(‰)$ results from AD 1394 to 2001, data from AD 1820 has been pin corrected but not shifted towards the mean value.

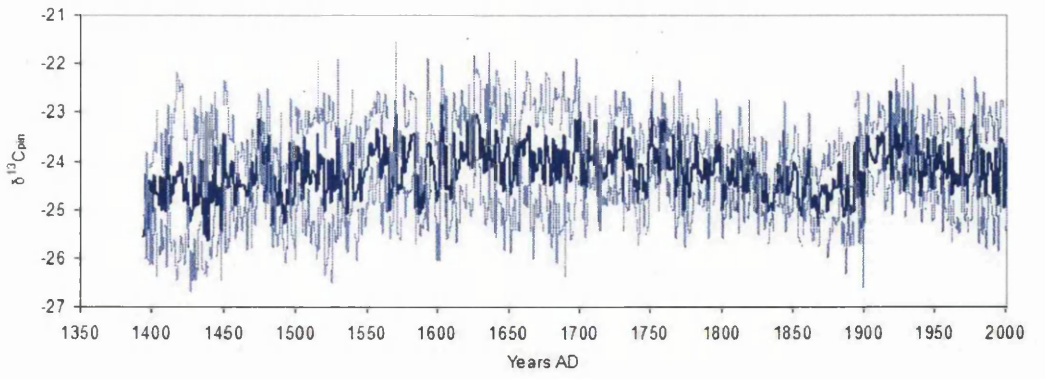

Figure 9.2: Mean $\delta^{13}C_{pin}(‰)$ values from AD 1394-2001 with 95% confidence limits around the mean value.

it was decided to cut the time series at AD 1394 from which point there are four trees in the series and a good common signal.

Figure 9.1 shows all the trees in the $\delta^{13}C$ series from AD 1394 to 2001, these results have been pin corrected ($\delta^{13}C_{pin}$) from AD 1820 onwards, but as yet have not been shifted towards the mean value. The mean $\delta^{13}C_{pin}$ value for these trees showing the 95% confidence limits in the mean value can be seen in Figure 9.2, while the 95% confidence interval and the range of $\delta^{13}C_{pin}$ can be seen in Figure 9.3.

The 95% confidence limits are narrower from AD 1700 onwards (Figure 9.2) and this is confirmed in Figure 9.3, which shows a mean 95% confidence limit of 0.81 overall (AD 1394-2001), a mean of 0.95 (AD 1394-1699) and 0.67 (AD 1700-2001). This improvement in the confidence post AD 1700 is due to the additional number of trees, from AD 1706 onwards there are (apart from a short period from AD 1880-1899 with 5 trees) a minimum of 6 trees in the series. Prior to AD 1706 there are there are never more than 5 trees in the series (this can be seen as the black line in Figure 9.3). The range of $\delta^{13}C_{pin}$ values is quite variable (as can be seen in Figure 9.3) however, there is little different on average prior or post AD 1700 with an overall mean range of 1.64 (AD 1394-2001) and a range of 1.54 prior to AD 1700 and 1.75 post AD 1700. This would suggest that were more trees added to the period from AD 1394 to 1705 the 95% confidence limits are likely to be as tight as those post AD 1706

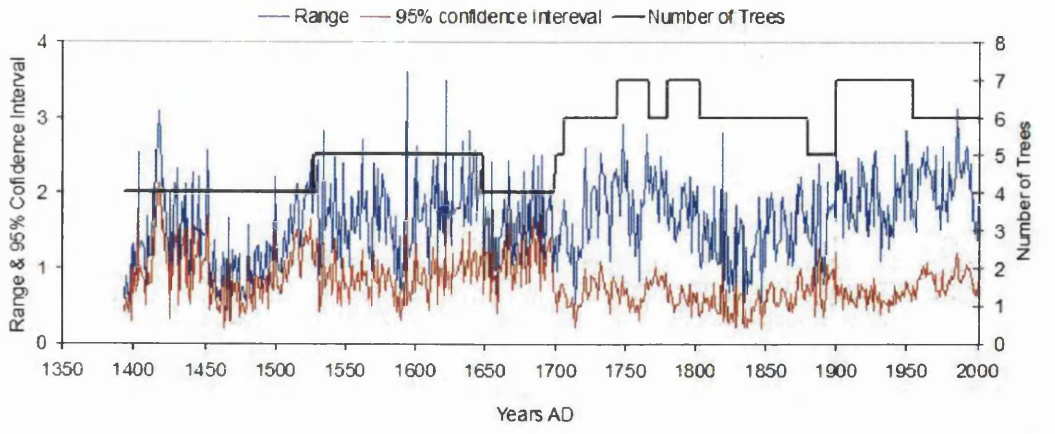

Figure 9.3: 95% confidence interval and range of isotope values from AD 1394-2001. The number of trees in the series are shown on the right hand axis

The temporal ranges of all the trees which make up the $\delta^{13}C_{pin}$ series from AD 1394-2001, can be seen in Figure 9.4. To prevent potential problems associated with off-setting the mean value as new trees are added to the series back through time it is important to shift these towards the mean value, as was described in Chapter 5. The trees at Forfjorddalen are long lived and so there is little problem with using overlapping trees which have been shifted to carry out this procedure. The three remaining trees to be shifted (128, 132 and 133) are shifted on the common period from AD 1527 to 1647 using the the mean shifted values of trees 63 and 166 to make this adjustment. This calculation is once again made using equation 9.1, where $\bar{x}$ is the mean δ^{13}C value for the trees already shifted (in this case Trees 63 and 166) over common period (AD 1527-1647), $\bar{n}$ is the mean δ^{13}C of the tree to be shifted over the common period and n is the individual δ^{13}C value of the tree to be shifted.

$$\delta^{13}C_{shift} = n - (\bar{n} - \bar{x}) \tag{9.1}$$

Figure 9.4: Temporal ranges of all the trees included in the $\delta^{13}C_{pin}(‰)$ series from AD 1394-2001. The trees in green are all those which span the shift period from AD 1800 to 1879 and so are shifted toward that mean value. The three trees in blue (128, 132 and 133) are not included in this period and so are shifted on the common period AD 1527-1647, using the mean shifted values of trees 63 and 166.

Figure 9.5 shows all the $\delta^{13}C_{pin}$ results for all trees from AD 1394 to 2001 shifted towards the mean value using equation 9.1 over common period. The values in this figure are much more homogeneous than those in Figure 9.1 and so the potential for off-sets in the mean value as new trees are introduced or leave the series are likely to be greatly reduced.

The mean of all the shifted $\delta^{13}C_{pin}$ results in Figure 9.5 with 95% confidence limits added can be seen in Figure 9.6. The process of shifting the results towards the mean has obviously improved the 95% confidence limits as can be seen by a comparing of Figures 9.6 and 9.2. The 95% confidence interval and the range for the shifted $\delta^{13}C_{pin}$ results can be seen in Figure 9.7. Again the reduction in range and the 95% confidence interval can be seen by comparing this with Figure 9.3 (for the un-shifted values). Figure 9.7 again shows a sharp improvement in the 95% confidence interval after about AD 1700, but again this is explicable by the increase in the number of the trees in the series after AD 1706. A summary of the comparison between the 95% confidence interval and the range of the pre and post shifted $\delta^{13}C_{pin}$ results for the entire period (AD 1394-2001) and the periods from AD 1394-1699 and AD 1700-2001 can be seen in Table 9.1.

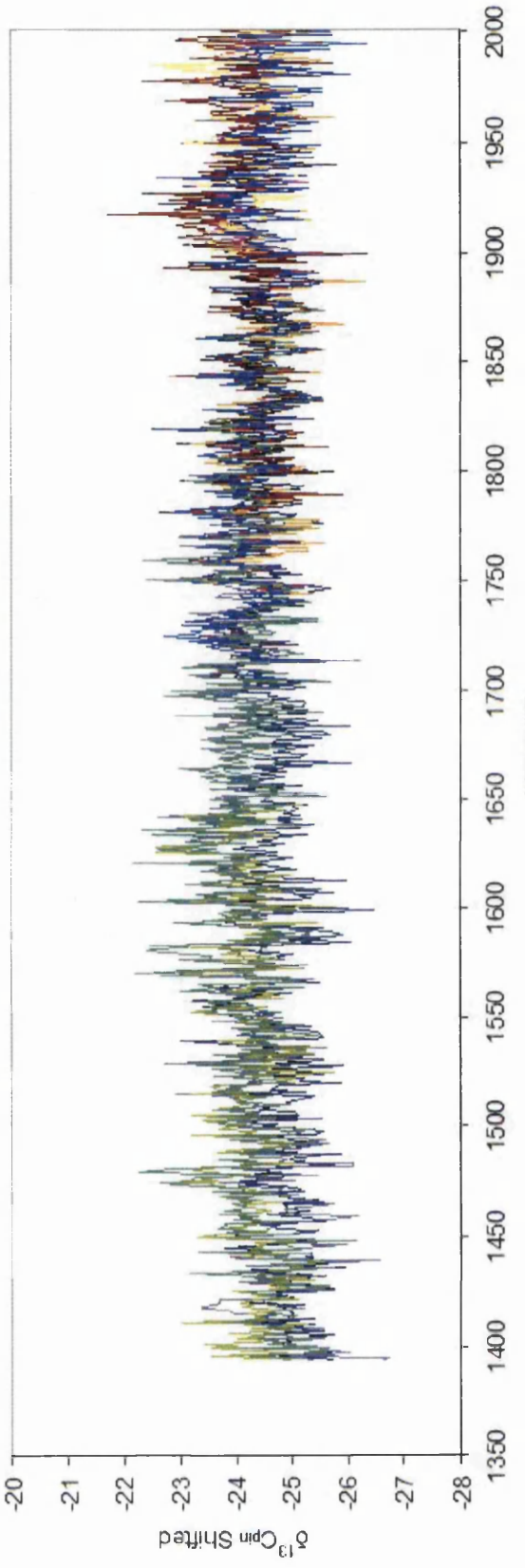

Figure 9.5: All $\delta^{13}C_{pin}$(‰) results from AD 1394 to 2001, data from AD 1820 has been PIN corrected and shifted towards the mean value using the common periods.

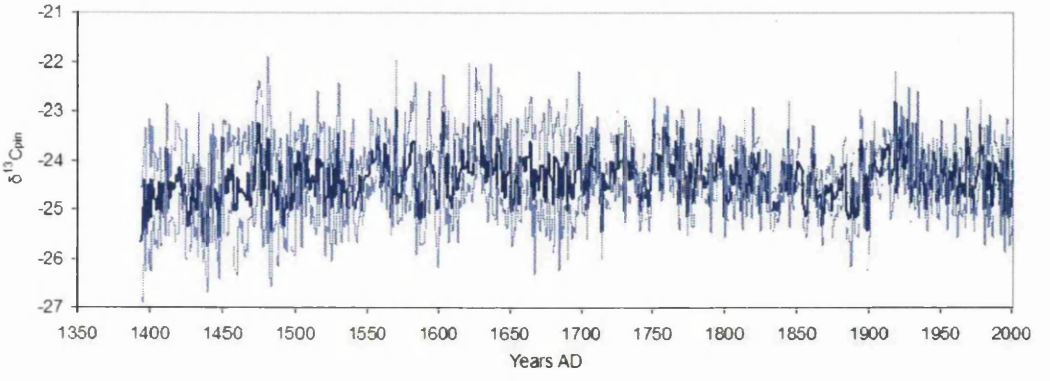

Figure 9.6: Mean $\delta^{13}C_{pin}(‰)$ shifted values from AD 1394-2001 with 95% confidence limits around the mean value.

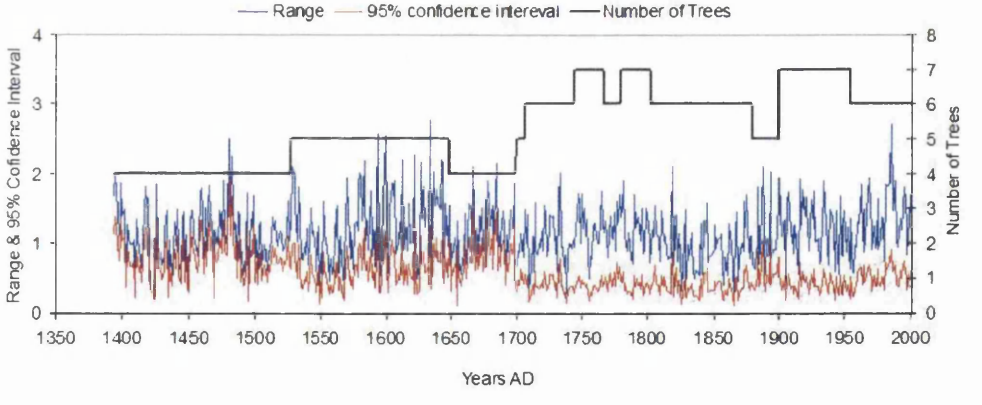

Figure 9.7: 95% confidence interval and range of isotope values from AD 1394-2001, with values shifted towards the mean using common periods. The number of trees in the series are shown on the left hand axis

	Range		95% Confidence Interval	
	$\delta^{13}C_{pin}$	$\delta^{13}C_{pin}$ Shifted	$\delta^{13}C_{pin}$	$\delta^{13}C_{pin}$ Shifted
AD 1394-2001	1.64	1.15	0.81	0.58
AD 1394-1699	1.54	1.16	0.95	0.73
AD 1700-2001	1.75	1.14	0.67	0.43

Table 9.1: Comparison of the range and 95% confidence interval for the $\delta^{13}C_{pin}$(‰) results pre and post shifting for the entire period (AD 1394-2001) and the periods from AD 1394-1699 and AD 1700-2001.

The common signal between $\delta^{13}C_{pin}$ results over the entire time series was again calculated using a 31 year running mean correlation and EPS the results of which can be seen in Figure 9.8, which also shows the number of trees in the time series at any one time. Figure 9.8 demonstrates how the EPS is linked to the number of trees in the series. For much of the period the EPS is near to, or in excess of the 0.85 threshold, while the maximum EPS in a 31-year running window (Figure 9.9) only drops below 0.85 at the very beginning of the sequence (31 year windows starting before AD 1420) and for one 31 year window beginning in AD 1534. There are however, quite a number of occasions (187 of the 594 correlations) when the EPS is below 0.85 and when the mean inter-tree correlation is below $r = 0.50$ (137 of 594 running correlations), however many of these are only marginal and would probably be improved by the addition of one or more trees.

As has already been shown, there is a period of low correlation between the $\delta^{13}C_{pin}$ results and temperature (AD 1880-1900, identified as number 4 on Figure 9.8), associated with a low common signal between trees. This means that there may be other periods of low correlation and that these may be recognisable by a low common signal, possible candidates have been numbered on Figure 9.8 (dated approximately: 1 - AD 1450-1460;

2 - AD 1535-1550; and 3 - AD 1640-1660). There are other periods which may be considered such as the early years of the nineteenth century and the AD 1620s, however the 4 listed would appear to be the largest events. Of the 4 events the largest dip in terms of inter-correlation is number 4 (AD 1880-1900) although the EPS is similar to the earlier events because the number of trees is greater. Unfortunately at the time of writing no oxygen isotopes are available for these earlier periods to help with further diagnosis, however these periods will be viewed with caution when a climate reconstruction is undertaken.

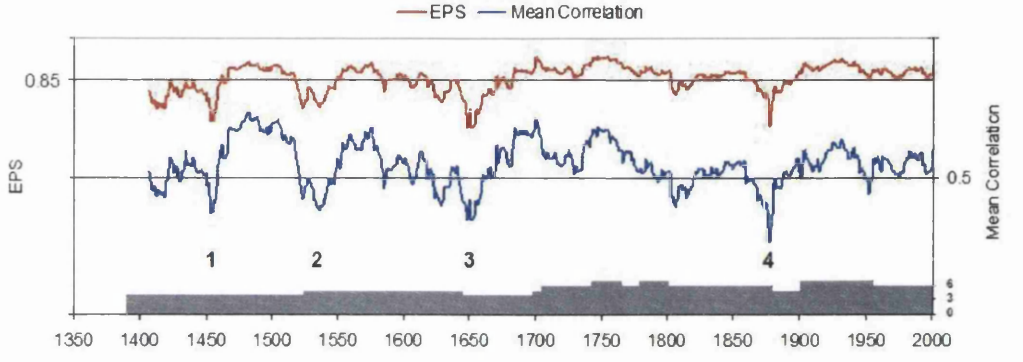

Figure 9.8: Running EPS (in red) and mean inter-series correlation (in blue) for all $\delta^{13}C(‰)$ results from AD 1394-2001. The total number of trees in the series at any given time is shown at the bottom in grey (with separate axis on the bottom left). Lines are drawn at the EPS threshold of 0.85 and mean inter series correlation of $r = 0.50$ (the scale on both axes is 0 to 1)

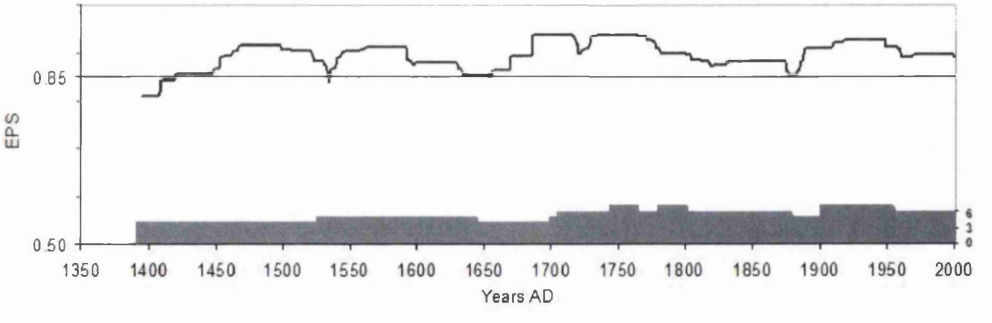

Figure 9.9: Maximum EPS in a 31 year running window from AD 1394 to 2001, the number of trees is again shown in grey at the bottom of the graph.

9.3 δ^{18}O Data Set

At the time of writing the δ^{18}O data available extends back as far as AD 1700, but only after AD 1765 are four simultaneous trees available in the time series, which has been found to be sufficient for climate reconstruction (Robertson et al., 1997b; McCarroll and Pawellek, 1998), and is the minimum number of trees which are considered for climatic reconstruction in this thesis. It is therefore from this point that the time series will be examined with a view to reconstructing precipitation using δ^{18}O results on their own and in combination with $\delta^{13}C_{pin}$. As much of this time series has already been examined in detail in Chapter 6 (as far back as AD 1810) it will only be briefly examined here.

Figure 9.10 shows all the trees in the time series from AD 1765 to 2001 and Figure 9.11 shows the trees after the values have been shifted towards the mean value. The mean $\delta^{18}O_{shifted}$ value with 95% confidence limits around it can be seen in Figure 9.12. As has already been noted, due to the slightly errant behavior of Tree 95 during the twentieth century, shifting the values to the mean of AD 1900 to 1954 has caused rather more variability prior to AD 1900 than post AD 1900. Unless Tree 95 is excluded or dealt with differently to the other trees this is unavoidable, and no good reason to exclude or deal with this tree as a special case was apparent.

The mean 31-year inter-correlation and EPS for all the trees in the time series can be seen in Figure 9.13, while the maximum EPS in a 31-year running widow can be seen

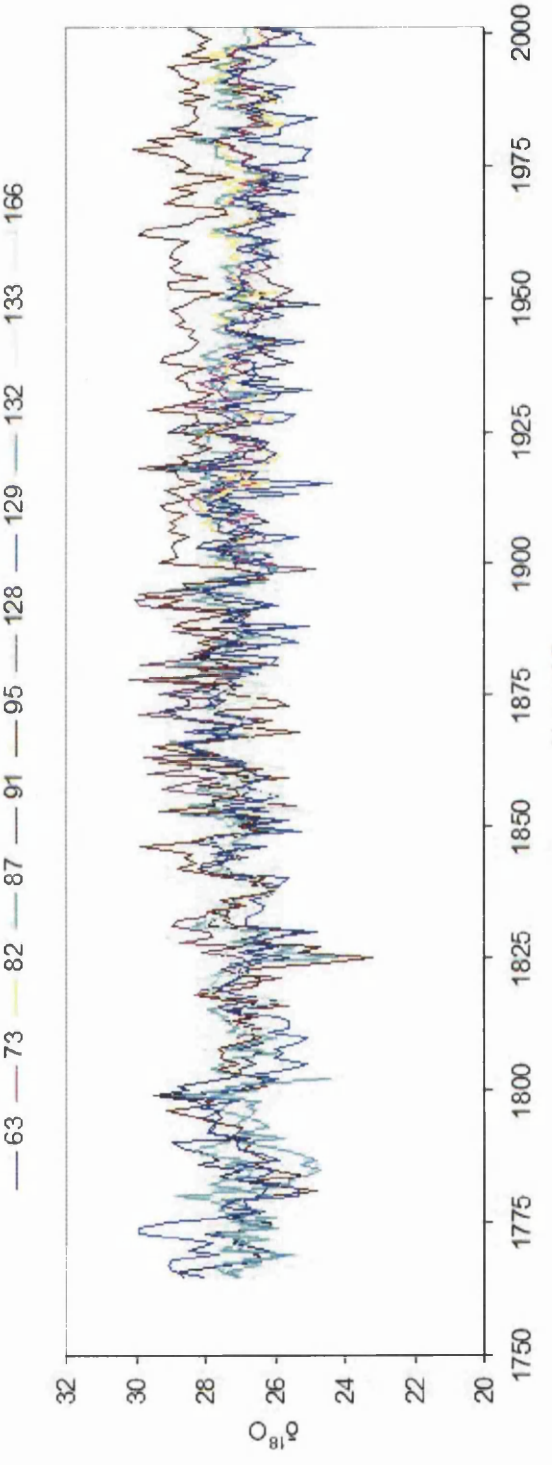

Figure 9.10: All raw $\delta^{18}O(‰)$ results from AD 1765 to 2001.

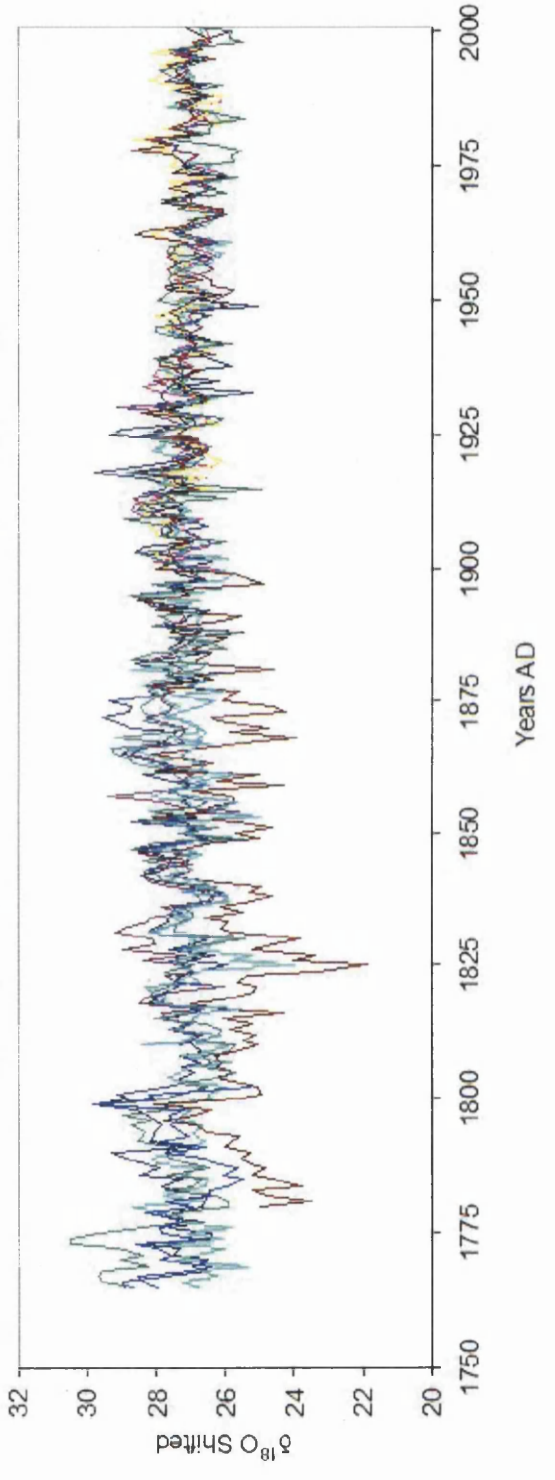

Figure 9.11: All $\delta^{18}O_{shift}(‰)$ results from AD 1765 to 2001, results have been shifted towards the mean using common periods.

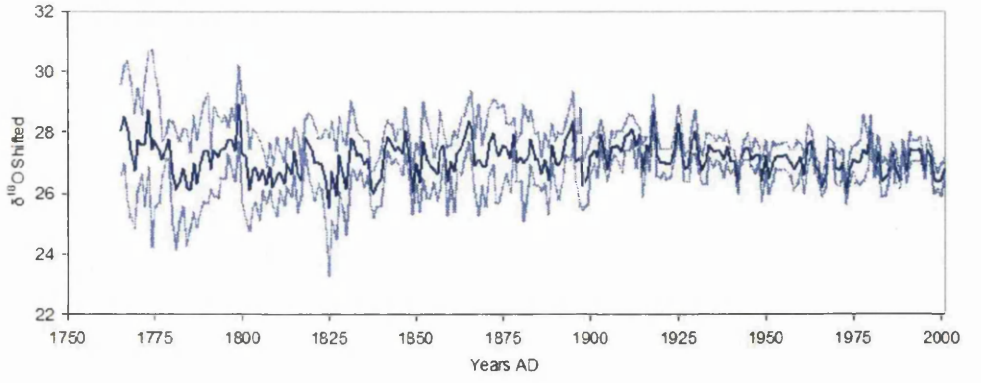

Figure 9.12: Mean $\delta^{18}O_{shift}(‰)$ shifted values from AD 1765-2001 with 95% confidence limits around the mean value.

in Figure 9.14. Both the EPS and inter-correlation are poorer for $\delta^{18}O$ than for $\delta^{13}C$, although the maximum EPS remains above the 0.85 level for the majority of the series. As discussed in previous chapter both $\delta^{18}O$ and $\delta^{13}C$ have a very poor common signal towards the end of the nineteenth century during the period of low corelation between isotopes and available climate parameters. It is interesting to note that the next most recent period of low common signal for $\delta^{13}C$ (Figure 9.8 , unnumbered) during the early years of the AD 1800s is a period of quite strong common signal for $\delta^{18}O$ (although the $\delta^{18}O$ signal dips soon after), this may suggest that this may not be a problematic period for $\delta^{13}C$ to reconstruct temperature and that simply one of two more trees are required to boost the common signal for $\delta^{13}C$. Were $\delta^{18}O$ available back to AD 1394 this comparison could be made to the other periods of low $\delta^{13}C$ EPS (Figure 9.8 numbers 1, 2 and 3).

In conclusion the $\delta^{18}O$ series appears robust back to AD 1790, before which the common signal falls away. This may however, have much to do with the limited number of tree early in the series. A precipitation reconstruction will be made using the series from AD 1765 to 2001, however caution will be exercised over the early period from AD 1765 to 1790 and the period of very low common signal during the second half of the nineteenth century.

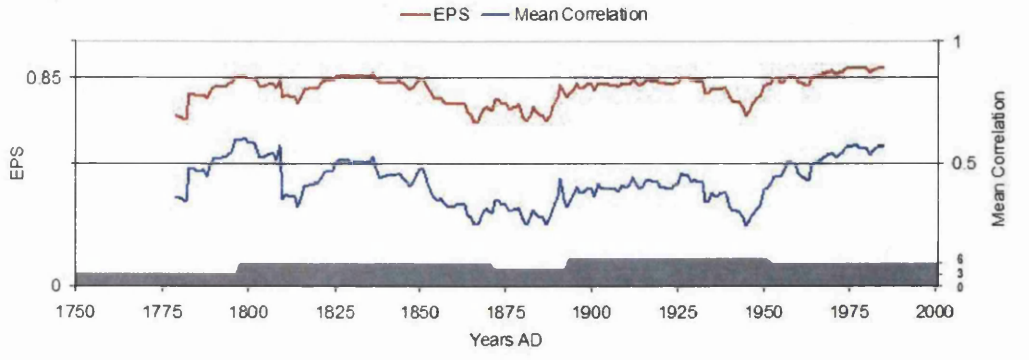

Figure 9.13: Running EPS (in red) and mean inter-series correlation (in blue) for all $\delta^{18}O$ results from AD 1765-2001. The total number of trees in the series at any given time is shown at the bottom in grey (with separate axis on the bottom left). Lines are drawn at the EPS threshold of 0.85 and mean inter-series correlation of $r = 0.50$ (the scale on both axes is 0 to 1)

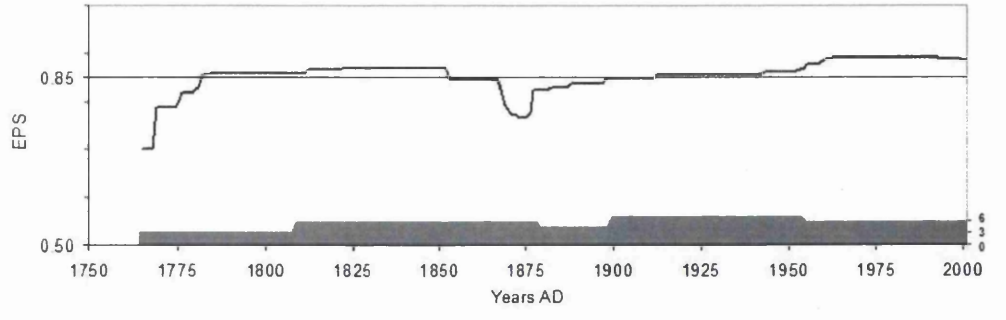

Figure 9.14: Maximum EPS in a 31 year running window from AD 1765 to 2001, the number of trees is again shown in grey at the bottom of the graph.

9.4 Temperature Reconstruction

Temperature at Forfjorddalen is reconstructed for the period AD 1394 to 2001 using a linear regression model based on $\delta^{13}C_{pin}$ and mean July and August temperature from Andenes over the period AD 1927 to 2001 and verified by a split data set method outlined in Chapter 5, the error in the reconstruction was estimated as 2 standard errors of the prediction ($\pm$1.614°C), this temperature reconstruction with estimated errors can be seen in Figure 9.15, this reconstruction can also seen as departures from the AD 1927 to 2001 mean temperature in Figure 9.16. The four periods of low EPS (Figure 9.8) are highlighted in Figure 9.17 as areas where the reconstruction may be in doubt.

What is perhaps most notable from Figures 9.15 and 9.16 is the multi-decadal variability in the reconstruction (especially when compared to the ring-width based reconstruction shown in Figure 9.20). The general pattern is one of gradual warming from the beginning of the record to a peak in the AD 1640s followed by further warm periods in the mid-eighteenth century and then a gradual decline to a cool phase at the end of the nineteenth century. The subsequent rapid warming from around AD 1900 to 1925 is a real phenomenon (according to all available climate records) but is not accurately captured by this reconstruction (see Figure 9.17), as previously discussed the isotope reconstruction leads actual temperature rise, following this there is a slight decline after which summer temperature remains generally stable for the rest of the twentieth century.

Cold conditions in northern Scandinavia at the end of the nineteenth century appear to have been widespread and are found in the long climate records available form this area (Klingbjer and Moberg, 2003; Moberg and Bergström, 1997). Recent climate reconstructions have also shown it be be one of the coldest phases in the past 500 years (Gagen et al., 2007; Grudd, 2008). Warm summer conditions in the mid-eighteenth century appear in the longest Scandinavian temperature record from Uppsala (Moberg and Bergström, 1997) and would seem to be in agreement with those found in this reconstruction (see Figure 9.18). The reconstructions of Grudd (2008) (based on maximum latewood density, see Figure 9.19) and Gagen et al. (2007) (based on $\delta^{13}C_{pin}$), both show

warm summer temperatures centered around AD 1760, as did Briffa et al. (1988). Both Lindholm and Eronen (2000) and Gagen et al. (2007) found sumer warmth in Scandinavia in the middle years of the seventeenth century (centered around AD 1650), although slightly later than the warmest period in this construction, which is centered around AD 1625 (see Figure 9.15). Interestingly the same feature appears in the reconstruction of Grudd (2008), although at a rather lower level (see Figure 9.19).

In terms of debates over recent global temperature rises (e.g. IPCC, 2007), Figure 9.16 suggests that there may have been several occasions over the part 600 years when the summer temperatures in northern Norway were higher than those of the late twentieth century. Notably the first half of the seventeenth and the mid-eighteenth centuries. It should of course be noted that as δ^{13}C can be affected by both temperature and precipitation (as previously discussed), thus anomalously high δ^{13}C values (taken in this reconstruction to represent high temperatures) could also represent very dry periods and while dry and warm conditions often go hand in hand this is not always the case (e.g. the late nineteenth century). The warm period in this reconstruction centered around AD 1760 is in agreement with the Uppsala temperature record (Moberg and Bergström, 1997) and the reconstruction of Grudd (2008). As the reconstruction of Grudd (2008)is based on density it should be generally independent of precipitation, and so the AD 1760s would seem likely to be a genuine warm episode. While there is no obvious reason to suspect the veracity of the warm period centered around AD 1625 an estimate of precipitation at this time (based on δ^{18}O) would be useful, unfortunately at the time of writing these data are not available.

9.4.1 Comparison with other records

The longest instrumental temperature record available for Scandinavia comes from Uppsala in southern Sweden (58°51'N and 17°38'E) which was initiated in AD 1722. This record has been homogenised by Moberg and Bergström (1997) who consider it a reliable record of southern Swedish temperature, although believe individual values before the AD 1860s, and particularly prior to AD 1750, to be less accurate. At almost 1000 km

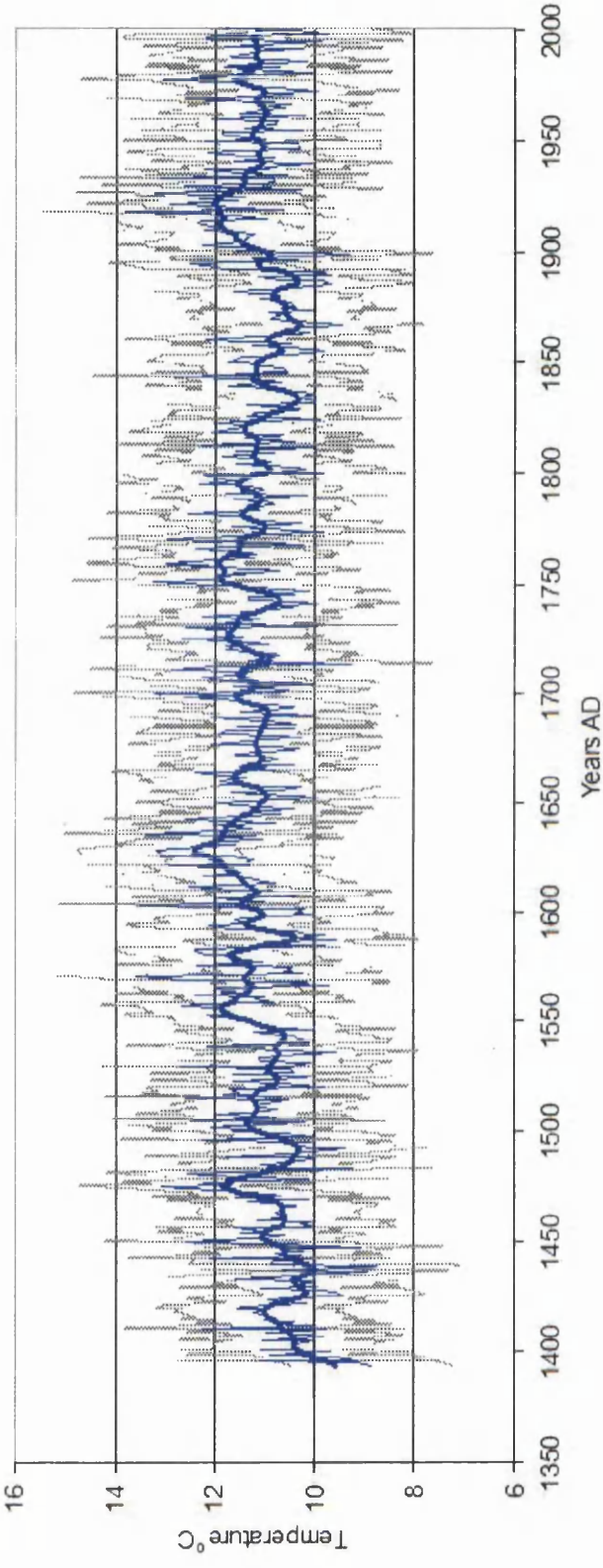

Figure 9.15: Reconstructed Forfjorddalen mean July and August temperature from 1394 to 2001 (blue line) using a linear regression model based on $\delta^{13}C_{pin}(‰)$, using the period from AD 1927 to 2001 for calibration, with an 11 year weighted and centered running mean (bold blue line), error in the reconstruction is represented by the grey dashed line (± 2 standard errors of the prediction).

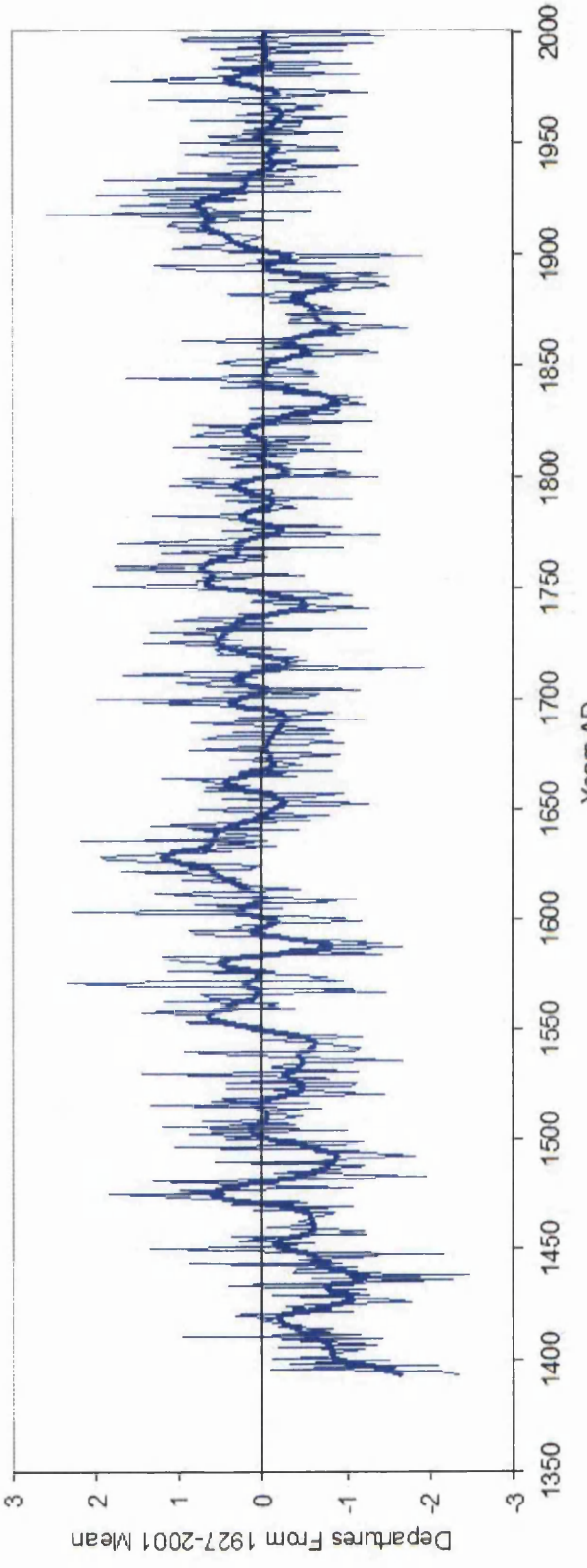

Figure 9.16: Reconstructed summer temperature (mean July and August) from Forfjorddalen (as repeated in Figure 9.15), shown as departures form the AD 1927 to 2001 mean temperature.

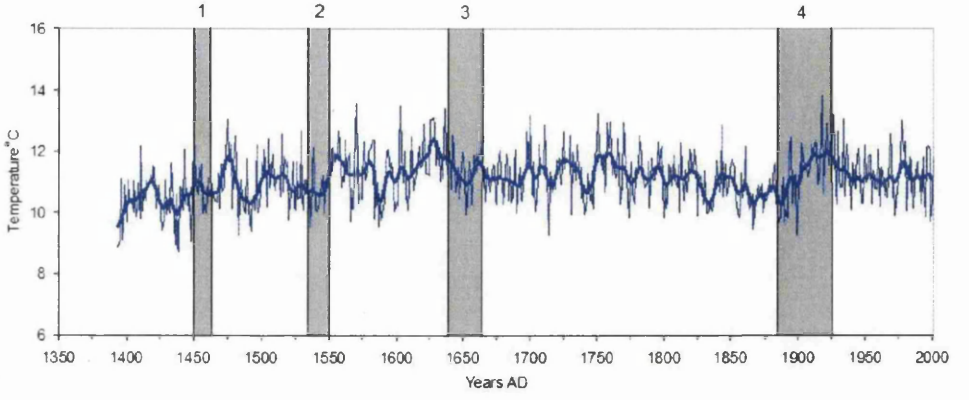

Figure 9.17: Reconstructed Forfjorddalen mean July and August temperature from AD 1394 to 2001 with areas of low between tree signal highlighted in grey and numbered : 1) AD 1450 to 1460; 2) AD 1535 to 1550; 3) AD 1640 to 1660; and 4) AD 1875 to 1925.

distance from Forfjorddalen (68°48'N and 15°44'E) and at almost exactly 10° of latitude south, there is little expectation that the temperature reconstruction from Forfjorddalen could be correlated with the Uppsala record on a year to year basis. However a visual comparison of the general trends in both data sets may prove useful to determine how realistic the low frequency component of the reconstruction from Forfjorddalen may prove to be (see Figure 9.18). Mean summer temperature from Uppsala is higher than that from Andenes and so both data sets have been normalised to aid comparison.

Figure 9.18 would seem to suggest that, apart from the period from AD 1900 to 1930 (which has already been discussed in detail) the general trends in both the Uppsala record and the reconstruction from Forfjorddalen are quite similar with a general decline in mean July and August temperature from AD 1750 to 1900, the brief cool event just prior to AD 1750 also match well in both records. This evidence suggests that the Forfjorddalen temperature reconstruction is valid as far back as AD 1722 and also reflects temperature trends on a regional basis.

Torneträsk in northern Sweden is the site of one of the world's longest tree-ring chronologies, at 7400 years (Grudd et al., 2002). Situated at 68°22'N and 19°06'E it is approximately 150 km east of Forfjorddalen. A comparison of the most recent temperature

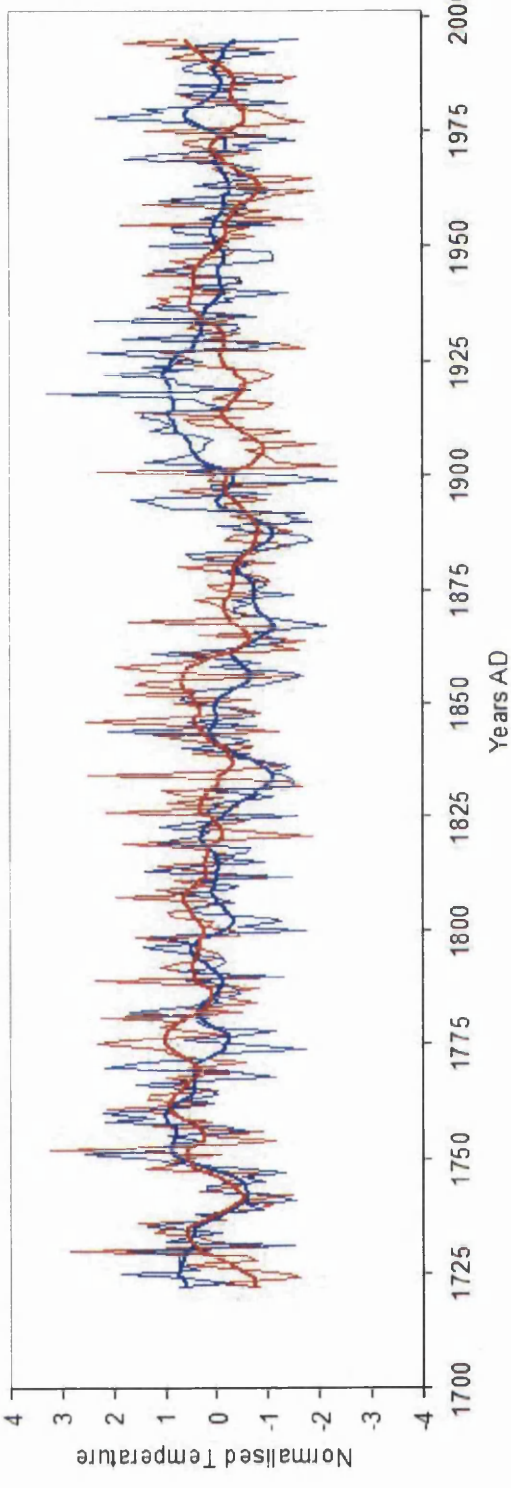

Figure 9.18: Reconstructed Forfjorddalen temperature, based on $\delta^{13}C_{pin}(‰)$, compared with the instrumental data from Uppsala (Moberg and Bergström, 1997), for July and August from AD 1722 to 1997, both data sets have been normalised and a centered running 11-year running mean has been added.

reconstruction from Torneträsk, based on maximum latewood density (Grudd, 2008) and the reconstruction from Forfjorddalen, based on $\delta^{13}C$, can be seen in Figure 9.19. The Torneträsk reconstruction is of April to August temperature while the Forfjorddalen one is of July and August and so the temperatures are rather different, to ease comparison both data sets have been normalised (mean 0, standard deviation 1).

Apart from the early twentieth century, there appears to be very good agreement between both these reconstructions back to around AD 1650 (Figure 9.19), prior to which they begin to diverge. It is interesting to note that the structure of the warm period in the Forfjorddalen reconstruction, centered around AD 1625, appears to be very similar to the same period in the Torneträsk reconstruction, except rather warmer. From AD 1394 to AD 1650 the Torneträsk reconstruction exhibits a general cooling trend while the Forfjorddalen reconstruction shows general warming. At only around 150 km distance one would expect more similarity between temperatures, especially considering that there is such good agreement post AD 1650. It therefore seems likely that one or both of these reconstructions have failed to capture the multi-decadal temperature trends in this area correctly prior to AD 1650. However, at this time it not possible determine which, if either, is nearer to the truth. Figure 9.19 would seem to suggest that the Forfjorddalen reconstruction may be considered reasonably accurate back to around AD 1650.

The only other published temperature reconstruction from Forfjorddalen is by Kirchhefer (2001), a comparison between this and the $\delta^{13}C_{pin}$ reconstruction from Figure 9.15 can be seen in Figure 9.20. What is immediately apparent from this comparison is that the reconstruction based on tree-ring widths lacks most of the multi-decadal variability of the $\delta^{13}C_{pin}$ reconstruction, although much of the year to year variability is the same ($r = 0.37$, between the two reconstructions). This is perhaps a good example of what Cook et al. (1995) called the *segment length curse*, where much of the multi-decadal climate variability is lost through statistical detrending of the growth trend in tree-ring widths. It should be noted that at the time of writing the tree-ring width based reconstruction

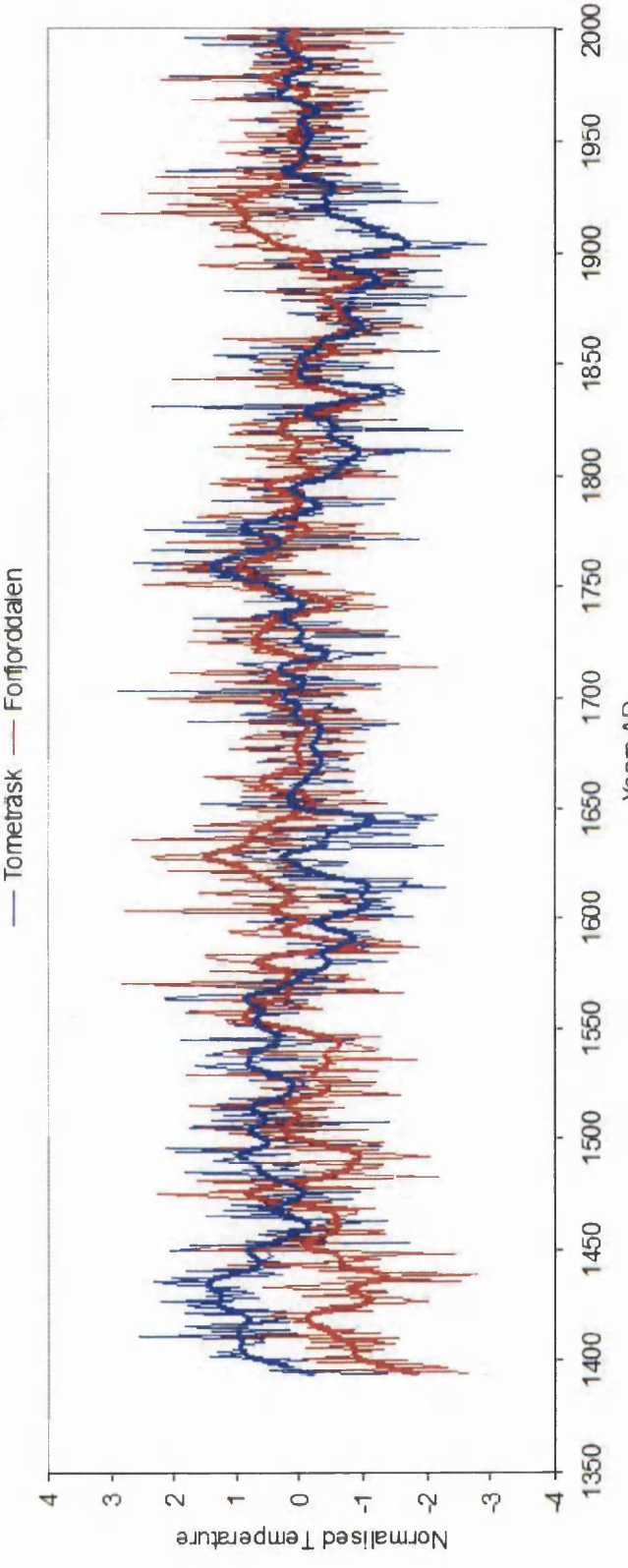

Figure 9.19: Reconstructed July and August Forfjorddalen temperature, based on $\delta^{13}C_{pin}$ (‰), compared with a maximum latewood density reconstruction from April to August for Torneträsk (Grudd, 2008), from AD 1394 to 2001, both data sets have been normalised and a centered running 11-year mean has been added.

at Forfjorddalen is being updated as part of the *Millennium Project* using more advanced statistical detrending techniques to allow for the retention more multi-decadal climate variability (Kirchhefer, *pers. comm.*). It may be possible that an analysis and combination of these two reconstructions may lead to a fuller understanding of the true temperature variability at Forfjorddalen over recent centuries.

9.5 Precipitation Reconstruction

A tentative reconstruction of precipitation, in the form of the Standardised Precipitation Index (SPI) of McKee et al. (1993), from AD 1765 to 2001 has been undertaken using a regression model based on $\delta^{18}O$ alone (Figure 9.21), and a multiple regression model using $\delta^{18}O$ and $\delta^{13}C_{pin}$ (Figure 9.22). Errors in these reconstructions were estimated as 2 standard errors of the prediction. A comparison of these two reconstruction can be seen in Figure 9.23.

Both Figures 9.21 and 9.22 suggest that precipitation in this area is quite variable. It has already been seen that there has been a large increase in both precipitation and precipitation variability during the twentieth century, which is not fully captured by either reconstruction. It appears that, if these reconstructions are at all accurate, it may have been even wetter in the early nineteenth century than at present. Both reconstructions suggest a similar pattern of a wet late twentieth century and early nineteenth century with a dryer interlude during the late nineteenth and early twentieth century, this period was also rather cold in this region and these cold and dry conditions have already been used as an explanation for problems with the $\delta^{13}C_{pin}$ record.

The period of seemingly dry conditions is also the period for which the two reconstructions depart from one another (Figure 9.23), the reconstruction based on $\delta^{18}O$ alone suggesting rather dryer conditions than the reconstruction based on $\delta^{18}O$ and $\delta^{13}C_{pin}$. This is also the period for which the inter-correlation between trees for both $\delta^{18}O$ and $\delta^{13}C_{pin}$

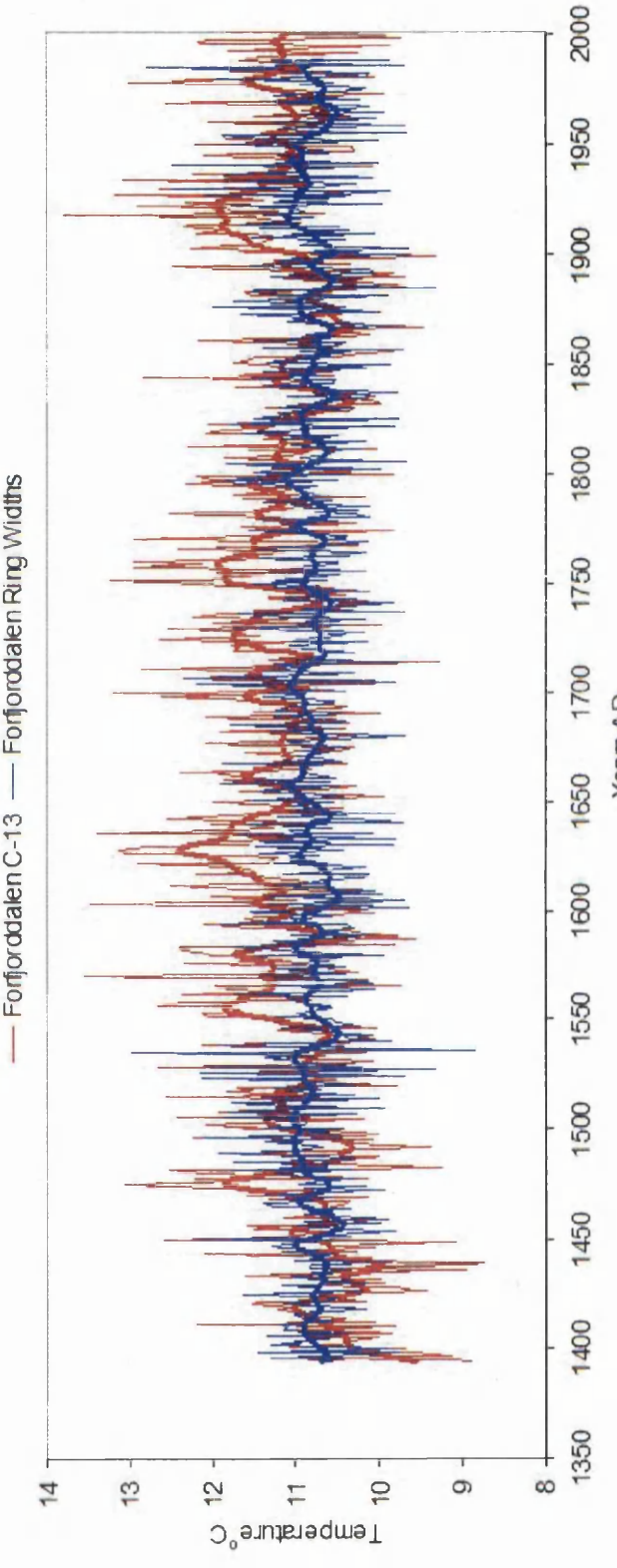

Figure 9.20: Reconstructed July and August Forfjorddalen temperature, based on $\delta^{13}C_{pin}(‰)$ (red line), and tree-ring widths (Kirchhefer, 2001)(blue line), from AD 1394 to 2001, a centered running 11-year mean has been added to both data sets.

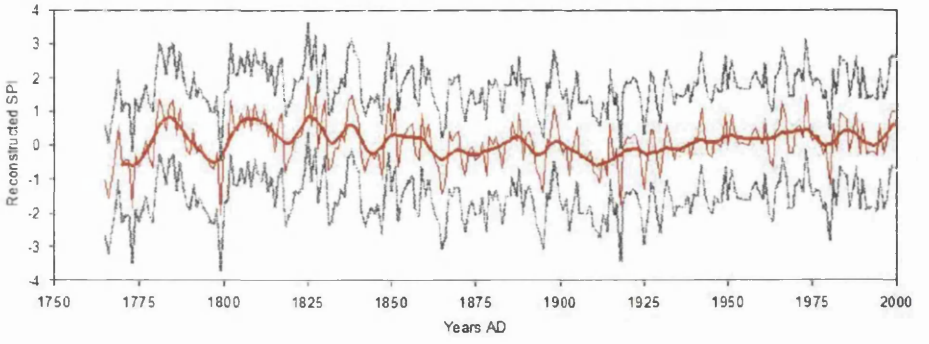

Figure 9.21: Reconstructed Forfjorddalen August SPI from AD 1765 to 2001 using a linear regression model based on $\delta^{18}O(‰)$, using the period from AD 1894 to 1997 for calibration, with an 11-year weighted and centered running mean, error in the reconstruction is represented by the grey dashed line (± 2 standard errors of the prediction).

is weak and so the uncertainly surrounding the reconstructions is high. The northern coastal precipitation record (Hanssen-Bauer and Føland, 1998), which begins in AD 1873 suggests that both of these reconstructions overestimate precipitation from AD 1873 to 1900, and especially the reconstruction based on $\delta^{18}O$ and $\delta^{13}C_{pin}$. Over most of the rest of the period the two reconstructions agree strongly.

When more $\delta^{18}O$ data are available it will be possible to compare this to the temperature reconstruction and establish a fuller picture of the climate at Forfjorddalen. An example of such a comparison can be seen in Figure 9.24, where the preliminary SPI reconstruction (based on $\delta^{18}O$) is plotted against the temperature reconstruction, with the SPI axis inverted. As has already been seen, temperature and precipitation (SPI) are reasonably well negatively correlated at this location, however towards the end of the nineteenth century there is a strong divergence between the two reconstructions. Although neither reconstruction is especially accurate for this period, the comparsion does suggest an unusual combination of cold and dry conditions. Such conditions may be the result of persistent blocking high pressure systems during this period. When a longer reconstruction of precipitation is available using $\delta^{18}O$ it should be possible to identify such unusual climatic conditions. Importantly it will also be useful in resolving whether

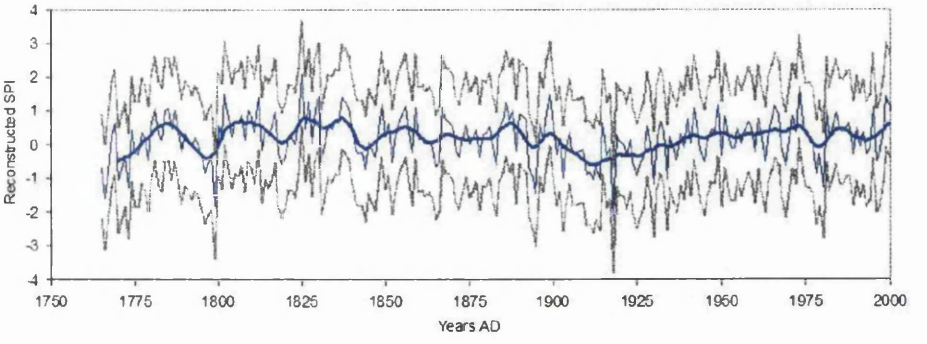

Figure 9.22: Reconstructed Forfjorddalen August SPI from AD 1765 to 2001 using a multiple regression model based on δ^{18}O(‰) and $\delta^{13}C_{pin}$(‰) , using the period from AD 1894 to 1997 for calibration, with an 11-year weighted and centered running mean, error in the reconstruction is represented by the grey dashed line ($\pm$2 standard errors of the prediction).

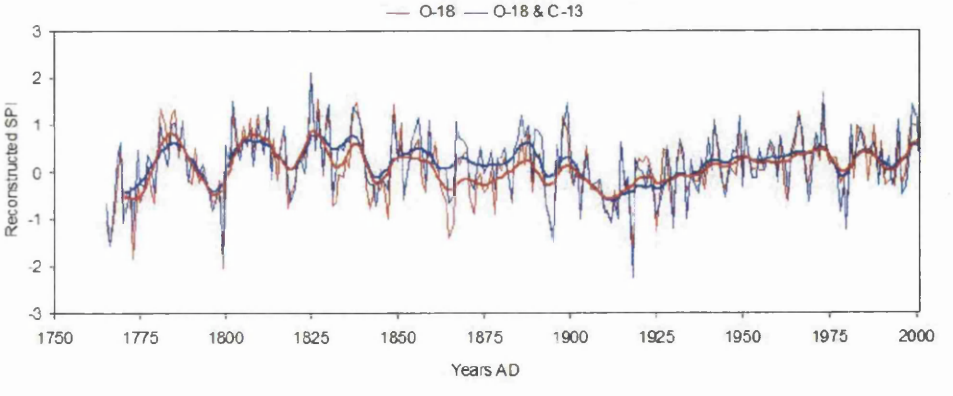

Figure 9.23: Comparison of the two SPI reconstructions from AD 1765 to 2001, based on δ^{18}O(‰) (Figure 9.21) and δ^{18}O(‰) and $\delta^{13}C_{pin}$(‰) (Figure 9.22).

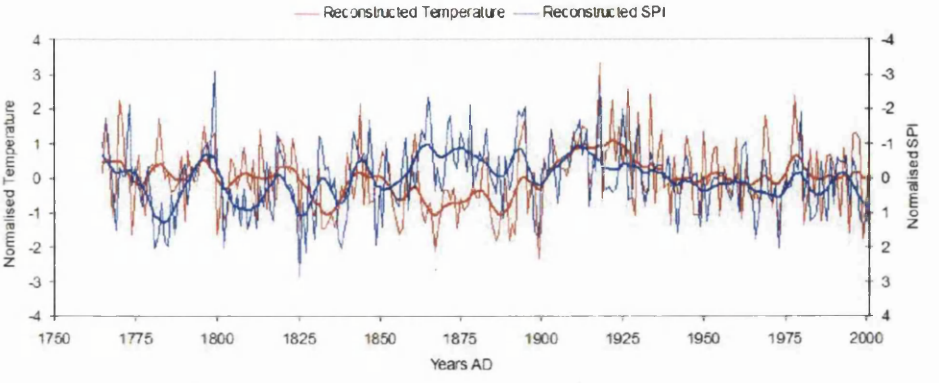

Figure 9.24: A comparison of reconstructed temperature and SPI from AD 1765 to 2001, both data sets have been normalised and the SPI (left hand) axis has been inverted (wetter towards the bottom)

anomalously high δ^{13}C values are the result of dry rather than warm conditions, such as the period centered around AD 1625 (Figure 9.15).

9.6 Regional Potential for Climate Reconstruction

It has already been established that the $\delta^{13}C_{pin}$ from Forfjorddalen correlates to some degree with the climate record from Tornedalen (Klingbjer and Moberg, 2003), 450 km distant, and bears visual comparison with the even more distant Uppsala record (Moberg and Bergström, 1997), around 1000 km distant. To further develop the regional potential of the isotope records from Forfjorddalen, spatial field correlations between the isotope data and meteorological data were made using the *Royal Netherlands Meteorological Institute* (KNMI) online *Climate Explorer* software (KNMI, 2008).

9.6.1 Temperature

The temperature reconstruction based on $\delta^{13}C_{pin}$ over the calibration period (AD 1927 to 2001) is compared to the Climatic Research Unit (CRU) gridded temperature data set

CRU (2008) using the KNMI software (KNMI, 2008) in Figure 9.25, with the locations of Forfjorddalen, Tornedalen and Uppsala shown. This shows an area of correlation in excess of $r = 0.70$ for a coastal area in the vicinity of Forfjorddalen and a rather larger area with a correlation in excess of $r = 0.60$. Tornedalen lies within an area of $r = 0.50$, which confirms the findings of the calibration exercise with Tornedalen record. Uppsala falls outside the region of significant correlations with Forfjorddalen ($p<0.01$). Based on the correlation contours in Figure 9.25, it would seen reasonable to expect the Forfjorddalen $\delta^{13}C_{pin}$ data to reconstruct temperature for a reasonably large area of the Atlantic Ocean. Unfortunately accurate sea surface temperature data are not available with which to check this supposition. However if the gridded area of the reconstruction is extended to include Svalbard (Figure 9.26), it appears that the Forfjorddalen temperature reconstruction correlates to some extent with Svalbard temperatures and by using these contours in conjunction with those in Northern Scandinavia it is possible to extrapolate areas in the Norwegian-Greenland Sea which may correlate with the Forfjorddalen reconstruction at greater than $r = 0.6$ and 0.7 (Figure 9.26). This area of the Norwegian-Greenland Sea off southern Svalbard is one that has been identified a key area of downwelling in the thermohaline circulation system (Schmitz, 1995) and so may be a key area for western European climate.

Reconstructing temperature in northwest Norway is one of the primary aims of this project and should prove of interest to a wider research community. However this research forms part of a larger research agenda (*The Millennium Project*) one of whose aims is to reconstruct temperatures over the past Millennium in Europe. It is hoped that by using various reconstructions a larger scale picture of European climate can be built up. One other such reconstruction is the tree-ring maximum latewood density reconstruction of Grudd (2008), which has already been compared to this reconstruction in Figure 9.19. A spatial correlation field using this reconstruction for April to August temperature can be seen in Figure 9.27, this correlates well with spring and summer temperatures over a large area northern and central Scandinavia.

By taking a simple mean of the normalised Forfjorddalen and Torneträsk reconstructions,

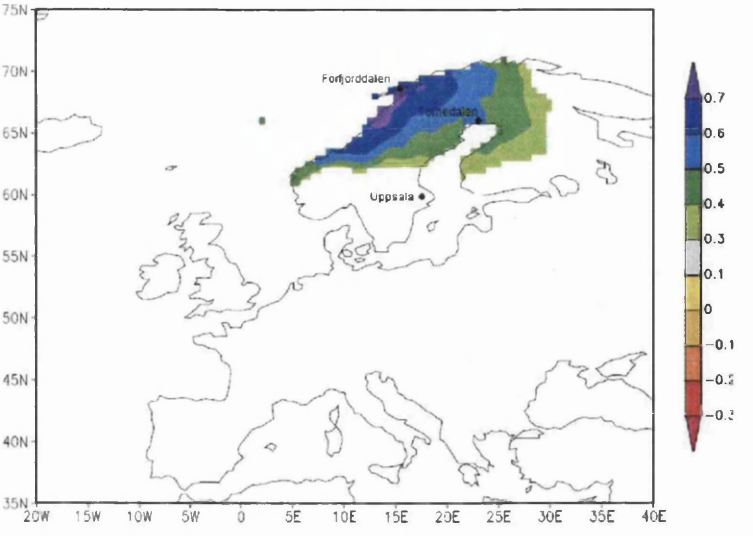

Figure 9.25: Spatial field correlation (KNMI, 2008) between reconstructed July and August Forfjorddalen temperature (based on $\delta^{13}C_{pin}(‰)$) and CRU (Climatic Research Unit) gridded July and August temperature CRU (2008) from AD 1927 to 2001. Only correlations with a significance of $p<0.01$ are shown.

the spatial field reconstruction in Figure 9.28 can be produced. This increases the area of correlation in excess of $r = 0.70$ to include most of northern and central Norway and much of northern Sweden. As the Forfjorddalen reconstruction is of July and August and the Torneträsk of April to August temperature, this method of combination is not ideal. However, it does highlight the great potential for regional climatic reconstructions from a small number of prudently chosen locations. As the Forfjorddalen and Torneträsk reconstruction appear to be in general agreement back to AD 1650, it would seem reasonable to expect that a combination of these two could successfully reconstruct climate over this region (Figure 9.28) to this date. Prior to this some work is required to resolve the differences in multi-decadal variability.

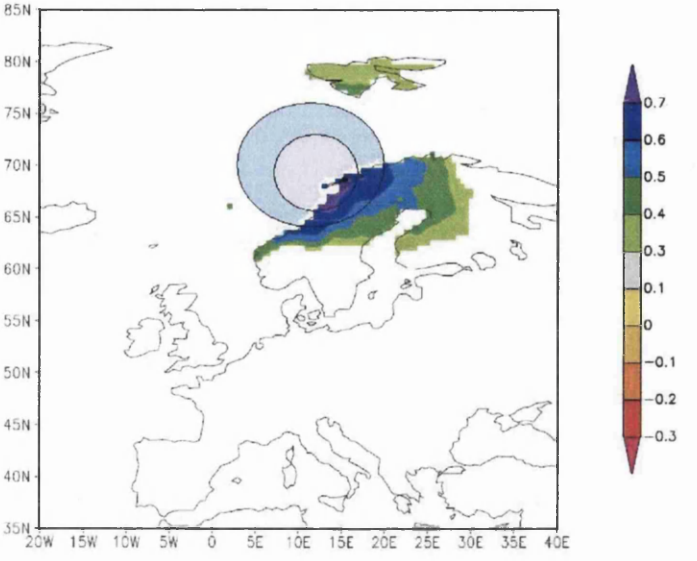

Figure 9.26: Spatial field correlation (KNMI, 2008) between reconstructed July and August Forfjorddalen temperature (based on $\delta^{13}C_{pin}(‰)$) and CRU (Climatic Research Unit) gridded July and August temperature CRU (2008) from AD 1927 to 2001. With an extrapolated area for temperature reconstruction in the Norwegian-Greenland Sea.

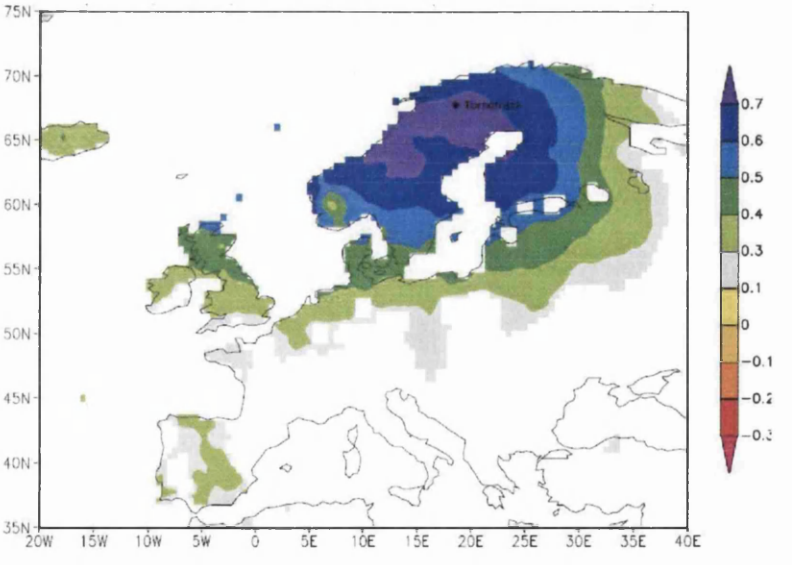

Figure 9.27: Spatial field correlation (KNMI, 2008) between reconstructed April to August Torneträsk temperature (based on maximum latewood density) (Grudd, 2008) and CRU (Climatic Research Unit) gridded July and August temperature (CRU, 2008) from AD 1900 to 2001.

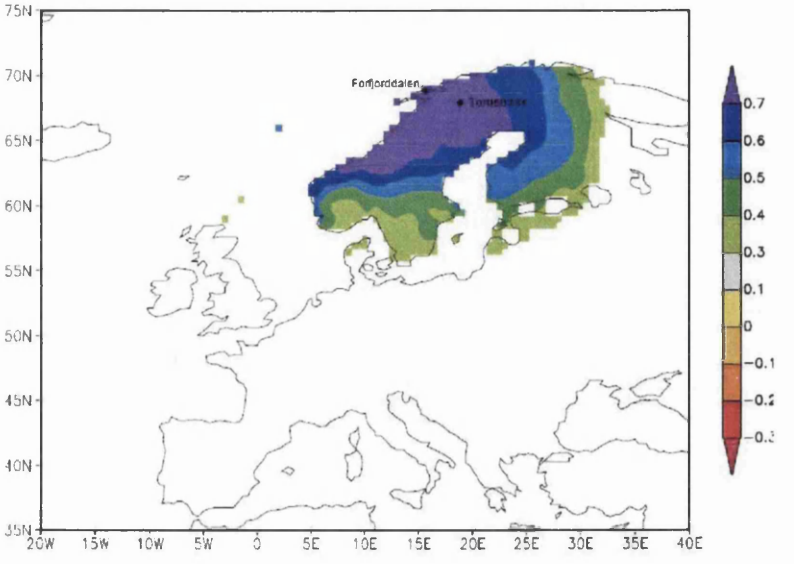

Figure 9.28: Spatial field correlation (KNMI, 2008) between a mean of the normalised Forfjorddalen and Torneträsk temperatures and CRU (Climatic Research Unit) gridded summer (June to August) temperature (CRU, 2008) from AD 1927 to 2001.

9.6.2 Precipitation

The precipitation reconstructions (SPI) (Figures 9.21 and 9.22) were compared to regional climate in the same manner as the temperature reconstructions using the KNMI software (KNMI, 2008) and the CRU gridded precipitation data (CRU, 2008). The results of these spatial correlations can be seen in Figure 9.30 (SPI reconstruction based on δ^{18}O) and Figure 9.30 (SPI reconstruction based on δ^{18}O and $\delta^{13}C_{pin}$). As would be expected, the correlations are lower than for the temperature reconstruction but small areas of northwest Scandinavia correlate at greater than $r = 0.6$ and a large maritime region of northern Scandinavia correlates at greater than $r = 0.50$. These data may confirm the finding of the calibration of δ^{18}O with precipitation data, which suggested that the δ^{18}O was best reflected in the regional coastal precipitation data assembled by Hanssen-Bauer and Føland (1998). It is interesting to note than in both Figures 9.29 and 9.30 the highest areas of correlation are not centered on the research site, this may either be a further indication of a more regionalised signal in the data or that the CRU gridded precipitation

data set CRU (2008) is not especially accurate for this region. The inclusion of Svalbard in the correlation field allows, once again, for an area of correlation (this time greater than $r = 0.50$) to be extrapolated into the Norwegian-Greenland Sea.

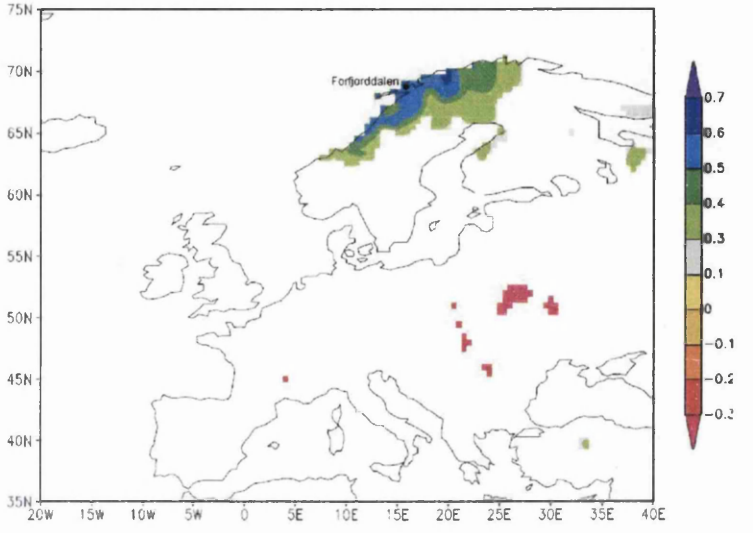

Figure 9.29: Spatial field correlation (KNMI, 2008) between SPI reconstruction based on $\delta^{18}O$ and CRU (Climatic Research Unit) gridded July and August temperature (CRU, 2008) from AD 1910 to 2001.

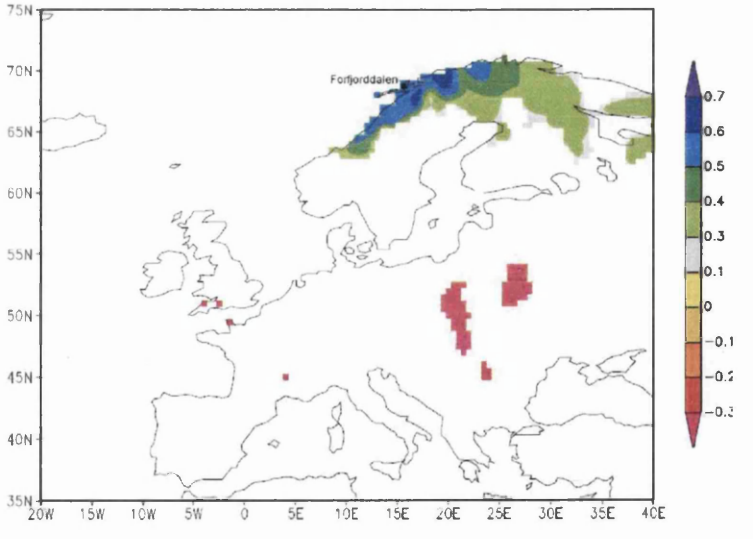

Figure 9.30: Spatial field correlation (KNMI, 2008) between SPI reconstruction based on $\delta^{18}O$ and $\delta^{13}C_{pin}$ and the CRU (Climatic Research Unit) gridded July and August temperature (CRU, 2008) from AD 1910 to 2001.

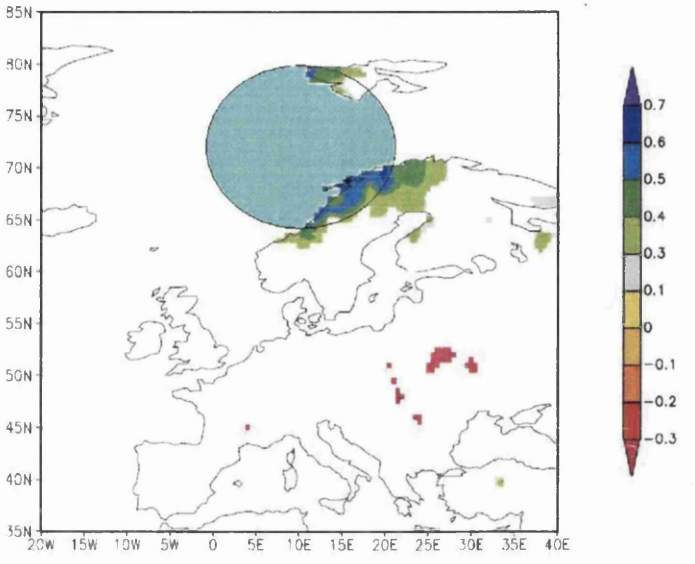

Figure 9.31: Spatial field correlation (KNMI, 2008) between SPI reconstruction based on δ^{18}O and CRU (Climatic Research Unit) gridded July and August temperature (CRU, 2008) from AD 1910 to 2001. With an extrapolated area of correlation, greater than r = 0.50 in the Norwegian-Greenland sea.

9.7 Conclusion

A temperature reconstruction in excess of 600 years (AD 1394 to 2001) has been constructed 9.15 using $\delta^{13}C_{pin}$ results from tree-ring latewood cellulose, calibrated against the local Andenes climate record for July and August. This reconstruction appears to be robust when compared to the long regional climate records from Scandinavia (Figures 9.18). It also compares well with the recent maximum latewood density reconstruction from Torneträsk (Grudd, 2008) back to around AD 1650, prior to this there is a divergence in the multi-decadal signal, although much of the higher frequency variability would appear to remain similar (Figure 9.19). When compared to the published tree-ring based temperature reconstruction from Forfjorddalen (Kirchhefer, 2001), the $\delta^{13}C_{pin}$ exhibits much more multi-decadal variability, while the tree-ring reconstruction remains essentially

a flat line (Figure 9.20). This would appear to demonstrate one of the potential pitfalls of longer time-scale climate reconstruction based on tree-ring widths alone, where the longer timescale variability is removed with the growth trend (Cook et al., 1995).

This temperature reconstruction suggests that in this area the summer temperatures of the late twentieth century are not anomalously warm when compared to that of the last six centuries (Figure 9.16), with a warmer period during the mid-eighteenth (confirmed by the Uppsala instrumental record (Moberg and Bergström, 1997) and the temperature reconstruction of Grudd (2008). The warmest period of the past 600 years appears to have been centered around AD 1625, and while this does not appear as a warm period in the records of Grudd (2008), Gagen et al. (2007) and Lindholm and Eronen (2000) have identified warm periods in the mid-seventeenth century. The coldest parts of the reconstruction in Figure 9.15 appear to be the late nineteenth century and at the beginning of the record in the early fifteenth century.

A tentative reconstruction of precipitation from AD 1765 to 2001 was also presented in the form of SPI, using a multiple regression model based on $\delta^{18}O$ and $\delta^{13}C_{pin}$ (Figure 9.22) and one based on $\delta^{18}O$ alone (Figure 9.21). Both reconstructions show a similar trend in precipitation since the middle of the eighteenth century, with wet periods surrounding a dryer late nineteenth century, although this is the period where both the $\delta^{18}O$ and $\delta^{13}C_{pin}$ records are suspect, with low between-tree correlation. Indeed, both these precipitation reconstructions appear to overestimate precipitation between AD 1873 to 1900. When a fuller precipitation reconstruction in made it should be possible to compare this with the temperature reconstruction (Figure 9.24) to identify periods with unusual climatic conditions (cold/dry and warm/wet), which may affect the $\delta^{13}C$ signal. It should also help in determining whether periods of positive $\delta^{13}C_{pin}$ values (such as the event centered around AD 1625) are a result of unusually dry (rather than unusually warm) conditions.

The spatial field correlations (Figures 9.25, 9.29 and 9.30) suggest that the temperature, and to a lesser extent, the precipitation reconstructions from Forfjorddalen have the potential to reconstruct climate at a more regional scale. When the temperature reconstruction is combined with the Torneträsk density reconstruction (Figure 9.28) the

area of correlation in excess of $r = 0.70$ extends over large areas of northern Scandinavia and demonstrates the possibility of a fully regional climate construction for Europe, using a relatively small network of well chosen sites.

10

Conclusion

10.1 Aims

This research has sought to determine whether climate at Forfjorddalen can successfully reconstructed using the stable isotopes of carbon and oxygen from tree-rings, and whether these isotopes contain additional palaeoclimatic information to that available from the existing tree-ring width series

10.2 Methodology

The reconstruction was made using the annually dated tree-rings of Scots pine (*Pinus sylvestris* L.). From the annual rings the latewood was cut and extracted to α-cellulose. Samples of this were weighed and the $\delta^{13}C$ and $\delta^{18}O$ values were measured using a mass spectrometer, with a mean of between four and seven trees being used to define each years value. In Chapter 4 the values of $\delta^{13}C$ were corrected for both the increase in light ^{12}C in the atmosphere, due to the increase combustion of fossil fuels since AD 1850, and for the increased amount of atmospheric of CO_2 to produce a $\delta^{13}C_{pin}$ value, which was then used for climate calibration and reconstruction.

10.3 Calibration with Climate

$\delta^{13}C_{pin}$ was calibrated against Andenes temperature from AD 1927 to 2001. The Andenes temperature record actually stretches back to AD 1869, however due to a very low inter-correlation between $\delta^{13}C_{pin}$ values this earlier period was not used for calibration. The correlation between $\delta^{13}C_{pin}$ and temperature over the calibration period was $r = 0.71$, explaining just over half the variability. The calibration was tested using a split data set method and verified using reduction of error (RE) and coefficient of efficiency (CE) statistics. $\delta^{13}C_{pin}$ also correlates with precipitation, much of which appears to be as a result of the co-variability of temperature and precipitation at this location, however, even at this wet location precipitation appears to be important when it falls below around a mean of 50mm for July and August, with the most positive $\delta^{13}C_{pin}$ values occurring only in very dry years, such as AD 1918. A calibration was also made with the longer, and more distant (450 km) Tornedalen temperature record (Klingbjer and Moberg, 2003), stretching from beginning in AD 1802. Although with lower correlation values, a successful calibration was undertaken, which importantly demonstrated that the $\delta^{13}C_{pin}$ record from Forfjorddalen was able to reconstruct temperatures prior to AD 1880, the period of low inter-tree correlation. When the problem period from AD 1800 to 1927 was removed and the early, less accurate, part of the Tornedalen record the two remaining periods were able to reconstruct each others temperatures successfully, despite a difference in mean temperature of nearly 1°C. This suggest that a reconstruction based on $\delta^{13}C_{pin}$ has potential for reconstruction lower frequency (multi-decadal) climatic variability.

There is no need for any correction of $\delta^{18}O$ values and calibration of these results was made using a regional precipitation data (Hanssen-Bauer and Føland, 1998) stretching from AD 1873 to 1997, and this data set converted to the Standardised Precipitation Index (SPI) (McKee et al., 1993). As with the $\delta^{13}C_{pin}$ data set the between tree correlation was very low for the period from AD 1873 (when the precipitation record starts) and AD 1896 and so the calibration was undertaken from AD 1896 to 1997. The correction

between SPI and $\delta^{18}O$ over this period is $r = 0.57$. A split data set and RE and CE statistics were again used to verify the calibration. The result of which was that $\delta^{18}O$ was able to successfully reconstruct precipitation and SPI, although this prediction was less good at predicting the larger magnitude precipitation events during the second half of the twentieth century.

10.4 Multiproxy

Various multiple regression models were attempted using a combination of $\delta^{13}C_{pin}$ and $\delta^{18}O$ and ring-widths to determine whether Multiproxy reconstructions could improve upon those using $\delta^{13}C_{pin}$ (temperature) and $\delta^{18}O$ (precipitation), with mixed results. A combination of $\delta^{13}C_{pin}$ and the ring-width residual chronology generally produced the highest correlation with temperature, but the RE and CE verification statistics were consistently better when using $\delta^{13}C_{pin}$. Based on this it was concluded that a temperature reconstruction based upon $\delta^{13}C_{pin}$ should prove be the most reliable. A multiple regression model based on $\delta^{18}O$ and $\delta^{13}C_{pin}$ produced the best overall correlation and RE and CE statistics for precipitation and SPI. However, a reconstruction based on $\delta^{18}O$ was almost as robust and it may prove prudent to use this reconstruction when attempting to determine whether high values in $\delta^{13}C_{pin}$ are as a result of high temperature rather than dry conditions, as it would be independent of $\delta^{13}C_{pin}$.

10.5 Conceptual Model

A conceptual model was presented in Chapter 7 to explain the the relationship between $\delta^{13}C$ and temperature and precipitation. It was suggested that under *normal* climatic condition at Forfjorddalen there is a negative correlation between temperature and precipitation. Under these conditions both temperature and precipitation act in the same direction on $\delta^{13}C$ (warm and dry both produce more positive $\delta^{13}C$, while cool and wet lead to more negative $\delta^{13}C$). It was argued that under *abnormal* conditions (warm/wet

and cool/dry) temperature and precipitation will act in opposite direction on $\delta^{13}C$ and lead to a confused signal. This should be especially important in cool/dry conditions, as precipitation is more important in determining $\delta^{13}C$ values when it is in short supply. It is argued that these (cool/dry) conditions generally prevailed in northwest Norway towards the end of the nineteenth and into the early years of the twentieth century, and this is generally supported by the available meteorological evidence. These conditions led to a hiatus in the $\delta^{13}C$ record, which produced a low between-tree correlation and an unreliable temperature reconstruction. Various suggestions of how such periods can be identified where no instrumental climate record is available, perhaps the most reliable being a low between-tree correlation. It was also suggested that using $\delta^{18}O$ as an independent estimator of precipitation should help in identifying such climatic anomalies.

10.6 Precipitation Reconstruction

A tentative reconstruction of summer (July to August) precipitation (SPI) was made from AD 1765 to 2001 using $\delta^{18}O$ and a multiple regression model using $\delta^{18}O$ and $\delta^{13}C_{pin}$, these suggests that wet conditions prevailed at Forfjorddalen during the late eighteenth and early nineteenth centuries and also during the second half of the twentieth century, with a dry period during the late nineteenth and early twentieth centuries. Instrumental data suggests that both these reconstructions overestimate precipitation during this dry period (especially the multiple regression model) and fail to capture the magnitude of the extreme precipitation events during the second half of the twentieth century. The $\delta^{18}O$ record is still however, incomplete. When all the $\delta^{18}O$ data are available it should be possible to make a full precipitation reconstruction from AD 1394 to 2001 which should help with interpretation of the $\delta^{13}C_{pin}$ temperature reconstruction, as well as being of interest in itself in helping to develop a fuller picture of climatic change in northern Fennoscandia.

10.7 Temperature Reconstruction

A temperature reconstruction using $\delta^{13}C_{pin}$ was made from AD 1394 to 2001 (Figure 10.1). This shows a significant amount of multi-decadal variability which was not present in the previous tree-ring width-based temperature reconstruction (Kirchhefer, 2001). This reconstruction has periods warmer than the late twentieth century in the mid-eighteenth and mid-seventeenth centuries, with cold periods in the early fifteenth and nineteenth centuries. Comparison with the long temperature record from Uppsala, initiated in AD 1722 (1000 km distant), suggest that the Forfjorddalen reconstruction may be robust until the early eighteenth century (apart from the period from around AD 1880 to 1925). A recent tree-ring density based temperature reconstruction from Torneträsk in north-western Sweden (Grudd, 2008) was also compared to the Forfjorddalen $\delta^{13}C_{pin}$ reconstruction, these appear to be in general agreement back to around AD 1650 from which point they diverge. The evidence from Uppsala and Torneträsk would seem to suggest that the summer warmth in this reconstruction is real, although the warmest period in the Forfjorddalen reconstruction centered around AD 1625 does not appear in the Torneträsk reconstruction of Grudd (2008). There is however evidence of warmth in the mid-seventeenth century in other tree-ring based reconstructions (Lindholm and Eronen, 2000; Gagen et al., 2007), although not entirely synchronous with the warmth in the Forfjorddalen reconstruction. The temperature reconstruction from Forfjorddalen suggests that late-twentieth century summer temperatures, in this area, are not unusually warm compared to those of the past 600 years.

10.8 Regional Climate Signal

Finally the potential of the Forfjorddalen isotope record for reconstructing more regional climate was explored. Spatial field correlation were made using the Forfjorddalen temperature and precipitation (SPI) reconstructions using the KNMI software (KNMI, 2008)

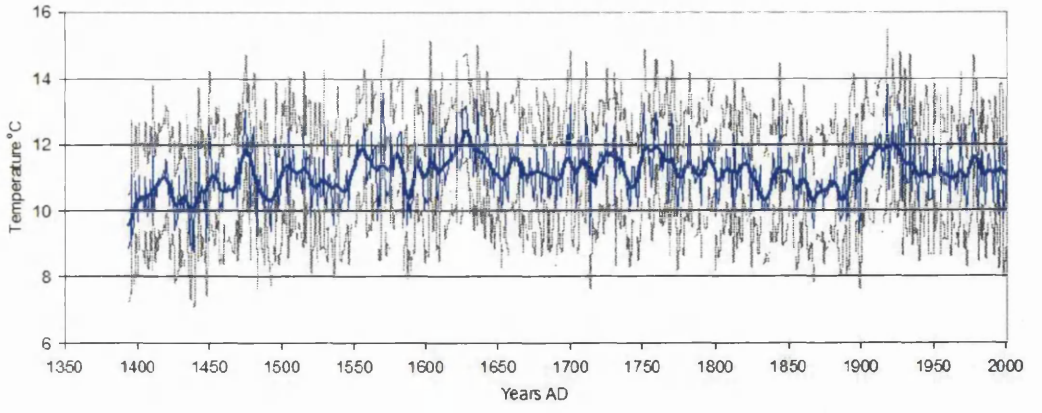

Figure 10.1: Reconstructed Forfjorddalen mean July and August temperature from AD 1394 to 2001 (blue line) using a linear regression model based on $\delta^{13}C_{pin}(‰)$, using the period from AD 1927 to 2001 for calibration, with an 11 year weighted and centered running mean (bold blue line), error in the reconstruction is represented by the grey dashed line (± 2 standard errors of the prediction).

and the CRU gridded temperature and precipitation data sets (CRU, 2008). The temperature reconstruction from Forfjorddalen correlated at greater than $r = 0.70$ with a small coastal area in the vicinity of Forfjorddalen and at greater than $r = 0.60$ with a large area of northwestern Scandinavia. Correlations with data from Svalbard suggest that it may also reconstruct a large and climatically key area of the Norwegian-Greenland Sea at greater than $r = 0.60$. When combined with the density based reconstruction from Torneträsk the resulting data set correlated with much of northern and western Scandinavia at greater than $r = 0.70$. As these two reconstructions are in general agreement back to AD 1650 a reconstruction using a combination of the two data sets should prove robust. Prior to this date work needs to be undertaken to homogenize these two series. This does demonstrate the potential for reconstructing much of European climate to this degree using a relatively small number of prudently chosen sites.

10.9 Further Research Potential

While this research has highlighted the great potential of stable isotopes from tree-rings to reconstruct both inter-annual and, perhaps more importantly, multi-decadal climatic variability there is still much work that needs to be undertaken that arises from this thesis. To engage further with the debate on natural climatic variability over the past 2000 years the isotope series (both $\delta^{13}C_{pin}$ and $\delta^{18}O$) at Forfjorddalen needs to be extended back as far as possible (based on data available at present AD 900 would seem a real possibility). Issues surrounding the departures in low frequency variability between the Forfjorddalen and Torneträsk reconstructions need to be resolved so that full regional climatic reconstructions can be made over the past millennium. The period of low correlation at the end of the nineteenth century needs to be more fully understood and the models presented in Chapter 7 further developed and applied to other locations which may be subject to such anomalies.

10.10 Conclusion

This thesis has demonstrated that stable isotopes from tree-rings ($\delta^{13}C_{pin}$ and $\delta^{18}O$), from this area of northern Fennoscandia, can successfully reconstruct summer temperatures and to a lesser degree precipitation. The available evidence suggests that they are able to capture not only the inter-annual climatic variability but also the more elusive multi-decadal variability, which is key to understating natural climatic variability and therefore to accurately predict future climate. It has also been shown how it may be possible to build a potentially European scale climatic reconstruction using climate proxies from a relatively small number of well chosen locations.

Bibliography

Alley, R. (2000). *The two-mile time machine: ice cores, abrupt climate change and our future* . Princeton University Press, Princeton.

Alley, R. (2003). Palaeoclimatic insights into future climate changes . *Phil. Trans. R. Soc. Lond. A*, 361:1831–1849.

Alley, R. and Agustsdottir, A. (2005). The 8k event: cause and consequences of a major Holocene abrupt climate change. *Quaternary Science Reviews*, 24:1123–1149.

Alley, R., Marotzke, J., Nordhaus, W., Overpeck, J., Peteet, D., Pielke, R., Pierrehumbert, R., Rhines, P., Stocker, T., Talley, L., and Wallace, J. (2003). Abrupt Climate Change . *Science*, 299:2005–2010.

Alley, R., Mayewski, P., Sowers, T., Stuiver, M., Taylor, K., and Clark, P. (1997). Holocene climatic instability: a prominent, widespread event 8200 yr ago . *Geology*, 25:483–486.

Ammann, W. and Germann, P. (1996). Treeline fluctuations recorded or 12,500 years by soil profiles, pollen and plant macrofossils in the central Swiss Alps . *Arctic, Antarctic, and Alpine Research*, 28:131–147.

Anderson, W., Bernasconi, S., and McKenzie, J. (1998). Oxygen and Carbon isotope record of climatic variability in tree ring cellulose (*Picea abies*): and example from central Switzerland (1913-1995). *Journal of Geophysical Research*, 103:31625–31636.

Anderson, W., Bernasconi, S., McKenzie, J., Saurer, M., and Schweingruber, F. (2002). Model evaluation for reconstrcting the oxygen isotopic composition in precipitation from tree ring cellulose over the last century . *Chemical Geology*, 182:121–137.

Baillie, M. (1995). *A slice through time: dendrochronology and precision dating*. Routledge, London.

Baillie, M. and Brown, D. (2003). Dendrochronlogy and the reconstruction of fine-resolution environmental change in the Holocene. In MacKay, A., Battarbee, R., Birks, J., and Oldfield, F., editors, *Global Change in the Holocene*, pages 75–91. Hodder, London.

Baillie, M. and Pilcher, J. (1973). A simple cross-dating program for tree-ring research. *Tree Ring Bulletin*, 33:7–14.

Barbour, M., Andrews, T., and Farquhar, G. (2001). Correlations between oxygen isotope ratios of wood constituents of Quercus and Pinus samples from around the world . *Australian Journal of Plant Physiology*, 28:335–348.

Barbour, M. and Farquhar, G. (2000). Relative humidity- and AB-induced variation in carbon and oxygen isotope ratios of cotton leaves . *Plant, Cell and Environment*, 23:473–485.

Barbour, M., Walcroft, A., and Farquhar, G. (2002). Seasonal variations in $\delta^{13}C$ and $\delta^{18}O$ of cellulose from growth rings of Pinus radiata . *Plant, Cell and Environment*, 25:1483–1499.

Battarbee, R. (2000). Palaeolimnological approches to climate change, with special regard to the biological record . *Quaternary Science Reviews*, 19:107–124.

Bell, M. and Walker, M. (1992). *Late Quaternary Enviromnetal Change: Physical and Human Perspectives*. Longman, London.

Biondi, F. and Waikul, K. (2004). DENDROCLIM2002: A C++ program for statistical calibration of climate signals in tree-ring chronologies . *Computers and Geosciences*, 30:303–311.

Bond, G., Broecker, W., Johnsen, S., McManus, J., Labeyrie, L. D., Jouzel, J., and Bonani, G. (1993). Correlations between climate records from North Atlantic sediments and Greenland ice . *Nature*, 365:143–147.

Bond, G., Kromer, B., Beer, J., Muscheler, R., Evans, M., Showers, W., Hoffmann, S., Lotti-Bond, R., Hajdas, I., and Bonani, G. (2001). Persistant solar influence on North Atlantic climate during the Holocene . *Science*, 294:2130–2135.

Borella, S., Leuenberger, M., and Saurer, M. (1999). Reducing uncertanties in $\delta^{18}O$ in tree rings: wood -cellulose comparison and method depedent sensitivity. *Journal of Geophysical Research*, 104:19267–19273.

Borella, S., Ménot, G., and Leuenberger, M. (2004). Sample Homogeneity and Cellulose Extraction from Plant Tissue for Stable Isotope Analyses. In de Groot, P., editor, *Handbook of Stable Isotopes Analytical Techniques*, volume 1, pages 507–522.

Bradley, R. (2000a). 1000 years of climate change . *Science*, 288:1353–1354.

Bradley, R. (2000b). Past global changes and their significance for the future . *Quaternary Science Reviews*, 19:391–402.

Bradley, R. (2001). Many citations support global warming . *Science*, 292:2011.

Bradley, R., Briffa, K., Cole, J., Hughes, M., and Osborn, T. (2003a). The climate of the last millennium . In Alverson, K., Bradley, R., and Pedersen, T., editors, *Paleoclimate, Global Change and the Future*, Global Change - The IGBP series (PAGES), pages 105–141. Springer, Berlin.

Bradley, R., Hughes, K., and Diaz, H. (2003b). Climate in Medieval time . *Science*, 302:404–405.

Bradley, R. and Jones, P. (1992a). *Climate Since A.D. 1500* . Routledge, London.

Bradley, R. and Jones, P. (1992b). Climatic variations over the last 500 years . In Bradley, R. and Jones, P., editors, *Climate since AD 1500*, pages 649–665. Routledge, London.

Brendel, O., Iannetta, P., and Stewart, D. (2000). A rapid and simple method to isolate pure alpha-cellulose. *Phytochemical Analysis*, 11:7–10.

Briffa, K. (2000). Annual climate variability in the Holocene: interpreting the message of ancient trees . *Quaternary Science Reviews*, 19:87–105.

Briffa, K. (2003). bristlecone pine . In Matthews, J., Bridges, E., Caseldine, C., Luckman, A., Owen, G., Perry, A., Shakesby, R., Walsh, R., Whittaker, R., and Willis, K., editors, *The Encyclopaedic Dictionary of Environmental Change*, page 690. Arnold, London.

Briffa, K. and Jones, P. (1989). Basic chronology statistics and assessment . In Cook, E. and Kairiukstis, L., editors, *Methods of dendrochronology : applications in the environmental sciences*, pages 137–152. Kluwer Academic Publishers, Dordrecht.

Briffa, K., Jones, P., Bartholin, T., Eckstein, D., Schweingruber, F., Karlén, W., Zetterberg, P., and Eronen, M. (1992). Fennoscandian summers from AD 500: temperature changes on short and long timescales . *Climate Dynamics*, 7:111–119.

Briffa, K., Jones, P., and Schweingruber, F. (1988). Summer temperature patterns over Europe: a reconstruction from 1750 A.D. based on maximum latewood density idicies of conifers. *Quaternary Research*, 30:36–52.

Briffa, K. and Osborn, T. (2002). Blowing hot and cold . *Science*, 295:2227–2228.

Briffa, K., Osborn, T., Schweingruber, F., Harris, I., Jones, P., Shiyatov, S., and Vaganov, E. (2001). Low-frequency temperature variations from a northern tree ring density network . *Journal of Geophysical Research*, 106:2929–2941.

Briffa, K., Osborn, T., Schweingruber, F., Jones, P., Shiyatov, S., and Vaganov, E. (2002a). Tree-ring width and density data around the Northern Hemisphere: Part 1, local and regional climate signals . *The Holocene*, 12(6):737–758.

Briffa, K., Osborn, T., Schweingruber, F., Jones, P., Shiyatov, S., and Vaganov, E. (2002b). Tree-ring width and density data around the Northern Hemisphere: Part 2, spatio-temporal variability and associated climate patterns . *The Holocene*, 12(6):759–789.

Broecker, W. (2001). Was the Medieval Warm Period Global . *Science*, 291:1497–1499.

Broecker, W. and Denton, G. (1990). The role of ocean-atmosphere reorganisations in glacial cycles . *Quaternary Science Reviews*, 9:305–341.

Brohan, P., Kennedy, J., Harris, I., Tett, S., and Jones, P. (2006). Uncertainty estimates in regional and global observed temperature changes: A new dataset from 1850. *Journal of Geophysical Research*, 111:D12106, doi:10.1029/2005JD006548.

Busuioc, A., Chen, D., and Hellström, C. (2001). Temporal and spatial variability of precipitation in Sweden and its link with the large-scale atmospheric circulation . *Tellus*, 53A:348–367.

Clark, P., Pisias, N., Stocker, T., and Weaver, A. (2002). The role of the thermohaline circulation in abrupt climate change. *Nature*, 415:863–869.

Clarke, G., Leverington, D., Teller, J., and Dyke, A. (2004). Paleohydraulics of the last outburst flood from glacial LAke Agassiz and the 8200 BP cold event. *Quaternary Science Reviews*, 23:389–407.

Cook, E., Briffa, K., Meko, D., Graybill, A., and Funkhouser, G. (1995). The 'segement length curse' in long tree-ring chronology development for palaeoclimatic studies . *The Holocene*, 5(2):229–237.

Cook, E., D'Arrigo, R., and Briffa, K. (1998). A reconstruction of the North Atlantic Oscillation using tree-ring chronologies from North America and Europe . *The Holocene*, 8(1):9–17.

Cook, E., D'Arrigo, R., and Mann, M. (2002). A well-verified, multiproxy reconstruction of the winter North Atlantic Oscillation index since A.D. 1400 . *Journal of Climate*, 15:1754–1764.

Cook, E., Esper, J., and D'Arrigo, R. (2004a). Extra-tropical Northern Hemisphere land temperature variability over the past 1000 years . *Quaternary Science Reviews*, 23:2063–2074.

Cook, E., Meko, D., Stahle, D., and Cleaveland, M. (1999). Drought reconstructions for the continental United States. *Journal of Climate*, 12:1145–1162.

Cook, E., Woodhouse, C., Eakin, C., Meko, D., and Stahle, D. (2004b). Long-term aridity changes in the western United States. *Science*, 306:1015–1018.

Coplen, T. (1995). Discontinuance of SMOW and PDB . *Nature*, 373:285.

Craig, H. (1954). Carbon-13 variations in Sequoia rings and the atmosphere . *Science*, 119:141–143.

Crowley, T. (2000). Causes of climate change over the past 1000 years . *Science*, 289:270–277.

Crowley, T. and Lowery, T. (2000). How warm was the Medieval Warm Period? . *Ambio*, 29(1):51–54.

CRU (2008). *Gridded temperature and precipitation* . http://www.cru.uea.ac.uk/.

Cullen, H., D'Arrigo, R., Cook, E., and Mann, M. (2001). Mutiproxy reconstructions of the North Atlantic oscillation . *Palaeoceanography*, 16:27–39.

Dahl, S. and Nesje, A. (1996). A new approach to calculating Holocene winter precipitation by combining glacier equilibrium-line altitudes and pine-tree limits: a case study from Hardangerjøkulen, central southern Norway . *The Holocene*, 6:381–398.

Danis, P., Masson-Delmotte, V., Stievenard, M., Guillemin, M., Daux, V., Naveau, P., and von Grafenstein, U. (2006). Reconstruction of past precipitation δ^{18}O using tree-ring cellulose δ^{13}C and δ^{18}O: A calibration study near Lac d'Annecy, France. *Earth and Planetary Science Letters*, 243:439–448.

Dansgaard, W. (1964). Stable isotopes in precipitaton. *Tellus*, 16:436–468.

Dansgaard, W., Johnsen, S., Clausen, H., Dahl-Jansen, D., Gundestrup, N., Hammer, C., Hvidberg, C., Steffensen, J., Sveinbjörnsdottir, B., Jouzel, J., and Bond, G. (1993). Evidence for general instability of past climates from a 250-kyr ice-core record . *Nature*, 364:218–220.

Darling, W. (2004). Hydrological factors in the interpretation of stable isotope proxy data present and past: a European perspective. *Quaternary Science Reviews*, 23:743–770.

D'Arrigo, R., Cook, E., Jacoby, G., and Briffa, K. (1993). NAO and sea surface temperature signatures in tree-ring records from the North Atlantic sector . *Quaternary Science Reviews*, 12:431–440.

D'Arrigo, R., Wilson, R., and Jacoby, G. (2006). On the long-term context for late twentieth century warming. *Journal of Geophysical Research*, 111(D3):doi:10.1029/2005JD006352.

Douglass, A. (1919). *Climatic Cycles and Tree-Growth, Volume I: a study of the annual rings of trees in relation to climate and solar activity* , volume 1. Carnegie Institution, Washington.

Douglass, A. (1928). *Climatic Cycles and Tree-Growth, Volume II: a study of the annual rings of trees in relation to climate and solar activity* , volume 2. Carnegie Institution, Washington.

Duquesnay, A., Breda, N., Stievenard, M., and Dupouey, J. (1998). Changes in tree ring $\delta^{13}C$ and water use effifciency of beech (*Fagus sylvatica* L.) in north-eastern France during the past century. *Plant, Cell and Environment*, 21:565–572.

Edwards, E. and McKee, T. (1997). *Characteristics of 20th century drought in the United States at multiple time scales*. Paper No. 634, Climatology Report No. 97-2. Colorade State University, Fort Collins, Colorado.

Edwards, T., Graf, W., Trimborn, P., Stichler, W., Lipp, J., and Payer, H. (2000). $\delta^{13}C$ response surface resolves humidity and temperature signals in trees . *Geochimica et Cosmochimica Acta*, 64(2):161–167.

Ehleringer, J. and Cerling, T. (1995). Atmospheric CO_2 and the ratio of intercellular to ambient CO_2 concentrations in plants. *Tree Physiology*, 15:105–111.

Ehleringer, J., Hall, A., and Farquhar, G. (1993). *Stable isotopes and plant carbon-water relations*. Academic Press, New York.

Epstein, S. and Yapp, C. (1976). Climatic implications of the D/H ratio of hydrogen in C-H groups in tree cellulose. *Earth and Planetary Science Letters*, 30:252–261.

Epstein, S., Yapp, C., and Hall, J. (1976). The determination of the D/H ratio of non-exchangeable hydrogen in cellulose extrected from aquatic and land plants . *Earth and Planetary Science Letters*, 30:241–251.

Eronen, M., Zetterberg, P., Briffa, K., Lindholm, M., Meriläinen, J., and Timonen, M. (2002). The supra-long Scots pine tree-ring record for Finnish Lapland: Part 1, chronology construction and initial inferences . *The Holocene*, 12(6).

Esper, J., Cook, E., and Schweingruber, F. (2002). Low-frequency signals in long tree-ring chronologies for reconstructing past temperature variability . *Science*, 295:2250–2253.

Esper, J. and Frank, D. (2004). Climate reconstructions: low-frequency ambition and high-frequency ratification . *Eos*, 85(12):113.

Evans, M. and Schrag, D. (2004). A stable isotope-based sapproach to tropical dendroclimatology. *Geochimica et Cosmochimica Acta*, 68(16):3295–3305.

Farmer, J. and Baxter, M. (1974). Atmospheric carbon dioxide levels as indicated by the stable isotope record in wood . *Nature*, 247:273–275.

Farquhar, G., Ehleringer, J., and Hubick, K. (1989). Carbon isotope discrimination and photosynthesis . *Annual Review of Plant Physiology and Plant Molecular Biology*, 40:503–537.

Farquhar, G., Henry, B., and Styles, J. (1997). A rapid on-line technique for the determination of oxygen isotope composition of nitrogen containing organic compounds and water. *Rapid Communications in Mass Spectrometry*, (11):1554–1560.

Farquhar, G., O'Leary, M., and Berry, J. (1982). On the relationship between carbon isotope discrimination and intercellular carbon dioxide concentration in leaves. *Australian Journal of Plant Physiology*, 9:121–137.

February, E. and Stock, W. (1999). Declining trends in the $^{13}C/^{12}C$ ratio of atmospheric carbon dioxide from tree rings of South African Widdringtonia cedarbergensis. *Quaternary Research*, 52:229–236.

Feng, X. (1998). Long-term c_i/c_a response of trees in western North America to atmospheric CO_2 concentration derived from carbon isotope chronologies. *Oecologia*, 117:19–25.

Feng, X. (1999). Trends in intrinsic water-ues efficiency of natural trees for the past 100-200 years: A respnse to atmospheric CO_2 concentrations. *Geochimica et Cosmochimica Acta*, 63:1891–1903.

Feng, X., Cui, H., Tang, K., and Conkey, L. (1999). Tree-ring δD as an indicator of Asian monsoon intensity . *Quaternary Research*, 51:261–266.

Feng, X. and Epstein, B. (1995a). Carbon isotopes iof trees from arid environmnets and implications for reconstructing atmospheric CO_2 concentrations. *Geochimica et Cosmochimica Acta*, 59:2599–2608.

Feng, X. and Epstein, S. (1994). Climatic implications of an 8000 year hydrogen isotope time series from Bristlecone Pine trees . *Science*, 265:1079–1081.

Feng, X. and Epstein, S. (1995b). Climatic temperature records in δD data from tree rings. *Geochimica et Cosmochimica Acta*, 59:3029–3037.

Folland, C., Karl, T., Christy, J., Clarke, R., Gruza, G., Jouzel, J., Mann, M., Oerlemans, J., Salinger, M., and Wang, S.-W. (2001). Observes climate variability and change . In Houghton, J., Ding, Y., Nouger, M., van der Linden, P., Dai, X., Maskell, K., and Johnson, C., editors, *Climate Change 2001: The Scientific Basis*, pages 99–181. Cambridge Univeristy Press, New York.

Francey, R., Allison, C., Etheidge, D., Trudinger, C., Enting, I., Leuenberger, M., Langenfelds, R., Michel, E., and Steele, L. (1999). A 1000-year high precision record of ^{13}C in atmospheric CO_2. *Tellus*, 51B:170–193.

Frencey, R. and Farquhar, G. (1982). An explanation for the $^{13}C/^{12}C$ variations in tree rings. *Nature*, 297:28–31.

Friedrich, M., Kromer, B., Spurk, M., Hofmamm, J., and Kaiser, K. (1999). Palaeo-environment and rasdicarbon calibration as derived from late glacial/early Holocene tree-ring chronologies. *Quaternary International*, 61:27–39.

Fritts, H. (1965). Tree-ring evidence for climatic changes in western North America. *Monthly Weather Review*, 93(7):421–443.

Fritts, H. (1976). *Tree Rings and Climate* . Academic Press, London.

Fritts, H. (1991). *Reconstructing Large-scale Climatic Patterns from Tree-Ring Data* . University of Arizona Press, London.

Gagen, M., McCarroll, D., and Edouard, J. (2004). Latewood width, maximum density, and stable carbon isotope ratios of pine as climate indicators in a dry subalpine environment, French Alps . *Arctic, Antarctic, and Alpine Research*, 36(2):166–171.

Gagen, M., McCarroll, D., Loader, N., Robertson, I., Jalkanen, R., and Anchukaitis, K. (2007). Exorcising the 'segment length surse': summer temperature reconstruction since AD 1640 using non-detrended stable carbon isotope ratios from pine trees in northern Finland. *The Holocene*, 17(4):435–446.

Grissino-Mayer, H. (2001). Evaluating crossdating accuracy: a manual and tutorial for the computer program COFECHA . *Tree-Ring Research*, 57(2):205–221.

Grove, J. (1988). *The Little Ice Age* . Methuen, London.

Grudd, H. (2008). Torneträsk tree-ring width and density AD 500-2004: A test of climate sensitivity and a new 1500-year reconstruction of north Fennoscandian summers. *Climate Dynamics*, in press.

Grudd, H., Briffa, K., Karlén, W., Bartholin, T., Jones, P., and Kromer, B. (2002). A 7400-year tree-ring chronology in northern Swedish Lapland: natural climatic variability expressed on annual to millennial timescales. *The Holocene*, 12(6):657–666.

Hansen, J., Ruedy, R., Sato, M., Imhoff, M., Lawrence, W., Easterling, D., Pedersen, T., and Karl, T. (2001). A closer look at United States and global surface temperature change. *Journal of Geophysical Research*, 106:23947–23963.

Hanssen-Bauer, I. and Føland, E. (1998). Annual and seasonal precipitation variations in Norway 1896-1997. KLIMA Report 27/98. Norweigian Meteorological Institute, Oslo.

Hanssen-Bauer, I. and Nordli, P. (1998). Annual and seasonal temperature variations in Norway 1876-1997. KLIMA Report 25/98. Norwegian Meteorological Institute, Oslo.

Hayes, M. (2006). Drought Indicies. National Drought Mitigation Centre, http://www.drought.unl.edu/whatis/indices.htm.

Hemming, D., Switsur, V., Waterhouse, J., Heaton, T., and Carter, A. (1998). Climate variation and the stable carbon isotope composition of tree ring cellulose: an intercomparison of *Quercus robur*, *Fagus sylvatica* and *Pinus sylvestris*. *Tellus*, 50B:25–33.

Holmes, R. (1983). Computer-assisted quality control in tree-ring dating and measurement. *Tree Ring Bulletin*, 43:69–78.

Huang, S. (2004). Merging information from different resorces for new insights into climate change in the past and future . *Geophysical Research Letters*, 31(L13205):doi:1029/2004GL019781.

Huang, S., Pollack, H., and Shen, P. (2000). Tempearure trends over the past five centuries reconstructed from borehole temperatures . *Nature*, 403:756–758.

Hughes, M. (2002). Dendrochronology in climatology – the state of the art . *Dendrochronologia*, 20:95–116.

Hughes, M. and Diaz, H. (1994). Was there a 'Medieval Warm Period', and if so, where and when? . *Climatic Change*, 26:109–142.

Hughes, M. and Funkhouser, G. (2003). Frequency-dependant climate signal in upper and lower forset border tree rings in the mountains of The Great Basin. *Climatic Change*, 59:233–244.

Imbrie, J. and Imbrie, K. (1979). *Ice Ages: solving the mystery* . Harvard University Press, London.

IPCC (1990). *Scientific Assessment of Climate change: Report of Working Group I*. Cambridge University Press, Cambridge.

IPCC (1996). *Climate Change 1995: The Science of Climate Change*. Cambridge University Press, Cambridge.

IPCC (2001). *Climate Change 2001: The Scientific Basis. Contributions of Working Group I to the Third Assessment Report of the Intergovernmetal Panel on Climate Change* . Cambridge University Press, Cambridge.

IPCC (2007). *Climate Change 2007: The Physical Science Basis. Contribution of Working Group I to the Fourth Assessment Report of the Intergovernmental Panel on Climate Change*. Cambridge University Press, Cambridge, UK and New York, NY, USA.

Jäggi, M., Saurer, M., Fuhrer, J., and Siegwolf, R. (2002). The relationship between the stable carbon isotope composition of needle bulk material, starch, and tree rings in *Picea abies*. *Oecologia*, 131:325–332.

Jansen, E., Overpeck, J., Briffa, K., Duplessy, J.-C., Joos, F., Masson-Delmotte, V., Olago, D., Otto-Bliesner, B., Peltier, W., Rahmstorf, S., Ramesh, R., Raynaud, D., Rind, D., Solomina, O., Villalba, R., and Zhang, D. (2007). Palaeoclimate. In Solomon, S., Qin, D., Manning, M., Chen, D., Marquis, M., Averyt, K., Tignor, M., and Miller, H., editors,

Climate Change 2007: The Physical Science Basis. Contribution of Working Group I to the Fourth Assessment Report of the Intergovernmental Panel on Climate Change. Cambridge University Press, Cambridge, UK and New York, NY, USA.

Jones, P., Briffa, K., Barnett, T., and Tett, S. (1998). High-resolution palaeoclimatic records for the last millennium: interpretation, integration and comparison with General Circulation Model control-run temperatures . *The Holocene*, 8(4):455–471.

Jones, P. and Mann, M. (2004). Climate over past millennia . *Reviews of Geophysics*, 42:1–42.

Jones, P. and Moberg, A. (2003). Hemispheric and large-scale surface air temperature variations: An extensive revision and update to 2001. *Journal of Climate*, 16:206–223.

Jones, P., New, M., Parker, D., Martin, S., and Rigor, I. (1999). Surface air temperature and its changes over the past 150 years . *Reviews of Geophysics*, 37:173–199.

Jones, P., Osborn, T., and Briffa, K. (2001). The evolution of climate over the last millennium . *Science*, 292:662–667.

Kagawa, A., Sugimoto, A., and Maximov, T. (2006a). $^{13}CO_2$ pulse-labelling of photoassimilates reveals carbon allocation within and between tree rings. *Plant, Cell and Environment*, 29:1571–1584.

Kagawa, A., Sugimoto, A., and Maximov, T. (2006b). Seasonal course of translocation, storage and remobilization of ^{13}C pulse-labeled photoassimilatein naturally growing Larix gmelinii saplings. *New Phytologist*, 171:793–804.

Keeling, C., Mook, W., and Tans, P. (1979). Recent trends in ^{12}C-^{13}C ratio of atmospheric carbon-dioxide. *Nature*, 277:121–123.

Keigwin, L. (1996). The Little Ice Age and Medieval Warm Period in the Sargasso Sea . *Science*, 274:1504–1508.

Keigwin, L. and Pickart, R. (1999). Slope water current over the laurentian fan on interannual to millennial time scales . *Science*, 286:520–523.

Kirchhefer, A. (2001). Reconstruction of summer temperatures from tree-rings of Scots pine (*Pinus sylvestris* L.) in coastal northern Norway . *The Holocene*, 11(1):41–52.

Kirchhefer, A. (2006). Forfjorddalen master chronology. Pers. Comm.

Kitagawa, H. and Matsumoto, E. (1995). Climatic implications of $\delta^{13}C$ variations in a Japanese cedar (Cryptomeria japonica) during the alst two millenia. *Geophysical Research Letters*, 22:2155–2158.

Klingbjer, P. and Moberg, A. (2003). A composite monthly temperature record from Tornedalen in northern Sweden, 1802-2002. *International Journal of Climatology*, 23:1465–1494.

KNMI (2008). *Climate explorer* . http://climexp.knmi.nl/start.cgi?someone@somewhere.

Knutson, D., Buddemeier, R., and Smith, S. (1972). Coral chronometers: seasonal growth bands in reef coral. *Science*, 177:270–272.

Krishnamurthy, R. and Epstein, S. (1985). Tree ring D/H ratio from Kenya, East Afica and its palaeoclimatic significance. *Nature*, 317:160–162.

Krishnamurthy, R. and Machavaram, M. (2000). Is there a stable isotope evidence for CO_2 fertilization effect? *Proceedings of Indian Academy of Sciences*, 109:141–144.

Körner, C. (2003). Carbon limitation in trees . *Journal of Ecology*, 91:4–17.

Körner, C. (2006). Plant CO_2 responses: an issue of definition, time and resourse supply. *New Phytologist*, 172:393–411.

Lamb, H. (1965). The early Medieval warm epoch and its sequel . *Palaeogeography, Palaeoclimatology, Palaeoecology*, 1:13–37.

Lamb, H. (1995). *Climate History and the Modern World* . Routlrdge, London, 2 edition.

Leavitt, S. (1994). Major wet interval in White Mountains medieval warm period experienced in $\delta^{13}C$ of bristlecone pine tree rings . *Climatic Change*, 26:299–307.

Leavitt, S. (2002). Prospects for reconstuction of seasonal environment from tree-ring $\delta^{13}C$: baseline findings from the Great Lakes area, USA . *Chemical Geology*, 192:47–58.

Leavitt, S. and Long, A. (1983). An atmospheric $^{13}C/^{12}C$ reconstruction generated through removal of climate effects from tree-ring $^{13}C/^{12}C$ measurements . *Tellus*, 35B:92–102.

Leavitt, S. and Long, A. (1984). Sampling stratergy for stable carbon isotope analysis of tree rings in pine. *Nature*, 311:145–147.

Leavitt, S. and Long, A. (1985). An atmospheric $^{13}C/^{12}C$ reconstruction generated through removal of climate effects from tree ring $^{13}C/^{12}C$ measurements. *Tellus*, 35B:92–102.

Lennon, J. and McCartney, P. (1965). Norwegian Wood . Parlophone, London.

Leuenberger, M. and Filot, S. (2007). Temperature dependancies of high-temperature reduction on conversion products and their isotopic signatures. *Rapid Communications in Mass Spectrometry*, 21(10):1587–1598.

Leuschner, H., Sass-Klaassen, U., Jansma, E., Baillie, M., and Spurk, M. (2002). Subfossil European bog oaks: population dynamics and long-tem growth depressions as indicators of changes in the Holocene hydro-regime and climate . *The Holocene*, 12(6):695–706.

Libby, L., Pandolfi, L., Payton, P., Marshall, J., Becker, B., and Giertz-Siebenlist, V. (1976). Isotopic tree thermometers . *Nature*, 261:284–290.

Linderholm, H. and Chen, D. (2005). Central Scandinavian winter precipitation variability during the past five centuries reconstructed from Pinus sylvestris tree rings . *Boreas*, 34:43–52.

Linderholm, H. and Molin, T. (2005). Early nineteenth century drought in central Sweden infered from dendrochronological and historical archives. *Climate Research*, 29:63–72.

Lindholm, M. and Eronen, M. (2000). A reconstruction of midsummer temperatures from ring-widths of Scots pine since AD 50 in Northern Fennoscandia. *Geografiska Annaler*, 82:527–535.

Lipp, J., Trimborn, P., Fritz, P., Moser, H., Becker, B., and Frenzel, B. (1991). Stable isotopes in tree ring cellulose and climatic change. *Tellus*, 43B:322–330.

Liu, Y., Ma, L., Leavitt, S., Cai, Q., and Liu, W. (2004). A preliminary seasonal precipitation reconstruction from tree-ring stable carbon isotopes at Mt. Helan, China, since AD 1804 . *Global Planetary Change*, 41:229–239.

Lloyd-Hughes, B. and Saunders, M. (2002). A drought climatology for Europe . *International Journal of Climatology*, 22:1571–1592.

Loader, N. and Buhay, W. (1999). Rapid catalytic oxidation of CO to CO_2 - on the development of a new approach to on-line oxyegen isotope analysis of organic matter. *Rapid Communications in Mass Spectrometry*, 13:1828–1832.

Loader, N., McCarroll, D., Gagen, M., Robertson, I., and Jalkanen, R. (2007). Extracting climatic information from stable isotopes in tree rings. In Siegwolf, R. and Dawson, T., editors, *Isotopes as indicators of ecological change*. Academic Press, San Diego. In Press.

Loader, N., Robertson, I., Barker, A., Switsur, V., and Waterhouse, J. (1997). An improved technique for the batch processing of small wholewood samples to a-cellulose . *Chemical Geology*, 136:313–317.

Loader, N., Robertson, I., Lücke, A., and Helle, G. (2002). Preparation of holocellulose from stable increment cores for stable carbon isotope analysis . *Swansea Geographer*, 37:1–9.

Loader, N., Robertson, I., and McCarroll, D. (2003). Comparison of stable carbon isotope ratios in the whole wood, cellulose and lignin of oak tree-rings . *Palaeogeography, Palaeoclimatology, Palaeoecology*, 196:395–407.

Loader, N. and Switsur, V. (1996). Reconstructing past environmental change using stable isotopes in tree rings. *Botanical Journal of Scotland*, 48:65–78.

Loader, N., Switsur, V., and Field, E. (1995). High-resolution stable isotope analysis of tree-rings: implications of 'microdendroclimatology' for palaeoenvironmental research. *The Holocene*, 5:457–460.

Lugina, K., Groisman, P., Vinnikov, K., Koknavena, V., and Speranskaya, N. (2006). Monthly surface air temperature time series area-averaged over the 30-degree latitude belts of the globe, 1881-2005. In *Trends: A Compendium of Data on Global Change*. Carbon Dioxide Information Analysis Center, Oak Ridge National Laboratory, U.S. Department of Energy, Oak Ridge, Tenn., USA.

Luterbacher, J., Xoplaki, E., Dietrich, D., Jones, P., Davies, T., Portis, D., Gonzalez-Rouco, J., von Storch, H., Gyalistras, D., Casty, C., and Wanner, H. (2002). Extending North Atlantic Oscillation reconstructions back to 1500 . *Atmospheric Science Letters*, 2:114–124.

MacFarlane, C., Warren, C., White, D., and Adams, M. (1999). A rapid and simple method for processing wood to crude cellulose fro analysis of stable carbon isotopes in tree rings. *Tree Physiology*, 19:831–835.

Madden, R. and Williams, J. (1978). The correlatin between temperature and precipitation in the United States and Europe . *Monthly Weather Review*, 106:142–147.

Mann, M. (2001). Climate during the past millennium . *Weather*, 56:91–102.

Mann, M. (2002). The value of multiple proxies. *Science*, 297:1481–1482.

Mann, M., Ammann, C., Bradley, R., Briffa, K., Jones, P., Osborn, T., Crowley, T., Hughes, M., Oppenheimer, M., Overpeck, J., Rutherford, S., Trenberth, K., and Wigley, T. (2003). On past temperatures and anomalous late-20th century warmt . *Eos*, 84:256.

Mann, M., Bradley, R., and Hughes, K. (1998). Global-scale temperature patterns and climate forcing oner the past six centuries . *Nature*, 392:779–787.

Mann, M., Bradley, R., and Hughes, K. (1999). Northern hemisphere temperatures during the past millennium: inferences, uncertainties and limitations . *Geophysical Research Letters*, 26:759–762.

Mann, M., Gille, E., Bradley, R., Hughes, M., Overpeck, J., Keimig, F., and Gross, W. (2000). Global temperature patterns in past centuries: an interactive presentation . *Earth Interactions*, 4(4):1–29.

Mann, M. and Hughes, K. (2002). Tree-ring chronologies and climate variability . *Science*, 296:848.

Mann, M. and Jones, P. (2003). Global surface temperatures over the past two millennia . *Geophysical Research Letters*, 30(15):doi:10.1029/2003GLO17814.

Marshall, J. and Monserud, R. (1996). Homeostatic gas-exchange parameters inferred from 13C/12C in tree rings of conifers during the Twentieth Century. *Oecologia*, 105:13–21.

Matthes, F. (1939). Report of the Comittee on Glaciers . *Transactions of the American Geophysical Union*, 20:518–523.

Matthews, J. and Briffa, K. (2005). The 'Little Ice Age': a re-evaluation of an evolving concept . *Geografiska Annaler*, 87A:17–36.

Matthews, J. and Kárlen, W. (1992). Asynchronous neoglacition and Holocene climatic change reconstructed from Norwegian glacio-lacustrine sequences . *Geology*, 20:991–994.

Mayewski, P., Rohling, E., Stager, J., Karlén, W., Maasch, K., Meeker, L., Meyerson, E., Gasse, F., van Kreveld, S., Holmgren, K., Lee-Thorp, J., Rosqvist, G., Rack, F., Staubwasser, M., Schneider, R. R., and Steig, E. (2004). Holocene climate variability . *Quaternary Research*, 62:243–255.

McCarroll, D., Gagen, M., Loader, N., Robertson, I., Anchukaitis, K., Los, S., Young, G., Jalkanen, R., Kirchhefer, A., and Waterhouse, J. (2007). Objective correction of tree ring stable carbon isotope chronologies for changes in the carbon dioxide content of the atmosphere. *In preparation.*

McCarroll, D., Jalkanen, R., Hicks, S., Tuovinen, M., Gagen, M., Pawellek, F., Eckstein, D., Schmitt, U., Autio, J., and Heikkinen, O. (2003). Multiproxy dendroclimatology: a pilot study in northern Finland . *The Holocene*, 13(6):829–838.

McCarroll, D. and Loader, N. (2004). Stable isotopes in tree rings . *Quaternary Science Reviews*, 23:771–801.

McCarroll, D. and Loader, N. (2006). Isotopes In Tree Rings . In Leng, M., editor, *Isotopes in Palaeoenvironmental Research*. Springer, Dordrecht.

McCarroll, D. and Pawellek, F. (1998). Stable carbon isotope ratios of latewood cellulose in Pinus sylvestris from northern Finland: variability and signal-strength . *The Holocene*, 8(6):675–684.

McCarroll, D. and Pawellek, F. (2001). Stable carbon isotopes ratios of Pinus sylvestris from northern Finland and the potential for extracting a climate signal from long Fennoscandian chronologies . *The Holocene*, 11(5):517–526.

McClanahan, T. and Multhiga, N. (2000). Tropical Pacific forcing of decadal SST variability in the western Indian Ocean. *Science*, 287:617–619.

McDowell, N., Phillips, N., Lunch, C., Bond, B., and Ryan, M. (2002). An investigation of hydraulic limitation and compensation in large, old Douglas fir trees. *Tree Physiology*, 22:763–774.

McIntyre, S. and McKitrick, R. (2003). Corrections to the Mann et. al. (1998) proxy database and northern hemispheric average temperature series. *Energy & Environment*, 14:751–771.

McIntyre, S. and McKitrick, R. (2005). Hockey sticks, proinciple components and spurious significance . *Geophysical Research Letters*, 32(L04703,):doi:10.1029/2004GL021750.

McKee, T., Doesken, N., and Kliest, J. (1993). The relationship of drought frequency and duration to time scales. In *Proceedings of the 8th Conference on Applied Climatology, 17-22 January*, pages 179–184, Anaheim, California. American Meteorological Society, Boston, MA.

Moberg, A. and Bergström, H. (1997). Homogenization of Swedish temperature data. Part III: The long temperature records from Uppsala and Stckholm. *International Journal of Climatology*, 17:667–699.

Moberg, A., Sonechkin, D., Holmgren, K., Datsenko, N., and Karlén, W. (2005). Highly variable Northern Hemisphere temperatures reconstructed from low- and high-resolution proxy data . *Nature*, 433:613–617.

Monserud, R. and Marshall, J. (2001). Time-series analysis of $\delta^1$3C from tree rings. I. Time trends and autocorrelation. *Tree Physiology*, 21:1087–1102.

Mook, W., M., K., Carter, A., and Keeling, C. (1983). seasonal, latitudinal, and secular variations in the abundance and isotopic-ratios of atmospheric carbon-dioxide. 1. Results from land stations. *Journal of Geophysical Research*, 88:915–933.

Nesje, A. and Kvamme, M. (1991). Holocene glacier and climatic variations in western Norway: evidence for early Holocene glacier demise and multiple Neoglacial events . *Geology*, 19:610–612.

Nesje, A., Matthews, J., Dahl, S., Berrisford, M., and Andersson, C. (2001). Holocene glacier fluctuations of Flatebreen and winter precipitation changes in the Jostedalsbreen region, western Norway, based on glaciolacustrine sediment records . *The Holocene*, 11(3):267–280.

NRC (2006). *Surface Temperature Reconstructions for the Last 2,000 Years*. The National Academies, Washington, D.C.

Ogilvie, A. and Jonsson, T. (2001). 'Little Ice Age' research: a perspective from Iceland . *Climatic Change*, 48:9–52.

O'leary, M., Madhavan, S., and Paneth, P. (1992). Physical and chemical basis of carbon isotope fractionation in plants . *Plant, Cell and Environment*, 15:1099–1104.

Osborn, T. and Briffa, K. (2006). The spatial extent of 20th-century warmth in the context of the past 1200 years. *Science*, 311:841–844.

Overpeck, J., Hughen, K., Hardy, D., Bradley, R.; Case, R., Douglas, M., Finney, B., Gajewski, K., Jacoby, G., Jennings, A., Lamoureux, S., Lasca, A., MacDonald, G., Moore, J., Retelle, M., Smith, S., Wolfe, A., and Zielinski, G. (1997). Arctic environmental change change of the last four centuries. *Science*, 278:1251–1256.

Parker, D., Basnett, T., Brown, S., Gordon, M., Horton, E., and Rayner, N. (2000). Climate observations - the instrumental record . *Space Science Reviews*, 94:309–320.

Petit, J., Jouzel, J., Raynaud, D., Barkov, N., Barnola, J.-M., Basile, I., Bender, M., Chappellaz, J., Davis, M., Delaygue, G., Delmotte, M., Kotlyakov, V., Legrand, M., Lipenkov, V., Lorius, C., Pépin, L., Ritz, C., Saltzman, E., and Stievenard, M. (1999). Climate and atmospheric history of the last 420,000 years from the Vostok ice coe, Antarctica . *Nature*, 399:429–435.

Phillips, R. (1978). *Trees in Britain, Europe and North America*. Pan Books Ltd, London.

Pilcher, J. (1989). Sample Preparation, Cross-dating, and Measurement. In Cook, E. and Kairiukstis, L., editors, *Methods of dendrochronology : applications in the environmental sciences*, pages 40–51. Kluwer Academic Publishers, Dordrecht.

Preston, T. and Owens, N. (1985). Preliminary $^{1}3C$ measurements using a gas chromatograph interfaced to an isotope mass spectrometer. *Biomedical Mass Spectrometry*, 12:510–513.

Raffalli-Delerce, G., Masson-Delmotte, V., Dupouey, J., Stievenard, M., Breda, N., and Moisselin, J. (2004). Reconstruction of summer droughts using tree-ring cellulose isotopes: a calibration study with living oaks from Brittany (western France) . *Tellus*, 56B:160–174.

Ramesh, R., Bhattacharya, S., and Gopalan, K. (1985). Dendroclimatological implications of isotope coherence in trees from the Kashmir Valley, India . *Nature*, 317:802–804.

Ramesh, R., Bhattacharya, S., and Gopalan, K. (1986). Climatic correlations in the stable isotope records of silver fir (Abies pindrow) trees from Kahmir, India . *Earth and Planetary Science Letters*, 79:66–74.

R.Development.Core.Team (2006). *R: A Language and Environment for Statistical Computing*. R Foundation for Statistical Computing, Vienna, Austria. http://www.R-project.org.

Rebetez, M., Saurer, M., and Cherubini, P. (2003). To what extent can oxygen isotopes in tree rings and precipitation be used to reconstruct past atmospheric temperatures? A case study . *Climatic Change*, 61:237–248.

Rinn, F. (1996). *Time series analysis and presentation*. Frank Rinn, Heidelberg.

Roberts, N. (1998). *The Holocene* . Blackwell, Oxford, 2nd edition.

Robertson, A., Overpeck, J., Rind, D., Mosley-Thompson, E., Zielinski, G., Lean, J., Koch, D., Penner, J., Tegen, I., and Healy, R. (2001a). Hypothesized climate forcing time series for the last 500 years. *Journal of Geophysical Research*, 106:14783–14803.

Robertson, I., Froyd, C., Walsh, R., Newbery, D., Woodborne, S., and Ong, R. (2004a). The dating of *dipterocarp* tree rings: establishing a record of carbon cycling and climatic change in the tropics. *Journal of Quaternary Science*, 19:657–664.

Robertson, I., Loader, N., McCarroll, D., Carter, A., Cheng, L., and Leavitt, S. (2004b). $\delta^{13}C$ of tree-ring lignin as an indirect measure of climate change . *Water, Air, and Soil Pollution: Focus*, 4:531–544.

Robertson, I., Rolfe, J., Switsur, V., Carter, A., Hall, M., Barker, A., and Waterhouse, J. (1997a). Signal strength and climate realtionships in $^{13}C/^{12}C$ ratios of tree ring cellulose from oak in southwest Finland . *Geophysical Research Letters*, 24:1487–1490.

Robertson, I., Switsur, V., Carter, A., Barker, A., Waterhouse, J., Briffa, K., and Jones, P. (1997b). Signal strength and climate relationships in $^{13}C/^{12}C$ ratios of tree ring cellulose from oak in east England . *Journal of Geophysical Research*, 102:19507–19519.

Robertson, I., Waterhouse, J., Barker, A., Carter, A., and Switsur, V. (2001b). Oxygen isotope ratios of oak in east England: implications for reconstructing the isotopic composition of precipitation. *Earth and Planetary Science Letters*, 191:21–31.

Roden, J., Lin, G., and Ehleringer, J. (2000). A mechanistic model fro interpretation of hydrogen and oxygen isotope ratios in tree-ring cellulose . *Geochimica et Cosmochimica Acta*, 64(1):21–35.

Ryan, M. and Yoder, B. (1997). Hydraulic limits to tree height and growth. *Bioscience*, 47:235–242.

Santrock, J. and Hayes, J. (1987). Adaptionof the Unterzaucher procedure for determination of oxygen-18 in organic substances. *Analytical Chemistry*, 59:119–127.

Sass-Klaassen, U., Poole, I., Wils, T., Helle, G., Schleser, G., and van Bergen, P. (2005). Carbon and Oxygen isotope dendroclimatology in sun-fossil Bog Oak tree rings - A preliminary study . *IAWA Journal*, 26(1):121–136.

Saurer, M. (2003). The influence of climate on the oxygen isotopes in tree rings . *Isotopes in Environmental Health Studies*, 39(2):105–112.

Saurer, M., Aellen, K., and Siegwolf, R. (1997a). Correlating $\delta^{13}C$ and $\delta^{18}O$ in cellulose of trees . *Plant, Cell and Environment*, 20:1543–1550.

Saurer, M., Borella, S., and Leuenberger, M. (1997b). $\delta^{18}O$ of tree rings of beech (*Fagus silvatica*) as a record of $\delta^{18}O$ of the growing season precipitation. *Tellus*, 49B:82–90.

Saurer, M., Robertson, I., Siegwolf, R., and Leuenberger, M. (1998a). Oxygen isotope analysis of cellulose: an interlaboratory comparison . *Analytical Chemistry*, 70(10):2074–2080.

Saurer, M., Schweingruber, F., Vaganov, E., Shiyatov, S., and Siegwolf, R. (2002). Spatial and temporal oxygen isotope trends at the northern tree-line in Eurasia . *Geophysical Research Letters*, 29(9):10–14.

Saurer, M., Siegenthaler, U., and Schweingruber, F. (1995). The climate-carbon isotope relationship in tree rings and the significance of site conditions. *Tellus*, 47B:320–330.

Saurer, M. and Siegwolf, R. (2004). Pyrolysis Techniques for Oxygen Isotope Analysis of Cellulose . In de Groot, P., editor, *Handbook of Stable Isotope Analytical Techniques, Volume 1*, volume 1, pages 497–522. Elsevier, Amsterdam.

Saurer, M., Siegwolf, R., Borella, S., and Schweingruber, F. (1998b). Environmental information from stable isotopes in tree rings of *Fagus silvatica*. In Beniston, M. and Innes, J., editors, *The Impacts of Climate variability on Forests*, pages 241–253. Springer, Berlin.

Saurer, M., Siegwolf, R., and Schweingruber, F. (2004). Carbon isotope discrimination indicates improving water-use efficiency of trees in northern Eurasia over the last 100 years. *Global Change Biology*, 10:2109–2120.

Schäfer, K., Oren, R., and Tenhunen, J. (2000). The effect of tree height on crown level stomatal conductance. *Plant, Cell and Environment*, 23:365–375.

Scheidegger, Y., Saurer, M., Bahn, M., and Siegwolf, R. (2000). Linking srtable oxygen and carbon isotopes with stomatal conductance and photosynthetic capacity: a conceptual model . *Oecologia*, 125:350–357.

Schleser, G. and Jayasekera, R. (1985). $\delta^{1}3C$ variation in leaves of a forest as an indication of reassimilated CO_2 from the soil. *Oecologia*, 65:536–542.

Schmitz, W. (1995). On the interbasin-scale thermohaline circulation . *Reviews of Geophysics*, 33:151–173.

Schulze, B., Wirth, C., Linke, P., Brand, W., Kuhlmann, I., Horna, V., and Schulze, E. (2004). Laser ablation-combustion-GC-IRMS–a new method for online analysis of intra-annual variations of d13C in tree rings . *Tree Physiology*, 24:1193–1201.

Schweingruber, F. (1988). *Tree Rings: Basics and Applications of Dendrochronology* . D. Reidel, Dordrecht.

Schweingruber, F. (1993). *Trees and Wood in Dendrochronology*. Springer-Verlag, Berlin.

Schweingruber, F., Kairiukstis, L., and Shiyatov, S. (1989). Sample Selection. In Cook, E. and Kairiukstis, L., editors, *Methods of dendrochronology : applications in the environmental sciences*, pages 23–35. Kluwer Academic Publishers, Dordrecht.

Seveinghaus, J. and Brook, E. (1999). Abrupt climate change at the end of the last glacial period inferred from trapped air in polar ice. *Science*, 286:930–934.

Sheu, D., Kou, P., Chiu, C., and Chen, M. (1996). Variability of tree ring $\delta^{13}C$ in Taiwan fir: growth effect and response to May-October temperatures. *Geochimica et Cosmochimica Acta*, 60:171–177.

Smith, T. and Reynolds, R. (2005). A global merged land and sea surface temperature reconstruction based on historical observations (1880-1997). *Journal of Climate*, 18:2021–2036.

Sonninen, E. and Jungner, H. (1995). Stable carbon isotopes in the tree rings of a Scots pine (*Pinus sylvestris* L.) from northern Finland. *Paläoklimaforschung*, 15:121–128.

Soon, W. and Baliunas, S. (2003). Proxy climatic and environmental changes of the past 1000 years . *Climate Research*, 23:89–110.

Spurk, M., Leuschner, H., Baillie, M., Briffa, K., and Friedrich, M. (2002). Depositional frequency of German subfossil oaks: climatically and non-climatically induced fluctuations in the Holocene . *The Holocene*, 12(6).

Sternberg, L., Anderson, W., and Morrison, K. (2003). Separating soil and leaf water ^{18}O isotopic signals in plant cell cellulose . *Geochimica et Cosmochimica Acta*, 67(14):2561–2566.

Sternberg, L., De Niro, M., and Savidge, R. (1986). Oxygen isotope exchange between metabolites and water during biochemical reactions leading to cellulose synthesis. *Plant Physiology*, 82:423–427.

Stine, S. (1994). Extreme and persistant drought in California and Patagonia during Medieval time . *Nature*, 269:546–549.

Stine, S. (1998). Medieval climate anomaly in the Americas . In Issar, A. and Brown, N., editors, *Water, Environment and Society in Times of Climate Change*, pages 43–67. Kluwer, Dordrecht.

Swanborough, P., Lamont, B., and February, E. (2003). $\delta^{13}C$ and water-use efficiency in Australian grassland and South African confiers over the last century. *Oecologia*, 136:205–212.

Switsur, V. and Waterhouse, J. (1998). Stable isotopes in tree ring cellulose . In Griffiths, H., editor, *Stable Isotopes: integration of biological, ecological and geochemical processes*, page 438. BIOS Scientific Publishers, Oxford.

Switsur, V., Waterhouse, J., Field, E., Carter, A., and Loader, N. (1995). Stable isotope studies in tree rings from oak - techniques and some preliminary results. *Paläoklimaforschung*, 15:129–140.

Tang, K., Feng, X., and Funkhouser, G. (1999). The $\delta^{13}C$ of tree rings in full-bark and strip-bark bristle cone pine trees in the White Mountains of California . *Global Change Biology*, 5:33–40.

Thompson, L., Davis, M., Mosley-Thompson, E., Sowers, T., Henderson, K., Zagorodnov, V., Lin, P.-N., Mikhalenko, V., Campen, R., Bolzan, J., Cole-Dai, J., and Francou, B. (1998). A 25,000-year tropical climate history from Bolivian ice cores . *Science*, 282:1858–1864.

Touchan, R., Funkhouser, G., Hughes, M., and Erkan, N. (2005). Standardized precipitation indexreconstructed from Turkish tree-ring widths . *Climatic Change*, 72:339–353.

Touchan, R. and Hughes, M. (1999). Dendrochronology in Jordan . *Journal of Arid Environments*, 42(4):291–303.

Trenberth, K. and Shea, D. (2005). Relationships between precipitation and surface temperature . *Geophysical Research Letters*, 32(L14703):doi:10.1029/2005GL022760.

Treydte, K., Esper, J., and Gärtner, H. (2004). Stabile isotope in der dendroklimatologie . *Schweiz. Z. Forstwes.*, 155(6):222–232.

Treydte, K., Schleser, G., Helle, G., Frank, D., Winiger, M., Haug, G., and Esper, J. (2006). The twentieth century was the wettest period in northern Pakistan over the past millennium. *Nature*, 440:1179–1182.

Treydte, K., Schleser, G., Schweingruber, F., and Winiger, M. (2001). The climatic significance of $\delta^{13}C$ in subalpine spruces (L. otschental, Swiss Alps). *Tellus*, 53B:593–611.

Tsuji, H., Nakatsuka, T., and Takagi, K. (2006). $\delta^{18}O$ of tree-ring cellulose in two species (spuce and oak) as proxies of precipitation amount and relative humidity in northern Japan. *Chemical Geology*, 231:67–76.

Tuomenvirta, H., Alexandersson, H., Drebs, A., Frich, P., and Nordli, P. (2000). Trends in Nordic and Arctic temperature extremes and ranges. *Journal of Climate*, 13:977–990.

Urey, H. (1947). The thermodynamic properties of isotopic substances . *Journal of the Chemical Society*, Pt 1:562–581.

Verheyden, A., Helle, G., Schleser, G., Dehairs, F., Beeckman, H., and Koedam, N. (2004). Annual cyclicity in high-resolution carbon and oxygen isotope ratios in the wood of the mangrove tree *Rhizophora mucronata*. *Plant, Cell and Environment*, 27:1525–1536.

Vose, R., Wuertz, D., Peterson, T., and Jones, P. (2005). An intercomparison of trends in surface air temperature analyses at the global, hemispheric and grid-box scale. *Geophysical Research Letters*, 32:L18718, doi:10.1029/2005GL023502.

Wahl, E. and Ammann, C. (2007). Robustness of the Mann, Bradley, Hughes reconstruction of Northern Hemisphere surface temperatures: examination of criticisms based on the nature and processing of proxy climate evidence. *Climatic Change*, 85(1,2):33–69.

Waterhouse, J., Barker, A., Carter, A., Agafonov, L., and Loader, N. (2000). Stable carbon isotopes in Scots pine tree rings preserve a record of the flow of the river Ob. *Geophysical Research Letters*, 27:3529–3532.

Waterhouse, J., Switsur, V., Barker, A., Carter, A., Hemming, D., Loader, N., and Robertson, I. (2004). Northern European trees show a progressively diminishing response to increasing atmospheric cardon dioxide concentrations . *Quaternary Science Reviews*, 23:803–810.

Werner, R. (2003). An online $^{18}O/^{16}O$ analysis: development and application . *Isotopes in Environmental Health Studies*, 39(2):85–104.

Werner, R., Kornexl, B., Roßmann, A., and Schmidt, H. (1996). On-line determination of $\delta^{18}O$ values of organic substances. *Analytica Chimica Acta*, 319:159–164.

Wigley, T., Briffa, K., and Jones, P. (1984). On the average value of correlated time series with applications in dedroclimatology and hydrometerorology . *Journal of Climate and Applied Meteorology*, 23:201–213.

Wilson, A. and Grinstead, M. (1977). $^{12}C/^{13}C$ in cellulose and lignin as palaeothermometers . *Nature*, 265:133–135.

Zimmerman, B., Schleser, G., and Brauning, A. (1997). Preliminary results of a Tibetan stable C-isotope chronology dating from 1200 to 1994. *Isotopes in Environmental Health Studies*, 33:157–165.

A

Raw Data

A.1 Andenes Temperature

	Jan	Feb	Mar	Apr	May	Jun	Jul	Aug	Sep	Oct	Nov	Dec
1868	-2.9	-3.8	-0.4	2.5	6.9	9.7	11.1	13.3	6.9	5.4	1.9	-1.3
1869	2.3	0.2	-0.2	2.1	4.8	9.3	11.1	10.3	8.7	1.8	0.7	-1.3
1870	-1.4	-2.3	-1.0	2.6	4.0	9.8	10.9	11.4	9.9	2.4	-0.9	-1.7
1871	0.9	-6.1	1.2	-0.2	3.5	7.1	10.7	9.7	6.1	4.2	-1.0	-2.7
1872	0.0	-0.8	-2.2	2.9	4.1	10.7	11.3	9.7	5.4	4.0	0.0	-2.7
1873	-1.3	-3.4	-1.4	-0.6	4.2	9.4	11.5	12.4	8.5	3.4	0.2	-1.2
1874	-1.5	-1.0	-1.7	1.3	3.7	6.5	9.1	10.6	7.9	5.4	0.6	-3.0
1875	-4.1	-1.6	-0.8	-1.2	6.8	7.9	10.8	9.4	6.4	4.0	0.6	-0.9
1876	0.8	-1.3	-2.6	-0.3	3.0	9.5	11.9	10.2	7.9	3.5	-1.0	-3.3
1877	-2.2	-4.6	-3.5	-0.5	3.5	6.9	9.3	9.0	6.2	1.9	2.2	0.6
1878	-0.4	-1.6	-2.0	1.5	5.1	8.4	10.0	8.8	8.4	5.2	0.6	-1.7
1879	-0.4	-3.6	-1.5	-0.1	3.6	5.9	10.0	12.5	9.4	3.6	0.2	-0.2
1880	0.6	-1.2	-1.5	0.0	3.8	6.7	8.9	11.2	8.6	0.5	-1.5	-2.9
1881	-4.8	-5.3	-4.8	-2.5	1.1	5.6	9.5	10.6	8.0	4.7	0.3	0.1
1882	-0.2	-3.0	-2.5	0.5	4.1	7.5	12.1	12.6	9.7	6.0	0.2	-2.3
1883	-0.4	0.4	-1.4	2.9	5.8	9.8	10.4	11.5	8.0	4.4	1.9	0.7
1884	-1.9	1.0	1.4	0.4	4.4	8.4	9.7	12.6	9.6	4.4	1.7	-1.7
1885	-1.1	-1.3	-1.8	1.3	2.5	6.6	10.0	9.5	7.2	2.4	0.1	-1.9
1886	-4.1	-0.5	0.4	1.6	5.2	9.2	10.6	11.6	7.4	6.2	2.9	-2.8
1887	1.6	1.1	-1.6	0.0	4.3	6.2	9.8	10.5	8.9	1.9	0.0	-3.9
1888	-2.0	-3.1	-4.6	-1.0	4.7	6.5	9.3	10.1	6.1	1.6	0.5	0.9
1889	-0.8	-3.7	-3.6	0.2	5.9	9.8	10.1	10.6	8.0	5.3	3.5	2.3
1890	0.5	0.8	0.4	2.2	6.6	9.1	9.3	11.9	9.4	1.7	1.4	2.1
1891	-1.0	1.3	-3.1	2.2	4.3	5.1	10.4	9.7	6.3	5.8	1.5	0.5
1892	-3.4	-2.8	0.1	0.6	2.9	6.1	9.2	9.2	8.0	1.9	2.4	-3.5
1893	-4.0	-5.4	-3.4	-0.5	4.1	8.4	8.0	9.2	4.9	3.7	-2.1	0.0
1894	0.3	-1.4	-0.8	4.8	5.7	11.2	11.8	10.5	5.5	2.9	2.1	-0.6
1895	-1.9	-1.7	-2.6	1.3	6.3	9.3	10.3	11.9	7.0	3.0	3.1	1.6
1896	-1.2	1.2	-0.5	2.5	5.0	7.4	12.5	10.4	9.0	3.1	0.5	0.6
1897	-0.4	-3.6	-3.3	3.4	6.4	7.2	9.0	10.8	8.5	5.7	1.2	0.2
1898	0.0	-3.0	-1.4	1.6	6.0	8.9	10.3	10.6	8.3	3.8	0.2	-2.4
1899	-3.8	-2.8	-4.6	-2.0	1.9	8.8	10.8	7.5	8.3	2.4	1.4	-1.4
1900	-1.7	-6.5	-1.9	-0.3	2.4	6.4	7.3	9.5	5.9	2.3	1.5	-2.7
1901	1.9	-4.4	-2.8	1.0	3.7	8.6	11.0	11.2	9.7	7.0	-0.6	-3.4

1902	-2.4	-2.4	-2.8	1.0	4.2	5.5	8.0	9.4	6.0	1.6	1.7	0.2
1903	-0.1	-0.6	0.9	1.5	4.8	6.4	8.0	10.6	7.4	-0.3	1.4	-0.1
1904	1.3	-4.4	0.8	3.3	3.2	7.0	9.5	9.7	8.4	4.2	-1.4	-3.3
1905	-1.7	-1.2	-1.0	0.2	4.8	7.8	11.1	11.3	7.9	2.5	-0.7	0.7
1906	0.6	-2.9	-3.7	2.4	3.7	7.3	10.7	8.5	7.8	3.9	1.6	-1.2
1907	-2.1	-0.5	0.9	3.1	3.5	10.9	10.1	9.7	5.7	5.2	3.3	-1.9
1908	-0.2	-2.8	-0.3	1.0	3.3	6.9	9.8	10.7	7.4	6.6	-0.7	-0.2
1909	0.7	-1.0	-3.2	0.4	2.3	6.8	9.4	10.3	7.4	4.5	-1.3	-1.9
1910	-2.2	0.8	0.9	1.3	5.7	7.8	9.1	9.4	6.9	3.5	-1.3	-0.7
1911	-0.2	-2.1	-0.6	0.4	5.4	6.4	9.9	11.0	8.6	2.0	1.8	1.5
1912	-2.7	-5.1	-0.8	-0.2	4.3	7.8	9.8	11.6	6.6	3.4	0.6	-1.3
1913	-1.5	-1.3	-0.6	1.9	5.1	6.7	10.6	11.0	7.3	2.1	2.8	-1.4
1914	-1.2	-1.1	-1.0	1.7	3.7	7.9	11.2	11.6	8.0	4.9	2.2	-0.1
1915	-2.6	-3.5	-3.9	0.5	2.4	6.0	11.5	9.9	6.0	4.3	-1.1	-6.4
1916	-1.2	-1.2	-3.8	0.9	3.8	7.8	12.6	10.3	6.7	1.4	2.2	-2.4
1917	-2.0	-4.2	-3.7	-2.0	1.5	8.6	8.1	11.1	7.2	3.5	0.6	-2.2
1918	-5.1	-1.6	0.6	1.5	4.0	8.3	11.8	9.9	7.5	4.2	3.4	-0.7
1919	-0.4	-4.1	-2.6	-0.9	6.2	9.3	9.8	9.7	7.2	2.4	-0.9	-3.0
1920	-1.5	-0.9	0.8	2.6	6.2	7.0	11.0	10.8	9.5	5.4	3.2	1.4
1921	-2.8	-0.9	0.5	3.9	5.2	7.4	9.4	10.1	6.9	2.5	0.3	-0.4
1922	-1.7	-1.4	-2.6	1.9	6.0	9.2	13.0	11.9	8.3	4.2	0.5	-2.0
1923	-0.6	-2.1	1.2	0.8	4.9	5.4	10.1	9.0	7.9	4.4	0.9	-1.4
1924	-0.1	-3.2	-3.2	0.4	4.7	7.1	11.9	12.7	8.9	6.6	2.4	1.4
1925	2.5	-0.8	-2.9	2.7	5.1	8.4	11.8	11.7	9.8	2.2	-0.5	-2.3
1926	-1.1	-1.8	-0.3	1.5	4.8	7.7	10.6	10.5	7.7	1.3	1.6	-1.9
1927	-2.6	0.0	-0.8	0.8	3.7	7.5	13.0	13.0	8.1	2.1	0.4	0.0
1928	0.0	0.4	0.7	1.7	4.2	9.1	10.1	10.9	7.9	3.6	0.9	0.5
1929	-1.4	-0.6	0.0	-1.1	5.4	7.6	8.9	10.3	8.3	3.8	2.9	3.1
1930	0.9	0.7	-1.0	4.0	6.1	9.5	12.9	13.9	7.8	4.5	1.0	1.6
1931	-1.2	-1.1	-1.4	2.9	5.0	6.8	11.6	9.9	6.4	3.2	3.4	1.4
1932	0.7	0.6	-0.6	1.4	4.1	7.6	10.8	10.5	6.6	3.2	1.9	3.4
1933	1.6	-3.3	-1.0	-0.4	4.3	10.0	11.2	11.4	9.4	5.0	2.6	1.4
1934	1.7	-0.9	0.1	1.0	5.6	7.0	13.5	14.5	12.1	5.5	2.5	1.1
1935	-0.1	-0.7	0.2	2.3	2.7	7.1	10.3	11.5	7.0	4.6	2.7	1.3
1936	-2.2	-4.1	-1.3	1.1	6.3	9.7	11.5	11.8	8.4	4.4	3.2	1.5
1937	0.6	-2.6	-1.7	4.5	6.5	8.7	12.7	12.6	9.2	6.3	2.1	-0.7
1938	0.6	1.5	-0.3	1.5	5.2	9.2	12.8	11.8	9.9	8.1	4.2	2.0
1939	-1.7	0.4	0.1	0.6	4.6	8.0	11.4	12.4	7.4	4.6	2.6	-0.5
1940	-0.9	-3.4	-3.5	-0.1	7.0	8.8	9.3	9.8	8.6	5.7	0.7	0.0
1941	-2.9	-3.0	-2.3	0.2	3.1	6.8	12.8	11.5	7.7	3.2	2.4	-1.5
1942	-3.0	-2.0	-3.3	1.5	3.0	8.3	10.2	10.5	8.2	3.9	1.7	0.0
1943	-2.9	-0.6	1.0	1.2	4.5	8.5	11.0	10.6	8.4	5.5	2.6	2.2
1944	-0.1	0.8	-0.8	-0.2	4.0	8.3	10.6	10.1	8.7	6.4	2.2	2.1
1945	-2.0	-0.6	-0.1	2.9	4.6	7.0	11.5	11.6	8.3	2.9	2.4	-0.4
1946	1.4	-3.9	-1.2	2.2	4.8	9.4	12.6	12.4	10.8	5.5	1.3	2.6
1947	0.8	-4.3	-3.8	0.9	4.5	8.4	11.0	11.1	9.1	4.6	0.4	-0.6
1948	-3.1	0.7	2.6	3.4	5.5	7.0	11.9	9.5	8.1	4.4	2.4	2.3
1949	0.0	1.1	-0.2	1.7	5.4	8.0	9.1	9.1	9.0	4.2	3.2	0.7
1950	-1.1	-1.3	0.3	3.7	4.3	8.9	11.4	13.3	10.1	6.9	2.9	0.3
1951	-2.3	-0.4	-1.3	1.8	3.7	6.2	9.3	11.9	8.7	7.8	-0.3	0.5
1952	-0.6	-1.2	-1.6	2.8	4.9	9.4	10.4	9.1	7.4	3.8	0.7	-2.0
1953	-0.8	-2.8	0.1	1.7	4.8	11.0	12.0	12.1	8.1	7.0	3.7	3.4
1954	0.3	-1.3	-0.5	1.8	6.7	7.3	13.6	11.6	8.7	4.3	1.4	1.8

1955	-1.9	-3.0	-1.3	0.0	3.7	6.0	9.6	10.5	9.6	3.6	0.4	-3.6
1956	-2.8	-2.7	0.6	0.1	5.5	7.9	11.5	10.7	7.3	4.6	1.0	1.0
1957	1.0	-2.1	0.0	2.9	4.4	6.7	11.6	11.2	9.1	4.7	3.1	-0.9
1958	-1.4	-3.6	-2.5	2.0	5.3	7.9	9.9	11.6	8.4	6.5	4.5	-1.1
1959	-2.4	2.7	3.1	3.0	5.5	8.3	10.5	11.2	7.7	5.6	3.5	0.6
1960	-1.3	-3.4	2.3	4.2	6.4	8.2	14.2	12.6	10.1	3.0	1.1	-0.5
1961	0.1	0.3	-0.2	0.2	5.5	9.6	12.2	12.2	9.5	8.3	3.9	-1.6
1962	-1.3	-0.9	-4.7	2.4	4.9	7.5	9.5	10.6	8.5	4.5	2.0	-1.8
1963	-2.3	-3.5	-2.3	2.3	8.2	8.8	10.5	12.4	10.0	6.0	0.8	0.6
1964	1.9	-1.9	1.2	1.9	6.3	7.1	11.2	10.5	7.3	6.9	1.4	0.6
1965	-1.5	-1.3	-2.2	2.0	3.2	7.8	8.6	10.1	10.0	5.0	-0.3	-3.4
1966	-3.7	-6.7	-3.1	-0.7	2.9	9.0	11.7	10.4	5.4	2.8	2.7	-0.5
1967	-3.2	-0.9	0.8	1.7	5.8	8.4	10.6	11.3	10.5	4.0	4.1	-2.9
1968	-4.0	-2.1	-1.9	1.2	3.5	7.8	9.0	9.6	7.3	1.1	2.7	1.8
1969	-1.8	-2.6	-1.0	1.6	4.8	9.4	12.7	13.2	8.4	5.3	0.4	-0.4
1970	-0.7	-4.9	-0.6	0.7	5.7	9.9	12.0	12.0	8.2	5.6	-0.1	0.4
1971	-1.4	-2.5	-2.9	0.7	5.0	9.4	10.1	11.2	7.7	3.9	-0.7	1.3
1972	1.2	-0.4	-0.1	1.4	5.5	11.6	13.5	11.6	7.2	4.1	1.0	3.0
1973	0.6	-2.3	-0.6	0.8	5.1	9.1	12.5	9.8	6.5	1.5	-1.2	-2.6
1974	0.1	-1.5	0.8	2.6	5.8	10.5	12.6	11.1	9.4	3.3	0.7	0.3
1975	-1.6	0.7	0.9	0.9	5.2	6.5	9.2	9.5	7.5	4.6	2.2	-2.3
1976	-4.7	-0.1	-0.9	-0.1	6.5	8.5	10.7	10.9	5.6	3.5	0.6	-2.3
1977	-3.0	-3.6	-1.8	-1.0	3.4	6.7	10.8	10.7	6.6	4.5	2.4	0.0
1978	-3.5	-4.1	-3.0	0.2	4.1	10.2	11.9	11.2	6.7	2.5	1.1	-3.9
1979	-3.4	-2.3	-1.6	0.8	4.7	8.6	12.4	11.7	7.5	3.2	0.8	-0.2
1980	-2.4	-2.5	-1.7	2.7	5.8	10.7	11.1	12.6	8.6	2.9	-1.1	-2.7
1981	-3.9	-2.5	-5.2	0.2	4.5	6.1	10.5	10.4	8.1	3.8	0.0	-3.7
1982	-3.7	0.8	-0.1	1.2	4.7	5.6	11.2	10.6	6.8	4.7	1.4	-0.4
1983	-1.3	-0.9	-0.9	2.8	7.0	8.1	10.6	9.2	8.8	3.3	-1.3	-1.9
1984	-3.0	0.8	-1.8	3.0	7.4	8.9	9.1	10.6	7.5	4.5	1.3	2.4
1985	-1.6	-5.2	-0.5	-0.7	4.3	7.5	12.8	12.6	7.1	4.7	0.3	-3.7
1986	-4.4	-2.5	0.2	0.0	7.1	9.5	10.4	10.2	6.2	4.9	1.9	-4.5
1987	-3.6	-4.5	-1.7	1.3	4.5	6.6	9.3	9.4	7.8	7.3	0.5	-2.4
1988	-1.4	-2.9	-2.7	-1.2	4.9	8.6	12.4	11.0	8.7	3.8	0.1	-1.6
1989	0.8	-0.8	0.6	3.9	5.6	9.3	9.6	12.5	8.0	3.8	2.5	-1.9
1990	-0.3	1.4	0.1	2.7	4.5	10.0	12.6	12.8	9.5	6.0	0.2	1.9
1991	0.5	-1.1	-0.8	2.8	4.6	10.1	10.9	11.7	6.6	5.1	1.6	1.5
1992	0.5	0.5	0.8	0.7	6.0	10.1	10.5	11.2	9.4	1.1	0.5	1.8
1993	0.2	-0.4	0.2	1.8	5.5	6.8	13.3	12.3	7.0	2.4	3.0	-2.0
1994	-3.8	-1.6	-0.5	3.1	5.1	7.9	10.6	11.4	7.8	3.2	1.0	1.3
1995	-0.5	-1.9	-0.3	0.3	5.1	8.5	9.7	9.4	7.4	3.6	-0.1	-2.1
1996	1.0	-4.1	-0.3	0.5	3.8	8.4	10.1	12.4	7.7	5.1	-0.3	-2.3
1997	-2.2	-2.3	-1.6	-0.8	4.3	10.2	11.7	13.0	9.2	3.4	0.9	0.8
1998	-1.5	-2.4	-2.2	0.7	4.8	9.0	13.6	12.5	8.5	4.6	-0.3	0.0
1999	-1.4	-2.4	-0.9	1.8	6.0	9.9	10.7	9.6	9.7	5.7	4.0	-1.9
2000	-0.5	-1.4	-1.5	0.3	6.3	7.9	10.1	10.6	9.0	7.5	2.7	-0.7
2001	0.5	-3.6	-3.5	0.6	4.9	9.5	10.9	11.1	9.7	5.0	1.3	-0.6

Table A.2: Monthly mean temperature data from Andenes (°C) (KNMI, 2008)

A.2 Andenes Precipitation

	Jan	Feb	Mar	Apr	May	Jun	Jul	Aug	Sep	Oct	Nov	Dec
1910	87	39	40	36	35	48	12	37	109	106	8	55
1911	76	46	70	62	29	50	62	63	85	83	37	50
1912	98	59	13	67	17	28	37	29	112	39	64	23
1913	23	44	61	46	36	54	44	68	121	103	41	84
1914	72	37	29	73	93	65	3	54	102	61	98	70
1915	54	26	94	47	100	69	56	38	72	60	50	37
1916	79	54	42	28	15	11	38	56	142	52	39	27
1917	89	77	66	26	88	92	88	35	92	74	110	137
1918	159	121	76	27	59	16	22	9	77	114	178	34
1919	25	45	51	51	20	54	32	80	158	98	48	33
1920	65	109	66	32	53	27	76	80	72	102	99	94
1921	87	117	53	76	133	74	48	94	127	148	76	60
1922	46	36	81	22	50	41	25	20	129	96	100	47
1923	62	93	71	33	70	60	105	18	50	63	60	96
1924	48	69	51	49	39	18	29	82	120	81	144	110
1925	68	50	35	49	39	55	37	37	70	106	146	57
1926	57	62	63	49	34	23	81	44	118	100	65	98
1927	38	89	49	20	47	37	4	52	60	84	29	82
1928	37	58	53	83	46	36	73	60	87	70	38	59
1929	99	32	98	33	24	22	38	33	97	76	46	28
1930	98	95	44	49	35	67	22	37	106	86	76	53
1931	30	42	107	23	60	42	73	64	90	95	42	113
1932	152	94	98	34	20	17	34	77	190	44	97	155
1933	74	68	87	60	18	9	50	56	61	98	82	120
1934	132	93	28	57	49	60	5	10	30	98	133	45
1935	119	57	58	21	80	58	36	45	47	52	49	58
1936	29	40	71	45	40	44	36	57	81	76	114	102
1937	54	43	18	28	51	61	24	42	114	124	157	55
1938	51	100	87	128	56	36	46	75	114	71	96	28
1939	56	87	42	54	83	47	25	48	118	97	60	89
1940	95	64	56	115	16	36	23	120	64	96	47	89
1941	154	28	53	38	69	44	43	67	103	126	42	71
1942	47	49	81	67	45	30	50	97	57	53	147	121
1943	12	87	106	91	104	68	59	54	82	87	155	110
1944	87	52	56	103	43	62	28	72	51	81	32	59
1945	64	36	136	63	36	26	33	48	61	167	129	67
1946	106	87	49	51	51	20	39	15	96	149	98	89
1947	41	86	93	41	53	73	36	102	131	137	64	102
1948	55	48	66	50	66	62	40	70	122	96	189	196
1949	101	99	50	99	101	22	62	96	125	176	43	20
1950	56	56	68	60	61	65	15	38	44	80	44	44
1951	64	20	100	63	51	53	63	109	110	184	82	116
1952	78	64	38	58	45	42	70	74	116	13	53	51
1953	124	52	153	70	38	6	43	44	68	115	101	67
1954	80	38	94	53	27	61	22	67	77	82	33	83
1955	95	52	60	88	23	51	52	68	50	142	99	53
1956	96	56	54	72	103	101	5	23	81	116	55	48
1957	87	22	45	65	38	80	6	90	29	138	80	65
1958	79	74	64	43	20	52	47	35	115	108	118	71

1959	96	117	89	27	61	49	98	101	138	146	38	39
1960	89	55	66	48	49	59	62	34	41	60	23	76
1961	62	114	138	68	34	66	34	25	171	37	108	130
1962	67	85	83	57	29	41	28	6	79	250	101	80
1963	102	51	42	47	52	17	89	24	140	89	83	121
1964	173	86	46	36	39	88	88	65	103	148	151	94
1965	62	81	90	40	33	38	62	26	76	135	94	56
1966	52	48	63	32	96	55	46	121	80	66	76	17
1967	99	52	60	91	18	95	99	92	78	122	84	76
1968	51	110	130	68	46	71	88	121	35	74	98	77
1969	47	15	67	42	19	73	66	27	133	180	90	85
1970	58	58	32	48	22	42	39	51	101	146	68	103
1971	112	43	61	65	41	56	76	129	130	232	120	79
1972	38	60	69	63	19	11	101	97	248	174	123	178
1973	119	95	178	60	50	96	40	185	46	207	151	151
1974	90	90	51	105	37	21	71	78	112	56	33	90
1975	105	189	139	58	98	111	137	107	216	173	153	135
1976	56	111	28	114	55	27	91	81	87	49	122	50
1977	74	45	130	46	35	77	36	89	67	126	88	100
1978	80	75	37	39	115	39	17	45	59	143	200	57
1979	35	73	20	17	69	54	13	60	142	101	38	171
1980	110	90	52	89	61	43	15	11	136	64	96	120
1981	206	66	79	109	19	48	52	76	77	68	56	93
1982	107	128	107	100	41	68	78	48	133	134	87	156
1983	87	115	71	13	49	111	131	210	59	123	161	121
1984	44	75	95	52	85	61	109	111	31	30	66	58
1985	91	39	50	50	48	38	68	105	104	259	127	120
1986	39	95	69	63	30	144	34	29	53	223	96	52
1987	68	68	7	78	63	15	80	51	26	139	79	182
1988	97	12	27	170	19	38	61	20	147	204	208	157
1989	233	130	54	28	128	62	105	47	185	145	123	149
1990	91	142	148	110	124	44	35	73	52	140	75	179
1991	161	57	64	88	79	32	59	59	134	179	104	179
1992	219	101	135	32	103	49	132	66	50	173	45	246
1993	153	207	198	90	51	15	44	24	70	153	33	38
1994	92	91	88	65	47	52	86	84	131	232	161	117
1995	115	86	99	72	22	47	91	236	91	195	233	83
1996	90	55	38	100	35	94	10	96	155	260	98	94
1997	187	136	99	89	65	10	32	89	156	131	38	64
1998	115	167	98	36	79	28	17	81	89	147	106	162
1999	84	128	64	83	36	58	91	78	92	139	225	89
2000	197	157	202	65	93	37	26	64	96	45	22	114
2001	100	72	38	76	116	34	105	58	81	164	139	76

Table A.4: Monthly mean precipitation data from Andenes (mm) (KNMI, 2008)

A.3 Tornedalen Temperature Data

	Jan	Feb	Mar	Apr	May	Jun	Jul	Aug	Sep	Oct	Nov	Dec
1802	-15.2	-11.7	-7.6	-0.6	2.4	13.0	13.3	10.8	6.9	2.7	-8.9	-17.7
1803	-18.6	-12.7	-8.4	1.3	9.6	13.6	16.0	15.5	7.8	3.6	-5.0	-15.9
1804	-17.0	-17.9	-10.1	1.5	6.7	11.2	17.5	13.0	9.3	3.2	-5.5	-15.4
1805	-9.7	-15.9	-8.3	-2.9	3.8	10.6	14.5	14.0	8.3	-4.4	-10.8	-15.0
1806	-11.4	-9.2	-8.6	1.3	6.5	11.4	13.3	16.0	10.2	0.6	-8.4	-10.1
1807	-17.9	-9.6	-10.0	-5.5	2.8	13.3	16.4	14.2	6.5	-2.2	-9.2	-12.1
1808	-8.7	-14.7	-9.0	-4.7	6.3	16.5	16.4	13.4	7.5	7.5	-4.1	-15.8
1809	-22.7	-17.7	-11.7	-7.1	3.7	13.1	14.9	14.2	8.2	1.9	-8.2	-1.2
1810	-16.9	-15.5	-11.5	-4.1	0.6	11.9	12.8	13.0	6.3	-0.4	-11.6	-14.1
1811	-10.3	-15.5	-3.8	-5.4	3.7	12.5	15.1	10.6	7.0	-1.0	-6.5	-14.0
1812	-11.8	-9.7	-12.6	-3.4	3.9	10.1	14.3	12.3	5.6	0.8	-11.5	-18.4
1813	-11.3	-11.6	-5.6	0.7	3.6	10.9	17.2	12.9	9.8	-2.4	-2.5	-13.4
1814	-22.7	-9.5	-10.3	0.3	4.2	13.2	17.2	12.9	8.1	1.2	-6.9	-17.2
1815	NA	NA	NA	NA	NA	NA	NA	NA	NA	NA	NA	NA
1816	-11.6	-22.3	-13.1	-2.1	1.1	11.4	15.4	12.1	9.0	0.6	-5.1	-9.2
1817	-9.5	-15.1	-11.5	-1.9	6.4	10.8	16.4	12.6	7.7	-0.6	-6.9	-19.6
1818	-10.2	-17.3	-10.5	-4.4	-0.5	11.6	18.7	9.9	8.2	3.1	-2.5	-4.0
1819	-7.4	-11.7	-8.8	-2.6	5.0	14.3	17.1	13.8	9.7	0.6	-10.9	-14.8
1820	-21.3	-11.7	-8.3	-1.8	5.0	14.4	14.7	12.5	9.0	0.7	-7.8	-14.9
1821	-14.6	-10.8	-6.9	-0.6	5.8	8.3	12.6	11.3	7.8	5.9	-8.5	-10.3
1822	-13.7	-3.7	-0.9	1.9	6.7	11.1	14.5	15.1	8.4	1.7	-8.7	-5.8
1823	-18.0	-12.5	-2.9	-0.4	6.2	11.8	15.4	12.7	6.2	2.5	-7.9	-9.7
1824	-12.5	-6.9	-5.1	-1.3	4.3	12.7	14.5	11.7	8.9	-1.4	-7.9	-12.4
1825	-8.6	-10.3	-5.6	0.7	4.8	12.6	13.7	13.2	6.6	4.3	-2.5	-6.4
1826	-11.3	-5.7	-1.4	-1.3	8.0	15.0	18.8	15.4	7.7	4.9	-2.3	-6.9
1827	-14.0	-12.4	-7.1	0.4	7.2	14.9	13.7	11.3	10.0	-0.4	-7.0	-4.1
1828	-14.7	-13.3	-9.5	-2.7	7.9	12.8	13.9	12.2	4.7	2.9	-5.6	-9.0
1829	-12.2	-17.6	-13.0	-5.5	5.9	12.5	16.0	11.0	9.1	0.7	-7.0	-7.7
1830	-12.5	-11.0	-5.2	-2.1	3.4	11.7	14.6	11.3	7.1	1.2	-2.0	-12.6
1831	-18.7	-12.1	-11.8	-0.6	5.6	14.9	16.1	13.7	7.0	1.6	-3.2	-10.9
1832	-8.4	-1.6	-3.1	1.8	4.5	13.1	12.7	9.9	5.2	4.4	-3.3	-5.0
1833	-5.8	-12.7	-11.3	-2.8	5.9	11.5	14.8	10.1	8.5	5.9	-2.6	-12.4
1834	-18.6	-8.7	-7.2	-0.1	5.0	9.3	15.7	15.1	7.0	0.3	-10.4	-10.3
1835	-11.8	-10.9	-7.6	-1.9	2.6	11.7	14.2	11.8	9.7	4.8	-8.8	-20.1
1836	-15.4	-14.1	-6.2	1.3	4.4	9.5	14.7	11.2	3.7	0.7	-6.7	-9.2
1837	-14.4	-4.5	-11.8	-3.7	5.0	9.4	12.7	12.2	7.7	2.2	-0.2	-7.6
1838	-16.5	-19.3	-10.5	-3.6	5.4	9.6	14.3	12.0	8.7	0.5	-9.2	-9.0
1839	-12.0	-11.3	-14.4	-4.1	6.9	10.9	15.3	12.6	7.6	6.3	-3.8	-11.6
1840	-14.3	-6.2	-5.9	-0.4	4.1	11.8	13.7	14.5	7.1	0.5	-5.3	-10.6
1841	-17.2	-12.6	-6.1	0.4	6.4	12.1	13.2	13.9	6.8	-1.0	-7.8	-5.3
1842	-8.0	-3.9	-7.0	-1.8	5.9	11.5	13.9	15.4	6.5	0.0	-12.1	-6.0
1843	-5.2	-11.8	-10.6	-5.4	3.7	9.9	15.5	16.5	8.6	-1.9	-4.8	-7.1
1844	-8.6	-19.0	-8.5	1.5	7.3	11.5	14.4	16.1	8.8	2.5	-6.8	-10.5
1845	-6.0	-17.8	-11.0	-4.2	3.7	11.0	15.3	15.1	8.4	0.0	-1.3	-8.4
1846	-13.6	-17.2	-4.4	-0.7	3.2	11.7	14.2	16.7	8.0	5.8	-2.0	-10.9
1847	-10.3	-16.4	-6.0	-5.6	2.8	14.0	14.8	15.6	9.9	2.4	0.8	-4.0
1848	-8.3	-8.8	-4.4	-0.1	5.1	10.3	12.5	13.0	8.2	0.5	-9.9	-11.3
1849	-19.9	-9.5	-9.0	-2.4	4.1	10.1	14.2	13.7	7.2	-0.1	-5.9	-11.7

1850	-17.7	-12.0	-11.4	-0.9	4.9	10.6	14.8	13.6	7.7	1.6	-7.0	-9.5
1851	-9.6	-10.1	-10.5	-0.5	4.2	11.6	14.9	12.3	9.2	4.0	-4.7	-5.8
1852	-16.3	-12.3	-5.0	-3.6	6.0	14.0	16.6	14.1	9.2	-3.0	-10.4	-12.2
1853	-9.0	-13.7	-14.6	-4.3	5.7	14.3	16.7	11.7	9.1	1.3	0.5	-7.7
1854	-12.7	-12.2	-3.2	-1.5	6.2	13.7	16.3	15.7	6.8	1.9	-5.8	-6.8
1855	-13.5	-18.2	-8.9	-0.8	4.9	13.2	17.8	12.3	6.5	-0.5	-5.5	-15.9
1856	-16.8	-13.9	-9.7	-1.8	2.6	10.4	14.0	10.3	6.5	0.9	-11.2	-16.5
1857	-18.7	-8.6	-6.1	-1.9	5.2	10.9	14.2	14.6	5.2	1.1	-4.8	-8.2
1858	-7.6	-10.1	-6.5	-1.3	7.9	14.5	18.8	13.9	8.1	1.1	-9.3	-10.7
1859	-8.7	-7.6	-8.0	-2.9	6.7	12.9	14.4	12.1	8.9	-0.2	-3.8	-8.4
1860	-12.8	-14.7	-6.6	-1.2	3.9	13.4	15.4	14.0	7.4	1.2	-3.4	-14.8
1861	-15.2	-11.6	-4.6	-2.1	2.7	13.3	18.5	15.4	6.8	3.9	-7.5	-5.2
1862	-18.7	-17.7	-12.8	-1.3	4.1	11.5	12.9	10.2	7.3	2.6	-0.5	-9.1
1863	-7.4	-4.9	-6.5	-1.4	3.2	13.3	12.9	11.5	9.8	3.3	-3.5	-9.6
1864	-9.5	-11.4	-9.6	-2.5	2.2	10.5	16.0	10.3	7.0	-4.5	-12.3	-6.6
1865	-11.1	-16.2	-12.1	-0.8	3.7	10.4	16.1	11.5	7.5	-1.4	-3.3	-5.1
1866	-8.7	-16.3	-14.4	-1.4	2.3	11.1	12.5	14.8	10.5	2.9	-7.8	-13.5
1867	-19.9	-10.6	-10.8	-6.9	-0.8	7.9	14.3	12.8	7.0	3.0	-10.8	-17.3
1868	-14.3	-14.0	-4.5	-1.6	6.0	12.0	14.9	15.3	6.8	2.0	-5.0	-12.3
1869	-9.1	-8.7	-7.5	-1.1	3.5	11.8	14.9	12.0	8.3	-1.1	-4.7	-6.5
1870	-10.8	-12.3	-9.0	-0.2	4.3	13.1	15.9	12.3	9.2	-0.2	-6.8	-14.4
1871	-13.7	-24.3	-3.1	-4.5	3.4	9.5	15.6	12.7	5.7	2.2	-8.7	-14.5
1872	-7.5	-7.5	-7.8	-0.8	4.6	14.2	16.1	12.3	4.9	3.5	-2.9	-11.6
1873	-9.8	-11.9	-8.2	-3.6	3.1	12.6	16.2	13.6	10.0	1.7	-4.2	-9.9
1874	-4.6	-6.6	-7.1	-0.8	2.9	9.3	13.8	12.1	8.1	5.6	-6.7	-14.8
1875	-18.6	-9.9	-8.0	-3.1	6.1	11.0	15.3	11.5	6.1	-0.8	-8.6	-13.6
1876	-11.0	-13.0	-7.9	-3.4	1.8	13.6	15.7	12.9	8.6	1.2	-6.8	-18.8
1877	-14.0	-14.9	-12.2	-5.3	2.1	9.0	15.1	10.6	4.7	0.0	0.5	-1.5
1878	-9.1	-8.2	-6.8	0.0	5.3	12.9	12.9	12.4	9.1	4.4	-4.0	-9.1
1879	-8.9	-14.0	-9.2	-1.9	4.2	10.4	15.4	15.2	10.0	1.1	-10.6	-8.1
1880	-8.8	-8.0	-6.5	-1.4	4.1	9.9	13.3	14.3	9.1	-4.5	-9.4	-14.0
1881	-14.9	-18.9	-12.7	-4.4	2.1	10.0	13.2	13.3	7.1	1.0	-3.4	-6.7
1882	-5.3	-8.3	-6.1	-1.8	5.1	10.7	14.1	16.1	9.3	2.9	-10.5	-12.8
1883	-11.3	-8.3	-7.2	0.7	6.4	15.3	15.0	12.8	6.8	1.6	1.0	-5.1
1884	-9.7	-9.1	-5.2	-2.7	2.8	11.6	15.2	12.0	9.7	4.2	-3.5	-11.3
1885	-13.3	-7.4	-7.4	-1.4	2.3	8.8	14.6	12.2	5.9	-1.2	-6.8	-10.8
1886	-15.8	-10.7	-7.4	-0.1	4.1	12.4	16.9	14.6	7.2	3.6	-0.5	-8.7
1887	-4.3	-3.6	-5.7	-1.0	6.2	11.7	14.3	12.9	9.5	-0.9	-5.7	-15.4
1888	-13.1	-16.0	-14.7	-5.3	3.3	10.0	14.3	12.6	7.5	-1.0	-8.9	-8.3
1889	-8.2	-14.8	-11.0	-1.1	7.0	14.1	13.8	13.2	8.0	4.1	0.6	-3.4
1890	-7.0	-6.7	-3.7	-0.6	6.8	12.8	14.0	13.7	9.7	0.3	-6.0	-6.4
1891	-12.0	-4.1	-8.9	-1.3	4.4	9.3	15.7	12.3	6.9	2.4	-4.6	-7.2
1892	-16.0	-15.0	-6.8	-3.2	3.3	10.0	13.4	11.8	8.0	0.0	-0.7	-12.0
1893	-17.0	-21.4	-11.4	-1.6	3.2	11.3	14.1	11.8	5.2	3.5	-6.4	-5.9
1894	-8.1	-7.9	-4.5	1.0	6.8	16.9	15.9	14.3	5.0	-1.4	-2.7	-6.5
1895	-14.6	-16.1	-10.3	-1.1	6.8	13.5	14.6	13.3	7.6	1.6	-3.0	-4.8
1896	-9.4	-6.8	-5.4	-1.0	5.3	12.5	18.5	13.0	8.2	1.8	-6.2	-10.1
1897	-10.8	-12.4	-11.3	1.1	9.2	11.7	15.8	12.9	9.0	4.0	-3.2	-8.7
1898	-6.4	-13.4	-9.7	-1.9	4.6	12.5	15.4	12.7	8.2	1.8	-4.0	-13.5
1899	-14.1	-15.0	-13.2	-2.5	2.4	11.6	17.1	10.2	8.7	1.2	-3.5	-9.3
1900	-11.9	-19.1	-9.2	-3.0	2.6	12.0	11.5	12.4	5.7	2.5	-2.1	-13.5
1901	-6.8	-17.8	-7.6	-0.6	4.4	14.4	17.9	14.0	9.2	6.0	-7.6	-13.8
1902	-15.1	-13.7	-12.1	-4.6	3.0	9.0	11.8	11.9	5.9	-2.1	-4.7	-7.9

1903	-12.2	-7.6	-3.0	-0.2	5.1	11.2	12.8	13.1	8.0	-1.8	-3.3	-4.9
1904	-4.2	-14.7	-9.6	-0.1	3.8	10.9	13.0	12.4	8.3	4.1	-7.3	-13.8
1905	-11.7	-10.3	-5.7	-3.5	5.3	13.8	15.3	12.8	7.4	-0.6	-3.6	-6.7
1906	-6.9	-8.2	-10.6	0.7	5.9	12.9	16.4	11.1	7.0	2.5	-4.6	-7.0
1907	-14.0	-6.5	-3.9	0.4	3.8	12.9	13.8	11.1	6.8	3.4	-0.2	-11.3
1908	-10.4	-10.6	-8.3	0.7	4.2	9.6	14.2	14.0	6.9	4.1	-7.2	-5.6
1909	-5.4	-12.0	-7.7	-4.1	2.2	11.5	15.2	12.4	8.7	5.0	-8.0	-8.2
1910	-10.1	-4.5	-4.9	-0.2	5.4	10.8	13.8	11.8	7.6	0.4	-4.6	-8.2
1911	-8.1	-12.9	-4.7	-1.5	5.7	9.7	13.8	14.1	8.3	0.1	-3.6	-3.7
1912	-14.9	-17.9	-5.5	-2.8	5.2	12.6	15.0	13.4	6.7	-0.6	-4.0	-7.6
1913	-12.1	-10.0	-6.8	0.0	5.6	11.4	17.3	13.6	8.2	0.0	-1.6	-9.9
1914	-11.3	-9.6	-6.9	0.5	4.6	11.4	17.2	11.5	7.7	1.1	-3.9	-5.2
1915	-12.9	-10.2	-11.7	-1.7	3.4	9.7	17.5	12.3	6.2	0.6	-8.2	-19.2
1916	-9.3	-7.9	-9.9	-0.9	3.8	11.3	18.1	11.2	6.3	-1.3	-1.2	-7.4
1917	-14.5	-14.5	-13.1	-2.8	2.7	12.2	13.7	16.2	7.7	3.9	-4.7	-8.8
1918	-15.9	-9.5	-5.2	-1.0	4.0	11.4	16.1	11.2	7.6	3.9	1.0	-7.4
1919	-8.7	-16.2	-7.8	-1.8	6.3	13.8	17.6	11.9	8.5	0.6	-7.0	-11.8
1920	-12.1	-7.4	-1.6	0.3	6.7	11.8	15.6	13.3	10.5	1.2	-0.2	-5.9
1921	-12.1	-11.1	-3.4	2.7	7.0	12.2	13.3	13.7	7.8	0.1	-9.4	-8.5
1922	-13.2	-12.8	-7.7	-1.2	5.4	13.7	15.7	12.5	9.2	0.5	-4.7	-11.4
1923	-6.2	-13.1	-5.4	-3.0	3.5	8.6	14.5	11.1	8.4	1.9	-3.9	-8.4
1924	-8.9	-13.7	-8.8	-1.9	4.4	9.9	17.1	15.7	10.3	5.3	-2.7	-4.3
1925	-2.3	-6.5	-9.8	0.3	5.7	12.6	19.6	13.6	8.1	0.8	-7.6	-11.6
1926	-13.5	-14.5	-5.7	-1.8	4.8	11.4	15.4	14.6	7.4	-1.1	-2.6	-10.8
1927	-12.6	-9.9	-6.2	-0.9	4.8	12.0	19.5	15.0	6.9	-1.1	-9.8	-9.9
1928	-9.3	-10.5	-5.2	-0.6	6.0	10.0	12.9	13.2	7.8	0.3	-5.1	-7.5
1929	-10.6	-15.0	-4.4	-3.9	4.9	12.2	13.5	12.6	8.3	3.0	0.7	0.1
1930	-3.3	-8.2	-5.7	0.2	8.1	13.5	17.8	15.2	5.6	2.4	-3.5	-7.2
1931	-11.8	-10.8	-8.0	-0.4	6.3	8.7	16.6	13.6	5.3	1.9	0.4	-6.1
1932	-4.6	-8.4	-6.1	0.3	4.9	10.5	16.7	13.9	7.9	0.0	-1.3	-1.0
1933	-6.7	-12.7	-8.5	-1.6	5.1	13.8	16.4	13.2	7.8	2.5	-6.2	-7.7
1934	-3.1	-8.8	-5.4	-2.1	6.9	12.1	18.0	15.3	12.0	3.4	-1.7	-4.5
1935	-8.2	-9.5	-6.9	-0.9	3.1	12.1	15.8	12.5	6.7	2.6	0.5	-4.1
1936	-10.5	-17.6	-9.6	-0.8	8.1	16.1	16.0	14.6	7.9	0.3	-0.3	-1.0
1937	-6.0	-13.3	-6.7	1.3	8.7	14.0	18.5	17.2	8.1	4.7	-1.3	-8.5
1938	-7.7	-3.9	-4.0	0.1	5.6	12.8	18.5	15.8	10.1	5.2	1.5	-2.7
1939	-9.2	-6.4	-5.8	-1.6	5.4	11.9	16.4	16.8	7.3	0.6	-0.5	-9.0
1940	-16.2	-14.2	-12.7	-1.9	7.4	12.8	15.3	13.4	9.3	3.7	-4.2	-9.7
1941	-14.8	-11.3	-9.6	-2.9	4.7	11.3	19.2	13.4	7.1	-1.2	-5.0	-15.1
1942	-17.0	-14.2	-11.4	-0.3	4.2	11.3	16.0	13.7	8.2	1.9	-3.1	-8.3
1943	-12.9	-4.9	-3.5	0.3	5.9	13.7	15.6	13.1	8.9	3.1	-0.4	-3.5
1944	-7.9	-7.2	-6.4	-3.4	4.0	11.0	15.9	13.4	8.7	5.3	-0.8	-2.1
1945	-12.5	-7.4	-7.5	0.9	5.7	12.1	17.4	15.9	7.0	-1.4	-3.9	-12.2
1946	-7.1	-13.6	-9.2	0.0	6.0	12.4	17.3	14.2	10.1	1.5	-3.5	-1.8
1947	-8.5	-18.0	-14.0	-0.8	6.3	14.2	17.2	13.5	10.2	2.1	-5.3	-8.8
1948	-14.4	-10.0	-4.3	1.3	7.2	11.9	16.2	11.3	8.6	1.9	-2.5	-3.2
1949	-5.9	-4.5	-6.7	-0.3	6.5	11.4	14.0	12.5	10.6	2.0	0.0	-6.0
1950	-16.5	-10.7	-5.8	1.5	6.7	13.3	15.7	15.6	8.8	4.8	-2.7	-6.3
1951	-15.1	-10.0	-8.1	0.3	3.6	10.3	13.1	16.0	9.3	6.0	-5.2	-5.8
1952	-8.2	-6.4	-9.4	-0.1	4.8	11.7	14.6	11.4	6.4	-1.4	-5.2	-9.9
1953	-10.6	-14.1	-4.0	0.6	5.6	17.1	15.0	13.1	7.0	4.5	0.0	-1.6
1954	-8.6	-15.2	-3.7	-1.3	8.5	10.3	16.1	13.9	9.4	0.9	-3.8	-2.3
1955	-12.9	-15.7	-8.7	-3.9	3.3	9.8	15.9	14.8	10.2	1.0	-7.6	-17.5

1956	-13.5	-16.2	-9.6	-4.4	4.7	12.4	15.0	11.4	7.6	0.7	-10.3	-8.6
1957	-7.0	-8.6	-9.5	-1.5	4.4	10.1	18.3	14.3	8.0	2.8	-2.2	-9.1
1958	-15.3	-13.2	-9.3	-2.9	4.1	12.1	13.7	14.3	8.7	3.2	1.2	-12.9
1959	-12.5	-5.3	-2.1	-1.3	6.6	12.2	15.5	14.2	6.8	2.2	-3.2	-8.8
1960	-14.2	-13.3	-6.7	-0.7	9.8	14.1	18.3	14.8	8.5	-2.4	-5.0	-6.5
1961	-9.3	-5.9	-3.6	-2.4	5.6	14.2	17.2	13.4	8.7	7.9	0.2	-10.4
1962	-11.1	-9.3	-14.5	1.2	6.1	10.8	13.3	11.4	7.4	4.0	-1.3	-12.2
1963	-13.7	-13.3	-11.5	0.1	8.3	11.6	14.2	14.4	10.8	3.3	-4.5	-7.9
1964	-4.5	-12.4	-8.4	-1.2	6.3	10.4	14.6	13.5	7.4	5.8	-3.4	-8.4
1965	-10.1	-10.1	-8.2	-1.0	3.7	12.1	13.8	11.8	9.8	2.8	-8.0	-13.0
1966	-19.0	-20.9	-11.9	-3.2	4.7	14.4	16.0	12.9	5.8	1.0	-0.2	-7.6
1967	-18.4	-7.6	-2.3	0.0	5.9	12.1	14.8	15.1	10.3	3.0	1.2	-16.5
1968	-18.5	-15.2	-5.7	-0.2	3.5	12.7	14.1	12.5	6.1	-2.8	-6.4	-3.3
1969	-13.2	-17.0	-10.1	-1.2	4.9	13.4	15.5	15.7	7.8	3.5	-4.7	-8.6
1970	-11.6	-18.0	-5.0	-2.5	6.0	14.7	16.5	14.5	8.0	2.4	-6.6	-6.4
1971	-8.9	-11.5	-11.3	-2.2	5.5	13.0	14.6	13.5	7.4	1.5	-8.3	-6.6
1972	-10.5	-10.1	-5.6	0.3	5.4	14.5	18.8	14.3	8.2	2.4	-5.8	-1.1
1973	-4.5	-8.6	-4.8	0.0	5.8	14.1	19.4	12.7	5.5	-1.5	-6.8	-14.2
1974	-6.4	-5.9	-4.6	0.8	5.7	14.5	15.6	13.9	10.8	2.1	-3.7	-3.3
1975	-7.6	-5.2	-2.1	0.0	7.2	11.1	14.1	12.4	9.9	3.0	-1.4	-8.4
1976	-15.6	-9.0	-8.9	-0.6	8.0	12.1	14.1	14.1	5.3	-0.1	-4.6	-8.7
1977	-10.0	-13.3	-5.0	-1.9	4.8	11.1	14.2	12.6	6.8	1.8	-3.3	-7.6
1978	-10.9	-16.0	-5.9	-1.5	7.7	12.7	14.6	12.5	7.2	1.4	-4.8	-18.1
1979	-15.9	-13.3	-4.4	-1.3	5.2	13.4	16.3	14.6	8.0	0.5	-2.1	-6.8
1980	-13.3	-15.1	-9.3	1.6	6.1	15.3	16.7	13.6	9.1	1.0	-8.9	-11.8
1981	-10.0	-12.7	-12.4	-0.1	5.2	9.9	15.1	12.2	7.3	2.8	-3.9	-15.7
1982	-16.5	-7.6	-3.2	0.3	5.3	9.8	15.5	13.9	8.2	2.3	-0.7	-6.0
1983	-7.7	-10.9	-5.6	2.1	8.4	12.3	15.7	12.4	9.3	2.5	-9.1	-10.8
1984	-12.7	-6.2	-9.1	0.8	9.3	13.4	14.3	12.8	6.9	3.2	-3.7	-5.3
1985	-20.2	-21.2	-7.0	-2.4	4.6	12.9	16.0	14.0	8.2	3.4	-5.0	-16.3
1986	-15.8	-12.9	-2.6	-0.9	6.1	14.7	15.1	10.7	5.3	3.9	-0.1	-13.8
1987	-19.4	-13.2	-9.1	-1.1	5.7	11.9	14.0	11.0	7.5	6.8	-4.7	-12.2
1988	-8.7	-9.7	-5.6	-1.3	6.7	14.8	18.3	13.3	9.7	2.4	-6.6	-11.0
1989	-5.6	-6.1	-1.4	2.2	7.1	13.3	14.8	14.0	9.5	1.4	-2.3	-9.8
1990	-12.7	-1.4	-3.7	1.0	7.0	13.1	15.7	14.4	7.6	3.4	-6.7	-3.2
1991	-8.8	-14.3	-6.3	0.8	4.9	11.3	16.0	15.1	6.8	3.2	-0.3	-4.1
1992	-5.4	-4.5	-1.7	-1.9	7.4	14.0	13.3	11.4	9.8	-4.7	-6.2	-2.0
1993	-6.9	-6.7	-4.1	-1.0	7.5	10.4	15.9	12.7	4.7	-0.1	-1.8	-8.2
1994	-13.9	-16.2	-6.8	2.0	5.2	12.6	16.4	14.4	8.0	1.8	-3.9	-2.9
1995	-6.9	-6.2	-2.4	-0.5	5.1	14.6	13.8	13.4	7.8	3.9	-6.6	-12.6
1996	-6.7	-12.8	-5.7	-0.4	5.1	11.6	14.3	16.0	7.7	4.4	-2.4	-9.5
1997	-8.9	-8.3	-3.8	-2.0	4.8	13.7	18.5	15.2	9.4	0.5	-3.9	-7.0
1998	-8.1	-12.6	-7.9	-1.5	6.0	12.4	16.6	12.7	8.5	2.9	-5.5	-7.6
1999	-13.1	-10.9	-5.2	1.7	5.4	14.0	15.8	11.9	9.9	3.7	0.6	-10.3
2000	-8.2	-7.6	-4.8	1.1	7.7	12.7	16.7	13.8	8.7	6.3	0.8	-6.3
2001	-5.6	-12.2	-8.3	0.6	6.2	14.4	16.4	13.9	10.1	3.3	-4.1	-10.4

Table A.6: Monthly mean temperature data from Tornedalen (°C) (Klingbjer and Moberg, 2003)

A.4 Northern Coastal Temperature

	Jan	Feb	Mar	Apr	May	Jun	Jul	Aug	Sep	Oct	Nov	Dec
1875	-1.29	0.33	0.16	-1.59	0.55	-0.51	-0.24	-1.22	-1.23	-0.41	-0.34	0.01
1876	1.66	0.05	-1.20	-1.03	-2.06	0.88	0.43	-0.72	0.30	-0.55	-1.61	-1.05
1877	0.13	-1.06	-1.70	-1.64	-1.59	-1.17	-0.03	-1.70	-1.33	-1.30	1.33	1.10
1878	1.10	0.67	-0.53	0.04	-0.38	-0.08	-0.65	-1.50	0.37	0.64	-0.54	-0.64
1879	0.78	-0.98	-0.03	-1.02	-0.88	-1.26	0.40	1.30	0.89	-1.01	-0.79	0.41
1880	1.55	0.33	0.05	-0.81	-1.57	-1.43	-0.73	0.50	0.86	-3.01	-1.67	-1.16
1881	-1.74	-1.46	-1.86	-3.00	-2.99	-1.81	-0.96	-0.03	0.11	-0.09	0.19	0.75
1882	1.13	-0.24	-0.50	-0.95	-0.77	-0.07	0.77	1.30	1.56	0.81	-1.20	-0.88
1883	0.97	1.06	-0.51	1.90	0.13	0.95	0.69	0.46	-0.04	0.06	0.95	0.83
1884	0.50	1.19	1.25	-0.77	-1.17	-0.29	0.02	1.13	1.30	0.14	0.38	-0.31
1885	0.40	0.63	-0.20	-0.26	-2.04	-1.62	-0.79	-1.19	-0.66	-1.73	-0.67	-0.38
1886	-1.51	0.69	0.69	0.04	-0.37	0.23	-0.48	0.19	-0.52	1.09	1.65	-1.00
1887	2.01	1.68	-0.19	-0.84	-0.88	-1.77	-0.82	-0.67	1.00	-1.62	-0.48	-1.18
1888	0.24	-0.40	-2.70	-2.06	-1.33	-1.45	-0.83	-0.66	-1.34	-1.85	-0.31	0.97
1889	0.83	-0.92	-1.44	-0.35	0.39	0.60	-0.30	-0.59	-0.19	0.63	2.09	1.59
1890	1.31	1.17	0.76	0.41	0.44	0.19	-0.92	0.08	0.73	-1.44	0.51	1.51
1891	0.58	1.57	-1.34	0.21	-1.00	-2.37	-0.53	-1.24	-1.19	0.79	0.36	0.86
1892	-0.63	-0.83	0.44	-0.98	-2.24	-2.10	-1.39	-2.14	-0.40	-1.53	1.40	-0.85
1893	-1.05	-1.98	-1.68	-1.38	-1.29	-0.67	-1.66	-1.64	-2.74	-0.30	-1.40	0.71
1894	0.79	0.34	0.40	2.56	0.19	1.56	0.39	-0.41	-1.73	-1.35	0.50	0.08
1895	-0.60	-0.40	-1.31	-0.73	0.17	0.25	-0.10	-0.32	-0.84	-0.62	1.01	0.87
1896	0.23	1.05	0.24	0.17	-1.00	-0.89	0.68	-0.76	0.42	-1.00	-0.48	0.43
1897	0.45	-0.73	-1.89	1.62	0.71	-0.85	-1.19	-0.10	0.20	1.05	-0.12	0.67
1898	1.37	-0.52	-0.68	0.60	0.31	0.13	-0.39	-0.49	0.45	-0.18	-0.10	-0.72
1899	-1.20	-0.44	-2.66	-2.52	-2.50	-0.24	0.70	-2.58	0.40	-0.96	0.60	-0.12
1900	0.28	-2.26	-0.73	-1.08	-2.14	-1.08	-2.42	-1.31	-1.41	-0.61	1.00	-0.75
1901	2.42	-1.22	-0.91	0.31	-1.13	0.04	0.16	0.25	1.45	1.70	-0.95	-0.91
1902	-0.46	-0.32	-1.49	-0.49	-1.12	-2.22	-1.74	-0.98	-1.44	-1.63	0.41	0.80
1903	0.96	0.88	1.26	-0.47	-0.68	-1.51	-1.51	-0.07	-0.16	-2.68	0.42	0.92
1904	1.98	-1.47	0.67	1.30	-1.56	-1.06	-1.26	-1.04	0.53	0.54	-1.90	-1.04
1905	-0.05	0.03	-0.14	-1.06	-0.64	-0.48	0.02	0.31	0.03	-1.72	-1.15	0.84
1906	1.11	-0.20	-2.13	0.04	-1.45	-1.09	-0.07	-1.89	-0.33	-0.09	0.15	-0.26
1907	-0.02	0.56	0.76	0.49	-1.72	0.76	-0.84	-1.59	-1.73	0.68	1.74	-0.45
1908	0.88	-0.26	0.23	-0.51	-1.84	-1.51	-0.72	-0.43	-0.37	1.30	-1.46	0.69
1909	1.86	0.24	-1.41	-0.79	-2.53	-1.38	-0.62	-0.78	-0.45	0.00	-1.90	-0.40
1910	0.08	1.49	1.13	-0.30	-0.08	-0.60	-1.03	-0.95	-0.69	-0.72	-1.48	0.20
1911	1.11	0.02	0.04	-0.89	-0.32	-1.34	-0.88	0.02	0.47	-1.46	0.03	1.40
1912	-0.57	-1.55	0.33	-1.05	-1.25	-0.16	-0.59	0.30	-1.03	-0.97	-0.14	-0.07
1913	0.46	0.34	0.19	0.46	-0.35	-1.38	-0.23	0.09	-0.39	-1.31	1.48	-0.27
1914	0.38	0.48	-0.02	0.45	-1.29	-0.53	0.49	0.20	0.10	0.04	0.54	0.38
1915	-0.51	-0.57	-1.74	-0.31	-2.34	-2.30	0.35	-0.14	-1.59	-0.09	-1.53	-2.54
1916	0.49	0.51	-1.59	-0.13	-0.81	-0.18	1.74	-0.52	-0.99	-1.81	0.81	-0.47
1917	-0.07	-0.97	-1.77	-2.67	-2.94	-0.40	-1.60	1.02	-0.42	-0.42	-0.26	-0.44
1918	-1.75	0.33	0.66	0.32	-0.91	0.05	1.28	-0.62	-0.27	0.23	1.92	0.06
1919	1.06	-0.96	-1.00	-1.73	0.66	0.69	-0.18	-1.30	-0.43	-1.48	-1.63	-0.92

1920	0.32	0.77	1.44	0.89	0.77	-0.79	0.29	-0.12	1.61	0.51	1.56	1.03
1921	-0.64	0.63	0.93	1.88	-0.03	-0.85	-0.99	-0.23	-0.70	-1.22	-0.73	0.01
1922	-0.17	0.26	-1.08	0.07	0.51	0.70	1.56	0.91	0.42	-0.35	-0.42	-0.66
1923	0.81	0.03	1.28	-0.76	-0.54	-2.22	-0.32	-1.09	0.10	-0.29	-0.43	-0.14
1924	1.00	-0.80	-1.45	-1.10	-0.82	-0.88	1.11	1.72	0.98	1.42	0.73	1.22
1925	2.40	0.34	-1.51	0.80	-0.18	0.14	1.33	1.06	1.02	-1.78	-1.40	-0.99
1926	0.40	0.08	-0.09	-0.16	-0.79	-0.10	-0.30	0.00	-0.03	-2.12	0.29	-0.46
1927	-0.39	0.52	0.11	-0.89	-1.21	-0.28	2.19	1.81	-0.20	-1.43	-0.87	0.06
1928	0.90	0.87	0.70	0.19	-0.84	0.17	-0.74	0.25	-0.26	-0.88	-0.34	0.51
1929	0.11	0.52	0.26	-2.49	0.14	-0.33	-1.29	-0.65	0.44	-0.51	1.35	2.01
1930	1.58	0.94	-0.25	1.57	0.75	0.79	1.82	2.51	-0.70	0.07	-0.09	1.18
1931	0.21	0.33	-0.95	0.44	-0.07	-1.31	1.02	-0.82	-1.57	-0.98	1.87	0.82
1932	1.36	0.89	-0.11	-0.34	-1.18	-0.71	0.30	-0.57	-1.26	-1.09	0.68	1.98
1933	1.95	-0.75	-0.34	-1.51	-0.85	1.34	0.47	0.43	1.26	0.11	0.42	0.65
1934	2.19	0.29	0.75	-0.59	0.29	-0.99	2.21	2.70	3.04	0.43	0.79	0.97
1935	0.83	0.31	0.19	0.21	-2.13	-0.89	-0.37	0.47	-0.87	-0.03	1.49	1.01
1936	-0.53	-1.11	-0.20	-0.43	0.91	0.83	1.10	0.70	0.11	-0.58	1.41	1.32
1937	1.38	-0.73	-0.78	2.77	0.98	0.42	2.33	1.70	0.62	1.07	0.60	-0.26
1938	1.10	1.55	0.27	-0.20	-0.53	0.49	1.57	0.62	1.46	2.04	1.98	1.31
1939	-0.07	0.96	0.32	-0.85	-0.93	-0.43	1.10	1.19	-0.65	-0.25	1.08	-0.05
1940	0.13	-1.00	-1.91	-1.34	1.45	0.28	-0.93	-1.07	0.21	0.28	-0.33	0.25
1941	-1.10	-1.02	-0.94	-1.17	-1.54	-1.36	2.36	0.31	-0.34	-1.30	0.43	-0.63
1942	-1.34	-0.55	-2.04	-0.33	-1.48	-0.56	-0.30	-0.13	0.00	-0.48	0.22	0.37
1943	-0.64	0.53	1.07	-0.23	-0.56	0.32	0.37	-0.63	0.35	0.72	0.43	1.41
1944	0.86	0.97	-0.19	-1.26	-1.35	-0.21	0.03	-0.72	0.40	1.09	0.46	1.32
1945	-0.56	0.66	0.63	0.89	-0.37	-0.45	1.02	0.69	-0.01	-1.26	0.80	-0.04
1946	1.50	-1.18	-0.33	0.51	-0.54	0.60	1.14	1.48	2.03	0.46	0.05	1.52
1947	1.00	-1.56	-2.23	-0.38	-0.50	0.58	1.23	0.25	0.83	-0.49	-0.93	-0.07
1948	-1.12	0.89	1.24	1.16	0.08	-0.88	1.45	-1.18	0.03	-0.60	0.61	1.39
1949	0.70	1.23	-0.12	-0.11	-0.18	-0.37	-1.12	-1.28	1.22	-0.27	1.51	0.60
1950	-0.02	0.21	0.46	1.48	-0.89	0.47	0.97	2.63	1.32	1.12	0.61	0.22
1951	-0.51	0.39	-0.82	-0.19	-1.84	-1.68	-1.27	1.73	0.84	1.74	-0.99	0.66
1952	0.25	-0.01	-0.81	0.99	-0.38	0.26	-0.35	-1.57	-1.10	-1.04	-0.72	-0.53
1953	0.40	-0.82	0.84	0.21	-0.73	2.84	1.20	1.17	0.07	1.50	1.71	1.82
1954	0.43	-0.09	0.06	-0.11	1.46	-0.64	1.77	0.27	0.20	-0.37	0.12	1.15
1955	-0.27	-0.74	-0.64	-1.62	-1.89	-1.93	-0.59	0.04	1.36	-0.94	-0.56	-1.56
1956	-0.49	-0.69	0.57	-1.41	-0.23	-0.54	0.49	-0.60	-0.63	-0.33	-0.49	0.70
1957	1.15	-0.17	0.10	0.37	-1.04	-1.54	0.93	-0.28	0.16	-0.06	1.00	-0.08
1958	-0.26	-1.50	-1.73	0.03	-0.84	-0.26	-0.66	0.88	0.68	1.12	2.25	-0.51
1959	-0.90	1.88	2.18	0.67	-0.33	-0.14	-0.16	0.20	-0.47	0.57	1.51	0.56
1960	-0.26	-0.86	1.51	1.69	0.71	-0.20	2.14	1.49	1.24	-1.78	-0.09	0.03
1961	0.77	0.97	0.35	-0.93	-0.17	0.49	0.75	0.48	1.03	2.31	1.70	-0.51
1962	0.11	0.31	-2.30	0.34	-0.62	-1.23	-1.10	-0.35	0.13	0.23	0.43	-0.35
1963	-0.26	-0.90	-0.88	0.74	2.15	0.24	-0.65	1.57	1.27	0.79	-0.52	0.58
1964	1.78	0.03	1.08	0.66	0.40	-1.09	-0.04	-0.37	-0.60	1.36	0.08	0.65
1965	0.05	0.21	-0.53	1.07	-1.34	0.03	-1.64	-0.91	1.62	0.50	-1.29	-1.23
1966	-0.99	-2.41	-1.17	-1.51	-1.27	0.93	-0.05	-0.61	-1.84	-1.01	0.79	0.22
1967	-0.98	0.55	1.04	-0.09	0.53	-0.60	-0.56	0.24	1.54	-0.31	2.02	-1.22
1968	-1.07	-0.24	-0.18	0.15	-1.51	-0.38	-1.26	-1.31	-0.17	-2.37	-0.16	1.07
1969	0.05	-0.72	-0.45	0.36	-0.37	0.87	0.44	2.25	-0.09	0.46	-0.93	0.20
1970	-0.27	-1.63	0.21	-0.75	0.44	0.91	0.55	0.70	0.12	0.23	-1.05	0.64
1971	0.32	-0.23	-1.57	-0.55	-0.22	0.36	-0.61	-0.17	-0.48	-0.40	-1.50	0.91
1972	0.91	0.57	0.45	0.42	0.56	2.11	1.59	0.27	-0.58	-0.06	0.27	2.02

1973	1.76	0.13	1.02	-0.40	-0.19	0.11	1.39	-1.24	-0.86	-1.66	-1.47	-0.57
1974	1.46	0.54	1.05	0.72	0.52	1.09	0.44	0.21	1.34	-0.42	-0.14	0.72
1975	0.67	1.28	1.12	-0.17	-0.40	-1.70	-1.34	-0.90	0.06	0.27	1.12	-0.12
1976	-0.83	1.03	-0.12	-0.67	1.02	-0.27	-0.42	-0.54	-2.04	-0.42	0.11	-0.40
1977	-0.39	-0.68	0.22	-1.50	-1.52	-1.38	-0.18	0.05	-0.90	0.38	0.50	0.71
1978	-0.49	-1.24	-0.41	-0.69	-0.37	0.75	0.95	-0.12	-0.75	-0.89	0.32	-1.54
1979	-0.92	-0.35	0.09	-0.02	-0.79	0.11	0.64	0.49	-0.51	-0.74	0.15	0.22
1980	-0.47	-0.02	-0.25	1.15	0.07	1.69	1.26	1.18	0.64	-1.00	-1.34	-0.77
1981	-0.48	0.18	-1.91	-0.45	0.92	-1.83	-0.58	-0.88	0.38	-0.30	-0.65	-1.73
1982	-0.97	1.13	0.85	0.06	-0.58	-1.86	-0.20	-0.24	-0.61	0.19	0.59	0.72
1983	0.85	0.45	0.18	1.40	1.43	-0.69	-0.36	-1.61	0.96	-0.59	-1.25	-0.14
1984	-0.33	1.27	-0.45	1.16	1.81	0.10	-1.11	-0.51	0.00	0.32	0.61	1.51
1985	-0.57	-1.53	0.24	-1.37	-0.74	-0.07	1.28	1.10	-0.46	0.51	-0.49	-1.27
1986	-1.34	-0.20	1.25	-0.80	1.24	0.62	-0.15	-0.44	-1.30	0.44	1.08	-1.27
1987	-1.28	-1.07	-0.55	0.38	-0.49	-0.41	-0.74	-1.32	0.01	2.07	0.34	-0.21
1988	0.56	-0.05	-0.58	-1.83	0.12	-0.05	1.61	0.51	0.91	-0.26	-0.68	-0.07
1989	1.71	0.96	1.28	1.96	-0.11	0.26	-1.12	0.99	0.36	-0.15	1.11	-0.20
1990	0.77	1.84	0.84	1.18	-0.79	1.07	0.71	1.17	0.98	0.87	0.04	1.40
1991	1.31	0.39	0.52	1.12	-0.94	0.55	0.12	0.70	-0.74	0.37	0.94	1.25
1992	1.67	1.15	1.26	-0.80	0.50	1.25	-0.67	-0.10	1.22	-2.62	-0.44	1.37
1993	1.31	0.87	0.66	0.23	0.15	-1.46	1.23	0.43	-0.71	-1.27	1.32	-0.11
1994	-0.71	-0.23	0.38	1.39	-0.59	-0.81	0.21	0.58	0.10	-0.82	0.14	1.35
1995	0.86	0.60	0.78	-0.60	-0.43	-0.37	-0.97	-1.19	0.19	0.06	-0.70	-0.28
1996	1.65	-0.72	0.50	-0.24	-1.10	-0.35	-0.44	1.87	-0.01	1.07	-0.36	-0.33
1997	0.61	0.22	0.14	-1.63	-0.83	0.83	1.41	1.47	1.27	-0.73	0.37	0.87

Table A.8: Indexed monthly mean Northern Coastal temperature data (Hanssen-Bauer and Nordli, 1998)

A.5 Northern Coastal Precipitation

	Jan	Feb	Mar	Apr	May	Jun	Jul	Aug	Sep	Oct	Nov	Dec
1873	0.37	0.72	0.66	0.04	0.97	0.79	0.86	0.68	0.42	0.72	0.75	0.58
1874	0.85	0.78	0.56	0.48	1.17	0.69	0.87	0.72	0.65	0.62	0.33	0.70
1875	0.39	0.56	0.84	0.13	0.82	0.79	0.96	1.02	0.63	0.53	0.63	0.64
1876	0.44	0.20	1.01	0.64	0.31	0.67	1.39	0.37	1.24	0.54	0.23	0.64
1877	0.18	0.41	0.93	0.56	1.35	0.53	0.59	0.90	1.02	0.53	0.40	0.63
1878	1.48	1.72	1.40	0.29	0.74	0.79	0.34	1.26	0.91	0.50	0.40	0.88
1879	0.26	0.52	1.09	0.47	0.37	0.44	0.55	0.65	0.65	1.27	1.37	0.72
1880	0.94	1.59	1.03	1.76	1.31	0.66	1.64	0.79	1.04	1.17	0.67	1.12
1881	0.35	1.73	1.82	0.80	0.90	1.02	0.85	0.41	0.48	1.00	0.72	0.85
1882	1.69	1.30	1.07	0.68	0.50	1.54	1.72	0.88	0.24	0.22	0.41	0.92
1883	0.57	1.86	0.32	1.05	0.95	0.12	0.45	0.93	1.03	0.43	0.85	0.78
1884	0.84	0.70	0.63	0.63	0.80	0.40	0.64	1.47	0.88	1.52	0.58	0.92
1885	0.50	0.99	0.47	0.67	1.06	1.42	0.59	0.45	0.49	0.98	1.27	0.78

1886	0.69	1.33	1.30	0.52	0.33	0.68	1.11	1.55	0.88	0.81	0.37	0.80
1887	1.25	1.76	0.95	1.68	0.76	0.57	0.71	0.55	0.55	1.11	0.34	0.85
1888	0.61	0.73	0.48	0.35	0.55	0.49	0.81	2.07	0.17	0.65	0.35	0.67
1889	0.36	1.08	0.40	0.97	1.07	0.55	0.73	1.06	0.25	1.43	0.58	0.78
1890	0.97	0.72	0.45	0.87	0.85	1.18	0.96	0.58	0.78	0.09	1.21	0.72
1891	2.05	0.95	0.44	0.58	1.27	0.35	0.46	1.41	0.48	0.59	0.65	0.82
1892	0.47	1.21	0.57	0.50	0.70	0.69	1.14	1.06	0.79	0.95	0.18	0.69
1893	0.28	1.34	1.20	0.47	0.93	0.74	0.98	0.83	0.39	1.03	0.26	0.66
1894	0.24	1.70	0.28	0.81	0.31	0.39	0.32	1.10	0.78	1.09	0.69	0.71
1895	0.85	0.14	1.18	0.87	0.83	0.84	1.11	1.91	0.68	2.02	0.42	0.82
1896	1.30	0.22	0.56	1.31	0.92	1.00	0.64	0.45	0.98	1.46	0.45	0.94
1897	0.91	0.17	0.25	0.94	1.06	0.77	0.69	0.95	0.87	1.96	0.78	0.84
1898	0.12	0.09	0.23	0.59	0.48	0.89	1.55	0.75	0.57	1.40	0.59	0.82
1899	1.16	0.64	0.41	0.90	0.45	0.92	1.60	0.40	1.01	1.54	0.24	0.84
1900	0.51	1.09	1.34	2.43	0.81	1.09	1.66	2.26	0.19	0.41	0.80	0.96
1901	0.87	1.39	0.35	1.36	0.81	0.76	1.46	0.40	0.87	2.33	0.17	1.07
1902	1.40	0.48	0.55	0.45	1.04	0.67	0.55	1.28	1.38	0.95	1.14	0.98
1903	1.95	0.79	0.21	0.48	0.98	0.92	0.79	0.93	0.22	1.35	1.00	0.88
1904	0.06	1.11	0.35	0.85	0.91	1.42	0.52	0.84	0.74	1.35	0.67	0.85
1905	1.62	0.22	0.47	1.59	0.67	1.30	0.48	0.86	0.50	1.04	1.48	1.02
1906	0.31	0.86	3.51	1.18	1.03	0.66	0.67	1.15	0.85	0.79	1.04	1.00
1907	1.03	1.94	0.52	0.51	0.72	0.84	0.58	2.10	0.30	0.63	0.38	0.93
1908	0.86	0.41	0.80	1.48	1.19	0.75	0.43	0.56	1.81	1.40	0.85	1.04
1909	1.13	0.19	0.59	0.70	0.59	0.63	1.48	0.98	0.47	0.68	1.40	0.92
1910	0.57	1.18	0.81	0.83	1.30	0.34	0.42	1.22	1.27	0.06	0.44	0.80
1911	1.17	0.97	1.51	0.71	0.99	1.00	0.88	0.81	1.26	0.36	0.38	0.95
1912	0.44	0.17	1.89	0.43	0.44	0.77	0.51	1.42	0.47	0.85	0.17	0.66
1913	0.97	1.08	0.98	0.87	1.10	0.78	0.93	0.79	1.08	0.69	0.96	0.88
1914	0.53	0.49	2.11	1.52	1.08	0.24	0.63	1.35	0.48	0.74	0.48	0.89
1915	0.22	0.85	1.34	2.56	1.10	1.02	0.82	0.84	0.50	0.83	0.21	0.74
1916	0.92	0.25	0.56	0.44	0.22	0.47	0.87	1.90	0.37	0.55	0.27	0.69
1917	1.21	0.54	0.65	1.85	1.45	1.07	0.52	1.07	0.37	0.80	1.19	0.91
1918	1.24	1.71	0.50	1.65	0.85	0.29	0.53	0.64	0.67	1.83	0.16	0.92
1919	1.18	0.75	1.47	0.40	0.97	0.37	0.96	1.75	1.00	0.40	0.16	0.81
1920	1.39	1.62	0.44	1.02	0.86	1.34	1.27	0.91	0.97	1.39	0.69	1.05
1921	1.23	0.99	1.42	2.12	2.07	0.96	1.31	1.57	1.21	0.92	0.74	1.23
1922	0.81	0.62	0.30	1.58	1.35	0.48	0.64	0.98	0.90	1.41	0.53	0.78
1923	0.42	1.17	0.43	1.01	1.18	1.09	0.38	0.76	0.36	0.54	0.68	0.69
1924	0.61	0.75	1.03	0.76	0.59	0.37	0.67	1.18	0.72	1.55	1.20	0.88
1925	0.59	0.73	1.06	0.72	1.05	0.80	0.51	0.79	1.17	1.36	0.34	0.93
1926	0.77	1.17	1.08	0.68	0.41	1.11	0.57	1.12	0.77	0.59	1.24	0.86
1927	1.52	0.97	0.41	0.70	0.73	0.25	0.61	0.74	0.78	0.36	0.84	0.71
1928	0.57	0.93	1.54	0.91	0.98	1.70	0.52	1.02	0.57	0.52	0.54	0.78
1929	0.45	2.74	0.90	0.76	0.76	0.80	1.14	0.88	0.60	0.33	0.47	0.90
1930	1.55	2.36	0.45	0.86	1.50	0.42	0.57	0.93	0.67	0.58	0.78	0.91
1931	0.16	1.49	0.15	1.37	1.07	0.78	1.08	1.19	1.17	0.39	1.27	0.86
1932	1.73	1.13	0.44	0.60	0.46	0.86	1.33	1.96	0.31	1.22	1.74	1.26
1933	0.60	1.23	1.02	0.37	0.15	0.84	0.80	0.88	0.80	1.26	1.90	0.94
1934	2.27	0.15	0.73	1.70	1.21	0.32	0.45	0.53	0.65	1.24	0.14	0.88
1935	0.77	1.06	0.37	1.92	0.79	0.69	0.45	0.54	0.36	0.19	0.49	0.68
1936	0.60	0.84	0.68	0.70	1.05	1.01	1.03	1.62	0.49	1.06	1.19	0.87
1937	0.38	0.38	0.47	1.31	1.53	0.28	0.60	0.99	0.91	1.39	0.69	0.80
1938	1.90	1.55	2.14	1.13	1.15	0.78	1.15	0.92	0.32	0.82	0.10	0.94

1939	1.62	0.53	1.27	1.34	1.69	0.37	0.68	1.53	0.75	0.61	1.16	0.96
1940	0.74	0.45	1.59	0.31	1.15	0.43	1.34	0.64	0.79	0.41	1.02	0.81
1941	0.51	0.92	0.44	1.11	0.98	0.67	1.01	1.58	0.99	0.47	0.76	1.00
1942	0.70	1.46	0.89	0.89	1.25	0.84	1.73	0.97	0.39	1.79	0.96	0.99
1943	1.22	1.69	1.99	1.49	0.81	0.65	0.80	0.62	0.71	0.96	1.86	1.02
1944	0.89	0.81	0.72	0.74	1.01	0.38	1.38	0.46	0.66	0.25	0.92	0.76
1945	0.58	1.89	1.50	0.86	0.59	0.50	0.80	0.58	1.46	1.54	0.49	0.96
1946	1.10	1.03	1.29	1.10	0.90	0.86	0.37	0.86	1.32	0.93	1.03	1.04
1947	0.52	0.69	1.06	0.97	1.25	0.86	1.02	1.51	1.28	0.31	0.64	0.87
1948	0.93	2.59	0.84	1.30	0.96	0.72	0.83	1.27	0.84	1.65	1.62	1.16
1949	1.58	1.20	1.11	1.80	0.53	1.01	1.00	1.31	1.26	0.44	0.43	1.09
1950	0.62	1.14	0.92	1.08	1.56	0.39	0.44	0.41	0.60	0.29	0.33	0.61
1951	0.12	1.34	1.03	0.90	1.09	1.22	0.87	0.99	1.18	0.56	1.28	0.89
1952	0.89	0.48	0.97	0.78	1.35	1.13	0.99	1.04	0.05	0.55	0.54	0.74
1953	0.82	4.04	1.25	0.89	0.29	0.53	0.51	0.90	1.16	1.31	0.90	1.17
1954	0.49	1.59	0.73	0.57	1.31	0.39	0.95	0.78	0.55	0.22	0.72	0.78
1955	0.64	1.52	1.27	0.59	1.17	0.75	0.99	0.55	1.02	1.16	0.37	0.88
1956	0.64	1.39	0.55	1.84	1.38	0.20	0.68	1.44	0.88	0.48	0.51	0.90
1957	0.21	0.86	1.37	1.01	1.81	0.30	1.04	0.33	0.99	1.06	1.18	0.94
1958	1.10	0.74	0.62	0.70	0.71	1.78	0.53	1.50	0.90	1.95	0.58	1.02
1959	1.75	1.57	0.50	1.80	1.17	1.33	1.24	1.49	0.89	0.27	0.19	1.01
1960	0.77	0.50	0.74	0.91	1.22	0.79	0.76	0.34	0.52	0.04	0.52	0.62
1961	1.86	2.05	0.73	0.69	2.04	0.83	0.61	1.45	0.43	1.57	0.84	1.11
1962	0.92	0.92	1.29	0.71	1.23	0.31	0.52	0.94	2.16	0.84	1.36	1.08
1963	0.82	0.78	1.03	0.76	0.38	1.29	0.50	1.67	1.01	0.44	1.46	1.02
1964	0.89	0.90	0.61	1.34	1.22	1.34	0.96	1.35	1.47	1.52	1.34	1.42
1965	1.38	1.42	0.80	0.57	0.69	1.10	0.50	0.56	1.27	0.67	0.24	0.81
1966	0.22	1.07	0.40	1.87	0.52	1.52	1.55	1.33	0.61	0.80	0.15	0.83
1967	0.70	1.32	1.37	0.38	1.64	1.46	0.79	0.71	0.70	0.68	0.52	0.89
1968	1.53	1.70	1.66	0.61	1.58	0.97	1.23	0.26	0.52	1.11	1.17	1.01
1969	0.17	1.18	0.84	0.31	0.92	1.08	0.40	1.13	1.69	0.63	0.68	0.83
1970	0.67	0.36	0.41	0.53	0.64	1.12	0.76	0.73	0.89	0.77	1.29	0.77
1971	0.73	0.94	0.96	1.50	0.56	1.36	2.39	1.09	1.46	1.18	1.22	1.26
1972	0.75	1.44	0.93	0.26	0.71	1.35	1.17	1.87	1.20	1.32	1.39	1.13
1973	1.11	2.63	0.90	0.90	1.57	0.74	2.07	0.44	1.15	1.19	1.06	1.24
1974	0.92	0.40	2.17	0.58	0.55	0.91	0.98	1.07	0.21	0.18	0.60	0.74
1975	2.82	1.17	0.66	1.65	1.64	1.35	1.23	1.80	1.53	1.51	2.17	1.60
1976	1.40	0.55	1.49	0.47	0.53	0.86	0.93	1.08	0.34	1.33	0.23	0.82
1977	0.33	1.91	0.40	1.03	1.33	0.61	0.84	0.95	0.95	0.68	1.11	0.89
1978	0.83	0.55	0.71	1.39	0.55	0.33	0.62	0.52	1.32	1.92	0.61	0.90
1979	1.14	0.36	0.36	1.59	1.24	0.35	0.71	1.33	0.63	0.45	0.87	0.76
1980	0.71	0.32	1.12	0.72	0.90	0.21	0.35	0.78	0.54	0.96	0.92	0.71
1981	0.63	0.82	2.02	0.36	0.65	1.07	1.26	0.61	0.38	0.42	0.53	0.89
1982	1.28	1.40	1.88	1.44	0.93	1.66	0.71	1.43	0.72	0.91	1.02	1.17
1983	1.61	0.86	0.12	0.63	1.57	1.68	2.72	0.83	0.93	1.81	1.19	1.26
1984	0.99	0.78	0.88	1.14	1.00	1.20	1.47	0.55	0.30	0.45	0.40	0.74
1985	0.41	0.67	1.12	0.80	0.76	0.82	1.37	1.40	2.47	0.72	0.85	1.12
1986	1.04	0.83	0.76	1.21	1.57	0.61	0.30	0.58	1.30	0.87	0.40	0.78
1987	0.92	0.13	0.90	1.29	0.49	0.83	0.71	0.26	0.80	0.96	1.91	0.85
1988	0.05	0.18	1.72	0.48	0.55	0.92	0.45	1.53	1.18	2.12	1.22	0.98
1989	1.69	0.66	0.44	2.68	0.83	1.20	0.70	1.56	0.76	1.03	1.89	1.30
1990	1.55	1.68	1.22	2.06	0.89	0.82	1.09	0.24	1.05	1.01	1.36	1.07
1991	0.30	1.02	0.69	1.73	0.68	0.81	0.77	1.41	0.78	1.30	1.76	1.09

1992	1.40	1.37	0.42	1.94	0.91	1.65	0.79	0.43	0.82	0.31	1.91	1.17
1993	2.13	2.42	0.66	1.43	0.83	0.65	0.74	0.51	1.04	0.59	0.35	0.99
1994	0.79	0.95	0.79	1.16	1.27	1.28	0.97	0.87	1.22	1.42	1.10	1.05
1995	0.94	1.14	0.94	0.81	1.51	1.31	2.32	0.61	1.47	1.45	0.91	1.18
1996	0.74	0.82	1.41	0.67	1.36	0.38	1.29	0.95	1.21	0.75	0.77	0.96
1997	1.01	1.78	1.88	1.68	0.27	0.38	1.05	1.69	1.15	0.48	0.63	1.18

Table A.10: Indexed monthly mean Northern Coastal precipitation data (Hanssen-Bauer and Føland, 1998)

A.6 Stable Carbon Isotope Data

	Tree 128	Tree 87	Tree 95	Tree 63	Tree 129	Tree 82	Tree 73	Tree 91	Tree 132	Tree 133	Tree 166
1394				-25.18					-25.76	-25.57	-25.74
1395				-24.95					-25.84	-25.31	-25.56
1396				-24.24					-24.08	-24.11	-24.63
1397				-25.15					-25.12	-25.48	-25.91
1398				-24.89					-24.80	-24.85	-26.07
1399				-24.44					-24.50	-24.12	-24.47
1400				-24.72					-24.73	-24.85	-26.05
1401				-24.18					-24.02	-24.01	-24.92
1402				-24.44					-24.01	-25.06	-25.06
1403				-24.34					-23.42	-24.96	-25.96
1404				-24.61					-24.17	-24.60	-25.42
1405				-25.22					-23.94	-25.25	-25.23
1406				-24.29					-23.58	-24.43	-24.93
1407				-25.02					-24.28	-25.16	-25.53
1408				-24.55					-24.67	-25.25	-24.90
1409				-24.09					-23.56	-24.87	-24.88
1410				-24.86					-24.19	-25.88	-25.21
1411				-23.83					-22.99	-23.61	-24.14
1412				-24.88					-24.18	-25.12	-25.35
1413				-24.44					-23.27	-24.85	-25.31
1414				-24.39					-23.80	-25.05	-25.48
1415				-24.48					-23.07	-24.78	-24.92
1416				-24.40					-22.97	-25.36	-25.14
1417				-24.29					-22.49	-25.01	-25.57
1418				-24.42					-22.50	-24.70	-25.21
1419				-24.70					-22.68	-24.89	-24.97
1420				-23.72					-22.81	-24.68	-24.88
1421				-23.67					-22.79	-24.96	-24.85
1422				-24.60					-23.82	-25.72	-25.17
1423				-24.29					-23.81	-25.03	-25.06
1424				-24.10					-23.61	-24.95	-24.83
1425				-24.40					-24.87	-24.51	-24.59
1426				-25.24					-23.97	-25.82	-25.96
1427				-24.84					-24.75	-25.29	-25.72
1428				-24.74					-23.92	-25.38	-26.03
1429				-24.21					-23.14	-25.07	-24.70
1430				-24.70					-23.77	-25.99	-25.33
1431				-24.48					-23.42	-25.74	-25.05
1432				-25.08					-24.55	-25.25	-24.82
1433				-24.10					-23.17	-25.05	-23.55
1434				-23.86					-23.39	-25.01	-25.01
1435				-23.74					-24.10	-25.33	-25.68
1436				-25.40					-24.86	-25.86	-25.94
1437				-24.34					-23.27	-25.40	-25.21
1438				-25.34					-24.94	-26.13	-25.76
1439				-25.24					-25.66	-26.03	-25.63
1440				-24.52					-23.19	-25.16	-24.79

	Tree 128	Tree 87	Tree 95	Tree 63	Tree 129	Tree 82	Tree 73	Tree 91	Tree 132	Tree 133	Tree 166
1441				-24.84					-22.99	-24.70	-25.26
1442				-24.79					-24.41	-25.45	-24.78
1443				-23.35					-23.09	-24.65	-21.31
1444				-24.06					-24.13	-25.27	-25.54
1445				-23.25					-24.24	-24.87	-25.46
1446				-24.14					-25.07	-25.10	-25.23
1447				-24.45					-23.82	-24.91	-25.02
1448				-24.73					-25.26	-25.62	-26.23
1449				-23.98					-23.79	-24.92	-25.22
1450				-23.12					-22.59	-23.88	-24.06
1451				-24.38					-22.81	-24.29	-25.38
1452				-24.84					-23.00	-25.04	-24.49
1453				-24.93					-23.59	-25.13	-24.61
1454				-24.20					-23.66	-24.28	-24.04
1455				-24.14					-23.89	-24.94	-24.21
1456				-24.09					-23.15	-24.52	-24.19
1457				-25.08					-24.29	-25.16	-25.14
1458				-24.93					-24.77	-24.95	-24.34
1459				-24.55					-25.29	-25.00	-24.79
1460				-24.04					-24.25	-24.60	-24.08
1461				-24.44					-24.05	-24.89	-24.79
1462				-24.77					-24.01	-25.22	-24.16
1463				-24.41					-23.97	-25.05	-24.41
1464				-24.35					-24.61	-24.56	-24.56
1465				-24.30					-24.86	-24.84	-24.31
1466				-25.03					-23.75	-25.41	-24.58
1467				-24.88					-24.45	-24.72	-24.77
1468				-24.24					-23.91	-24.29	-24.15
1469				-24.45					-24.23	-25.48	-25.20
1470				-24.23					-23.43	-24.32	-23.97
1471				-24.68					-23.83	-25.00	-24.53
1472				-24.53					-23.93	-24.74	-24.45
1473				-24.24					-23.15	-24.06	-23.69
1474				-23.42					-23.15	-24.20	-23.02
1475				-23.18					-22.81	-23.30	-23.24
1476				-23.88					-24.15	-24.26	-23.51
1477				-23.79					-23.24	-23.87	-23.63
1478				-24.81					-24.56	-25.14	-24.84
1479				-23.81					-24.02	-24.53	-24.12
1480				-24.19					-23.85	-24.10	-22.62
1481				-23.80					-23.04	-23.71	-23.22
1482				-24.52					-25.21	-24.59	-24.24
1483				-25.47					-25.22	-25.65	-25.03
1484				-24.78					-23.80	-24.72	-25.00
1485				-24.42					-24.03	-24.63	-24.07
1486				-24.59					-23.86	-24.94	-25.10
1487				-25.09					-24.16	-24.76	-25.46
1488				-25.32					-24.45	-25.05	-24.82
1489				-23.81					-23.14	-24.24	-24.36
1490				-24.48					-24.21	-24.83	-24.95
1491				-24.56					-24.32	-25.26	-25.22

	Tree 128	Tree 87	Tree 95	Tree 63	Tree 129	Tree 82	Tree 73	Tree 91	Tree 132	Tree 133	Tree 166
1492				-24.90					-24.76	-25.62	-25.80
1493				-24.90					-24.25	-25.61	-24.67
1494				-24.40					-24.72	-24.92	-24.28
1495				-24.51					-24.11	-25.43	-25.41
1496				-23.66					-22.86	-23.77	-24.14
1497				-24.89					-24.11	-24.67	-25.28
1498				-25.04					-24.31	-24.93	-25.35
1499				-24.74					-23.51	-24.27	-25.73
1500				-23.96					-23.04	-24.53	-24.30
1501				-24.23					-23.64	-24.77	-24.10
1502				-23.53					-23.11	-24.12	-24.05
1503				-24.14					-23.40	-24.01	-24.37
1504				-25.00					-24.21	-24.83	-25.15
1505				-23.34					-22.77	-23.79	-24.10
1506				-24.58					-23.42	-24.91	-24.82
1507				-24.54					-23.54	-24.83	-24.47
1508				-23.91					-23.03	-24.17	-24.05
1509				-24.12					-23.52	-24.62	-24.98
1510				-24.40					-23.50	-24.67	-25.34
1511				-24.36					-23.37	-24.92	-24.38
1512				-24.54					-23.19	-24.56	-24.48
1513				-24.75					-23.01	-24.73	-24.78
1514				-24.86					-23.30	-25.21	-25.04
1515				-23.72					-22.03	-23.79	-24.14
1516				-24.73					-23.32	-25.02	-25.00
1517				-24.08					-23.01	-24.28	-24.03
1518				-24.16					-23.26	-24.16	-24.54
1519				-24.25					-22.72	-24.46	-24.29
1520				-25.34					-23.85	-25.66	-25.35
1521				-24.62					-23.35	-25.41	-25.25
1522				-24.67					-23.48	-25.63	-24.65
1523				-24.05					-22.88	-24.90	-24.00
1524				-25.02					-23.49	-25.58	-25.11
1525				-24.71					-23.88	-26.32	-24.50
1526				-24.11					-23.00	-24.74	-23.97
1527	-24.10			-25.02					-23.36	-25.57	-24.92
1528	-23.40			-25.40					-24.07	-25.21	-24.70
1529	-22.28			-24.17					-21.88	-24.15	-24.00
1530	-23.85			-25.05					-23.14	-25.58	-25.21
1531	-24.39			-24.97					-24.67	-25.30	-24.66
1532	-23.86			-24.35					-23.76	-24.85	-24.23
1533	-23.18			-24.47					-24.53	-24.67	-24.17
1534	-24.03			-24.11					-23.18	-26.00	-25.04
1535	-24.24			-23.91					-24.01	-25.40	-24.50
1536	-24.98			-24.34					-24.73	-25.93	-25.54
1537	-23.84			-23.57					-24.16	-25.36	-24.86
1538	-23.47			-23.39					-23.51	-24.59	-25.12
1539	-23.50			-22.48					-23.20	-24.27	-24.58
1540	-24.42			-24.82					-24.05	-25.25	-25.25
1541	-24.07			-25.02					-24.32	-25.27	-25.38
1542	-23.58			-24.99					-23.39	-25.46	-25.86

	Tree 128	Tree 87	Tree 95	Tree 63	Tree 129	Tree 82	Tree 73	Tree 91	Tree 132	Tree 133	Tree 166
1543	-23.88			-24.93					-23.49	-25.44	-25.24
1544	-24.16			-24.68					-23.97	-25.07	-24.43
1545	-24.04			-24.29					-23.05	-24.80	-24.55
1546	-24.74			-24.81					-24.02	-25.33	-25.29
1547	-24.29			-24.09					-24.34	-25.11	-24.55
1548	-24.39			-24.25					-22.69	-24.69	-25.09
1549	-23.83			-23.78					-23.60	-24.94	-24.60
1550	-23.84			-23.54					-23.95	-25.17	-24.36
1551	-23.94			-23.51					-23.60	-24.77	-24.75
1552	-24.37			-22.87					-23.41	-23.78	-23.82
1553	-23.43			-22.99					-23.66	-23.95	-24.02
1554	-24.11			-23.14					-23.17	-25.10	-23.94
1555	-23.96			-22.88					-23.02	-24.81	-24.34
1556	-23.70			-23.67					-22.87	-24.34	-24.17
1557	-23.26			-22.65					-22.89	-24.12	-23.59
1558	-23.18			-22.70					-23.12	-24.10	-24.34
1559	-24.23			-24.10					-23.39	-25.43	-24.72
1560	-24.06			-23.60					-23.73	-24.99	-24.40
1561	-24.25			-24.47					-22.62	-25.33	-24.58
1562	-23.31			-23.59					-22.58	-24.44	-23.40
1563	-24.76			-23.47					-23.18	-24.96	-24.03
1564	-23.84			-23.20					-23.00	-24.80	-24.09
1565	-23.54			-23.31					-22.97	-25.01	-24.24
1566	-24.80			-24.96					-24.36	-25.34	-25.55
1567	-24.30			-24.07					-24.08	-25.34	-25.10
1568	-24.61			-24.38					-24.53	-25.36	-24.95
1569	-23.71			-23.09					-22.77	-23.73	-23.33
1570	-23.70			-22.50					-21.31	-23.66	-22.70
1571	-23.90			-23.98					-23.10	-24.89	-23.46
1572	-24.24			-24.34					-24.33	-25.75	-24.82
1573	-24.77			-24.09					-23.17	-25.47	-24.99
1574	-24.47			-24.00					-24.38	-25.35	-24.69
1575	-24.16			-24.04					-23.23	-24.83	-24.34
1576	-23.81			-23.57					-22.07	-24.33	-23.64
1577	-24.41			-24.27					-23.26	-25.28	-23.94
1578	-23.80			-24.22					-23.24	-24.88	-23.97
1579	-24.19			-24.48					-23.17	-24.33	-23.54
1580	-24.00			-23.60					-23.19	-24.79	-22.80
1581	-24.01			-23.48					-22.87	-24.77	-22.85
1582	-24.02			-22.84					-22.72	-24.23	-23.51
1583	-24.21			-23.91					-22.97	-23.33	-22.85
1584	-24.89			-25.55					-24.01	-25.16	-25.41
1585	-24.73			-24.66					-23.82	-24.74	-24.61
1586	-24.73			-24.43					-23.11	-24.80	-24.22
1587	-24.95			-25.16					-24.60	-25.36	-25.45
1588	-23.95			-25.39					-24.29	-24.75	-24.76
1589	-24.86			-25.15					-24.46	-25.23	-25.19
1590	-24.72			-24.74					-24.38	-25.09	-24.83
1591	-24.31			-25.02					-24.00	-25.05	-24.75
1592	-23.62			-23.90					-23.55	-24.52	-24.16
1593	-22.45			-23.29					-22.97	-26.06	-23.61

	Tree 128	Tree 87	Tree 95	Tree 63	Tree 129	Tree 82	Tree 73	Tree 91	Tree 132	Tree 133	Tree 166
1594	-23.46			-23.42					-23.20	-24.10	-23.98
1595	-23.90			-23.81					-23.64	-24.42	-24.67
1596	-23.37			-23.82					-23.42	-24.64	-24.29
1597	-24.17			-24.11					-23.25	-24.50	-24.10
1598	-23.55			-24.91					-24.28	-24.98	-24.22
1599	-23.50			-25.96					-24.15	-25.11	-25.38
1600	-24.21			-25.03					-23.90	-24.90	-25.12
1601	-24.05			-24.18					-23.78	-26.39	-25.18
1602	-23.13			-23.55					-23.06	-24.72	-24.10
1603	-21.80			-23.18					-22.58	-23.42	-23.09
1604	-22.85			-24.49					-23.71	-24.12	-23.54
1605	-23.38			-24.82					-23.92	-25.17	-24.05
1606	-22.85			-24.54					-22.80	-24.27	-23.89
1607	-23.42			-25.23					-24.15	-25.41	-24.72
1608	-24.12			-24.68					-23.63	-25.40	-24.75
1609	-24.66			-24.41					-24.63	-25.34	-24.91
1610	-23.00			-24.21					-23.42	-24.90	-24.12
1611	-23.12			-23.62					-22.54	-24.20	-23.48
1612	-23.81			-24.28					-22.72	-24.75	-23.99
1613	-24.01			-25.45					-23.01	-25.38	-24.16
1614	-23.98			-24.38					-23.10	-24.91	-24.89
1615	-23.52			-24.19					-23.01	-25.56	-24.12
1616	-23.80			-23.64					-23.63	-24.22	-24.58
1617	-22.95			-23.76					-22.61	-24.72	-23.85
1618	-23.52			-24.58					-23.21	-24.71	-23.93
1619	-23.26			-24.16					-23.02	-25.05	-24.21
1620	-23.45			-23.93					-23.23	-24.02	-24.52
1621	-22.93			-23.72					-21.55	-25.04	-22.55
1622	-23.49			-23.93					-23.55	-24.88	-24.54
1623	-23.51			-24.47					-22.91	-24.95	-24.56
1624	-23.88			-23.98					-23.16	-24.75	-24.94
1625	-23.59			-23.81					-23.23	-24.23	-24.54
1626	-22.62			-24.21					-21.69	-23.16	-23.66
1627	-23.20			-23.43					-21.95	-23.80	-22.99
1628	-22.61			-23.68					-21.96	-23.16	-23.69
1629	-22.72			-24.06					-22.28	-23.37	-23.69
1630	-23.72			-24.33					-22.73	-24.54	-24.38
1631	-22.67			-23.88					-22.49	-24.28	-24.20
1632	-22.90			-24.22					-22.45	-24.45	-24.35
1633	-23.52			-24.17					-23.34	-25.33	-24.85
1634	-22.05			-24.74					-23.38	-24.50	-24.44
1635	-23.56			-23.77					-23.83	-25.11	-24.59
1636	-21.86			-23.81					-22.12	-23.72	-22.84
1637	-23.11			-24.56					-22.71	-24.39	-23.97
1638	-23.23			-24.86					-23.24	-24.82	-24.44
1639	-22.93			-24.61					-22.52	-24.34	-25.36
1640	-23.60			-24.25					-22.67	-24.22	-23.59
1641	-24.54			-24.64					-22.79	-25.29	-24.71
1642	-23.26			-24.26					-21.69	-23.81	-23.79

	Tree 128	Tree 87	Tree 95	Tree 63	Tree 129	Tree 82	Tree 73	Tree 91	Tree 132	Tree 133	Tree 166
1643	-23.54			-24.63					-22.11	-23.62	-24.23
1644	-23.07			-24.32					-23.45	-24.70	-24.47
1645	-24.44			-24.48					-23.44	-25.33	-24.61
1646	-24.13			-24.60					-22.67	-24.35	-24.26
1647	-23.95			-24.47					-23.38	-25.82	-25.34
1648	-23.29			-24.74					-23.18		-24.55
1649	-23.80			-23.93					-23.34		-24.35
1650	-23.42			-23.98					-22.65		-23.97
1651	-23.89			-24.08					-22.91		-24.74
1652	-25.18			-24.61					-23.65		-25.29
1653	-24.69			-24.47					-23.92		-24.64
1654	-23.97			-23.85					-23.57		-24.68
1655	-23.09			-23.58					-22.82		-25.23
1656	-24.23			-24.56					-23.52		-24.69
1657	-24.47			-24.66					-23.74		-25.13
1658	-23.38			-23.44					-23.45		-23.92
1659	-24.04			-23.74					-23.06		-24.03
1660	-23.26			-24.31					-22.91		-23.77
1661	-23.96			-24.34					-22.92		-24.25
1662	-23.56			-23.77					-22.70		-24.12
1663	-23.37			-24.38					-22.45		-24.08
1664	-23.36			-23.81					-22.51		-23.35
1665	-24.28			-24.81					-23.07		-24.57
1666	-23.90			-24.17					-22.96		-24.10
1667	-24.52			-25.55					-23.11		-24.54
1668	-24.19			-23.79					-22.83		-24.40
1669	-24.22			-24.43					-23.38		-24.12
1670	-24.24			-24.60					-23.37		-24.69
1671	-24.02			-24.75					-23.16		-24.26
1672	-23.68			-24.15					-23.05		-24.02
1673	-23.95			-24.39					-22.51		-24.11
1674	-24.40			-24.65					-23.40		-25.02
1675	-24.54			-24.86					-23.58		-24.92
1676	-23.85			-24.09					-23.06		-24.03
1677	-23.18			-24.25					-22.50		-23.85
1678	-23.54			-24.98					-22.70		-24.37
1679	-24.12			-24.48					-23.30		-24.14
1680	-24.64			-25.14					-23.34		-24.88
1681	-24.38			-25.00					-23.09		-24.49
1682	-23.75			-23.78					-22.78		-23.86
1683	-24.28			-23.89					-22.57		-23.88
1684	-24.36			-25.49					-22.97		-24.81
1685	-23.65			-24.12					-22.83		-24.43
1686	-24.51			-24.93					-23.48		-24.86
1687	-24.62			-24.53					-23.33		-24.89
1688	-23.29			-23.92					-22.72		-25.07
1689	-23.78			-23.84					-22.90		-23.29
1690	-24.31			-25.01					-23.41		-25.93
1691	-24.15			-24.53					-23.58		-24.98
1692	-23.78			-24.29					-22.83		-24.24

	Tree 128	Tree 87	Tree 95	Tree 63	Tree 129	Tree 82	Tree 73	Tree 91	Tree 132	Tree 133	Tree 166
1693	-24.70			-24.69					-23.57		-24.48
1694	-24.29			-24.73					-23.48		-25.22
1695	-24.22			-24.69					-22.85		-24.58
1696	-24.06			-24.11					-22.55		-24.60
1697	-23.83			-24.44					-22.93		-24.12
1698	-23.16			-24.05					-22.21		-23.10
1699	-23.74			-24.08					-23.21		-24.17
1700	-22.84			-23.01				-23.57	-22.14		-23.24
1701	-24.43			-24.39				-24.88	-23.92		-24.21
1702	-24.26			-24.72				-25.11	-23.67		-24.76
1703	-24.17			-23.88				-24.34	-23.03		-24.15
1704	-25.25			-24.86				-24.99	-23.70		-25.12
1705	-24.77			-24.41				-24.88	-23.52		-25.17
1706	-23.79			-23.41	-24.67			-24.24	-22.76		-23.81
1707	-23.58			-23.51	-23.90			-23.88	-22.26		-23.91
1708	-24.51			-24.07	-23.95			-24.46	-23.02		-23.91
1709	-23.61			-23.70	-24.07			-24.26	-23.26		-24.47
1710	-24.01			-23.57	-24.15			-24.70	-23.49		-24.48
1711	-22.60			-22.85	-23.44			-23.65	-22.73		-23.60
1712	-23.31			-23.40	-23.51			-24.88	-23.29		-23.72
1713	-24.78			-24.08	-24.78			-25.06	-24.07		-25.03
1714	-25.37			-25.05	-25.10			-25.55	-25.32		-25.00
1715	-23.95			-23.95	-23.79			-24.33	-23.92		-24.29
1716	-24.22			-23.41	-24.54			-24.39	-23.74		-24.71
1717	-24.80			-24.01	-24.31			-24.68	-23.73		-24.91
1718	-24.51			-23.85	-23.92			-24.43	-23.80		-24.95
1719	-24.53			-24.30	-23.56			-24.94	-23.94		-24.87
1720	-23.76			-23.82	-23.23			-24.16	-23.12		-24.66
1721	-23.14			-23.65	-23.51			-25.56	-22.96		-24.17
1722	-23.62			-23.17	-22.93			-24.66	-23.71		-24.59
1723	-24.53			-23.69	-23.91			-24.76	-23.71		-25.02
1724	-23.43			-23.39	-23.36			-24.78	-23.63		-24.59
1725	-23.53			-22.82	-22.48			-23.86	-22.78		-24.14
1726	-24.18			-23.66	-22.96			-24.93	-23.16		-24.95
1727	-24.27			-23.40	-23.10			-24.41	-22.71		-24.81
1728	-24.13			-23.61	-22.94			-24.37	-22.80		-24.90
1729	-24.07			-23.25	-23.76			-24.59	-22.57		-24.46
1730	-23.73			-22.52	-22.84			-23.95	-22.83		-24.07
1731	-25.03			-24.44	-24.72			-25.39	-23.98		-25.40
1732	-23.89			-22.59	-23.23			-24.49	-22.61		-25.12
1733	-25.03			-23.19	-23.23			-24.45	-22.73		-24.67
1734	-24.04			-24.10	-24.04			-25.07	-22.80		-24.98
1735	-23.64			-23.26	-23.43			-23.94	-22.26		-24.48
1736	-23.61			-23.75	-23.41			-24.32	-22.72		-24.47
1737	-23.98			-24.24	-24.03			-24.93	-23.03		-24.67
1738	-23.88			-23.50	-23.82			-24.69	-23.14		-24.64
1739	-24.51			-24.68	-24.26			-24.78	-23.94		-25.03
1740	-24.18			-24.16	-23.91			-25.04	-23.48		-25.52
1741	-24.50			-24.80	-24.82			-25.73	-23.47		-25.72
1742	-24.12			-24.44	-24.97			-25.25	-23.39		-25.60

	Tree 128	Tree 87	Tree 95	Tree 63	Tree 129	Tree 82	Tree 73	Tree 91	Tree 132	Tree 133	Tree 166
1743	-23.98			-23.98	-23.88			-24.61	-22.75		-25.07
1744	-23.82	-24.85		-23.87	-23.84			-24.48	-22.87		-24.95
1745	-23.88	-25.50		-24.69	-24.73			-25.30	-23.26		-24.95
1746	-24.27	-24.60		-24.94	-24.29			-24.47	-23.30		-25.02
1747	-24.80	-25.27		-25.15	-24.76			-25.12	-23.08		-25.34
1748	-23.73	-25.16		-24.63	-24.22			-25.81	-22.88		-24.93
1749	-23.71	-23.70		-23.93	-23.44			-24.77	-22.54		-24.33
1750	-23.65	-23.91		-24.19	-23.49			-24.05	-22.11		-24.17
1751	-23.16	-23.55		-22.89	-22.47			-23.94	-21.51		-23.34
1752	-23.69	-23.85		-24.28	-23.07			-24.14	-22.69		-24.18
1753	-23.88	-23.65		-24.09	-23.42			-24.03	-22.80		-24.01
1754	-23.91	-23.97		-24.64	-23.72			-24.51	-23.05		-24.49
1755	-23.26	-23.90		-23.91	-23.38			-24.75	-22.71		-24.22
1756	-23.95	-24.83		-24.36	-24.30			-25.32	-23.53		-24.88
1757	-23.54	-24.48		-24.11	-24.57			-24.70	-23.67		-24.44
1758	-22.97	-23.63		-22.86	-23.31			-23.94	-22.22		-23.79
1759	-23.07	-24.60		-23.57	-23.61			-23.99	-22.90		-23.58
1760	-23.21	-23.48		-22.95	-23.24			-23.59	-22.75		-22.75
1761	-23.58	-24.75		-22.99	-23.88			-23.93	-22.83		-24.06
1762	-23.88	-24.95		-24.10	-23.98			-24.83	-23.11		-24.17
1763	-23.62	-24.59		-24.09	-23.85			-24.14	-22.72		-24.32
1764	-23.51	-25.45		-23.95	-24.04			-24.77	-23.21		-24.38
1765	-24.18	-25.44		-23.33	-23.84			-25.03	-22.65		-24.42
1766	-23.51	-24.38		-22.99	-22.98			-24.02	-22.10		-24.19
1767		-25.02		-23.53	-24.05			-24.38	-23.00		-24.11
1768		-25.76		-24.45	-24.92			-25.27	-23.40		-24.45
1769		-25.00		-23.89	-23.90			-25.51	-23.59		-24.62
1770		-23.54		-22.45	-23.16			-23.80	-22.09		-24.16
1771		-24.29		-23.51	-22.88			-24.07	-22.10		-24.47
1772		-25.24		-23.24	-23.45			-24.86	-23.00		-24.79
1773		-24.59		-24.12	-23.48			-24.83	-23.33		-25.18
1774		-25.65		-24.91	-24.20			-25.64	-24.05		-25.61
1775		-25.40		-24.50	-23.82			-24.62	-22.92		-24.88
1776		-24.54		-23.61	-23.32			-24.89	-22.76		-24.50
1777		-25.49		-25.04	-23.71			-25.03	-23.30		-24.42
1778		-25.63		-24.78	-23.93			-25.16	-23.90		-25.08
1779		-23.93		-24.23	-23.07			-24.90	-23.31		-25.38
1780		-23.85	-24.39	-24.55	-23.61			-24.40	-22.91		-24.60
1781		-24.77	-24.23	-24.56	-23.35			-24.40	-23.28		-24.46
1782		-23.91	-22.47	-23.98	-22.59			-24.33	-22.58		-24.19
1783		-24.56	-23.55	-23.61	-23.05			-24.52	-22.87		-24.30
1784		-24.86	-24.32	-24.26	-23.54			-25.19	-23.25		-24.37
1785		-24.46	-23.93	-24.36	-24.05			-24.42	-23.35		-24.77
1786		-24.58	-24.47	-24.65	-23.79			-24.96	-23.61		-24.97
1787		-24.87	-25.04	-23.91	-23.97			-24.67	-23.54		-24.75
1788		-24.36	-24.81	-24.14	-24.00			-24.88	-23.27		-24.56
1789		-24.50	-23.99	-23.66	-23.41			-24.54	-23.02		-24.52
1790		-25.35	-25.77	-24.36	-23.98			-25.72	-23.69		-24.46
1791		-24.82	-24.01	-23.33	-23.21			-24.74	-22.77		-24.25
1792		-25.11	-24.07	-24.61	-23.90			-24.56	-22.98		-24.20
1793		-23.90	-24.22	-24.60	-24.37			-24.77	-23.15		-25.01

	Tree 128	Tree 87	Tree 95	Tree 63	Tree 129	Tree 82	Tree 73	Tree 91	Tree 132	Tree 133	Tree 166
1794		-24.30	-23.93	-24.69	-23.79			-25.27	-23.50		-24.38
1795		-24.38	-23.95	-24.25	-23.74			-24.19	-22.84		-24.11
1796		-24.42	-22.88	-23.09	-24.30			-24.39	-22.22		-24.69
1797		-24.21	-23.82	-24.07	-23.85			-24.58	-23.38		-24.13
1798		-24.49	-23.36	-23.25	-23.83			-24.60	-22.57		-24.05
1799		-23.87	-23.72	-24.11	-23.14			-24.18	-22.25		-24.14
1800		-25.63	-25.22	-25.21	-24.69			-25.63	-23.93		-24.71
1801		-25.08	-24.47	-24.30	-24.22			-24.85	-22.98		-25.07
1802		-25.40	-24.85	-24.71	-24.70			-25.03	-24.01		-24.91
1803		-24.43	-24.75	-24.70	-24.76			-25.48			-24.75
1804		-23.59	-24.08	-24.10	-23.70			-24.57			-24.60
1805		-24.20	-24.66	-24.04	-23.49			-24.13			-24.46
1806		-24.65	-24.92	-24.50	-23.66			-25.43			-23.90
1807		-24.46	-24.92	-23.53	-23.82			-24.36			-24.63
1808		-23.91	-23.86	-23.69	-23.09			-24.33			-24.83
1809		-24.31	-24.66	-24.01	-23.50			-24.82			-25.11
1810		-24.74	-24.41	-24.32	-23.87			-24.95			-24.95
1811		-23.86	-24.81	-23.41	-23.99			-23.93			-24.71
1812		-25.10	-25.52	-24.57	-24.38			-25.31			-25.25
1813		-23.34	-23.80	-22.40	-23.70			-24.49			-24.44
1814		-23.86	-24.44	-24.24	-23.42			-24.70			-24.46
1815		-24.36	-24.85	-24.39	-24.61			-25.53			-24.99
1816		-24.10	-24.58	-23.53	-24.16			-24.52			-24.39
1817		-24.81	-24.81	-24.03	-24.35			-25.11			-24.53
1818		-25.18	-25.09	-23.88	-24.69			-24.82			-24.26
1819		-23.73	-24.42	-21.95	-24.34			-24.75			-24.22
1820		-24.11	-23.82	-23.68	-23.74						-24.39
1821		-24.64	-24.52	-23.68	-24.36			-24.01			-23.96
1822		-23.75	-23.41	-24.35	-24.23			-25.41			-24.59
1823		-23.83	-23.50	-23.67	-23.81			-24.38			-23.84
1824		-24.05	-24.55	-24.32	-23.87			-24.40			-24.10
1825		-24.89	-25.03	-24.74	-25.01			-25.86			-24.95
1826		-24.57	-23.95	-23.72	-24.10			-24.60			-24.55
1827		-24.16	-24.39	-24.13	-24.12			-24.51			-24.84
1828		-24.37	-24.76	-23.62	-23.19			-25.04			-24.97
1829		-24.91	-24.84	-24.49	-24.79			-25.12			-24.80
1830		-24.81	-24.90	-24.10	-24.54			-25.57			-25.22
1831		-23.80	-24.13	-23.73	-23.81			-25.07			-24.91
1832		-24.86	-24.58	-24.32	-24.85			-25.99			-25.62
1833		-24.55	-24.74	-24.38	-24.94			-25.65			-25.94
1834		-24.69	-24.73	-24.75	-25.28			-24.93			-25.43
1835		-24.76	-24.63	-24.63	-24.93			-25.18			-24.95
1836		-24.95	-25.14	-24.25	-24.97			-25.53			-25.23
1837		-24.86	-24.84	-24.49	-24.81			-24.87			-25.15
1838		-24.74	-24.38	-24.04	-24.33			-24.46			-24.91
1839		-24.84	-24.54	-24.16	-24.65			-24.95			-24.73
1840		-23.97	-23.77	-23.89	-23.50			-24.65			-24.41
1841		-24.24	-25.10	-23.99	-23.88			-24.40			-24.73
1842		-24.88	-24.60	-24.23	-24.12			-24.77			-25.27

	Tree 128	Tree 87	Tree 95	Tree 63	Tree 129	Tree 82	Tree 73	Tree 91	Tree 132	Tree 133	Tree 166
1843		-23.88	-24.53	-24.08	-24.11			-24.05			-25.33
1844		-22.96	-22.98	-23.34	-23.09			-23.37			-24.50
1845		-25.66	-25.17	-23.71	-24.47			-24.97			-24.32
1846		-24.67	-23.66	-23.29	-23.82			-24.48			-24.68
1847		-24.72	-24.85	-24.54	-24.42			-24.71			-24.97
1848		-24.87	-23.96	-24.35	-24.57			-24.91			-25.31
1849		-24.67	-24.49	-23.36	-24.52			-24.93			-24.62
1850		-24.29	-23.86	-23.72	-24.48			-24.45			-24.74
1851		-24.81	-23.63	-22.88	-24.03			-24.80			-24.31
1852		-24.10	-23.50	-23.72	-23.53			-24.68			-24.96
1853		-24.65	-23.76	-22.94	-24.22			-25.71			-24.81
1854		-25.10	-24.08	-23.72	-24.38			-25.65			-25.43
1855		-25.34	-23.97	-24.37	-24.53			-25.52			-25.56
1856		-25.75	-24.33	-24.48	-25.27			-25.39			-25.42
1857		-25.52	-24.57	-24.44	-24.80			-24.92			-25.44
1858		-24.54	-23.93	-23.62	-23.99			-24.70			-24.78
1859		-25.04	-24.37	-24.11	-24.78			-24.96			-25.44
1860		-24.14	-23.88	-23.59	-24.21			-24.22			-24.81
1861		-24.62	-23.85	-22.77	-23.20			-24.53			-23.99
1862		-25.34	-23.97	-23.40	-24.03			-25.29			-24.88
1863		-24.89	-24.12	-24.18	-24.49			-25.92			-25.75
1864		-25.19	-24.32	-24.21	-24.84			-25.28			-25.29
1865		-24.85	-24.45	-24.24	-24.45			-25.51			-25.23
1866		-24.16	-24.34	-24.79	-24.36			-25.51			-24.92
1867		-26.08	-25.15	-24.95	-25.10			-25.56			-25.19
1868		-25.87	-24.14	-24.94	-24.71			-25.38			-25.36
1869		-25.01	-24.50	-24.35	-24.41			-25.00			-24.88
1870		-24.76	-23.98	-23.88	-24.66			-25.36			-24.81
1871		-24.62	-24.53	-23.40	-24.48			-24.56			-24.75
1872		-25.08	-24.85	-23.87	-24.41			-25.32			-25.18
1873		-24.75	-23.38	-24.18	-23.85			-25.95			-25.49
1874		-25.56	-24.21	-24.01	-24.51			-25.47			-25.97
1875		-25.25	-23.39	-23.71	-24.42			-24.95			-25.60
1876		-25.31	-24.57	-23.79	-24.79			-25.64			-25.39
1877		-25.00	-23.98	-24.06	-24.64			-25.21			-25.16
1878		-24.41	-24.45	-23.75	-24.80			-24.82			-25.16
1879		-25.15	-23.96	-23.41	-23.87			-25.16			-25.10
1880		-25.10	-24.62	-23.77	-24.07			-25.24			
1881		-24.66	-24.21	-23.90	-24.74			-24.73			
1882		-24.65	-23.45	-23.65	-23.88			-24.95			
1883		-24.28	-23.47	-23.94	-23.46			-25.11			
1884		-25.45	-24.79	-24.64	-23.32			-25.26			
1885		-25.01	-24.50	-24.81	-25.07			-25.75			
1886		-25.28	-24.47	-24.76	-25.32			-25.36			
1887		-26.41	-24.07	-24.08	-25.22			-25.22			
1888		-24.98	-24.25	-23.42	-24.94			-25.05			
1889		-24.06	-23.88	-23.94	-24.56			-25.50			
1890		-25.60	-24.77	-24.51	-25.18			-24.87			
1891		-24.97	-25.32	-24.77	-24.54			-25.68			

	Tree 128	Tree 87	Tree 95	Tree 63	Tree 129	Tree 82	Tree 73	Tree 91	Tree 132	Tree 133	Tree 166
1892		-25.45	-24.42	-24.85	-24.80			-24.99			
1893		-24.73	-22.64	-23.68	-24.52			-24.04			
1894		-24.04	-23.46	-22.81	-23.85			-24.44			
1895		-24.12	-23.33	-22.67	-23.17			-24.42			
1896		-25.06	-25.10	-23.86	-24.14			-25.61			
1897		-24.89	-24.01	-23.42	-23.71			-25.24			
1898		-24.17	-23.46		-24.26			-25.09			
1899		-25.54	-25.53	-24.18	-24.72			-26.70			
1900		-25.13	-23.92	-24.15	-25.05	-24.63	-24.81	-25.56			
1901		-23.94	-24.00	-23.06	-24.13	-23.28	-23.08	-25.42			
1902		-24.38	-24.06	-23.29	-24.32	-24.17	-23.40	-25.35			
1903		-23.90	-23.11	-22.61	-24.13	-22.92	-22.80	-24.86			
1904		-23.90	-23.99	-23.32	-24.00	-23.54	-22.85	-24.64			
1905		-24.23	-23.72	-23.37	-24.14	-23.97	-23.35	-24.75			
1906		-24.55	-23.42	-23.82	-24.93	-24.18	-22.64	-24.60			
1907		-24.89	-22.90	-24.17	-24.39	-24.05	-23.03	-24.90			
1908		-24.78	-23.53	-24.23	-24.31	-24.11	-23.27	-24.73			
1909		-24.79	-23.52	-23.92	-23.43	-24.13	-23.11	-24.80			
1910		-23.98	-23.38	-23.39	-24.45	-23.29	-22.26	-24.33			
1911		-24.54	-23.41	-23.37	-24.05	-23.98	-22.79	-24.32			
1912		-24.45	-22.92	-23.54	-24.07	-23.57	-22.76	-24.21			
1913		-23.90	-23.19	-23.33	-23.90	-23.77	-22.46	-23.96			
1914		-23.77	-23.65	-23.40	-23.80	-23.76	-22.46	-23.92			
1915		-25.60	-23.58	-23.14	-25.05	-24.58	-23.85	-24.36			
1916		-24.85	-22.78	-23.82	-24.59	-24.52	-23.57	-24.12			
1917		-24.90	-23.36	-23.58	-24.33	-24.00	-23.15	-24.61			
1918		-22.54	-21.70	-22.63	-23.28	-22.93	-21.64	-24.03			
1919		-25.52	-23.85	-24.16	-25.00	-24.60	-23.29	-24.95			
1920		-24.71	-22.88	-24.13	-24.11	-23.56	-22.84	-24.68			
1921		-24.62	-23.35	-23.75	-24.10	-23.86	-23.13	-23.82			
1922		-24.15	-23.91	-22.34	-23.19	-23.24	-22.03	-23.50			
1923		-24.53	-23.95	-23.28	-24.15	-24.33	-23.11	-24.45			
1924		-24.64	-22.79	-22.83	-23.50	-24.26	-22.63	-24.13			
1925		-24.63	-23.69	-23.83	-24.16	-25.02	-22.67	-24.38			
1926		-24.54	-23.58	-23.78	-24.05	-23.86	-22.99	-23.61			
1927		-24.17	-22.29	-22.50	-23.50	-23.88	-21.70	-23.30			
1928		-24.30	-24.39	-24.62	-24.65	-24.54	-22.90	-25.43			
1929		-25.39	-24.21	-24.85	-25.17	-24.55	-23.69	-25.00			
1930		-23.87	-23.76	-22.84	-23.66	-23.14	-22.14	-24.13			
1931		-24.31	-23.94	-23.77	-24.61	-24.54	-23.45	-25.05			
1932		-24.92	-23.84	-24.13	-24.82	-24.29	-24.19	-24.60			
1933		-25.08	-23.78	-24.17	-24.60	-24.00	-23.85	-25.20			
1934		-23.24	-22.75	-22.42	-22.54	-23.51	-23.40	-23.93			
1935		-24.96	-23.98	-24.92	-24.91	-24.93	-23.52	-24.61			
1936		-24.77	-23.74	-24.28	-23.92	-24.16	-22.94	-24.16			
1937		-24.29	-23.32	-23.15	-23.51	-23.66	-22.84	-24.47			
1938		-24.74	-24.30	-24.08	-24.75	-24.54	-23.49	-24.51			
1939		-25.08	-23.52	-24.64	-24.90	-23.95	-23.59	-24.28			
1940		-25.43	-24.47	-25.45	-24.95	-24.24	-24.03	-25.20			
1941		-24.66	-23.56	-24.39	-23.98	-23.81	-22.35	-24.85			
1942		-24.96	-24.26	-24.32	-24.76	-24.37	-23.32	-24.93			

	Tree 128	Tree 87	Tree 95	Tree 63	Tree 129	Tree 82	Tree 73	Tree 91	Tree 132	Tree 133	Tree 166
1943		-25.15	-23.96	-25.07	-24.91	-23.72	-23.24	-24.83			
1944		-24.86	-23.94	-24.56	-24.45	-23.49	-22.73	-24.54			
1945		-24.30	-23.64	-23.89	-23.94	-23.36	-22.43	-24.11			
1946		-24.42	-23.85	-25.09	-23.56	-23.81	-22.63	-24.44			
1947		-25.68	-24.78	-24.41	-24.83	-24.50	-23.50	-25.24			
1948		-25.18	-24.66	-24.54	-24.92	-24.22	-23.65	-25.75			
1949		-25.26	-24.66	-24.44	-25.38	-24.07	-23.74	-25.35			
1950		-24.74	-23.69	-24.18	-23.95	-22.91	-21.93	-23.97			
1951		-24.97	-24.35	-24.60	-24.60	-23.90	-22.78	-25.04			
1952		-24.89	-23.92	-23.69	-24.86	-23.84	-23.42	-24.98			
1953		-23.91	-23.93	-24.14	-23.99	-23.41	-22.57	-24.97			
1954		-24.30	-23.66	-23.85	-23.54	-23.68	-22.95	-24.82			
1955		-25.55	-23.95		-25.20	-24.73	-23.80	-25.27			
1956		-24.52	-23.92		-24.22	-24.30	-23.03	-24.47			
1957		-25.11	-24.27		-24.32	-24.06	-22.78	-24.75			
1958		-25.34	-24.45		-24.83	-23.95	-23.07	-25.04			
1959		-24.81	-24.16		-25.34	-24.01	-23.21	-25.25			
1960		-24.71	-23.91		-24.29	-23.07	-22.42	-23.83			
1961		-24.90	-25.23		-24.86	-23.61	-22.68	-24.88			
1962		-26.01	-24.48		-24.91	-23.75	-23.80	-25.68			
1963		-24.88	-23.56		-24.07	-24.06	-22.69	-24.91			
1964		-25.18	-23.54		-24.63	-24.85	-22.58	-24.92			
1965		-25.36	-24.22		-24.88	-24.11	-23.23	-25.59			
1966		-25.16	-23.83		-24.54	-24.45	-22.94	-25.28			
1967		-25.13	-23.66		-24.93	-24.42	-23.52	-25.73			
1968		-24.79	-23.45		-25.27	-23.75	-23.40	-25.06			
1969		-24.52	-22.71		-23.62	-23.65	-22.42	-23.61			
1970		-24.98	-23.74		-23.41	-23.46	-22.48	-24.47			
1971		-25.38	-24.16		-24.80	-24.53	-23.63	-25.30			
1972		-25.56	-24.01		-24.27	-23.94	-23.74	-24.72			
1973		-25.57	-24.56		-25.45	-24.58	-24.10	-25.39			
1974		-25.02	-24.06			-24.13	-23.22	-25.30			
1975		-24.51	-23.97		-25.44	-24.22	-22.86	-25.19			
1976		-24.74	-23.77		-24.56	-24.28	-22.85	-24.39			
1977		-24.84	-23.78		-24.20	-23.91	-22.98	-24.14			
1978		-23.92	-22.32		-23.55	-23.22	-22.31	-23.80			
1979		-25.01	-23.84		-23.77	-23.24	-22.61	-24.17			
1980		-24.31	-23.90		-25.35	-23.22	-22.22	-24.12			
1981		-25.64	-25.09		-25.33	-24.07	-23.76	-24.91			
1982		-24.84	-24.37		-25.32	-23.54	-23.46	-25.14			
1983		-24.76	-24.08		-24.53	-22.72	-22.96	-24.31			
1984		-25.44	-24.59		-25.19	-23.34	-23.10	-25.43			
1985		-25.44	-23.80		-23.88	-22.36	-23.11	-24.93			
1986		-25.69	-25.72		-24.64	-24.38	-23.11	-25.47			
1987		-25.75	-24.02		-24.68	-24.11	-23.32	-24.67			
1988		-25.35	-23.19		-23.81	-23.79	-23.41	-24.31			
1989		-24.85	-24.05		-24.17	-23.52	-22.50	-24.58			
1990		-24.97	-24.17		-24.31	-23.65	-22.74	-24.88			

	Tree 128	Tree 87	Tree 95	Tree 63	Tree 129	Tree 82	Tree 73	Tree 91	Tree 132	Tree 133	Tree 166
1991		-25.27	-24.44		-24.21	-24.09	-22.80	-25.07			
1992		-25.37	-24.33		-25.48	-24.17	-23.34	-25.95			
1993		-24.68	-23.65		-23.87	-23.27	-22.59	-25.18			
1994		-25.07	-23.44		-24.78	-23.51	-23.27	-25.34			
1995		-25.81	-24.49		-26.12	-24.44	-23.82	-25.27			
1996		-24.48	-22.94		-24.34	-23.35	-22.84	-24.14			
1997		-24.55	-23.04		-24.11	-23.49	-22.64	-24.16			
1998		-24.23	-23.63		-23.77	-24.20	-22.51	-24.13			
1999		-25.24	-24.39		-25.55	-25.50	-24.24	-25.51			
2000		-24.85	-24.00		-25.51	-24.42	-23.72	-25.58			
2001		-24.69	-23.50		-24.39	-23.18	-22.80	-24.74			

Table A.13: Raw $\delta^{13}C$ (‰) data

A.7 Stable Oxygen Isotope Data

	Tree 63	Tree 73	Tree 82	Tree 87	Tree 91	Tree 95	Tree 129	Tree 132	Tree 166
1765	28.93			26.79			28.63	27.94	
1766	29.02			27.21			29.54	28.38	
1767	27.75			26.24			29.69	28.54	
1768	26.48			26.71			29.54	27.01	
1769	26.90			25.32			28.23	26.42	
1770	26.52			27.41			29.07	27.93	
1771	27.49			26.88			28.39	27.61	
1772	27.31			25.99			29.13	27.93	
1773	28.32			27.66			30.49	28.59	
1774	26.45			26.09			30.50	26.76	
1775	26.41			27.08			29.68	27.81	
1776	27.62			25.83			28.43	27.91	
1777	26.59			27.47			27.14	27.22	
1778	27.83			27.26			27.35	27.66	
1779	27.47			27.81			27.47	28.31	
1780	26.69			28.69		24.98	25.92	26.90	
1781	26.61			26.63		23.48	25.90	27.74	
1782	26.50			27.76		24.76	26.24	26.45	
1783	27.56			27.21		25.20	27.73	26.44	
1784	27.85			26.53		23.74	26.90	25.94	
1785	27.22			26.48		24.69	26.61	25.50	
1786	28.50			27.27		25.24	27.68	26.07	
1787	27.90			26.65		24.82	26.46	25.63	
1788	28.27			27.91		25.28	26.97	26.19	
1789	28.85			28.13		25.53	27.65	26.61	

	Tree 63	Tree 73	Tree 82	Tree 87	Tree 91	Tree 95	Tree 129	Tree 132	Tree 166
1790	29.27			27.21		25.27	27.72	27.75	
1791	27.02			26.88		26.01	27.47	26.54	
1792	28.20			26.60		25.75	28.55	27.89	
1793	28.03			26.83		25.60	28.41	27.04	
1794	28.05			26.87		26.55	28.31	27.25	
1795	27.81			26.64		26.80	28.66	27.61	
1796	27.99			27.32		27.78	28.16	27.40	
1797	28.21			27.29		26.86	28.94	27.65	
1798	28.61			27.01		26.43	27.64	27.19	
1799	29.80			27.67		28.04	29.48	29.78	
1800	28.81			26.40		25.57	27.68	28.04	
1801	29.14			26.48		24.90	27.37	28.22	
1802	27.74			25.95		25.06	26.49	25.18	
1803	27.24			26.94		25.57	27.38		
1804	27.31			27.66		26.25	26.20		
1805	26.87			27.35		25.74	25.69		
1806	27.23			27.03		26.21	26.62		
1807	26.71			25.81		26.13	26.36		
1808	27.32			27.23		26.27	26.63		
1809	26.64			26.48		25.72	25.91		
1810	26.91			25.83	27.33	25.06	25.67		28.43
1811	27.07			27.19	26.91	25.46	26.79		26.76
1812	26.66			26.86	26.79	25.09	26.20		26.15
1813	27.36			27.34	27.64	25.88	26.16		27.58
1814	27.01			27.17	27.05	25.17	26.56		26.89
1815	27.74			27.77	27.69	26.08	28.06		26.90
1816	27.01			27.16	27.83	24.26	26.84		26.74
1817	26.78			26.78	26.71	26.10	26.60		25.53
1818	28.23			27.78	28.50	27.01	27.70		27.98
1819	27.98			27.75	28.32	25.77	28.15		27.71
1820	27.78			27.68	27.58	25.15	28.12		28.16
1821	27.35			27.47	26.02	25.09	27.63		28.31
1822	27.38			27.56	27.30	25.66	27.44		26.74
1823	27.31			26.99	27.72	25.36	27.30		26.99
1824	26.82			27.11	26.95	23.31	27.73		26.81
1825	25.89			24.04	27.16	21.84	26.85		27.36
1826	27.10			25.88	28.34	24.01	27.62		27.44
1827	26.26			25.24	27.14	23.35	26.57		26.77
1828	27.64			27.08	28.93	25.24	27.39		27.35
1829	26.91			26.22	28.00	24.64	26.56		26.90
1830	26.48			26.00	28.10	23.84	25.43		26.81
1831	28.18			28.21	29.18	25.75	27.44		28.12
1832	28.12			27.80	29.02	26.13	27.46		27.97
1833	27.62			27.29	28.23	25.91	27.34		27.13
1834	27.68			27.47	28.17	26.60	26.96		26.98
1835	27.31			27.08	27.23	25.52	26.91		27.60
1836	27.50			26.95	27.80	26.12	27.32		27.08
1837	26.51			25.88	26.43	25.25	26.65		26.11
1838	26.34			25.94	26.26	24.58	26.82		25.90
1839	26.67			26.00	26.05	25.32	26.47		27.28

	Tree 63	Tree 73	Tree 82	Tree 87	Tree 91	Tree 95	Tree 129	Tree 132	Tree 166
1840	26.82			26.68	27.60	24.96	26.22		26.42
1841	27.96			27.63	28.24	26.57	27.84		26.66
1842	28.47			27.34	28.35	27.46	27.89		27.71
1843	27.79			27.37	28.29	26.95	28.25		26.92
1844	27.64			27.56	26.96	27.26	27.73		27.14
1845	27.60			27.09	27.95	27.04	28.40		27.13
1846	27.91			26.65	27.12	28.52	26.83		26.89
1847	28.69			27.08	28.52	27.20	28.68		28.14
1848	27.35			26.55	27.11	26.29	27.99		27.00
1849	26.48			25.52	26.61	25.00	25.80		26.75
1850	27.13			27.18	27.24	25.67	27.38		27.12
1851	26.80			26.51	26.86	24.60	26.19		27.00
1852	28.75			28.51	27.12	25.60	28.54		27.81
1853	27.53			27.17	28.08	28.00	26.82		24.92
1854	26.66			28.25	25.60	26.40	28.07		26.51
1855	26.84			26.92	27.27	26.46	26.88		26.19
1856	27.22			27.04	27.81	25.66	26.50		25.62
1857	26.98			28.12	29.42	25.76	27.22		26.94
1858	27.77			27.76	27.87	26.92	27.48		27.69
1859	27.05			27.16	26.68	24.25	26.74		26.46
1860	27.55			27.33	27.37	26.24	27.19		26.81
1861	28.40			26.56	26.97	25.01	27.47		25.67
1862	27.11			26.77	27.59	28.02	27.57		26.74
1863	27.72			28.22	27.84	26.34	28.63		26.59
1864	28.25			27.53	28.07	27.03	28.75		27.03
1865	28.96			28.21	28.69	28.14	29.16		27.24
1866	28.71			28.84	28.43	26.73	29.30		26.85
1867	27.85			26.47	27.18	25.56	27.59		26.71
1868	27.64			27.69	27.34	23.93	29.20		26.76
1869	27.39			26.75	27.18	25.86	27.66		26.53
1870	28.70			26.77	27.15	24.73	27.09		26.74
1871	29.23			27.22	27.95	26.24	28.36		26.98
1872	29.57			27.57	28.26	26.43	28.15		27.85
1873	28.79			27.83	27.65	24.22	28.37		27.31
1874	28.74			27.31	27.53	24.65	28.47		26.72
1875	29.36			27.75	27.87	26.06	28.18		26.28
1876	27.92			28.00	27.79	25.84	27.91		27.53
1877	28.22			27.93	27.44	25.58	27.62		26.09
1878	27.97			28.43	28.25	28.12	27.91		27.09
1879	26.77			27.98	27.30	26.30	27.21		26.49
1880	27.62			26.21	27.49	26.87	27.74		
1881	27.63			28.70	27.27	24.54	26.72		
1882	28.61			26.74	27.55	26.81	26.55		
1883	28.02			27.36	28.09	26.80	28.67		
1884	26.56			27.08	27.41	26.42	28.07		
1885	27.62			27.61	27.39	26.90	25.93		
1886	27.23			26.27	26.93	26.21	26.52		
1887	27.53			26.97	27.40	25.95	27.65		
1888	25.47			26.71	26.72	27.58	25.60		
1889	27.73			26.77	27.91	27.37	28.13		

	Tree 63	Tree 73	Tree 82	Tree 87	Tree 91	Tree 95	Tree 129	Tree 132	Tree 166
1890	27.15			26.82	27.28	26.06	27.57		
1891	27.08			26.68	27.19	25.54	27.96		
1892	26.46			27.34	27.45	27.98	26.53		
1893	28.05			28.18	28.08	27.31	27.29		
1894	28.15			26.74	28.30	28.56	28.24		
1895	28.76			28.82	28.70	27.06	28.65		
1896	27.10			26.14	27.34	27.32	27.29		
1897	27.67			27.74	27.46	24.86	28.08		
1898	26.61			26.08	26.53	25.19	26.74		
1899	27.40			25.74	26.91	25.71	26.82		
1900	27.50	26.20	27.91	26.71	27.21	28.00	26.93		
1901	26.37	28.06	27.40	27.69	27.43	27.45	27.74		
1902	26.68	26.90	27.70	25.93	27.45	27.53	28.05		
1903	28.57	27.56	28.10	27.37	27.91	27.64	28.56		
1904	28.35	26.50	27.30	26.98	27.54	27.58	26.91		
1905	26.94	26.46	26.97	26.91	26.95	27.10	25.96		
1906	26.78	26.85	28.00	27.51	27.81	27.75	27.90		
1907	27.23	27.23	28.00	27.33	27.82	27.53	27.59		
1908	26.51	27.46	28.29	27.60	27.76	27.66	27.65		
1909	27.17	26.64	27.23	26.86	27.41	27.19	28.89		
1910	27.44	28.46	28.33	27.54	28.20	27.81	27.20		
1911	27.27	28.67	28.32	26.99	27.95	27.92	28.56		
1912	28.01	28.60	28.47	27.92	28.35	27.21	28.35		
1913	27.56	27.85	27.61	27.65	28.62	27.58	25.96		
1914	28.38	28.20	27.74	28.02	27.76	27.86	27.79		
1915	27.78	26.47	26.39	26.89	27.60	26.83	24.97		
1916	27.70	27.77	27.71	27.96	27.13	27.39	27.34		
1917	28.38	26.56	26.57	27.64	27.30	27.54	27.07		
1918	29.75	28.63	27.84	28.85	28.68	28.61	28.48		
1919	28.61	26.37	26.51	27.57	27.72	27.07	27.00		
1920	27.56	27.18	26.02	26.78	27.09	27.48	26.77		
1921	27.49	27.52	26.40	27.30	27.12	26.86	26.58		
1922	26.69	27.17	26.62	28.08	26.54	26.51	26.93		
1923	26.47	26.43	26.69	27.79	27.52	27.14	26.99		
1924	27.10	27.45	27.69	27.70	27.00	26.78	28.04		
1925	29.39	28.05	28.40	28.27	28.22	27.40	28.39		
1926	29.00	27.52	27.37	27.54	27.96	27.17	27.63		
1927	27.10	26.58	26.17	27.23	27.34	26.87	26.37		
1928	27.33	26.48	26.74	26.78	27.75	26.96	26.02		
1929	27.31	27.36	27.91	27.46	28.45	28.32	27.20		
1930	29.12	29.04	27.63	27.60	27.27	27.41	28.04		
1931	27.61	27.21	26.47	27.46	27.62	26.80	26.62		
1932	26.63	26.77	26.77	26.22	27.80	26.45	26.45		
1933	25.24	27.82	27.16	27.48	27.87	27.17	26.82		
1934	27.34	28.41	27.14	27.69	27.64	27.20	27.68		
1935	26.19	27.57	27.63	27.10	28.06	27.54	27.23		
1936	27.26	28.04	27.63	27.26	27.12	27.24	27.16		
1937	26.86	27.95	27.58	27.89	27.46	26.66	27.27		
1938	25.81	26.91	27.46	27.25	27.25	27.93	27.17		
1939	26.48	27.36	27.69	27.96	27.38	27.82	28.04		

	Tree 63	Tree 73	Tree 82	Tree 87	Tree 91	Tree 95	Tree 129	Tree 132	Tree 166
1940	26.68	27.05	27.11	27.52	26.25	27.11	27.47		
1941	27.03	27.53	26.46	27.40	26.91	27.04	27.17		
1942	26.14	26.82	26.27	26.15	26.08	26.83	25.77		
1943	26.70	27.21	27.04	27.01	27.04	27.12	27.40		
1944	27.61	27.45	27.23	27.62	26.97	26.98	28.00		
1945	27.67	27.55	27.86	27.31	26.68	27.54	28.02		
1946	27.49	26.96	27.19	26.80	26.87	27.27	27.15		
1947	27.80	27.05	28.02	27.40	26.55	27.39	26.36		
1948	27.66	26.85	27.39	27.17	27.13	27.66	27.04		
1949	25.03	26.43	26.54	26.31	25.98	27.20	27.19		
1950	26.74	27.52	27.55	27.41	26.30	26.98	27.94		
1951	26.53	26.35	26.18	26.43	25.94	26.14	27.71		
1952	27.64	26.76	27.23	26.56	25.71	27.67	27.48		
1953	27.10	27.01	27.30	27.17	26.42	27.73	27.54		
1954	27.44	27.48	27.19	27.31	26.40	26.62	27.65		
1955		26.76	27.52	27.04	26.77	27.51	27.57		
1956		27.24	27.39	27.39	26.32	27.66	27.23		
1957		26.97	27.10	26.40	26.58	27.34	27.46		
1958		26.18	27.48	26.29	26.39	27.67	26.54		
1959		26.36	27.24	26.03	26.88	27.56	27.70		
1960		27.09	27.53	26.64	26.78	27.42	27.63		
1961		26.39	27.25	25.78	26.24	27.11	26.60		
1962		27.12	28.14	27.21	27.03	28.59	27.41		
1963		27.61	27.80	27.62	27.64	28.36	27.31		
1964		26.95	27.21	26.55	26.96	27.15	26.63		
1965		26.87	26.75	26.31	26.46	26.93	27.07		
1966		25.98	26.56	26.25	25.96	26.05	26.03		
1967		26.60	26.95	26.36	26.27	26.11	27.36		
1968		27.44	27.67	27.56	27.02	27.86	26.87		
1969		27.20	27.45	27.47	27.00	27.45	27.80		
1970		26.87	27.54	26.90	26.75	26.92	25.95		
1971		26.39	27.12	26.41	26.25	27.64	26.57		
1972		27.18	27.65	26.56	26.79	26.93	27.00		
1973		26.09	26.49	25.62	26.12	25.87	25.64		
1974		26.11	26.90	26.71	26.49	27.54	27.01		
1975		27.01	27.63	26.40	27.17	27.09	27.26		
1976		27.06	27.40	27.19	27.13	27.29	25.72		
1977		26.78	27.47	27.51	26.79	27.57	25.76		
1978		27.44	27.96	27.51	27.49	28.73	25.55		
1979		27.36	27.53	27.42	27.37	27.61	26.27		
1980		28.43	28.63	28.23	28.00	28.29	27.63		
1981		26.73	26.83	26.51	26.96	26.75	26.45		
1982		27.14	27.82	27.53	27.50	27.64	26.44		
1983		26.86	25.75	26.08	26.29	27.15	26.31		
1984		26.54	26.99	26.16	26.99	26.84	25.40		
1985		26.87	26.12	26.33	26.56	26.99	26.59		
1986		27.55	27.44	27.67	27.34	26.94	27.37		
1987		26.15	26.24	27.39	26.84	27.40	27.10		
1988		26.14	26.08	26.71	26.53	26.60	26.40		
1989		27.63	27.64	27.55	27.40	27.40	26.90		

	Tree 63	Tree 73	Tree 82	Tree 87	Tree 91	Tree 95	Tree 129	Tree 132	Tree 166
1990		26.73	27.03	26.80	26.55	26.96	26.03		
1991		27.15	28.23	27.57	27.75	26.91	27.14		
1992		27.19	27.86	26.87	27.43	27.36	27.62		
1993		27.04	27.40	27.34	27.08	27.43	27.91		
1994		27.17	27.93	27.66	27.46	27.69	26.91		
1995		26.78	26.81	26.75	26.92	26.28	26.58		
1996		27.41	28.17	27.10	27.58	27.31	27.04		
1997		27.10	27.35	27.30	27.26	26.68	27.63		
1998		26.55	26.75	26.68	26.37	26.90	25.46		
1999		26.35	26.52	26.54	26.45	26.50	25.87		
2000		26.57	26.67	26.73	25.76	26.94	25.83		
2001		26.43	26.76	26.67	26.86	27.20	26.93		

Table A.15: Raw $\delta^{18}O$ (‰) data